



Resilience assessment: Methodological challenges and applications to critical infrastructures

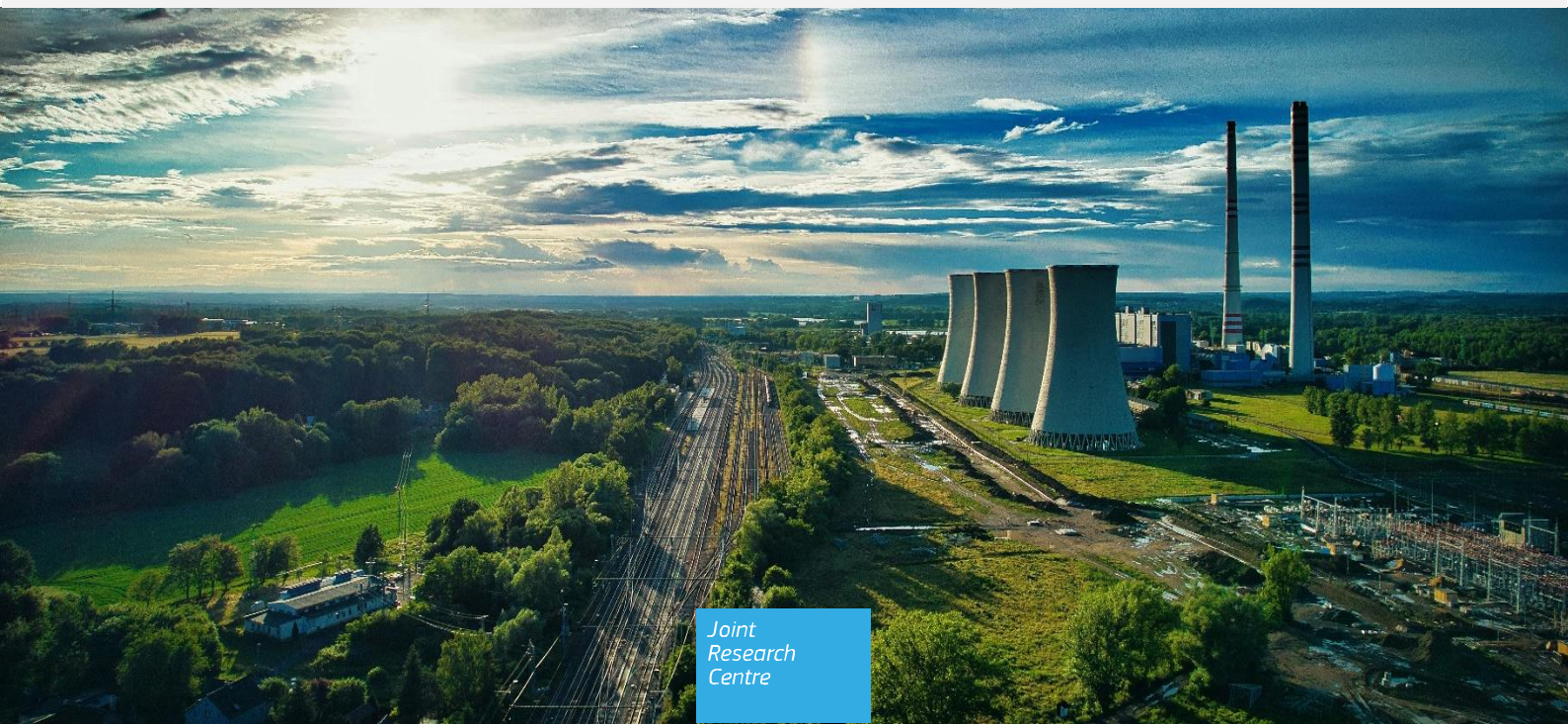
Proceedings of the 63rd ESReDA Seminar

Joint Research Centre, Ispra, Italy

25-26 October 2023

Kopustinskas, V., Foretic, H., Asensio Bermejo, I.

2024



This document is a publication by the Joint Research Centre (JRC), the European Commission's science and knowledge service. It aims to provide evidence-based scientific support to the European policymaking process. The contents of this publication do not necessarily reflect the position or opinion of the European Commission. Neither the European Commission nor any person acting on behalf of the Commission is responsible for the use that might be made of this publication. For information on the methodology and quality underlying the data used in this publication for which the source is neither Eurostat nor other Commission services, users should contact the referenced source. The designations employed and the presentation of material on the maps do not imply the expression of any opinion whatsoever on the part of the European Union concerning the legal status of any country, territory, city or area or of its authorities, or concerning the delimitation of its frontiers or boundaries.

Contact information

Name: Vytis Kopustinskas

Address: E. Fermi 2749, Ispra (VA), 21027, Italy

Email: vytis.kopustinskas@ec.europa.eu

Tel.: +39 0332 786257

EU Science Hub

<https://joint-research-centre.ec.europa.eu>

JRC139101

PDF ISBN 978-92-68-20482-5 doi:10.2760/2808748 KJ-01-24-002-EN-N

Luxembourg: Publications Office of the European Union, 2024

© European Union, 2024



The reuse policy of the European Commission documents is implemented by the Commission Decision 2011/833/EU of 12 December 2011 on the reuse of Commission documents (OJ L 330, 14.12.2011, p. 39). Unless otherwise noted, the reuse of this document is authorised under the Creative Commons Attribution 4.0 International (CC BY 4.0) licence (<https://creativecommons.org/licenses/by/4.0/>). This means that reuse is allowed provided appropriate credit is given and any changes are indicated.

How to cite this report: European Commission, Joint Research Centre, *Resilience assessment: Methodological challenges and applications to critical infrastructures*, Kopustinskas, V., Foretic, H. and Asensio Bermejo, I. editor(s), Publications Office of the European Union, Luxembourg, 2024, <https://data.europa.eu/doi/10.2760/2808748>, JRC139101.

Contents

| | |
|--|-----|
| Abstract | 3 |
| Acknowledgements | 4 |
| 1 Introduction..... | 5 |
| 2 Seminar papers and presentations..... | 6 |
| Plenary talk 1 – Igor Linkov: Infrastructure Resilience: State of Science and Practice | 6 |
| Plenary talk 2 – Ivo Häring: Analytical resilience quantification approaches (resilience analytics) to classify and rank first principle risk and resilience modelling and simulation methods | 31 |
| Plenary Talk 3 – Marta Poncela Blanco: Risk preparedness regulation in the electricity sector: aims and challenges | 52 |
| 2.1 Resilience of Ukraine's critical energy infrastructure. Challenges of war time..... | 66 |
| 2.2 On the resilience of the European Union natural gas system..... | 71 |
| 2.3 Resilience enhancement of gas transmission system by remote control deployment of valves: methodology of indicator analysis and case study | 86 |
| 2.4 Application of metaheuristic algorithms for finding strategy of optimal response to natural gas supply disruptions..... | 90 |
| 2.5 Hydrogen electrolyzers as a flexible source for the optimal operation of the distribution grid | 95 |
| 2.6 Risk and resilience-informed decision-making for strategic territorial risk management: from methodologies to practical implementation for infrastructures exposed to mountain natural hazards | 107 |
| 2.7 Towards a modular co-simulation framework for the assessment of cascading effects among critical infrastructures and the impact on citizens | 110 |
| 2.8 Remaining Useful Life of hydraulic steel structures under high-cycle fatigue Presentation of the chair Medelia and preliminary study of a lock gate..... | 121 |
| 2.9 Resilience Metrics for Interdependent Infrastructure Systems: Characterization in full-scale Application | 130 |
| 2.10 A territorial view of the infrastructure resilience..... | 133 |
| 2.11 Use of Multi-Criteria Decision Analysis for assessing the resilience of Critical Entity systems..... | 140 |
| 2.12 The main topics of discussion and research on issues of modelling systemic changes in urban systems | 141 |
| 2.13 Impacts of Climate Change on interdependent Critical Energy Infrastructure: Direct and Cascading Effects across Energy Production, Transport and Demand | 144 |
| 2.14 Fragility assessment of power grid infrastructure towards climate resilience and adaptation..... | 154 |
| 2.15 Feasibility Study: Improving Low-Inertia Power System Resilience By Novel Load Shedding Method Including Control of Synchronous Condensers' Power Injections | 164 |
| 2.16 An innovative methodology for risk-based resilience assessment to prioritize grid interventions against natural threats in the Italian power system | 174 |
| 2.17 The Resilience Assessment in Electricity sector: How to get started, holistic or segmented view? | 189 |
| 2.18 Modelling of power disruption scenarios by PyPSA in the Baltic region..... | 201 |
| 2.19 The Impact of Small Hydro Power Plants on the Adequacy of a Power System with High Penetration of Renewable Energy Sources | 208 |
| 2.20 Evaluation matrix to select appropriate countermeasures for Offshore Wind Farm protection | 220 |
| 2.21 Addressing the Risk of Prolonged Periods of Low Renewable Generation in Power Systems Resilient Planning..... | 232 |

| | |
|--|------------|
| 2.22 Assessing risk of water damage to buildings under current and future climates | 239 |
| 2.23 Flood resilience and sustainability in bridge climate adaptation..... | 242 |
| 2.24 An Empirical Model for Predicting Landslide Runout Distance in Malaysia | 245 |
| 2.25 Complex Systems Resilience to Hybrid Threats | 256 |
| 3 Conclusions of the Seminar | 257 |
| Annexes | 258 |
| Annex 1. Programme of the Seminar as presented..... | 258 |
| Annex 2. Plenary speakers | 260 |
| Annex 3: About the Seminar..... | 262 |
| Annex 4: About ESReDA organisation and activities | 265 |

Abstract

These proceedings are the outcome of the 63rd ESReDA Seminar on “Resilience assessment: Methodological challenges and applications to critical infrastructures” that took place at the European Commission’s Joint Research Centre’s (JRC) premises in Ispra, Italy, on 25-26 October 2023. A broad spectrum of resilience topics were covered, with sessions addressing different infrastructure sectors: energy sector (electricity, gas, hydrogen), transport sector (rail, road, air and maritime), other critical infrastructures, networks and entities, urban development, public sector and government. The seminar aimed at addressing resilience due to different hazards or threats, such as: disruptions of infrastructures due to aging or technical failures, natural events, intentional attacks or emerging threats, hybrid being an example. This seminar brought together researchers, practitioners and decision-makers from academia, operators, industry, governing bodies, to discuss theories, concepts, and experiences of resilience assessment methodologies and applications. The proceedings include 3 plenary speeches and 25 full papers or extended abstracts.

Acknowledgements

The organisation of the 63rd ESReDA Seminar was a huge effort of many JRC staff and ESReDA members. The authors of this report are particularly thankful for full support of the JRC Directorate C Director Habil dr. Piotr Szymański and his office team, Unit C3 – Energy Security, Distribution and Markets hierarchy – Head of Unit Kristine Vlagsma and her deputy Gianluca Fulli. The authors are very thankful for the time and attention from ESReDA Board of Directors and in particular ESReDA President dr. Mohamed Eid.

The Seminar would not be a successful event without dedication of the JRC Ispra Conference Service Team, Catering, Logistics, Security and Procurement Services. All and each service member deserves a big thank you!

We would like to thank every participant for attending and contributing to the 63rd ESReDA Seminar. We hope that the seminar provided a platform for stimulating discussion and debate and that participants were able to take the opportunity to form new, collaborative links and share their knowledge of resilience techniques and their applications in practice, with like-minded engineers and scientists.

Special thanks goes to Virginie Petitjean, Unit secretary, for her full dedication, extreme efforts and creativity that made a lot of last minute requests happen.

The last, but not least ‘thank you’ goes to the Technical Programme Committee for their efforts during the review process of the seminar contributions.

Authors

Vytis Kopustinskas, Hrvoje Foretić, Isabel Asensio Bermejo

1 Introduction

Research in resilience of infrastructure systems has been constantly increasing during the last decade and is expected to grow further. Although the term resilience was used in material science already in 19th century, the current meaning of system resilience originates from research in ecology back in 70s. Self-repairable computer systems, being developed also in the same decade for space and defence applications, could be considered as examples of resilience applications in engineering. Resilience applications in technical systems domain have evolved most significantly during the last two decades and the term resilience has already been transferred to the policy domain, as the Directive on the Resilience of Critical Entities (CER Directive) went into force in January 2023 and replaced the Critical Infrastructure Directive, published in 2008.

Two fundamental points in the resilience domain were addressed by the Seminar: 1. the methodological development of resilience assessment from a conceptual framework to modelling approaches, and 2. the metrics for resilience assessment and development of quantitative tools for decision-making. The 63rd ESReDA seminar was a forum for exploring these points and other related questions. Aim was to discuss theories, concepts, and experiences of resilience assessment methodologies and applications. Authors were invited to present their proposals and discuss successes and/or failures and to identify future needs in resilience research. Participants presented new ideas, scientific papers, conceptual papers, case studies and cross-sectoral research on this topic with examples and applications of infrastructures exposed to both technological and natural hazards or threats.

The seminar saw the presentation of three plenary speakers: Igor Linkov, Senior Science and Technology Manager with the US Army Engineer Research and Development Center (ERDC), and Adjunct Professor with Carnegie Mellon University, Ivo Häring, Senior Scientist in the Department Safety and Resilience of Technical Systems at Fraunhofer Ernst-Mach-Institute (EMI), and Marta Poncela Blanco, Policy Officer at the European Commission, Directorate General for Energy, Energy Security and Safety unit.

These proceedings contain 3 plenary speeches and 25 papers presented at the seminar with authors spread across academia and industry. A broad spectrum of resilience topics were covered, with sessions addressing different infrastructure sectors: energy sector (electricity, gas, hydrogen), transport sector (rail, road, air and maritime), other critical infrastructures, networks and entities, urban development, public sector and government. The seminar aimed at addressing resilience due to different hazards and threats, such as: disruptions of infrastructures due to aging or random failures, natural disasters, intentional attacks or man-made hazards, emerging threats (e.g. hybrid).

The seminar has attracted a good mix of academic and industrial participants from many European and overseas countries. There were authors coming from universities, research institutes and industrial companies in Austria, Belgium, Cyprus, France, Germany, Greece, Italy, Latvia, Lithuania, Malaysia, Netherlands, Norway, Poland, Portugal, Romania, Spain, Ukraine, United Kingdom and United States of America.

The editorial work for this report was supported by the Joint Research Centre of the European Commission in the frame of JRC support to ESReDA activities.

2 Seminar papers and presentations

Plenary talk 1 – Igor Linkov: Infrastructure Resilience: State of Science and Practice

Igor Linkov, Senior Science and Technology Manager, US Army Engineer R&D Center, University of Florida, USA

*This presentation does not necessarily reflect
the views of the United States Government, and
is only the view of the author*

Infrastructure Resilience: State of Science and Practice

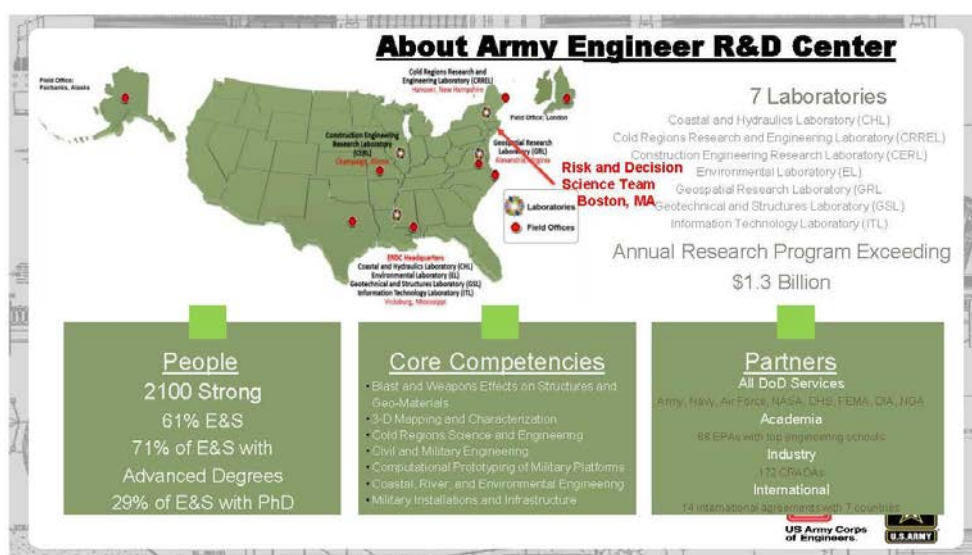
Igor Linkov, PhD

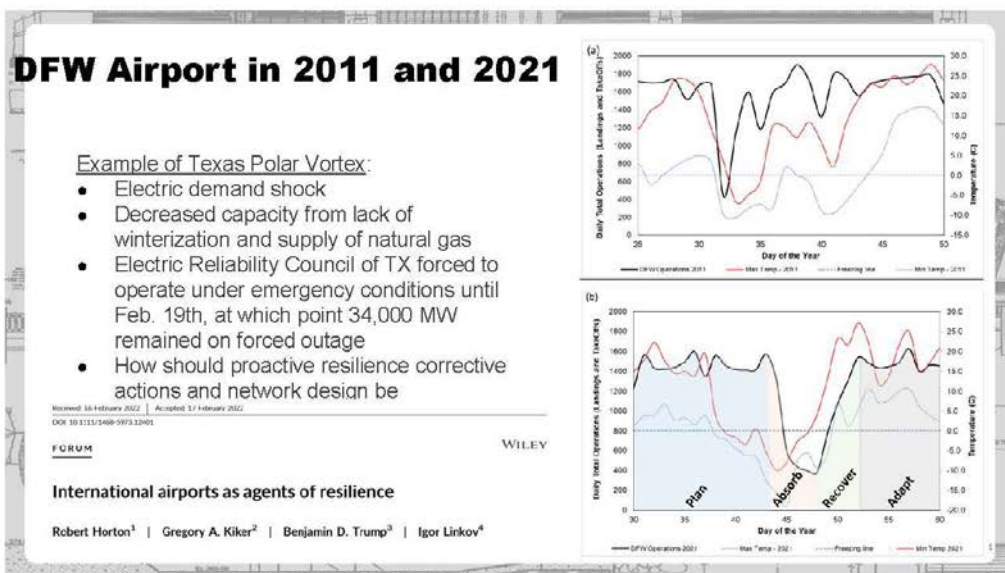
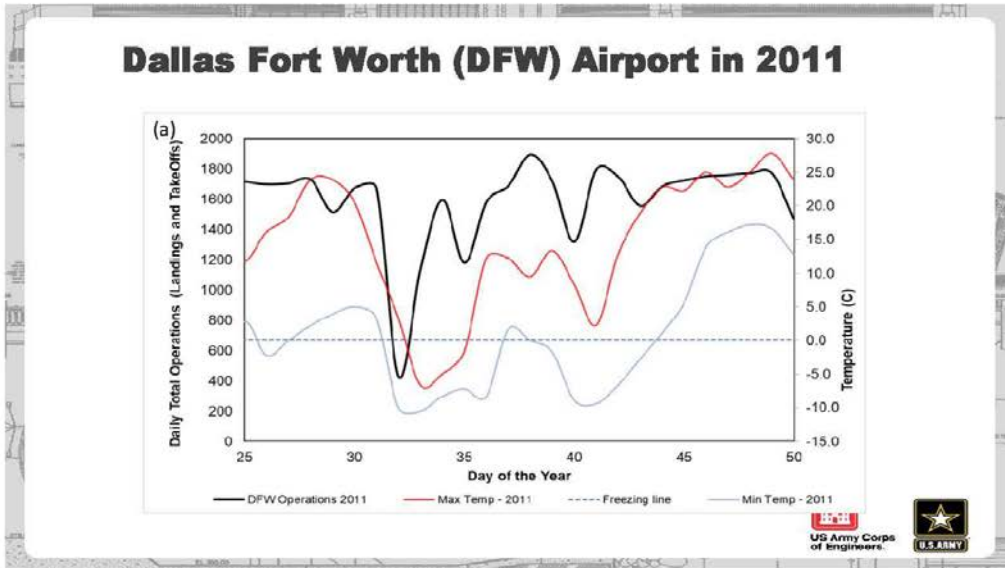
Senior Science and Technology Manager (SSTM),
US Army Engineer R&D Center;

Adjunct Professor, Carnegie Mellon University and
University of Florida

i.linkov@yahoo.com

25 October 2023





Outline

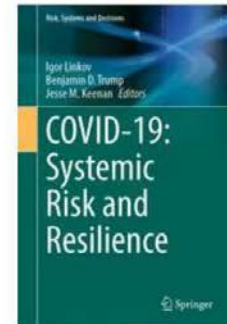
Data: IAEA Model intercomparisons – very significant uncertainty driven by judgment of modelers

Science and Crisis: Historical perspectives (Venice), Decision Maker Needs in New England, Need for Resilience

From Safety and Reliability to Resilience: Taxonomy, Measurements, Efficiency/Resilience, By Design and by Intervention

AI/Vision for Data: Project Examples

Conclusion: Resilience science and practice may be difficult to implement in the sea of noise, clear vision is required



International Atomic Energy Agency Model Intercomparisons

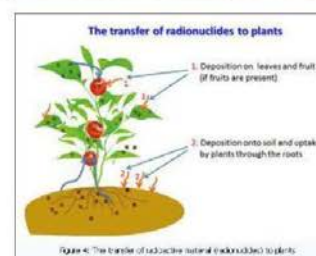
- Multiple types of uncertainty strongly affect modeling results
 - parameter, model, scenario
 - Understanding uncertainty is essential to:
 - Conduct analysis consistent with current regulatory guidance
 - Gain trust and confidence
- Generally:
- Conclusions can be generalized to a wide range of models and situations.



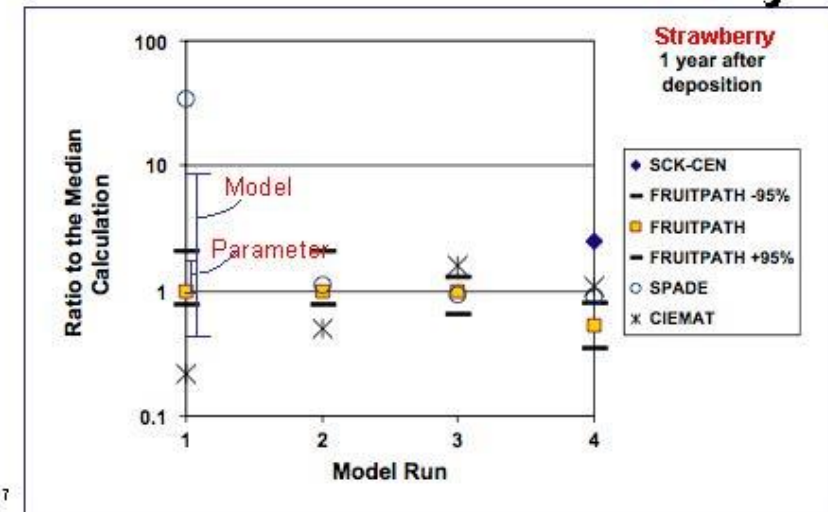
Risk Analysis, Vol. 28, No. 6, 2008

Model Uncertainty and Choices Made by Modelers: Lessons Learned from the International Atomic Energy Agency Model Intercomparisons†

Igor Linkov^{1*} and Dmitriy Burmistrov²

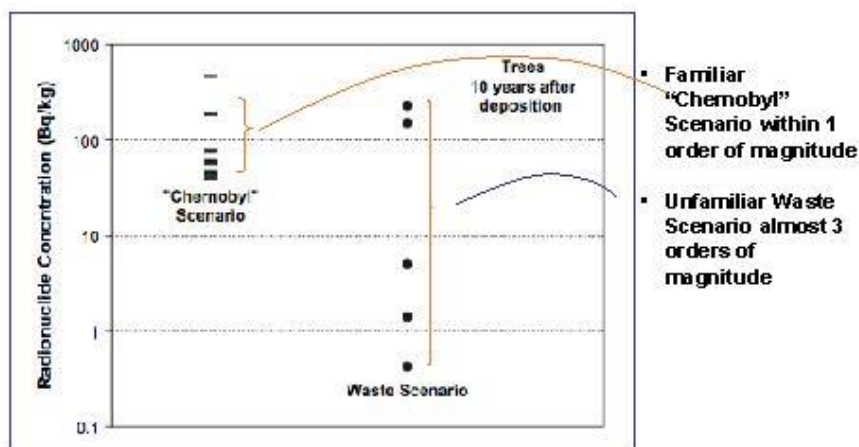


Model vs. Parameter Uncertainty

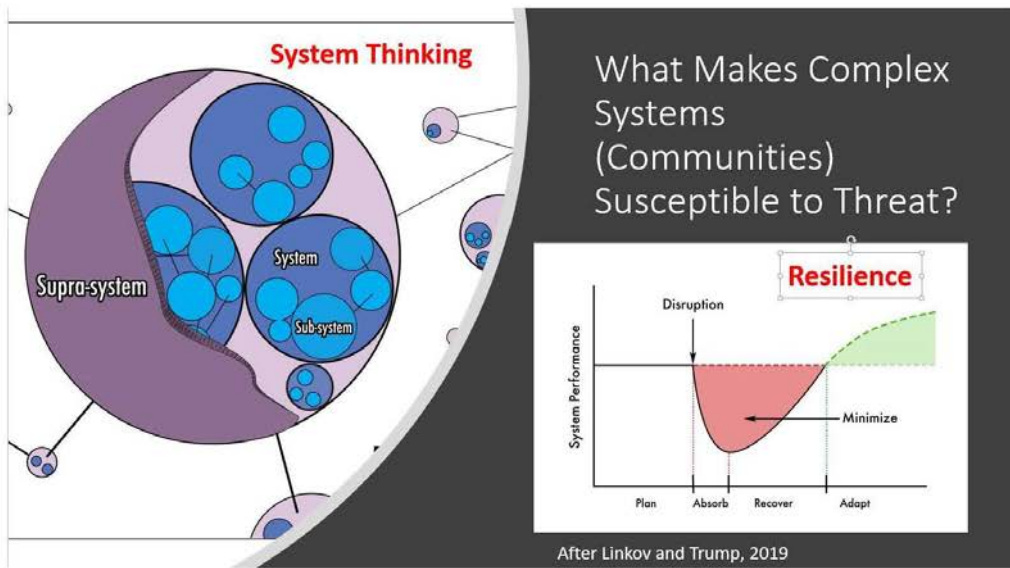


7

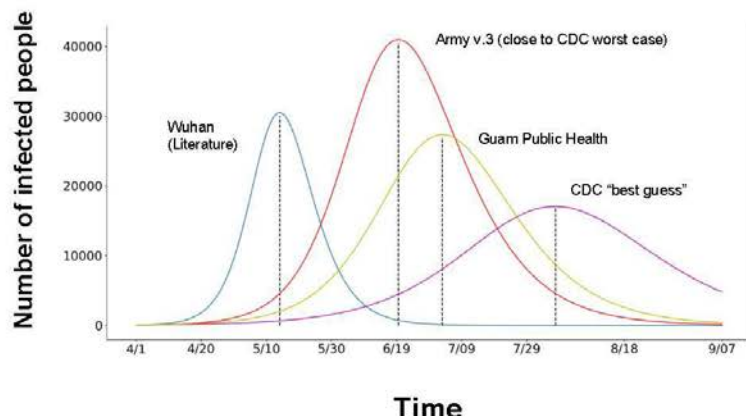
"Modeler" Uncertainty (Subjectivity)



4

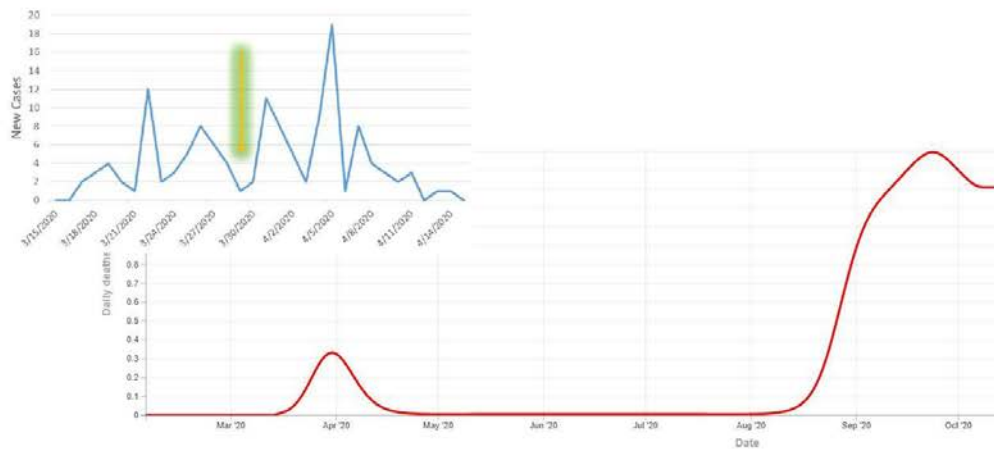


Comparison of different SEIR models



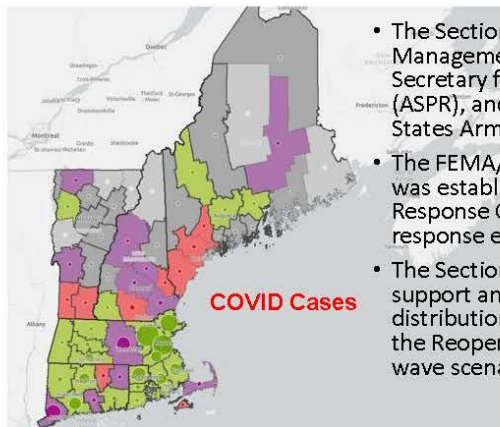
11

What Actually Happened in Guam?



6

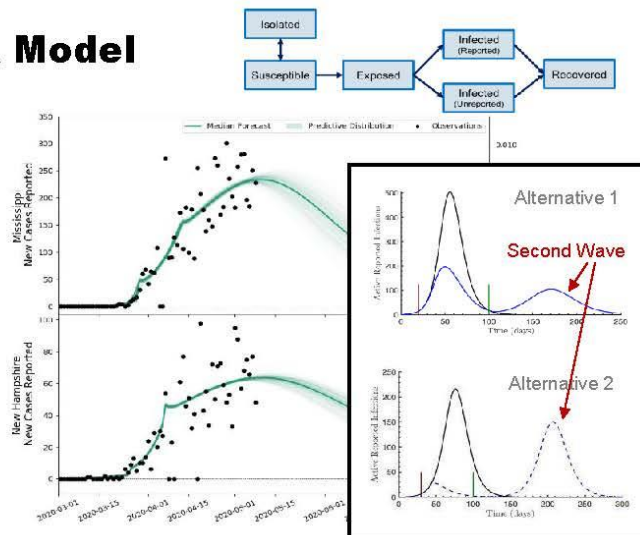
COVID in FEMA/ASPR Reg. 1: Resilience



- The Section is co-led by the Federal Emergency Management Agency (FEMA) and the Assistant Secretary for Preparedness and Response (ASPR), and includes personnel from the United States Army Corps of Engineers (USACE)
- The FEMA/ASPR Region 1 Data Analytics Section was established to support the Regional Response Coordination Center (RRCC) COVID-19 response efforts
- The Section provides modeling and analysis to support and inform decisionmakers on the distribution of resources, fatality management, the Reopening of America efforts, and second wave scenarios

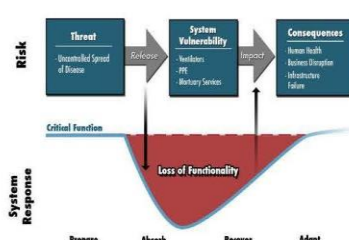
ERDC SEIR Model

- Adapted SEIR approach - Splits Infected population into "reported" and "unreported"
- Dynamics statistically combined with observations and SME knowledge
- Parameters updated daily with new data
- Model parameters change with varying social distancing restrictions
- Prediction uncertainty from unconstrained parameters is characterized



Goal: Moving Towards Resilience

- Goal: Translating region-specific COVID-19 and socio-political realities into an actionable plan
- Transition from risk- to resilience-based analytics



- Systems Approach to systemic risks combining epidemiological, infrastructure and public health models and evaluation
- Integration of socio-cultural specificity of state/territory

AN ANALYTICAL PERSPECTIVE ON PANDEMIC RECOVERY

Health Security
Volume 18, Number 3, 2020
DOI: 10.1089/hs.2020.0057

Benjamin D. Trump, Todd S. Bridges, Jeffrey C. Cegan, Susan M. Cibulsky, Scott L. Greer, Holly Jarman, Brandon J. Lafferty, Melissa A. Surette, and Igor Linkov

15

1 Don't conflate risk and resilience

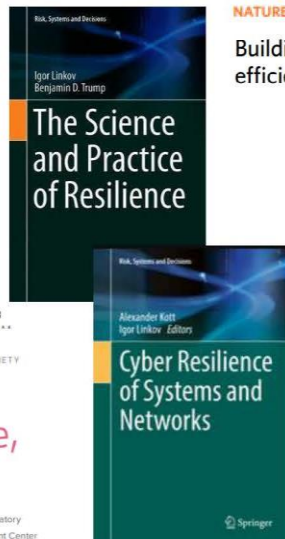
'Risk' and 'resilience' are fundamentally different concepts that are often conflated. Yet maintaining the distinction is a policy necessity. Applying a risk-based approach to a problem that requires a resilience-based solution, or vice versa, can lead to investment in systems that do not produce the changes that stakeholders need.

30 | NATURE | VOL 555 | 3 MARCH 2018

COMPUTER PUBLISHED BY THE IEEE COMPUTER SOCIETY

2 To Improve Cyber Resilience, Measure It

Alexander Kott, U.S. Army DEVCOM Army Research Laboratory
Igor Linkov, U.S. Army Engineer Research and Development Center



NATURE ENERGY

Building resilience will require compromise on efficiency

3

nature

COMBINE RESILIENCE AND EFFICIENCY IN POST-COVID SOCIETIES



4 Cyber Resilience: by Design or by Intervention?

Alexander Kott, U.S. Army DEVCOM Army Research Laboratory
Maureen S. Golan, U.S. Army Engineer Research and Development Center and Credere Associates
Benjamin D. Trump, U.S. Army Engineer Research and Development Center and University of Michigan
Igor Linkov, U.S. Army Engineer Research and Development Center and Carnegie Mellon University

8

Risk -- “a situation involving exposure to danger [threat].”

Don't conflate risk and resilience

'Risk' and 'resilience' are fundamentally different concepts that are often conflated. Yet maintaining the distinction is a policy necessity. Applying a risk-based approach to a problem that requires a resilience-based solution, or vice versa, can lead to investment in systems that do not produce the changes that

Security -- “the state of being free from danger or threat.”

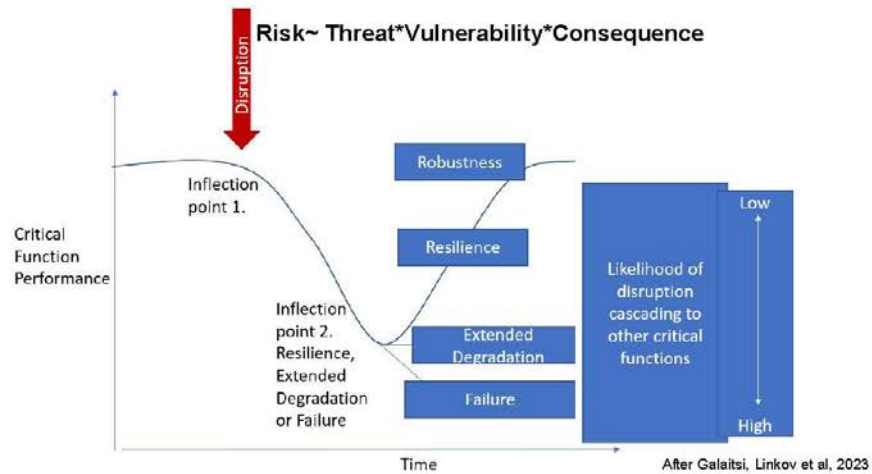
Igor Linkov, Benjamin D. Trump,
US Army Corps of Engineers,
Cincinatti, Ohio, USA.
Jeffrey Kelder University of
Massachusetts Boston, USA.
igor.linkov@usace.army.mil

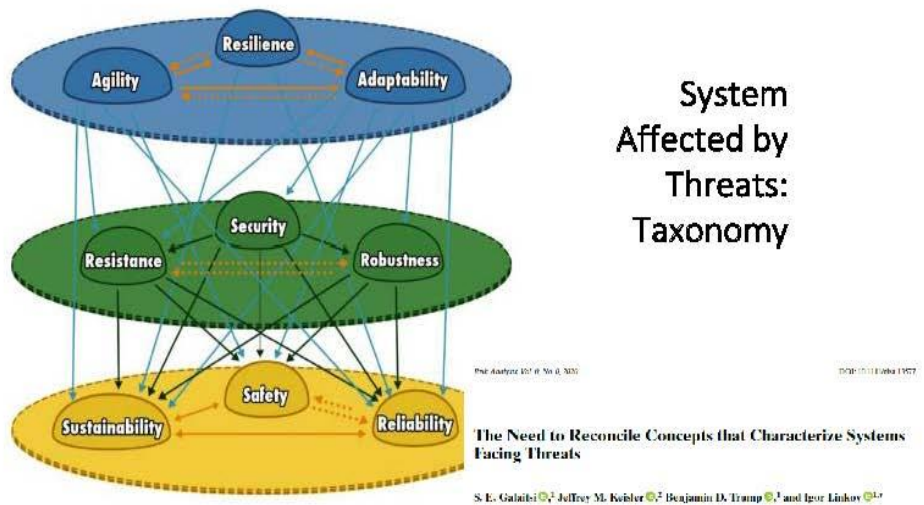
Reliability -- “the quality of performing consistently well.”

Resilience -- “the capacity to recover quickly from difficulties.”

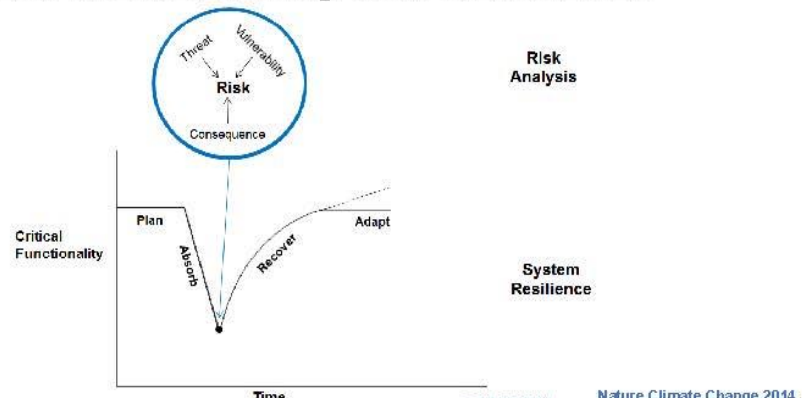
Definitions by Oxford Dictionary

Risk and Resilience at the Time of Crisis





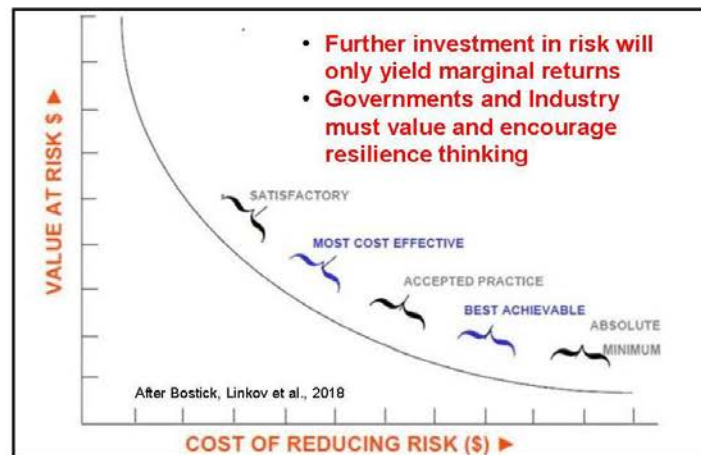
System Risk/Security and Resilience



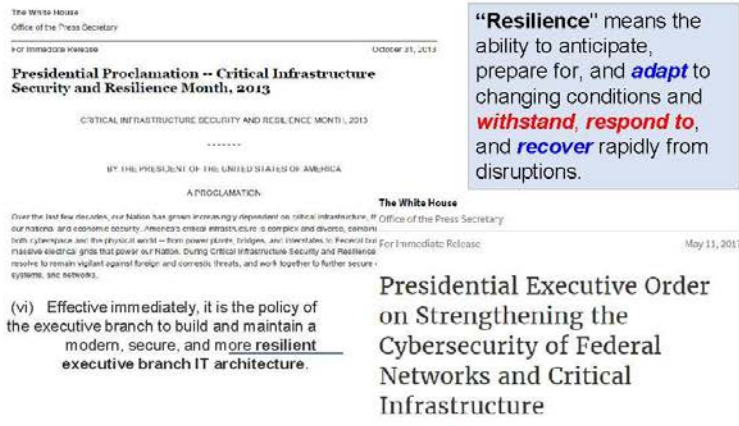
Evolution of Risk Assessment

- 1970's- Risk=Probability x Consequence
- 1980's- Risk=Hazard x Exposure x Consequence
=Threat x Vulnerability x Consequence
- 2000's- Risk~ $f(H \times E \times E_{ff})$

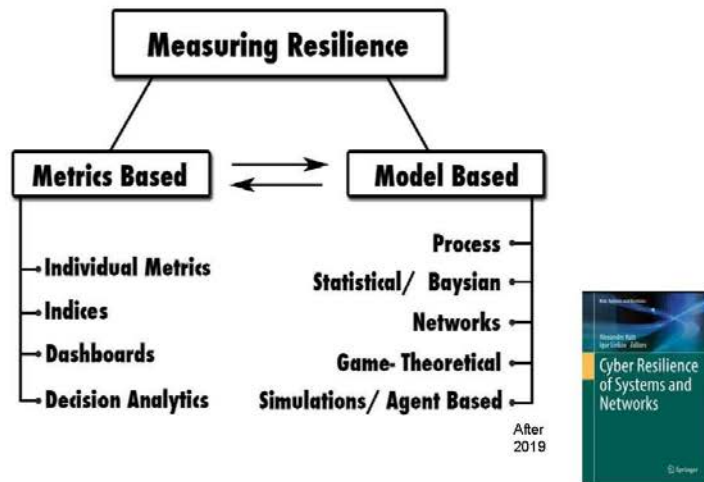
Cost of Buying Down Risk



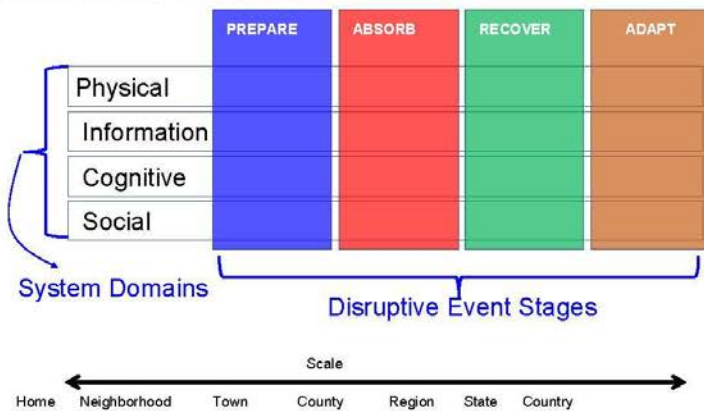
Calls for Resilience



How to Quantify Resilience?



Resilience Matrix



Assessment using Stakeholder Values

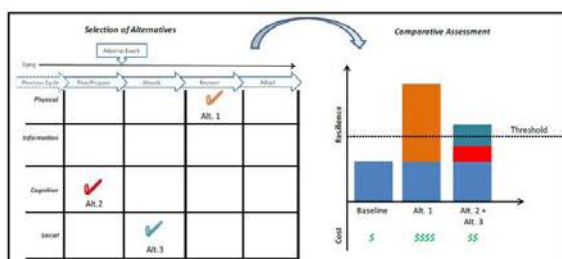


Figure 5: Comparative Assessment of Resilience-Enhancing Alternatives

Use developed resilience metrics to comparatively assess the costs and benefits of different courses of action

After Fox-Lent et al., 2015

26

Short Communication

Metrics for energy resilience

Paul E. Koege^a, Zachary A. Collier^a, James Mancillas^b, John A. McDonagh^b, Igor Linkov^{b,*}

Resilience Matrix: Energy

| | Plan and Prepare for | Refs Absorb | Refs Recover from | Refs Adapt to | Refs |
|--|-----------------------|---|--|---|---------------------|
| Physical | | | | | |
| Reduced reliance on energy/increased efficiency | A,B, E,F, I,J,K | Design margin to accommodate range of potential changes | B,C: I,J,K reconfiguration and/or system reorganization | C,D: F,I,J,K flexible network architecture to facilitate modernization and new system integration | C,D, E,F, K |
| Energy source diversity/ local sources | A,E, F,H, K | Limited performance degradation under changing conditions | B,C: I,J,K Capability to monitor and control portions of system | B,L: Sensors, data collection and visualization capabilities to track system performance trending | D,E, L,K |
| Energy storage capabilities/ pre-logged equipment | B,H, K | Operational system protection (e.g., pressure relief, circuit breakers) | I,K: Fuel flexibility | C,D: Ability to use new/alternative fuel sources | C,F, H |
| Redundancy of critical capabilities | D,E, F,G, I,K | Backup power for critical components (e.g., generators, pumps) | D,I: Capability to re-route energy from available sources | C,D: Update system configuration/ functionality based upon lessons learned | C,D, I,P,I, K |
| Preventative maintenance on energy systems | I,K | Investigate and repair damaged/ degraded systems | E,I,J,K: Investigate and repair malfunctioning controls or sensors | I: Replace obsolete or damaged assets and introduce new assets | A,C, D,I, K |
| Sensors, controls and communication links to support awareness and response | H,I, K | Capability for independent local/sub-network operation | D,K: Energy network flexibility to re-establish service by priority | F,I,J,K: Integrate new interface standards and operating system upgrades | D,I, K |
| Proactive measures from external attack (physical/cyber) | A,D, I,K | Alternative methods/equipment (e.g., paper copy, flashlights, radios) | B,H: Backup communication, lighting, power systems for repair/recovery operations | I,K: Update response equipment/supplies based upon lessons learned | D,I |
| Information | | | | | |
| Capabilities and services centralized based on criticality or performance requirements | B | Environmental condition monitoring and event warnings broadcast | E,F: Information available to operators and customers regarding customer/community needs | D,I: Identify event, incident point of entry, associated vulnerabilities and impacts identified | A,D, H,I, K |
| Internal and external system dependencies identified | B,G, H | System status, trends, margins available to operators and customers | D,E: Recovery progress tracked, synthesized and available to operators and stakeholders | D,I: Event data and operating environment forecasts utilized to evaluate future conditions/ events | D,H, I,K |
| Design, control, operational and maintenance data archived and protected | B,I, J,K | Critical systems data monitored, anomalies alarmed | E,F: Investigate and repair damaged systems | K: Updated information about emergency alternatives and emergent technologies available to managers and stakeholders | D,F, H,I |
| Vendor information available | B | Operational/troubleshooting/response procedures available | G,I,K: Location, availability and ownership of energy, hardware and software resources available to restoration teams | K: Maintenance information updated consistent with system modeling | F,I,K |

Table I The cyber resilience matrix

| Plan and prepare for | Absorb | Recover from | Adapt to |
|---|--|---|--|
| Physical | | | |
| (1) Implement consequences for critical assets (M2, M18, 20) | (1) Signal the compromise of assets or services [M18, 20] | (1) Investigate and repair malfunctioning controls or sensors [M17] | (1) Review asset and service configuration in response to recent event [M17] |
| (2) Implement consequences for critical services [M18, 20] | (2) Use redundant assets to continue services [M18, 20] | (2) Assess servicecast damage | (2) Phase out obsolete assets and introduce new assets [M17] |
| (3) Assess impact of network structure and interconnection to system components and to the environment | (3) Isolate cyber resources to defend against attack [M16] | (3) Assess distance to functional recovery | |
| (4) Redundancy of critical physical infrastructure | | (4) Safely dispose of impenetrable assets | |
| (5) Redundancy of data physically or logically separated from the network [M24] | | | |
| Information | | | |
| (1) Catalog assets and services based on sensitivity or resilience requirements [M63] | (1) Observe assets for critical services and assets [M22] | (1) Log events and sessions during event [M17, 22] | (1) Document incident's impact and cause [M17] |
| (2) Documentation of certificates, qualifications and policies of critical hardware and/or software providers | (2) Efficiently and effectively transmit relevant data to reasonable stakeholders/ decision makers | (2) Review and compare systems before and after the event [M17] | (2) Document time between problem discovery/detection and recovery [M17] |
| (3) Proper plans for surge and containment of classified or sensitive information | | (3) Anticipate future system states post-recovery | |
| (4) Identify external system dependencies (i.e., internet providers, electricity, water) [M31] | | | |
| (5) Identify internal system dependences [M63] | | | |
| Cognitive | | | |
| (1) Anticipate and plan for system states and events [M16] | (1) Use a decision making protocol or aid to determine when event can be considered "continued" | (1) Review physical assets in order to make decisions | |

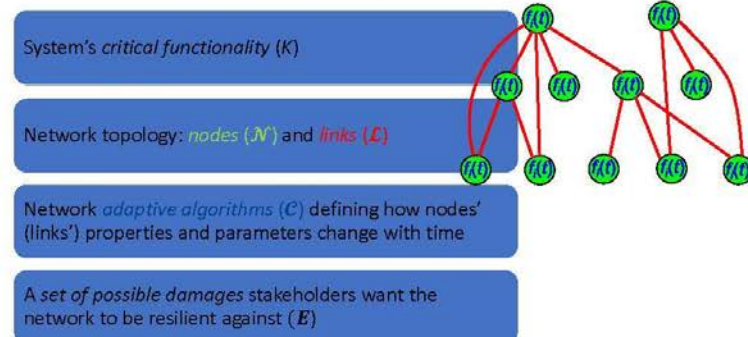
Environ Syst Decis (2013) 33:471–476
 DOI 10.1007/s10669-013-9485-y

PERSPECTIVES

Resilience metrics for cyber systems

Igor Linkov · Daniel A. Eisenberg ·
 Kenton Plourde · Thomas P. Seager ·
 Julia Allen · Alex Kott

Network-based Resilience Theory?



$$R = f(\mathcal{N}, \mathcal{L}, \mathcal{C}, \mathcal{E})$$

29

Poor Efficiency:

System cannot not accommodate a large volume of commuters driving at the same time.

Traffic congestions are predictable and are typically of moderate level.



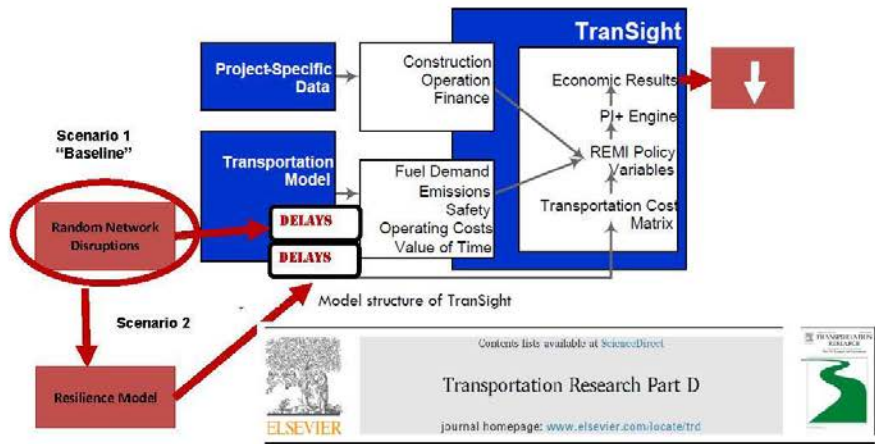
Lack of Resilience:

System cannot recover from adverse events (car accidents, natural disasters)

Traffic disruptions are not predictable and of variable scale.



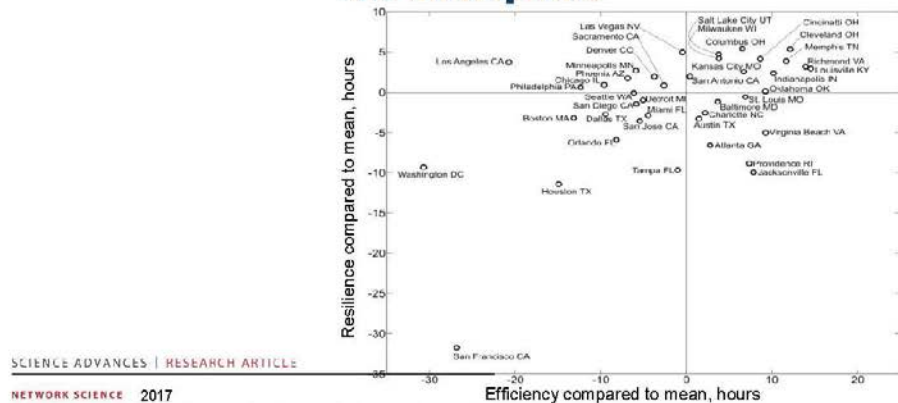
15



Lack of resilience in transportation networks: Economic implications



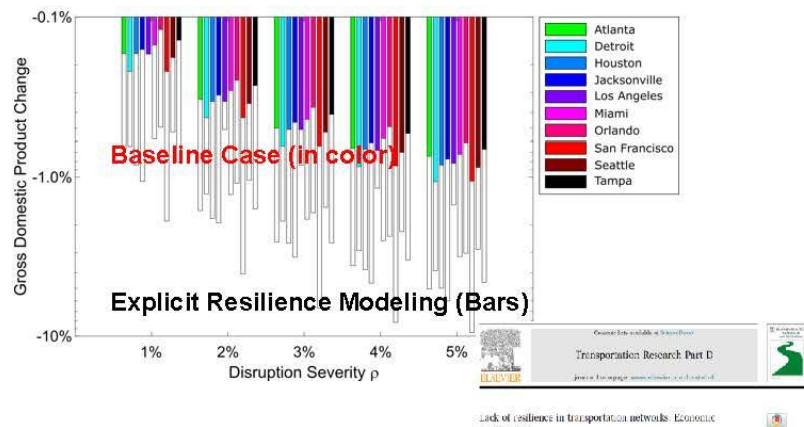
Resilience vs Efficiency at 5% disruption



Resilience and efficiency in transportation networks

Alexander A. Ganin,^{1,2} Maksim Kitsak,² Dayton Marchese,² Jeffrey M. Keisler,^{3*}
Thomas Seager,² Igor Linkov²⁺

Lack of Resilience: Impact on GDP



II2 COMPUTER PUBLISHED BY THE IEEE COMPUTER SOCIETY

Cyber Resilience by Design or by Intervention?

Alexander Kott, U.S. Army DEVCOM Army Research Laboratory
Maureen S. Gelan, U.S. Army Research and Development Directorate
Benjamin D. Tramp, U.S. Boeing Research and Development, University of Michigan
Igor Linkov, U.S. Army Research and Development Center, Carnegie Mellon University

| | Risk management | R&D | R&I |
|-------------------|--|---|---|
| Objective | Harden individual components | Design components to be self-reorganizable | Rectify disruption to components and stimulate recovery by external actors |
| Capability | Predictable disruptions, acting primarily from outside the system components | Either known/predictable or unknown disruptions, acting at a component or system level | Failure in the context of societal needs; there may be a constellation of networks across systems |
| Consequence | Vulnerable nodes and/or links fail as a result of a threat | Degradation of critical functions in time and capacity to achieve system's function | Degradation of the critical societal function due to cascading failure in interconnected networks |
| Actor | Either internal or external to the system | Internal to the system | External to the system |
| Corrective action | Either loosely or tightly integrated with the system | Tightly integrated with the system | Locally |
| Stages/ analytics | Prepare and absorb (the risk is a product of a threat, vulnerability, and consequences, and is time independent) | Recover and adapt (explicitly modeled as time to recover system function and the ability to change system configuration in response to threats) | Pre (exist) to (recover) to (rebuild) to (societal) |

NATIONAL STRATEGIC COMPUTING RESERVE: A BLUEPRINT

A report to the
NATIONAL SECURITY COUNCIL, COMMISSIONER OF CYBERSECURITY AND TELECOMMUNICATIONS, CHIEF INFORMATION OFFICER, AND THE SECRETARY OF DEFENSE FROM THE NATIONAL STRATEGIC COMPUTING RESERVE

October 2013

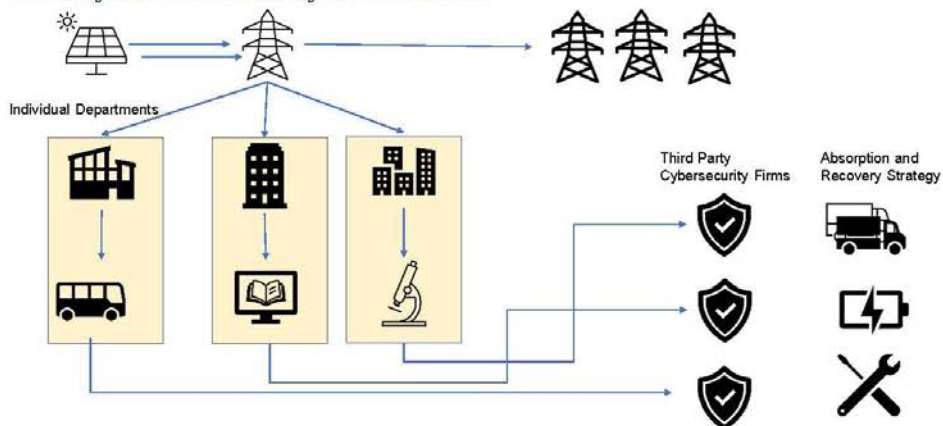
Case Study: University of Texas at Austin



- UT Austin became the first PEER Certified Campus in the world.
- PEER Certification by GBCI matches LEED certification for power system efficiency, day-to-day reliability and overall resiliency
- Four Main Considerations for Certification:
 - Reliability and Resiliency
 - Energy Efficiency and Environment
 - Operational Effectiveness
 - Customer Contribution

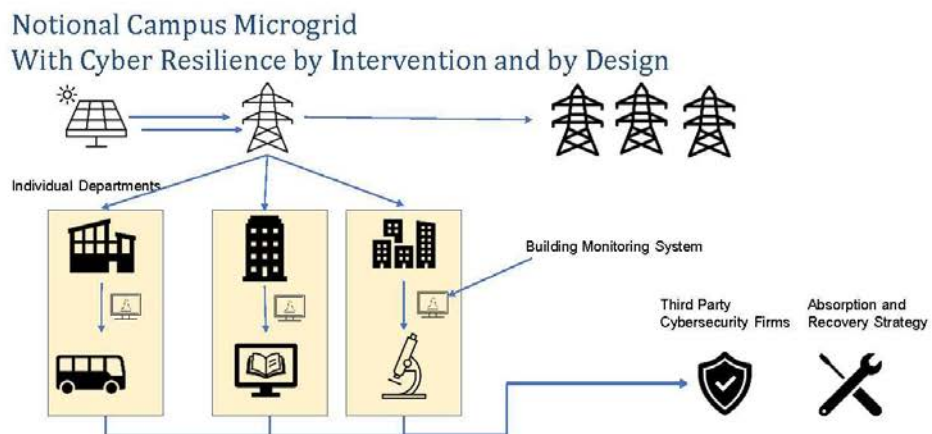


Notional Campus Microgrid With Cyber Resilience by Intervention

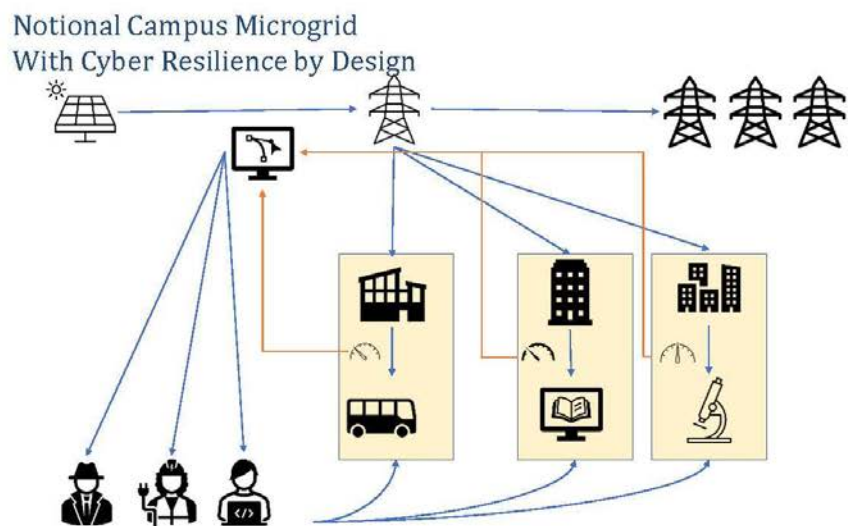


38

18



37



38

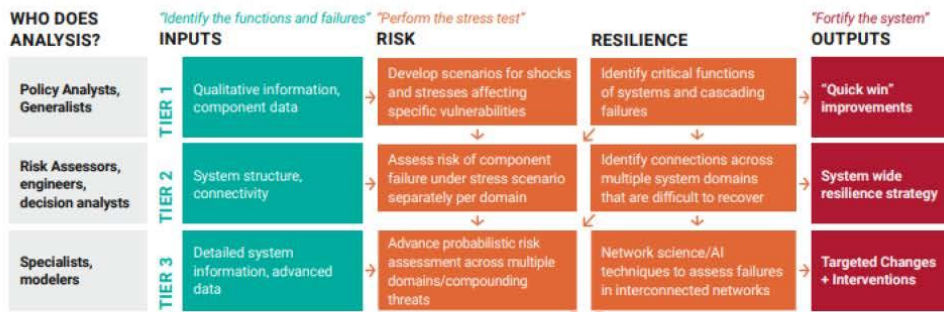
19



578 | Nature | Vol 603 | 24 March 2022

Stress-test the resilience of critical infrastructure

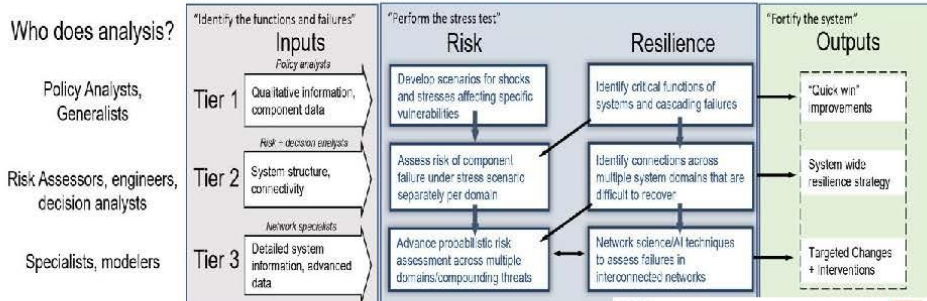
INTEGRATED RISK/RESILIENCE STRESS TESTING



40

Integrated Risk/Resilience Stress Testing

How Do We Increase Resilience In Complex, Interconnected Infrastructure?



Three-Tiered Approach:

Tier 1: Define and identify more important critical functions & risks

Tier 2: Refine with interconnections, and define KPI

Tier 3: Asset-level data-driven analysis

International Journal of Disaster Risk Reduction
Volume 62, Number 132, 10323

Resilience stress testing for critical infrastructure

Parikhoo^{1,2}, A. Asif, S. Bhowmik, D. Tramp^{3,4}, Md. M. Islam⁵, Shafiqur Reza⁶, M. Ehsan Haider⁷, Md. Golam Ali⁸, Md. Golam Md. Hossain⁹, Md. Golam Md. Hossain¹⁰, Md. Golam Md. Hossain¹¹

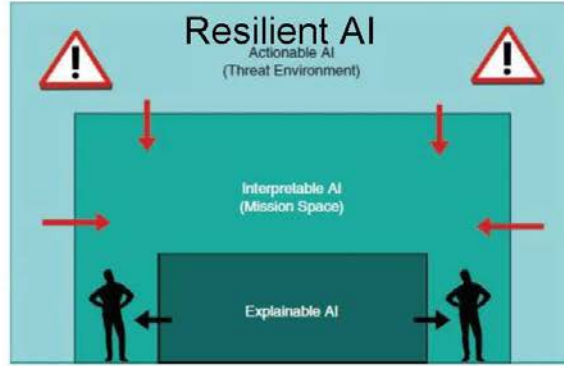


Cybertrust: From Explainable to Actionable and Interpretable Artificial Intelligence

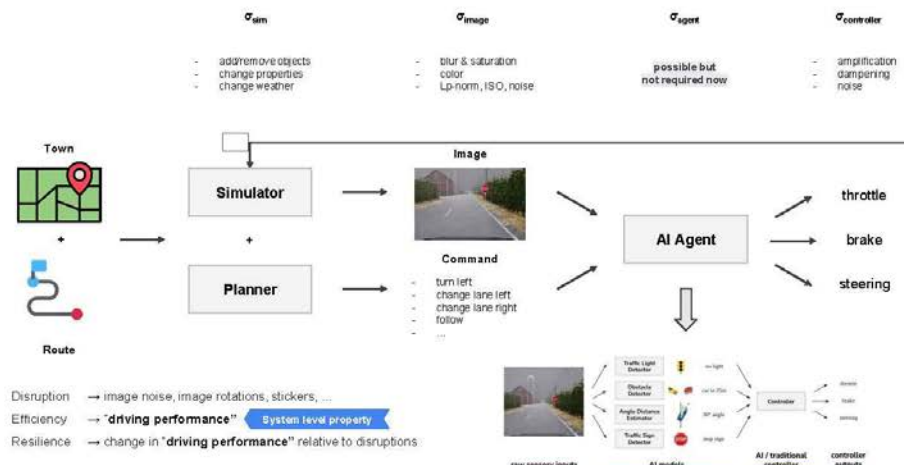
Igor Linkov, Stephanie Galaitis, and Benjamin D. Trump, U.S. Army Corps of Engineers
Jeffrey M. Keisler, University of Massachusetts
Alexander Kott, U.S. Army Futures Command

TABLE 1. The typology of human-AI assessments of decision strategy.

| Human | AI | |
|-------|--------------|-----------|
| | Yes | No |
| No | Disagreement | Agreement |



Resilient AI



AI-DRIVEN RESILIENCE ARCHITECTURE

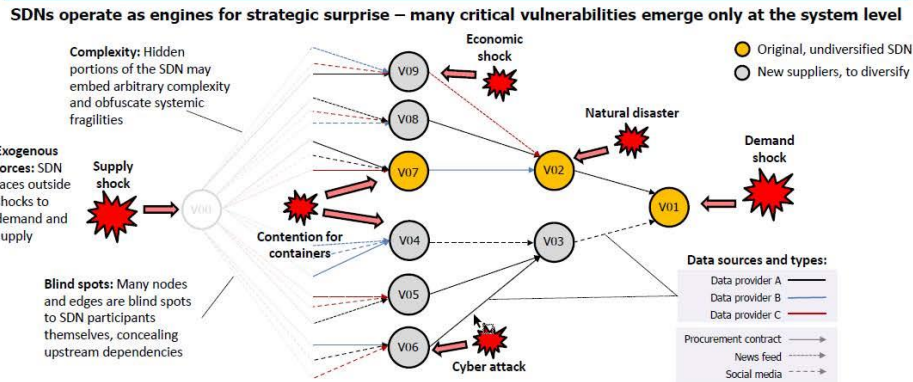


Integrating Energy and Computing Networks





Supply-and-Demand Networks – challenges

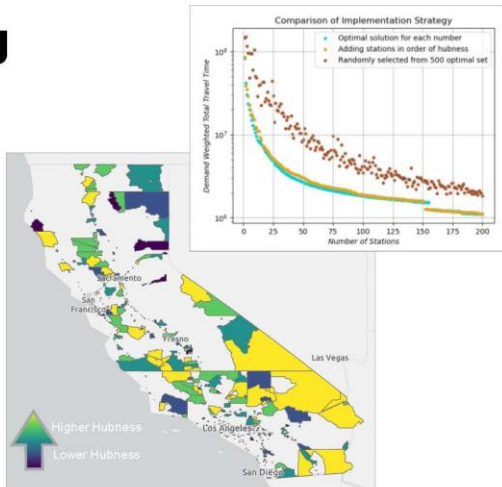


AI/Machine Learning for Resilient Supply Chains in CA



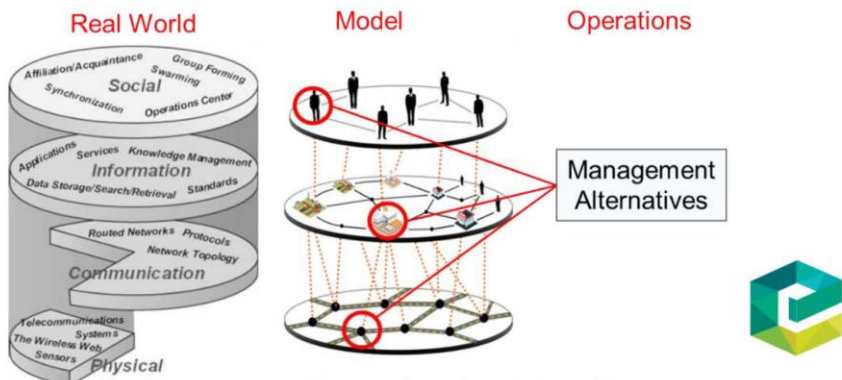
Hydrogen Refueling Stations

- **Motivation:** California has new legislation requiring move towards zero emission freight trucks
- **Problem:** How can we convert current refueling stations to hydrogen refueling stations without interruption to the shipping industry in California?
- **Solution:** Find the optimal candidate locations for this conversion and suggest priority rankings



47

Vision for System Resilience: Social Science/Communication Integration



The case for value chain resilience

Igor Linkov, Savina Carluccio, Oliver Pritchard, Aine Ni Bhreasail,
Stephanie Galatsi, Joseph Sarkis and Jeffrey M. Keisler

Management Research Review
© Emerald Publishing Limited
2040-8269
DOI 10.1108/MRR-08-2019-0353

24

References

- 1) Linkov, I., Roslycky, L., Trump, B. (2020). *Resilience of Hybrid Threats: Security and Integrity for the Digital World*. IOS Press.
- 2) Trump, B., Hussain, K., Linkov, I. (2020). *Cyber Resilience in Arctic* IOS Press.
- 3) Hynes, W., Trump, B.D., Linkov, I. (2020). A Resilience Approach to dealing with COVID-19 and future systemic shocks. *Environment, Systems, Decisions*, 40(2).
- 4) Golen, M.S., Linkov, I. (2020). Trends in Resilience Analytics in Supply Chain Modeling in the Context of the COVID Pandemic. *Envr. Systems and Decisions*, 40(2).
- 5) Linkov, I., Trump, B. (2019). *The Science and Practice of Resilience*. Springer, Amsterdam.
- 6) Kott, A., Linkov, I. eds (2019). *Cyber Resilience in Systems and Networks*. Springer, Amsterdam.
- 7) Kurtt, M., Keenan, J.M., Sagan, M., Linkov, I. (2019). Defining resilience for the US building industry. *Building Research and Innovation*, 47: 480.
- 8) Linkov, I., Trump, B.D., Keesler, J.M. (2018). Risk and resilience must be independently managed. *Nature* 555:30.
- 9) Bostick, T.P., Lambert, J.H., Linkov, I. (2018). Resilience Science, Policy and Investment for Civil Infrastructure. *Reliability Engineering & System Safety* 175: 19-23.
- 10) Massaro, E., Garin, A., Linkov, I., Vesagnani, A. (2018). Resilience management of networks during large-scale epidemic outbreaks. *Science Reports* 8:1859.
- 11) Marchese, D., Reynolds, E., Bates, M.E., Clark, S.S., Linkov, I. (2018). Resilience and sustainability: similarities and differences. *Sig Total Environ.* 613-614:1275-83.
- 12) Trump, B., Florin, M.V., Linkov, I. eds. (2018). *IRGC Resource Guide on Resilience* (vol. 2): Domain of resilience for complex interconnected systems. Switzerland.
- 13) Florin, M.V., Linkov, I., eds. (2017). *International Risk Governance Council (IRGC) Resource Guide on Resilience*. International Risk Governance Center, Switzerland.
- 14) Linkov, I., Palma-Oliveira, J.M., eds (2017). *Risk and Resilience*. Springer, Amsterdam.
- 15) Garin, A., Kisak, M., Keesler, J., Seager, T., Linkov, I. (2017). Resilience and efficiency in transportation networks. *Science Advances* 3:e1701079.
- 16) Marchese, D., Linkov, I. (2017). Can You Be Smart and Resilient at the Same Time? *Environ Sci Technol* 2017, 51, 5887-5898.
- 17) Connally, E. B., Allen, C. R., Hatfield, K., Palma-Oliveira, J. M., Woods, D. D., & Linkov, I. (2017). Features of resilience. *Environ Systems and Decisions*, 37(1), 46-50.
- 18) Thonisson, H., Lambert, J.H., Cardenas, J.J., Linkov, I. (2017). Resilience Analytics with Application to Power Grid of a Developing Region. *Risk Analysis* 37:1288.
- 19) Gisladottir, V., Garin, A., Keesler, J.M., Kepner, J., Linkov, I. (2017). Resilience of Cyber Systems with Over- and Under-regulation. *Risk Analysis* 37:1844.
- 20) Bakkerssen, L., Fox-Lent, C., Read, L., and Linkov, I. (2016). Validating Resilience and Vulnerability Indices in the Context of Natural Disasters. *Risk Analysis* 37:982.
- 21) Garin, A., Massaro, E., Keesler, J., Kott, A., Linkov, I. (2016). Resilient Complex Systems and Networks. *Nature Scientific Reports* 6, 19540.
- 22) Linkov, I., Larkin, S., Lambert, J.H. (2015). Concepts and approaches to resilience in governance. *Environment, Systems, and Decisions* 35:219-228.
- 23) Fox-Lent, C., Bates, M. E., Linkov, I. (2015). A Matrix Approach to Community Resilience Assessment. *Environment, Systems, and Decisions* 35(2):205-219.
- 24) Larkin, S., Fox-Lent, C., Linkov, I. (2015). Benchmarking Agency and Organizational Practices in Resilience Decision Making. *Environ. Syst., & Dec.* 35(2):185-195.
- 25) DiMese D., Collier Z.A., Linkov I. (2015). Systems Engineering Framework for Cyber Physical Security and Resilience. *Environment, Systems, and Decisions* 35:201.
- 26) Linkov, I., Fox-Lent, C., Keesler, J., Della-Sala, S., Sweeney, J. (2014). Plagued by Problems: Resilience Lessons from Venice. *Environment, Systems, and Decisions* 34:378.
- 27) Linkov, I., Kroger, W., Leyermann, A., Renn, O. et al. (2014). Changing the Resilience Paradigm. *Nature Climate Change* 4:407.
- 28) Roegge, P., Collier, Z.A., Mancillas, J., McDonagh, J., Linkov, I. (2014). Metrics for Energy Resilience. *Energy Policy Energy Policy* 72:249.
- 29) Park, J., Seager, T., Linkov, I. (2013). Integrating risk and resilience approaches to catastrophe management in engineering systems." *Risk Anal.*, 33(3), pp. 358.



Plenary talk 2 – Ivo Häring: Analytical resilience quantification approaches (resilience analytics) to classify and rank first principle risk and resilience modelling and simulation methods

Ivo Häring¹, Julia Rosin¹, Sebastian Ganter¹, Jörg Finger¹, Mirjam Fehling-Kaschek¹, Kris Schroven¹, Benjamin Lickert¹, Alexander Stolz¹, Stephen Crabbe²

¹Fraunhofer EMI, Freiburg, Germany, Emails: {haering; rosin; ganter; finger; fehling-kaschek; schroven; lickert; stolz}@emi.fraunhofer.de

²Work done at Fraunhofer EMI, Current affiliation: Crabbe Consulting, Erfurt, Germany, Email: stephen@crabbe-consulting.com

Abstract

Risk control and resilience of critical infrastructures (CI) and similar cyber physical socio technical systems are increasingly requested by legal regulations and emerging technical standards at international, European (ECI) and national levels, e.g. the German KRITIS umbrella law. Along with the increase of knowledge, the number of methods for CI protection (CIP) assessment is growing. For industrial, enterprise and organizational practitioners as well as academia increasingly guidance is needed to select, tailor, extend or newly develop resilience assessments in a better-informed way.

The contribution starts by providing a schematic how resilience analysis and management within a given framework is expected to use risk and resilience analytical approaches and how these request input from model-based simulation of resilience properties, among other methodological inputs. After methodological clarifications and gaps identification, the focus is on providing representative analytical risk and resilience assessment approaches to identify their expected inputs as well as to give a list of representative resilience simulation approaches.

The following analytical resilience assessment approaches are discussed along with their main requested input information: (i) Classical risk on resilience approach along with generalized acceptance criteria, also (ii) resolved with respect to a set of resilience dimensions such as disruption types, system layers, technical resilience capabilities, and resilience cycle ordering along with risk aversion aware evaluation options; (iii) resilience propagation layer expansion for overall disruptions events propagation through assessment layers as a logic or temporal forward problem; and (iv) abstract probabilistic resilience dependency and causal modelling (resilience belief network), e.g. starting with classical or extended Markov or Petri models.

For these resilience analytics approaches, the question is addressed which existing and emerging model-based first-principle physical-engineering simulative methods are suited to provide sufficient information to feed their requests to assess the level of risk control and resilience of systems under investigation? In particular, the following approaches are considered: (a) single- and multi-point mass ersatz models along with initial conditions, loading models and failure models; (b) dynamic material and structural simulation, including coupled models, e.g. air-structure and fluid-structure coupling; and (c) topologic, static and transient network flow simulations.

With the presented approach, the suitability of simulation methods is assessed regarding their capability to provide inputs to analytical system analysis requests. To this end 15 key requests of the 4 considered resilience analytical methods are identified, in particular coverage of disruptions, coverage of all resilience cycle phases and system layers, capability to assess mitigation measures, identification of causality chains (inference) between system properties and observed resilience, also conditional given system resilience modifications and specific treatments. Each representative resilience simulation method is assessed regarding these benchmarks revealing its strengths and weaknesses regarding resolution, coverage, dependency modeling, and causality simulation capability as well as how they could be combined. Possible extensions of the approach are indicated to even better guide CI system resilience assessments regarding selection of model-based system resilience quantification.

1 Introduction

System design and system thinking is increasingly holistic and demanding. Expectations on modern systems include availability, reliability, durability, adaptivity, smartness, self-learning capability, safety, security, robustness, resilience, cost-efficiency, low carbon footprint, participation in cyclic economy, societal, psychological and ethical acceptance, legal acceptability, user satisfaction, attractiveness, inclusiveness, etc.

The term system comprises here small technical systems up to large scale multi-country wide socio technical systems. In particular critical infrastructures (CI) are distributed, smart interconnected cyber-physical-human (CPH) systems.

The present article addresses the challenge of how to assess a subset of the above desirable system properties analytically informed and driven quantitatively. Namely, systemic properties related to resilience. The working definition for resilience adopted is that a system is resilient if its performance (e.g. percentage of consumers sufficiently supplied with communication services) and non-performance functions over time [1] (e.g. percentage of households with electrical energy supply disruption) are within acceptable bands for all types of possible disruption events before, during and after such disruptions [2] [3]. In a narrower definition of resilience, disruptions can be restricted to major events and focus is on system (non-)performance during and after events only, and risk analysis before such events.

The term analytical comprises formal mathematical expressions as well as algorithmic processes (see e.g. terms as respectively used in [4]) and system analysis schemes that can be conducted using templates, such as tables and matrices (see e.g. [5] [6]). These approaches can in principle be conducted and be understood with "paper, pencil and rubber". The term quantitatively refers to results in terms of numbers, percentages, curves, etc., as opposed to qualitative labels and relative orderings only.

An appropriate working definition addressing the research question is that within a natural science, technology, engineering and mathematics (STEM) [7] perspective resilience analysis and management of systems (in a broader sense) comprises context, concepts, processes, and methods (see Figure 1 below), see also [8] [9]. The main focus of the STEM sciences are their disciplinary and interdisciplinary methods. This working definition does not exclude other types of disciplinary methods. A research question reads: Which STEM inspired methods are useful for a given system to determine its resilience?

In as far as analytical system assessment methods are more abstract and conceptual and as they are closer to system management, evaluation and decision making, the article sets out to show that they can be used to classify system resilience quantification approaches, in particular approaches that use large-scale models, simulation and data analysis. This is challenging since at first sight it is not clear whether an analytical method is just the theory or algorithm of a model-based resilience quantification simulation. Hence the article needs to show that such a distinction can be made.

To this end, the article introduces the notion of first principle or ab initio resilience quantification methods. The working assumption is that models can be defined and be parametrized with real world data such that simulation results can be achieved to assess resilience of systems as well as related properties, in particular without scaling or shifting of results. Hence such models claim to cover all significant effects relevant to model systemic resilience, which is challenging.

The article relates in parts to ISO 31000 [10] framework and its list of methods [11]. The presented analytical assessment approaches and the first-principle simulation approaches are generic and can be used in various domains, depending on the cyber-physical threats considered, e.g. business continuity as covered in [12], community resilience [13], emergency response [14], and cyber resilience [15] [16]. They can be used to fulfill regulatory requirements of the EU directive 2022/2557 on the resilience of critical entities (CER) [17] and the directive on a high common level of cybersecurity across the Union (NIS-2) [18], within such EU policies as the EU Security Union Strategy for 2020-2025 [19] and the EU Counter-Terrorism-Agenda [20].

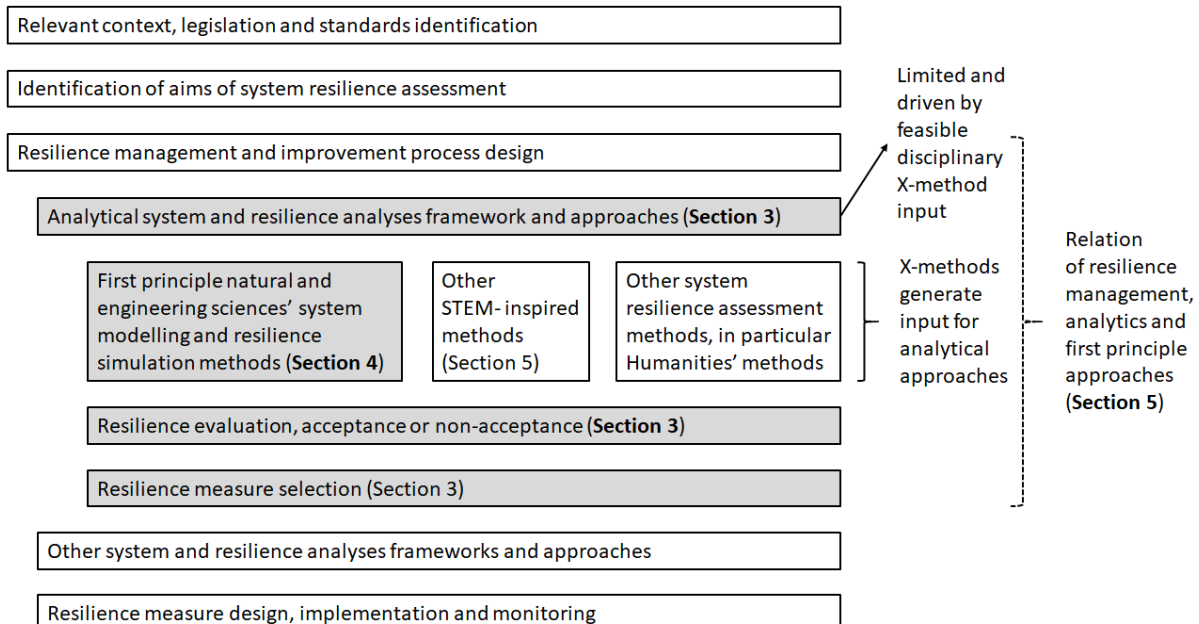
The article is structured as follows, see Figure 1. Section 0 gives an overview of existing approaches in literature to classify, sort and rank methods for system resilience assessment, in particular of critical infrastructures. A schematic gives an overview how resilience quantification method properties can be characterized with the help of analytical resilience approaches. This will elucidate that analytical system analysis methods of resilience of systems "ask the right questions" that need to be answered by first principle resilience modelling and simulation methods, e.g., if a certain given disruption leads to a critical system performance loss or which disruption out of a known set of disruptions leads to critical system loss.

Section 0 gives compact formal expressions of analytical system resilience assessment methods. This provides the basis to define properties of system modeling and simulation methods that make them sufficient to fulfill requests of analytical assessment methods.

Section 0 describes representative first-principle system resilience quantification approaches. This will show required modelling data and parameterizations. It will allow to assess which inputs they can deliver for system resilience analytical methods.

Section 0 discusses the results of section 0 and section 0 by giving a list of system modelling and simulation properties that are desirable from the perspective of key analytical system resilience assessment approaches. A list of simulation properties is provided by comparing the representative simulation approaches. Finally, a matrix is presented that shows which representative simulation approaches can be used for which analytical approaches. This will also allow to identify links between resilience analytics and resilience simulation, as well as distinctions between both. Section 0 gives conclusion and outlook.

Figure 1. System risk and resilience analysis and management framework and main contributions of present article.



2 Today's gaps of resilience quantification methods classification and present approach

Existing reviews on resilience definitions and metrics cover a wide range. First generic reviews are compared. In [21] the focus is on respective formal expressions, rather than their use within resilience management processes, leading to a bottom-up classification of existing quantifications. In [22] the use of resilience quantities within system design and development processes is the key motivation of classification. The review article [23] follows a capability-to-X systematic for sorting of overall resilience assessment approaches. Already in [24] order of magnitude resilience levels are proposed that are expected to be used to assess degree of criticality of combinations of disruption events and system performance function disturbance, rigor of resilience quantification as well as implementation.

On the other hand, resilience frameworks are reviewed and compared. In this case focus is less on quantities but generic definitions, overall process requirements and process steps. CI-independent reviews include [25], which uses a dimensional literature analysis, the resilience dimension [3] resilience capabilities, and flow charts for illustration. In [26] a first broad uptake of classical resilience engineering concepts [27] takes place, in particular organizational effects in development, production and operation of high risk systems. In [28] several CI types, system layer perspectives and time-horizons are covered as relevant for cities. In [24] a (semi-)quantitative system (non-)performance function based framework is presented for quantification and improvement of resilience, including sample methods and process accompanying generic resilience level quantities. In [29] a panarchy (infinity sign) such as process [30] is proposed that comprises explicitly overall risk and resilience management steps as well as disruption response steps in case of crisis events. Note that all the described frameworks go beyond tailoring of the generic risk analysis and management scheme according to ISO 31000 [10] to application of yet another domain (see e.g. urban [31] [32], football stadium public security management [33]) as well as beyond ad hoc frameworks in societal security research [34] as employed after the 9/11 event. They are also not generic extensions of ISO 31000 for overall risk and resilience management, e.g. [35] for an example.

Domain specific resilience framework reviews cover smart grids [36], coupled CI in cities [37], power grids and their related ICT grids [38], and telecommunication grids [39] [40]. Regarding resilience quantification, the

dependence on CI domains is mirrored by domain specific reviews. Examples include drinking water systems [41], electrical power grids [42], and transportation systems [43]. In recent years, there seems to emerge a trend towards more CI domain specific reviews regarding frameworks as well as quantification recommendations, indicating the need for more generic systemic resilience assessment approaches that can be tailored to domains.

However, the majority of articles on resilience quantification provide for their application specific contexts, frameworks or process, if any, respectively, and description of the method or sequence of methods used, as well as standard, tailored or novel risk and resilience quantities, see the articles inspected by the above cited reviews. In the light of this observation the question arises if beyond foundational notions of resilience and resilience engineering tangible analytical properties of such approaches can be identified and be used for classification, selection and directed tailoring and extension of resilience processes and methods.

3 Resilience analytics methods and their input and simulation capability requests

Section 0 lists several generic analytical approaches that can be used to classify system modelling and simulation approaches to quantify resilience of systems. Only the first two can be characterized as tabular or matrix supported [44] [45] [6] [46]. The last two methods allow for graphical representation. All of them can be evaluated qualitatively and quantitatively.

3.1 Risk on resilience approach considering multiple resilience dimensions and concepts

Starting from the classical notion of overall risk R of a system caused by a collection of N_R independent risk events E_i with risks R_i , each characterized by a measure of its probability P_i and its consequence C_i , an obvious request of resiliency is to require that all possible risks are considered including:

- all types of risk, e.g. natural, natural-technical, man-made including accidental, intentional (e.g. corruption-routed, sabotage), and malicious (e.g. crime, terrorism), e.g., labeled by i_1
- for all phases before, during and after disruptions, e.g., labeled by i_2 ;
- for all system layers such as physical, engineering, cyber, organizational, ecological, economical and societal, e.g., labeled by i_3 ;
- for all phases of the resilience or catastrophe response cycle such as preparation, detection, prevention, absorption, response, recovery, adoption and learning, e.g., labeled by i_4 ; etc.

or by using any other single or combination of such resilience dimensions [46] [47].

Hence, even when assuming for simplicity independency of risks, resilience assessment needs to require that for a finite multi-index $i = (i_1, i_2, \dots)$, see e.g. [48] [49] [50] [35],

$$R_i = P_i C_i \text{ are acceptable, } i = 1, \dots, N_R, \text{ and } \sum_{i=1}^{N_R} R_i \text{ is acceptable.} \quad (1)$$

Thus, *degree of coverage of (combined) risk types and vectors*, e.g. empirical terrorism threat types [51] [52], classified cyber threat types according to cyber security assessment schemes [53], etc., as well as of combined threats [54], *of resilience dimensional perspectives and assumption of independency of single risks or not are distinction options of resilience modelling and simulation approaches*.

3.2 Resilience aversion approaches

When introducing risk on resilience acceptance measures, e.g. within ISO 31000 framework as in [31] [33] [32] using a risk criticality matrix, that depends on risk type and resilience dimensions considered, equation (1) can be extended to

$$R_i = P_i C_i \leq R_{crit}(i, P_i, C_i), \quad i = 1, \dots, N_R, \quad \text{and} \quad \sum_{i=1, C_i \in C_j}^{N_R} R_i \leq R_{crit}(C_j), \quad (2)$$

where criteria for single risks depend in the most general case on risk type and values of probability and consequence, respectively, to take account of risk aversion [55]. Collective risk criteria in (2) depend on consequence types $\{C_j\}_{j=1, \dots, N_C}$ that cover, not necessarily orthogonal, all consequence types, e.g. number of fatalities, injured, environmental loss quantities, and monetary loss.

Thus, *types or risk criteria that can be employed are distinction options including individual risk criteria, profile risk criteria (taking into account exposition of objects and persons), location dependency and collective risk*

criteria, see e.g. [56] [57] for a sample application of all of these. In addition, in as far as *risk on resilience aversion can be considered*, see e.g. within statistical analysis [58], database assessment [59], hazard-analysis (HA) such as [60], failure modes-and effects (FMEA) such as approaches [61], or by using FN-curves [56] [62].

3.3 Disruption event propagation through logic or temporal resilience assessment layers

Several analytical resilience assessment approaches ask for causality assessments. By definition of section 0, resilience of systems in a narrower sense can only be observed on the condition that a disruption or at least potential disruption has already occurred. For formalization, if for instance $E_{i_1}, i_1 = 1, 2, \dots, N_1$ are events that may cause disruption events, let $E_{i_2}, i_2 = 1, 2, \dots, N_2$ be unsuccessful preparation, detection and prevention activities or events, let $E_{i_3}, i_3 = 1, 2, \dots, N_3$ be initial absorption and damage events, which are low if system is robust, let $E_{i_4}, i_4 = 1, 2, \dots, N_4$ be initial system stabilization events, let $E_{i_5}, i_5 = 1, 2, \dots, N_5$ be intermediate recovery events, let $E_{i_6}, i_6 = 1, 2, \dots, N_6$ be final recovery events, and let $E_{i_7}, i_7 = 1, 2, \dots, N_7$ be final adoption and learning effects or events related to the system under threat.

Then it can for instance be asked if prevention activities are successful, e.g. in terms of concepts of operation (CONOPS) and preparation [63], access control [64] [65], detection [66] [67], or geometrical layout and physical barriers [68] [69] [70] [71] [72] [73]. To this end, for each event set $\{E_{i_1}\} \dots \{E_{i_7}\}$ we assume that the overall event space Ω is covered, the events are mutually orthogonal and the last events covers all other events not yet labeled explicitly, i.e., respectively,

$$\bigcup_{\iota=1,2,\dots,N_*} E_\iota = \Omega, \quad E_\iota \cap E_\kappa = \emptyset, \text{ if } \iota \neq \kappa, \quad E_{N_*} = \Omega \setminus \bigcup_{\iota=1,2,\dots,N_*-1} E_\iota. \quad (3)$$

Then in case of successful prevention the sums over conditional probabilities of damage event occurrence, see e.g. [74] for options to determine event probabilities and [75] [71] for database-driven event frequency determination, should be small in case of successful prevention considering all possible threats, see e.g. [76] for an all terrorism threats quantitative approach,

$$\sum_{i_2=1}^{N_2} \sum_{i_1=1}^{N_1} P(E_{i_2}|E_{i_1}) P(E_{i_1}) = ! \text{ min.} \quad (4)$$

Initial risk of damage consequences $C(E_{i_3})$ after threat absorption (classical naïve risk without considering recovery) should be small, for instance in terms of loading strength [77], e.g., in case of mechanical loading impact absorption due to high ductility [78], or combined resistance mechanisms [79] in case of (complex) blast effects [80],

$$\sum_{i_3=1}^{N_3} \sum_{i_2=1}^{N_2} \sum_{i_1=1}^{N_1} C(E_{i_3}) P(E_{i_3}|E_{i_2}) P(E_{i_2}|E_{i_1}) P(E_{i_1}) = ! \text{ min.} \quad (5)$$

The system should be stabilized after absorption of disruption, i.e. chances (positive risks, see e.g. [3] [81] [82]) of stabilization events post disruption should be maximized in terms of their consequences $C(E_{i_4})$,

$$\sum_{i_4=1}^{N_4} \sum_{i_3=1}^{N_3} \sum_{i_2=1}^{N_2} \sum_{i_1=1}^{N_1} C(E_{i_4}) P(E_{i_4}|E_{i_3}) P(E_{i_3}|E_{i_2}) P(E_{i_2}|E_{i_1}) P(E_{i_1}) = ! \text{ max.} \quad (6)$$

The system should exhibit further intermediate recovery chances, showing related consequence behavior $C(E_{i_5})$,

$$\sum_{i_5=1}^{N_5} \sum_{i_4=1}^{N_4} \sum_{i_3=1}^{N_3} \sum_{i_2=1}^{N_2} \sum_{i_1=1}^{N_1} C(E_{i_5}) P(E_{i_5}|E_{i_4}) P(E_{i_4}|E_{i_3}) P(E_{i_3}|E_{i_2}) P(E_{i_2}|E_{i_1}) P(E_{i_1}) = ! \text{ max.} \quad (7)$$

Similarly, the system should exhibit consequence signatures of final recovery $C(E_{i_6})$,

$$\sum_{i_6=1}^{N_6} \sum_{i_5=1}^{N_5} \dots \sum_{i_3=1}^{N_3} \sum_{i_2=1}^{N_2} \sum_{i_1=1}^{N_1} C(E_{i_6}) P(E_{i_6}|E_{i_5}) P(E_{i_5}|E_{i_4}) \dots P(E_{i_3}|E_{i_2}) P(E_{i_2}|E_{i_1}) P(E_{i_1}) = ! \text{ max,} \quad (8)$$

as well as for uptake of overall learning and adoption $C(E_{i_7})$,

$$\sum_{i_7=1}^{N_7} \sum_{i_6=1}^{N_6} \dots \sum_{i_3=1}^{N_3} \sum_{i_2=1}^{N_2} \sum_{i_1=1}^{N_1} C(E_{i_7}) P(E_{i_7}|E_{i_6}) \dots P(E_{i_2}|E_{i_1}) P(E_{i_1}) = ! \text{ max.} \quad (9)$$

Already in equation (5) it might be necessary to write instead of $P(E_{i_3}|E_{i_2})$ the more complex conditional expression $P(E_{i_3}|E_{i_2}, E_{i_1})$ indicating that the occurrence of E_{i_3} depends on both the occurrence of E_{i_2} and E_{i_1} . This holds true as soon as there is a dependence on the trajectory through the exhaustive event layers as defined in (3) with obvious generalizations up to equation (9). The described formalism (3) to (9) can be understood as a generalized Markov process where each propagation joins two different Markov spaces going

beyond stepwise extension and contraction of Markov spaces for resilience system analysis as described in [83] without memory (generalization of classical Markov model as e.g. applied in [84] [85]) as notated and with memory in case of the extensions just discussed at the beginning of the present text paragraph. However, (5) to (9) contain in addition consequence and effect quantification and time separation is replaced by consideration of logical response, resilience or catastrophe management cycle step phases, see e.g. [45] [86] [46].

Hence, first principle risk and resilience simulation should be able to *assess effect of preparation, detection and prevention of potential disruption events*, be able to *determine initial damage effects*, possibly averaged over objects at risk, over large scale areas or over threat source variations, see e.g. in the case of explosion events [80] [73] and in case of physical impact events [87] [68] [57]. Furthermore, *post event stabilization, intermediate system at risk behavior up to final recovery, as well as of learning and adoption* are asked for.

3.4 Causal resilience dependencies, resilience inference, resilience intervention effect

Next, time-ordered or logic dependence as used in (3) to (9) is further lifted and just causal dependency and inference is asked for influencing resilience performance of a socio-technical CI system. For instance, one may ask for the probability that a learning event labelled with ι_7 takes place modelled by random variable E_7 in case a recovery event labelled with ι_6 described by recovery random variable E_6 , knowing that realizations for random variables describing system threat loading $E_1 = \iota_1$, prevention effects $E_2 = \iota_2$, etc. up to and including intermediate response behavior $E_5 = \iota_5$ are given, using repeatedly the chain rule of probability, see e.g. [88] [89],

$$\begin{aligned} P(E_7 = \iota_7, E_6 = \iota_6, E_5 = \iota_5, \dots, E_2 = \iota_2, E_1 = \iota_1) &= P(E_7 = \iota_7 | E_6 = \iota_6, E_5 = \iota_5, \dots, E_2 = \iota_2, E_1 = \iota_1) \\ &\quad \cdot P(E_6 = \iota_6 | E_5 = \iota_5, \dots, E_2 = \iota_2, E_1 = \iota_1) P(E_5 = \iota_5 | E_4 = \iota_4, \dots, E_2 = \iota_2, E_1 = \iota_1) \cdot \dots \\ &\quad \cdot P(E_2 = \iota_2 | E_1 = \iota_1) P(E_1). \end{aligned} \quad (10)$$

More interestingly, causal inferences may be asked for. For instance, what is the effect of threat absorption (robustness) level on learning and adoption level without considering all the other effects, which are here threat type, prevention success, immediate stabilization effect, intermediate, and final recovery,

$$\begin{aligned} P(E_7 = \iota_7 | E_3 = \iota_3) &= \frac{P(E_7 = \iota_7, E_3 = \iota_3)}{P(E_3 = \iota_3)} \\ &= \frac{\sum_{\substack{\kappa_1=1,2,\dots,N_1 \\ \kappa_2=1,2,\dots,N_2 \\ \kappa_4=1,2,\dots,N_4 \\ \vdots \\ \kappa_6=1,2,\dots,N_6}} P(E_7 = \iota_7, E_6 = \kappa_6, \dots, E_3 = \iota_3, E_2 = \kappa_2, E_1 = \kappa_1)}{\sum_{\substack{\kappa_1=1,2,\dots,N_1 \\ \kappa_2=1,2,\dots,N_2 \\ \kappa_4=1,2,\dots,N_4 \\ \vdots \\ \kappa_7=1,2,\dots,N_7}} P(E_7 = \kappa_7, E_6 = \kappa_6, \dots, E_3 = \iota_3, E_2 = \kappa_2, E_1 = \kappa_1)}. \end{aligned} \quad (11)$$

In (11) we loop over all nuisance random variables, which are not relevant for the present question.

Also, the specific effect of resilience interventions on causal relations can be determined, for instance if we require that the successful early detection of threats, i.e. random discrete variable E_2 has a corresponding value ι_2 , we can determine whether it influences the effect of high robustness on high learning as given in (12).

$$\begin{aligned} P(E_7 = \iota_7 | E_3 = \iota_3, E_2 = \iota_2) &= \frac{P(E_7 = \iota_7, E_3 = \iota_3, E_2 = \iota_2)}{P(E_3 = \iota_3, E_2 = \iota_2)} \\ &= \frac{\sum_{\substack{\kappa_1=1,2,\dots,N_1 \\ \kappa_4=1,2,\dots,N_4 \\ \kappa_5=1,2,\dots,N_5 \\ \vdots \\ \kappa_6=1,2,\dots,N_6}} P(E_7 = \iota_7, E_6 = \kappa_6, \dots, E_4 = \kappa_4, E_3 = \iota_3, E_2 = \iota_2, E_1 = \kappa_1)}{\sum_{\substack{\kappa_1=1,2,\dots,N_1 \\ \kappa_4=1,2,\dots,N_4 \\ \kappa_5=1,2,\dots,N_5 \\ \vdots \\ \kappa_7=1,2,\dots,N_7}} P(E_7 = \kappa_7, E_6 = \kappa_6, \dots, E_4 = \kappa_4, E_3 = \iota_3, E_2 = \iota_2, E_1 = \kappa_1)}. \end{aligned} \quad (12)$$

Hence the question arises if the ab-initio resilience simulation model is capable to *contribute to a Bayesian network (belief network, decision network)* or generalizations thereof such as dynamic Bayesian networks (see e.g. [90] [91] [92]) or influence diagrams (see e.g. [93] [94]) allowing for the computation of joint probability functions of resilience-relevant events, whether the approach *allows for resilience inferencing* (determination of effects given causes, e.g. on average better recovery levels given robustness measures independent of

threat events) as well as *resilience intervention effect assessment* (determination of effect of resilience improvement (intervention, treatment) measures on resilience causal relations).

Table 1 lists in its first column the identified resilience simulation method capabilities as requested for input to analytical system resilience analysis methods. Depending on the resilience assessment process selected, see Figure 1, a single simulation method or several methods could be necessary to cover the requested input of the overall assessment process.

4 First-principle resilience modelling and simulation methods and their properties

Sample resilience modelling and simulation methods are selected somewhat aligned with the historic and more recent development of resilience analysis of single structural members (section 0), structures and areas (section 0), and finally graphs, technical grid systems, socio-technical and human cyber-physical learning systems (section 0).

4.1 Single and multiple degree of freedom ersatz models

Single point mass ersatz models with single degree of freedom (SDOF) have been used successfully to describe the behavior of structural members under static, quasi-static and dynamic loads [79], in particular for modeling blast effects on structures [95] [96] [97], and earth quake resilience modelling [98], or against wind loads [99]. The basic idea is expressed by the partial vector differential equation of first order, corresponding initial conditions, and failure criteria,

$$m \frac{d}{dt} \begin{bmatrix} x(t) \\ v(t) \end{bmatrix} = \begin{bmatrix} v(t) \\ F_{ext}(x, v, t) + F_{res}(x, v) \end{bmatrix}, \quad \begin{bmatrix} x(t_0) \\ v(t_0) \end{bmatrix} = \begin{bmatrix} x_0 \\ v_0 \end{bmatrix}, \quad |x(t)| \leq x_{crit}, |v(t)| \leq v_{crit}, |a(t)| \leq a_{crit}, \quad (13)$$

where $m = const.$ is the ersatz mass of the point mass model, $x(t)$ the position of the point mass, $v(t) = \frac{d}{dt}x(t) = \dot{x}(t)$ its velocity, $a(t) = \frac{d^2}{dt^2}x(t) = \ddot{x}(t)$ its acceleration, $F_{ext}(x, v, t)$ is the external force on the point mass depending on its position, velocity and time, $F_{res}(x, v)$ is the response force of the point mass, typically forcing it back to its initial or another stable position, x_0 is the initial position, v_0 is the initial velocity, x_{crit} is a critical displacement, v_{crit} a critical velocity and a_{crit} a critical acceleration.

Generalizations comprise multiple point masses resulting in multiple degree of freedom (MDOF) models (i.e., respectively position and velocity) [100], for instance to describe more complex structural members, in particular sacrificial layers, or to describe multi storage buildings [101]. If more than a single degree of freedom of the point mass is considered behavior of several ersatz mass points in a plane [102] or even in three-dimensional space can be considered.

Regarding parameterization effort such modelling approaches require rather little experimental input. For instance, SDOF models assuming for simplicity Hook's law or an arctan elastic-plastic response, only require parameters for dimensionless Hook's constant or two parameters, respectively, and corresponding critical displacement with suitable assumptions [79]. Nevertheless, effects of geometry and material can be assessed provided sufficient validated SDOF parametrizations are available, see e.g. [103] [104] [105].

In summary, single and multiple point mass models allow to model system response model, loading model and failure criteria explicitly. They can be designed to cover a wide range of predefined geometries and material properties for at least order of magnitude estimates of failure behavior. They are well suited for a large number of buildings or structural elements, where lack of data limits the use of more detailed models and in case of large statistical or systematic variations of systems under risk. Models can easily be scaled to adopt to modified conditions by applying dimensionless formulations.

4.2 Physical-engineering coupled continuum simulation

An intuitive example is the effect of blast (shock waves in air) on structures [106]. In this case computational fluid dynamics (CFD) for the blast propagation is coupled with computational structural dynamics (CSD) codes.

Fluid dynamics is described by conservation equations of compressible fluid flow [106]. In integral form they can be applied to an arbitrary moving and deforming volume (arbitrary Lagrangian Eulerian (ALE) formulation [107]) and can be solved on time dependent grids in three-dimensional space thus allowing deformable and moving bodies, e.g. if structures subjected to blast are deformed or overthrown [106],

$$\frac{d}{dt} \int_V U dV = \oint_S (L + K) n dS, \quad (14)$$

$$U = (1, \rho, \rho \mathbf{v}, e^{tot})^T, \quad L = (\mathbf{v}, 0, -\underline{\underline{\sigma}}, -\underline{\underline{\sigma}}\mathbf{v} + \mathbf{q})^T, \quad K = U(\mathbf{w} - \mathbf{v}),$$

where the column matrix U contains the set of conservative time and position-dependent variables density ρ , mass flow density $\rho \mathbf{v}$ and total energy per volume $e^{tot} = e + v^2/2$ with the internal energy e , material velocity is given by the vector \mathbf{v} with absolute value $v = |\mathbf{v}|$, $\underline{\underline{\sigma}}$ is the stress tensor, and \mathbf{q} is the heat flux vector, \mathbf{w} is the externally supplied velocity field, the column matrix L is the Langrangian flux density, and the column matrix K is the convective flux density. The equality in (14) ensures the conservation equations for mass, momentum and energy in an abstract form (geometrical conservation law for the size of the control volume) [106].

To solve (14) in a unique way an equation of state is missing (EOS). In case of air the compressible fluid can be considered as inviscid (without friction) and not heat-conducting. In this case $\mathbf{q} = 0$ and $\underline{\underline{\sigma}} = -p \mathbf{E}$, where EOS $p = p(\rho, e)$ is used and the unit matrix \mathbf{E} , i.e. $\sigma_{ij} = p \delta_{ij}$ using three-dimensional Kronecker delta. For instance using the calorically perfect gas approximation [108], $p = \rho(\gamma - 1)e$, with $\gamma = C_p/C_v$, the adiabatic index and $e = C_v T$ the internal energy per unit mass, where C_p is the specific heat capacity at constant pressure and C_v is the specific heat capacity at constant volume.

Structural dynamics is described using a Lagrangian description with primitive variables (see e.g. [109]), where the conservation of mass, momentum and energy respectively read [106], using the material derivative $\frac{D}{Dt} = \frac{\partial}{\partial t} + \mathbf{v} \cdot \operatorname{div}(\bullet)$, \mathbf{f} being the vector of body forces, and again neglecting heat flow for fast processes,

$$\frac{D\rho}{Dt} + \rho \operatorname{div}(\mathbf{v}) = 0, \quad \frac{D\mathbf{v}}{Dt} = \mathbf{f} + \frac{1}{\rho} \operatorname{grad}(\underline{\underline{\sigma}}), \quad \frac{De}{Dt} = \mathbf{f}\mathbf{v} + \frac{1}{\rho} \operatorname{div}(\underline{\underline{\sigma}}\mathbf{v}). \quad (15)$$

Equation (15) needs as an additional equation a material model of the form $\underline{\underline{\sigma}} = \underline{\underline{\sigma}}(\underline{\underline{\epsilon}}, \underline{\dot{\epsilon}}, T)$, where $\underline{\underline{\epsilon}}$ is the strain tensor, $\underline{\dot{\epsilon}} = \frac{1}{2}(\operatorname{grad}(\mathbf{v}) + \operatorname{grad}(\mathbf{v})^T)$ is the strain rate tensor and in general for the temperature $T = T(e, \rho)$ holds [106], see [110]. Equation (14) and (15) are propagated using initial and boundary conditions, respectively.

Coupling of the compressible fluid and the structural simulation is required for all coupling surfaces S_{cpl} of the structure that are surrounded by the fluid, excluding possibly boundary conditions, e.g. bottom of wall or house [106]. In general, at the surface the marital velocity \mathbf{v} for fluid and solid must be equal, the surface stress (traction) $\mathbf{t} = \underline{\underline{\sigma}}\mathbf{n}$, the temperature T , and the heat flux \mathbf{qn} [106]. Due to inviscid fluid, only stress and tension perpendicular to surface is possible, also only velocities of solid perpendicular to surface have influence on fluid. Furthermore, heat conduction is neglected and hence the last two conditions are dropped. So, the remaining boundary conditions for all coupling surface points $\mathbf{r} \in S_{cpl}$ read, e.g. $p_{fluid} = p_{fluid}(\mathbf{r})$, [106]

$$p_{fluid} = -\mathbf{n}(\underline{\underline{\sigma}}_{struct}\mathbf{n}), \quad \mathbf{n}\mathbf{v}_{fluid} = \mathbf{n}\mathbf{v}_{struct}. \quad (16)$$

In summary, we see that for solving such coupled continuum equations for structural resilience response and counter measure assessment, at least the following inputs are required: geometrical information, boundary condition information, e.g. where and how are objects fixed, how are they connected, material model information for fluids in terms of equation of state (e.g. air, water, compressed gases, etc.) and material model in case of structures (e.g. steel, concrete, window glass, brick walls, etc.). This is confirmed by applications of the approach for assessing efficiency of blast walls [111], transport infrastructure [112], or structures under seismic excitation [113]. Within such frameworks loading conditions are part of the model or are dynamic boundary conditions, e.g., to simulate free field explosions. Effort for such simulations is significant in terms of expertise and also often regarding simulation time due to the need to assess multiple scenarios. The models claim predictive capability, thus also improved scenarios can be assessed and optimal protection mechanisms can be identified. Statistical and expected systematic variations can be covered, however, even single scenario computations are relative resource intensive.

4.3 Graphical and physical-engineering network simulation

Network or graph structures are suitable to describe classical infrastructures such as supply (e.g. water distribution [114], electricity [115], gas [116], oil), disposal networks (wastewater, waste), transportation [117] (railways [118], urban transport [119], highways, main airports), health care, hospitals, banking backbones as well as more recent critical infrastructures such as mobile communication grids (radio masts, space-based), internet and mobile digital services, and cyber grids [120]. Basic modelling elements include vertices, nodes or points, and their potential single or multi-directional connections called edges, links or lines. Under reasonable assumptions, the type of graph is in general an undirected multigraph allowing for loops,

$$G = (V, E), \quad V = \{v_i\}_{i=1,2,\dots,N_V}, \quad (17)$$

$$E = \{e_i\}_{i=1,2,\dots,N_E/2} \\ = \left\{ e_1 = (v_{i_1}, v_{i_2}), e_2 = (v_{i_3}, v_{i_4}), \dots, e_{N_E/2} = (v_{i_{N_E-1}}, v_{i_{N_E}}) \mid v_{i_1}, v_{i_2}, \dots, v_{i_{N_E}} \in V \right\},$$

where V is a nonempty finite set of N_V distinct vertices and E is a non-empty set of $N_E/2$ edges. By definition edges are directed (e.g. for e_1 from v_{i_1} to v_{i_2}) and may connect with the same vertex, e.g. when an airplane flies back to start airport in case of disruption, as well as the same two vertices may be connected with several edges, e.g. when there are two distinct railway transportation routes between two cities. Also, some vertices may not be connected at all with any other vertices by an edge.

Edges may be colored as sources (producer) or sinks (consumer) or both (prosumer) of objects or services distributed via the graph (colored graph or network). Then such questions may be formalized and answered for supply grids (and similarly for disposal and mixed grids):

- (i) Number of consumers connected with any producer (supplied consumers);
- (ii) Number of (completely or in parts) alternative connections along distinct edges (degree of redundancy of supply);
- (iii) Ranking of vertices or edges regarding criticality for supply of defined subset of consumers (how many vertices are not supplied anymore if vertex or edge fails);
- (iv) Number of alternative sources for each vertex consumer;
- (v) Minimum number of vertices or edges to achieve isolation of one up to all sources;
- (vi) Distance between sources and consumers in terms of minimum number of vertices in between;
- (vii) Number and scale (e.g. in terms of sources per consumer) of islanding options in terms of independent sub-graphs ensuring supply of all consumers.

If additional information is available for vertices or edges more quantitative grid assessments are feasible. Additional information may include abstract capacity statements such as minimum and maximum inflow at each vertex (e.g. maximum capacity of freshwater well), minimum and maximum outflow at each vertex (e.g. minimum and maximum consumption of hospital), and minimum and maximum throughput for each edge (e.g. capacity of electrical power line section):

$$\{v_i^{in\ min}\}, \quad \{v_i^{in\ max}\}, \quad \{v_i^{out\ min}\}, \quad \{v_i^{out\ max}\}, \quad \{e_j^{through\ min}\}, \quad \{e_j^{through\ max}\}, \quad (18)$$

Already (17) and (18) lead to some consistency requirements, when asking for a possible solution of the graph. If $v_i^{in\ min} > 0$ for some vertex, i.e. vertex is source, then there must be a single directed edge e_j away from v_i , in case $v_i^{in\ min} > v_i^{out\ max}$, i.e. vertex cannot consume all it generates, such that at least $v_i^{in\ min} - v_i^{out\ max} \leq e_j^{through\ min}$. Alternatively, there must be several edges away from e_j such that the minimum inflow can be directed in further graph parts. In this way, for each vertex and edge certain requirements must be fulfilled. This shows that solution options may be restricted or be lost in case of disruptions, i.e., lost vertices or edges. On the other hand, often vertices and edges can be assumed to have very high throughputs, such that bus solutions can be found, i.e. only connection to source matters for consumers and sufficient over source input, as in case of local electricity distribution grids [86]. If (18) quantities are given, even in a statistical form (i.e. probability of flow connection), and if there are many nodes and edges between sources and consumers, e.g. multiple pipeline segments, stations, hierarchies of distribution, also percolation questions (flow throughput at system level) may be formulated, e.g. in transportation networks for cities [117].

Finally, if further additional information for edges is provided, e.g. such as distance along edge $r_j = r(e_j)$, height-profiles or a least height differences between vertices, cross-sections per resolved edges, dynamic flow simulations are accessible, for instance for gas grids [121] [122] [123] beyond graphical models [124], also in case of major disruptions where some vertices are not supplied anymore. More detailed simulations could even consider environmental temperatures and related heat flows, external pressures, cross-section changes and bending of pipelines, or corrosion effects due to gas flow.

Graphical-topological or quantified network models are simulation approaches of choice for genuine network critical infrastructures. In the first case many generally known quantities and effects can be searched for within a given network, e.g. regarding optimal selection of hierarchy levels and nearest neighbor connections given certain disruption patterns. CI networks are spatial-temporal cyber-physical systems, where the challenge is to avoid oversimplification while too much detail renders quantitative physics-engineering simulation impossible. An option could be to add additional network properties only if found necessary to explain observed or reasonably expected effects, while allowing for emergent grid properties to occur due to a comprehensive set of potential disruptions.

5 Classification of simulation methods regarding usefulness for resilience analytics

Section 0 allows to define key properties of first principle simulation methods as relevant for analytical resilience assessment on system level. The simulation approaches are listed in the first column of Table 1 as presented in section 4. For the first-principle model-based resilience simulation methods, section 0 identified feasible contributions at an abstract level. The present section now resolves more specifically to which analytical resilience assessment step the sample methods can contribute. Resilience assessment schemes or frameworks as indicated in Figure 1 are not resolved, since they are considered more arbitrary when compared to the requests of analytical quantification schemes of risk control and resilience enhancement as presented in section 0.

Table 1 shows that the basic point mass ersatz model, the coupled continuum simulation as well as the graph and network theory approach (see column headings 1 to 3) can contribute to almost all requirements of analytical system resilience assessment (see first column items 1 to 15), see the graded green color coding in Table 1. If not understood as an abstract way to model system static and dynamic loading and response, in particular in case of the point mass ersatz models, the first two models are rather restricted in their coverage of possible threats and resilience measures to mechanical-physical static and dynamic events. The graph theory or network theory based approach is more flexible, requires however the modeling of corresponding types of systems as well as interdependencies, e.g. organizational/operator and cyber effects on physical grid.

Regarding dynamic unfolding of event chains as disruptions occur, the ersatz model is a limited description of representative points' movements, the continuum model covers time evolution of physical-engineering models where snapshots can be interpreted, see Table 1 for more details. However, both lack coverage of response and recovery beyond built-in material-structural properties, e.g. elastic behavior, shape memory or self-healing effects, e.g. actual rebuilding models or similar due to their low abstraction level. Thus, causal chain generation and the assessment of effect of resilience improvement measures and treatments of undesired causal dependencies is restricted to structural-material prevention, improved elastic response or graceful absorption or system mechanical-structural degradation with acceptable consequences.

The model parameters in general increase from left to right in Table 1. However, the coupled continuum modelling uses this for specific higher structural-material system resolution. Whereas the graph and network models require more parameters for providing more dependencies between subsystems in terms of structural-topological information and in terms of coupling strengths and subsystem modeling, in particular when going beyond input-output models, see e.g. [125] [126] [127].

For instance, when studying the resilience of power grids in the context of the energy transition in Germany [128], a physical-engineering network simulation approach is used to model the influence of larger or smaller power outages on power-dependent and in general interdependent critical infrastructure elements of a city, including, *inter alia*, hospitals, medical practices, food shops, industrial sites, water supply, and police stations. Damage cascades are triggered and can be quantified based on the mutual interdependencies to assess the gradual decay of public services and economy over hours, days and weeks.

An efficient combination and joint employment of the three detailed first principle simulation approaches of Table 1 is that point mass models can be used to summarize coupled fluid-mechanical simulations of disruption event effects. Then the former can be used to provide resource-efficient input for assessing local dependencies

Table 1. Classification of first principle simulation methods of resilience of systems. Table gives contribution of simulation methods (listed from left to right) to requests of analytical system resilience analysis methods. Green color coding grade indicate suitability of simulation model for providing input to analytical risk and resilience assessment requests.

| Resilience analytics request versus fulfillment by system resilience simulation | 1. Single and multiple degree of freedom ersatz models | 2. Physical-engineering coupled continuum simulation | 3. Graph based and physical-engineering Network simulation |
|--|--|---|---|
| 1. Coverage of risk on resilience types, including combined threat vectors | As is restricted to mechanical loading threats | Restricted to mechanical fluid-dynamic threat subset. Covers time dependent and resonance effects. | Only disruptions covered that can be related to at least one sub-grid. Matching between threat type and system aspect modeled use of corresponding graph is necessary. E.g. to model cyber effects on physical grids. |
| 2. Resilience dimensions covered, e.g. system layers, technical resilience capabilities | Physical-engineering layer only | Physical-engineering layer only; Could model interface to steering systems and cyber systems, by modelling actuator with high resolution. | See above |
| 3. Assumption of independency of single risks on systemic resilience | Not assumed as sequential loadings and resonance effects can be covered. However, loadings need to fit in model frame. | Not assumed. Dynamic boundary conditions can cover up to long-term dynamic mechanical loadings. Type of threat is limited. | No, as simultaneous and sequential transient considerations are feasible |
| 4. Overall Risk acceptance criteria employable, e.g. individual, profile risk, location dependent, collective | If several ersatz models are considered for all objects at risk | Complex damage models can be built based physical-engineering criteria, e.g. maximum strain, stress, deformation, etc. | Vertices, edges and sub-grids can be assessed to obey these quantities or proxies thus individual and collective criteria are accessible |
| 5. Consideration of resilience aversion feasible | Within evaluation process feasible | See left | Could be built into model by aggregating counter effects in case of partially major losses in part of grid. |
| 6. Determination of effect of preparation, detection and prevention and of disruptions | Not explicitly. Effect on ersatz model must be assumed. | Prevention efforts can be part of simulation of unfolding physical threat potential, e.g. using dynamic change of geometry of objects at risk | Could be considered in terms of changing capabilities of vertices and edges to prevent event, to fast response, in case of similar attacks. Also, overall weakening effects can be considered. |
| 7. Determination of initial or maximal damage effects after absorption | Yes, in terms of maximal elongation | Yes, based on physical engineering effects, e.g. displacement, expected crack-distribution, etc. | Yes, based on multiple qualitative and quantities measures, e.g. customers served, response time, consideration of regions, etc. However, requires quantification of graph model. |
| 8. Determination of immediate response, | No | Only if part of modelled response mechanism of | Yes, by assuming (immediate) repair schemes and by |

| | | | |
|--|---|---|---|
| e.g. stabilization post disruption | | structures | comparing their efficiency. Suited for $N - 1$ redundancy assessment, common cause and root cause assessment. |
| 9. Coverage of intermediate recovery steps | No, requires ersatz model sequence, i.e. beyond single model | Only if response can be incorporated in material models and failure modes | Yes, by using (long-term) repair and improvement models. |
| 10. Final asymptotic system recovery or improvement assessment | See above | See above | Yes, see above |
| 11. Effects of adoption and learning of system regarding control and resilience | Model parameters can be modified | System geometry, material and failure mechanisms can be modified; | Yes, see above. In addition, learning thresholds can be defined covering architectural and parametric changes based on past event evaluation. |
| 12. Contribution to structure of Bayesian network or generalizations | Only within restricted application domain if already covered model parameter ranges are considered. | Required is generic model that describes variation options at system model level covering structural changes and material changes. Can be used to identify potential effects of disruptions on system at risk and its response options. | Graph or network can be translated or abstracted into dependency network, e.g. by assuming that vertices that are connected also affect each other along allowed edge directions or beyond. Insight expected if such direct mapping are abstracted. |
| 13. Parametrization of probabilistic graphical models | As above | Quantification of response paths. Restricted to dependencies that can be modeled in physical-structural domain. | Effects can be resolved and quantified up to highest network resolution. However, restricted to properties modeled with (extended) graphical network |
| 14. Causal inference for resilient systems | As above | Quantification of cause-effect paths on system variations | Causal inference can be very high resolving, or abstract when averaging over realization options, e.g. effect of nearest neighbor disruption, etc. |
| 15. Assessment of effect of resilience interventions | As above | Comparison of cause-effect paths on system variations in presence of additional resilience interventions | Yes, by considering structural and quantitative modified networks, or by adding dynamic modifications to network |

and effects of disruption events within graph and network simulations. However, if spatial distribution and analysis matter to cover common cause effects as caused by large scale loadings such as (sea) floods, storm loading, impact or explosive loading, the simulation on these scales is required to take account of cascading effects and resulting common cause effects. An approach in this direction is [129].

Further model-based simulation methods of system resilience include system structure and dynamics informed Monte-Carlo simulation of agents (see e.g. for an airport checkpoint application example [130] [131]), random matrix theory applied for modelling of partially unknown systems (see e.g. for an application to distributed edge communication system for vehicles [132]), structural assessment based on probabilistic frameworks (e.g. [133]), as well as application domain specific physical-engineering simulations for modelling of physical hazard or disturbance propagation, e.g. of effect of disturbances on short-range ultrasound communication [82], of fragments in air [134] [56], or with very high resolution of potential initial unintended triggering events of explosions [135].

6 Conclusions

The paper provided an approach to better classify and select for application purposes first-principle resilience simulation methods that claim to generate model-based (socio) technical simulation of risk control and resilience. Such approaches compute, ideally without any rescaling, risk and resilience quantities based on controlled and understandable model properties and parameters.

The assumption was made that for resilience management and improvement frameworks are employed that can be summarized using joint risk control and resilience analytical approaches. For instance, in terms of: nested tables and matrices to summarize results, e.g. on system elements, system functions, potential threats and disruptions; risk and resilience ranking on system level using different risk and resilience quantitative aspects; and risks on resilience can be evaluated and the most suitable counter measures can be selected and implemented.

Any such framework was assumed to be fed from one or more formal risk control and resilience assessment analytical approach, several of which were introduced and characterized. This ranged from risk on systemic resilience approaches and their risk aversion aware evaluation, to incorporating resilience dimensional aspects for risk control and resilience quantification, to logic and temporal dependency chains as extension of conditional vulnerability expressions and finally causal dependencies using probabilistic belief networks.

Such formal analytical overall risk and resilience (semi) quantification approaches were found to be sufficiently well defined to derive requirements on expected outputs from first-principle approaches. If the latter can provide valuable input to analytical approaches it can be expected that they fit well into current resilience assessment frameworks. Strengths and weaknesses of the simulation approaches can be identified regarding their application scope, level of (spatial) resolution, types of known and unknown threats covered, coverage of systemic aspects, flexibility to extend simulations, number of parameters needed, resources needed for set-up and operation of models and simulation runs.

Regarding the sample simulations considered it was found in summary that abstract quantitative ersatz models are flexible and predictive within pre-evaluated application domains only. Computational continuum mechanical simulations are highly resolving but limited to corresponding threats, response and recovery mechanisms. Graph based approaches are flexible regarding subsystem dependencies but require additional input for quantitative predictive network modelling. Different system layers can be covered, however, coupling models add additional challenges regarding parameterization and different time scales during modelling.

Future system resilience quantification classification could significantly extend the list of resilience analytical approaches considered as well as the number of numerical ab-initio simulations. As requests of analytical methods overlap, it can be expected that a certain convergence of resilience analytical classification options will be identified. This is expected to be somewhat in contrast with the set of methods for systemic risk control and resilience assessment methods, as they are expected to cover more and more seldom, rare, unexpected and unexampled disruption effects. This requires an increasing model complexity, e.g. using system-informed variations of Monte-Carlo simulations (classical, pseudo, surrogate), and random matrix system theory. The presented approach could be used to guide resilience simulation model complexity increase using overall systemic resilience assessment relevancy, in particular to ensure that key requests are covered such as coverage, option for identification of causal chains or dependencies, inference on failure root causes and resilience treatment efficiency assessment for key causal dependencies.

Acknowledgements

Work presented has been supported by German BMBF project RESIST on Resilient power grids for the energy transformation (Resiliente Stromnetze für die Energiewende, Founding contract number: 03SF0637) [128], and in parts by the BMBF project OCTIKT (Founding contract number: 01IS18064A) [136] as well as the EU projects eFORT (Grant Agreement ID: 101075665) [137], SecureGas (Grant Agreement ID: 833017) [138], RESISTO (Grant Agreement ID: 786409) [139], SnowBall (EC Grant agreement ID: 606742) [140], ENCOUNTER (Grant agreement ID: 285505) [141], and EDEN (Grant agreement ID: 313077) [142].

References

1. Häring I, Schäfer J, Vogelbacher G, Fischer K, Riedel W, Faist K, et al. From event to performance function-based resilience analysis and improvement processes for more sustainable systems. *IJSMSS*. 2021;5:90. doi:10.1504/IJSMSS.2021.115784.
2. Thoma K, Scharte B, Hiller D, Leismann T. Resilience Engineering as Part of Security Research: Definitions, Concepts and Science Approaches. *European Journal for Security Research*. 2016;1:3–19. doi:10.1007/s41125-016-0002-4.
3. Häring I, Ebenhöch S, Stoltz A. Quantifying Resilience for Resilience Engineering of Socio Technical Systems. *European Journal for Security Research*. 2016;1:21–58. doi:10.1007/s41125-015-0001-x.
4. Mohammadnazari Z, Aghsami A, Rabbani M. A hybrid novel approach for evaluation of resiliency and sustainability in construction environment using data envelopment analysis, principal component analysis, and mathematical formulation. *Environment, Development and Sustainability*. 2023;25:4453–90. doi:10.1007/s10668-022-02210-z.
5. Finger J, Hasenstein S, Siebold U, Häring I. Analytical resilience quantification for critical infrastructure and technical systems. In: Walls L, Revie M, Bedford T, editors. *ESREL 2016*; 25.-29.09.2016; Glasgow, Scotland. Routledge, Taylor & Francis Group: CRC Press; 2016. p. 2122–2128. doi:10.1201/9781315374987-322.
6. Häring I, Fehling-Kaschek M, Miller N, Faist K, Ganter S, Srivastava K, et al. A performance-based tabular approach for joint systematic improvement of risk control and resilience applied to telecommunication grid, gas network, and ultrasound localization system. *Environment Systems and Decisions*. 2021;41:286–329. doi:10.1007/s10669-021-09811-5.
7. Koonce D, Zhou J, Anderson C, Hening D, Conley V. What is STEM? In: 2011 ASEE Annual Conference & Exposition; 6/26/2011 - 6/29/2011; Vancouver, BC: ASEE Conferences; 6/26/2011 - 6/29/2011. 22.1684.1-22.1684.9. doi:10.18260/1-2--18582.
8. Häring I, Scharte B, Hiermaier S. Towards a novel and applicable approach for Resilience Engineering. In: Stal M, Sigrist D, Wahlen S, Portmann J, Glover J, Bernabe N, et al., editors. *IDRC*; 28.08-01.09.2016; Davos. Davos: GRF; 2016. p. 272–276.
9. Häring I, Scharte B, Stoltz A, Leismann T, Hiermaier S. Resilience engineering and quantification for sustainable systems development and assessment: socio-technical systems and critical infrastructures. In: Linkov I, Florin M-V, Trump B, editors. *IRGC Resource Guide on Resilience*. Lausanne: International Risk Governance Center; 2016. p. 81–89.
10. ISO 31000. Risk management — Guidelines 2018-02;ICS: 03.100.01. 2nd ed. Geneva, Switzerland: International Organization for Standardization (ISO).
11. ISO 31010. Risk management - Risk assessment techniques 2019-06;03.100.01. 2nd ed. Geneva, Switzerland: International Organization for Standardization.
12. ISO/TS 22317. Security and resilience — Business continuity management systems — Guidelines for business impact analysis 2021-11;03.100.01. 2nd ed.
13. ISO 22319. Security and resilience — Community resilience — Guidelines for planning the involvement of spontaneous volunteers 2017-04;03.100.01. 1st ed.
14. ISO 22320. Security and resilience — Emergency management — Guidelines for incident management 2018-11;03.100.01. 2nd ed.
15. BSI-Standard 200-1. BSI-Standard 200-1, Managementsysteme für Informationssicherheit (ISMS) 2017-08.
16. ISO/IEC 27001. Information security management systems 2022-10;35.030; 03.100.70.
17. Directive (EU) 2022/2557. Directive (EU) 2022/2557 of the European Parliament and of the Council of 14 December 2022 on the resilience of critical entities and repealing Council Directive 2008/114/E: CER; 2022-12.
18. Directive (EU) 2022/2555. Directive (EU) 2022/2555 of the European Parliament and of the Council of 14 December 2022 on measures for a high common level of cybersecurity across the Union, amending Regulation (EU) No 910/2014 and Directive (EU) 2018/1972, and repealing Directive (EU) 2016/1148 (NIS 2 Directive); 2022-12.
19. European Comission (EC). Communication from the Comission to the European Parliament, the European Council, the Council, the European economic and social Committee and the Committee of the Regions on the EU Security Union Strategy, COM(2020) 605 final. 2020. <https://ec.europa.eu/futurium/en/system/files/ged/communication-eu-security-union-strategy.pdf>. Accessed 22 Sep 2023.
20. European Comission (EC). Communication from the Comission to the European Parliament, the European Council, the Council, the European economic and social Committee and the Committee of the Regions: A

- counter-terrorism agenda for the EU: anticipate, prevent, protect, respond, COM(2020) 795 final. 2020. <https://db.eurocrim.org/db/en/doc/3542.pdf>. Accessed 22 Sep 2023.
21. Hosseini S, Barker K, Ramirez-Marquez JE. A review of definitions and measures of system resilience. *Reliability Engineering & System Safety*. 2016;145:47–61. doi:10.1016/j.ress.2015.08.006.
 22. Yodo N, Wang P. Engineering Resilience Quantification and System Design Implications: A Literature Survey. *Journal of Mechanical Design* 2016. doi:10.1115/1.4034223.
 23. Mottahedi A, Sereshki F, Ataei M, Nouri Qarahasanlou A, Barabadi A. The Resilience of Critical Infrastructure Systems: A Systematic Literature Review. *Energies*. 2021;14:1571. doi:10.3390/en14061571.
 24. Häring I, Sansavini G, Bellini E, Martyn N, Kovalenko T, Kitsak M, et al. Towards a Generic Resilience Management, Quantification and Development Process: General Definitions, Requirements, Methods, Techniques and Measures, and Case Studies. In: Linkov I, Palma-Oliveira JM, editors. *Resilience and Risk*. Dordrecht: Springer Netherlands; 2017. p. 21–80. doi:10.1007/978-94-024-1123-2_2.
 25. Curt C, Tacnet J-M. Resilience of Critical Infrastructures: Review and Analysis of Current Approaches. *Risk Analysis*. 2018;38:2441–58. doi:10.1111/risa.13166.
 26. Madni AM, Jackson S. Towards a Conceptual Framework for Resilience Engineering. *IEEE Systems Journal*. 2009;3:181–91. doi:10.1109/JSYST.2009.2017397.
 27. Woods DD. Four concepts for resilience and the implications for the future of resilience engineering. *Reliability Engineering & System Safety*. 2015;141:5–9. doi:10.1016/j.ress.2015.03.018.
 28. Mohebbi S, Zhang Q, Christian Wells E, Zhao T, Nguyen H, Li M, et al. Cyber-physical-social interdependencies and organizational resilience: A review of water, transportation, and cyber infrastructure systems and processes. *Sustainable Cities and Society*. 2020;62:102327. doi:10.1016/j.scs.2020.102327.
 29. Häring I, Ganter S, Finger J, Srivastava K, Agrafioti E, Fuggini C, Botella F. Panarchy Process for Risk Control and Resilience Quantification and Improvement. In: Baraldi P, Di Maio F, Zio E, editors. *ESREL2020 and PSAM15*; Venice, Italy (virtual). Singapore: Research Publishing; 2020. p. 2481–2488.
 30. Allen CR, Angeler DG, Garmestani AS, Gunderson LH, Holling CS. Panarchy: Theory and Application. *Ecosystems*. 2014;17:578–89. doi:10.1007/s10021-013-9744-2.
 31. Baumann D, Häring I, Siebold U, Finger J. A web application for urban security enhancement. In: Thoma K, Häring I, Leismann T, editors. *9th Future Security – Security Research Conference*; September 16 – 18, 2014; Berlin, Germany. Stuttgart: Fraunhofer Verl.; 2014. p. 17–25.
 32. Finger J, Ross K, Häring I, Restayn E-M, Siebold U. Open Chance and Risk Management Process Supported by a Software Tool for Improving Urban Security. *European Journal for Security Research*. 2021;6:39–71. doi:10.1007/s41125-021-00072-6.
 33. Siebold U, Hasenstein S, Finger J, Häring I. Table-top urban risk and resilience management for football events. In: Podofillini L, Sudret B, Stojadinović B, Zio E, Kröger W, editors. Boca Raton, London, New York: CRC Press Taylor & Francis Group a Balkema book; 2015. p. 3375–3382.
 34. Dörr A, Häring I. Introduction to methods applied in hazard and risk analysis. In: Gebbeken N, Thoma K, editors. *3. Workshop Bau-Protect, Buildings and Utilities Protection*; 28.-29.10.2008; Munich. Neubiberg: Universität der Bundeswehr München; 2008.
 35. Häring I. Introduction to Risk Analysis and Risk Management Processes. In: Häring I, editor. *Risk Analysis and Management: Engineering Resilience*. 1st ed. s.l.: Springer-Verlag; 2015. p. 9–26. doi:10.1007/978-981-10-0015-7_2.
 36. Huang G, Wang J, Chen C, Guo C, Zhu B. System resilience enhancement: Smart grid and beyond. *Front. Eng.* 2017;4:271. doi:10.15302/J-FEM-2017030.
 37. Haggag M, Ezzeldin M, El-Dakhakhni W, Hassini E. Resilient cities critical infrastructure interdependence: a meta-research. *Sustainable and Resilient Infrastructure*. 2022;7:291–312. doi:10.1080/23789689.2020.1795571.
 38. Nait Belaid Y, Coudray P, Sanchez-Torres J, Fang Y-P, Zeng Z, Barros A. Resilience Quantification of Smart Distribution Networks—A Bird's Eye View Perspective. *Energies*. 2021;14:2888. doi:10.3390/en14102888.
 39. Fehling-Kaschek M, Faist K, Miller N, Finger J, Häring I, Carli M, et al. A systematic tabular approach for risk and resilience assessment and Improvement in the telecommunication industry. In: Beer M, Zio E, editors. *ESREL*; 22–26 September 2019; Hannover, Germany. Singapore: Research Publishing Services; 2019. p. 1312–1319.
 40. Miller N, Fehling-Kaschek M, Haab G, Faist K, Stoltz A, Häring I. Resilience analysis and quantification for Critical Infrastructures. In: Soldatos J, Philpot J, Giunta G, editors. *Cyber-Physical Threat Intelligence for Critical Infrastructures Security: A Guide to Integrated Cyber-Physical Protection of Modern Critical Infrastructures*. [S.l.]: Now Publishers; 2020. p. 365–384. doi:10.1561/9781680836875.ch20.

41. Quitana G, Molinos-Senante M, Chamorro A. Resilience of critical infrastructure to natural hazards: A review focused on drinking water systems. *International Journal of Disaster Risk Reduction*. 2020;48:101575. doi:10.1016/j.ijdrr.2020.101575.
42. Panteli M, Mancarella P, Trakas DN, Kyriakides E, Hatziargyriou ND. Metrics and Quantification of Operational and Infrastructure Resilience in Power Systems. *IEEE Trans. Power Syst.* 2017;32:4732–42. doi:10.1109/TPWRS.2017.2664141.
43. Ahmed S, Dey K. Resilience modeling concepts in transportation systems: a comprehensive review based on mode, and modeling techniques. *J Infrastruct Preserv Resil* 2020. doi:10.1186/s43065-020-00008-9.
44. Schoppe C, Zehetner J, Finger J, Siebold U, Häring I. Risk assessment methods for improving urban security. In: Nowakowski T, Młyńczak M, Jodejko-Pietruczuk A, Werbińska-Wojciechowska S, editors; 14.-18.09.2014; Wrocław, Poland. London: CRC Press; 2014. p. 701–708.
45. Häring I, Gelhausen P. Technical safety and reliability methods for resilience engineering. In: Haugen S, Barros A, van Gulijk C, Kongsvik T, Vinnene JE, editors. 28-th European Safety and Reliability Conference (ESREL); 17–21 June 2018; Trondheim, Norway: CRC Press; 2018. p. 1253–1260.
46. Häring I. Technical Safety and Reliability Methods for Resilience Engineering. In: Häring I, editor. *Technical Safety, Reliability and Resilience: Methods and Processes*. 1st ed. Singapore: Springer Singapore; Imprint: Springer; 2021. p. 9–26. doi:10.1007/978-981-33-4272-9_2.
47. Häring I, Schäffer L, Restayn E-M, Vogelbacher G, Stoltz A, Finger J. Formalization of Questionnaire-based Score Card Risk Control and Resilience Assessment for Critical Infrastructure Operators and Companies Countering Covid-19. In: Castanier B, editor. 31st European Safety and Reliability Conference (ESREL 2021); 19–23 September 2021; Angers, France. Chennai: Research Publishing Services; 2021. p. 2862–2869.
48. Schoppe CA, Häring I, Siebold U. Semi-formal modeling of risk management process and application to chance management and monitoring. In: Steenbergen RDJM, van Gelder P, Miraglia S, Vrouwenvelder, A. C. W. M, editors. ESREL 2013; 29.09.-02.10.2013; Amsterdam, The Netherlands. Boca Raton, Fla.: CRC Press; 2013. p. 2019–2026.
49. Finger J, Hasenstein S, Siebold U, Häring I. Analytical resilience quantification for critical infrastructure and technical systems. In: Walls L, Revie M, Bedford T, editors; 25-29.09; Glasgow. London: Taylor & Francis Group; 2016. p. 2122–2128.
50. Kaplan S, Garrick BJ. On The Quantitative Definition of Risk. *Risk Analysis*. 1981;1:11–27. doi:10.1111/j.1539-6924.1981.tb01350.x.
51. Siebold U, Häring I. Terror Event Database and Analysis Software. In: Elsner P, editor. *Future Security: 4th Security Research Conference*; 29.09-01.10.2009; Karlsruhe, Germany: Fraunhofer Verlag; 2009. p. 85–92.
52. Gary LaFree. Terrorism open source databases. In: Muro D, Wilson TK, editors. *Contemporary terrorism studies*. Oxford, United Kingdom: Oxford University Press; 2022. p. 113–135.
53. Häring I, Sudheendran V, Sankin R, Hiermaier S. Joint functional safety ISO 26262 and cybersecurity STRIDE/HEAVENS assessment by developers within MBSE SPES framework using extended SysML diagrams and minor automations. In: PSAM16, editor; 27.-31.06.2022.; Honolulu, O'ahu, Hawaii, USA; 27.-31.06.2022,
54. Wells EM, Boden M, Tseytlin I, Linkov I. Modeling critical infrastructure resilience under compounding threats: A systematic literature review. *Progress in Disaster Science*. 2022;15:100244. doi:10.1016/j.pdisas.2022.100244.
55. Häring I. Risk Acceptance Criteria. In: Häring I, editor. *Risk Analysis and Management: Engineering Resilience*. Singapore: Springer Singapore; 2015. p. 313–342. doi:10.1007/978-981-10-0015-7_17.
56. Häring I, Schönherr M, Richter C. Quantitative hazard and risk analysis for fragments of high-explosive shells in air. *Reliability Engineering & System Safety*. 2009;94:1461–70. doi:10.1016/j.ress.2009.02.003.
57. Häring I, Pfeiffer M, Vogelbacher G, Stottmeister A, Restayn E-M, Ross K, von Ramin M. Risk and Resilience Analysis of Public Civil Buildings Against Shelling with Explosive Sources in Urban Contexts. *Eur J Secur Res (European Journal for Security Research)*. 2019;1:37. doi:10.1007/s41125-019-00046-9.
58. Vogelbacher G, Häring I, Fischer K, Riedel W. Empirical Susceptibility, Vulnerability and Risk Analysis for Resilience Enhancement of Urban Areas to Terrorist Events. *Eur J Secur Res (European Journal for Security Research)*. 2016;1:151–86. doi:10.1007/s41125-016-0009-x.
59. Häring I. More Elaborate Database Analysis for Risk and Resilience Analysis. In: Haring I, editor. *Risk Analysis and Management: Engineering Resilience*. 1st ed. s.l.: Springer-Verlag; 2015. p. 61–89. doi:10.1007/978-981-10-0015-7_4.
60. Häring I. Hazard Analysis. In: Häring I, editor. *Technical Safety, Reliability and Resilience: Methods and Processes*. 1st ed. Singapore: Springer Singapore; Imprint: Springer; 2021. p. 127–159. doi:10.1007/978-981-33-4272-9_8.

61. Häring I. Failure Modes and Effects Analysis. In: Häring I, editor. Technical Safety, Reliability and Resilience: Methods and Processes. 1st ed. Singapore: Springer Singapore; Imprint: Springer; 2021. p. 101–126. doi:10.1007/978-981-33-4272-9_7.
62. Häring I. Risk Computation and Visualization. In: Häring I, editor. Risk analysis and management: Engineering resilience. Singapur: Springer; 2015. p. 251–270. doi:10.1007/978-981-10-0015-7_14.
63. Ganter S, Balbi A, Finger J, Schäffer L, Bolletta F, Fuggini C, et al. Conceptual Model and CONOPS for Secure and Resilient Gas Critical Infrastructure. In: Soldatos J, Praça I, Jovanović A, editors. Cyber-Physical Threat Intelligence for Critical Infrastructures Security: Securing Critical Infrastructures in Air Transport, Water, Gas, Healthcare, Finance and Industry. Norwell: Now Publishers; 2021. p. 308–326. doi:10.1561/9781680838237.ch13.
64. Fischer K, Häring I, Riedel W. Risk-based resilience quantification and improvement for urban areas. In: Beyerer J, Meissner A, Geisler J, editors. Stuttgart: Fraunhofer Verlag; 2015. p. 417–424.
65. Häring I. Risk Mitigation and Chance Enhancement Measures for Improving Resilience. In: Häring I, editor. Risk analysis and management: Engineering resilience. Singapur: Springer; 2015. p. 343–352. doi:10.1007/978-981-10-0015-7_18.
66. Rehak D, Lovecek T, Hromada M, Walker N, Haring I. Critical Infrastructures Resilience in the Context of a Physical Protection System. In: Shinkuma R, Xhafa F, Nishio T, editors. Advances in Engineering and Information Science Toward Smart City and Beyond. Cham: Springer International Publishing; 2023. p. 1–33. doi:10.1007/978-3-031-29301-6_1.
67. Cammarata G, Giunta G, F. Sutton L, Orizio R, Le Pham T, Sebastio S, et al. Data Visualisation for Situational Awareness in Industrial Critical Infrastructure: an InfraStress Case Study. In: Soldatos J, Praça I, Jovanović A, editors. Cyber-Physical Threat Intelligence for Critical Infrastructures Security: Securing Critical Infrastructures in Air Transport, Water, Gas, Healthcare, Finance and Industry. Norwell: Now Publishers; 2021. p. 83–106. doi:10.1561/9781680838237.ch4.
68. Voss M, Häring I, Fischer K, Riedel W, Siebold U. Susceptibility and vulnerability of urban buildings and infrastructure against terroristic threats from qualitative and quantitative risk analyses. In: PSAM11 and ESREL 2012; 25 - 29 June 2012; Helsinki, Finland. Red Hook, NY: Curran; 2012. p. 5757–5767.
69. Fischer K, Riedel W, Häring I, Nieuwenhuijs A, Crabbe S, Trojaborg S, et al. Vulnerability Identification and Resilience Enhancements of Urban Environments. In: Dangschart JS, Feilmayr W, Frey O, Haselsberger B, Lenes T, Verlic M, editors. EURA-Conference 2012; 20.-22.09.2012; Vienna; 20.-22.09.2012.
70. Fischer K, Riedel W, Häring I, Nieuwenhuijs A, Crabbe S, Trojaborg SS, et al. Vulnerability Identification and Resilience Enhancements of Urban Environments. In: Aschenbruck N, Martini P, Meier M, Tölle J, editors. Berlin, Heidelberg: Springer; 2012. p. 176–179. doi:10.1007/978-3-642-33161-9_24.
71. Schäfer J, Kopf N, Häring I. Empirical risk analysis of humanitarian demining for characterization of hazard sources. In: Thoma K, Häring I, Leismann T, editors. 9th Future Security - Security Research Conference; September 16 - 18, 2014; Berlin, Germany. Stuttgart: Fraunhofer Verl.; 2014. p. 598–602.
72. Riedel W, Fischer K, Stoltz A, Häring I. Modeling the vulnerability of urban areas to explosion scenarios. In: Stewart MG, Netherton MD, editors. Callahan, NSW: Centre of Infrastructure Performance and Reliability, School of Engineering, University of Newcastle; 2015. p. 469–478.
73. Häring I, Ramin M von, Stottmeister A, Schäfer J, Vogelbacher G, Brombacher B, et al. Validated 3D Spatial Stepwise Quantitative Hazard, Risk and Resilience Analysis and Management of Explosive Events in Urban Areas. *Eur J Secur Res (European Journal for Security Research)*. 2019;4:93–129. doi:10.1007/s41125-018-0035-y.
74. Häring I. Hazard Event Frequency, Distribution of Objects and Success Frequency of Avoiding Hazards. In: Haring I, editor. Risk Analysis and Management: Engineering Resilience. 1st ed. s.l.: Springer-Verlag; 2015. p. 233–249. doi:10.1007/978-981-10-0015-7_13.
75. Fischer K, Siebold U, Vogelbacher G, Häring I, Riedel W. Empirische Analyse sicherheitskritischer Ereignisse in urbanisierten Gebieten. *Bautechnik*. 2014;91:1–12. doi:10.1002/bate.201300041.
76. Fischer K, Hiermaier S, Riedel W, Häring I. Morphology Dependent Assessment of Resilience for Urban Areas. *Sustainability*. 2018;10:1800. doi:10.3390/su10061800.
77. Häring I, Gürke G. Hazard densities for explosions. In: Soares CG, Zio E, editors. European Safety and Reliability Conference (ESREL) 2006; 18-22 September 2006; Valencia, Spain: Taylor and Francis Group, London; 2006. p. 1987–1994.
78. Domanescu M, Cimellaro GP, Xie L, Bruneau M, Wu Z, Didier M, et al. Present and future resilience research driven by science and technology. *IJSMSS*. 2021;5:50–89. doi:10.1504/IJSMSS.2021.115783.
79. Fischer K, Häring I. SDOF response model parameters from dynamic blast loading experiments. *Engineering Structures*. 2009;31:1677–86. doi:10.1016/j.engstruct.2009.02.040.

80. Häring I. Hazard Propagation III: Free Field Blast and Complex Blast: Empirical-Analytical Expressions and Scaled Experiments. In: Haring I, editor. Risk Analysis and Management: Engineering Resilience. 1st ed. s.l.: Springer-Verlag; 2015. p. 155–166. doi:10.1007/978-981-10-0015-7_8.
81. Häring I, Scheidereiter J, Ebenhöch S, Schott D, Reindl L, Koehler S, et al. Analytical engineering process to identify, assess and improve technical resilience capabilities. In: Čepin M, Briš R, editors. ESREL 2017; 18–22 June 2017; Portoroz, Slovenia. Boca Raton: CRC Press; 2017. p. 159. doi:10.1201/9781315210469-136.
82. Jain AK, Schott DJ, Scheithauer H, Häring I, Höflinger F, Fischer G, et al. Simulation-Based Resilience Quantification of an Indoor Ultrasound Localization System in the Presence of Disruptions. Sensors. 2021;21:6332. doi:10.3390/s21196332.
83. Häring I, Nikhilesh S, Teo P-W, Vogelbacher G, Alexander R, Asihvarya JK, et al. Dynamically resolving and abstracting Markov models for system resilience analysis. In: Brito MP, Aven T, Baraldi P, Čepin M, Zio E, editors. ESREL 2023; 3.-7.9.2023; Southampton, UK; 2023. p. 241–248.
84. Häring I, Satsrisakul Y, Finger J, Vogelbacher G, Köpke C, Höflinger F. Advanced Markov modeling and simulation for safety analysis of autonomous driving functions up to SAE 5 for development, approval and main inspection. In: ESREL 2022, editor. ESREL 2022; 28.08.–01.09.2022; Dublin, Ireland; 2022. p. 104–111. doi:10.3850/978-981-18-5183-4_R03-02-012-cd.
85. Häring I, Sunil MKR, Teo P-W, Mayur D, Nikhilesh S, Jörg F, et al. Overall Markov diagram design and simulation example for scalable safety analysis of autonomous vehicles. In: Brito MP, Aven T, Baraldi P, Čepin M, Zio E, editors. ESREL 2023; 3.-7.9.2023; Southampton, UK; 2023. p. 2261–2268.
86. Tomforde S, Gelhausen P, Gruhl C, Häring I, Sick B. Explicit Consideration of Resilience in Organic Computing Design Processes. In: ARCS Workshop 2019 and 32nd International Conference on Architecture of Computing Systems; 20.-23.05.2019; Copenhagen, Denmark. Berlin, Germany: VDE Verlag GmbH; 2019. p. 51–56.
87. van der Voort M, Radtke F, van Amelsfort R, Khoe YS, Wosnitza A, Voss M, Häring I. Recent developments of the KG Software (Klotz group engineering software). In: Explosives Safety Board, Alexandria, Virginia, editor. 34th DDESB Seminar; 13.-15.07.2010; Portland, Oregon; 2010. 16 pp.
88. Lee C-J, Lee KJ. Application of Bayesian network to the probabilistic risk assessment of nuclear waste disposal. Reliability Engineering & System Safety. 2006;91:515–32. doi:10.1016/j.ress.2005.03.011.
89. Tong Q, Gernay T. Resilience assessment of process industry facilities using dynamic Bayesian networks. Process Safety and Environmental Protection. 2023;169:547–63. doi:10.1016/j.psep.2022.11.048.
90. Wu ZY, Sun HB, Liu SK. A dynamic Bayesian network model for structural time-dependent reliability with deterioration. In: Deodatis G, Ellingwood BR, Frangopol DM, editors. 11th International Conference on Structural Safety and Reliability; 16–20 June 2013; New York, USA. 1st ed. London: Taylor & Francis Group; 2014. p. 1191–1197.
91. Tabandeh A, Gardoni P, Murphy C, Myers N. Societal Risk and Resilience Analysis: Dynamic Bayesian Network Formulation of a Capability Approach. ASCE-ASME J. Risk Uncertainty Eng. Syst., Part A: Civ. Eng. 2019. doi:10.1061/AJRUA6.0000996.
92. Kammouh O, Gardoni P, Cimellaro GP. Probabilistic framework to evaluate the resilience of engineering systems using Bayesian and dynamic Bayesian networks. Reliability Engineering & System Safety. 2020;198:106813. doi:10.1016/j.ress.2020.106813.
93. Buchanan RK, Goerger SR, Rinaudo CH, Parnell G, Ross A, Sitterle V. Resilience in engineered resilient systems. Journal of Defense Modeling & Simulation. 2020;17:435–46. doi:10.1177/1548512918777901.
94. Gerber Machado P, Oliveira Ribeiro C de, Oller do Nascimento CA. Risk analysis in energy projects using Bayesian networks: A systematic review. Energy Strategy Reviews. 2023;47:101097. doi:10.1016/j.esr.2023.101097.
95. Riedel W, Niwenhuijs A, Fischer K, Crabbe S, Heyenes W, Müllers I, et al. Quantifying urban risk and vulnerability – a toolsuite of new methods for planners. In: Thoma K, Häring I, Leismann T, editors. 9th Future Security - Security Research Conference; September 16 - 18, 2014; Berlin, Germany. Stuttgart: Fraunhofer Verl.; 2014. p. 8–16.
96. Ziehm J, Häring I. Risk Analysis for a German Harbour within the Project ECSIT. In: Ender J, editor. 6th Future Security Research Conference; September 5th - 7th, 2011; Berlin, Germany. Stuttgart: Fraunhofer Verl.; 2011. p. 201–207.
97. Stolz A, Fischer K, Roller C, Hauser S. Dynamic bearing capacity of ductile concrete plates under blast loading. International Journal of Impact Engineering. 2014;69:25–38. doi:10.1016/j.ijimpeng.2014.02.008.
98. Vaseghiamiri S, Mahsuli M, Ghannad MA, Zareian F. Surrogate SDOF models for probabilistic performance assessment of multistory buildings: Methodology and application for steel special moment frames. Engineering Structures. 2020;212:110276. doi:10.1016/j.engstruct.2020.110276.

99. Bezabeh MA, Bitsuamlak GT, Tesfamariam S. Nonlinear Dynamic Response of Single-Degree-of-Freedom Systems Subjected to Along-Wind Loads. II: Implications for Structural Reliability. *J. Struct. Eng.* 2021; doi:10.1061/(ASCE)ST.1943-541X.0003124.
100. Döge T, Häring I. Differential equation of motion for single and multiple degree of freedom systems. In: Gebbeken N, Thoma K, editors. 3. Workshop Bau-Protect, Utilities and Building Protection; 28.-29.10.2008; Bad Reichenhall, Germany; 2008. 16 pp.
101. Marsaco S, Noori AZ, Cimellaro GP. Resilience assessment for the built environment of a virtual city. In: COMPDYN 2017. p. 2043–2055.
102. Qiao H, Huang P, Domenico D de, Wang Q. Structural control of high-rise buildings subjected to multi-hazard excitations using inertial-based vibration absorbers. *Engineering Structures*. 2022;266:114666. doi:10.1016/j.engstruct.2022.114666.
103. Mayrhofer C. Reinforced masonry walls under blast loading. *International Journal of Mechanical Sciences*. 2001;44:1068–80.
104. Riedel W, Mayrhofer C, Thoma K, Stolz A. Engineering and Numerical Tools for Explosion Protection of Reinforced Concrete. *International Journal of Protective Structures*. 2010;1:85–101. doi:10.1260/2041-4196.1.1.85.
105. Zhang X, Hao H, Wang Z. Experimental study of laminated glass window responses under impulsive and blast loading. *International Journal of Impact Engineering*. 2015;78:1–19. doi:10.1016/j.ijimpeng.2014.11.020.
106. Klomfass A, Heilig G, Thoma K. Analysis of blast loaded structures by numerical simulation. *WIT Transactions on The Built Environment*. 2005;403–12. doi:10.2495/FSI050391.
107. Souli M, Ouahsine A, Lewin L. ALE formulation for fluid–structure interaction problems. *Computer Methods in Applied Mechanics and Engineering*. 2000;190:659–75. doi:10.1016/S0045-7825(99)00432-6.
108. Lv Y, Ihme M. Discontinuous Galerkin method for multicomponent chemically reacting flows and combustion. *Journal of Computational Physics*. 2014;270:105–37. doi:10.1016/j.jcp.2014.03.029.
109. Ryzhakov P, Oñate E, Rossi R, Idelsohn SR. Lagrangian FE methods for coupled problems in fluid mechanics. Barcelona: International Center for Numerical Methods in Engineering; 2010.
110. Rees DWA. Mechanics of solids and structures: Empirical College Press; 2000.
111. Jin M, Hao Y, Hao H. Numerical study of fence type blast walls for blast load mitigation. *International Journal of Impact Engineering*. 2019;131:238–55. doi:10.1016/j.ijimpeng.2019.05.007.
112. Valsamos G, Casadei F, Solomos G, Larcher M. Risk assessment of blast events in a transport infrastructure by fluid-structure interaction analysis. *Safety Science*. 2019;118:887–97. doi:10.1016/j.ssci.2019.06.014.
113. Rosin J, Mykoniou K, Butenweg C. Analysis of base-isolated liquid storage tanks with 3d FSI-analysis as well as simplified approaches. In: 16th World Conference on Earthquake Engineering; 09.-13.01.2017; Santiago, Chile. Red Hook, NY: Curran Associates Inc; 2017. 14 pp.
114. Pagano A, Sweetapple C, Farmani R, Giordano R, Butler D. Water Distribution Networks Resilience Analysis: a Comparison between Graph Theory-Based Approaches and Global Resilience Analysis. *Water Resour Manage*. 2019;33:2925–40. doi:10.1007/s11269-019-02276-x.
115. Kandaperumal G, Pandey S, Srivastava A. AWR: Anticipate, Withstand, and Recover Resilience Metric for Operational and Planning Decision Support in Electric Distribution System. *IEEE Trans. Smart Grid*. 2022;13:179–90. doi:10.1109/TSG.2021.3119508.
116. Yang Z, Su H, Du X, Zio E, Xiang Q, Peng S, et al. Supply resilience assessment of natural gas pipeline network systems. *Journal of Cleaner Production*. 2023;385:135654. doi:10.1016/j.jclepro.2022.135654.
117. Dong S, Mostafizi A, Wang H, Gao J, Li X. Measuring the Topological Robustness of Transportation Networks to Disaster-Induced Failures: A Percolation Approach. *J. Infrastruct. Syst.* 2020. doi:10.1061/(ASCE)IS.1943-555X.0000533.
118. Bhatia U, Kumar D, Kodra E, Ganguly AR. Network Science Based Quantification of Resilience Demonstrated on the Indian Railways Network. *PLoS ONE*. 2015;10:e0141890. doi:10.1371/journal.pone.0141890.
119. Aydin NY, Duzgun HS, Wenzel F, Heinemann HR. Integration of stress testing with graph theory to assess the resilience of urban road networks under seismic hazards. *Nat Hazards*. 2018;91:37–68. doi:10.1007/s11069-017-3112-z.
120. Pirbhulal S, Gkioulos V, Katsikas S. Towards Integration of Security and Safety Measures for Critical Infrastructures Based on Bayesian Networks and Graph Theory: A Systematic Literature Review. *Signals*. 2021;2:771–802. doi:10.3390/signals2040045.
121. Ganter S, Srivastava K, Vogelbacher G, Finger J, Vamanu B, Kopustinskas V, et al. Towards Risk and Resilience Quantification of Gas Networks based on Numerical Simulation and Statistical Event Assessment.

- In: Baraldi P, Di Maio F, Zio E, editors. ESREL2020 and PSAM15; Venice, Italy (virtual). Singapore: Research Publishing; 2020. p. 819–826.
122. Kopustinskas V, Vamanu B, Ganter S, Finger J, Häring I, Zalitis I, Zemite L. Gas network modelling to support pipeline hub area risk assessment study. In: Remenyte-Prescott R, Sanderson K, Kopustinskas V, Simola K, editors; 4.-5.5.2022; Grenoble, France; 2005. p. 159–162.
123. Zalitis I, Dolgicers A, Zemite L, Ganter S, Kopustinskas V, Vamanu B, et al. Mitigation of the impact of disturbances in gas transmission systems. International Journal of Critical Infrastructure Protection. 2022;39:100569. doi:10.1016/j.ijcip.2022.100569.
124. Praks P, Kopustinskas V, Masera M. Probabilistic modelling of security of supply in gas networks and evaluation of new infrastructure. Reliability Engineering & System Safety. 2015;144:254–64. doi:10.1016/j.ress.2015.08.005.
125. Liu X, Ferrario E, Zio E. Resilience Analysis Framework for Interconnected Critical Infrastructures. ASCE-ASME J Risk and Uncert in Engng Sys Part B Mech Engng 2017. doi:10.1115/1.4035728.
126. Hiermaier S, Hasenstein S, Katja F. Resilience Engineering - How to handle the unexpected. In: Nyssen A-S, Jaspar M, Woods D, editors. 7-th REA-Symposium; 26.-29.06.2017; Liège, Belgium; 2017. p. 92–97.
127. Cimellaro GP, Crupi P, Kim HU, Agrawal A. Modeling interdependencies of critical infrastructures after hurricane Sandy. International Journal of Disaster Risk Reduction. 2019;38:101191. doi:10.1016/j.ijdrr.2019.101191.
128. RESIST. Resiliente Stromnetze für die Energiewende (RESIST), BMBF-Projekt. 2021–2024. <https://www.enargus.de/pub/bscw.cgi?op=enargus.eps2&q=EB6010&v=10&s=13&id=7686958>; <https://strom-resist.de/>; <https://www.emi.fraunhofer.de/de/geschaeftsfelder/sicherheit/forschung/Resiliente-Stromnetze-fuer-die-Energiewende-RESIST.html>. Accessed 19 Sep 2023.
129. Lukau E, Martini T, Rosin J, Finger J, Vetter J, Neuhäuser S, et al. Towards a modular co-simulation framework for the assessment of cascading effects among critical infrastructures and the impact on citizens. In: 61th ESReDA Seminar on Technological disruptions triggered by natural events: identification, characterization, and management; 22.-23.09.2022: Publications Office of the European Union, Luxemburg, Joint Research Center.
130. Jain AK, Satsrisakul Y, Fehling-Kaschek M, Häring I, van Rest J. Towards Simulation of Dynamic Risk-Based Border Crossing Checkpoints. In: Baraldi P, Di Maio F, Zio E, editors. ESREL2020 and PSAM15; Venice, Italy (virtual). Singapore: Research Publishing; 2020. p. 4446–4452.
131. Jain AK, Ruiter J de, Häring I, Fehling-Kaschek M, Stolz A. Design, Simulation and Performance Evaluation of a Risk-Based Border Management System. 2023;15:12991 (22 pages). doi:10.3390/su151712991.
132. Shi Y, Lv L. Complexity Assessment with K-Weighted Entropy for Cloud-Edge-Vehicle System. In: 2021 IEEE International Conference on Smart Internet of Things (SmartIoT); 13–15 August 2021; Jeju, Republic of Korea (Online Event); 2021. p. 294–300. doi:10.1109/SmartIoT52359.2021.00054.
133. Stocchi A, Richard B. Sensitivity of engineering demand parameters as a function of structural typology and assessment method. Nuclear Engineering and Design. 2019;343:151–65. doi:10.1016/j.nucengdes.2019.01.006.
134. Formalization of a quantitative risk analysis methodology for static explosive events; 2011.
135. Ebenhöch S, Nau S, Häring I. Validated model-based simulation tool for design optimization of exploding foil initiators. Journal of Defense Modeling & Simulation. 2015;12:189–207. doi:10.1177/1548512914557834.
136. OCTIKT. Ein Organic-Computing basierter Ansatz zur Sicherstellung und Verbesserung der Resilienz in technischen und IKT-Systemen, German BMBF Project, Förderkennzeichen: 01IS18064A. 2018–2021. <https://projekt-octikt.fzi.de/>; <https://www.softwaresysteme.dlr-pt.de/de/resilienz.php>; https://www.softwaresysteme.dlr-pt.de/media/content/Projektblatt_OCTIKT_01IS18064.pdf; Accessed 19 Sep 2023.
137. eFORT. Establishment of a Framework for Transforming current EPES into a more resilient, reliable and secure system all over its value chain, EU-project, Grant agreement ID: 101075665. 2022–2026. <https://cordis.europa.eu/project/id/101075665>. Accessed 23 Sep 2023.
138. SecureGas. Securing the European gas network, EU H2020 project, 2019–2021, Grant agreement ID: 833017. 2019–2021. <https://cordis.europa.eu/project/id/833017/en>; <https://www.securegas-project.eu/>. Accessed 19 Sep 2023.
139. RESISTO. Resilience enhancement and risk control platform for communication infrastructure operators: EC Grant agreement ID: 786409. 2018–2021. <https://cordis.europa.eu/project/id/786409>. Accessed 19 Sep 2023.

140. SnowBall. Lower the impact of aggravating factors in crisis situations thanks to adaptative foresight and decision-support tools, EC Grant agreement ID: 606742. 2014-2017.
<https://cordis.europa.eu/project/id/606742>. Accessed 19 Sep 2023.

141. Encounter. Explosive neutralisation and mitigation countermeasures for IEDs in urban/civil environment (ENCOUNTER), Grant agreement ID: 285505. 2012-2015.
<https://cordis.europa.eu/project/id/285505>. Accessed 19 Sep 2023.

142. EDEN. End-user driven demo for CBRNE (EDEN), Grant agreement ID: 313077. 2013-2016.
<https://cordis.europa.eu/project/id/313077>. Accessed 19 Sep 2023.

Plenary Talk 3 – Marta Poncela Blanco: Risk preparedness regulation in the electricity sector: aims and challenges

Marta Poncela Blanco, Policy Officer at the European Commission, Directorate General for Energy, Energy Security and Safety Unit, Brussels



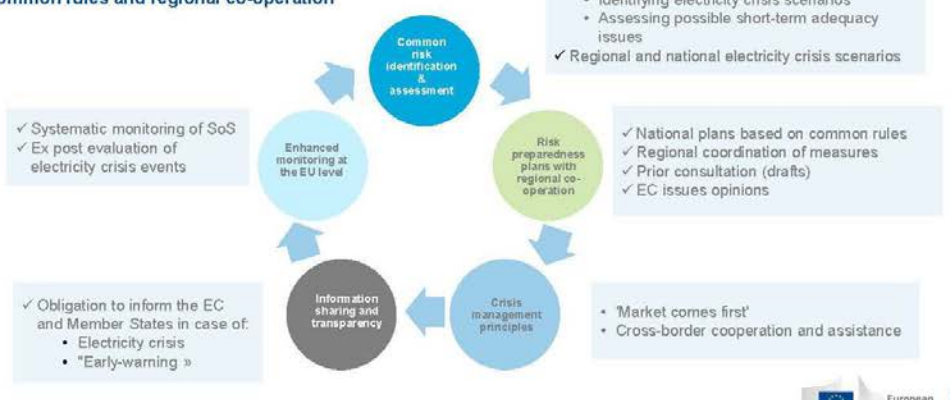
The slide has a blue background with white text and icons. It includes the European Commission logo at the top left and bottom right. The main text reads: 'Review of current national rules and practices relating to risk preparedness in the area of security of electricity supply (Contract ENE/1/B4/ADM/2015 623/SI2.7.17(65)) Final report'. Below this, it says 'Carried out by Ispra for the European Union and Research Project Research'. At the bottom, it says 'May 2016'. To the right, there is a section titled 'Starting point (2014-2016)' with the question 'How are electricity crisis managed in Europe?'. This is accompanied by a grid of nine icons representing various aspects of risk preparedness, such as a person holding a 'RISK' sign, a group of people, a lightbulb, a bell, a hard hat, and a medical cross.

Energy Union: security and single electricity market are key pillars

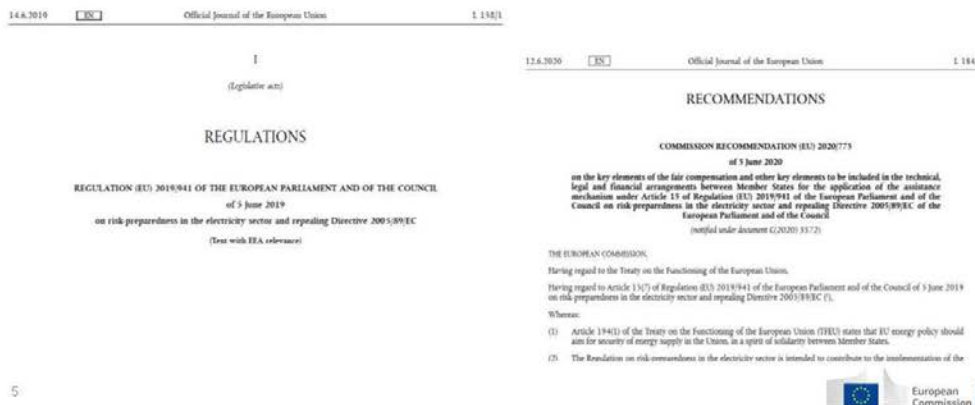


New approach: Risk Preparedness Reg

Risk Preparedness Regulation (EU) 2019/941
Common rules and regional co-operation



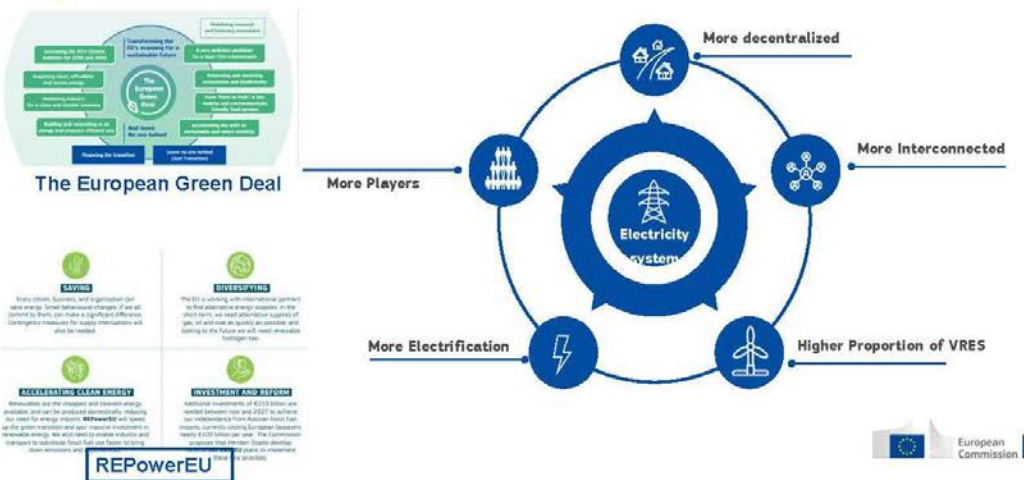
Risk Preparedness Regulation



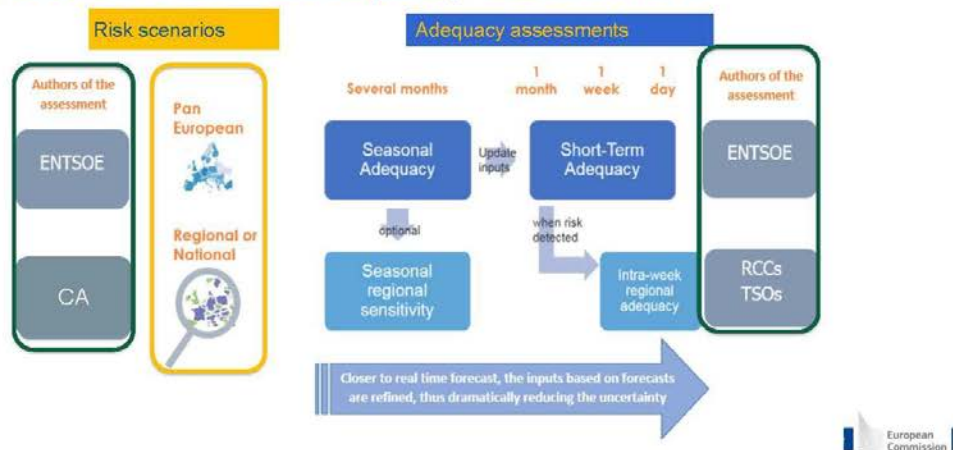
Overall framework



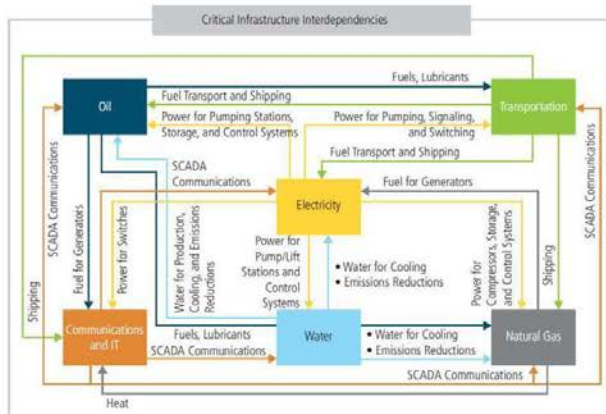
Current context



Risk assessment. The combined tools of crisis scenarios and adequacy assessment



Identification of risk scenarios



Source of the figure: DOE (2017)

Threats:

- rare and extreme natural hazards;
- accidental hazards going beyond the N-1 security criterion;
- consequential hazards i.e. fuel shortages;
- malicious attacks: cyber and/or physical.



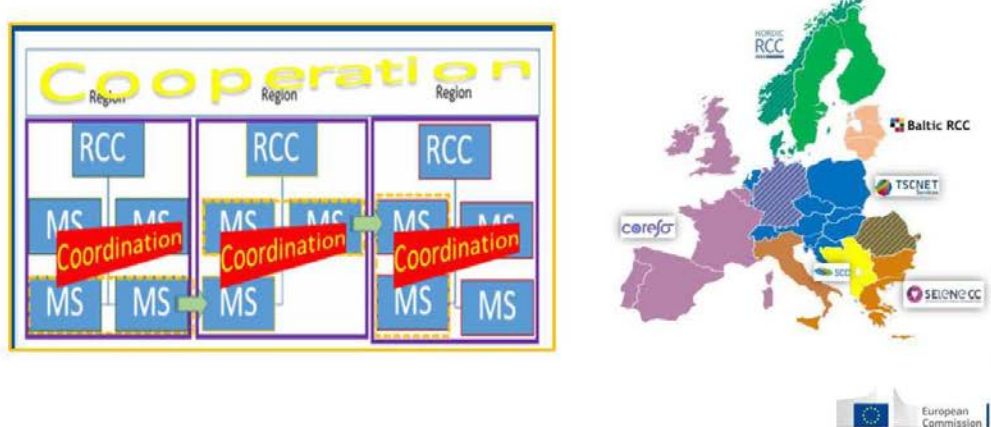
Identification of risk scenarios

Considering:

- a consideration of all **relevant national and regional circumstances**, including any subgroups;
- interaction and correlation of risks across **borders**;
- **simulations** of simultaneous electricity crisis scenarios;
- **ranking** of risks according to their impact and probability;
- principles on how to handle **sensitive information** in a manner that ensures transparency towards the **public**.



MSs' cooperation framework under risk preparedness regulation



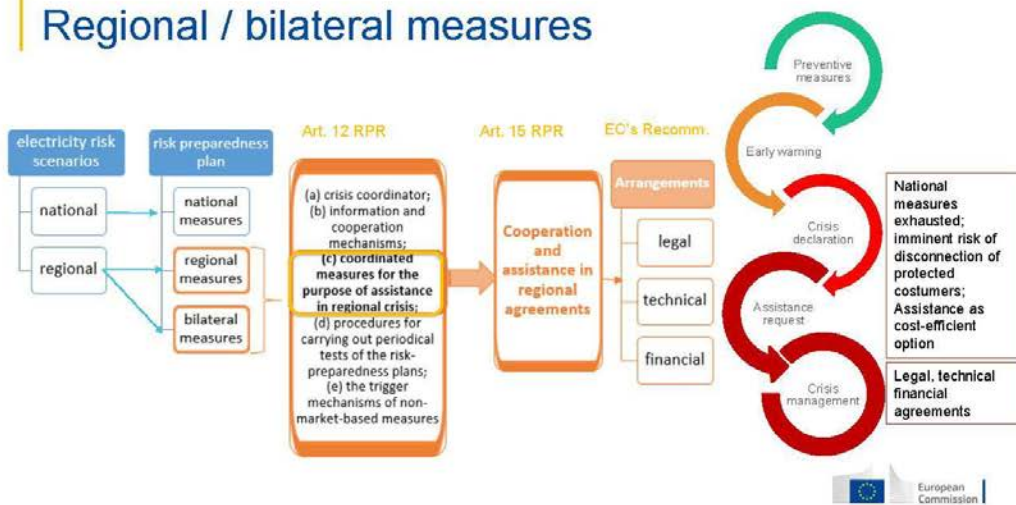
European Commission

Basic principles for cooperation and assistance in the risk preparedness regulation

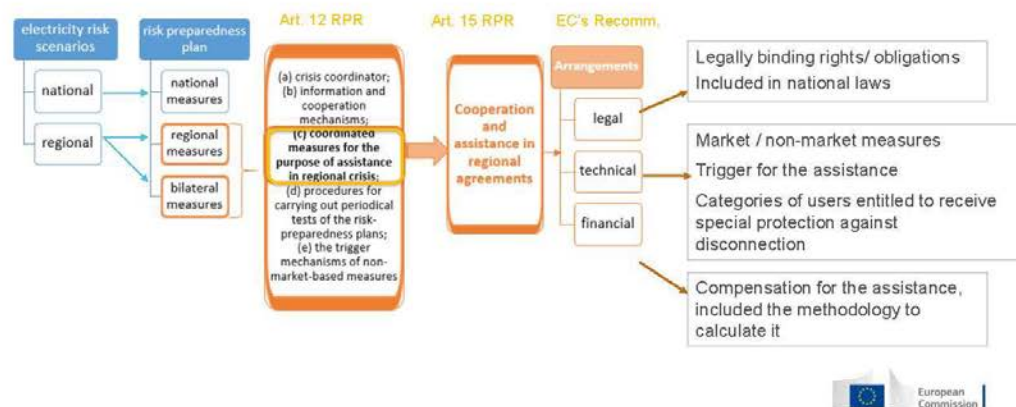
| | |
|---|---|
| Solidarity | • to prevent or manage electricity crises when MSs has the technical ability to offer assistance to a MS in crisis in order to protect public safety and national security. |
| Harmonization | • EU-Harmonized approach towards the prevention, preparation for and management of electricity crises to give transparency to the regional and bilateral agreements |
| Cost-efficiency | • Cooperation allows a more efficient use of resources, guarantees the operation of the electricity market until all options are exhausted before the activation of non-market based measures. |
| Effectiveness | • Coordination allows a timely and effective resolution of the emergency |
| Form of the assistance agreement | • Legally binding agreements, with clearly defined rights and obligations of the parties of the agreement |
| Fairness | • The assistance in case of crisis should be adequately remunerated and the methodology for the calculation of the remunerating should be agreed ex-ante. At the same time, assisting MSs shall not seek for profits. |

European Commission

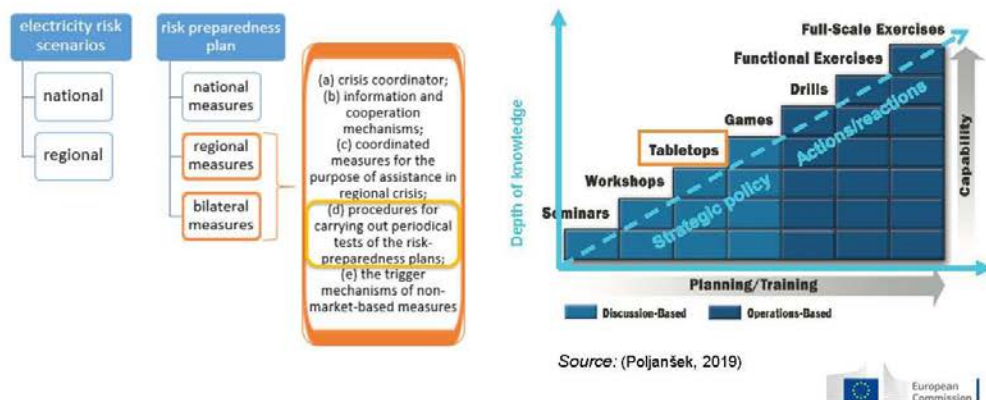
Regional / bilateral measures



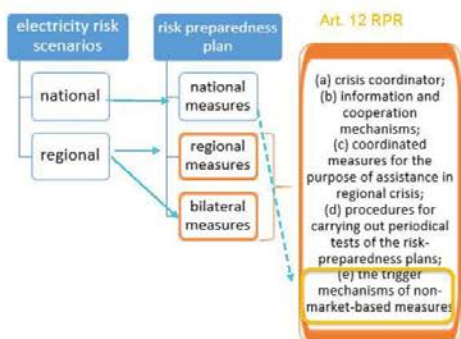
Regional / bilateral measures



Regional exercises to test the plans



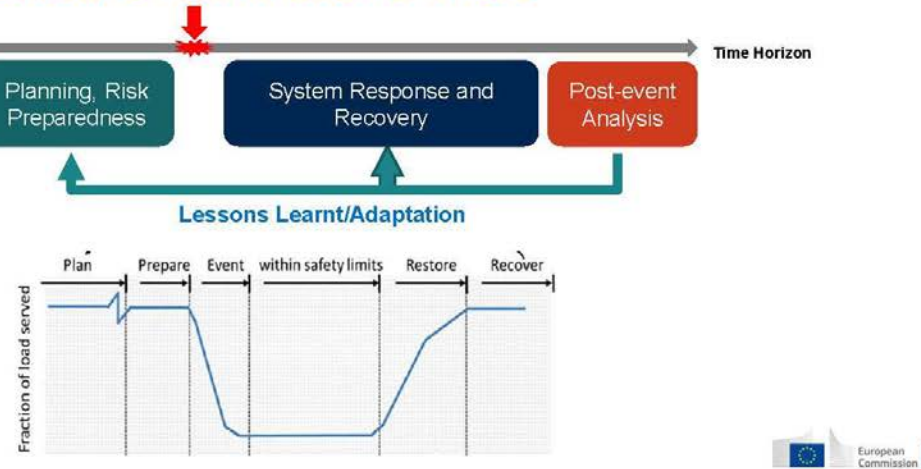
Non-market-based measures



- Last resort to protect public safety and personal security
- Only if all options provided by the market have been exhausted or where it is evident that market-based measures alone are not sufficient
- Not unduly distort competition and the effective functioning of the internal electricity market.
- Be necessary, proportionate, non-discriminatory and temporary.
- The competent authority shall inform relevant stakeholders in its Member State of the application of any non-market-based measures.



Lessons learnt after a crisis



Roadmap for implementation



Risk preparedness plans and EC opinion

Screenshot of the European Commission website showing risk preparedness plans and EC opinions for the electricity sector.

The page title is "Risk preparedness plans in the electricity sector by national competent authorities and Commission's opinions".

The URL is https://energy.ec.europa.eu/topics/energy-security/security-electricity-supply/risk-preparedness-plans-electricity-sector-national-competent-authorities-and-commissions-opinions_en

The page lists risk preparedness plans for Austria and Belgium, along with their respective EC opinions and national websites.

| Member State |
|--------------|
| Austria |
| Belgium |

What happened during this time



Brussels, 2.6.2020
SWD(2020) 104 final

RISKS AND CHALLENGES at a glance:

Short-term:

- ensuring energy supply,
- movement and availability of specialised energy workers,
- movement and access for Euratom safeguards inspectors,
- access to components and raw materials that are critical for energy,
- access to protective equipment and medical testing for energy workers,
- business continuity of critical energy infrastructure,
- preparedness to rebound of energy demand,
- cyber and hybrid threat preparedness.

Long-term:

- uncertainty regarding the duration of the pandemic,
- specialised workforce unavailability or lower resilience,
- additional unexpected contingencies, including extreme weather events, reliability of critical supply chains,
- impact of delays of postponing maintenance,
- large project delays and investment reductions,
- non-realistic emergency stockholding for upcoming calendar years,
- loss of control of critical energy assets.

COMMISSION STAFF WORKING DOCUMENT

ENERGY SECURITY: GOOD PRACTICES TO ADDRESS PANDEMIC RISKS



What happened past winter



 European Commission

Lessons learnt from the past winter

ACER
European Union Agency for the Environment
of Energy Regulators



Main mitigating measures reported

- Supply-sided:
 - Replenishment of gas storage
 - Replacement of gas by coal and other fuels,
- Demand-sided
 - Energy saving campaigns, energy efficiency
 - Ad-hoc DSR products
- Multi-stakeholder coordination
- Price caps,

 European Commission

Lessons learnt from the past winter

1. **Contribution of neighbours** to security of supply is crucial: some MSs recorded historical high imports during the winter.



2. **Consumer awareness** played a significant role, e.g. some NRAs reported that higher levels of demand savings/shifting was observed following awareness campaigns.



23

European Commission

Lessons learnt from the past winter



Key findings from the energy crisis

- The common European framework and integrated market were essential to shelter Member States against the risks of the energy crisis
 - sector interconnectivity key in overcoming uncertain gas supplies and increased outages
 - multi-level coordination essential for secure supply of electricity
- Any emergency necessarily calls for trade-offs and compromises; yet some approaches outperform others.
 - Some measures come with **adverse effects** (e.g. affordability measures hinder demand reduction)
 - **no-regret measures**, (e.g. energy efficiency, RES) should be prioritised

Recommendations:

- Accelerate and strengthen the integration of the European electricity market.
- Further reinforce inter-institutional and cross-border cooperation in security of supply.
- Prepare well-balanced and coordinated emergency measures sufficiently in advance, prioritising measures that contribute to the decarbonisation objectives.

24

European Commission

12

Challenges and areas of improvement



Risk scenario
identification
methodology



Regional and
bilateral measures



Plans for future
development of the
system

25



New regional electricity crisis scenario identification

Top-down
approach

Simultaneous
threats

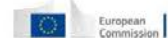
Cross-border
focus

More interaction
and earlier with
stakeholders

simulations

quantitative versus qualitative impact assessment

26



13

Bilateral and regional measures

- Size and position of countries
- **Financial agreements**
- Triggers for assistance

27



Keep in touch



ec.europa.eu/



[europeancommission](#)



europa.eu/



[@EuropeanCommission](#)



[@EU_Commission](#)



[EUTube](#)



[@EuropeanCommission](#)



[EU Spotify](#)



[European Commission](#)

28



2.1 Resilience of Ukraine's critical energy infrastructure. Challenges of war time.

Andrii Davydiuk, G.E. Pukhov Institute for modelling in energy engineering, Kiev, Ukraine, andrey19941904@gmail.com

Abstract

During the Russian-Ukrainian war, Russia has launched mass rocket attacks on critical energy infrastructure facilities and carried out cyberattacks targeting vital information systems within the energy sector [1, 2]. The objective behind these actions against Ukraine is to inflict economic damage, exert psychological pressure on the population, diminish the defensive capabilities, and provoke cascading effects on the economies of other European and global countries.

Following the disruption of energy facilities in Ukraine, the primary cascading effects have resulted in issues with communication, logistics, water supply, and financial services. Problems in these sectors have triggered irreversible consequences in fields such as healthcare, food industry, military operations, and so forth.

The purpose of this article is to illustrate the most critical impacts of combat actions on the energy infrastructure using Ukraine as an example. Specifically, it aims to establish the interdependencies of other sectors of the economy on energy and the dependence of the energy sector on other economic sectors. Additionally, it seeks to identify possibilities to minimize Russia's influence on Ukraine's energy infrastructure.

1 Russian activity on energy front

During the annexation of Ukrainian territories, Russia seizes objects of critical energy infrastructure in Ukraine. Since the beginning of the war, significant changes in Ukraine's energy infrastructure in 2014 can be highlighted. Specifically, the cessation of services by certain fuel and energy complex facilities due to their occupation in the territory of the Autonomous Republic of Crimea and the Kherson region. The halt of coal exports from the seized mines due to the impossibility of transportation (destruction of enterprises, transport routes, blockade of mine operations, enrichment plants, coal extraction). Sabotage of transportation infrastructure for supplying coal to Luhansk Thermal Power Station. Shelling of thermal power plants (TPPs) and disabling TPP equipment, power lines, transformers. As a result, on July 3, 2014, at Sloviansk Thermal Power Plant, there was damage and ignition of two self-consumption transformers, with a fuel oil tank of 2,000 tons. The damage led to the disconnection of the last two power transmission lines: 330 kV "Sloviansk TPP - Zmiivska TPP" and 220 kV "Sloviansk TPP - LYP". In June 2014, in the Sloviansk district, 11 power transmission lines and 88 transformer substations were eliminated, limiting power supply to certain settlements and enterprises. During the night of October 8, 2014, 14 artillery shells hit the territory of Luhansk Thermal Power Station; the station was shelled with small arms. One shell hit the station block, causing its shutdown. On October 9, the TPP transformer was damaged. Overall, out of 22 high-voltage power lines near the station, 18 were damaged. Transformer substations in Luhansk and Donetsk were repeatedly disabled. On June 7, an electric substation was blown up at Luhansk Airport, which provided power to the airport. On June 8, a transformer substation was blown up in Mariupol, resulting in the discontinuation of power supply to the television center and TV tower, halting television broadcasting. In May-June 2014, there were three explosions on the high-pressure gas pipeline Urengoy-Pomary-Uzhhord in the Ivano-Frankivsk region. On June 17, there was an explosion on a section of the Urengoy-Pomary-Uzhhord gas pipeline in the Poltava region. All incidents shared a common feature - explosive devices were placed on the ground under the gas pipeline. The interruption of transit (supply) of gas did not occur due to the existence of a branched gas pipeline system (backup pipelines and bypass routes) [3]. In the Luhansk and Donetsk regions, gas networks and gas distribution stations that supplied gas to settlements were repeatedly damaged. The destruction of enterprise infrastructure, both due to hostilities and for the purpose of selling as scrap metal (dismantling of industrial enterprises, mines, railway and tram tracks), and their export for scrap (looting and plundering) [4]. Repeated damage to water supply systems and pumping stations near Sloviansk, Shchastia, and Stanytsia Luhanska. In June 2014, pumping stations near Sloviansk were repeatedly damaged. Militants repeatedly seized the pumping station, shelled it, and obstructed its repair. On June 7, 2014, a bridge transporting coal to Luhansk TPP was blown up. It was impossible to restore the bridge due to resistance from militants [5].

In 2015, Russia's destructive impact on Ukraine's energy infrastructure persisted, including the halt of coal exports from captured mines due to the impossibility of transportation (destruction of enterprises, transport routes, blockade of mine operations, enrichment plants, coal extraction). Sabotage of transportation infrastructure for supplying coal to Luhansk and Vuhlehirksa Thermal Power Stations [6]. Shelling of thermal

power plants (TPPs) and disabling TPP equipment, power lines, transformers). Since the summer of 2014, Luhansk Thermal Power Station has been repeatedly under fire, resulting in a complete shutdown of the station's internal generating capacity and, consequently, disruption of electricity supply to consumers (generating units, power lines, transformer substation on the station's territory were disabled). On March 10, 2015, due to shelling, two high-voltage lines, 220 kV "Lysychanska" and 110 kV "Novoaydarska," damaged 6 km from Luhansk TPP, were automatically disconnected, leading to the shutdown of TPP generating units. The shutdown of TPP operations (as well as damaged lines) resulted in a complete cessation of electricity supply to the northern, non-occupied regions of Luhansk Oblast due to the emergence of alternative power sources. Transformer substations in Luhansk and Donetsk were repeatedly without power. On July 27, 2015, Vuhlehirskaya TPP was deliberately shelled with artillery guns. Critical elements were disabled as a result of the shelling, leading to the station's shutdown [7]. On July 28, Donetsk Oblast suffered extensive power outages after Vuhlehirskaya TPP was shelled with mortars, causing the shutdown of one power unit. Most of Luhansk Oblast was left without electricity [8]. On August 3, 2015, Vuhlehirskaya TPP ceased operations again due to continuous shelling, as departure lines 330 kV "Donbas-1" and "Donbas-2" were taken out of service [5]. On February 17, 2015, Vuhlehirskaya TPP, along with other consumers in Donetsk Oblast, lost gas supply due to water supply issues from the main branch "Novopokrov-Kramatorsk." In Luhansk and Donetsk Oblasts, gas networks and gas distribution stations supplying gas to settlements were repeatedly damaged. On June 12, 2015, due to targeted artillery shelling, the "Kramatorsk-Donetsk" main gas pipeline was damaged. This route had no alternative pipelines or other gas supply routes. Large cities - Mariupol, Berdyansk, and nearby towns faced the threat of gas supply disruption. Companies and the population were forced to suspend operations (gas consumption). The destruction of enterprise infrastructure, both due to combat actions and for the purpose of selling as scrap metal (dismantling of industrial enterprises, mines, railway and tram tracks). Troitske village (Luhansk Oblast) was left without electricity in June 2015 due to shelling; however, restoring electricity was impossible as transformers were cut for scrap metal by local residents. Repeated damage to water supply systems and pumping stations near Popasna, Shchastia, and Stanytsia Luhanska. In May 2015, repair teams near Mayorsk (Donetsk Oblast) were shelled, disrupting repair work on the "Seversky Donets - Donbas" canal. In June 2015, residents of Krasnohorivka and neighboring Maryinka in Donetsk Oblast lived without electricity for more than two weeks and faced water supply problems (due to pump shutdown). Snipers from the Donetsk People's Republic shot at electricians, preventing them from carrying out repair work. From June 2014 to June 2015, ten personnel of Donetskoblenergo's repair team were killed, and 16 were injured [5].

In 2016, in the temporarily occupied Horlivka, a group of militants led by the head of the power grid enterprise, established by the 'DNR' authorities, seized the premises of the Donbas Power System (ES) of the state enterprise 'NEC 'Ukrenergo' [9].

In 2022, in the first days of the invasion, on February 24-25, the Chernobyl Nuclear Power Plant was seized. The military vehicles of the occupiers entering the territory raised a significant amount of radioactive dust, leading to an increase in the radiation background. Russian invaders captured the Zaporizhzhia Nuclear Power Plant on March 3-4, despite the heroic attempts of the residents of Enerгодар and the Ukrainian Armed Forces to prevent this. The occupants bombed the training center and later declared ZNPP as 'property of Rosatom.' Officially, Rosatom did not recognize this. On March 16, due to enemy shelling, a high-voltage power line ZNPP - Kakhovska 750 kV was damaged. Repairmen from NEC 'Ukrenergo' fixed it on March 19. Currently, 2 out of 6 power units are operational at the NPP. The capture of the Zaporizhzhia Nuclear Power Plant, which accounts for about 30% of electricity generation in Ukraine [10], and the blowing up of the dam at the Kakhovska Hydroelectric Power Station [11] by Russia confirms the prioritization of Russia's goals in the energy sector. Since the start of Russia's full-scale invasion in 2022, Ukraine has had a surplus of electricity and continues to be a supplier of cheap electricity to the countries of the European Union. Therefore, the cascading effects of disrupting Ukrainian energy infrastructure extend beyond Ukraine's borders. The Ohtyrka Thermal Power Plant was completely bombed by Russian occupiers. It provided electricity and heat energy to enterprises and residents of the city of Ohtyrka. The Luhansk Thermal Power Plant was shelled from the occupied territories of Luhansk region. The neutron source nuclear facility was a scientific nuclear facility bombed by Russian occupiers in Kharkiv on March 6. It has been switched to 'long-term shutdown' mode. Research conducted at the facility for peaceful purposes was funded by international projects. Also, Russian occupiers are systematically destroying and looting green energy facilities: shooting at solar panels and stealing equipment. Some of these objects belong to foreign investors. Aviation strikes and artillery bombardments by Russian occupiers caused significant damage to Ukraine's gas transportation network. According to one of the largest gas suppliers, as of March 5, 2022, 58,000 households were left without gas [12]. In November 2022, a Russian mass rocket attack on energy infrastructure objects led to blackouts at all Ukrainian NPPs: power units were emergency shut down and switched to diesel generators - the last hope for

power supply. 'It was a real threat of repeating the 'Fukushima' scenario and a nuclear catastrophe that would affect all humanity. This is nothing but nuclear terrorism,' emphasized Herman Halushchenko. Ukrainian energy infrastructure facilities were rebuilt under Russian control from the very beginning of the full-scale invasion, and since October 2022, Russians have pursued its complete destruction. About 50% of the energy infrastructure suffered from shelling [13]. In light of this, the energy front, where Russia is waging war against Ukraine and the EU, can be distinctly highlighted.

The existence of this issue poses additional risks in Russia's use of the cyber domain in their multi-domain operations. Research conducted by CERT-UA experts confirms the connection between cyberattacks and kinetic attacks on critical infrastructure. Even if it's impossible to directly influence the system's operation in cyberspace, sensitive data about electricity generation volumes, supply networks, peak loads, equipment used, and more become valuable information for causing maximum damage [14]. Since the start of Russia's full-scale military invasion into Ukraine, over 1,200,000 cyberattacks have been carried out on energy infrastructure objects, whereas in the entire year of 2021, there were 900,000 recorded. This was stated by the Deputy Minister of Energy for Digital Development, Digital Transformations, and Digitization, Farid Safarov, speaking at the Energy Security Forum 2022 [15]. It's crucial to separately consider dependencies on the technologies used and equipment supplies, as these factors also create additional stability issues.

2 Recovering model

In light of the above, the question of restoring critical energy infrastructure arises. Let's describe a mathematical damage accumulation model that takes into account these indicators.

E_i - Energy system component i;

$R_i(t)$ - Repair rate of component i at time t;

$D_i(t)$ - Damage level of component i at time t;

C_{ij} - Dependency coefficient between components i and j;

P_i - Priority of restoring component i;

T - Total time for recovery.

$$D_i(t+1) = D_i(t) + \sum_j C_{ij} \cdot R_j(t) \quad (1)$$

This equation shows how damage accumulates in component i over time based on repair rates of interdependent components. It helps to describe repair rate model:

$$R_i(t) = f(D_i(t), P_i, \text{other factors}) \quad (2)$$

The repair rate function could be dependent on the current damage level, priority, and various other factors influencing the restoration process. After this we can describe objective function:

$$\text{Minimize } \sum_i \int_0^T R_i(t) dt \quad (3)$$

This objective function could represent minimizing the overall repair time for all components.

Constraints could involve resource limitations, interdependencies, and priorities:

$$\sum_i R_i(t) \leq \text{Resources available at time } t \quad (4)$$

Based on this the resilience function aims to provide a quantitative measure or assessment of how well the critical energy infrastructure can absorb disturbances, recover functionality, and continue operating efficiently. It helps in decision-making processes by evaluating different strategies to enhance the system's resilience against various threats or disruptions.

$$\text{Resilience} = f(\text{Damage Level}, \text{Restoration Time}, \text{Resource Allocation}, \text{other factors}) \quad (5)$$

3 Lessons learnt

The application of a 'response plan,' involving the use of law enforcement and armed forces in predefined measures for preventing the seizure and protection of critical energy infrastructure upon reaching a specified threat level (acts of terrorism); Conducting explanatory work among the population, armed forces, and law enforcement regarding the importance of ensuring the functioning of critical energy infrastructure; Implementation of additional organizational and technical measures to protect critical infrastructure from

accidental damage; Establishing a communication system between conflicting parties, involving representatives of the conflict and impartial parties. Avoiding the placement of military formations (command centers) on or near critical energy infrastructure. Coordination of the protection of energy infrastructure in areas of armed conflict between armed forces and law enforcement agencies to prevent looting. Diversification of generation capacities across the country and decentralization of the energy system to enhance its resilience and adaptability. Introduction of modern, highly maneuverable, and more environmentally friendly generating capacities to strengthen the energy system's maneuverability. Increase the share of renewable energy sources in the energy system, tapping into the significant potential of clean and sustainable energy. Initiation of efforts to phase out and ultimately abandon the use of coal in line with commitments to Ukraine for reducing CO_2 emissions and contributing to global climate change mitigation efforts. Exploration of further possibilities to enhance the efficiency of nuclear and hydro energy use while maintaining an optimal energy balance.

4 Conclusions

Research in the field of resilience is crucial for Ukraine not only during wartime but also in the post-war reconstruction period, where the best practices in implementing energy sector resilience need to be considered. Such experience will also be valuable for countries facing unstable climatic conditions and increased risks of natural disasters.

Hence, research on the resilience of the energy sector in Ukraine is important not just for the country itself but also for other nations. Ukraine and the EU are not the sole examples of energy cooperation globally, but presently stand as a unique instance of a country at war with substantial energy potential and numerous dependencies in the energy sector. This example allows for an analysis of resilience under heightened risks based on real events and their consequences. This analysis aims to develop approaches and methodologies for stress-testing critical energy sector assets and other related industries.

Specifically, research in resilience aims to support decisions regarding the restoration of existing infrastructure, construction of new facilities, restructuring of power grids, and implementation of alternative energy sources. An example of resilience is seen in the transition of Ukrainian businesses and citizens to alternative sources of electricity such as generators, batteries, and the implementation of electricity outage schedules during the winter of 2023. The integration of alternative sources leads to increased service costs, which also restrict access for financially disadvantaged citizens. Therefore, organizational procedures and technical solutions form the basis of resilience, yet their implementation requires comprehensive risk management research.

Acknowledgements

The work was carried out under the W911NF-22-2- 0153 "AI Methods and Tools for Integrating Resilience Analytics and Edge Computing for Energy Systems" grant funded by US Army Engineering Research and Development Centre.

References

- "Verkhovna Rada of Ukraine. "Together - Against Russian Aggression - Missile attacks of the Russian Federation have created significant problems for the energy system, but in a few days they will be liquidated - Chairman of the Committee on Energy and Housing - Official Portal of the Verkhovna Rada of Ukraine." November 11, 2022. [Link: <https://www.rada.gov.ua/news/razom/229018.html>]
- State Service for Special Communications and Information Protection of Ukraine. "CERT-UA Has Processed over 2,000 Cyberattacks against Ukraine Year to Date." December 30, 2022. [Link: <https://cip.gov.ua/ua/news/cert-ua-vid-pochatku-roku-opracyuvala-bilshe-dvokh-tisyach-kiberatak-na-ukrayinu>]
- M. Honchar, A. Chubik, O. Ishchuk. "Hybrid war of the Kremlin against Ukraine and the EU: energy component." [Link: http://gazeta.dt.ua/energy_market/gibridna-viyna-kremlja-proti-ukrayini-i-yes-energetichniy-komponent_.html]
- "DNR" created a separate "State enterprise "Vtorchormet", which massively sold scrap metal. Mobile brigades on "Gazelles" with installed metal cutters cut everything, from cables and rails to enterprise workshops. [Link: http://gazeta.dt.ua/macrolevel/blokada-bezgluzda-y-neschadna_.html; Militants open liquor and vodka factories in Donbas and cut enterprises for scrap metal. [Link: <http://tyzhden.ua/News/136938>]

National Institute for Strategic Studies. "Problems of protecting energy infrastructure in conditions of hybrid warfare." [Link: <https://niss.gov.ua/doslidzhennya/nacionalna-bezpeka/problemi-zakhistu-energetichnoi-infrastrukturi-v-umovakh-gibridnoi>]

"The railway was blown up in Lugansk region, which delivers coal to Vuglegirska TPP." [Link: http://www.loga.gov.ua/oda/press/news/2015/06/12/news_66168.html]

Militants severely damaged Vuglegirska TPP. PHOTO. [Link: <http://uainfo.org/blognews/1437999336-boyoviki-seryozno-poshkodili-vuglegirsku-tes-foto.html>]

Most of Luhansk region remained without electricity after the shelling of TPP in Schastia. [Link: <http://www.unian.ua/war/1105540-bilsha-chastina-luganskoji-oblasti-zalishisya-bez-svitla-pislyu-obstrilu-tes-u-schasti.html>]

"Pravda." [Link: <https://www.pravda.com.ua/news/2016/07/2/7113493/>]

Ministry of Foreign Affairs of Ukraine. "Statement of the Ministry of Foreign Affairs of Ukraine on the Endangering Situation at the Zaporizhzhia NPP." June 23, 2023. [Link: <https://www.kmu.gov.ua/news/zaiava-mzs-ukrainy-shchodo-zahrozlyvoi-sytuatsii-na-zaporizkii-aes>]

Ministry of Foreign Affairs of Ukraine. "Statement of the Ministry of Foreign Affairs of Ukraine Regarding the Russian Terrorist Act at the Kakhovka HPP." June 06, 2023. [Link: <https://mfa.gov.ua/en/news/zayava-mzs-ukrayini-shchodo-teroristichnogo-aktu-rosiyi-na-kahovskij-ges>]

"Kosatka Media." [Link: <https://kosatka.media/category/blog/news/kakie-poteri-ponesla-ukrainskaya-energetika-iz-za-rossiyskogo-vtorzheniya>]

"50 energy infrastructure facilities in Ukraine damaged, Russia is responsible for this - Herman Halushchenko." [Link: <https://www.kmu.gov.ua/news/poshkodzheni-50-enerhetychnoi-infrastruktury-ukrainy-rosiia-maie-vidpovisty-za-tse-herman-halushchenko>]

State Service for Special Communications and Information Protection of Ukraine. "Cyber, artillery, propaganda: general overview of the dimensions of Russian aggression." 2023. [Link: <https://cip.gov.ua/en/news/kiberataki-artileriya-propaganda-zagalnii-oglyad-vimiriv-rosiiskoyi-agresiyi>]

"From the beginning of the war, over 12 million cyber attacks on the energy sector have been recorded - Farid Safarov." [Link: <https://www.kmu.gov.ua/news/z-pochatku-vijni-zafiksovano-ponad-12-mln-kiberatak-na-energosektor-farid-safarov>]

2.2 On the resilience of the European Union natural gas system

Rebecca Schill, Ricardo Fernández-Blanco, Nuria Rodríguez Gómez, Anca Costescu, Ricardo Bolado Lavín
Joint Research Centre, European Commission, Petten, Netherlands

Rebecca.Schill@ec.europa.eu, Ricardo.Carramolino@ec.europa.eu, Nuria.Rodriguez-Gomez@ec.europa.eu,
Anca.Costescu@ec.europa.eu, Ricardo.Bolado-Lavin@ec.europa.eu

Abstract

Resilience is, in a broad sense, the capacity to withstand or recover quickly from difficulties / shocks. This paper focuses on the resilience of energy systems, specifically on the European Union (EU) natural gas system. The energy crisis started at the second half of 2021 has tested its ability to recover from a difficult situation. Before the energy crisis, the EU gas system relied heavily on Russian gas to meet its seasonal gas consumption. Almost two years later, the natural gas sector has proved resilient to adverse events jeopardizing the security of gas supply of the EU such as the decay of flows from Russia, gas price spikes or low levels of gas in storage. These triggering events have obliged policy makers to react swiftly in 2022 by adopting temporal regulations in record time, namely the new gas storage Regulation (EU) 2022/1032 and Regulation (EU) 2022/1369 on coordinated demand-reduction measures for gas, among others. The natural gas sector, as well as society, have also proactively implemented these political actions. The ultimate outcome has been the shift from a status quo relying on Russian gas to a new paradigm in which one of the main suppliers to the EU is the liquefied natural gas from all possible sources. This paper analyses how the resilience of the EU gas system has been tested since the beginning of the energy crisis by using publicly available data from ENTSOG Transparency Platform, ENaGaD database, and Gas Infrastructure Europe. In particular, we describe the triggering events of the energy crisis, the political proposals to strengthen the security of gas supply, and the consequences of such political reactions.

1 Introduction

A resilient system can be exposed to a shock, experience the negative impact of this shock, and then recover to its original state, or one of equal quality. Enhancing a system's resilience therefore shifts the focus of common risk management strategies, which is minimising the likelihood and impact of defined risk scenarios, to maximising the impacts a system can withstand without a lasting loss of function. Assessing resilience prioritises assessing the system's crisis preparedness, crisis response, and recovery period (Hosseini, Barker, & Ramirez-Marquez, 2016). Thus, the impact assessment is expanded to include not only system damage but also the cost of recovery efforts (Vugrin, Warren, & Ehlen, 2011). From this perspective, the likelihood of a shock occurring is no longer in focus, as real-world systems are certain to eventually be disrupted in some form.

This is especially true for large-scale, complex systems exposed to a combination of technical, environmental, social, and political risks, such as the natural gas system of the European Union (EU). This system involves not only the natural gas infrastructure, but also the overarching policy and market framework of the EU and Member States (MSs), the geopolitical relations with external suppliers, and finally, the gas consumers within its boundaries.

The function of the EU natural gas system is to provide a secure, affordable gas supply to the EU citizens. The EU has been working to improve the security of gas supply (SoS) since 2010, with the adoption of Regulation (EU) No 994/2010 (Regulation (EU) No 994/2010 of the European Parliament and of the Council concerning measures to safeguard the security of gas supply and repealing Council Directive 2004/67/EC, 20 October 2010), which was replaced and enhanced by Regulation (EU) 2017/1938 (Regulation (EU) 2017/1938 of the European Parliament and of the Council concerning measures to safeguard the security of gas supply and repealing Regulation (EU) No 994/2010, 25 October 2017) several years later. This regulation is the reference legal text to safeguard the security of gas supply and strengthens the concept of solidarity among the EU MSs in case of need, which is vital for ensuring the gas flow to the EU (Fleming, 2019). However, this regulation has been supported by recently adopted legislative acts to face the current energy crisis, which has been characterised mainly by geopolitical and economic risks. Recent policy actions in the field of security of energy supply have been deemed necessary to counteract the potential deterioration of the security of supply in the EU.

This paper reviews main drivers of the energy crisis as well as the legislative actions carried out by the European Commission (EC) during 2022 and 2023. In addition, we evaluate whether the EU natural gas system proved itself resilient during and after the 2022 energy crisis using the following metrics: (i) Underground Gas storage (UGS) filling level, (ii) gas demand reduction, (iii) gas supply diversification (share of

gas from Liquefied Natural Gas (LNG)), (iv) new infrastructure in the natural gas system, and (v) price developments.

This paper is structured as follows. Section 0 briefly describes the triggering events of the energy crisis. Section 0 presents the legislative actions adopted by the EC in 2022 and 2023 in response to the crisis. Section 0 analyses the reaction of the natural gas system of the European Union before and after the adoption of the preventive measures. Finally, Section 0 duly concludes the paper.

2 Triggering events of the energy crisis

The 2022 energy crisis was brought on by a combination of factors. The accelerated economic recovery after the COVID-19 pandemic already strained energy supplies in 2021 (IEA). At this point, coming out of the winter 2020/2021 gas withdrawal season, EU gas storage facilities were more depleted than they were on average after the previous winters. Gas price volatility already began increasing during the following summer of 2021, and the injection season did not recover gas storages to the typical filling level observed in the last years. Overall, the EU storages were 77% filled, but UGS facilities owned or operated by Gazprom, the Russian state-owned energy corporation, remained especially depleted with a filling level below 30% by 1 November 2021 (Fernandez Blanco Carramolino, et al., 2023). This left the EU gas system vulnerable to supply disruptions during peak demand periods in the cold winter months.

When the gas supply from Russia started to diminish in winter 2021/2022, the combination of these factors exacerbated the issue into an energy crisis. Gas and electricity prices spiked for the first time in winter 2021/2022 (Gil Tertre, Martinez, & Rivas Rábago, 2023). During this winter, the natural gas imports from Russia via Ukraine and Nord Stream I dropped by 107 TWh compared to the previous winter, representing a loss of 7% of total pipeline imports. The Russian invasion of Ukraine on 24 February 2022 worsened the political tension between Russia and the EU with severe impacts on the gas supply. On 31 March 2022, one day prior to the start of the gas storage injection season, Russia issued a decree mandating payments for natural gas supplies be made in roubles. At this point, EU storages were depleted to a filling level of 27%. In April 2022, Russia halted the gas supply to several EU countries (Bulgaria, Poland, Finland), and by June, with the capacity reduction of Nord Stream I, the gas flows from Russia to the EU were less than 30% of the average of the preceding five years (European Commission Directorate-General for Energy, 2022). The flow via Nord Stream I was completely halted on 1 September 2022, according to the ENTSOG Transparency Platform (ENTSOG, n.d.), and the following sabotage of the pipelines on 26 September 2022 rendered this interruption permanent (Jacobsen & Abnett, 2022). Overall, the EU natural gas system had to cope with 18% lower pipeline imports in the summer of 2022 compared to the summer of 2021 (Fernandez Blanco Carramolino, et al., 2023).

Reduced nuclear and hydroelectric energy generation pressured the electricity supply during this summer, which in turn further burdened the gas supply (Gil Tertre, Martinez, & Rivas Rábago, 2023). The average seasonal gas price saw an almost ten-fold increase between winter 2020/2021 and summer 2022, and an all-time high price of 315 €/MWh was reached in August 2022.

As opposed to the simple model of a system in equilibrium, which experiences a single shock, an impact, and then recovery, the EU natural gas system was repeatedly exposed to a multitude of difficulties over a long period of time, which eventually cumulated into a crisis. The system needed to prove its resilience to all of these shocks in a continuous manner, thus reacting quickly albeit smoothly to keep the security of gas supply by means of political actions or proposals. These political developments could be viewed as mitigation and preventive measures and are further described in the next Section 0.

3 Political proposals as mitigation measures

EU policy interventions are a key part of the resilience of the EU natural gas system. Before the 2022 energy crisis, several regulations had already put in place collective risk management strategies to protect the internal gas market and especially vulnerable customers such as households and businesses. When these preparations were insufficient to handle the extent of the 2022 crisis, EU policy-makers reacted quickly to coordinate an improved joint crisis response of the MSs.

3.1 Preceding regulations

Strengthening the natural gas system has been an EU priority since the First Gas Directive 98/30/EC of 1998 but was first secured in regulation in 2010 (Directive 98/30/EC of the European Parliament and of the Council concerning rules for the internal market in natural gas, 22 June 1998). **Regulation (EU) No 994/2010** on the security of natural gas supply in the EU was created after a commercial dispute led to Russia temporarily

stopping the supply of gas to Ukraine on 1 January 2009 (Regulation (EU) No 994/2010 of the European Parliament and of the Council concerning measures to safeguard the security of gas supply and repealing Council Directive 2004/67/EC, 20 October 2010). The regulation recognized the European dependency on third countries for natural gas and the resulting need to increase and to diversify the supply. Preceding directives 98/30/EC (Directive 98/30/EC of the European Parliament and of the Council concerning rules for the internal market in natural gas, 22 June 1998) and 2003/55/EC (Directive 2003/55/EC of the European Parliament and of the Council concerning common rules for the internal market in natural gas and repealing Directive 98/30/EC, 26 June 2003) liberalised the EU natural gas market, which now required new safeguards for security of supply within the limits of a reasonable burden on the market.

The regulation confronted the experiences of the previous years that had unveiled a risk of MSs acting unilaterally in crises and thus jeopardizing the internal gas market and the security of supply. Solidarity and coordination became key tools for the primary goal of security of gas supply. Risk assessments, preventive action plans, and emergency plans became the tools for each MS to evaluate their security of supply and coordinate with other MS. The regulation also mandated enabling bi-directional flow capacity between MS, with exceptions. Households and their corresponding district heating systems, as well as essential social services were defined as protected customers, and optional protections for small and medium-sized enterprises were introduced. An infrastructure standard ("N-1 criterion") was defined: the entire gas demand should be covered in the case that the single infrastructure delivering the largest share of the total gas supply to a country or region was interrupted. Additionally, a supply standard was defined to ensure a sufficient supply to cover the demand of protected customers during extremely cold periods and periods of high demand. Three crisis levels were defined: early warning, alert, and emergency.

After the Russo-Ukrainian dispute escalated with the Russian annexation of Crimea on 20 February 2014, the 2010 security of supply regulation was replaced by **Regulation (EU) 2017/1938** (Regulation (EU) 2017/1938 of the European Parliament and of the Council concerning measures to safeguard the security of gas supply and repealing Regulation (EU) No 994/2010, 25 October 2017). A stress test exercise in October 2014 had revealed insufficiencies in the preceding regulation, specifically a need to strengthen and enhance existing solidarity and cooperation mechanisms in the Union. Risk groups of MSs were defined to create joint risk assessments, to further improve MSs preventive action and emergency plans using an EU-wide simulation of gas supply and disruption scenarios as input. Bi-directional capacity exemptions were re-examined under a broader scope of EU-wide security of supply, not only the scope of neighbouring MSs. The regulation also added the category of solidarity protected customers, next to protected customers, which could no longer include MSEs, and educational and public administration services. Solidarity flow capacity was clearly prioritized over storage filling firm capacities.

3.2 Reactions to the crisis

As electricity prices increased by 200% year-on-year in October 2021, the European Commission published a non-binding communication on the "energy prices toolbox", which included suggested tools for MS to support gas consumers to handle price spikes, such as tax exemptions for vulnerable households and authorising the deferral of electricity bills (Tackling rising energy prices: a toolbox for action and support, 2021).

On 24 February 2022, Russia invaded Ukraine. Within weeks, the Commission published the **REPowerEU** plan (REPowerEU Plan, 18 May 2022), another non-binding communication on short-term measures to protect consumers from price hikes and on securing the winter gas supply. It also defined three longer-term measures to secure affordable and sustainable energy supplies in the EU: (i) save energy via enhanced energy efficiency, (ii) diversify energy supplies, and (iii) boost renewable energies.

As uncertainty over the security of gas supply in winter 2022 rose, the **Regulation (EU) 2022/1032** on gas storage was proposed in March 2022 and then adopted on 30 June 2022 (Regulation (EU) 2022/1032 of the European Parliament and of the Council of 29 June 2022 amending Regulations (EU) 2017/1938 and (EC) No 715/2009 with regard to gas storage, 30 June 2022). This regulation recognized that existing security of supply measures were insufficient in addressing increasing geopolitical risks, as was proven by the Russian weaponisation of the gas supply. Throughout the summer, gas supplies from Russia were interrupted in several countries and by June, gas flows from Russia had been reduced to less than a third of the average of the five preceding years. The regulation specifically highlighted the importance of UGS in buffering pipeline supply disruptions and introduced a general filling target of 80% by 1 November 2022, and of 90% by the same date of each year from 2023 onwards, with some exceptions. The storage filling levels were to be monitored and a number of tools were suggested to implement the targets, for example mandated minimum gas filling levels and discounts on tariffs. However, the solidarity mechanism was clearly prioritised over storage filling in case of emergency. Collaboration between MS with and without storages was encouraged.

As was previously declared in the REPowerEU communication, improving gas storage utilization was not the only means of securing the gas supply in the EU for the winter. The **Regulation (EU) 2022/1369** on gas demand reduction was proposed in July 2022, and adopted on 5 August 2022 (Council Regulation (EU) 2022/1369 on coordinated demand-reduction measures for gas, 5 August 2022). It encouraged MS to voluntarily reduce their gas demand by at least 15% from 1 August 2022 to 31 March 2023, compared to a reference period from 1 August to 31 March during the five preceding years. In case of a Union alert, this reduction would be mandated, with some limits in place (e.g. in case of an electricity crisis), and avoiding market distortion. Protected customers were once again clearly prioritized, and the importance of coordination among MS was highlighted. MS were encouraged to monitor the gas demand of industry, households and services, and the gas input for electricity and heat separately.

As energy prices remained high at the start of winter 2022, **Regulation (EU) 2022/1854** was adopted on 6 October 2022 to protect consumers from high electricity prices by reducing demand and temporarily shifting the costs to energy producers via a revenue cap and a solidarity contribution (Council Regulation (EU) 2022/1854 on an emergency intervention to address high energy prices, 6 October 2022).

In December, two further regulations were adopted: **Regulation (EU) 2022/2576** on enhancing the solidarity mechanism (Council Regulation (EU) 2022/2576 enhancing solidarity through better coordination of gas purchases, reliable price benchmarks and exchanges of gas across borders, 19 December 2022) and **Regulation (EU) 2022/2578** on the market correction mechanism (Council Regulation (EU) 2022/2578 establishing a market correction mechanism to protect Union citizens and the economy against excessively high prices, 22 December 2022). The former was adopted on 19 December 2022 and introduced a joint purchasing platform for EU MSs to aggregate their demand of gas, LNG, and hydrogen to lower prices and allow for more equal access to energy. Fair allocation was to be performed by a temporarily contracted service provider. Increasing transparency was especially highlighted, for the common purchasing process as well as for LNG and gas storage facilities, including via data gathering and publishing by ACER. Solidarity protections were more specifically defined and expanded to include critical gas volumes needed to secure the electricity supply. Trading venues were given the responsibility to temporarily contain the extent of intra-day price volatility by defining price boundaries. As this intra-day mechanism only reduced price volatility on a short-term basis, Regulation (EU) 2022/2578 on the market correction mechanism was adopted only days later (Council Regulation (EU) 2022/2578 establishing a market correction mechanism to protect Union citizens and the economy against excessively high prices, 22 December 2022). It defined price thresholds, monitored by ACER, which would trigger a temporary dynamic bidding limit to reduce price volatility in the medium-term. This market correction mechanism was not triggered.

4 Reactive natural gas system

EU policy can steer the natural gas system using several components aside from obvious measures on improving the gas network itself and its infrastructure to enhance resilience. A strong gas storage strategy increases resilience as storages can buffer potential supply shortages. Diversifying the gas supply in terms of gas sources (pipeline versus LNG) and gas suppliers also allows the system to absorb shortages from individual suppliers with reduced impact on the security of supply. Cooperative market measures such as joint purchasing can mitigate crisis effects, and in case they prove themselves insufficient, demand-side measures, while potentially costly, are the most direct way of ensuring essential demand can be covered and of preventing curtailment of gas supply to vulnerable customers such as households. In the following subsections, we analyse the reaction of these parts of the natural gas system to the crisis and to the EU policy interventions.

The data of the natural gas system come from the ENTSOG Transparency Platform (ENTSOG, n.d.), and the data collected by Gas Infrastructure Europe (GIE) on underground gas storages and LNG terminals, namely the AGSI+ Transparency Platform (GIE, n.d.) and the ALSI Transparency Platform (GIE, n.d.). The data from ENTSOG is downloaded and processed by using the package eurogastp¹ developed by the Joint Research Centre (JRC) (Jung, et al., 2022). The reader is referred to **Error! Reference source not found.** of the Appendix for an overview of the main parameters analysed in the next subsections in the last six seasons ranging from the winter 2020/2021 until the summer of 2023.

4.1 Gas in storage

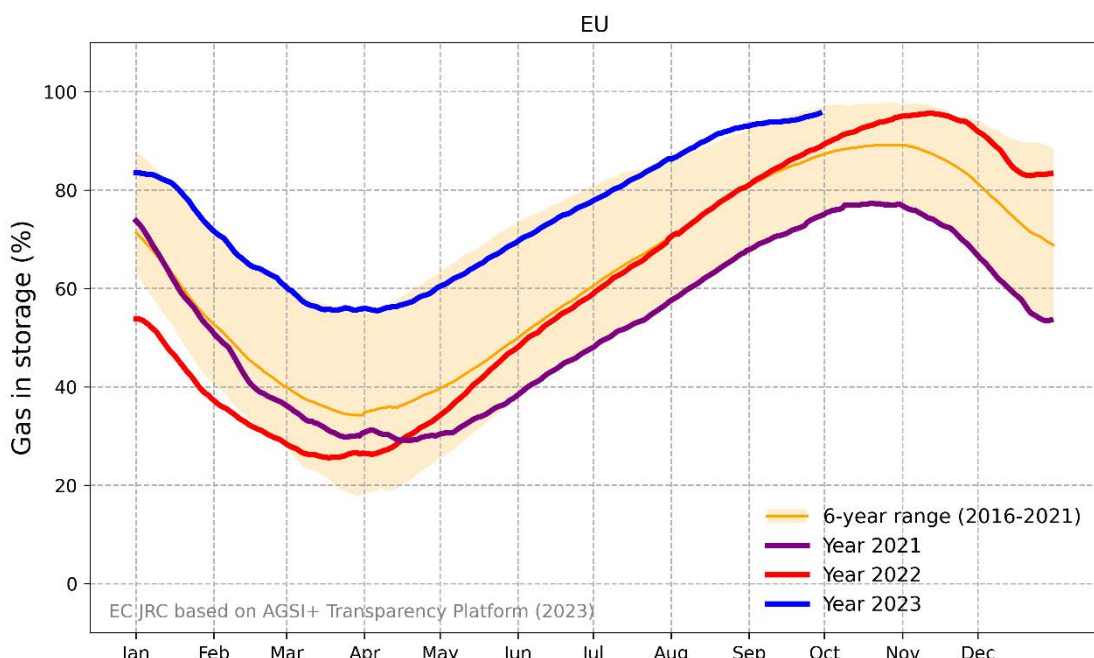
¹ <https://github.com/ec-jrc/eurogastp>.

The first EC regulation after the start of the energy crisis was devoted to gas storage facilities (Regulation (EU) 2022/1032 of the European Parliament and of the Council of 29 June 2022 amending Regulations (EU) 2017/1938 and (EC) No 715/2009 with regard to gas storage, 30 June 2022). Based on the gas storage developments at the beginning of the heating season of 2021/2022, this regulation was intended to (i) prevent low levels of gas in storage of UGSs in the EU by 1 November, and (ii) carry out storage certifications to avoid underutilisation of UGSs and reinforce the security of supply in the EU.

As previously mentioned, a driving factor of the energy crisis in 2021 were low filling levels of natural gas storage facilities in the EU. 19 of the MSs have gas storage facilities in their respective territories. As shown in **Figure 2**, the filling levels between June and December 2021 (in purple) were the lowest in six years². The filling levels remained significantly below average during the winter of 2021/2022, and only began to overlap the six-year range again in March 2022. The Regulation (EU) 2022/1032 on gas storages was proposed in March 2022 (Regulation (EU) 2022/1032 of the European Parliament and of the Council of 29 June 2022 amending Regulations (EU) 2017/1938 and (EC) No 715/2009 with regard to gas storage, 30 June 2022) and was a key driver of storage filling, as the levels surpassed the preceding six-year average in September 2022. The 80% filling target on 1 November 2022 was overshot, even surpassing the 90% filling level set for the beginning of winter the following year.

Note also that the storage filling levels after winter 2021/2022 never fell below 25%, indicating that the security of gas supply was not in critical danger from the storage perspective. The period after April 2022, when EU gas storages were being refilled faster than during the previous years, shows the system's ability to recover quickly in terms of UGS. The EU net injections were 33% higher than the 11-year average and 18% higher than the 6-year average (Fernandez Blanco Carramolino, et al., 2023). In contrast, the net extractions during winter 2022/2023 (around 360 TWh – see **Error! Reference source not found.** in the Appendix) were the lowest of the last seven winter seasons, being 39% lower than the 7-year average (2015–2022).

Figure 2. Filling level of EU natural gas storage (%) in 2021 (purple), 2022 (red), and 2023 (blue) compared to the six-year range between 2016 and 2021.



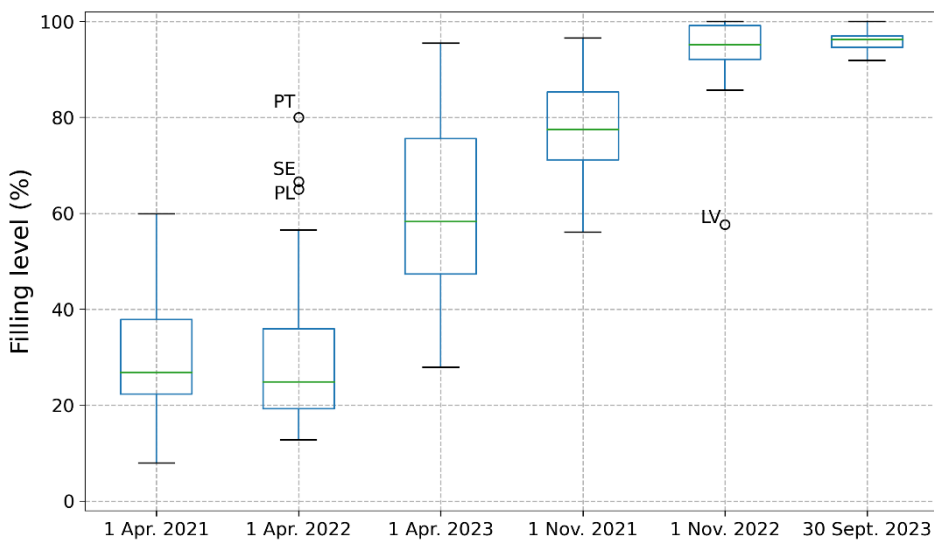
Reference (Fernandez Blanco Carramolino, et al., 2023) provides an exhaustive analysis of the underground gas storage developments during 2022 compared to historical figures. **Figure 3** shows the dispersion of the

² The gas storage filling levels were the lowest since 2011 (last year in which data are available in AGSI+ Transparency Platform) during July–December 2021, however the plot is limited to years 2016–2023.

relative filling levels across EU countries at the beginning of the injection season and on 1 November (when the filling target was set at 90% in the EU). We have adopted the filling level on 30 September in 2023 as a proxy of 1 November. At the start of the winter season, the dispersion of the filling level across Member States is visibly lower in 2023 compared to 2020 and 2021. The main reason for this behaviour relies on the minimum storage obligations imposed by the Gas Storage Regulation (Regulation (EU) 2022/1032 of the European Parliament and of the Council of 29 June 2022 amending Regulations (EU) 2017/1938 and (EC) No 715/2009 with regard to gas storage, 30 June 2022). The filling levels at the beginning of the injection season in 2023 are remarkably high with a median around 60%. This can be explained by the mild weather conditions of the past winter 2022/2023 combined with the need to save gas for the upcoming winter 2023/2024.

The certification of gas storages has allowed to fill the facilities owned or operated by Gazprom in record time, as explained in (Fernandez Blanco Carramolino, et al., 2023). This was mainly motivated by the Regulation on gas storage. As indicated in the JRC report (Fernandez Blanco Carramolino, et al., 2023), half of the Gazprom-related storage capacity was allocated in Germany, while the other half was split essentially between Austria and the Netherlands. After the implementation of the Gas Storage Regulation, storage filling levels corresponding to Gazprom-related storages increased by 71 and 67 percentage points in Austria and Germany, respectively, on the same day one year later.

Figure 3. Boxplot of the country-specific filling levels on 1 April and 1 November in 2021-2023. We show the filling level on 30 September 2023 instead of 1 November 2023.



Source: JRC based on AGSI+ Transparency Platform, 2023.

4.2 Natural gas consumption

The second regulation adopted by the EC, i.e., the **Regulation (EU) 2022/1369** on gas demand reduction (Council Regulation (EU) 2022/1369 on coordinated demand-reduction measures for gas, 5 August 2022), recommended a voluntary gas consumption reduction of 15% at EU level from August 2022 until March 2023 to save gas for the winter. The actual reduction reached 17.9% compared to the average from the reference period August 2017-March 2022. Although the measure was not mandatory, the cooperation of consumers of natural gas encouraged by the national governments was positive and the reduction was above the 15% target.

The European Commission published a preliminary analysis of the demand reduction developments until January 2023 (SWD(2023) 63 final, 2023). This report discusses the possible sources of reduction and points out three categories: savings due to behavioural changes and energy efficiency, fuel switching to carbon-intensive or clean fuels, and demand destruction. Those categories could be further classified into structural or non-structural. For instance, the gas consumption reduction by households due to favourable weather conditions would be non-structural because a change in the weather conditions might reverse the reduction.

Eurostat provides monthly data of gas consumption (IC_CAL_MG) that allows the calculation of the demand reduction, and data of gas consumption for electricity and heat generation (TI_EHG_MAP) (Statistical Office of the European Union, n.d.). The gas consumption for electricity generation was reduced by 8.3% in the period August 2022- March 2023 (i.e. 55.5 TWh). The largest part of the total gas consumption reduction is due to other sectors, namely the distribution and industrial sector. In other words, 10% of the demand decline can be attributed to the power sector (55.5 TWh) while the other 90% was linked to the distribution and industrial sectors (519.5 TWh).

A further sectoral contribution to the gas consumption reduction, e.g. households versus industry, is challenging due to a lack of sectoral breakdown in Eurostat. One could resort to ENaGaD, the JRC in-house database collecting data published by gas Transmission System Operators with daily granularity of gas consumption by electricity and heat producers, distribution and industrial users (Zaccarelli, Giaccaria, Feofilovs, & Bolado-Lavín, 2021).

ENaGaD is composed of daily time series of the national demand of natural gas for each of the 25 MSs with a transmission system. The series is available from 2015 to 2023 (March) in energy units. Values are mainly collected from the transparency platform of National Transmission System Operators in compliance with Regulation (EC) No 715/2009 (Regulation (EC) No 715/2009 of the European Parliament and of the Council on conditions for access to the natural gas transmission networks and repealing Regulation (EC) No 1775/2005, 13 July 2009) or directly from the ENTSOG Transparency Platform (ENTSOG, n.d.). Whenever possible, the daily demand is further divided into consumption by electricity and heat producers, by industrial users and by

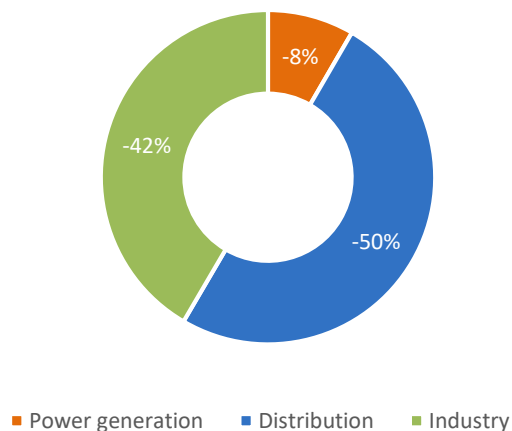
the gas consumed in the distribution sector (including households, public buildings, commerce, small enterprises...). The daily values are then aggregated to get the monthly values.

The breakdown of the daily gas consumption by industrial and distribution sector in the ENaGaD database is complete for 11 Member States (BE, DE, EL, FR, HR, IT, LU, NL, PL, PT and RO). We have added Spain to this group because there was a consumption increase up to 40% in the power sector during the period of analysis. For Spain, we have assumed a 50% split consumption between the distribution and power sectors. We have focused the analysis on these 12 Member States that comprise 87% of the gas consumption of the EU in the period of analysis August 2022–March 2023 (hereinafter referred to as EU12).

Figure 4 shows the EU12 decomposition of the demand reduction per sector in the period August 2022 – March 2023. The largest contributor to the demand reduction is the distribution sector, responsible for 50% of the total reduction, followed by the industry sector, which is responsible for 42%. The power generation sector only contributes to 8% of the reduction due to the low electricity production from renewables (hydro) and the lack of electricity production from nuclear in France (Gil Tertre, Martinez, & Rivas Rábago, 2023).

It is difficult to quantify whether the gas consumption was reduced due to the price and weather conditions, or the destruction of industrial demand. In the SWD(2023) 63 final of the European Commission (SWD(2023) 63 final, 2023), there is an estimation of the gas demand reduction induced by the temperature (mild weather conditions). One-sixth of the gas demand reduction in the period August – December 2022 can be attributed to the weather, i.e. around 5 bcm of the 30 bcm saved in total during that period.

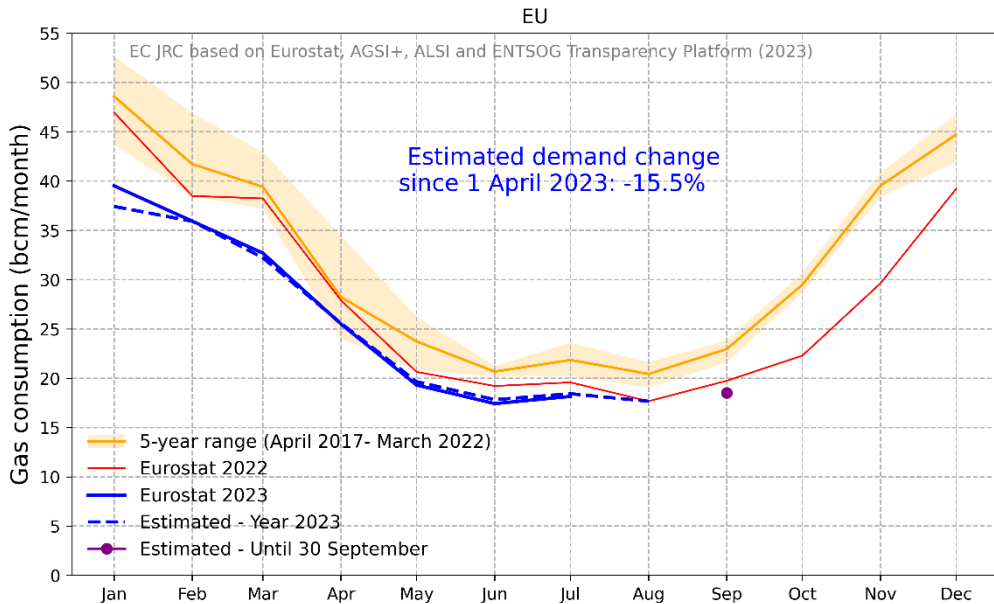
Figure 4. Sectoral contribution to the EU12 gas reduction in the period August 2022 – March 2023.



Source: JRC based on ENaGaD and Eurostat, 2023.

This regulation has been prolonged to cover the period comprising April 2023 until March 2024 as adopted by Council Regulation (EU) 2023/706 in March 2023 (Council Regulation (EU) 2023/706 amending Regulation (EU) 2022/1369 as regards prolonging the demand-reduction period for, 30 March 2023). Monitoring this measure is essential to keep track of the accumulated demand reduction in case there are major deviations that could hinder the final target, thus affecting the security of gas supply for the winter 2023/2024. Eurostat compiles monthly data for the gas consumption in EU member states but there is a delay of 55 days after the reference month. To overcome this issue, the JRC estimates the gas consumption for those periods in which Eurostat does not provide data or the time series are incomplete. The methodology consists in a mass balance model combined with a least square method to estimate the domestic gas production in the EU by using the data from ENTSOG, AGSI+ and ALSI Transparency Platforms. **Figure 5** shows the gas consumption from Eurostat, the estimated one by the JRC, and the average and range of the reference period April 2017 – March 2022 according to the Council Regulation (EU) 2023/706 (Council Regulation (EU) 2023/706 amending Regulation (EU) 2022/1369 as regards prolonging the demand-reduction period for, 30 March 2023). The accumulated gas consumption reduction from April 2023 until 30 September 2023 is 15.5%, using gas demand estimations by the JRC for the values of August and September 2023. This shows that the political system around the gas sector is cooperative and reactive given the voluntary nature of this preventive measure.

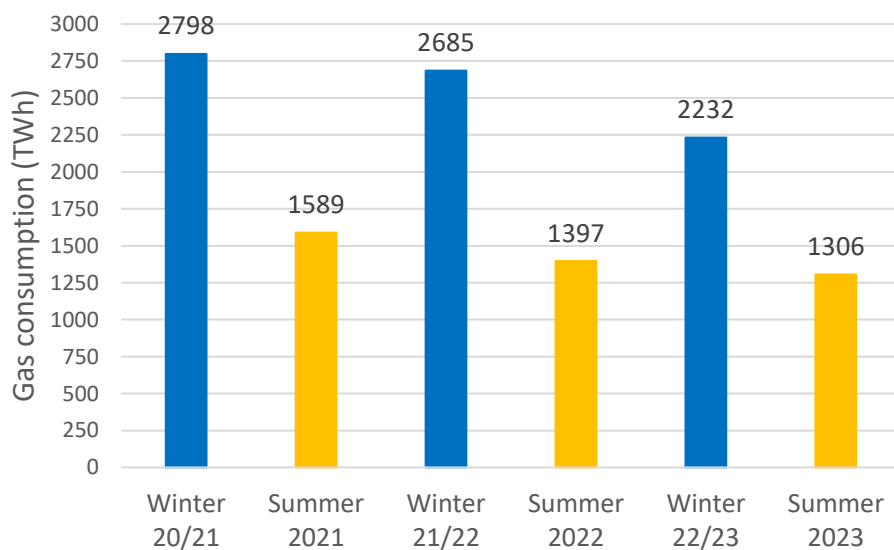
Figure 5. EU gas consumption (bcm/month) in 2022 (red) and the first half of 2023 (blue) compared to a five-year range between April 2017 and March 2022 (orange), including a demand estimation between January and September 2023.



Source: JRC based on ENTSOG, AGSI+, ALSI Transparency Platforms, and Eurostat, 2023.

When looking at the gas consumption per season (**Figure 6**), the general trend is a decrease in the total gas consumption in both winter and summer seasons. In the winter of 2021/2022, even before the adoption of the legislative actions on coordinated demand reduction measures, the natural gas consumption of the EU decreased by 4% compared to the winter 2020/2021. A possible reason behind this decrease is the gas price hike observed in the last quarter of 2021 and the first half of 2022. In fact, in the summer of 2022, the gas demand decreased by 12% compared to the previous summer. The Regulation (EU) 2022/1369 was very effective during the winter of 2022/2023 with an observed reduction of 17% with regard to the winter 2021/2022. In the summer 2023, the reduction is moderate compared to the summer of 2022 (just 7%), when the Regulation (EU) 2022/1369 was already adopted (by 5 August 2022).

Figure 6. Gas consumption (TWh) of the European Union in the last six seasons (winter 2020/2021 to summer 2023).



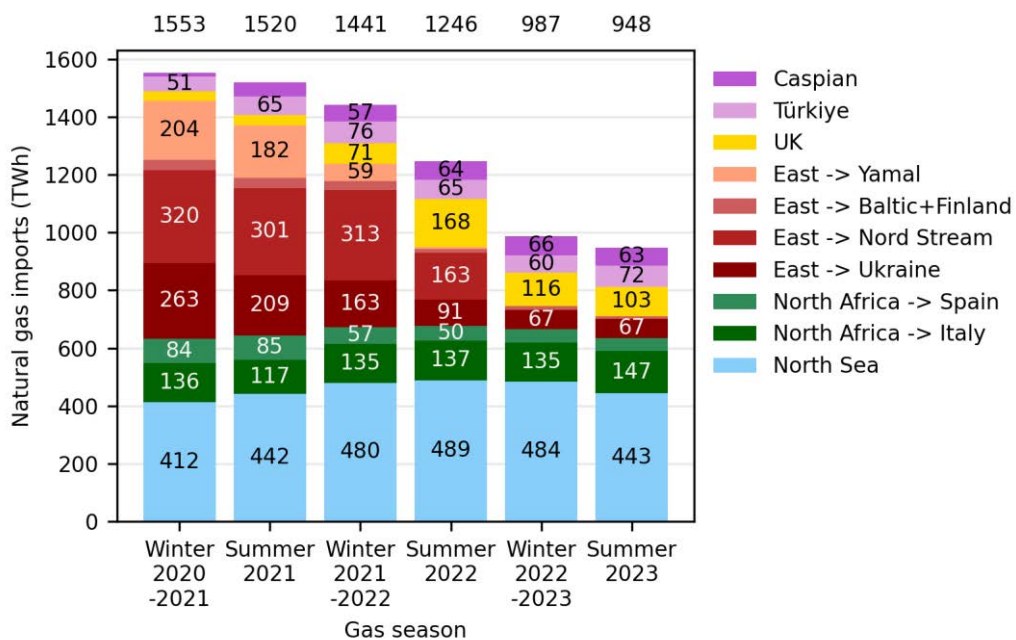
Source: JRC based on ENTSOG, AGSI+, ALSI Transparency Platforms, and Eurostat, 2023.

4.3 Supply diversification

At the start of the energy crisis, there was a slight decline of pipeline gas flows to the European Union. In the winter of 2021/2022, the pipeline gas flows fell by 7% compared to the previous winter 2020/2021 (see **Figure 7**). This reduction was substantial in the following seasons and currently we can observe a decrease in pipeline flows of more than one third in winter and summer compared to pre-crisis levels. **Figure 7** visualises how the distribution of countries supplying pipeline gas to the EU changed over the six gas seasons surrounding the energy crisis. The figure shows that these deficits are mainly caused by the halt of gas supplies by Russia through the routes Nord Stream, Eastern Yamal, and Baltic+Finland. In addition, the gas flows via Ukraine have substantially dropped to 67 TWh per season, when this route used to transport up to 263 TWh in winter 2020/2021 and 209 TWh in the summer of 2021. Essentially, gas imports from the East decreased by 90% in the last two seasons compared to pre-crisis levels.

The cessation of flows from Russia was gradually compensated by a moderate increase of the remaining routes and mainly by an increase of LNG supplies. The diversification of supplies has been at the core of the energy security policy of the European Commission, greatly interlinked with EU foreign policy (European External Action Service, 20 May 2022). Norwegian gas supplies rose by 17% in winter 2021/2022 compared to the previous winter, and by 11% in summer 2022 with regard to the summer of 2021. The pipeline gas via Norway has come back to pre-crisis levels in the summer of 2023. The gas flows via the Caspian route have steadily increased to reach 63-66 TWh per season, as have flows via the UK, which have risen to more than 100 TWh per season. Finally, gas pipeline flows from North Africa to Italy have slightly increased over the last two seasons, although the gas deliveries to Spain have decreased below 50 TWh/season.

Figure 7. Natural gas pipeline imports (TWh) by route for winter and summer gas season between 2020 and 2023. Total imports per season are displayed above the graph.



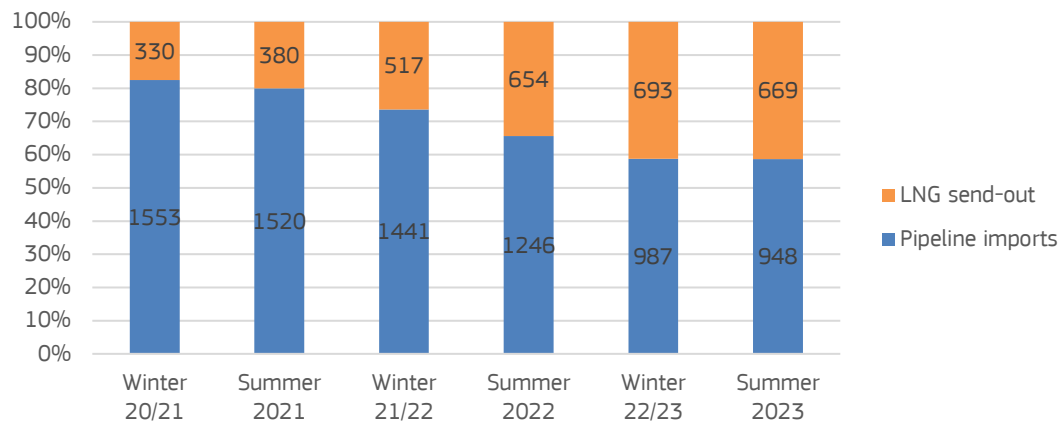
Source: JRC based on ENTSOG Transparency Platforms, 2023.

Figure 8 shows the change of paradigm in the EU natural gas system. The main contributor to offset the missing Russian pipeline gas deliveries has been the gas in liquid form. In winter 2020/2021 and summer 2021, the piped natural gas represented around 82% of the gas imports, while this share has drastically decreased to around 60% in the last two seasons.

The success of the rapid increase of LNG deliveries is in part attributable to the diplomatic relations carried out in 2022 by the European Commission in order to diversify the gas supplies (European External Action Service, 20 May 2022). Several agreements were reached with the United States, Egypt, Israel, Japan, Korea, and Qatar. **Figure 9** compares the LNG exports to the EU by country and the United States is currently the

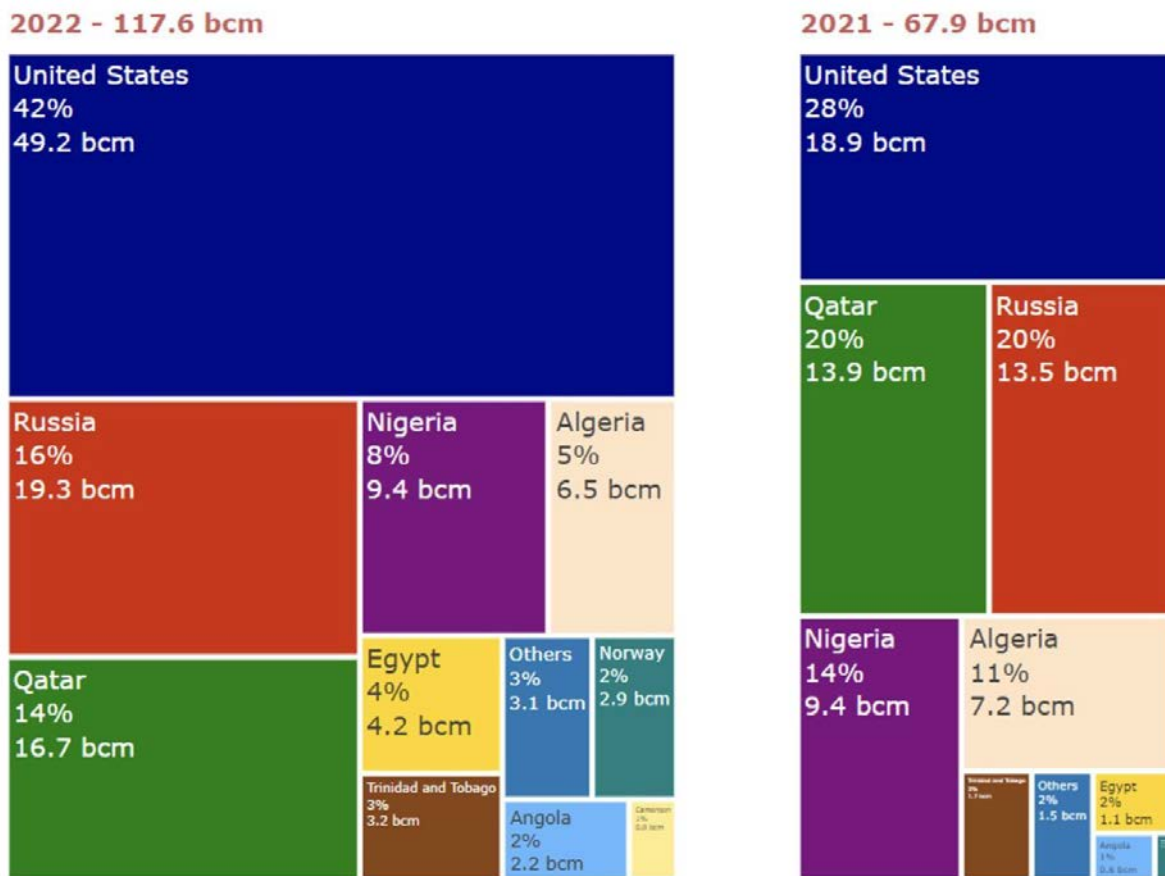
main LNG supplier. LNG exports from the United States have increased by 160% in 2022 compared to 2021, thus representing around 40% of the total LNG exports. Natural gas from Russia continued to play a role in the form of LNG with a share of 16% of total LNG exports to the EU.

Figure 8. Development of share of gas imports (TWh) via pipeline and LNG throughout the gas seasons from winter 2020/2021 to summer 2023.



Source: JRC based on ENTSOG and ALSI Transparency Platforms, 2023.

Figure 9. LNG exports to the EU by country in 2021 and 2022 (Gil Tertre, Martinez, & Rivas Rábago, 2023).



Source: (Gil Tertre, Martinez, & Rivas Rábago, 2023), European Commission based on Refinitiv, 2023.

4.4 Pipeline infrastructure and bidirectional flow capacities

The new pipeline and LNG infrastructure has been key to transitioning to a new paradigm in the natural gas system of the EU. These projects have been discussed at a country level in the reports presented by the European Commission to analyse the progress of the REPowerEU one year after its launch (Directorate-General for Energy, 24 May 2023). The pipeline projects that started operation in 2022 are the following:

- Gas interconnector Poland-Lithuania (GIPL), completed in May 2022 (2.4 bcm/year to Lithuania and 1.9 bcm/y to Poland).
- Poland-Slovakia interconnector, completed in August 2022 (5.7 bcm/y to Poland and 4.7 bcm/y to Slovakia).
- Denmark-Poland interconnector (Baltic pipe), completed in October 2022 (10 bcm/year to Latvia and 3.7 bcm/y to Lithuania). Full capacity from January 2023.
- Interconnector Greece-Bulgaria, completed in October 2022 (3 bcm/y to Bulgaria and 3 bcm/y to Greece).
- Enhancement of Lithuania-Latvia interconnector, completed in December 2022 (4.1 bcm/y to Latvia and 3.7 bcm/y to Lithuania).

Offshore solutions have been carried out by the Netherlands, Germany, Finland, and Italy in record time. These countries have resorted to floating storage and regasification terminals (FSRU) to transport the LNG to their respective territories. In total, there are 6 FSRU terminals currently in operation with a total regasification capacity of 35 bcm/y and three additional FSRU terminals are expected to be commissioned in 2023. There is one new LNG terminal in operation (0.13 bcm/y) and three to be commissioned in 2023/2024 with a total capacity of 23.3 bcm/y. In short, 35.1 bcm/y of new regasification capacity can be found in the EU, while 35.3 bcm/y is to be expected by 2023/2024. The LNG terminals already in operation or to be commissioned soon are:

- FSRU terminal in Eemshaven (the Netherlands), completed in September 2022 with a regasification capacity of 8 bcm/y. Its daily regasification capacity in ALSI Transparency Platform is 249.6 GWh/d.
- Three FSRU terminals in Germany, i.e. Wilhelmshaven, Lubmin and Elbehafen, which started operations by December 2022, April 2023, and March 2023, respectively, with a total regasification capacity of 20.5 bcm/y. Their daily regasification capacities in ALSI Transparency Platform are 152.5, 155.8, and 61.6 GWh/d, respectively.
- FSRU terminal in Piombino (Italy), completed in April 2023 with a regasification capacity of 5 bcm/y. Its daily regasification capacity in ALSI Transparency Platform is 146.7 GWh/d.
- FSRU terminal in Inkoo (Finland), completed in December 2022 with a regasification capacity of 5.5 bcm/y.
- FSRU terminal in Alexandroupolis (Greece) which is to be commissioned by December 2023 with a regasification capacity of 5.5 bcm/y.
- Expansion of LNG terminal in Świnoujście (Poland), to be commissioned by December 2023 with a regasification capacity of 8.3 bcm/y.

Bi-directional flow capacity was already defined as another key tool to increase the security of supply in the EU in 2017 via Regulation (EU) 2017/1938. Enabling bi-directional flow between EU MSs is mandatory, unless exceptions are granted. This strategy was crucial during the energy crisis, as it supported the partial replacement of interrupted flows. A specific example for this is the Yamal pipeline, which until 2021 transported major gas flows from Russia and Belarus in the east to western European countries via Poland. The Yamal pipeline transported 263 TWh from Poland to Germany at Mallnow border transfer station in 2020, and after the reduction in flows from Russia in 2021, the pipeline supported flows in the opposite direction, transporting 33 TWh of gas to Poland from Germany (ENTSOG, n.d.). A detailed view of the changes in the net flow direction between EU MSs throughout several gas seasons surrounding the energy crisis is visualised in the JRC report (Fernandez Blanco Carramolino, et al., 2023).

4.5 Gas price developments

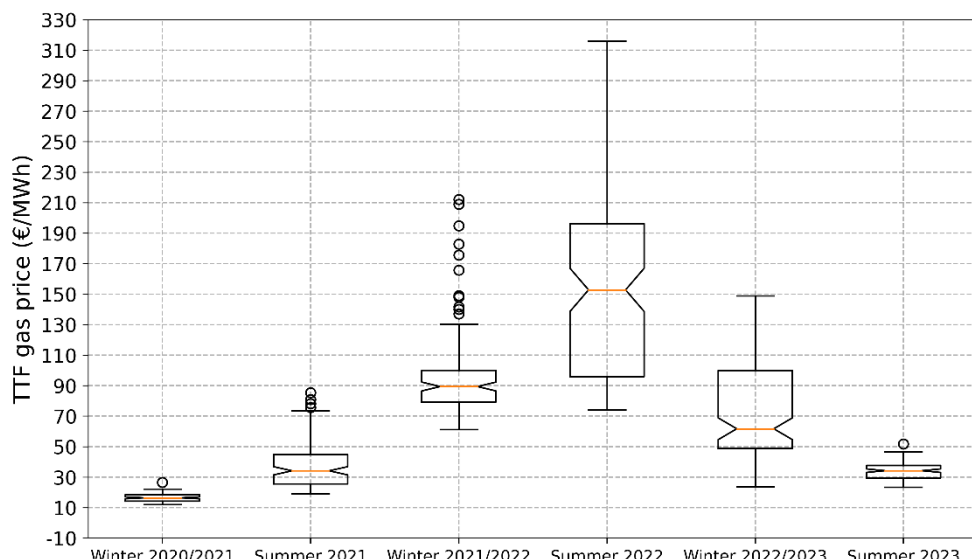
One of the most important trading hubs for natural gas is the Title Transfer Facility (TTF) Virtual Trading Point, operated by Gasunie Transport Services B.V., in the Netherlands. Typically, before the energy crisis, the day-ahead price traded at the Dutch TTF hub was closer to the day-ahead price from other EU trading hubs

for natural gas, such as the Spanish Punto Virtual de Balance, Belgian Zeebrugge, or the French Point d'Échange de Gaz (ACER, 2023). However, the energy crisis caused day-ahead price spreads among various gas trading hubs to increase significantly, especially from the end of February 2022 onwards. Therefore, we analyse the TTF day-ahead price for natural gas for the last six seasons, as represented in **Figure 10**.

The price stability is clear when looking at the day-ahead prices in winter 2020/2021, just before the start of the energy crisis. In that winter, the average price was around 17 €/MWh and the daily price oscillated between 10 and 30 €/MWh. We can observe an increase of the average price in the subsequent three seasons, i.e. during summer 2021, winter 2021/2022, and summer 2022. The average price increased up to 150 €/MWh on average in summer 2022. As previously mentioned, the price shock is not a static event and the EC policies have reacted to these price developments, e.g. with the market correction mechanism Regulation at the end of 2022 (Council Regulation (EU) 2022/2578 establishing a market correction mechanism to protect Union citizens and the economy against excessively high prices, 22 December 2022). The unprecedented price volatility has also increased over those four seasons, thus creating price uncertainty in the gas market. The first price spike happened on 21 December 2021 in which gas price reached around 180 €/MWh. The second price spike was at the start of the war in Ukraine with 210 €/MWh. During the summer 2022, there was a steady increase of day-ahead gas prices until attaining an all-time high price of circa 315 €/MWh at the end of August 2022.

In winter 2022/2023 and summer 2023, we can observe a clear reduction of average prices and price volatility, being the average price equal to 34 €/MWh in the summer of 2023 while its maximum peak was around 50 €/MWh. The price stabilization could have been driven by several factors: (i) the filling of gas storages at the beginning of the winter due to the Gas Storage Regulation, (ii) the reduction of gas demand incentivised by the Regulation (EU) 2022/1369, (iii) the mild winter 2022/2023 thus keeping a non-negligible amount of natural gas stored in EU gas storage facilities (around 55% of filling level), and (iv) the reliance on LNG supply for both winter (to satisfy the gas consumption) and summer (for ensuring the injection of gas in storages).

Figure 10. Boxplot of the daily TTF price (€/MWh) per season from winter 2020/2021 to summer 2023.



Source: JRC, 2023.

5 Discussion and conclusions

The 2022 energy crisis has tested the EU natural gas system's ability to absorb abrupt and drastic changes to its supply and market. Despite the decreasing flows from Russia and the price hike during 2022, the natural gas system has returned to a new status quo predominantly pushed by the political actions carried out in the last two years, and the mild weather conditions during the heating season.

The current natural gas system is characterised by a higher share of LNG supply than in previous years to partially replace the missing import pipeline gas flows from Russia. The gas supply has become less

dependent on individual gas exporters and on pipeline gas. This allows the system to adapt more quickly and flexibly to changes to the geopolitical stances of both natural gas exporters and the EU on the importing side that could affect the security of supply in the future. LNG terminals are the new cornerstone of the EU natural gas system, together with UGS facilities, which provide the flexibility needs required in winter and summer. The EU natural gas system has been reinforced by new infrastructure projects, such as the new FSRU LNG terminals in the Netherlands, Germany, and Finland, and the pipelines that started operation in 2022. Hardening the gas infrastructure has helped to implement the policy measures in a timely and effective way (minimum storage obligations and reduction of consumption of natural gas). These recovery efforts of strengthening the infrastructure and retaining high storage filling levels have increased energy security, but at a high cost.

The new equilibrium is also marked by a lower natural gas consumption, which has been one of the collateral impacts of the energy crisis. Not all demand reductions in the EU were achieved by increased energy efficiency alone – a fraction of the demand was certainly destroyed by consumers who could not afford to pay the exceptionally high prices. Moreover, the energy crisis is still ongoing and the natural gas sector should remain vigilant in order to keep the security of supply at all times. The return of the gas consumption to pre-crisis levels could increase the need for higher LNG send-out flows, which would affect in turn the prices in the gas market. Additionally, despite the high storage levels buffering the system for winter 2023/2024, uncertainty remains, for example in the LNG market and the weather conditions affecting the thermosensitive gas consumption.

Handling these challenges will require strong cooperation and solidarity between MSs, as adopted in Regulation (EU) 2022/2576. The implementation of the Regulation needs to be monitored and reviewed in light of new threats, and its benefits and successes should be communicated to encourage continued support for solidarity in policy and society. In light of the uncertain geopolitical situation and compounding crises increasing pressure onto the European Union, solidarity fatigue in society could endanger the successful implementation of a collaborative resilience policy in the EU. Encouraging solidarity and collaboration on a political and societal level may also aid the recovery from economic damages caused by demand destruction during the energy crisis.

The EU natural gas system has proved itself resilient to the extent that the supply of natural gas was consistently secured despite the abrupt decline of pipeline supply from Russia in a time of low gas levels in storage and extremely high energy prices. The system has formed a new status quo of strengthened cooperation between the MSs. The natural gas system's resilience was supported by diversified supply, reduced demand, reinforced infrastructure, and a strong storage strategy.

Disclaimer

The views expressed here are purely those of the authors and may not, under any circumstances, be regarded as an official position of the European Commission.

References

- [1] S. Hosseini, K. Barker and J. E. Ramirez-Marquez, "A review of definitions and measures of system resilience," *Reliability Engineering & System Safety*, vol. 145, pp. 47-61, 2016.
- [2] E. D. Vugrin, D. E. Warren and M. A. Ehlen, "A resilience assessment framework for infrastructure and economic systems: Quantitative and qualitative resilience analysis of petrochemical supply chains to a hurricane," *Process Safety Progress*, vol. 30, no. 3, pp. 280-290, 2011.
- [3] Regulation (EU) No 994/2010 of the European Parliament and of the Council concerning measures to safeguard the security of gas supply and repealing Council Directive 2004/67/EC, Brussels: Official Journal of the European Union, 20 October 2010.
- [4] Regulation (EU) 2017/1938 of the European Parliament and of the Council concerning measures to safeguard the security of gas supply and repealing Regulation (EU) No 994/2010, Brussels: Official Journal of the European Union, 25 October 2017.
- [5] R. Fleming, "A legal perspective on gas solidarity," *Energy Policy*, vol. 124, pp. 102-110, 2019.
- [6] IEA, *Global Energy Crisis*.
- [7] R. Fernandez Blanco Carramolino, R. Schill, A. Costescu, J.-F. Vuillaume, D. Jung, H. Filipe Calisto, J. Ichaso Franco, L. Lo Presti, D. Pozo Camara, N. Rodriguez Gomez and R. Bolado Lavin, "Monitoring the security of gas supply in the European Union," Publications Office of the European Union, Luxembourg, 2023.

- [8] M. Gil Tertre, I. Martinez and M. Rivas Rábago, Reasons behind the 2022 energy price increases and prospects for next year, Centre for Economic Policy Research, 2023.
- [9] European Commission Directorate-General for Energy, "Annual Activity Report 2022," European Commission, Brussels, 2022.
- [10] ENTSOG, "ENTSOG Transparency Platform," [Online]. Available: <https://transparency.entsog.eu/>. [Accessed 1 July 2023].
- [11] S. Jacobsen and K. Abnett, Nord Stream ruptures revealed as Europe grapples with gas plan, Copenhagen/Brussels, 2022.
- [12] Directive 98/30/EC of the European Parliament and of the Council concerning rules for the internal market in natural gas, Brussels: Official Journal of the European Communities, 22 June 1998.
- [13] Directive 2003/55/EC of the European Parliament and of the Council concerning common rules for the internal market in natural gas and repealing Directive 98/30/EC, Brussels: Official Journal of the European Union, 26 June 2003.
- [14] Tackling rising energy prices: a toolbox for action and support, Brussels: European Commission, 2021.
- [15] REPowerEU Plan, Brussels: European Commission, 18 May 2022.
- [16] Regulation (EU) 2022/1032 of the European Parliament and of the Council of 29 June 2022 amending Regulations (EU) 2017/1938 and (EC) No 715/2009 with regard to gas storage, Brussels: Official Journal of the European Union, 30 June 2022.
- [17] Council Regulation (EU) 2022/1369 on coordinated demand-reduction measures for gas, Brussels: Official Journal of the European Union, 5 August 2022.
- [18] Council Regulation (EU) 2022/1854 on an emergency intervention to address high energy prices, Brussels: Official Journal of the European Union, 6 October 2022.
- [19] Council Regulation (EU) 2022/2576 enhancing solidarity through better coordination of gas purchases, reliable price benchmarks and exchanges of gas across borders, Brussels: Official Journal of the European Union, 19 December 2022.
- [20] Council Regulation (EU) 2022/2578 establishing a market correction mechanism to protect Union citizens and the economy against excessively high prices, Brussels: Official Journal of the European Union, 22 December 2022.
- [21] GIE, "AGSI+ Transparency Platform," [Online]. Available: <https://agsi.gie.eu/>. [Accessed 1 July 2023].
- [22] GIE, "ALSI Transparency Platform," [Online]. Available: <https://alsi.gie.eu/>. [Accessed 1 July 2023].
- [23] D. Jung, J.-F. Vuillaume, R. Fernandez Blanco Carramolino, H. Filipe Calisto, N. Rodriguez Gomez and R. Bolado Lavin, "Tools for analysing the European natural gas system with public data – The Python package eurogastp," EUR 31281 EN, Publications Office of the European Union, Luxembourg, ISBN 978-92-76-58764-4, doi:10.2760/153669, JRC130771., 2022.
- [24] SWD(2023) 63 final, "Analysis of coordinated demand reduction measures for gas, Accompanying the document REPORT FROM THE COMMISSION TO THE COUNCIL, review on the functioning of Regulation (EU) 2022/1369 on coordinated gas demand reduction," Brussels, 2023.
- [25] Statistical Office of the European Union, "Eurostat," [Online]. Available: <https://ec.europa.eu/eurostat/web/main/home>. [Accessed 5 July 2023].
- [26] N. Zaccarelli, S. Giaccaria, M. Feofilovs and R. Bolado-Lavín, "The European Natural Gas Demand database (ENaGaD)," Publications Office of the European Union, Luxembourg, 2021.
- [27] Regulation (EC) No 715/2009 of the European Parliament and of the Council on conditions for access to the natural gas transmission networks and repealing Regulation (EC) No 1775/2005, Brussels: Official Journal of the European Union, 13 July 2009.
- [28] Council Regulation (EU) 2023/706 amending Regulation (EU) 2022/1369 as regards prolonging the demand-reduction period for, Brussels: Official Journal of the European Union, 30 March 2023.
- [29] European External Action Service, "Energy policy is at the centre of EU foreign policy," 20 May 2022.
- [30] Directorate-General for Energy, REPowerEU - one year on, European Commission, 24 May 2023.
- [31] ACER, "Market Correction Mechanism. Preliminary data report," European Union Agency for the Cooperation of Energy Regulators, 2023.

2.3 Resilience enhancement of gas transmission system by remote control deployment of valves: methodology of indicator analysis and case study

Bogdan Vamanu, Horia Hulubei National Institute of Physics and Nuclear Engineering, Bucharest, Romania
bvamanu@nipne.ro

Vytis Kopustinskas, European Commission, Joint Research Centre (JRC), Ispra, Italy
vytis.kopustinskas@ec.europa.eu

Vladislavas Daškevičius, Andrius Dagys, AB Amber Grid, Vilnius, Lithuania
v.daskevicius@ambergrid.lt, a.dagys@ambergrid.lt

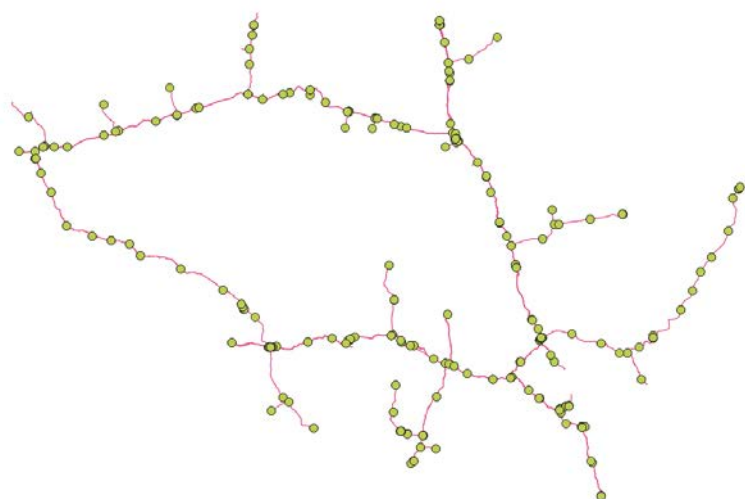
Abstract

The paper presents a study that aims to develop a priority list of main valves of the gas transmission network that should be connected to SCADA for remote monitoring and control. Remotely controlled valves are necessary to quickly localize accidents, minimize methane release into atmosphere and enable rerouting of the gas flow to ensure security of supply. Although the highest system resilience is achieved when connecting all main valves, this process is long and therefore must be prioritized as not all valves have the same importance for the system operation.

Extended abstract

The work presented was co-funded under Horizon 2020 framework by SecureGas project. The study aims to develop a priority list of main valves of the gas transmission network that should be connected to SCADA for remote monitoring and control. The priority list involved development of a multi-criteria decision tool [1] as many different parameters should be considered for connection of a valve to SCADA. The gas network used for a case study was a realistic topology of a real network, but slightly simplified only for computational purposes. The study used the network GIS geodatabase and all calculations were performed by using QGIS software platform. The whole network valves topology is shown in Figure 1. The total number of valves is 1356. However not all valves are eligible for the SCADA connection. The number of valves that were analysed for possible SCADA connection is significantly lower and includes 349 valves that were priority ranked.

Figure 11. The gas network topology of all valves



Each parameter was quantified on a unified scale and then the total priority score was obtained by applying a specific weighting scheme [2, 4]. The following quantitative and qualitative criteria were used for the ranking: pipeline importance in terms of security of supply [3]; pipeline diameter; type of customers served and

demand volumes (protected, industrial); valve accessibility (distance to the roads); land use parameters and hazard zones (forest areas, flood areas, swamps); costs of installation and maintenance; networks topology (number of valves in close vicinity, within 300 meters). These criteria were further developed and applied for the valve topology in QGIS software, obtaining individual scores of some indicators directly from QGIS computational routines.

The final priority list of over 500 valves strongly depends on weights that individual indicators are assigned. The weights were assigned by experts applying expert judgment techniques (Table 1).

Table 2: Structure of the resilience indicator framework.

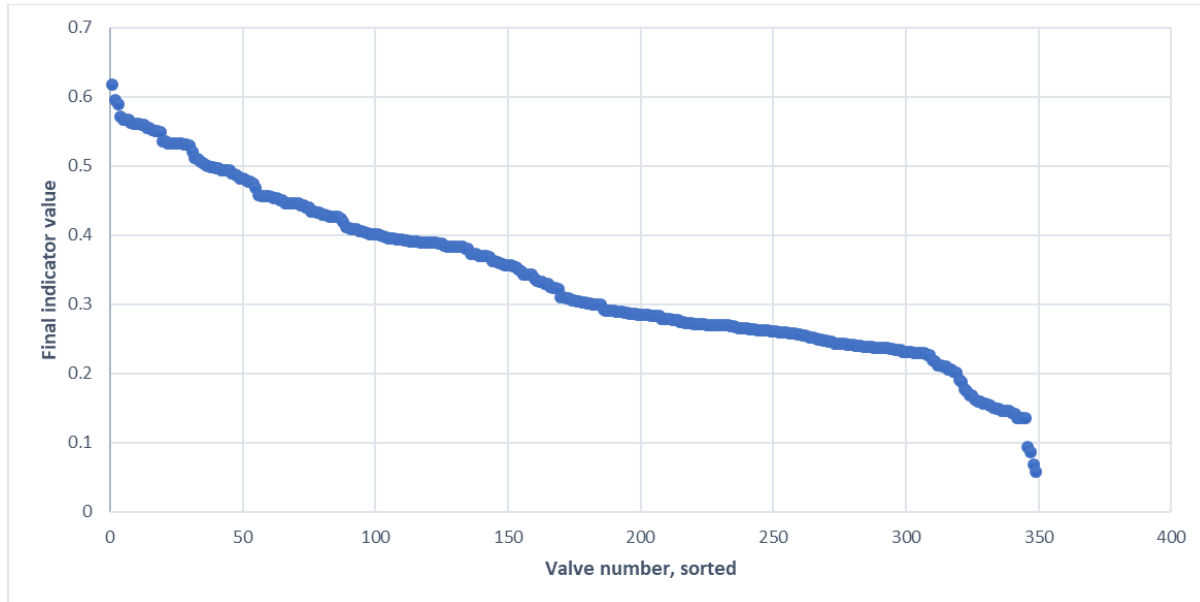
| Indicator ID | Description | Importance Score | Weighting factor |
|--------------------------------|--|-------------------------|-------------------------|
| Topological indicators | | | |
| T1 | Pipeline diameter | 10 | 0.124 |
| T2 | Distance to GDS (only if branch) | 5 | 0.062 |
| T3 | Gas consumption (sum of all GDS (DSS) in a branch) | 9 | 0.111 |
| T4 | Clustering within 300 meters | 8 | 0.099 |
| Geographical indicators | | | |
| G5 | Off-road/bad road distance to valve | 4 | 0.049 |
| G6 | River crossing | 10 | 0.123 |
| G7 | Wet land area (wet land ratio in a line) | 6 | 0.074 |
| G8 | Forest area (forest area length ratio in a line) | 4 | 0.049 |
| Safety indicators | | | |
| S9 | Residential area (ratio in a line) | 8 | 0.099 |
| S10 | Absence of internal diagnostics | 10 | 0.124 |
| S11 | Reduced pressure pipeline segments | 7 | 0.086 |

Each valve ranking indicator shown in Table 1 was assessed individually and computed independently from the others as described in the section above. In order to be numerically comparable, the numerical scale must be the same for all indicators. The scale used in this study is a real value range [0, 1] where 0 means the lowest priority for the SCADA connection and 1 – is the highest priority. For the scale normalization, the indicators T1-T4 and G5 were normalized by dividing each value by the maximum value of each indicator. The remaining indicators were already in the scale of [0, 1] as they are either binary or ratios.

Furthermore, each numerical indicator value is multiplied by the weighting factor, shown in the last column of Table 1. After multiplication, all individual indicators are summed up to produce the final indicator value, which allows to prioritise the valves. Due to weighting factor applied, and noting that the sum of all weighting factors is equal to 1, the range of the final indicator value is again in the range of [0, 1]. This allows easy ranking of the valves for SCADA connection by simply ranking them in descending order. The valves appearing on the top are those with the highest priority.

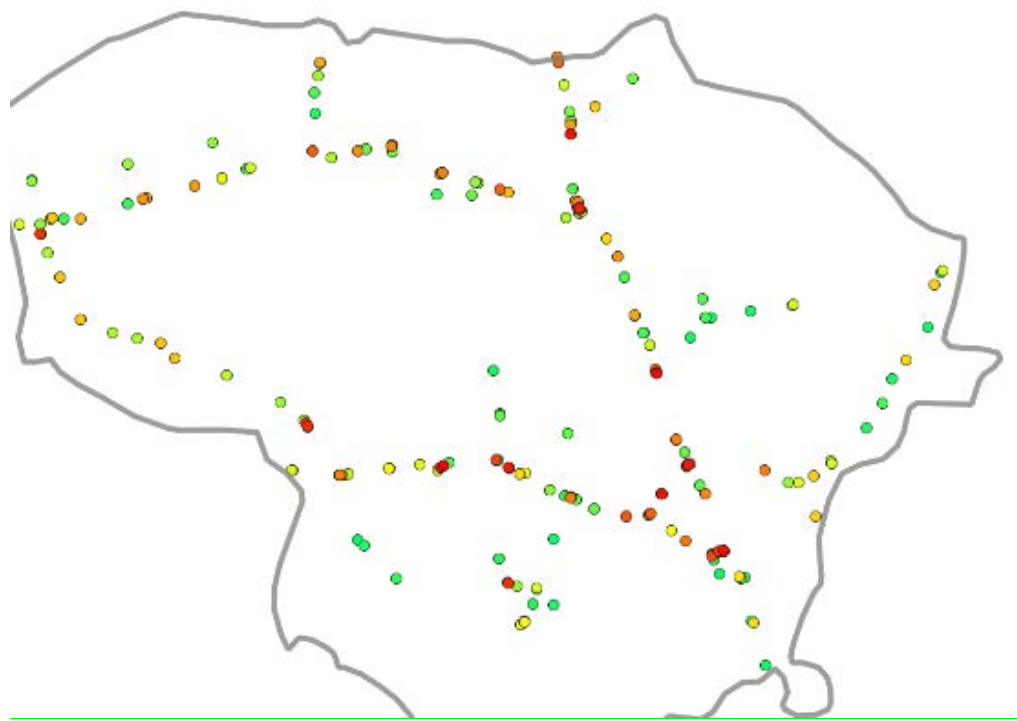
The ranking results of 349 valves are shown graphically in Figure 2. As you see, the highest ranked valve obtained the final indicator value 0.62, and the lowest – 0.06. Note that the first 3 highest ranked valves and the last 4 lowest ranked valves are slightly detached from the middle group of valves that are ranked more continuously. This result is typical in ranking tasks and some items always have extreme values. however, in general the ranking is rather smooth and homogenous across the whole range.

Figure 2. The ranking results of 349 valves



In addition, the valves were visualised in QGIS software platform for easier navigation and search. Figure 3 shows all 349 valves with priority colours: red – highest priority, green – lowest priority.

Figure 3. Prioritisation of all valves



The priority ranking of the valves for SCADA connection is an important operational task to help planning the network control activities. The methodology developed and implemented relies on correct information in the GIS geodatabases and therefore completeness and correctness of GIS geodatabases is essential for obtaining correct priority ranking of the valves. The application of the methodology illustrates how GIS geodatabase can be efficiently used to obtain important operational findings and results.

References

1. B. Vamanu, A. Gheorghe, P. Katina, Critical Infrastructures: Risk and Vulnerability Assessment in Transportation of Dangerous Goods, Springer, 2016. doi: 10.1007/978-3-319-30931-6.
2. Vamanu, B., Martišauskas, L., Karagiannis, G., Masera, M., Krausmann, E., Kopustinskas, V., Development of indicator framework for critical energy infrastructure, European Commission, Ispra, 2021, JRC125802.
3. V.Kopustinskas, P.Praks, Identification of the main contributors to the security of supply in a gas transmission network, Proceedings of PSAM14 conference, IAPSAM, 2018.
4. Kopustinskas V., Praks P., Methodology to assess resilience of critical energy infrastructure - Project CEI-Resilience, Deliverable 1, European Commission, Ispra, 2018, JRC115179.

2.4 Application of metaheuristic algorithms for finding strategy of optimal response to natural gas supply disruptions

Ivars Zalitis, Laila Zemite and Aleksandrs Dolgicers, Riga Technical University, Institute of Power Engineering, Latvia, Ivars.Zalitis@rtu.lv, Laila.Zemite@rtu.lv, Aleksandrs.Dolgicers@rtu.lv

1 Introduction

Modelling-based risk and resilience analysis for gas networks (GNs) has seen continuous development. One of such approaches considers mainly the network structure and its flowrate limitations and combines the Monte-Carlo method with the maximum flow algorithm for various resilience analysis tasks [1], [2]. This allows one to perform probabilistic simulation-based analysis while considering main network supply and transmission capabilities as well as structure. The proposed solution applies a more detailed approach to both physical modelling of GN operation and potential demand curtailment simultaneously achieving a boost in performance. There are methods and software tools, which even simulate integrated gas-electricity systems (IEGSs) [3] sometimes incorporating transient simulations [4] when analysing their normal and post-contingency operation. In comparison the proposed method avoids the additional computational complexity and burden of transient simulations by operating with several steady-state simulations (SSSs) throughout the disruption event, which are then linked with a secondary optimisation layer. Furthermore, regular model updates during simulations allows for better representations of pressure regulators (PRs), gas storages, operation of bi-directional or multi-directional compressor stations (CSs) and their network-wise control than some methods that model IEGSs. Additionally, the proposed method provides an option to consider consumer groups, their proportions and differentiate their supply priority levels for any demand node, which is not observed by the authors to be present for other known solutions.

This work describes a framework for an updated version of the method for synthesis of an optimal response strategies (ORSs) to GN disturbances, which ensures maximum possible supply of gas to highest priority consumers [5]. An ORS consists of necessary demand curtailment levels and decisions on utilisation of available reserve sources. Simultaneously, this algorithm determines the minimum value of expected unsupplied gas due to a disruption for identification of critical GN elements and other resilience analysis tasks. The proposed method addresses the disconnection between individual time intervals or points of disruption duration optimised separately in [5], which can lead to slightly sub-optimal solutions when considering the whole track of disturbance mitigation, while avoiding full complexity associated with the dynamic programming. This is achieved essentially by separation of ORS synthesis process into two stages. First, an “inner” layer of the genetic algorithm (GA)-based optimisation is performed for each specific time interval identifying sets of near optimal solutions. The term “near” is defined as *genome* distance from optimum found. When a set of possible “ad hoc” optimums is collected second or “outer” layer of GA is utilised to find the most optimal combination (or trajectory) of these solutions for the whole disturbance duration. Such an approach reduces variable space and computation burden while maintaining precision. Furthermore, the new method has more flexibility to adapt gas supply rates from gas sources during a disruption, which allows to generate more diverse solution variants for the outer layer to operate with.

2 The proposed method framework

The inner GA layer operates on the same principles as the original method [5] selecting optimal demand curtailment levels for a modelled gas transmission system local demand and transit demand nodes and activating reserve sources if necessary for each time interval during a disturbance:

$$\min_{F_{\text{OBJ}} \in [0, \infty)} F_{\text{OBJ}} = \min_{V_{\text{CURTi}} \in [0, V_{\text{DEM}i}]} \sum_{i=1}^{MS} (K_{Pi} V_{\text{CURTi}}), \quad (1)$$

where F_{OBJ} — the objective function: the total weighted volume of unsupplied gas, m³;

MS — the number of nodes in a GN graph;

K_{Pi} — the penalty coefficient for demand curtailment of node i of a GN graph;

V_{CURTi} — the volume of curtailment or gas not supplied to node i of a GN graph, m³;

i — GN graph node index;

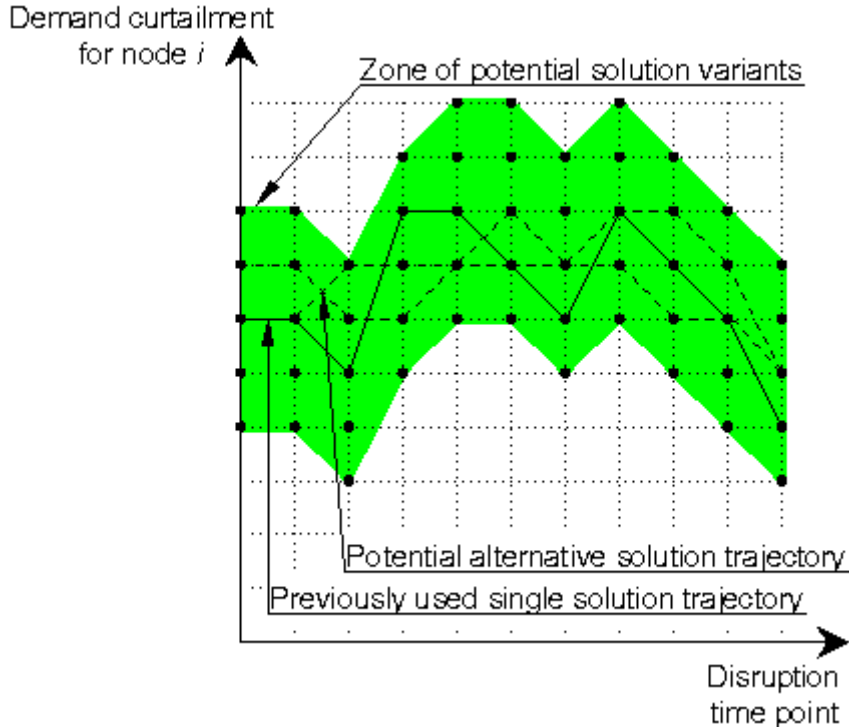
$V_{\text{DEM}i}$ — the total demanded gas volume for node i of a GN graph, m³.

The physical limitations both for pipelines and non-pipeline elements described in [5] also remain in power. All of the PR and CSs control mechanics and the consumer categorisation with specific curtailment limits defined by a user for each category will be considered as described in [5] as well. Thus, the merits of the original method compared to other existing methods will be retained.

The First major change of the inner GA layer is to allow the optimisation to define boundaries of gas supply rates for all sources (including transit reserve supply) in each time interval so that the total expected available gas volume supplied during the whole disruption is not exceeded. To some extent the original method [5] allows to manually redefine source supply profiles and to define and automatically consider impact of underground storage depletion on maximum withdrawal rate. However, the addition of automatic consideration of different gas consumption rates for all sources will enable more flexibility to generate solution variants necessary to generate best possible ORSs.

The second change is related to use of potential optimal solutions. Instead of selection of one solution with a minimal F_{OBJ} value, 5–10 best solutions from a final population are chosen. If necessary additional boundaries for genetic similarity to a present best solution or potential differences in F_{OBJ} may can be applied when selecting the solution group for a particular time interval. It is important to note, that genome similarity or genetic distance can be used as a quantitative metric permitting one to consider a set of possible solutions as a metric space. Furthermore, the logic-based ORS refinement with a smaller step of demand curtailment changes from [5] are applied to all of the selected solutions. Essentially, this change provides a zone of potential sub-optimal solutions during a disruption instead of one solution trajectory (Figure 1). These solution groups will already exclude solutions that are unacceptable due to GN limitations or excessive demand curtailment, thus, avoiding the complexity caused by consideration of all of potential solutions in a real life GN faced by the dynamic programming or single GA layer performing optimisation for a whole duration of a disturbance.

Figure 12. Transition from a single trajectory to a zone of potential solution variants.

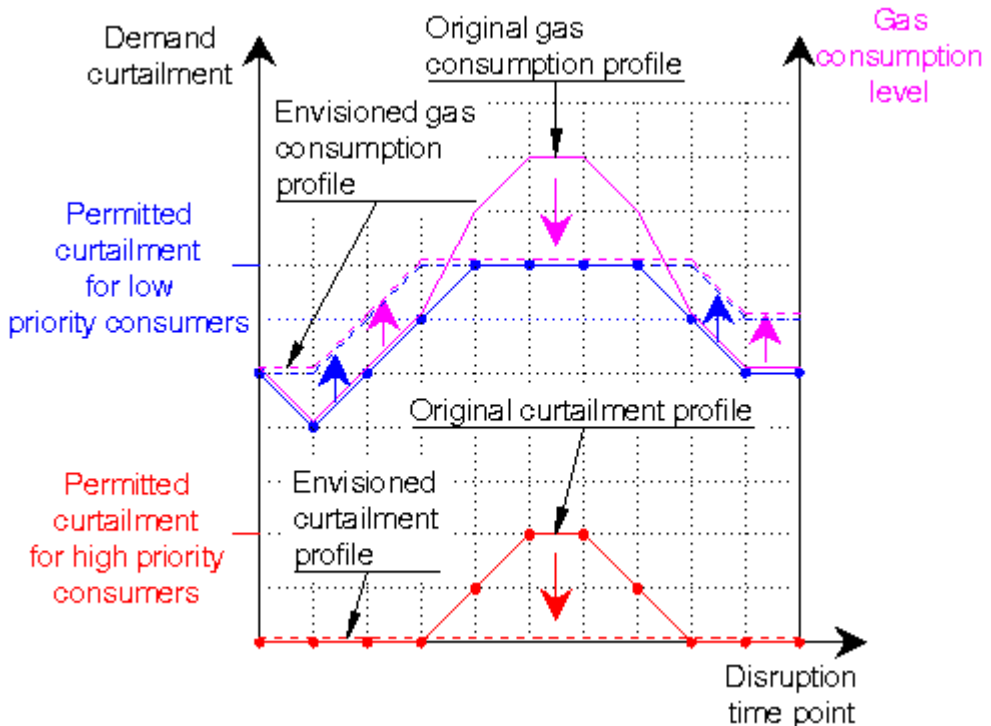


When such solution groups have been obtained for the whole duration of a disturbance the outer GA layer is activated. The outer layer operates utilising the same objective function (1) only extended to a sum of weighted unsupplied gas volume for all of the time intervals of a disruption defined by a user. The most substantial difference compared to the inner layer are the envisioned decision variables, which are the selected and now fixed solution variants not the particular demand curtailment volumes of individual demand nodes. Thus, the task of the outer GA layer is only the selection of the most optimal trajectory of solutions from the pre-defined zone of potentially sub-optimal solutions.

3 Envisioned results

The change from the original method [5] to this two layer optimisation is proposed as this should allow to shift demand curtailment profiles of lower priority consumer groups or nodes and total gas consumption profiles within the duration of a disturbance (Figure 2). Thus, one could avoid potential curtailment of higher priority consumers during peak demand simply because a gas consumption rate is assumed pre-defined and fixed for each time interval. To a smaller degree than shown in Figure 2 this issue was observed in [5] for a scenario where only the gas remaining within the pipelines (*Linepack*) was available as a GN network part was disconnected from all real sources. However, it is foreseen that the automatic ability to modify the gas supply rates from active and reserve gas sources will also provide ORS with even lower volumes of unsupplied gas due to the new flexibility when the GN limits allow it.

Figure 2. Envisioned resulting shift in demand curtailment and gas consumption profiles.



As one can see the intended improvement in flexibility of the existing method for generation of ORSs comes at a cost of larger memory use, scale of which should not pose significant problem for modern computers, and a larger computational burden for the inner optimisation layer generating the zone of potential solutions. The addition of the outer optimisation layer in comparison will result only in a fraction of computational work, as it is not foreseen to need to perform SSSs to verify the technical feasibility of the selected solution variants.

4 Conclusions

Methods for risk and resilience analysis of transmission networks of natural gas and other gaseous fuels is continuously evolving. One of directions for development of such methods is implementation of mathematical modelling of GN operation, where one often seeks to consider more technical aspects of network capabilities and operation than previous works when performing risk or resilience analysis. To some extent this what the proposed method and its previous version pursue while attempting to limit the computational burden so that this solution can be applied to large scale real-life networks.

The proposed method builds upon previously developed method for minimisation of impact of disruptions on gas supply. The original method optimises gas demand curtailment and decides on use of reserve sources during a disruption while considering detailed consumer categorisation and various technical aspects of GN operation, which allows the proposed method to also have the same edge over many other existing solutions.

The proposed method intends to permit more flexibility for supply rates from gas sources during a disruption, which was previously pre-defined and fixed for each time interval. Furthermore, instead of utilising only one best solution from a last population obtained by the inner GA layer, a group of potential solutions will be saved to obtain a zone of potential solutions in comparison to a one solution trajectory during a disruption. These two changes to the inner optimisation layer will permit the new outer GA-based optimisation layer to achieve more flexibility and find ORSs with even lower expected demand curtailment for various disruption scenarios.

The future work entails refinement of mechanics for effective changes of gas supply rates for gas sources based on the total available gas volume and technical or organisational limits for specific time intervals. This will be followed by implementation and testing of the overall methodological framework described in this work.

References

1. Kopustinskas, V., and Praks, P., Effect of investments to security of gas supply: A probabilistic cost-benefit case study, In: M. Cepin and R. Bris (Eds.) Safety and Reliability – Theory and Applications, Proceedings of the 27th European Safety and Reliability conference, Portorož, Slovenia, June 18-22 2017. pp. 177–181. DOI: 10.1201/9781315210469.
2. Senderov, S.M., and Vorobev, S.V. Approaches to the identification of critical facilities and critical combinations of facilities in the gas industry in terms of its operability. Reliability Engineering and System Safety, Vol. 203, 2020, pp. 1-11. DOI: 10.1016/j.ress.2020.107046.
3. Bao, Z., Jiang, Z., and Wu, L. Evaluation of bi-directional cascading failure propagation in integrated electricity-natural gas system. International Journal of Electrical Power and Energy Systems, Vol. 121, 2020, pp. 1-10. DOI: 10.1016/j.ijepes.2020.106045.
4. Pambour, K.A., Erdener, B.C., Bolado-Lavin, R., and Dijkema, G.P.J. SAInt – A novel quasi-dynamic model for assessing security of supply in coupled gas and electricity transmission networks. Applied Energy, Vol. 203, 2017, pp. 829-857. DOI: 10.1016/j.apenergy.2017.05.142.
5. Zalitis, I., Zemite, L., Ganter, S., Kopustinskas, V., Vamanu, B., Finger, J., Fuggini, C., Bode, I., Kozadajevs, J. and Haring, I. Mitigation of the Impact of Disturbances in Gas Transmission Systems. International Journal of Critical Infrastructure Protection, Vol. 39, 2022, pp. 1-17. DOI: 10.1016/j.ijcip.2022.100569.

2.5 Hydrogen electrolyzers as a flexible source for the optimal operation of the distribution grid

Irina Oleinikova and Basanta Raj Pokhrel, Department of Electric Energy, Norwegian University of Science and Technology, Norway, irina.oleinikova@ntnu.no, basanta.r.pokhrel@ntnu.no

Marius Rasmussen and Sofie Lorentzen, Department of Electric Energy, Norwegian University of Science and Technology, Norway, marius.rasmussen@ntnu.no, sofie.lo@stud.ntnu.no

Abstract

The share of low-emission hydrogen production is expected to increase dramatically over the next decade, from 10% in 2020 to 70% in 2030. This trend is expected to continue as more and more countries recognize the importance of hydrogen in achieving Net Zero emissions. The purpose of this paper is to explore the potential role of low-emission hydrogen produced through electrolysis in the future energy system, and to examine the implications for the distribution grid when it is used to provide electricity for electrolysis. Additionally, the paper will discuss which electrolysis technologies are most suitable for optimal operation and can help avoid unnecessary upgrades to the electrical distribution grid. As well as it will demonstrate how the flexible operation of a water electrolyser can be utilized to minimize the impacts of electrification. Real network data has been used to create a realistic network model in the simulation tool DlgSILENT Power Factory. Real load data has been implemented in the software to enable simulations based on daily, weekly, and yearly cases, forming the basis for scenario creation.

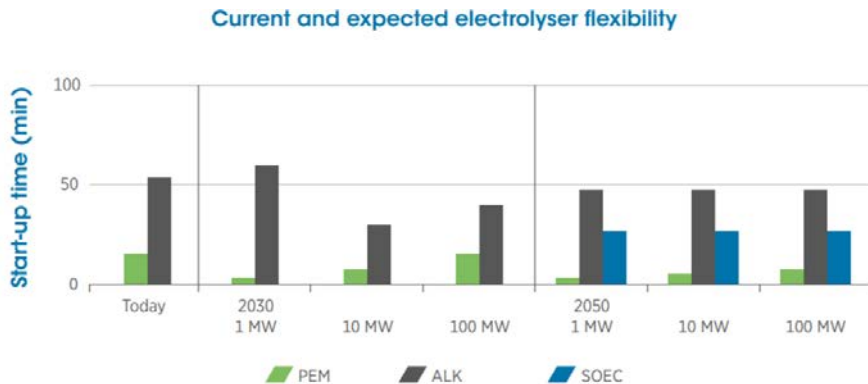
1 Introduction

It is estimated that 40% of the energy used for hydrogen production in 2030 will come from electricity [1]. Of this electricity, 2700 TWh should be generated from renewable sources. The share of low-emission hydrogen production is expected to increase dramatically over the next decade, from 10% in 2020 to 70% in 2030 [2]. The targets for electrolysis capacity installation have more than doubled from 2021 to 2022, from 74 GW in 2021 to 145-190 GW in 2022 [1]. This trend is expected to continue as more and more countries recognize the importance of hydrogen in achieving Net Zero emissions. According to recent plans, the European Union (EU) has set a goal of installing 40 GW of electrolyzers by 2030[3], with the primary goal of developing renewable hydrogen using wind and solar energy. Electrolysis is considered the most viable path for achieving this goal, and the EU has set a target of installing 6 GW of renewable hydrogen electrolyzers by 2024. Norway has set ambitious goals to reduce its greenhouse gas emissions in the coming decades. By 2050, Norway plans to become a low-emission society in which 90-95% of greenhouse gases are eliminated [4].

To meet the goal of net zero emissions by 2050, it is necessary to phase out hydrogen production from fossil fuels and coal and adopt more sustainable methods, such as hydrogen production from natural gas with carbon capture and storage, or hydrogen produced through electrolysis using renewable electricity. While the former significantly reduces the carbon footprint, the latter has the potential to almost eliminate emissions completely.

Therefore, electrolysis may play a crucial role in the transition to a net zero society, and it is important to investigate how to implement this technology in the daily grid operations.

Figure 13. Trend of electrolyser flexibility development.



Electrolysers can add flexibility to the demand side of the power grid, and improvements in startup times are expected in the future [5]. The trend is shown in Figure 13 above.

2 Hydrogen production

Electrolysers are a key technology for the development of a low emission society, as they use renewable or nuclear electricity to produce low-emission hydrogen. Despite their potential, only about 0.1% of the world's hydrogen production currently comes from water electrolysis [6]. However, it is expected that this will significantly increase in the future. From 2020 to 2021, the installed capacity of electrolysers increased by almost 70%, or 210 MW, to reach 510 MW [6]. It is anticipated that the electrolyser capacity will reach 1 GW by this year, and potentially even 1.4 GW if all planned projects are completed. To minimize costs, it is optimal to operate an electrolyser within the range of lowest hydrogen cost. One of the examples is to have a model to identify the optimal trails for the SOECs to be operated economically over the extended periods of time, with minimum degradation rate [7].

Figure 14. Mix of hydrogen production [6]

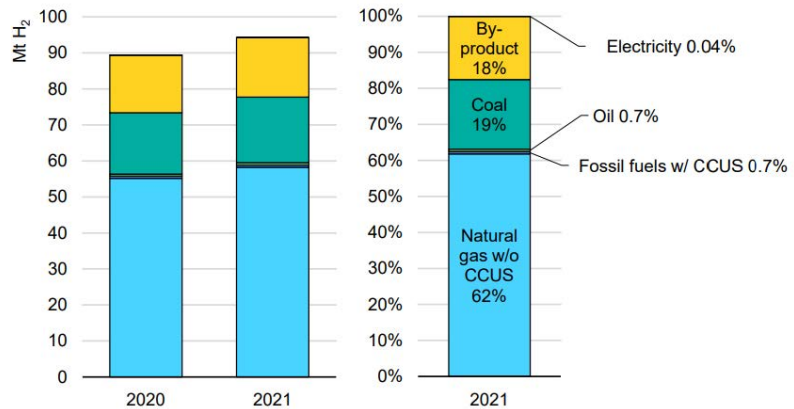


Figure 14 visualizes the share of globally produced hydrogen with different technologies, namely with electricity, as a byproduct, with coal, oil, and natural gas with and without carbon capture, utilization, and storage. According to IRENA classification [8] exist different shades of hydrogen, listed below.

2.1 Grey hydrogen

Grey hydrogen represented more than 80% of the produced hydrogen in 2021, according to the graph in Figure 14, and is produced from coal or natural gas i.e., mainly methane [8]. The process performed is either producing hydrogen by steam methane reforming, in which as the name indicates methane is used, or coal gasification. Both processes involve large CO₂ emissions and is unsuitable for a future net zero society.

2.2 Blue hydrogen

Blue hydrogen only represented 0.7% of the produced hydrogen in 2021, according to Figure 14. Blue hydrogen is very much similar as grey hydrogen but provides an 85% – 95% capture of the emitted carbon. This method allows continuation in usage of the already existing equipment for production of grey hydrogen

but with significantly lower greenhouse gas emissions. Production of blue and grey hydrogen do both require fossil resources, making them vulnerable to fluctuations in prices [8].

2.3 Turquoise hydrogen

Turquoise hydrogen is still in the interface between demonstration and market uptake. The process uses natural gas and does not produce CO₂ [8]. Instead, the carbon atoms from the methane molecules are turned into solid carbon black through pyrolysis.

2.4 Green hydrogen

Green hydrogen only represented 0.04% of the produced hydrogen in 2021 and is produced through electrolysis with renewable electricity as the energy source. Despite its low fraction of the total hydrogen production, the interest for green hydrogen has increased significantly over the last years and is well suited for the net zero route. However, there are several barriers such as expensive production, need for infrastructure and lower efficiency that need to be overcome for the upscaling of green hydrogen to take place [8].

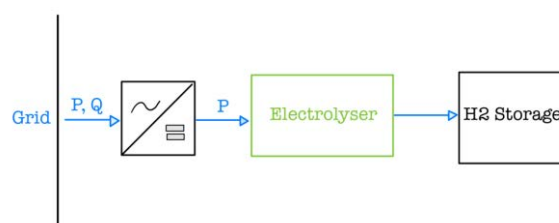
Producing hydrogen through electrolysis requires a reliable and resilient electricity grid. Distribution network operators might need more regulations in place to ensure efficient handling of bottlenecks and maintain quality. The current trend of electrification is already putting the grid under strain and adding electrolyzers for hydrogen production will further increase the demand for upgrades. To avoid unnecessary upgrades to the grid, one alternative could be to design electrolyzers with some flexibility, allowing them to reduce their energy consumption during times of peak power demand. This comes at the cost of reduced hydrogen production, but optimal solutions may be found by maximizing the combined utility value of delayed grid reinforcements and the flexibility of electrolyser operations.

3 Electrolysers connected to the grid

Electricity production and consumption must be balanced to maintain a stable grid. When demand for electricity decreases, production must decrease as well, while when demand increases, production must increase. This balance is maintained with power reserves, which must always have a certain amount of available capacity. If production exceeds demand, downregulation is performed, while if consumption exceeds production, upregulation must be carried out[9]. The integration of RES into the grid can introduce instability due to the unpredictable nature of their production, which cannot be controlled. As a result, they are not able to contribute to grid balancing, except through the undesirable process of curtailing production.

The operational patterns for hydrogen production will have different consequences for the distribution grid, depending on the economic feasibility of production. Therefore, it is important to develop various scenarios and analyse the specific consequences for each case. By simulating hydrogen production from a specific grid, the impacts of importance would be clearer and optimal operation of hydrogen production could be more accurately defined. This could help to better understand the optimal ways to integrate hydrogen production into the grid as shown in Figure 15. As energy-intensive technology, electrolyzers can be operated to support the grid by regulating the input power based on the grid's condition, to deliver system services, participating in ancillary markets.

Figure 15. Layout for the grid connected electrolyser system [10]



Different solutions such as energy storage, demand response, and curtailment of variable renewable energy sources in combination with hydrogen technology have been suggested to manage the energy flows and increase the flexibility of the grid considering the rapid dynamics of the electrolyzers.

4 Electrolysers as a flexible load

The flexibility of an electrolyser refers to its ability to adapt to different loading conditions, ramp up or down production quickly, start up quickly from both cold and warm states, and minimize standby losses. Cold start up is the time it takes for the electrolyser to start up from ambient temperatures, while warm start up is the time it takes to start up when the system is already warm or in standby mode.

Heat is generated when an electrolyser operates at lower loads, such as below 30% of its nominal capacity [3]. This can result in increased energy consumption and hydrogen production costs. On the other hand, operating an electrolyser above its nominal load, as is possible with Proton exchange Membrane (PEM) electrolysis, can cause the stack to degrade faster due to the additional stress of the overload. In addition, higher cooling costs may be incurred as more cooling of the system is required. Large electrolyser systems can shut down part of the system completely, allowing for a wider practical load range. On smaller systems, the load range may be limited by the components that require cooling or heating to operate at thermoneutral conditions. The practical minimum load for alkaline electrolysis is around 20-25% of the nominal load. Operating below this level can result in increased impurities in the produced gases, as the current density decreases, and the amount of contamination remains constant. Therefore, it is recommended to operate an alkaline electrolyser at 100% of its nominal capacity. PEM electrolysis technology has better flexibility, as it can be operated across the full range from 0-100%, and in some cases even up to 150-160% for a short period of time [3]. However, additional cooling and a properly dimensioned power supply may be necessary to support operation in these overload scenarios.

4.1 Dynamic behaviour

Both PEM and alkaline electrolysis systems require some time to heat up and maintain a certain temperature during standby mode. PEM systems take only seconds to transition from standby mode to nominal load when the systems are warm and pressurized, while alkaline systems take 1 to 5 minutes to do the same [3]. Although alkaline electrolysis is not suitable for low loads and therefore not suitable for variable renewable energy sources (VRES), it has the lowest cost for large systems. On the other hand, PEM electrolysis is more suited for VRES but is more expensive due to the use of expensive or rare materials. In terms of flexibility, PEM is generally better suited than alkaline electrolysis, as the latter has previously demonstrated relatively poor dynamic behaviour while PEM operates well during dynamic operation. As a result, alkaline electrolysis systems are typically operated in continuous mode, despite having a practical load range of 20-100% of nominal load. PEM systems, on the other hand, can ramp up to the MW scale in less than 10 seconds, but may require 5-20 minutes for cold start up [11]. However, this start-up time is significantly shorter than that of alkaline electrolysis, as shown in Figure 13, and is expected to continue decreasing in the coming years. As the enhancement in the start-up times can be expected in future, electrolyzers can be considered as the potential source of flexibility in the demand side of the power grid.

4.2 Economics

The economic feasibility of using electrolyzers for grid balancing services depends on various factors. One important factor to consider is the reduced income from not producing hydrogen, also known as the price of curtailed hydrogen. To determine if electrolyzers are economically viable for balancing services, the income loss from curtailed hydrogen should be subtracted from the income gained from participation in the grid balancing market.

The value of participating in the grid balancing market varies among countries, depending on the availability of fast-controllable power sources [12]. For instance, Norway has a large capacity for hydroelectric power, with approximately 85 TWh of energy storage in water reservoirs. This acts as a "giant battery", reducing the need for grid services in Norway. In contrast, countries with more conventional power plants, such as nuclear and coal, which have slower controllable generators, are more likely to profit from grid balancing services provided by electrolyzers [12]. Then it would be possible to have a gradually increasing share of renewable energy sources, increasing the need for grid balancing services.

It is worth noting that due to the high electricity share from hydro power in Norway, power generation is fast-controllable, leading to lower profitability for grid services compared to other countries. Despite having a large hydrogen production capacity, Norway has lower values for curtailed hydrogen than the other European countries considered [9]. In addition to the impact of curtailed hydrogen prices, the economic performance of an electrolyser depends on its utilization in terms of full load hours, at the low level of full load hours may allow the electrolyser to be available for grid balancing services when needed. On the other hand, a higher utilization of the electrolyser with a higher number of full load hours may limit its potential for grid balancing services. However, the duration of power peaks may electrolyser to lose a significant amount of time

operating at full load. Therefore, providing grid balancing services in short time intervals may be economically beneficial if it can prevent or at least delay the reinforcement of existing cables and lines to some extent.

5 Technology in the grid perspective

To maintain focus of this study is on the grid integration, therefore following assumptions are considered:

- This study does not specifically concentrate on the modelling of the hydrogen storage or the dimensioning of a hydrogen storage facility. It is assumed that the storage of hydrogen necessary for the different scenarios is feasible without explicitly examining the storage aspect.
- Real-time control of the water electrolyser is not modelled as it falls outside the scope of this study, which primarily focuses on the power system perspective.
- Only a portion of the distribution network is modelled, specifically one radial of the grid. This assumption arises from various factors, like to construct a realistic and agile network model.
- Insights into critical infrastructure are limited.
- The investments and costs associated with implementing an electrolyser of the chosen size will not be considered due to the same reasons stated above.

5.1 Modelling

In this study investigation is focused on the optimum utilization of green hydrogen and explore the impact of integrating electrolyser into the distribution grid operation. To accomplish this test network have been modelled in DigSILENT power factory and various case studies have been studied. As actual data both electrical equipment and load was obtained from the real distribution grid, to obtain precise simulations.

5.1.1 Network Model

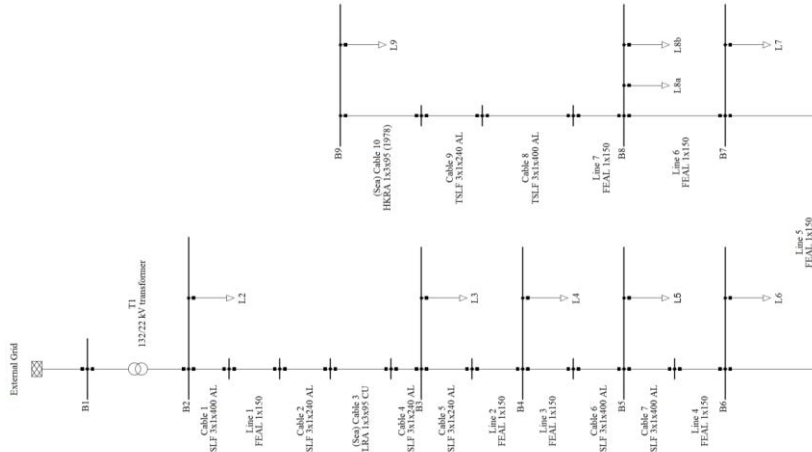
The test network is based on the radial 22 kV distribution grid. There are nine primary connection points, labelled as B1-B9, 19 buses in total interconnecting the cables, lines, and a transformer.

Table 3: Network parameters

| Transformer | Overhead Lines | Cables | System Voltage | Remarks |
|-----------------------|---|---|---|---|
| 210 MVA, 132/22 kV | FEAL 1x150 | Aluminium with cross-section of either 240 or 400 mm ² | 22 kV | Transmission between B3-B3: Combination of cables and overhead lines |
| YNd11 | Steel core with outer layers of aluminium | Copper with cross-section of either 95 mm ² | Remain constant in the entire radial from the transformer | |

Source : Elmea,2023 ; <https://www.elmea.no/>

Figure 16. Model of the test network



Although actual line are three phases, single line diagram of the test network is shown above in Figure 16 [10] and technical details are found in Table 3.

5.1.2 Modelling of Water Electrolyser

PEM (proton exchange membrane) electrolyser dynamics are ascribed to the coupling of various physical phenomena represented as a complex system with non-linear relations Figure 17 [13]. Mathematical model of electrolyser unit can be represented via electrical model demonstrating auxiliary system, electro-chemical domain, fluidic as well as mass transfer domain etc [14] [15]. Flexibility behind water electrolyser can be characterised by the capacity to perform at various power levels which is primarily dependent on the stack potential.

In this work, electrolyser model is developed using DIgSILENT Simulation Language (DSL) with the data source: NEL PEM MC500 electrolyser system. Although DSL modelling is typically utilized for dynamic (time-continuous) process and control, we simplified the control where only power consumption is considered to control the electrolyser. This is due to the focus of the research, which is to explore the impact into the network. It was assured to preserve the characteristics of electrolyser to rapidly ramp up and down.

Figure 17. System representation of a PEM electrolyser plant

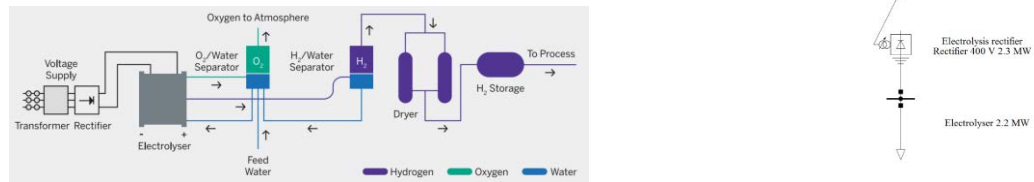


Figure 18. Electrolyser model with the components considered.

Model of electrolyser thus developed is as shown above in Figure 18. Further details of electrolyser modelling can be found in [10].

5.2 Simulation scenarios

In order to assess the most suitable technology for optimal operation and figure out how the flexible operation of water electrolyser can be utilized to minimize the impacts of electrification, three most relevant scenarios have been chosen for the analysis: Scenario A, Scenario B and Scenario C.

6 Result and Discussions

6.1 Scenario A: Base Case

Scenario A refers the base case i.e., current grid at the Figure 15, and winter load variation, without considering the use of electrolyser. The load variation plot in Figure 19 represent typical weekday in a worst way.

Figure 19. Load variation (day with highest consumption in without considering electrolyser)

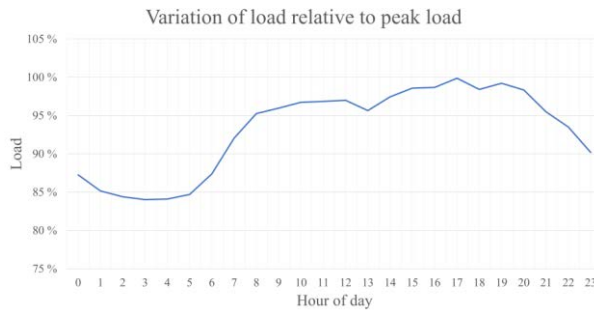
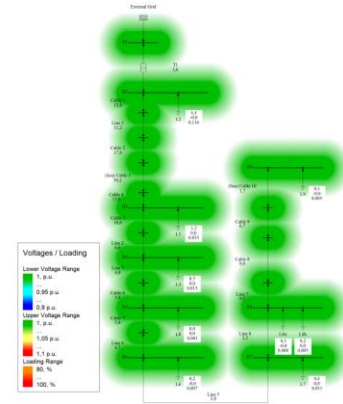


Figure 20. Network with heat map illustrating voltage level throughout the network



Scale in the left side of the network in Figure 20 represent voltage threshold and loading range. White boxes are with key parameter info like active power in MW, reactive power in MVar and current in kA. It is observed that system has sufficient capacity to meet peak power demand without reliability or stability issues.

6.2 Scenario B: Current Grid with Electrolyser

In this case, electrolyser is implemented in the existing grid and was operated in the peak loading condition as mentioned in section 6.1.

Figure 21. Line loading of existing grid with electrolyser

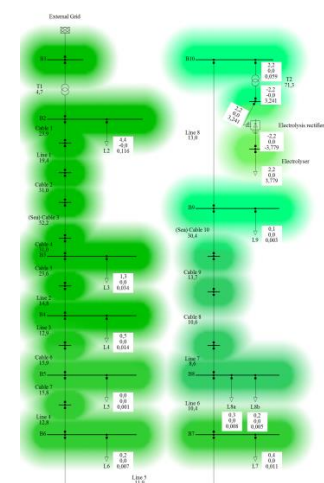
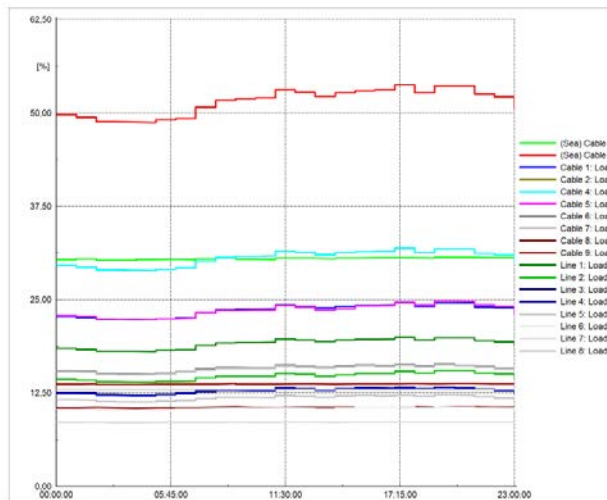


Figure 22. Heat map illustrating existing network voltage status when operating with electrolyser

As shown in the figures Figure 21 and Figure 22 above, it is observed that with implementing 2.214 MW electrolyser there is minor impact (lightning of green colour) in voltage near the point of coupling however it is still within limit. Maximum line loading is only about 50%.

6.3 Scenario C: Future Grid with Electrolyser

In this case also same network is considered however, loading of the line are based on highest forecasted load profiles for 2050 by Statnett i.e. loads are increased by 114%. In addition, ferry charging point (FCP) is added at the end of radial. For details information about the set up please refer to [10]. This network set up will be used for the future scenarios discussed below.

a) Scenario C 1 Future Daily

Figure 23. Cable 3 loading with FCP and electrolysis operating at 100%

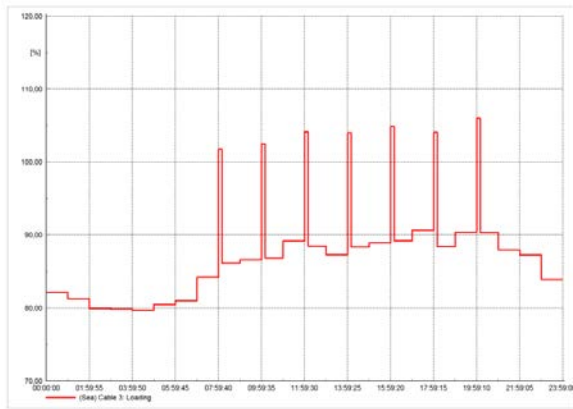
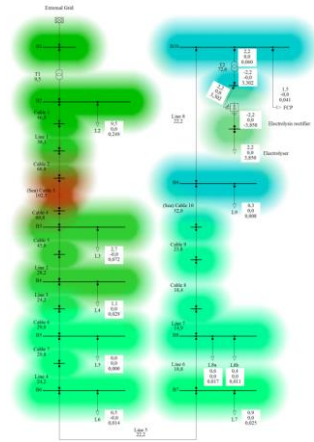


Figure 24. Illustration of network voltage distribution in a heat map



The heat map presented in Figure 24 is for the case for peak daily load with electrolyser operating at 100% and at the same time ferry charging drawing 100% power all day. Overloading (red colour in heat map) of the sea cable-3 (102.5%) is observed with potential thermal stress. Additional voltage drops (blue) are measured which are close to lower limit. For the more realistic scenarios for the flexible solutions, ferry charging schedule (7 different timings) with varying operating scenarios (73% - 91%) for electrolyser is implemented. It is observed that when the operation of electrolyser is minimised, the voltage loss is reduced. So, significant trade off can be achieved.

b) Scenario C 2 Future Weekly

Same network with electrolyser operating at 100% as mentioned above is used in this case as well but loading scenarios depicts the typical weekday and weekend day. From this analysis variation in consumption pattern will be observed.

Figure 25. On average weekday: line loading

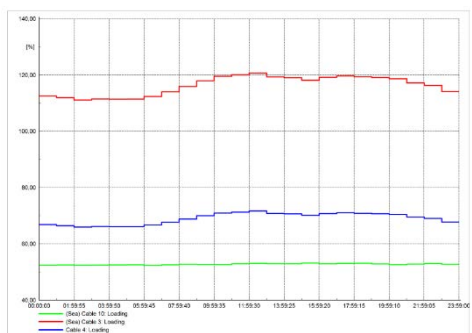
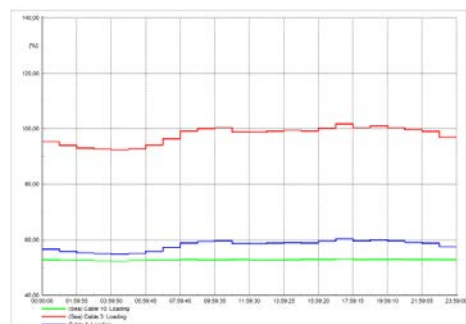


Figure 26. On average weekend day: Line loading



It is observed that during weekdays maximum line loading was up to 100% however in weekend days it recharges up to 120% as shown in

Figure 25. On average weekday: line loading

Figure 26. On average weekend day: Line loading

and **Error! Reference source not found.** above. This is due to more typical residential load which has increased useage during the weekend. So, by adjusting hydrogen production and storage utilization according to the load trends, the grid can be capable to accommodate more fluctuating loads and can have less overload situations even in peak periods.

c) Scenario C 3 Future Yearly

This scenario is to understand monthly hydrogen production and demand from fishing fleets to figure out the trade off with grid operation.

Figure 27. Yearly line loading with electrolyser operating at 100%

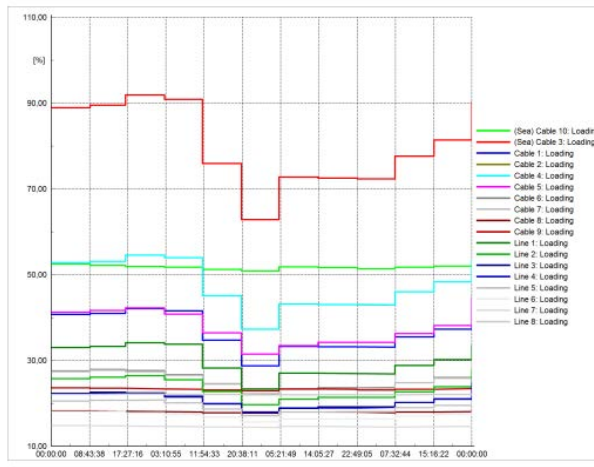


Figure 28. Heat map showing voltage distribution across the network

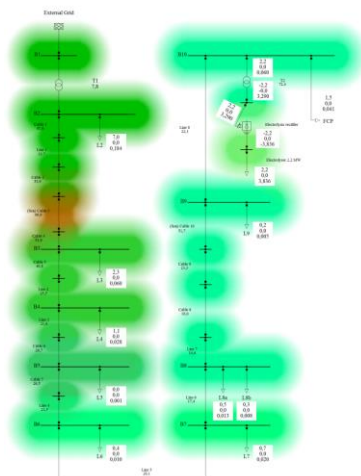


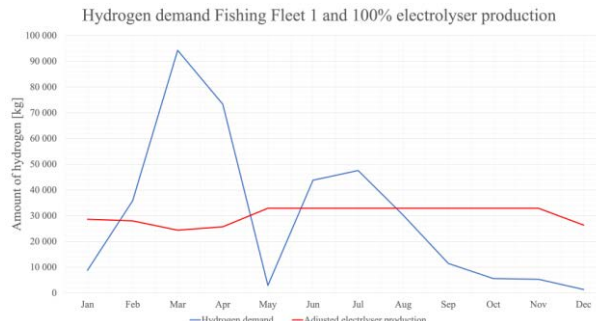
Figure 27 and Figure 28 shows that cable-3 is the most stressed cable which is operating almost 100% during first 4 months however rest 4 lines are below 60%.

So, electrolyser can be operated with variable load that can lead boost grid to flatten the load profile. To calculate the flexible solution from electrolyser, surplus energy available after fulfilling the hydrogen demand of fishing fleet was calculated which was 8%. So, 8% of hydrogen production can be utilised for the grid services. Further, by determining the periods when hydrogen demand exceeds maximum production capacity of electrolyser, load shifting requirement for particular months can be identified. Effect can be seen in Figure 29 and Figure 30 below.

Figure 29 Average loading of the cable 3 by month with different operating strategy for electrolyser



Figure 30. Adjusted electrolyser production and hydrogen demand for fishing fleet



Analysis shows that in this particular case, electrolyser can operate 2500 full load hours that can give sufficient low price however operation exceeding 6000 full load hours may result in increase in hydrogen price. For example, if electrolyser is operated at 92% capacity i.e., 8000 full load hours, may result higher hydrogen cost in comparison to period when operated at lower capacity.

7 Conclusions

Electrolysis may play a crucial role in the transition to a net zero society, and it is important to understand how to implement this technology in the power grid. It is clear what electrolyzers can add flexibility to the demand side of the power grid, and technological improvements in startup times and opportunities are expected in the future.

The findings of this study suggest that hydrogen from electrolysis has the potential to play a significant role in the transition to a net zero society. While it requires a reliable and resilient electricity grid. Advances in electrolysis technologies and optimization strategies can help minimize the impact of renewables on the grid operation. Alkaline electrolysis is the most widely used method for large-scale hydrogen production, but proton exchange membrane (PEM) electrolysis has the potential to provide the best characteristics for grid balancing services and operate as a flexible load. This can be achieved through strategies such as adjusting energy consumption to match available grid capacity. However, this may come with a cost and potentially increase the price of hydrogen per unit.

The operational patterns for hydrogen production will have different consequences for the distribution grid, depending on the economic feasibility of production side. For future work it would be interesting to develop various operational scenarios and analyse the specific consequences for each case. By simulating hydrogen production from a specific grid, the impacts of importance would be more clear and optimal operation of hydrogen production could be more accurately defined. All these is important to better understand the optimal ways to integrate hydrogen production into the grid.

Acknowledgements

The authors gratefully acknowledge the contributions of ZEROKYST KSP partners and researchers involved for their inputs during different meetings and discussions.

References

- [1] "Hydrogen," IEA. Accessed: Sep. 26, 2023. [Online]. Available: <https://www.iea.org/energy-system/low-emission-fuels/hydrogen>
- [2] "Net Zero by 2050." Accessed: Sep. 25, 2023. [Online]. Available: <https://www.iea.org/reports/net-zero-by-2050>
- [3] "A hydrogen strategy for a climate-neutral Europe." Accessed: Sep. 25, 2023. [Online]. Available: https://knowledge4policy.ec.europa.eu/publication/communication-com2020301-hydrogen-strategy-climate-neutral-europe_en
- [4] "Hydrogen, electrofuels, and CCUS in a Nordic context." Accessed: Sep. 25, 2023. [Online]. Available: <https://www.nordicenergy.org/publications/hydrogen-electrofuels-ccu-and-ccs-in-a-nordic-context/>
- [5] "Hydrogen: A renewable energy perspective." Accessed: Sep. 25, 2023. [Online]. Available: <https://www.irena.org/publications/2019/Sep/Hydrogen-A-renewable-energy-perspective>
- [6] "Global Hydrogen Review 2022." Accessed: Sep. 25, 2023. [Online]. Available: <https://www.iea.org/reports/global-hydrogen-review-2022>

- [7] M. Naeini, J. S. Cotton, and T. A. Adams, "An eco-technoeconomic analysis of hydrogen production using solid oxide electrolysis cells that accounts for long-term degradation," *Front Energy Res*, vol. 10, Sep. 2022, doi: 10.3389/fenrg.2022.1015465.
- [8] International Renewable Energy Agency., "Green hydrogen : a guide to policy making," Abu Dhabi, 2020.
- [9] F. Zenith, M. N. Flote, M. Santos-Mugica, C. S. Duncan, V. Mariani, and C. Marcantonini, "Value of green hydrogen when curtailed to provide grid balancing services," *Int J Hydrogen Energy*, vol. 47, no. 84, pp. 35541–35552, Oct. 2022, doi: 10.1016/j.ijhydene.2022.08.152.
- [10] M. Rasmussen and S. Lorentzen, "Potential of Hydrogen Technology for Coastal Electrification: Minimizing Distribution Grid Impacts through Flexibility," 2023.
- [11] International Renewable Energy Agency., *Hydrogen : a renewable energy perspective*. 2019.
- [12] F. Zenith, "Grid services and electrolyzers ." Accessed: Sep. 26, 2023. [Online]. Available: <https://www.haeolus.eu/?p=1143>
- [13] "The world's most efficient and reliable electrolyzers ." Accessed: Sep. 26, 2023. [Online]. Available: <https://nelhydrogen.com/wp-content/uploads/2020/03/Electrolyzers-Brochure-Rev-D.pdf>
- [14] S. Sood et al., "Generic Dynamical Model of PEM Electrolyser under Intermittent Sources," *Energies* (Basel), vol. 13, no. 24, p. 6556, Dec. 2020, doi: 10.3390/en13246556.
- [15] A. Chandrasekar, D. Flynn, and E. Syron, "Operational challenges for low and high temperature electrolyzers exploiting curtailed wind energy for hydrogen production," *Int J Hydrogen Energy*, vol. 46, no. 57, pp. 28900–28911, Aug. 2021, doi: 10.1016/j.ijhydene.2020.12.217.

2.6 Risk and resilience-informed decision-making for strategic territorial risk management: from methodologies to practical implementation for infrastructures exposed to mountain natural hazards

Tacnet, J.-M., Univ. Grenoble Alpes, INRAE, CNRS, IRD, Grenoble INP, IGE, 38000 Grenoble, France. jean-marc.tacnet@inrae.fr

Bérenguer, C., Univ. Grenoble Alpes, CNRS, Grenoble INP, GIPSA-lab, 38000 Grenoble, France. Christophe.berenguer@grenoble-inp.fr

Chahrour,N., Univ. Grenoble Alpes, CNRS, Grenoble INP, GIPSA-lab and Grenoble Alpes University, INRAE, IGE nour.chahrour@grenoble-inp.fr

Carladous S., French National Forest Office, simon.carladous@onf.fr

1 Context

People, assets and infrastructures located in mountain territories are highly exposed to natural phenomena that induce both direct consequences (damage) on objects but also indirect, remote consequences. In these areas, critical infrastructures such as transport, energy, communication, water networks disruption due to either rockfalls, floods, snow avalanches or landslides can have severe long-term, remote, economic, social consequences which somehow characterize the territory resilience including therefore a temporal dimension. To reduce risk, local authorities, state, infrastructures managers often build structural protection measures. For instance, torrent check dams control material volume and flow through stabilization of bed scouring and banks. More than 21,000 old protection works, including 14,000 check dams, are registered in French public forests. Those works are highly exposed to phenomena effects, to severe climatic conditions and are often located in non-easily accessible areas: they are therefore submitted to deterioration with consequences on their efficacy and the risk level on areas where protected assets are located downstream. Assessing their actual effectiveness is a key issue in maintenance decision-making (Carladous et al., 2016a, b). In this context, being able to assess the status of the protection works, their maintainability and to choose the best maintenance strategy remain challenging decision-making issues for stakeholders.

Several scientific and methodological developments have been proposed to both characterize the efficacy of protection works, to support related decisions processes such as identifying the best maintenance strategies and also finally to analyse the effects of deterioration on risk levels. This presentation presents a global picture of the natural risk management context and the interest of proposing integrated, pluridisciplinary and complementary methodologies. It recalls recent findings but also connect them to decisions contexts and stakeholders' needs for research to implementation and real-life decision contexts.

2 Some pluridisciplinary methodological developments

2.1 Analysing the efficacy of protection works

The efficacy of a system may be an ambiguous concept. For a (risk) protection work, it can be defined as the level of objective achievement according three features: structural, functional, and economic. Its assessment is based on the comparison of its capacity with the chosen objectives. Nevertheless, due to ageing and deterioration the nominal capacity of a structure may be reduced. When analysing structural pathology, field practitioners focus on structural and functional features. A first essential step is to define and assess degradation criteria that can affect structural stability and the functional service of each structure or cluster of structures. This analysis based on inspection done by experts is the basis to propose maintenance strategies. A pluridisciplinary, integrated process is proposed to assess this efficacy using multicriteria, multi-feature (structural, functional, and economic) and multiscale (check dam, device, and watershed) analysis. Those developments combine functional analysis and multi-criteria decision methods (MCDMs) in a context of imperfect information (Carladous et al., 2016a, b).

2.2 Analysing the deterioration process and prioritizing maintenance strategies

Protection structures that reduce the risk caused by natural hazards protect infrastructures and are there part of critical systems. Their deterioration over time influences their level of performance and can lead to dramatic consequences. In the context of natural hazards, identifying and analysing dependencies between the structure and the environment, and supporting decision-making for choosing the best maintenance

strategy with limited budgetary resources remain challenging. New approaches are proposed to go beyond traditional methods used in safety and reliability analysis and to develop a comprehensive approach that permits incorporating possible interactions when modelling system's deterioration and provides information for analysing cascading effects prioritizing maintenance actions. Recent developments couple (1) numerical models that account for the dynamic deterioration of check dams and retention dams (Chahrour et al., 2021, 2022b) based on civil and hydraulic engineering expertise, and (2) a decision-aiding model, based on surrogate stochastic models built with e.g. stochastic Petri nets, that compares the evolution of the system deterioration and the associated incurred costs when subjected to maintenance operations.

2.3 Developing practical tools and frameworks for operational risk management decision-aiding

Practitioners need operational risk management frameworks. To help local authorities to manage multiple risks in mountain areas and choose the best strategy, the French ministry for Ecological Transition has designed and promotes the new French framework called Mountain Risk Management and Prevention Strategy (STePRiM). It consists in a new innovative framework to help local authorities choosing and funding their risk management strategies in mountain areas. A first step of risk diagnosis and protection works' status analysis is first carried out over a large area and is then followed by a step of prioritization between possible options in collaboration with local stakeholders. Risk analysis is here directly linked to risk evaluation and finally decisions related to the choice, the location and the scheduling of risk reduction strategies and actions (Carladous and Tacnet, 2022; Tacnet et al., 2022).

3 Perspectives and challenges

The objective of merging science, engineering and decision-aiding open new research perspectives dedicated to critical infrastructures risk and resilience assessment. Combining disciplines, approaches developed for industrial, technological assets and infrastructures for application to natural and NATECH risks is a promising challenge. Improving knowledge about cascading effects between natural and technological risks, including the evolution of vulnerability are important issues. Linking the level of protection works or systems with the downstream risk and resilience levels is one of the next on-going challenges (Chahrour et al., 2022a). Merging technical analysis and decision-making processes is key for effective territorial risk and resilience management. New spatial group decision-aiding methods are required to associate all stakeholders.

References

- 1 Carladous S, Tacnet J-M. Stratégie Territoriale de Prévention des Risques en Montagne (STePRiM) – Guide méthodologique pour la mise en œuvre - version de travail. Ministère de la Transition Ecologique et Solidaire (MTES), Direction Générale de la Prévention des Risques (DGPR), Service des Risques Naturels et Hydrauliques (SRNH), Bureau des Risques Naturels Terrestres (BRNT); 2022.
- 2 Carladous, Simon and Tacnet, Jean-Marc and Batton-Hubert, Mireille and Dezert, Jean and Marco, Olivier, 2019. Managing protection in torrential mountain watersheds: A new conceptual integrated decision-aiding framework. Land Use Policy, Elsevier, Vol. 80, 464-479, 10.1016/j.landusepol.2017.10.040
- 3 Carladous,S., Piton,G., Tacnet,J.-M., Philippe,F., Nepote-Vesino,R. et al.(2016a). From the restoration of French mountainous areas to their global management: historical overview of the Water and Forestry Administration actions in public forests. 13th INTERPRAEVENT Conference, May 2016, Lucerne, Switzerland.
- 4 Carladous,S., Tacnet,J.-M.,Batton-Hubert, M., 2016b. Protection structures against natural hazards: from failure analysis to effectiveness assessment. 13th Congress INTERPRAEVENT 2016, May 2016, Lucerne, France.
- 5 Chahrour, N., Bérenguer, C., & Tacnet, J.-M. (2023 – accepted,under press). Incorporating Cascading Effects Analysis in the Management Process of Torrent Check Dams Against Natural Hazards. Reliability Engineering & System Safety.
- 6 Chahrour, N., Piton, G., Tacnet, J.-M., & Bérenguer, C. (2024). A Surrogate Deterioration Model of Debris Retention Systems Towards Cost-Effective Maintenance Strategies and Increased Protection Efficacy. Engineering Structures, Volume 300, 2024, 117202, ISSN 0141-0296, <https://doi.org/10.1016/j.engstruct.2023.117202>.
- 7 Chahrour, N., Piton, G., Tacnet, J.-M. and Bérenguer, C. (2022b). Decision-Aiding Towards Improved Resilience of a Deteriorating Debris Retention System Subject to Maintenance Strategies. 60th ESReDA Seminar On Advances in Modelling to Improve Network Resilience, Grenoble, France.

- 8 Chahrour, N., Tacnet, J.-M. and Berenguer, C. 2022a. Economic Efficacy Assessment of Deteriorating Protection Structures Subjected to Natural Phenomena in Mountains. ICASP14 - 14th International Conference on Applications of Statistics and Probability in Civil Engineering. https://hal.science/hal-04245183/file/ChahrourEtAL_ICASP14_2023.pdf
- 9 Chahrour,C., Tacnet,J.-M., Bérenguer,C. (2021b). Deterioration Modelling and Preventive Maintenance of Critical Torrential Protection Structures towards Improved Resilience – A Petri Net based Approach. R. Remenyte-Prescott; V. Kopustinskas. Modelling the Resilience of Infrastructure Networks - An ESReDA Project Group Report, Det Norske Veritas, pp.166-181, 2021, 978-2-930928-11-1. (hal-03408080)
- 10 Chahrour, N., Nasr, M., Tacnet, J.M. and Bérenguer, C. (2021a). Deterioration modeling and maintenance assessment using physics-informed stochastic petri nets: Application to torrent protection structures. Reliability Engineering System Safety 210, 107524.
- 11 Curt,C., Tacnet, J.-M., 2018. Resilience of critical infrastructures: review and analysis of current approaches. Risk Analysis, 2018, pp.18. (hal-02607701)
- 12 ESREDA. Modelling the Resilience of Infrastructure Networks: an ESREDA (European Safety, Reliability & Data Association) project group report. Remenyte-Prescott R, Kopustinkas V, editors. Norway: Det Norske Veritas AS; 2021.
- 13 Tacnet, J.-M., Carladous S., Sassus, Ripert, E., Lagleize, P. , Stephan, A., Calmet, C., Gili, 2022. Risk, resilience in Mountain Risk Management and Prevention Strategy (STePRiM). Proc. 60th ESReDA Seminar (ESReDA 2022) - Advances in Modelling to Improve Network Resilience, Grenoble, France
- 14 Tacnet,J.-M., Dezert,J., Curt, C., Batton-Hubert, M., Chojnacki, E., 2014. How to manage natural risks in mountain areas in a context of imperfect information? New frameworks and paradigms for expert assessments and decision-making. Environment Systems and Decisions, 2014, Volume 34 (Issue 2), pp 288-311, 10.1007/s10669-014-9501-x, <https://hal-emse.ccsd.cnrs.fr/emse-00995011/file/P033.pdf>
- 15 Tacnet J-M, Mermet E, Zadonina K, Deschates M, Humbert P, Dissart J-C, et al. Road network management in the context of natural hazards: a decision-aiding process based on multi-criteria decision making methods and network structural properties analysis. Proceedings of the International Snow Science Workshop (ISSW 2013), 7-11 october 2013, Grenoble, France. Grenoble, France; 2013. p. 95–106.
- 16 Tacnet J-M (coord. Decision Support Guidelines - Methods, procedures and tools developped in PARAmount (WP7 report) - hal-03639896. European Regional Development Fund - Alpine Space Progam - Interreg IV - PARAmount projet: imProved Accessibility: Reliability and safety of Alpine transport infrastructure related to mountainous hazards in a changing climate. <http://www.paramout-project.eu/>; 2012. see also <https://cv.hal.science/nour-chahrour> ; <https://cv.hal.science/christophe-berenguer> ; <https://cv.hal.science/jean-marc-tacnet>

2.7 Towards a modular co-simulation framework for the assessment of cascading effects among critical infrastructures and the impact on citizens

Till Martini^{1,2}, Julia Rosin², Joanna Zarah Vetter^{1,2}, Stefan Neuhäuser^{1,2}, Eridy Lukau^{1,3}, Faruk Catal^{1,3}, Maurizio Boigk^{1,4}, Maik Simon^{1,4}, Michael Monteforte^{1,4}, Michael Gerold^{1,5}, Windy Phung^{1,5}, Steffen Dietze⁵, Jörg Finger², Patrick Brausewetter⁴, Steffen Nicolai⁵

¹Fraunhofer Center for the Security of Socio-Technical Systems SIRIOS, Berlin, Germany

²Fraunhofer Institute for High-Speed Dynamics, Ernst-Mach-Institute, EMI, Freiburg, Germany

³Fraunhofer Institute for Open Communication Systems FOKUS, Berlin, Germany,

⁴Fraunhofer Institute for Transportation and Infrastructure Systems IVI, Dresden, Germany

⁵Fraunhofer Institute of Optronics, System Technologies and Image Exploitation IOSB, IOSB-AST, Ilmenau, Germany

Corresponding Author: Dr. Till Martini, Till.Martini@emi.fraunhofer.de

Abstract

Public safety is confronted with an increasing number of threats, such as natural disasters, terrorist attacks, cyber-attacks and more. In many cases, these lead to significant disruptions of critical infrastructures affecting a large number of citizens. A better understanding of the complex interplay of critical infrastructures in such scenarios can support authorities and organizations responsible for security. To address this, a modular co-simulation framework is presented that simulates the effects of disasters on critical infrastructures and their direct impact on citizens. The framework captures interdependencies and cascading effects by simulating multiple domains such as water, energy, gas, and telecommunications. It also includes building damage analyses and emergency response decisions. Grounded in physical principles and real-world data, this versatile framework serves as a valuable tool for public-safety assessment and training for safety personnel.

1 Introduction

Determining the vulnerability of urban areas and its critical infrastructure to natural calamities like flood, heavy rainfall, and severe storm events but also anthropogenic disasters like terror attacks has become an increasingly important research topic in recent decades due to the worldwide increasing frequency and intensity of such events. The failure or impairment of critical infrastructure can have a severe impact leading to sustained supply shortages and significant disruptions to public safety. Especially, hidden dependencies and unforeseen or unexpected cascading effects between multiple critical infrastructures pose potentially high possibilities for danger to citizens.

In terms of increasing resilience of an urban area but also its critical infrastructure, it is essential for decision makers, agencies, governments, and infrastructure providers to gain a comprehensive understanding of not only the vulnerability and failure probabilities of individual critical infrastructure. It is also important to consider the conditional impact that the degradation or failure of one infrastructure can potentially have on another critical infrastructure. In the past, several research groups identified risks and hazards that arise from cascading effects in interconnected systems of the built environment and critical infrastructure. The authors of 1 give an overall summary of the current progress and challenges concerning community resilience and the identification of system interdependencies. Although researchers identified and investigated some interdependencies between critical infrastructure systems, these findings have so far been used in few cases to couple simulations of the individual components of an urban system. Some projects offer possibilities to evaluate and visualize the interdependencies of critical infrastructure systems by developing tools like SAT (*Severity Assessment Tool*) 2 or CReDo (*Climate Resilience Demonstrator*) 3 for decision-making and optimization purposes. Nevertheless, the individual functionalities of different critical infrastructures or the state of the built environment are not simulated using engineering models and other simulation methods; instead, they are often data driven. Coupled simulations are mostly used for critical infrastructures such as water, electricity, and gas networks (e.g. 4 5). However, the interdependencies to the built environment and emergency response systems are not treated in most projects. In 6 an interdependent networked community resilience modelling environment (IN-CORE) is implemented. The authors use a service-oriented architecture that supports the integration of various services, including analyses for buildings and the built environment using fragility curves, simulation of infrastructure networks, and various hazard scenarios. However, the

authors do not address the simulation methods that were used. Also, emergency response systems, which are crucial for using such a system for training purposes, are not included in the analysis.

Therefore, a methodology is developed that enables the virtual representation of infrastructure vulnerability and functional impairments of an urban district in a hazard situation. Within the presented framework multiple simulation modules for diverse critical infrastructures and services such as water, energy, gas, and telecommunication are incorporated. These simulation modules are built upon engineering models that are grounded in physical principles, standards or (geo-referenced) real-world data, enabling them to make predictions about the state of the modelled system based on specific conditions. The framework also includes scenario-specific building damage that is analysed based on probabilistic engineering models. Furthermore, an agent-based simulation of emergency operations and services by first responders, modelling quick responses and actions to critical incidents is incorporated into framework. The inclusion of these two aspects, which both impact or are impacted by the state of other critical infrastructures, is a novelty, as it enables the structural assessment of critical infrastructure facilities and explores cascading effects that hinder the work of emergency responders.

In general, the developed methodology allows insights before, during and after a disaster and can offer a deeper understanding of cascading effects and chain reactions caused by major impacts on critical infrastructure from severe natural events or deliberate attacks. The framework is developed using the example of an urban heavy rainfall event with flooding and considers the mentioned aspects of gas, water, power supply, communication networks, emergency services, and building structures. However, due to its modular structure and integration into the *Fraunhofer Open Source SensorThings API Server FROST 7*, it is versatile and can be expanded to cover additional hazard scenarios and infrastructure aspects. It enables various applications, such as decision support tools for authorities and infrastructure operators, as well as training tools in the field of public safety.

2 State of the technology and model overview

The simulation of the individual components of the infrastructure networks (gas, power supply, drinking water, telecommunication) as well as the emergency response and building vulnerability each on its own is already a comprehensive tool for functionality and resilience assessment analysis. Therefore, for each component a separate simulation tool is developed that meets the specific requirements and functions of the component. Each tool works independently on its own and represents an autonomous simulation tool, which is described in the following paragraphs for all components. The communication between the individual simulators is described in section 0.

2.1 Simulation of extreme contingencies in urban gas distribution networks

A multitude of tools to study disruptions on the operation of gas grids have been described in the literature: The *ProGasNet*-code 8 is based on the maximum flow algorithm together with failure rates and can be used to perform statistical risk assessment regarding the supply situation of gas consumers. The *GEMFLOW*-code 9 allows to simulate probabilistic time-dependent gas supply disruptions in a flow model without accounting for realistic flow physics. The *TIGER2*-model 10 is a dispatch model of the European gas market based on capacity constraints and the mass-balance equation able to optimize natural gas flow under physical and economic restrictions while neglecting the gas pressure distribution and friction. An important open-source software project aiming at static analyses of balanced fluid systems of incompressible or compressible media is *pandapipes* 11 which allows solving for pressure and velocity distributions. The software *SAInt* 12 allows for transient hydraulic simulation of gas systems together with modelling of electric power systems using an augmented AC-Optimal power flow model. *SIMONE* 13 offers a transient gas flow solver for optimization of design and operation of large and complex gas systems. *Synergi™Gas* 14 can be used for optimizing network operations, planning and design, and performing "what-if" or other operational analyses based on a steady-state approach. The *GasNetSim*-code 15, 16 aims at a compromise between physical accuracy and computational efficiency by providing more detailed and realistic predictions of the gas flow than *GEMFLOW* and *ProGasNet* while incorporating more simplifications than the commercial tools *SAInt*, *SIMONE* and *Synergi™Gas*. A flow regulator approach for ensuring a robust solution for highly disrupted gas network scenarios constitutes a unique feature of the *GasNetSim*-code. Therefore, the implementation presented in this contribution of the gas network simulation module is based on the *GasNetSim*-code.

Natural gas grids can be modelled as networks with nodes (representing, i.e., sources, consumers, junctions) which are connected by directed one-dimensional edges (representing, i.e., pipeline segments, compressors, regulators, valves). The respective network graph attributed with operating parameters like source pressures, consumer demands or compressor, regulator, and valve properties as well as pipeline characteristics like

lengths, diameters, inclinations, and roughness values constitutes the input for the gas module. The dynamics of natural gas, as a mixture of gaseous hydrocarbons, are governed by the laws of thermodynamics as well as hydrodynamics ensuring the conservation of mass as well as momentum under the influence of inertia, friction, gravity, and external forces from, e.g., compressors (see, e.g. 15, 16). Assuming isothermal and steady-state conditions, which are reasonable assumptions in the context of urban gas distribution networks, the state of the resulting system is completely described by the pressures at all nodes and the flow rates through all edges. Values for these variables can be obtained as the solution of a system of coupled non-linear differential equations of motion. Integrating the equations of motion in sections along the longitudinal direction of the edges yields a system of coupled non-linear algebraic equations describing the average flow rate through each section as well as the pressure at each node (see, e.g. 15, 16 for details). These form the set of output variables of the gas module associated with the respective elements. When receiving an arbitrary gas network graph as input, the gas module automatically sets up the corresponding system of non-linear algebraic equations built from the topology information and the attributes of the input graph. Solvability is ensured by checking mathematical solvability of the input graph as well as by utilizing the *flow-regulator concept* introduced in 15, 16 enabling physical solutions that may be far from design-point operation. To enhance robustness, the solution is found by iterated linearization in conjunction with a least-square method.

2.2 Simulation of urban power distribution grids

Various software solutions are available for modelling and simulating power distribution grids, including both commercial and open-source options. A comprehensive overview of these tools is available in 17. Further tools that have been used in literature for coupled simulations with other supply grids are summarized in the following. *Pandapower* is an open-source Python package that can perform static and quasi-static power grid analyses 18. By combining *pandapower* with *pandapipes*, multi-energy grids are simulated 11. *OpenDSS* is another open-source software for simulating distribution power grids. In 19, a co-simulation between a distribution grid and communication network is realised with *OpenDSS* and *OMNeT++*, a software for simulating communication networks. In 20, an integrated multi-energy system consisting of a power and gas grid is modelled using the commercial tool *PSS®SincaL*. The authors use the co-simulation tool *OpSim* to connect both simulations and conduct discrete time steps of uniform length. Another commonly used commercial tool is *PowerFactory* by *DIGSILENT*. In 21, examples of coupling with other systems are provided. *PowerFactory* offers flexibility and interoperability with additional tools through its Python application programming interface (API) 22, while maintaining high accuracy of results 23. In addition, *PowerFactory* presents a wide range of different components and a comprehensive library of models for them.

To address the need for a flexible and modular interface tool that allows for adjustment of grid parameters through a user-friendly graphical user interface (GUI), this paper presents an implementation of a power grid simulation module using the simulation software *DIGSILENT PowerFactory*, controlled by a Python application through an API developed by *DIGSILENT*. A geo-referenced power grid can be imported into the software as input, but a modelling of the network from scratch is also possible. Analogously to the gas network, nodes and edges form the network graph. In principle, all voltage levels can be analysed with *PowerFactory*, but for the urban setting of this paper, the middle voltage (MV) grid was chosen, which describes the inner-city supply conditions with sufficient accuracy. The MV grid consists of lines, transformers, terminals, various generation units, and consumers. The parameter data for the components of the MV grid come from various public sources. The grid model is stored in *PowerFactory*'s internal *Oracle®* database. The grid state is calculated by load flow calculation based on the *Newton-Raphson* method (see 24) and is described using the load of the components, as lines and transformers, and by the voltages at the terminals.

2.3 Simulation of drinking water networks

EPANET 25 is the most widely used tool for hydraulic simulations of drinking water distribution networks. It can be used as a standalone command-line tool and provides a basic network editor. *EPANET* is also used as the computational engine for numerous free and commercial drinking water network modelling and simulation software, since most drinking water network simulation tools have the capability to import and export *EPANET* INP files. Some examples of open-source attempts to enhance the functionality of *EPANET* are *WNTR* 26 and *QGISRed* 27. *WNTR* provides a Python wrapper that adds advanced analysis capabilities to hydraulic simulations. On the other hand, *QGISRed* integrates *EPANET* with *QGIS Software* 28, a comprehensive open-source GIS package. Python libraries do not provide user-friendly interfaces by themselves to non-Python experts and QGIS-extensions are restricted to the QGIS interface. Therefore, a GIS-like software with its own GUI based on the developing tools .NET and C# using *EPANET* as the computational engine is developed as a part of this research.

Drinking water pipeline networks in *EPANET* are described as an ordered graph consisting of nodes connected by links. The nodes in the network represent tanks, reservoirs and junctions, while the links represent pipeline sections, valves, and pumps. Each network element has a set of parameters, as detailed in the EPANET manual 29. The developed software offers the functionality to assign coordinates to *EPANET* objects in a specific spatial reference system (SRS) 30. It also allows the storage of the entire network (graph), along with all parameters, in a relational *PostGIS* database 31. Additionally, spatial operations can be performed on the data, and additional information such as population density can be incorporated into calculations. While initially developed for *Windows*, the software can be adapted to run on any platform supported by the .NET framework. In addition, the software wrapper includes support for various standard interfaces.

2.4 Simulation of (LTE/5G) cellular network coverage in disaster-stricken areas

The communication simulation module calculates the effects on the cellular network coverage that arise from critical infrastructure failures within urban or sub-urban areas. The primary objectives of this module are firstly, to generate forecasts on remaining cellular network coverage in a disaster-stricken area and secondly to evaluate the citizens' ability to receive alerts and warnings from authorities as well as their ability to initiate emergency calls. To conduct these simulations for the simulated target area, the module actively monitors the power supply of mobile base stations that are typically deployed atop buildings and calculates the areal overall cellular-network coverage. Mobile base stations in general function as pivotal cellular network antennas, provisioning mobile network services towards cell phone users. In this case the simulation-module recreates LTE and 5G networks based on the information about all cellular network antennas deployed in the simulated target area.

Network simulation is a widely employed research methodology that serves multiple purposes, including validation 32 and comprehension of diverse network models and protocols 33. This methodology proves invaluable in assessing network protocol performance 33 and crafting mobility and signal propagation models for real-world scenarios 34. Notably, the simulation of cellular networks (such as LTE-networks) has been explored in prior research, encompassing link-level and system-level analyses in 35 using an *OMNeT++* based approach as presented in 36 and 37 through a system-level approach utilizing *MATLAB*®.

In addition to the approaches in the field, this mobile-network simulation approach aims at simulating large-scale city-based mobile network topologies with a massive amount of network nodes. The ability to conduct large-scale analysis is required for the assessment of crisis outcomes and post-disaster communication between citizens and authorities, especially in residential areas. The approach shall further be useful for the evaluation of suitable post-disaster emergency communication strategies that may be deployed by authorities in a post-disaster scenario such as *Void-Communication* as described in 38, depending on the remaining state of the cellular network.

The core foundation of the simulation module rests upon a system-of-systems architecture of several integrated submodules. The major submodule includes a *NS-3* based discrete event simulation framework 39. This submodule recreates the network topology, based on real-world data that contains the positions, and configurations of each mobile base station in the target area. It is therefore mainly responsible for the establishment of network scenarios and signal processing calculations within an LTE or 5G network. The LTE architecture modules and signaling models as well as functionalities that are used are integrated in *NS-3* and have been introduced in 40 and 41.

The simulated base stations are configured with the respective height, transmission power, bands, bandwidth and corresponding channels, and are connected to a simulated evolved packet core (EPC) as core network 42. 5G networks are simulated as non-stand-alone architecture, which is realized as 5G base stations connected to an EPC core network 43. The scenarios further include randomly placed user equipment (in-house and outdoors) that acts as cell phones. The connection between each user equipment and base station, based on distance, received signal strength and positioning, simulates the cell selection process and is used to determine the maximum range of each cell. The occurrence of a non-functioning base station changes the current cellular network topology within the submodule and thus the maximum range of each cell.

2.5 Simulation environment of the emergency response

The emergency response simulation presented here is being developed to assist in evaluating disaster management plans in conjunction with expert knowledge and provides recommendations for crisis situations. Already known approaches of disaster management simulation use four typical techniques 44: Monte Carlo simulations, discrete-event simulations, system dynamics, and agent-based simulations. Here, the agent-based modeling approach is used, in which different types of abstract agents interact with their environment

to fulfill assigned tasks. Agent-based modeling provides an effective way to simulate complex problems by accurately representing them through simple activities. Examples of the use of agent-based modeling are given in 45 and 46. In 45, agent-based modeling and simulation for crowd evacuation are analyzed from a methodological and empirical perspective. Specifically emergency plans are investigated with the aim of evaluating their feasibility. In 46, resource allocation across two locations is considered in a major incident using agent-based simulation.

Here, multiple sub-modules, namely *Incident Generator*, *Detectors*, *Control Center*, *Depots* and *Tactical Units*, are combined to a comprehensive emergency response simulation module. In a first step, incidents are generated using a time-based or probabilistic approach based on available open data. These incidents can originate from the areas of fire, technical, medical, police, power grid, drinking water network, gas network, telecommunication and combinations of these. The other infrastructure simulators presented in this publication can also trigger incidents, e.g. gas leaks triggered by the gas simulation module (see paragraph 0), water pipe burst triggered by the drinking water simulation module (see paragraph 0), and so on.

In the second step, the occurred incidents are detected and then reported to the *Control Center*. Possible detectors can be civilians, tactical units, but also automatic alarm systems. The incident is forwarded from the *Detector* to the *Control Center* by sending an emergency call. The *Control Center* sets up and manages missions resulting from incoming emergency calls, by using mission keywords. Resources are assigned and distributed in an optimal way. Resources are tactical units that comprise different types of vehicles from fire, police, and medical departments. Tactical units recognise on-site whether the mission keyword is correct. If necessary, they can request new resources via the *Control Center*. The units communicate with each other to ensure a successful mission. The routing of vehicles depends on their characteristics and can be adjusted due to factors such as size or weight restrictions, activation of signalling systems or roadblocks.

In total, the emergency response simulation enables the detailed evaluation of different scenarios. This evaluation focuses on operational principles, such as alerting, deployment sequence, access routes, and optimal positioning of tactical units, in conjunction with expert knowledge. It is advantageous to provide these evaluations as well as the visualizations of the simulation to staff members in a familiar operational command and administration software environment. Currently, the *MobiKat* 47 application is utilized for this purpose, including its application in staff training sessions.

2.6 Hazard vulnerability assessment of the built environment

The built environment is subject to aging, changes in occupancy and usage requirements. Lacking adequate design provisions or mitigation measures for existing buildings and increasing hazard frequency and intensity can often result in severe damage 48. In general, structural and non-structural damage is distinguished. While the latter primarily affects the usage of structures, the former can also lead to a threat to human life. Even though not every building and infrastructure system is needed immediately after a hazardous event, it is important that critical infrastructures remain operational, or the operational failure is considered in the emergency response.

Flood damage is often provided as a function of equivalent monetary losses and water level 49, 50. However, this does not directly address the type (structural or non-structural) and the extent of structural damage (crack opening, partial or total collapse). To evaluate the structural performance, hazard intensity measures such as flow velocity, flood elevation, debris transport/impact loads, critical water level differences (between interior and exterior), and subsoil parameters are proposed in the literature 50. Depending on a building class (e.g. RC, masonry, timber, high rise, low rise), fragility curves can then be defined and used to determine the probability of exceeding a certain damage level state as a function of intensity indicators. These curves can be obtained from empirical data of past damage situations 50 or generated with the help of simulations. Simulations are typically based on a deterministic approach that does not allow for a proper incorporation of uncertainties 51, 52. Recently, probabilistic methods have been increasingly used for flood vulnerability calculation. For example, fragility curves were developed for flood exposure of North American wood-frame and steel buildings 53 or for tsunami loaded Asian RC buildings with masonry infilled wall 54. However, the developed fragility curves strongly depend on regional construction methods and the considered loading condition and cannot easily be transferred to other regions/buildings, e.g., urban structures in Central/Western Europe. Therefore, in this contribution fragility curves are derived using probabilistic analyses for typical German buildings to assess flood risk at the urban scale.

Vulnerability is assessed for a portfolio of buildings that have similar characteristics in terms of performance in a hazard situation. To organize the buildings into different categories, the urban mixed-use pattern is divided into a certain number of building types, each representing a building class, e.g., typical 19th/20th

century historical masonry residential building or RC administrative building built after 1945. The variability in geometry, material strength and other relevant input parameters within a building class are considered in the analysis by means of a probabilistic distribution. The proposed probabilistic framework consists of three different sequential modules. Within the first module, a representative structural system within a building class is generated from a 3D city model. For this purpose, the building type is first extracted from the city model using the building age and geometric footprint of the building. The frequency of its occurrence as well as the geometric bounds of its dimensions in plan and elevation are evaluated. Information on the internal load-bearing structure, which cannot be extracted from the city model, is supplemented from literature studies or individual reference objects with a known structural system. A set of different structural models, representative of a specific building class, is derived by considering the uncertainty and adjusting input parameters based on their statistical distribution. A Python-based environment is being developed to access and manipulate the geometrical models created by the previous module and transfer them to an appropriate software package for structural analysis (e.g., RFEM®, Ansys®). The second module then executes the structural analysis. Loading scenarios (both standard loading and loads due to the hazardous events) can be applied as well as structural modifications (element stiffnesses, section and thickness variations). The third module collects and evaluates the analysis results to derive the fragility curves, describing the probability of reaching or exceeding a certain damage as a function of the intensity measure. All developed software tools are fully coupled, and the consecutive modules are executed automatically in series for integration of the results in the overall process.

In the first phase of the project, the analyses are limited to the complex investigations of structural damage to flood loading. However, the concept is equally applicable to all components and installations and will also be used to determine the vulnerability of non-structural elements in the future. In addition, the investigation of further natural disaster scenarios as well as man-made hazards is foreseen in order to provide a general-purpose tool for vulnerability determination of built environment.

3 Proposed co-simulation framework implementation details

The aim of this research is to create a simulation framework which is able to cover diverse crisis-related aspects regarding cascading effects among critical infrastructures and their consequences for citizens for various contingency scenarios. To this end, a system architecture allowing for the coupled and synchronized orchestration of the presented simulator modules is developed. This so-called co-simulation framework is implemented as a microservice-based architecture with each module as an independent microservice. This modular approach ensures scalability as well as maximum flexibility in development and integration. For communication and synchronization measures, an event-based communication pattern is implemented containing events and messages that are exchanged via publish-and-subscribe together with a rule-based translation between domain-specific parameter spaces. While heterogenous in principle, each of the modules presented in section 0 works in a similar manner as a mapping from domain-specific input data to simulation results as data output which might contribute to the input for other modules in subsequent simulation steps. For each module, the set of required input data and related output data is called its current *world model*. For a coupled operation, relevant elements of the individual world models have to be sharable among all the modules. To ensure this kind of interoperability between the modules with the aforementioned scalability and flexibility in mind, a common data model serving as an interface for all modules has to be introduced.

In this work, physical and also abstract elements of the simulated domains are interpreted as geo-referenced *things* equipped with *sensors* able to take thing-specific, time-resolved measurements. The inspiration is drawn from design and development in the *IoT* (internet of things) sector. This analogy elevates the modelled systems to the concept of a *digital twin*: While the input data can partly be specified through real-world sensor data, where available, simulated results can be used to complement the information content of the system state where no measured data is available. Moreover, the *IoT* sector offers standardized, well-established data models tailored to sensing entities like the *OGC SensorThings API* standard 55. The *SensorThings API* standard provides a concept of various entities in specified relations and serves as a foundational concept that strictly specifies how data models have to be structured and stored so that other modules can subsequently read and understand them.

Figure 31. Mapping of the world-model elements (white boxes) to the *SensorThings API* entities (orange boxes).

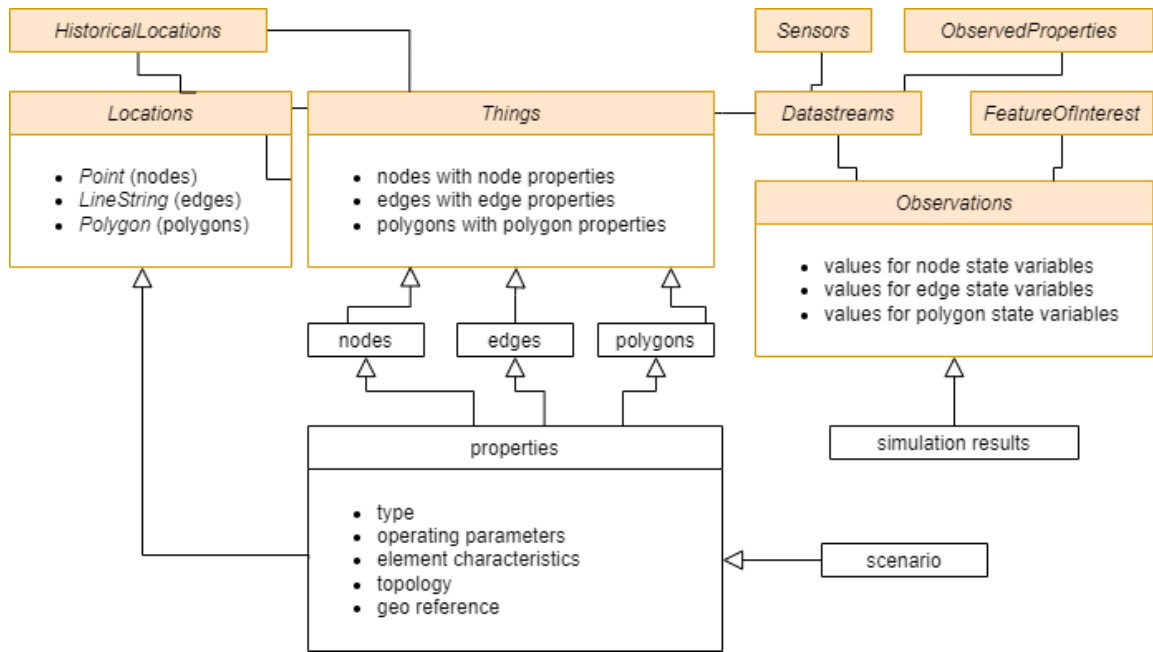


Table 1. Domain-specific world-model elements and their classification as *SensorThings API* entities.

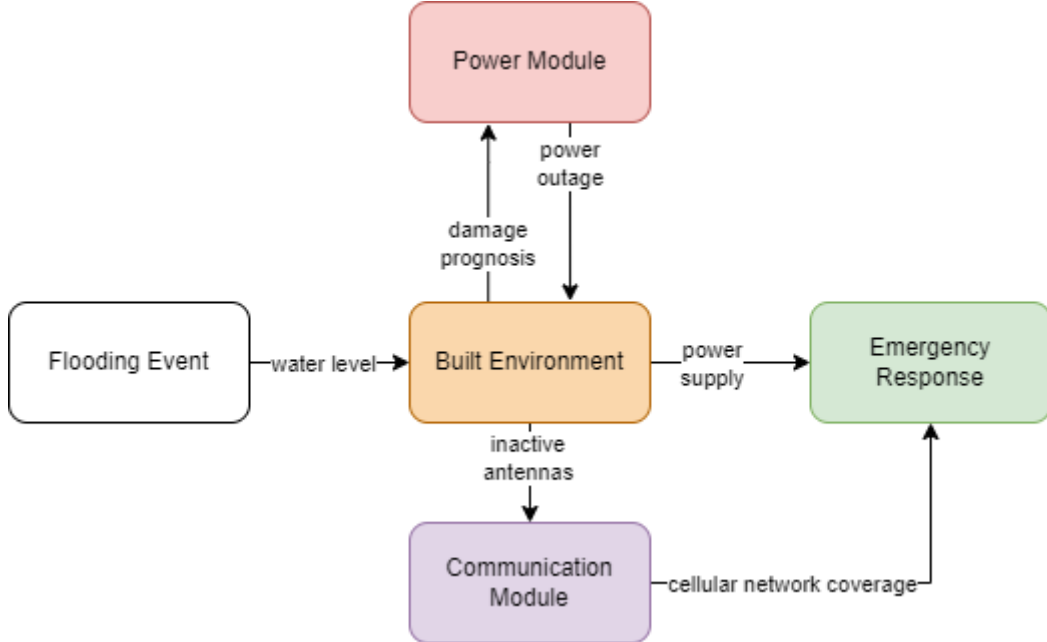
| Module | Power | Communication | Gas | Built Environment | Water | Emergency Response |
|---|---|--|--|---|--|---|
| <i>SensorThings API</i> | | | | | | |
| Things | <ul style="list-style-type: none"> • Terminals • Lines | <ul style="list-style-type: none"> • Coverage Area • Mobile Base Stations | <ul style="list-style-type: none"> • Node elements • Edge elements | <ul style="list-style-type: none"> • Buildings | <ul style="list-style-type: none"> • Node elements • Link elements | <ul style="list-style-type: none"> • Incidents • Tactical units • Depots |
| Locations (geo-referenced geometries) | <ul style="list-style-type: none"> • Polygons (terminals) • LineStrings (lines) | <ul style="list-style-type: none"> • Polygons (Base Stations) • Points (enbLocation) | <ul style="list-style-type: none"> • Points (nodes) • LineStrings (edges) | <ul style="list-style-type: none"> • Polygons (buildings) | <ul style="list-style-type: none"> • Points (nodes) • LineStrings (links) | <ul style="list-style-type: none"> • Points |
| HistoricalLocations | not used | | | | | cf. Locations |
| Datastreams | <ul style="list-style-type: none"> • Voltage at terminals • Load at lines | <ul style="list-style-type: none"> • Received Signal Strength Indicator (RSSI) • Radio Link Quality • Throughput/ Data rate | <ul style="list-style-type: none"> • Pressures at nodes • Flow rates through edges | <ul style="list-style-type: none"> • Probability of damage classes for buildings | <ul style="list-style-type: none"> • Pressure • Head • Demand • Demand Deficits • Flows • Velocity • Headloss • Status | <ul style="list-style-type: none"> • Incidents properties • Tactical Units properties • Depot properties |
| Sensors | cf. Datastreams | | | | | |
| Observed Properties | cf. Datastreams | | | | | |
| Observations | cf. Datastreams | | | | | |
| Feature Of Interest | not used | | | | | |

The *FROST* server implementation 7, 56 of the *SensorThings API* is employed in this work. Each simulator module's world-model elements, relevant for inter-module interactions, are stored on its dedicated *FROST*-server instance (see 7). The elements of the simulated domains are stored as *Things* with *Locations* and properties constituting the input data for the simulator module. *Datastreams*, defined by respective *Sensors* and *ObservedProperties*, can be related to the *Things* in order to store the (simulated) measurement values as *Observations* from the simulator output data. Entities on the *FROST* server can be created, read, updated, or deleted via *FROST*'s *RESTful API*. A detailed overview over the domain-specific world-model elements which need to be shared between the modules and their classification as *SensorThings API* entities is shown in Table 1.

Interactions between the different domains based on innate simulation results are initiated by mutual changes to other modules' world models. These are implemented as translation rules. These translations have to be defined for each possible change in one module and its implications to the other world models, thereby facilitating an interface between the modules on a world-model level. Furthermore, changes in one module's world model have to trigger a simulation run of said module in response which can be realized by event-based message exchange. For this purpose, the *FROST*-inherent *MQTT*-broker is used by each module to monitor or broadcast changes to world-model elements.

For example (see Figure 32): When the building module calculates the probability for severe structural damage due to rising water levels for a specific building in an area affected by flooding, it updates its world model with the relevant information. Subsequently, the power module must be informed about possible consequences for its world model, e.g., if the damaged building is a critical building such as a transformer station. If so, the power module therefore recalculates the state of the power grid which, in turn, might yield a set of buildings without electricity in the building module's world model. Buildings with base stations on their roofs, which are affected by the power outage, result in a change within the communication module's world model triggering updates to the predicted cellular network coverage of the affected area. Finally, the information about cell-phone coverage and the power supply situation of certain buildings might be of importance to the emergency response module affecting the agent-based simulation of the units.

Figure 32. Exemplary cascading effects caused by a flooding event.



4 Conclusion

This paper introduces a simulation framework that aims to assess and understand the interdependencies and cascading effects between critical infrastructures in urban or sub-urban areas during disasters. The framework consists of multiple simulation modules, including those for water, energy, gas, telecommunication, building damage analysis, and emergency response. The claim to reproduce cascading effects within the simulation, mandates a coupled instead of an insular modelling of infrastructures. This requires defined ways of communication and translation between the modules. The proposed system architecture is a microservice-based architecture. With event-based messaging and translation rules from the

microservices' outputs to inputs, it allows for communication between the simulation modules and manages their mutual triggering. The exchange of messages is facilitated through the common data model based on the *OGC SensorThings API* standard.

The presented architectural concept serves not only the requirement of scalability, since new modules may be introduced in a straightforward manner if they conform to the world-model protocol, but also serves the requirements in an environment where numerous developers and modules must collaborate in an interdisciplinary environment.

The presented research is to be understood as an introduction to the newly developed concept. After detailing the building blocks, it also lays out the roadmap for further development: The performance of the presented modules that are already integrated into the simulation framework has to be validated against real-world data with a special focus on their interdependencies. This validation also has to encompass the data and assumptions which go into the modelling of the real-world systems since each digital twin can only be as good as the data foundation and its simplifications. The inclusion of additional simulation modules must be carried out to scrutinize the claim of scalability and flexibility of the approach. The number and dimension of contingency scenarios which can be covered by this cross-domain coupled simulation framework also has to be enriched to offer versatile application possibilities.

Conceivable options include "what-if" analyses with a focus on vulnerability and resilience of coupled socio-technical systems, training applications for relief units and task forces, or infrastructure managers and even integration into decision-support software used by decision makers, authorities, and organizations with security responsibilities. Incorporating these kind of simulation results with complementing real-world data obtained from, e.g., drone reconnaissance or spontaneous helpers into different stages of the crisis management cycle, can assist authorities with proactively staying *ahead of the crisis*.

Acknowledgments

The authors' interdisciplinary research and development, as presented in this paper, is conducted within the Fraunhofer Center for the Security of Socio-Technical Systems (Fraunhofer SIRIOS) funded by the German federal government and the state of Berlin.

References

- 1 Koliou, M., van de Lindt, J., McAllister, T., Ellingwood, B., Dillard, M., Cutler, H., State of the research in community resilience: progress and challenges, Sustainable and Resilient Infrastructure, Vol. 5(3) pp. 131-151, 2020.
- 2 Deshmukh, A., Ho Oh, E., Hastak, M., Impact of flood damaged critical infrastructure on communities and industries, Built Environment Project and Asset Management, Vol. 1(2) pp. 156-175, 2011.
- 3 Hayes, S., Dent, C., Mawdsley, B., Collingwood, T., CReDo: an overview, Centre for Digital Built Britain, Cambridge, 2022.
- 4 Wang, Y., Yu, J. -Z., Baroud, H., Generating Synthetic Systems of Interdependent Critical Infrastructure Networks, in IEEE Systems Journal, Vol. 16(2), pp. 3191-3202, 2022.
- 5 Arrighi, C., Perngolato, M., Castelli, F., Indirect flood impacts and cascade risk across interdependent linear infrastructures. Natural Hazards and Earth System Sciences, Vol. 21(6) pp. 1955-1969, 2021.
- 6 van de Lindt, J., Kruse, J., Cox, D., Gardoni, P., Lee, J., Padgett, J., McAllister, T., Barbosa, A., Cutler, H., Van Zandt, S., Rosenheim, N., Navarro, C., Sutley, E., Hamideh, S., The interdependent networked community resilience modeling environment (IN-CORE), Resilient Cities and Structures, Vol. 2(2) pp. 57-66.
- 7 Fraunhofer-Institut für Optronik, Systemtechnik und Bildauswertung IOSB. Fraunhofer Open Source SensorThings API Server (FROST), 2023. <https://github.com/FraunhoferIOSB/FROST-Server>.
- 8 Praks, P., Kopustinskas, V., Masera, M., Probabilistic modelling of security of supply in gas networks and evaluation of new infrastructure. Reliability Engineering and System Safety, Vol. 144 pp. 254-264, 2015.
- 9 Sziksza, A., Monforti, F., GEMFLOW: A time dependent model to assess responses to natural gas supply crises. Energy Policy, Vol. 39(9), pp. 5129-5136, 2011.
- 10 Lochner, S., Dieckhöner, C., Tiger: infrastructure and dispatch model of the European gas market. Institute of Energy Economics at the University of Cologne, 2010.
- 11 Lohmeier, D., Cronbach, D., Drauz, S. R., Braun, M., Kneiske T. M., Pandapipes: An open-source piping grid calculation package for multi-energy grid simulations. Sustainability, Vol. 12(23), 2020.

- 12 Pambour, K. A., Cakir Erdener, B., Bolado-Lavin, R., Dijkema, G. P., SAInt - A novel quasi-dynamic model for assessing security of supply in coupled gas and electricity transmission networks. *Applied Energy*, Vol. 203 pp. 829-857, 2017.
- 13 SIMONE Research Group and LIWACOM Informationstechnik GmbH. SIMONE software. <https://www.liwacom.de/>. Accessed: 2023-05-09.
- 14 DNV. Synergi™ Gas. <https://www.dnv.com/services/hydraulic-modelling-and-simulation-software-synergi-gas-3894>, Accessed: 2023-06-07.
- 15 Ganter, S., Srivastava, K., Vogelbacher, G., Finger, J., Vamanu, B. I., Kopustinskas, V., Häring, I., Stolz, A., Towards Risk and Resilience Quantification of Gas Networks based on Numerical Simulation and Statistical Event Assessment. 30th European Safety and Reliability Conference and 15th Probabilistic Safety Assessment and Management Conference, ESREL/PSAM 2020. E-Proceedings. 2020.
- 16 Ganter, S., Kopustinskas, V., Zalitis, I., Vamanu, B., Finger, J., Martini, T., Dolgicers, A., Zernite, L., Fuggini, C., Häring, I., Stolz, A., A highly robust gas network simulation approach through an inherently solvable problem formulation for network states far from intended design points. Submitted to Applied Mathematical Modelling. 2023
- 17 Ringkjøb, H.K., Haugan, P. M., Solbrekke, I. M., A review of modelling tools for energy and electricity systems with large shares of variable renewables. *Renewable and Sustainable Energy Reviews* Vol. 96, pp. 440-459, 2018.
- 18 Thurner, L., et al., Pandapower – An Open-Source Python Tool for Convenient Modeling, Analysis, and Optimization of Electric Power Systems. *IEEE Transactions on Power Systems*, Vol. 33(6), pp. 6510-6521, 2018.
- 19 Troiano, G.O., Ferreira, H.S., Trindade, F.C.L., and Ochoa, L.F., Co-Simulator of Power and Communication Networks Using OpenDSS and OMNeT++. 2016 IEEE Innovative Smart Grid Technologies Asia, pp. 1094-1099, 2016.
- 20 Drauz, S.R., Spalthoff, M., Würtenberg, M., Kneiske, T.M., Braun, M., A Modular Approach for Co-Simulations of Integrated Multi-Energy Systems: Coupling multi-energy grids in existing environments of grid planning & operation tools. 2018 Workshop on Modeling and Simulation of Cyber-Physical Energy Systems (MSPCES), pp. 1-6, 2018.
- 21 Stifter, M., Schwalbe, R., Andrén, F., Strasser, T., Steady-state co-simulation with PowerFactory. 2013 Workshop on Modeling and Simulation of Cyber-Physical Energy Systems (MSPCES), pp. 1-6, 2013.
- 22 Caballero-Peña, J., Cadena-Zarate, C., Osma-Pinto, G., Hourly characterization of the integration of DER in a network from deterministic and probabilistic approaches using Co-simulation PowerFactory-Python. *Alexandria Engineering Journal*, Vol. 63, pp. 253-305, 2023.
- 23 Monsalve, C., Ruhe, S., Khabourtli, S., Nicolai, S., Netzkapa: Simulation Tool for Assessing the Integration of Electrical Vehicles in Distribution Grids, 2019 IEEE PES Innovative Smart Grid Technologies Europe (ISGT-Europe), pp. 1-5, 2019.
- 24 Grainger, J.J., and Stephenson, W. D., *Power System Analysis*. McGraw-Hill. 1994.
- 25 Rossman, L.A., EPANET: A public domain software package for modeling drinking water distribution systems. *Environmental Modelling & Software*, Vol. 15(6-7), pp. 647-653, 2000.
- 26 Klise, K.A., Bynum, M., Moriarty, D., Murray, R., A software framework for assessing the resilience of drinking water systems to disasters with an example earthquake case study. *Environmental Modelling & Software*, Vol. 95, pp. 420-31, 2017.
- 27 Martínez Alzamora, F., Lerma, N., Ayala, H.J., Vegas, Niño, O., Upgrade of the GISRed application for the free analysis of WDN under GIS environment, 17th International Computing & Control for the Water Industry Conference, CCWI 2019.
- 28 QGIS. <https://www.qgis.org/en/site/>. Accessed: 2023-09-27.
- 29 Rossman, L., Woo, H., Tryby, M., Shang, F., Janke, R., Haxton, T., EPANET 2.2 User Manual. U.S. Environmental Protection Agency, Washington, DC, EPA/600/R-20/133, 2020EPANET Manual, 2020.
- 30 Chang, K. *Introduction to Geographic Information Systems*. McGraw-Hill. 2008.
- 31 PostGIS. <https://postgis.net/>. Accessed: 2023-09-27.
- 32 Wrulich, M., Weiler, W., Rupp, M., HSDPA performance in a mixed traffic network. *VTC Spring 2008 - IEEE Vehicular Technology Conference*, 2008.
- 33 Jardosh, A.P., et al., Real-world environment models for mobile network evaluation, *IEEE Journal on Selected Areas in Communications* 23.3 pp. 622-632, 2005.
- 34 Hahn, S., et al., Impact of realistic pedestrian mobility modelling in the context of mobile network simulation scenarios, 2015 IEEE 81st Vehicular Technology Conference (VTC Spring), 2015.
- 35 Rupp, M., Schwarz, S., Taranetz, M., *The Vienna LTE-advanced simulators* Springer-Verlag, 2016.
- 36 Ikuno, J.C., Wrulich, M., Rupp, M., System level simulation of LTE networks. 2010 IEEE 71st Vehicular Technology Conference, 2010.

- 37 Johnson, D.B., Validation of wireless and mobile network models and simulation. DARPA/NIST network simulation validation workshop, 1999.
- 38 Lukau, E., Schiller, J., Meissen, U., Towards efficient post-blackout emergency communication based on citizens' smartphone state of charge, Proceedings of the 20th International ISCRAM Conference, 2023.
- 39 Piro, G., Baldo, N., Miozzo, M., An LTE module for the ns-3 network simulator. SimuTools, 2011.
- 40 Baldo, N., et al., An open source product-oriented LTE network simulator based on ns-3, Proceedings of the 14th ACM international conference on Modeling, analysis and simulation of wireless and mobile systems, 2011.
- 41 Virdis, A., Stea, G., Nardini, G., SimuLTE-A modular system-level simulator for LTE/LTE-A networks based on OMNeT++, 4th International Conference on Simulation and Modeling Methodologies, Technologies And Applications (SIMULTECH), IEEE, 2014.
- 42 Liu, G., et al., 5G deployment: Standalone vs. non-standalone from the operator perspective. IEEE Communications Magazine Vol. 58(11) pp. 83-89, 2011.
- 43 Hayashi, T., Evolved packet core (epc) network equipment for long term evolution (lte), Fujitsu Scientific and Technical Journal Vol. 48(1), pp. 17-20, 2011.
- 44 Mishra, D., Kumar, S., Hassini, E., Current trends in disaster management simulation modelling research. Annals of Operations Research, 283(1-2) pp. 1387-1411, 2019.
- 45 Piccione, A., Pellegrini, A., Agent-based Modeling and Simulation for Emergency Scenarios: A Holistic Approach. 2020 IEEE/ACM 24th International Symposium on Distributed Simulation and Real Time Applications (DS-RT), pp. 1-9, 2020.
- 46 Hawe, G., Coates, G., Wilson, D., Crouch, R., Agent-based simulation of emergency response to plan the allocation of resources for a hypothetical two-site major incident. Engineering Applications of Artificial Intelligence, Vol. 46 (Part B), pp. 336-345, 2015.
- 47 Brausewetter, P., Hahmann, S., MobiKat: GroBräumige Einsätze vernetzt bewältigen, gis.Business, 3(2019), pp. 14-16, 2019.
- 48 Maiwald, H., Schwarz, J., Abrahamczyk, L., Kaufmann, C. Das Hochwasser 2021: Ingenieuranalyse der Bauwerksschäden. Bautechnik 99, Vol. 12, pp. 878-890, 2022.
- 49 Neubert, M., Naumann, T., Hennersdorf, J., & Nikolowski, J., The geographic information system-based flood damage simulation model HOWAD. Journal of Flood Risk Management, 9(1), 36-49, 2016.
- 50 Schubert, J., Sanders, B., Structural Damage Prediction in a High-Velocity Urban Dam-Break Flood: Field-Scale Assessment of Predictive Skill. Mechanics, 138(10), 2012.
- 51 Handmer, J., The chimera of precision: Inherent uncertainties in disaster loss assessment. International Journal of Mass Emergencies and Disasters, Vol. 20, pp. 325–346, 2020.
- 52 Wagenaar, D., De Bruijn, K.M., Bouwer, L.M., De Moel, H., Uncertainty in flood damage estimates and its potential effect on investment decisions. Natural Hazards and Earth System Sciences, Vol. 16, pp. 1–14, 2016.
- 53 Nofal, O.M., van de Lindt, J.W. Minimal Building Flood Fragility and Loss Function Portfolio for Resilience Analysis at the Community Level. Water, Vol. 12, pp. 2277, 2020.
- 54 Waenpracha, S., Foytong, P., Suppasri, A., Tirapat, A., Thanasisathit, N., Maneekul, P., Ornhammarath, T. Development of Fragility Curves for Reinforced-Concrete Building with Masonry Infilled Wall under Tsunami. Advances in Civil Engineering, Vol. 2023, Article ID 8021378, 15 pages, 2023.
- 55 Liang, S.H., & Khalafbeigi, T., van der Schaaf, H., OGC SensorThings API Part 1: Sensing Version 1.1. OGC® Implementation Standard. 2021.
- 56 Hertweck, P., Hellmund, T., van der Schaaf, H., Moßgraber, J., Blume, J.W., Management of Sensor Data with Open Standards, 16th International Conference on Information Systems for Crisis Response and Management, ISCRAM 2019. Conference proceedings, 2019.

2.8 Remaining Useful Life of hydraulic steel structures under high-cycle fatigue Presentation of the chair Medelia and preliminary study of a lock gate

Julien Baroth¹, Vincent Michaud², Rafael Estevez³, Arnaud Isaac²

¹3SR Lab, Univ. Grenoble Alpes, CNRS, Grenoble INP, Institute of Engineering Univ. Grenoble, France

²ARTELIA/SPRETEC, Echirolles, France

³SIMAP Lab, Univ. Grenoble Alpes, CNRS, Grenoble INP, Institute of Engineering Univ. Grenoble, France

Corresponding author: julien.baroth@univ-grenoble-alpes.fr

Abstract

This work aims to characterize damage and lifetime of welded steel structures based on probabilistic fatigue design. This proposal presents a new research program (Medelia) to tackle and address several challenges related to this important field, gathering researchers and engineers at Grenoble-Alpes University and SPRETEC/ARTELIA company. The idea is to identify some drawbacks regarding usual fatigue verification of steel structures under high-cycle fatigue, to develop a fatigue study methodology of such structures composing hydraulic structures. Following a probabilistic S-N curves at the origin of Eurocodes, we propose a probabilistic approach based on fracture mechanics, applied to finite element models. A case study is introduced, which is a focus on connections of a lock gate. The resulting stochastic finite element allows plotting cumulative distribution function (CDF) of damage and remaining useful life (RUL).

List of abbreviations and definitions

| | |
|-----------|---|
| SFE | Stochastic finite element analysis |
| S-N curve | Stress vs Number of load cycles |
| P-S-N | Probabilistic fatigue curves |
| ASME | American Society of Mechanical Engineers |
| EdF | Electricité de France: the main French supplier of electricity managing nuclear and hydroelectric plants |
| CNR | Compagnie Nationale du Rhône: French company managing facilities such as dams or hydroelectric plants along the Rhône river |
| RCC-M | Design and Construction Rules for Mechanical Components |
| RUL | Remaining Useful Life |

1 Introduction

The ageing of the hydraulic works in France and around the world leads managers to choose between several scenarios: service life extension, repairs, reinforcements, or even complete replacement. The financial stakes are often very high, given the costs of manufacturing, construction and operating losses during shutdowns. Managers are therefore asking for as much information as possible to assess the remaining life and the level of risk associated with each of the aforementioned scenarios. In the case of welded steel structures such as turbine runners, lock gates, it is crucial to characterize and model the vulnerability of mechanically welded joints and the remaining useful life (RUL) of hydraulic structures.

1.1 Medelia chair purpose

The engineering mechanics company SPRETEC, member of ARTELIA group, has initiated the Medelia research chair with the INP foundation and the support of two mechanical engineering laboratories (3SR and SIMAP) at Grenoble Alpes University (UGA). The aim of this industrial chair is to develop knowledge of fatigue, fracture and the durability of hydromechanical structures, for an initial period of four years (2023-2026).

In all industrial sectors, operators such as Compagnie Nationale du Rhône (CNR) or Electricité de France (EdF) face with an increasing rate of problems linked to the ageing of their equipment, and in particular related to fatigue. This is due to the fact that industries developed strongly in the 2 or 3 post-war decades, bringing

equipment to 50–60 years of use today. This is the case in the nuclear, hydraulic, materials handling and civil engineering sectors, among others.

In the field of hydromechanics, changes in operating conditions, in particular frequent variations in operating dimensions, can also lead to load variations or start and stop costs not originally anticipated (Savin et al. 2020). Vibration phenomena linked to machinery or hydrodynamic effects can also cause fatigue failure. Finally, climate change and its effects (droughts, more frequent and higher floods, high temperatures, etc.) could also generate greater variability in equipment loading conditions. Equipment concerned includes lock gates, pipes, ball valves, turbines, tanks, aspirators, alternators, etc. At a first stage, we focus on mechanically-welded structures such as in lock gates, but the aim of the Chair is to develop a methodology that can be applied to other types of equipment.

1.2 Probabilistic fatigue analyses

Fatigue calculations carried out in practice are usually based on finite element models and normative post-processing of cyclic stresses: Eurocodes 3 (EC3, 2005), CODAP (2005), etc. These fatigue calculations result in estimates of cumulative damage, reflecting an indicative level of degradation. These estimates are subject to uncertainty at various levels. These include e.g.

- cyclic (or even vibratory) loading history of these components, supplied by the operators (number of daily cycles, water level, thermal stresses, etc.);
- material characteristics (quality of welding, fatigue limits, roughness, residual stresses, stress sign, etc.);
- geometrical: presence of cracks or defects, reduction in thickness due to corrosion, manufacturing tolerances...
- boundary conditions: bond stiffness, non-linear contact;
- fatigue calculation methods (damage estimates, service life, probability of failure, etc.).

In the context, estimating a remaining useful life (RUL) can only be uncertain, despite the many existing fatigue studies on steel structures. Figure 1 displays the variation of the stress amplitude applied to the mechanical system vs the number of cycles to failure (i.e. service life). Red and green curves are denoted S-N curves, or fatigue curves or Wöhler's curves.

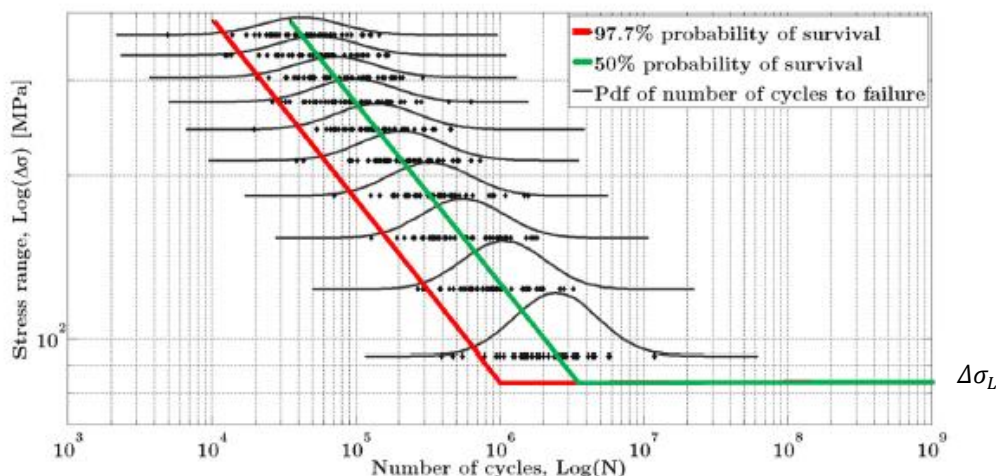


Figure 1. Stress amplitude variation at failure as a function of the number of cycles (S-N or Wöhler curve), illustrating the probability density functions of design lifetimes, as well as the quantiles at 2.3% and 50%, equal to the respective probabilities of 97.7 and 50% of a longer life (from Rocher et al., 2020). $\Delta\sigma_L$ denotes the fatigue endurance limit.

The principle of probabilistic fatigue calculation is to enrich fatigue calculation by taking into account uncertainties. In Figure 1 are plotted the probability density functions of the growing numbers of cycles to failure (i.e. service life), showing probabilities of exceeding a target service life (Rocher et al. 2020), which can be updated after inspection, e.g. in the case of offshore structures, taking into account inspection data (DNV, 2015, in van Jole 2016).

Just a few publications have been published on the fatigue assessment of lock gates, using stochastic finite element models, e.g. (Ramancha et al., 2022) and (Estes et al. 2004). The fatigue study of rivets is also the subject of recent work (Jiang et al., 2017). This type of study highlights influencing factors by prioritizing their effects on fatigue life. Some works also use a Bayesian approach, i.e. they take into account new observations over time to update predictions.

In the following, this paper first presents the Medelia Chair strategy, before presenting the methodological framework to be applied. Finally, some preliminary results are proposed.

1.3 Medelia chair strategy

Fatigue calculation rules of the Eurocode type are not very well suited to older structures. Indeed, the S-N curves of the Eurocode, although reputed to be conservative (97,7% probability of survival in Fig. 1), are designed for structures built with contemporary requirements (in particular, in compliance with EN 1090). An evaluation method has been proposed by the European Joint Research Centre (JRC, 2008), and recently adopted by CETIM in its recommendations (Depale B & Bennebach, 2020). In accordance to this framework, we therefore wish to go further than the Eurocode rules by proposing an alternative methodology based on the following axes:

1 - Refine fatigue criteria by studying the effects of parameters not taken into account in the Eurocode: one can consider e.g. steel grades, weld quality, roughness, corrosion, average stress, stress sign (partially taken into account in Eurocode), the level of reliability required, residual stresses, etc. Brand et al. (1999) e.g. gathers interesting parametric studies that should be used and completed.

2 - Enriching calculations with probabilistic approaches to fatigue. The Wöhler curves of the Eurocode are established for a certain level of reliability, which is generally not questioned. A probabilistic approach to influential parameters can also enrich fatigue analysis.

3 - Fracture mechanics calculations on weak points of a structure could also enrich and complete the previous points, in particular by assessing the influence of the presence of a crack on a constructive detail.

These preliminary working axes are likely to evolve during the course of the chair, in order to best serve the objective of developing complementary fatigue calculation tools to help operators to make the right decisions.

2 Proposed method

Several types of coupling are possible to achieve probabilistic characterization, with different precision levels. These couplings depend on the computational cost of the numerical models involved or the level of nonlinearity of these models. They also depend on the possibility of practically implement a mechanical-probabilistic coupling. The planned fatigue analysis is built on the expertise of the chair members: analytical and finite element models developed by SPRETEC, stochastic finite element (SFE) and fracture mechanics methods developed by the holders of the chair. We focus particularly in a two-scale SFE approach (connections and structure) to predict remaining useful life, before proposing a preliminary fatigue study of the welded connection of a lock gate.

2.1 Two-scale stochastic finite element framework

The methodology is summarized in figure 2, with the aim of formalizing the framework of our work, by arbitrarily defining our calculation models, analytical or finite element (FE), at the scale of a steel connection or structure, as a model M , a transfer function between an input parameter vector \mathbf{x} and a mechanical response \mathbf{y} . The central light gray box describes current practice in design offices: based on modeling assumptions (materials, geometry, boundary conditions, loads, etc.), the vector \mathbf{x} of descriptive parameters of the structure is defined. This vector feeds the mechanical study, which may call a series of calculations and models (analytical FE analysis...). For example, at the scale of a given mechanically-welded connection, for a given principal direction, the maximum stress is a component of \mathbf{y} , associated with the "S-N" fatigue curve of Eurocode 3, leading to the estimation of a number of cycles to failure N , as well as an elementary damage d by relativizing n by the total number N of cycles to failure, from which we can deduce the RUL as a function of an operating scenario for the structure concerned. The vector \mathbf{x} is decomposed into two sub-vectors \mathbf{x}_1 and

\mathbf{x}_2 , \mathbf{x}_2 modelling the parameters that can contribute to the correction of the fatigue curve. Parameters \mathbf{x}_1 , which have an impact on mechanical behavior, concern

(i) loads: water level (for a lock gate), thermal (data from thermal models or measurements), vibrations (data from measurements and/or FE models), friction (from literature and/or measurements), weight, etc.

(ii) geometry: construction dimensions, as the steel plates thickness, weld thickness (manufacturing tolerances, on-site observations/measurements...), etc.

(iii) mechanical characteristics: Young's modulus, yield strength, or even ultimate strength...

These \mathbf{x}_1 parameters are the ones that feed the M model, and are more or less well known. Each of them can be modeled by a random variable based on a mean value and a standard deviation obtained by gathering data from operators, on-site observations, scientific and technical literature, fictitious data, etc.

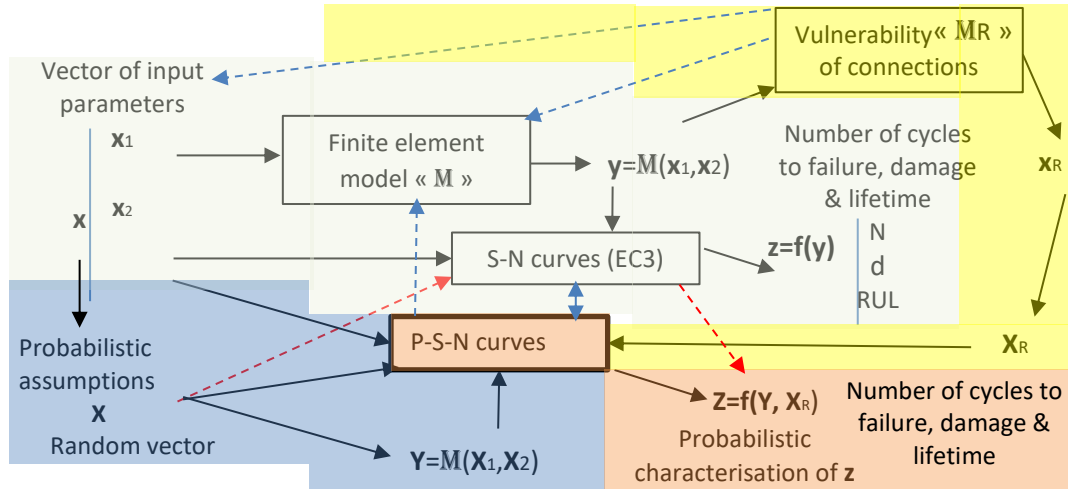


Figure 2. Probabilistic framework of fatigue analysis proposed within the Medelia chair.

The vector \mathbf{x}_2 is also used to denote the parameters that affect the Wöhler curves (P-S-N curves):

- material characteristics (literature and/or site measurements);
- mainly on-site observations: weld quality, roughness, corrosion;
- from M models or measurements: average stress, sign of stress;
- reliability target...

The vectors \mathbf{x}_1 and \mathbf{x}_2 are therefore not distinct; \mathbf{x} is the fusion of the two.

The blue box concerns the use of probabilistic assumptions and ad-hoc modelling, such that the parameters \mathbf{x} can be modelled using a random vector \mathbf{X} , as input to the model M , leading to a vector random response \mathbf{Y} . From this response, the use of regulatory fatigue curves (dotted red arrow) enables probabilistic characterization of the output z modelled using a random vector $\mathbf{Z} = (N, d, DV)$. Probabilistic fatigue curves (P-S-N) can also be defined.

The yellow box shows the use of modelling at the scale of connections identified as vulnerable at the end of the M calculation, with or without cracks. Fracture mechanics enables a more detailed characterization of the harmfulness of the crack. At the end of this study, \mathbf{x}_R represents information such as dissipation energy rates or stress intensity factors, that could be used to revise the M model, or the fatigue curves.

The bottom-right pink box reflects the combined result of fracture mechanics and probabilistic \mathbf{Z} modeling approaches, leading to a RUL characterization: Statistical moments (mean, variance), confidence interval, probability density function (PDF), cumulative distribution functions (CDF) can then be deduced.

2.2 Application to the study of a lock gate

Fig. 3a presents an overview of the half of a lock gate, modelled using a FE model (Ansys, 2021). The detailed description of this model (geometry, material, loads, bounding conditions) is gathered in Michaud (2021). For confidentiality reasons, only a few characteristics are given. From the FE calculations, some connections with higher stresses are identified. Fig. 3b represents a local description of one of these connections, between

vertical and horizontal panels. Due to the processing, an initial horizontal region is not welded and acts as an initial crack. Taking advantage of the symmetries (vertical and horizontal), a quarter of the region of interest is considered, loaded under uniaxial tension and at the bottom the displacement is fixed along the vertical direction to account for the symmetry plane (Fig. 3c). A FE model at the scale of the assembly is built (Abaqus, 2023).

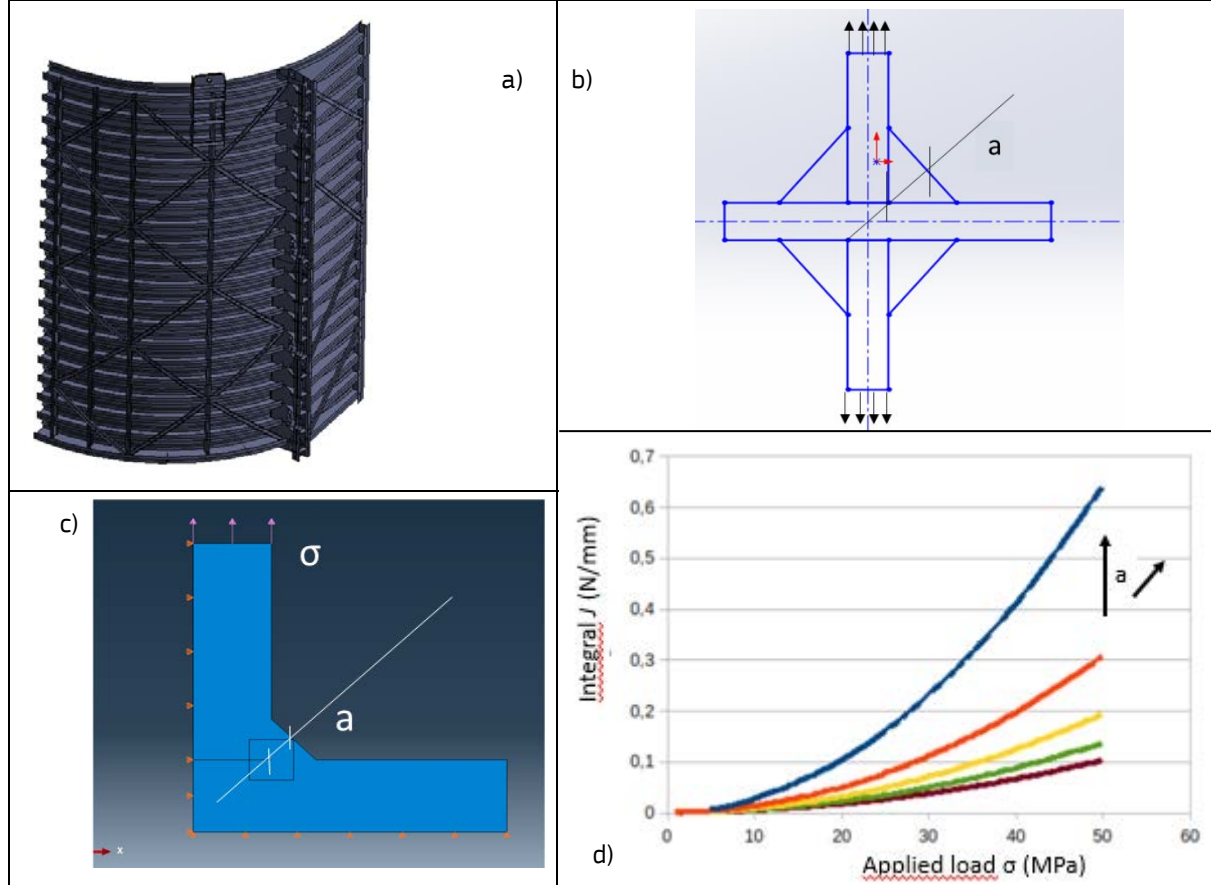


Figure 3. Overview of the half of a lock gate (a) and focus on a welded connection (b), reduced description (c) and calculation of the loading acting the crack (horizontal line in 'd') depending on the welded thickness a (d).

In Fig. 3d, the magnitude on the load level in terms of J-integral versus the prescribed tension remote stress σ on the top of the vertical panel is reported, with respect to the thickness a of the welded region (oblique length in Fig. 3b and 3c). The J-Integral (Rice, 1968) characterises the load level on the crack and corresponds to the strain energy released rate. We observe that the increase of the welding thickness induces an increase on the load acting on the crack (J-integral). As this thickness a can be variable, this originates the probabilistic load to be considered in the sequel.

2.2.1 Eurocode fatigue calculation

The Eurocode 3 (EC3) cumulative damage calculation method is an approach for assessing the progressive damage of steel structures subjected to repeated loads. This method involves calculating the level of cumulative damage at each point of the structure, integrating the effects of repetitive loading cycles. The calculation is based on the concept of remaining useful life (RUL), which is defined as the remaining service life of the structure before reaching a predefined level of damage. This residual service life is determined by comparing the cumulated damage level at each point of the structure with the corresponding allowed damage limit. The cumulated damage is defined such that $d = \sum \frac{n_i}{N_i}$, with N_i the total number of cycles to failure and n_i the number of the past cycles, where $i \in [1, r]$, r being the number of principal stress applied to each connection.

Let denote by $\Delta\sigma$ the stress amplitude, $\Delta\sigma_L$ the fatigue endurance limit (see Fig. 1), and $\Delta\sigma_p$ the weight stress amplitude such that

$$\Delta\sigma_p = \gamma_{Ff} \frac{1}{K_s} \cdot \gamma_{MF} \cdot \Delta\sigma , \quad (1)$$

with γ_{Ff} and γ_{MF} partial safety coefficients, K_s a reduction factor (due to dimension effect) if the thickness of the plates $e > 25\text{mm}$ (7.2.2, EC3, 2005), such that

$$K_s = \left(\frac{25}{e}\right)^{0.25} \quad (2)$$

The total number N_i of loading cycles to failure is then calculated as follows

$$(3) \quad \begin{aligned} \text{if } \Delta\sigma_p &< \Delta\sigma_L & \text{then } N_i &\rightarrow +\infty \\ \text{if } \Delta\sigma_L &< \Delta\sigma_p < \Delta\sigma_D & \text{then } N_i &= 5 \cdot 10^6 \left(\frac{\Delta\sigma_D}{\Delta\sigma_p}\right)^5 \\ \text{if } \Delta\sigma_D &< \Delta\sigma_p & \text{then } N_i &= 2 \cdot 10^6 \left(\frac{\Delta\sigma_C}{\Delta\sigma_p}\right)^3 \end{aligned} \quad \left. \right\}$$

where $\Delta\sigma_C$: reference value of the fatigue resistance for $N_C = 2 \cdot 10^6$ millions de cycles and $\Delta\sigma_D$: fatigue limit for constant stress amplitudes, a number of cycles N_D .

We arbitrarily set $n_i = 255000$ loading cycles (past service life of the gate), $\gamma_{Ff} = 1$, $\gamma_{MF} = 1.35$, and the thickness e reaches 40 mm (Michaud, 2021). For such a number of cycles, a significant cumulated damage has been found (Michaud, 2021). The idea is to complete this first indicator using probabilistic analyses and fracture mechanics.

2.2.2 Preliminary probabilistic analysis of the welded connection

A complex SFE analysis could be conducted using the FE model of the lock gate. In this first methodological presentation, we are simply interested in the maximum stress amplitude σ transmitted to the weld, and we arbitrarily consider it can be modelled using a Gaussian random variable, with a coefficient of variation of 10 %. Propagating this variability through the set of equations (3), using Monte-Carlo simulation. Fig. 4 displays the resulting PDF and CDF of the number of loading cycles to failure. From this graph, one can deduce that the probability of failure for the past service life of the gate ($2.55 \cdot 10^5$ cycles) already leads to around 10, that confirms the necessity at least to repair the concerned connection, with no allowable remaining useful life.

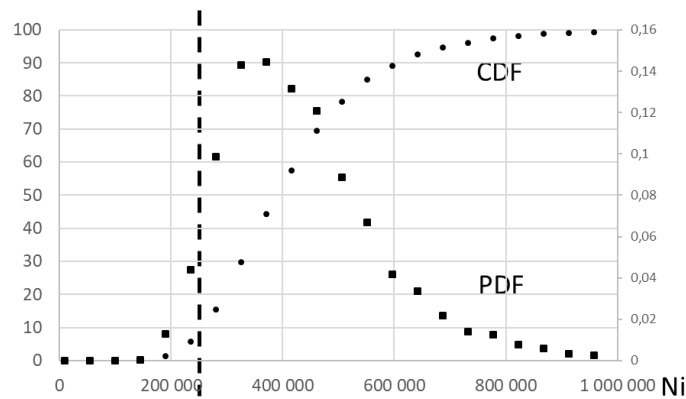
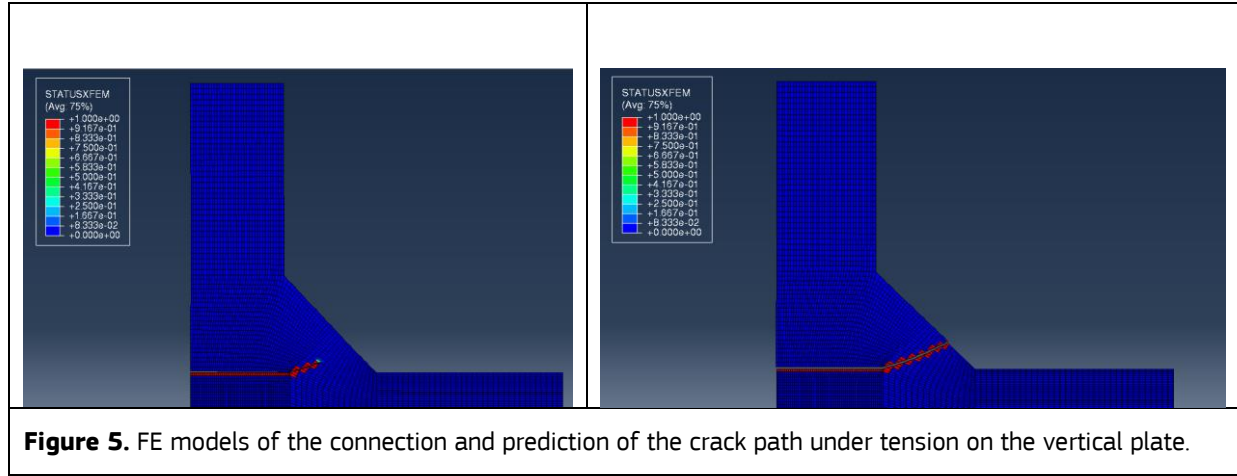


Figure 4. Cumulative distribution function (CDF) and probability distribution function (PDF) of the number of cycles to failure of the connection. The dashed vertical line indicates the past service life already leads to a 10% probability of failure, that seems already high to allow a remaining useful life

2.2.3 SFE analysis of a welded connection

A stochastic finite element model of the connection is deduced from the FE model of the assembly. The description of the model and boundary conditions are presented in Fig. 3. In Figure 4, we illustrate how a crack propagation can be modelled with cohesive zones inserted "on the fly" with phantom nodes (Abaqus, 2023). The fracture parameters are the energy release rate $G_c = 10 \text{ J/m}^2$ and maximum strength $T_{\max} = 100 \text{ MPa}$, for illustrative purpose, the elastic properties being those of a standard steel with Young modulus $E = 200 \text{ GPa}$ and $\nu = 0.3$. In the case of tension at the top of the vertical panel, the calculation shows how the crack grows with an inclined crack path (Fig. 5). Using this method, the studied connection of the lock gate is also modelled.



The stochastic collocation method (Baroth et al. 2007) is used to propagate the 10% load variability through the FE model. As a result, Fig. 6a presents the PDF and CDF of the strain energy release rate, also known as « integral J ». One can deduce from this graph the 90% confidence interval, defined by the bounds corresponding to the 5 and 95% quantiles, corresponding to J values approximately equal to 20 and 55 N/mm² respectively. This graph can also be interpreted as meaning that the probability of exceeding 55 is 5%, which could be considered as a "characteristic value" of J , as defined in the Eurocodes (ECO, 2002).

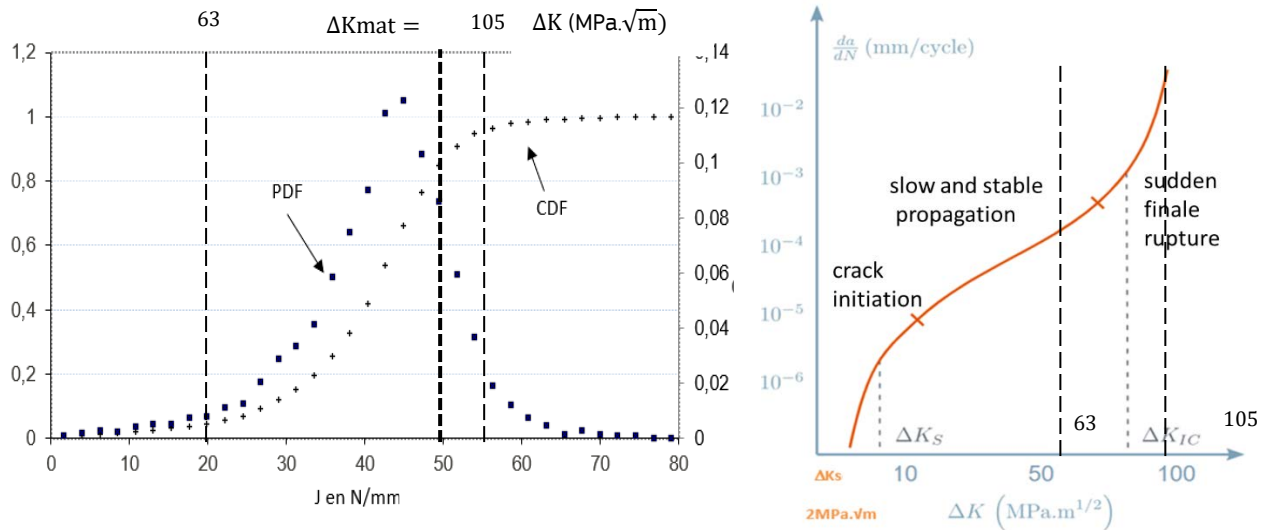


Figure 6. Characterization of the severity of the crack of the assembly: PDF and CDF of the integral J (a) ; Paris Law evolution (b)

In this work, we point out that this J distribution can be also used to estimate a range of corresponding stress intensity factor (ΔK) range, remembering the well-known relation between J and ΔK and Young's modulus E .

$$\Delta K = \sqrt{JE} \quad (4)$$

Indeed, deducing that the 90% confidence interval on the stress intensity factors is around [63;105] MPa. \sqrt{m} . This range can be compared to the evolution of the crack propagation velocity estimated by the famous Paris law, giving the rate of growth of a fatigue crack. da/dN is the fatigue crack growth for a load cycle N . The material coefficients C and m are obtained experimentally and also depend on environment, frequency, temperature and stress ratio.

$$\frac{da}{dN} = C \Delta K^m \quad (5)$$

Given the operating conditions of the lock gate, using the British standard (BS 7910, 2019), we build the evolution Fig. 5b, defining three zones, before crack initiation, the slow and stable propagation, and a sudden and brutal rupture. These three zones are delimitated by two stress intensity factor ranges ΔK_s and ΔK_{IC} , estimated around 2 and 99 MPa \sqrt{m} respectively. The 90% confidence interval from Fig. 5a has been reported in Fig. 5b, including the critical stress intensity factor range ΔK_{IC} of 99 MPa. \sqrt{m} . Coming back to the CDF in Fig. 5a, one can read a probability to exceed ΔK_{IC} of 10% to reach a sudden and finale rupture. Once again, this result confirms the necessity at least to repair the concerned connection, with no allowable remaining useful life.

3 Conclusions

This article has presented the chair Medelia and a preliminary framework to contribute to the evaluation of damage and remaining useful life of hydromechanical structures. Mechanical-probabilistic coupling is proposed to better understand the behavior of such aging structures, in order to help managers to decide to repair or not connections or whole structure, and for the future to highlight design parameters, that could be crucial to better control. Until now, the regulatory study allows to estimate a cumulated damage indicator, that should be completed. Recent studies highlight e.g. that a unique estimator of damage is not enough when damage level increases, it is at least useful to conduct several damage estimations in different operating conditions (Savin et al., 2021).

For the sake of illustration, the case of the FE model of a lock gate is introduced, a “critical” connection being selected and studied. From a deterministic regulatory point of view, damage estimation alerts on the nocivity of the connection. The novelty in this work is to use both fracture mechanics and probabilistic analyses to provide two complementary indicators of the damage level of the connection: the probability to exceed the critical stress intensity factor range and the distribution of loading cycles to failure. These two indicators show clearly that the connection must be repaired in this case.

This preliminary study opens the route to more detailed investigation of early stages of fatigue crack growth, using the last 3 damage indicators, applying such methodology to all potentially dangerous connections identified or using available in situ observations.

Acknowledgements

Authors are grateful for the support provided by ARTELIA-SPRETEC within the Chair Medelia agreement with the Grenoble INP Partnership Foundation. The Chair Medelia partners shall not in any circumstances be deemed liable for the content of this publication which is only binding its author.

Authors are also grateful to Hana Abidi and Bintou Coulibaly for their contributions in their internships.

References

- 1 Abaqus, Standard User's Manual, Version 2020.
- 2 Abidi H., Initiation à la fiabilité et à la fatigue probabiliste : Application aux portes d'écluses de navigation, Master thesis, ENSE3, 2023.
- 3 Ansys, Workbench, R1, 2021.
- 4 Baroth J., Chauvière C., Bressolette P., Fogli M., An efficient SFE method using Lagrange Polynomials: application to nonlinear mechanical problems with uncertain parameters. Comp. Meth. Appl. Mech. Engrg., n° 196, pp. 4419-4429, 2007.
- 5 Brand A, Flavenot J.F., Gregoire R., Tournier C. Technological data on fatigue, Senlis, CETIM; 1999, 4e ed., 383 p.
- 6 BS 7910, Guide to methods for assessing the acceptability of flaws in metallic structures, 2019.
- 7 CODAP, code de construction des appareils à pression non soumis à la flamme, SNCT, 2005.

- 8 Coulibaly, B., Analyse de la nocivité de défauts de structures métalliques mécanosoudées, Mémoire de stage de fin d'études, Master 2 Génie Mécanique, Polytech'Lille, 2023.
- 9 Depale, B & Bennebach, M., Durée de vie résiduelle (DVR) des structures et équipements : problématique et applications aux appareils de levage / Residual Life of Structures and Equipment_Problems and Application to Crane, CETIM, 2020.
- 10 DNV GL, "Probabilistic methods for planning of inspection for fatigue cracks in offshore structures," Recommended Practice, 2015.
- 11 Eggen, A.O., Belsnes, M. Operation related maintenance and reinvestment costs for hydropower scheduling. Energy Syst (2023).
- 12 EN 1990, Eurocode 0. 2002. Bases of Structural Design. Brussels: CEN.
- 13 EN 1993-1-9. Eurocode 3: Design of steel structures - Part 1-9: Fatigue [Authority: The European Union Per Regulation 305/2011, Directive 98/34/EC, Directive 2004/18/EC]; 2005.
- 14 JRC, JRC43401, Assessment of Existing Steel Structures: Recommendations for Estimation of Remaining Fatigue Life, EUR 23252 EN – 2008.
- 15 Michaud, V., Ecluse de Bollène, Fatigue de la porte aval, Notes de calcul, SPRETEC, 2021.
- 16 Rocher, B., Schoefs, F., François, M., Salou, A., Caouissin, A.L., A two-scale probabilistic time-dependent fatigue model for offshore steel wind turbines, International Journal of Fatigue 136 (2020) 105620.
- 17** Savin, O., Badina, C., Baroth, J., Charbonnier, S., Bérenguer, C. Start and stop costs for hydro power plants: a critical literature review. In: Proceedings of the 30th European Safety and Reliability Conference and the 15th Probabilistic Safety Assessment and Management Conference, 2020.
- 18 Savin, O., Baroth, J., Badina, C., Charbonnier, S., Bérenguer, C.: Damage due to start-stop cycles of turbine runners under high-cycle fatigue. Int. J. Fatigue 153, 106458 (2021).
- 19 Stefanou, G., 2009. The stochastic finite element method: Past, present and future. Computer Methods in Applied Mechanics and Engineering 198, 1031–1051. doi:10.1016/j.cma.2008.11.007.
- 20 van Jole, J.A., Development of a Method for Assessment of the Remaining Fatigue Life of Steel Structures of Existing STS Cranes, master thesis, Delft university of technology, 2016.

2.9 Resilience Metrics for Interdependent Infrastructure Systems: Characterization in full-scale Application

Paolo Trucco and Boris Petrenj, Politecnico di Milano, School of Management, Italy paolo.trucco@polimi.it, boris.petrenj@polimi.it

1 Introduction

The growing need for managing Critical Infrastructure (CI) resilience has spurred significant research endeavours, resulting in the proposal of various metrics to capture the resilience properties of CI systems. Effectively capturing all resilience dimensions and quantifying them to create a holistic resilience assessment is a challenging task. Thus, choosing the most suitable metric for a particular application is a key decision for the analyst, potentially affecting the validity of the results. It requires careful consideration of the properties, key strengths, and limitations inherent in existing metrics.

In this paper we summarize a study on the characterization of the most representative resilience metrics, suitable for the analysis of interdependent infrastructure systems, based on a critical evaluation of their adoption in a full-scale CI resilience assessment

2 State of the art review

We depart from a systematic literature review to identify quantitative technical resilience metrics applicable to networked infrastructure systems, used to interpret quantitative data that describe infrastructure performance/functionality during disruptions. The searching on Scopus and Web of Science databases resulted in a list of 360 unique publications across various application domains.

A systematic process narrowed the metrics down to 20, focusing on quantitative technical resilience metrics and prioritizing new and recent advancements when multiple papers covered the same metrics. Similar metrics were then streamlined, favouring the most recent or comprehensive ones. Metrics requiring extensive non-technical information were excluded, and the study favoured composite and ‘valid metrics’ [1], resulting in the final selection of 7 metrics for quantitative analysis in the experimental campaign.

Table 1. List of the selected resilience metrics as representative of each group

| Type | Reference | Equation(s) | Metric Code |
|------------------------------------|---|---|-------------|
| Metrics built on the RLT | Chen and Miller-Hooks, 2012 [2] | $R_c(T) = \frac{\sum_{w=1}^W c_w(T)}{\sum_{w=1}^W C_w(T)}$; $R_d(T) = \frac{\sum_{w=1}^W d_w(T)}{\sum_{w=1}^W D_w(T)}$ | A1, A2 |
| Metrics built on the RLT | Ouyang and Wang, 2015 [3] | $R_c(T) = \frac{\int_0^T c(t) dt}{\int_0^T C(t) dt}$; $R_d(T) = \frac{\int_0^T d(t) dt}{\int_0^T D(t) dt}$ | B1, B2 |
| Composite Resilience Metrics (CRM) | Nan and Sansavini, 2017 [4] | $R = RO \times \left(\frac{RAPI_{RP}}{RAPI_{DP}} \right) \times (TAPL^{-1}) \times RA$ | C |
| CRM with service segmentation | Goldbeck, Angeloudis, and Ochieng, 2019 [5] | $R = \frac{MSP}{RLT \times TLD}$ | D |
| Case-specific Resilience Metrics | Kilanitis and Sextos, 2019 [6] | $f_p = 100 \times \sum f_j$ | E |

A1, B1: c – actual capacity of the system; C - theoretical capacity of the system; (of node w at time t)

A2, B2: d – demand successfully satisfied; D – actual demand; (at node w at time t)

C: RO – Robustness; $RAPI$ – Rapidity; $TAPL$ – Time Average Performance Loss; RA – Recovery Ability

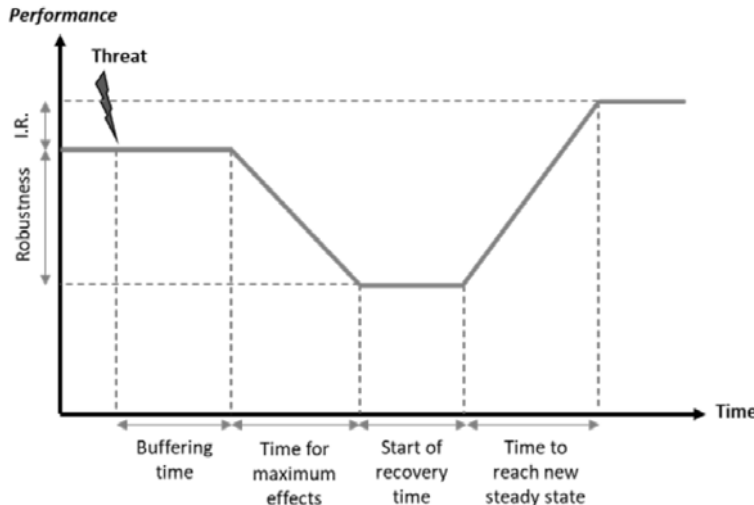
D: MSP – minimum system performance; RLT – resilience loss triangle; TLD – total length of disruption;

E: f – importance factors of links that are functional during each phase of the disruption

3 Benchmarking Framework

The selected metrics (Table 1) were assessed against the six main parameters that define the disruption profile (aka ‘Resilience Loss Triangle’): Robustness; Buffering time; Time for maximum effects; Start of recovery time; Time to reach new steady-state and Improvement ratio (Figure 1). These parameters were taken as a reference to systematically assess and compare the ability of each resilience metric to capture the influence of the system’s structural and operational conditions on its resilience profile.

Figure 1. Key parameters of the resilience loss triangle considered in the comparative assessment.



To comprehensively evaluate and fairly compare the selected resilience metrics, five evaluation criteria were established. First, **sensitivity** assessed a metric’s capability to detect changes in system properties. Second, **flexibility** measured a metric’s adaptability to different performance measures. Third, **selectivity** evaluated a metric’s ability to detect specific system changes while isolating their contribution to overall resilience. Fourth, **generality** assessed a metric’s suitability for assessing resilience across diverse network types and purposes. Finally, **scalability** determined a metric’s capacity to provide size-independent resilience measurements, crucial for comparing systems of varying sizes.

4 Experimental Setting and Procedure

The evaluation process employs the DMCLe tool (Dynamic Functional Modelling of Vulnerability and Interdependencies of CIs [7]) which analyses interdependent CI systems. For the empirical setting, we use a significant portion of the transportation network connecting Italy and Switzerland. The DMCLe model aligns with simulation-based resilience metric assessment requirements, accounting for interdependencies, measuring resilience on a system-of-systems level, and considering service disruptions. The case study’s heterogeneity and relevance for generalization make it valuable, and the simulator is validated through replication of a real event in the Lombardy region (Italy).

The analysis aimed to assess whether variations in resilience parameters affected the selected metrics. Assuming a steady-state level post-disruption recovery equal to the original level (Improvement ratio=1), a single replicate 2^k factorial design was employed, with k representing the number of factors (here, five resilience properties) and 2 indicating two levels for each factor (coded as lowest=0; highest=1). This design allowed 32 independent simulations without confounding effects. Each simulation simulated the complete loss of the Brogeda customs station’s functional integrity for 36 hours, a strategic choice based on its criticality from the Vital Node Analysis. To mitigate noise in the experiments, careful selection of values for factor codes 0 and 1 was crucial. Higher variations between low and high factor levels yielded more reliable results, reducing the risk of erroneous conclusions due to random variability.

The performance assessment approach, based on Goldbeck et al. [5], used **Service Level** as the main performance indicator at the system level. Flexibility of metrics was tested using **Service Capacity** as an alternative indicator. Sensitivity to changes in resilience parameters was assessed through two rounds of experiments, with the second addressing time variability in service demand.

5 Main results

Based on the assessment summary (Table 2), we can recommend a combined approach for analysing resilience in complex interconnected systems. A qualitative analysis (e.g. using metrics A and B) aids in visualizing system dynamics and the contribution of various factors to overall resilience. A quantitative analysis (e.g. employing metric C) allows for objective scenario comparison within a system and, with precautions, across different system topologies.

Table 2. Summary of the assessed properties of the selected resilience metrics: marginal fit (*), substantial fit (**) and full fit (***)

| | Metrics A1, A2, [2] | Metrics B1, B2 [3] | Metric C [4] | Metric D [5] | Metric E [6] |
|-------------|---------------------|--------------------|--------------|--------------|--------------|
| SENSITIVITY | ** | *** | *** | ** | *** |
| FLEXIBILITY | ** | *** | ** | * | *** |
| SELECTIVITY | ** | ** | *** | ** | * |
| GENERALITY | ** | ** | *** | ** | * |
| SCALABILITY | *** | *** | ** | *** | *** |

6 Conclusions

This research addresses the challenges of assessing specific resilience aspects in networked infrastructure systems, providing valuable insights into the properties of various resilience metrics. Specifically, we assess their ability to capture the influence of both structural and operational conditions on the resilience profile of the system. These findings can inform decisions, including the development of resilience-enhancing strategies. However, the study's limitation lies in its focus on a complex transportation network, and different networked systems may exhibit distinct responses to disruptions.

References

- [1] Najarian, M. and Lim, G. J. (2019). "Design and assessment methodology for system resilience metrics". Risk Analysis 39. 9. pp. 1885–1898.
- [2] Chen, L. and Miller-Hooks, E. (2012). "Resilience: an indicator of recovery capability in intermodal freight transport". Transportation Science 46.1, pp. 109– 123.
- [3] Ouyang, M. and Wang, Z. (2015). Resilience assessment of interdependent infrastructure systems: With a focus on joint restoration modeling and analysis. RESS 141, pp. 74–82. [4] Nan, C. and Sansavini, G. (2017). A quantitative method for assessing resilience of interdependent infrastructures. RESS 157, pp. 35–53.
- [5] Goldbeck, N., Angeloudis, P. and Ochieng, W. Y. (2019). Resilience assessment for interdependent urban infrastructure systems using dynamic network flow models. Reliability Engineering & System Safety, 188, 62–79.
- [6] Kilanitis, I. and A. Sextos (2019). Integrated seismic risk and resilience assessment of roadway networks in earthquake prone areas. Bulletin of Earthquake Engineering 17.1, pp. 181–210.
- [7] Galbusera, L., Trucco, P., Giannopoulos, G. (2020). Modeling interdependencies in multisectoral critical infrastructure systems: Evolving the DMCI approach. Reliability Engineering & System Safety, 203, 107072.

2.10 A territorial view of the infrastructure resilience

David Javier Castro Rodriguez, Politecnico di Torino, Italy, david.castro@polito.it

Antonello Barresi, Politecnico di Torino, Italy, antonello.barresi@polito.it

Micaela Demichela, Politecnico di Torino, Italy, micaela.demichela@polito.it

Abstract

The challenge to make cities and, more in general, the territories inhabited or exploited by humans safe, and resilient, includes mitigation and adaptation strategies against disaster, as a central issue in achieving sustainability. A tool to measure local vulnerability from a multi-risk approach is proposed and discussed. The tool consists of a mathematical framework for the territorial vulnerability assessment that integrates multiple indicators clustered into three factors defined as sensitivity, pressures, and hazards, weighted according to a participatory procedure. These include the infrastructures at the service of the territories and the effects of their disruption. Cascade effects can be also considered in the model, as mutual influences among factors, to keep into account, as an example, climate change related phenomena. Space-dependent analyses using the Geographical Information System were developed from the multiple nested indicators to project the vulnerability index onto a homogeneous grid in the territory of interest. Thematic maps referring to the systemic vulnerability by different sensitivity components were generated. The tool contributes to increasing the awareness of territorial vulnerability and offers support to resilience-based decision-making in designing technical measures of policies at a local scale, whose managers are potentially disoriented by more complex models. A municipality in North-West Italy was used as a case study, concerning the process/energy infrastructures, within the research activities of the Responsible Risk Resilience Centre from the Polytechnic of Turin to test the vulnerability matrix. Further research is required to implement the framework in different scenarios and develop the model's temporal behaviour.

1 Introduction

The Sustainable Development Goals (SDGs) issued in 2015 for the United Nations Agenda, highlight the necessity to strengthen the resilience and the adaptive capacity in all sectors against the different natural hazards and disasters, in line with the Sendai Framework for Disaster Risk Reduction 2015–2030 (United Nations, 2015a; 2015b). In this context, contemporary challenges and uncertainties expose cities and local communities to multiple and non-linear risk factors that require a spatial planning approach to integrate the dimensions of complexity and unpredictability. This situation calls for new methods and tools to frame territorial vulnerability (Brunetta et al., 2019) and thus enhance resilience (Galderisi, 2012) and adaptation in the context of sustainable development goals. Central to spreading awareness and building adaptation policies is the availability of specific data and analysis to measure resilience. In this sense, vulnerability assessment is the first part of operationalizing resilience, often interpreted as a buzzword and a term challenging to put into an operational context (Brunetta et al., 2020).

Vulnerability, often considered as the counter position to resilience, is to be understood as the predisposition of the elements of the system to be damaged by hazard events, punctuality, or continuous pressures over time (IPCC, 2012), while resilience is, in fact, the coping capacity of the elements of the system. Consequently, the measurement of vulnerability lends itself to using quantitative methodologies based on multivariate analysis of representative indicators.

New challenges faced by people involved in disaster risk management are the so-called high-impact and low-probability events (HILP), such as technological events triggered by natural hazards (Natech). Even if this kind of event presents a small likelihood (often neglected by operators), in case of occurrence, it may cause severe damage to individuals, infrastructure, environment, and society, being particularly complex because often it is the result of cascading events (Mesa-Gómez et al., 2020). Furthermore, there is some evidence suggesting that an increase in the frequency of certain types of Natech, may be linked to climate change (Ricci et al., 2021).

In this line, the Italian National Adaptation Plan serves as a notable instance of a climate change adaptation strategy advanced by EU member states. It acknowledges the issue of NaTech events as one of the sectoral vulnerabilities related to climate change and recommends sector-specific measures and best practices to ensure effective adaptation to climate change in the industrial sector (Centro Euro-Mediterraneo sui Cambiamenti climatici, 2017). Regarding the industries, they are no longer perceived as isolated facilities, but

as part of larger, interconnected socio-ecological and technological systems (SETSS), that consider the entire production process and its impacts on human beings and the environment.

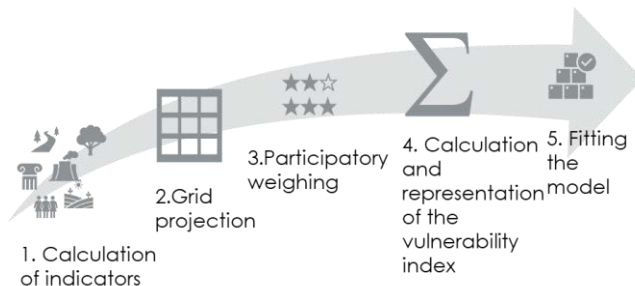
Considering everything described above, this contribution develops a territorial view of the infrastructure vulnerability, integrating elements of one industrial case study and the multi-hazard context where the facility is located. This case serves as a proof of concept to assist the decision-making process about the interaction among critical infrastructures and the multiple hazards belonging to the territories.

2 Tool for assessing the territorial vulnerability.

The tool proposed by Beltramino et al. (2022), to determine vulnerabilities at the local scale, represents the cornerstone of this case study. This multidisciplinary tool has been developed by the Responsible Risk Resilience Centre (R3C) from Polytechnic of Turin, to respond to the first objective of the project Measuring Resilience (Brunetta et al., 2019), which consists of the assessment and spatial representation of the systemic vulnerability of a territory.

In a nutshell, the multidisciplinary tool consists of a mathematical framework capable of quantifying the vulnerability in a territory, integrating multiple indicators clustered into three factors defined as sensitivity (S), pressures (P), and hazards (H), weighted according to a participatory procedure. It ensures not only the estimation of different stressors and hazards according to impacting sensible elements belonging to the location of interest, but also the necessities of the stakeholders expressed as a coefficient of interest. In addition, in the mathematical equation for the estimation of the systemic vulnerability consider factors for both, the impact of climate change, and the temporal character of the pressures. The vulnerability matrix follows five steps as depicted in Figure 1.

Figure 33. Steps to implement the vulnerability matrix.



2.1 Selection and Calculation of Indicators

The starting point for the creation of the tool is the selection of a set of sensitivity, pressure, and hazard indicators and their calculation using GIS tools. They were selected following a discussion with stakeholders from the area under study and a review of the principal spatial government plans and territorial instruments, highlighting the Municipality specificities.

The definition and calculation of the indicators is the most consistent and time-consuming phase of this work. Each of the 21 indicators selected has followed a process of data collection and calculation in a GIS environment. Further details about the description and calculation of each indicator can be found in Beltramino et al. (2022).

2.2 Indicators Grid Projection and Representation

These indicators were nested in layers onto a grid of homogeneous cells (200 x 200 m) which covers the municipality combining all the relationships and elements examined and allowing an overall reading of the critical territorial aspects. For their attribution into the grid, spatial join operations through a specific field identifier (FID) were assigned to each cell. Depending on the geometry of the input data (point, line, polygon) the attribution of the values obtained for each indicator to the grid was carried out according to five criteria: (i) point count (Cultural heritage consistency-B1, Floods-ALA), (ii) sum of the point values (Energy consumption intensity-A3, RES energy selfsufficiency-B3, Earthquakes-SIS), (iii) weighted sum of linear (Road infrastructure density-B5) or areal elements (Landscape sensibility-A1, Ecological Quality-A2, Building construction characteristics-B2, Communication infrastructure density-B4, Density of productive activities-C4, Soil consumption-CDS, Building obsolescence-OBS, Wildfires-IBO, Lands slides-FRA), (iv) average value of areas within the cell (Population density-C1, Elderly component-C2, Immigrant Component-C3, Aging population-OLD) and (v) intersection between input polygons and each cell (Flash floods-ALU, Major Industrial Risk-RIR).

2.3 Participatory weighing

The relationship between each sensitivity indicator and pressure and hazard indicator was weighted using a crossing matrix procedure (row by column). In this phase, a participatory methodology was used, involving a team of 13 researchers participating in the project, where an interactive version of the matrix, evaluated the degree of relationship between each indicator using an ordinal Likert scale, where: 0, no relationship; 1, weak relationship; 2, strong relationship; 3, very close relationship.

2.4 Calculation and Representation of the Vulnerability Index

The formula for determining the systemic vulnerability was implemented in a spreadsheet which involved not only the weights described in 2.3. section, but also the 21 columns corresponding to the indicators of S, P, and H, and the 2550 rows (one entrance for each 200x200 m cell that subdivides the territory). More details about the methodology and its mathematical framework can be found in Beltramino et al. (2022).

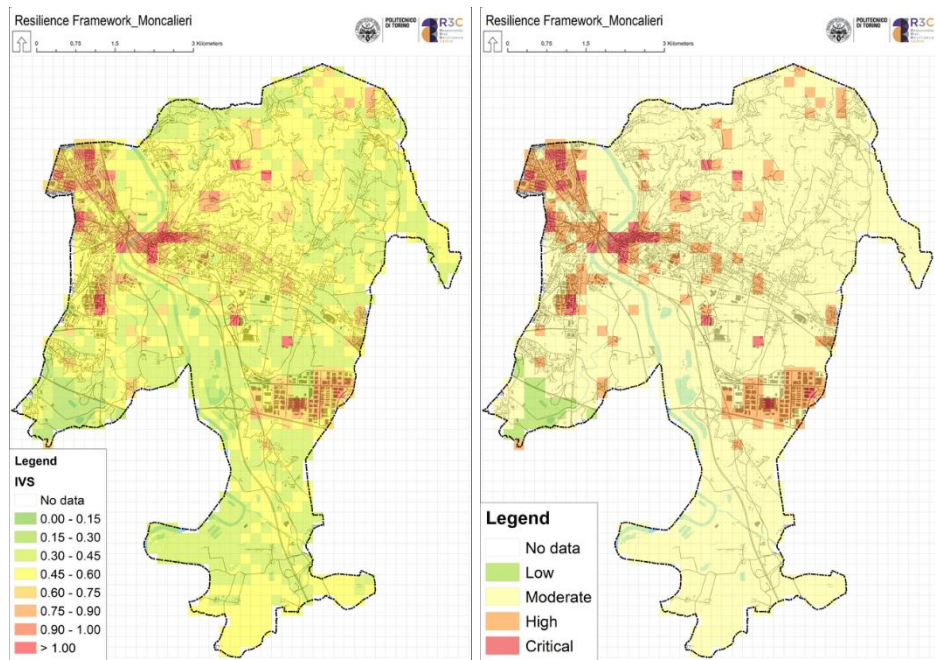
2.5 Fitting the model

Since the indicators depend on the availability of spatial data, and some assumptions should be made for the calculation and spatialization of the indicators, uncertainties are introduced to the model. Then, it is important to verify statistically as a single variable (central tendency, dispersion, shape, possible outliers, etc.) the behavior of each column (2550 values of each indicator). In addition, a representative sample of the 2550 values of each indicator and the critical points were spatially checked through the expertise of the planners and stakeholders in the territory under analysis.

3 Systemic Vulnerability assessment in the municipality of Moncalieri, Italy.

The principal output of this methodology consisted of colored maps using both, numerical scales (Figure 2 a), and qualitative scales (Figure 2 b), suitable for reading by non-experts, representing the systemic vulnerability through an ordinal scale of four categories (Low-green, Moderate-yellow, High-orange, and Critical-red).

Figure 2. Final systemic vulnerability map (a) numerical scale (b) qualitative scale.

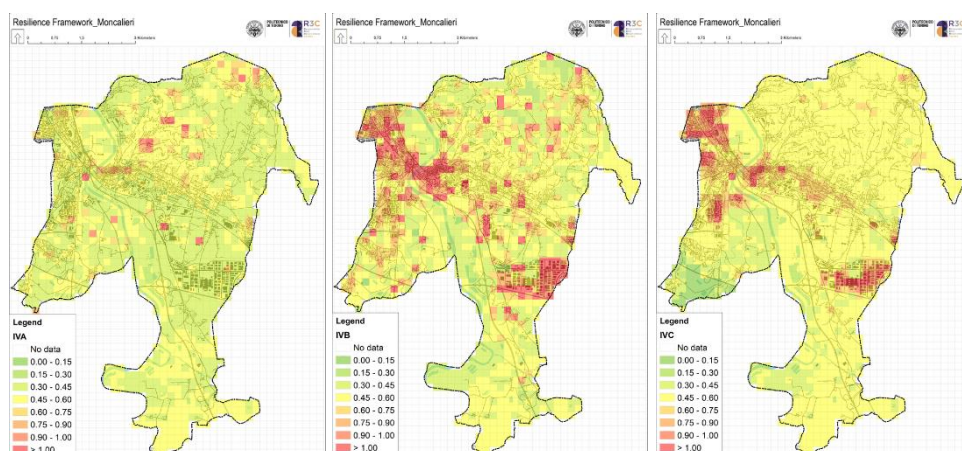


Source: Beltramino et al. (2022)

The three most vulnerable areas correspond to the historical center, the industrial areas, and the most anthropized area in the north-north-west. Other scattered areas identify situations characteristic of punctual elements of the territory. Indeed, during the step described in the 2.5 subsection, most of these areas were verified, providing consistency concerning the presence of elements that determined the territorial vulnerability.

Furthermore, the systemic vulnerability can be deployed by the three components of Sensitivity (Environment and Landscape-A; Building, Heritage, and Infrastructures-B; Economy and Population-C) as represented in Figure 3.

Figure 3. Systemic vulnerability maps (a) IVA: vulnerability index component A, (b) IVB: vulnerability index component B, (c) IVC: vulnerability index component C.



Source: Beltramino et al. (2022)

The values obtained, represented in the three maps, show the values of the vulnerability index divided according to the components IVA, IVB, and IVC.

Focus the analysis on component B (Building, Heritage, and Infrastructures) according to the scope of this article, the most vulnerable areas are those with the highest density of built-up areas, road infrastructures, and the presence of cultural heritage buildings, with a substantial impact on the pressure indicator OBS (obsolete buildings) and the presence of some industries.

The next section presents an application of the vulnerability matrix in an industrial context, to determine its vulnerabilities against the principal Natech factors.

4 Vulnerability deployment focus in a Critical Infrastructure

4.1 General description of the plan

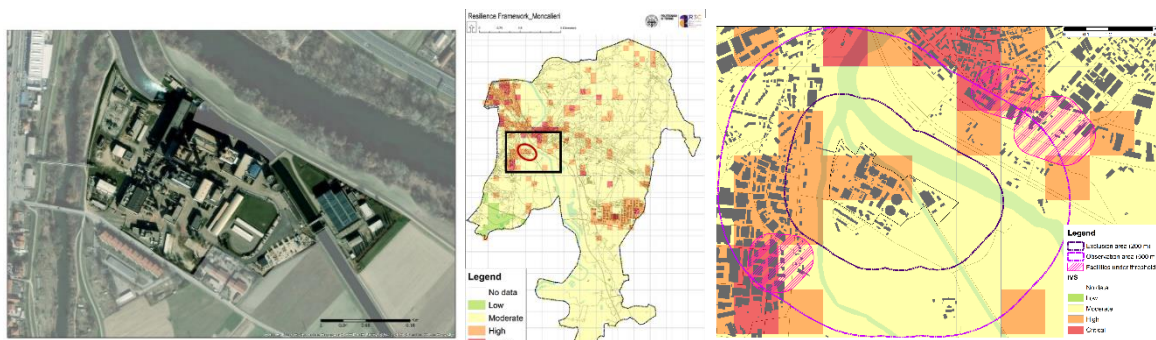
The establishment corresponded with a typical industrial typology clustered in the macro-sector "Power production" according to the description given by Casson Moreno et al. (2018). Its specific activity is the power production from the combustion of hydrocarbons. The unitary operations that are carried out in the plant are both chemical and physical. The activities also include auxiliary technical systems necessary for the production plant's operation, such as compressed air, treated wastewater, steam production, and warehousing. Within all the processes and functions of the plant, the following items were identified: atmospheric storage tanks, tall structures such as chimneys and process columns and equipment, heat exchangers, complex systems of pipelines, complex electrical networks, and water treatment organs.

4.2 Territorial Vulnerability Associated with an Industrial Context

The area of interest corresponds to an industrial context that not only includes the plant inside the fence, but also the entire environment with which the facility interacts, comprehending approximately 280 hectares and conformed by 70 exhaustive homogeneous cells. Figure 4 recreate some elements of interest for the industrial context.

Figure 4. Industrial context.

- a) Industrial satellite view b) location of the industrial context within the municipality c) IVS for the industrial context.



Source: Castro et al. (2023).

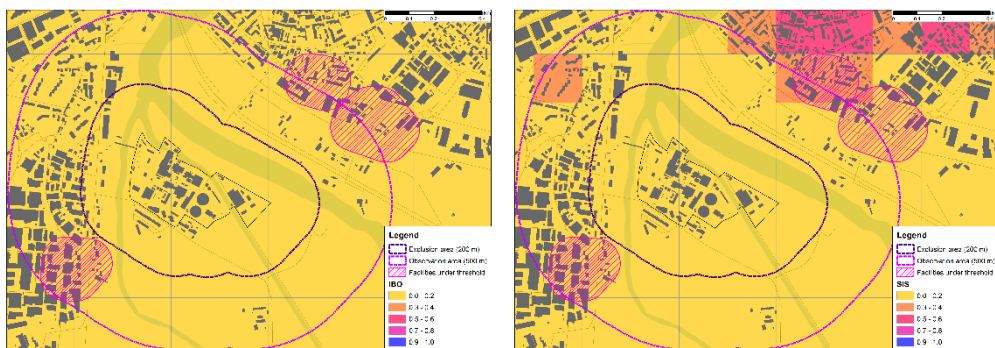
The systemic vulnerability analysis according to the visual field yielded approximately 65% of the cells with moderate vulnerability (yellow), 26% with high vulnerability (orange), and 9% with critical vulnerability (red). It is important to remark that the few critical vulnerability cells corresponded to areas that only partially intersect the observation area (farther than 500 m). In contrast, within the perimeter of the plant, more than 50% of the occupied area is found with a coloration corresponding to high vulnerability, while another 3 orange cells are included within the exclusion area in case a major accident occurs.

In addition, it can be also appreciated how different binding areas applied to other neighbor plants may interact with the observation area, being able to cause domino effects. Therefore, the zone analyzed is highly vulnerable to the mutual interaction between both industrial and external hazards, susceptible to suffering cascading events that may harm the environment, the population, and the infrastructure.

In this line, a components breakdown for IVS was carried out up to the pressure and hazards able to impact the industrial context.

Regarding the breakdown, this section just highlighted the contrast between the less relevant and the significative indicators as potential disruptive elements. Then, Figure 5 starts illustrating the vulnerability representation of two natural hazards that were not considered significant to the industrial context. On the other hand, Figure 6 presents a vulnerability representation of two significant indicators.

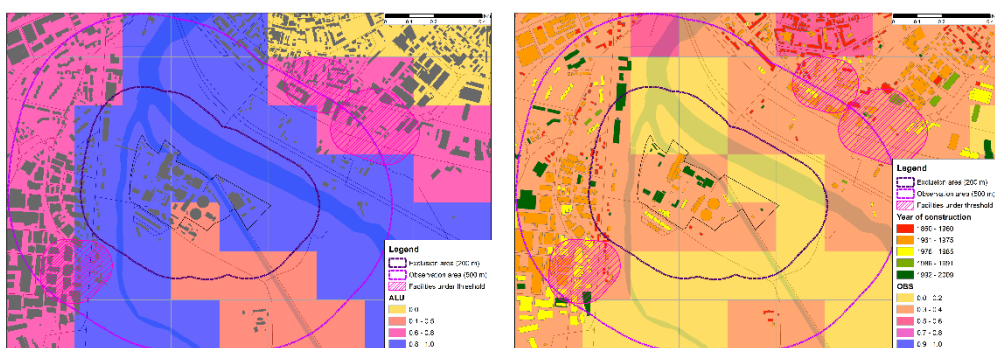
Figure 5. Vulnerability representation of natural hazards is not significant to the industrial context. a) Wildfires (IBO). b) Earthquakes (SIS).



Source: Castro et al. (2023).

It can be appreciated from the analysis that both hazards, earthquakes, and wildfires although they should not be completely disregarded, the industrial context vulnerability against these hazards is low.

Figure 6. Vulnerability representation of natural hazards and pressures significant to the industrial context. a) Floods (ALU). b) building obsolescence (OBS).



Source: Castro et al. (2023).

Moving to Figure 6 a), in contrast, it is not difficult to note how practically all the cells in the exclusion area, including those in the internal perimeter of the plant, are critically vulnerable to the impact of floods. The rest of the visual field in the industrial context alternates between critical and high vulnerability. The potential impact of this natural hazard is conditioned by the proximity of the plant location to the bed of a river which bifurcates on both sides of it. According to the European Commission (2022), this kind of natural hazard may trigger several damaged modes to industrial items such as buckling, rupture of pipes and connections, overfilling of process equipment, displacement and overturning of structures, and pushed objects against the equipment provoking the puncturing phenomena.

Moreover, Figure 3b shows building obsolescence as a linear and generalized trend that affects gradually the industrial context cells. In addition, it is important to note how the punctual elements in the plant area are categorized according to the year of construction. From this, it can be perceived that some process areas and the round structures corresponding to storage tanks had more than 50 years of construction. Then, a specific analysis should be done as proposed by Milazzo and Bragatto (2019).

5 Conclusions

The tool offers a comprehensive approach to measuring territorial vulnerability by integrating relevant indicators and considering systemic factors, territorial peculiarities, and stakeholder interests. Its multi-risk concept and spatial analysis enable scalable and replicable applications, fostering increased awareness and supporting detailed local policy planning.

The tool potentialities could be applied to assess the vulnerabilities of the critical infrastructure within territories of interest, such as Industrial contexts. The analysis enabled the systemic vulnerability at levels of components or indicators, individuating the most prominent to cause disruptions. The picture must be completed. From vulnerability to resilience. Data availability and quality is a criticality. This introduces uncertainties that must be addressed.

Acknowledgments

This study was carried on within the activities of the Interdepartmental Centre R3C (Responsible Risk Resilience Centre – r3c.polito.it) of Politecnico di Torino, that co-funded the PhD of David Castro Rodriguez. This study is a part of the activities of the RETURN Extended Partnership and received funding from the European Union Next-GenerationEU (National Recovery and Resilience Plan – NRRP, Mission 4, Component 2, Investment 1.3 – D.D. 1243 2/8/2022, PE0000005) – SPOKE TS 2 *Studio condotto nell'ambito del Partenariato Esteso RETURN, finanziato dall'Unione Europea – NextGenerationEU (Piano Nazionale di Ripresa e Resilienza – PNRR, Missione 4 Componente 2, Investimento 1.3 – D.D.1243 2/8/2022, PE0000005–SPOKE TS 2

References

1. Beltramino, S., M. Scalas, D.J. Castro Rodriguez, G. Brunetta, F. Pellerey, M. Demichela, A. Voghera, A. Longhi, G. Mutani, O. Caldarice, G. Miraglia, E. Lenticchia, and L. La Riccia (2022). Assessing territorial vulnerability: Testing a multidisciplinary tool in Moncalieri, Italy, *TeMA. Journal of Land Use, Mobility, and Environment* 15 (3), 355–375. <http://dx.doi.org/10.6092/1970-9870/9069>
2. Brunetta, G., Caldarice, O., Tollarin, N., Rosas-Casals, M., & Morató, J. (2020). Urban Resilience for Risk and Adaptation Governance. *The Resilient Cities* book.
3. Brunetta, G., Ceravolo, R., Barbieri, C.A., Borghini, A., De Carlo, F., Mela, A., Beltramo, S., Longhi, A., De Lucia, G., Ferraris, S., Pezzoli, A., Quagliolo, C., Salata, S., & Voghera, A., (2019). Territorial Resilience: Toward a Proactive Meaning for Spatial Planning. *Sustainability*, 11(8), 2286. <https://doi.org/10.3390/su11082286>
4. Castro Rodriguez, D.J., Beltramino, S., Scalas, M., Pilone, E., Demichela, M., 2022. Territorial Representation of a Vulnerability Associated with the Seveso Installations in a Nord Italian Case Study, in Proceedings of 32nd European Safety and Reliability Conference (ESREL 2022), Research Publishing Services, pp. 1463–1470. https://doi.org/10.3850/978-981-18-5183-4_R25-02-574-cd
5. Centro Euro-Mediterraneo sui Cambiamenti Climatici, 2017. Piano Nazionale di Adattamento ai Cambiamenti Climatici (PNACC) - Prima stesura per la consultazione pubblica. https://www.minambiente.it/sites/default/files/archivio_immagini/adattamenti_climatici/documento_pnacc_luglio_2017.pdf
6. European Commission (2022). Joint Research Centre, Necci, A., Krausmann, E. NaTech risk management: guidance for operators of hazardous industrial sites and national authorities. Publications Office of the European Union.
7. Galderisi, A., & Ferrara, F. F. (2012). Enhancing urban resilience in face of climate change: a methodological approach. *TeMA-Journal of Land Use, Mobility and Environment*, 5(2), 69-88. <https://doi.org/10.6092/1970-9870/936>
8. IPCC (2012). Field, C.B., Barros, V., Stocker, T.F., Qin, D., Dokken, D.J., Ebi, K.L., Mastrandrea, M.D., Mach, K.J., Plattner, G.-K., Allen, S.K., Tignor, M., & Midgley P.M. (Eds.) Retrieved from Cambridge University Press, The Edinburgh Building, Shaftesbury Road, Cambridge CB2 8RU ENGLAND, 582 pp.
9. Mesa-Gómez, A., J. Casal, and F. Muñoz (2020). Risk analysis in Natech events: State of the art. *Journal of Loss Prevention in the Process Industries* 64, 104071.
10. Milazzo, M.F. and P. Bragatto (2019). A framework addressing a safe aging management in complex industrial sites: The Italian experience in «Seveso» establishments. *Journal of Loss Prevention in the Process Industries* 58, 70–81.
11. United Nations (2015a). Transforming our world: The 2030 agenda for sustainable development (A/RES/70/01).
12. United Nations (2015b). Sendai framework for disaster risk reduction 2015-2030. Office for Disaster Risk Reduction (UNISDR). UNISDR/GE/2015 - ICLUX EN5000 1st Ed., Switzerland.

2.11 Use of Multi-Criteria Decision Analysis for assessing the resilience of Critical Entity systems

Frédéric Petit, European Commission, Joint Research Centre (JRC), Ispra, Italy

frederic.petit@ec.europa.eu

Extended abstract

The Directive (EU) 2022/2557 on the resilience of critical entities emphasizes the need to identify European Critical Entities subject to specific requirements and implement strategies for enhancing the resilience of critical entities (CE). In the context of this directive, resilience is defined as the “critical entity’s ability to prevent, protect against, respond to, resist, mitigate, absorb, accommodate and recover from an incident (i.e., disruptive events).” [1]. Enhancing CE resilience requires therefore taking appropriate and proportionate security and emergency management measures to assess vital functions, prevent incidents, protect critical infrastructure (CI) assets, raise awareness about infrastructure interdependencies, and mitigate the consequences resulting in respect of all-hazards, whether natural, manmade, accidental or intentional, but also emerging and hybrid threats.

The Directive (EU) 2022/2557 defines eleven sectors, and it is challenging to find an approach adapted to assess the resilience of all these systems that differ significantly in their organizations, operations, technical specificities, and management procedures. However, operations research and multi-criteria decision analysis (MCDA) can be the solution to define the criticality and compare the resilience attributes of various entities and infrastructures.

MCDA uses a systematic and logical set of procedures for analysing complex problems with multiple objectives (that could appear conflicting at first sight) and supporting decision-making. It utilizes a “divide and conquer” philosophy in which hard-to-define, high-level objectives are successively divided into lower-level, more easily understood, defined, and evaluated objectives. MCDA develops meaningful and useful measurement scales for objectives, examines trade-offs among conflicting objectives, and incorporates uncertainty and risk attitudes as appropriate. The concepts of MCDA and value-focused techniques have been successfully implemented in the United States to construct indices to compare possible resilience and protective measures enhancement alternatives for all types of CI and National Critical Functions in an all-hazards approach. They are also used to assess the resilience of electric power distribution systems and to support decision-making on energy policies, initiatives, and project investments.

This presentation will discuss the possible use of MCDA for implementing the Directive (EU) 2022/2557 by:

- Describing MCDA principles and techniques; and
- Illustrating how these techniques can be used to characterize the criticality of CE and to prioritize alternatives in enhancing the resilience and protection of CI assets and CE systems.

References

1. Directive (EU) 2022/2557 of the European Parliament and of the Council of 14 December 2022 on the resilience of critical entities and repealing Council Directive 2008/114/EC – available at <https://eur-lex.europa.eu/legal-content/EN/TXT/?uri=CELEX%3A32022L2557>, accessed on September 30, 2023.

2.12 The main topics of discussion and research on issues of modelling systemic changes in urban systems

Katarzyna Goch, Institute of Geography and Spatial Organization Polish Academy of Sciences;
kgoch@twarda.pan.pl

Przemysław Śleszyński, Institute of Geography and Spatial Organization Polish Academy of Sciences,
psleszyn@twarda.pan.pl

Andrzej Affek, Institute of Geography and Spatial Organization Polish Academy of Sciences,
a.affek@twarda.pan.pl

Extended abstract

Knowledge about urban systems from a global perspective has become critical to shaping a sustainable future. Global urban areas are inhabited by more than a half of the globe's population and this share is rapidly growing. Moreover, they are the main centres of economic growth, resulting in the highest consumption of energy and natural resources and the highest CO₂ emissions (Acuto, Parnell, and Seto, 2018; Elmqvist et al., 2019; McPhearson, Haase, et al., 2016), whose dynamics and processes are globally territorialized (Sassen, 2004; Taylor, 1997). Thus, a synthetic and in-depth understanding of global urban systems is essential for shaping the future living conditions in a sustainable and fair way.

Urban systems are dynamic, human modified environments that encompass legal, functional, infrastructural and social components, both interrelated and interacting with each other (Acuto, Parnell, and Seto, 2018; Frank, 2017; McPhearson, Pickett, et al., 2016; Meerow, Newell, and Stults, 2016). Urban systems can be perceived as Complex Adaptive Systems (CAS) (Kok, Loeber, and Grin, 2021; McPhearson et al., 2022). According to the CAS concept, an adaptive system is a collection of multiple interacting elements that evolve and adapt over time to their environment, with the environment also adapting to the processes taking place. In this context, urban systems can be considered as complex, hierarchical, self-organising systems, emerging from the interaction between humans and nature (Levin et al., 2013). Important in the context of urban systems research is their property to move over time to one of many possible states, related to the intrinsic characteristics of CAS: complexity, highly dynamic and distributed structure, and indeterminism and non-linearity of the processes involved (Oughton et al., 2018).

The creation or implementation of new institutions, rules or behavioural norms in urban systems results in exogenous change and/or endogenous evolution (Polhill et al., 2016), which reactively affects the urban system. Either driven by a rapid disturbance or by gradual evolution, they can lead to fundamental changes in behaviour and/or system structure - to the systemic change (Polhill et al., 2016). However, with regard to the study of complex urban systems, the impact of systemic changes is not sufficiently explored (Grimm et al., 2017); both in terms of the occurrence of systemic change as an inherent feature of the system under study (Polhill et al., 2016; van Strien et al., 2019; Verstegen et al., 2016) or systemic change as a goal towards sustainable transformation (Wolfram and Frantzeskaki, 2016).

The primary goal of this study was to determine the current state of knowledge on the implementation of the non-stationary nature in models representing urban systems. In order to determine the state of the art in an explicit and repeatable way, we conducted a systematic literature review, in accordance with the PSALSAR method (Mengist, Soromessa, and Legese, 2020). We used five search databases for this study: Google Scholar, Web of Science Core Collection, Scopus, IEEE Xplore, and ScienceDirect. No time constraint for the searched studies was assigned. The query used for the search was based on the combination of phrases capturing: 1. the systemic component, 2. the urban environment, 3. the connotation of the change in the environment and 4. the modelling component, marking the conceptualization of the change in the urban system. We applied eligibility criteria to the results of the literature search to exclude works that did not support the research question.

Data extraction from publications collected in the database was done in a two stage process. Firstly, we analysed the words used in the abstracts and, on the basis of the most frequently occurring phrases related to the topic of the review, we defined broad thematic groups. Subsequently, during the abstracts screening, we revised and refined the division into thematic groups. Based on the content of the abstracts, each analysed publication was quantitatively assessed on a scale of 1-3 for fit into the relevant thematic groups, according to the scoring method proposed by Śleszyński et al. (2023): zero points were assigned, if there was no reference to a thematic group; one point was assigned, if at least one-two sentences referred to a thematic group; two points were assigned, if at least several sentences referred to a thematic group; and three points

were assigned if the whole abstract, or its substantial part, referred to a thematic group. In case of difficulties in assigning points, keywords and article titles were taken into account.

Systemic literature search resulted in a database of 94 works covering the topic of systemic change in urban systems. The investigated works cover seven non-exclusive thematic groups: (1) land-use change, (2) planning and policies for sustainable development, (3) climate change, (4) resilience, (5) infrastructure, (6) systems approach, and (7) global scale models. The number of works is growing in time, with one work per year found for the period before 2009, increasing to 12 works found for the year 2022. Based on the assessment of the collected abstracts we demonstrated that the majority of works fit into the group “planning and policies for sustainable development” followed by “infrastructure”, “climate change”, “systems approach”, “land-use change”, “resilience”, and “global scale models”. For thematic groups “climate change” and “planning and policies for sustainable development” the number of points is significantly higher in the recent publications (after 2012 and 2016, respectively). On the other hand, for the thematic group “systems approach” the number of points is significantly lower before 2011. For the groups “resilience” and “global scale models”, works were identified starting from 2013, with average number of points per year relatively low (<0.3). These results point to the emerging fields of studies of urban resilience and global urbanisation for potential exploration in the context of quantitative urban research.

References

- Acuto, M., S. Parnell, and K.C. Seto, ‘Building a Global Urban Science’, *Nature Sustainability*, Vol. 1, No. 1, 2018, pp. 2–4.
- Elmqvist, T., E. Andersson, N. Frantzeskaki, T. McPhearson, P. Olsson, O. Gaffney, K. Takeuchi, and C. Folke, ‘Sustainability and Resilience for Transformation in the Urban Century’, *Nature Sustainability*, Vol. 2, No. 4, 2019, pp. 267–273.
- Frank, B., ‘Urban Systems: A Socio-Ecological System Perspective’, *Sociology International Journal*, Vol. 1, No. 1, 2017.
- Grimm, N.B., S.T.A. Pickett, R.L. Hale, and M.L. Cadenasso, ‘Does the Ecological Concept of Disturbance Have Utility in Urban Social-Ecological-Technological Systems?’, *Ecosystem Health and Sustainability*, Vol. 3, No. 1, 2017, p. e01255.
- Kok, K.P.W., A.M.C. Loeber, and J. Grin, ‘Politics of Complexity: Conceptualizing Agency, Power and Powering in the Transitional Dynamics of Complex Adaptive Systems’, *Research Policy*, Vol. 50, No. 3, 2021, p. 104183.
- Levin, S., T. Xepapadeas, A.-S. Crépin, J. Norberg, A. de Zeeuw, C. Folke, T. Hughes, et al., ‘Social-Ecological Systems as Complex Adaptive Systems: Modeling and Policy Implications’, *Environment and Development Economics*, Vol. 18, No. 2, 2013, pp. 111–132.
- McPhearson, T., E.M. Cook, M. Berbés-Blázquez, C. Cheng, N.B. Grimm, E. Andersson, O. Barbosa, et al., ‘A Social-Ecological-Technological Systems Framework for Urban Ecosystem Services’, *One Earth*, Vol. 5, No. 5, 2022, pp. 505–518.
- McPhearson, T., D. Haase, N. Kabisch, and Å. Gren, ‘Advancing Understanding of the Complex Nature of Urban Systems’, *Ecological Indicators*, Vol. 70, 2016, pp. 566–573.
- McPhearson, T., S.T.A. Pickett, N.B. Grimm, J. Niemelä, M. Alberti, T. Elmqvist, C. Weber, D. Haase, J. Breuste, and S. Qureshi, ‘Advancing Urban Ecology toward a Science of Cities’, *BioScience*, Vol. 66, No. 3, 2016, pp. 198–212.
- Meerow, S., J.P. Newell, and M. Stults, ‘Defining Urban Resilience: A Review’, *Landscape and Urban Planning*, Vol. 147, 2016, pp. 38–49.
- Mengist, W., T. Soromessa, and G. Legese, ‘Method for Conducting Systematic Literature Review and Meta-Analysis for Environmental Science Research’, *MethodsX*, Vol. 7, 2020, p. 100777.
- Oughton, E.J., W. Usher, P. Tyler, and J.W. Hall, ‘Infrastructure as a Complex Adaptive System’, *Complexity*, Vol. 2018, 2018, pp. 1–11.
- Polhill, J.G., T. Filatova, M. Schlüter, and A. Voinov, ‘Modelling Systemic Change in Coupled Socio-Environmental Systems’, *Environmental Modelling & Software*, Vol. 75, 2016, pp. 318–332.
- Sassen, S., ‘The Global City: Introducing a Concept’, *Brown J. World Aff.*, Vol. 11, 2004, p. 27.

Śleszyński, P., A.R. Khavarian-Garmsir, M. Nowak, P. Legutko-Kobus, M.H.H. Abadi, and N.A. Nasiri, 'COVID-19 Spatial Policy: A Comparative Review of Urban Policies in the European Union and the Middle East', *Sustainability*, Vol. 15, No. 3, 2023, p. 2286.

van Strien, M.J., S.H. Huber, J.M. Andries, and A. Grêt-Regamey, 'Resilience in Social-Ecological Systems: Identifying Stable and Unstable Equilibria with Agent-Based Models', Application/pdf, 2019, p. 23 p.

Taylor, P.J., 'Hierarchical Tendencies amongst World Cities: A Global Research Proposal', *Cities*, Vol. 14, No. 6, 1997, pp. 323–332.

Versteegen, J.A., D. Karssenberg, F. van der Hilst, and A.P.C. Faaij, 'Detecting Systemic Change in a Land Use System by Bayesian Data Assimilation', *Environmental Modelling & Software*, Vol. 75, 2016, pp. 424–438.

Wolfram, M., and N. Frantzeskaki, 'Cities and Systemic Change for Sustainability: Prevailing Epistemologies and an Emerging Research Agenda', *Sustainability*, Vol. 8, No. 2, 2016, p. 144.

2.13 Impacts of Climate Change on interdependent Critical Energy Infrastructure: Direct and Cascading Effects across Energy Production, Transport and Demand

Ricardo Tavares da Costa, Elisabeth Krausmann and Marta Poncela, European Commission Joint Research Centre (JRC), Ispra, Italy, ricardo.tavares-da-costa@ec.europa.eu, elisabeth.krausmann@ec.europa.eu, marta.poncela@ec.europa.eu

Abstract

In this paper the authors explore the impacts of climate change on critical energy infrastructure, focusing on both direct and indirect effects across multiple dimensions of the energy sector, from production to storage, transport and demand. In addition to analysing the influence of climate hazards, such as extreme weather events, the study also briefly explores the effects of meteorological variability on operating conditions and weather-dependent electricity generation and energy demand, illustrated by the example of a dunkelflaute event. The paper contributes to a more complete understanding of how climate change may affect the energy sector, by paying attention to the interdependency of critical energy infrastructure, encompassing electricity and fossil fuels. It highlights the need for proactive measures to reduce climate risk and enhance the climate resilience of critical entities, while continuing on the path of greenhouse gas reduction and the energy transition.

1 Introduction

The ongoing trend in greenhouse gas (GHG) emissions is driving up the global average temperature, which affects the Earth's climate. Some of these changes may even become irreversible, a phenomenon known as climate tipping points. While an effective reduction of GHG emissions is essential across all sectors of society in an effort to prevent more dire consequences from climate change, managing climate risk and increasing resilience must also be at the top of each country's agenda, as some of the severe impacts of climate change are already being felt and are unavoidable for decades to come.

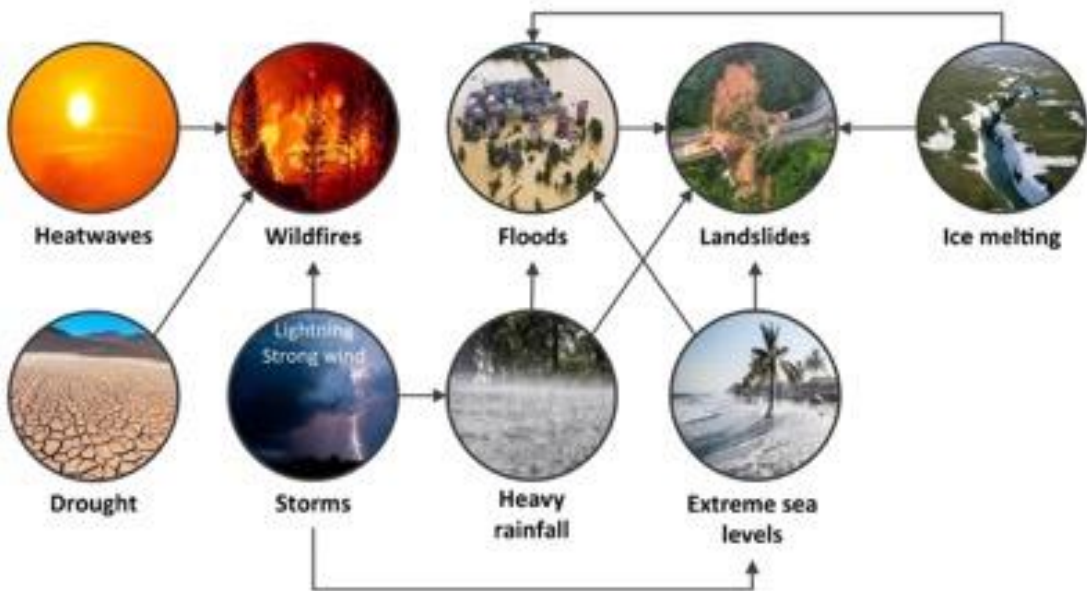
Climate change, stemming from a combination of natural processes and greenhouse gas emissions resulting from human activities, induces changes in various climate variables such as temperature, precipitation (rainfall, snowfall, ice accumulation and hail), wind patterns and humidity levels. These changes manifest in two ways: 1) changes in the mean values of these variables, referred to as climate averages, and 2) changes in their extremes, which encompass the lowest and highest values within each variable. As we depart from a climatic optimum, various unprecedented impacts to critical energy infrastructure (CEI) are expected.

2 Climate change as a driver of impacts

Overall, *changes in climate averages* have wide-ranging effects on various operational conditions for CEI, weather-dependent electricity generation and energy demand. For example, increased temperatures and low river flows threaten the operation of thermal power plants with once-through cooling systems (e.g., Henry and Pratson, 2019). At the same time heatwaves can reduce generation and transmission efficiency and abruptly increase the demand for electricity for air conditioning and ventilation. These compounding events increase the risk of electricity shortfall.

On the other hand, *changes in climate extremes* are represented by changes in the frequency, intensity, timing, duration and location of climate hazards (e.g., heatwaves, drought, floods etc.), and are often characterised as events with low probability of exceeding a high-intensity level, or a high probability of exceeding a low-intensity level. Both cases are important, as low intensity events happening often can lead to cumulative impacts (e.g., frequent repairs) and disturbances, while high-intensity events that are uncommon may catch operators unprepared and lead to catastrophic consequences. Climate hazards may happen simultaneously and self-reinforce, as shown in Figure 1, resulting in diverse consequences. A wildfire, for example, may be triggered by lightning and aggravated by a windstorm, leading to multiple impacts.

Figure 34. The interplay between climate hazards gives rise to intricate chains of impact.



Source: JRC, 2023.

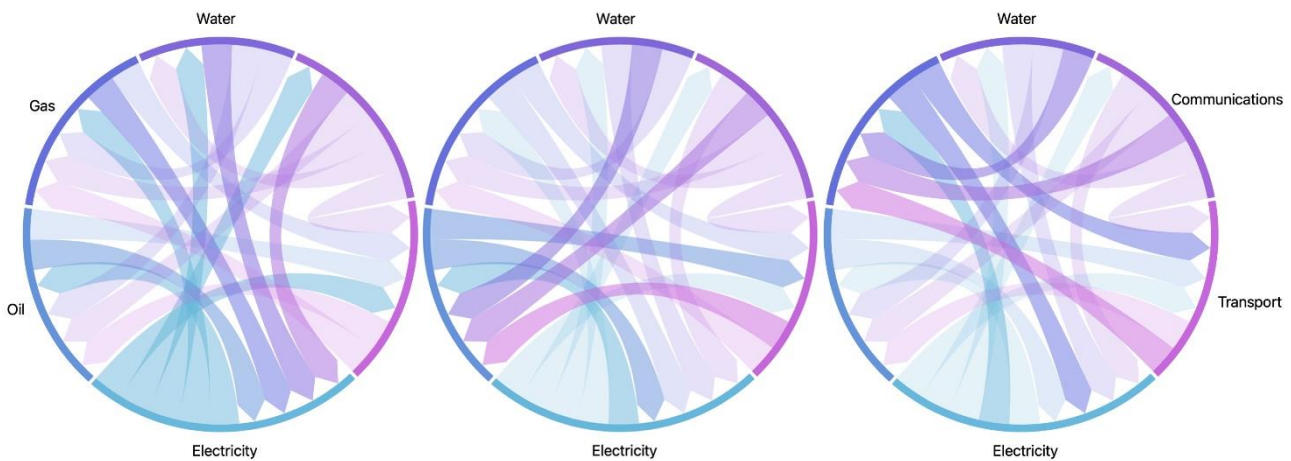
It is also important to recognise that modern energy systems are not only at risk of direct impacts of climate change, but are also at risk of indirect impacts. An energy system of systems has components with different degrees of vulnerability (e.g., narrow operating limits). If a single or multiple components fail, or an electric circuit shuts itself off to prevent damage (due to a fault condition being detected), and countermeasures are not in place or effective, a disturbance may quickly propagate within an energy system. This means that a failure in any point of an energy system may quickly cascade to a large-scale disruption. Further, because of the high interdependency, and reliance on services delivered by other critical infrastructure (e.g., water, telecommunications, transport), disruptions can propagate across sectors.

For example, in November 2006, the intentional but insufficiently coordinated, transmission line switch-off in an EU Member State led to the overloading and automatic disconnection of other lines and the splitting of the Central Europe Synchronous Area. A generalised blackout cascaded across sectors and EU Member States and beyond EU borders (van der Vleuten and Lagendijk, 2010). If CEI can be disrupted by human error at scales that extend beyond national borders, then they may also be disrupted by climate change with its regional or even global impacts. Moreover, the risk of disaster or an energy crisis may increase as a result of economic and population growth (greater demand for energy and exposure), ageing infrastructure, electrification of other sectors and lack of investment, as well as inadequate planning and coping capacity.

Similarly, a disruption in any critical infrastructure sector, which an energy system depends upon, may lead to its disruption or exacerbate already existing challenges. This was the case of the 2022 floods in Nigeria, for example, that halted liquefied natural gas exports at a time when Europe was seeking to replace Russian gas.

Given their vast geographical coverage, sometimes narrow operational limits and growing maintenance and replacement needs, critical infrastructures may face increased climate risk. In Figure 2, the interdependency between energy systems and across critical infrastructure sectors is illustrated.

Figure 35. Critical infrastructure Interdependency with a focus on energy systems, namely electricity, oil and gas. On the left side the dependencies that the electricity sector presents, in the middle the dependencies of the oil sector and in the right side the dependencies of gas. Labels are the same for each graph.



Source: JRC, 2023.

3 Climate change impacts on electricity, oil and gas

Given the vulnerability and exposure of CEI to climate hazards, it is imperative to assess the impacts of climate change on CEI, particularly on electricity, oil and gas. To gain a deeper understanding of these impacts, Table 1 outlines examples of possible direct and cascading effects resulting from climate change on the electricity, oil and gas infrastructure. This should shed some light on CEI-related structures, equipment and components that may be at risk, but also on other effects that could trigger an energy crisis or exacerbate already challenging operational conditions. It should underscore the necessity of proactive measures to ensure resilience and sustainability in the face of climate change.

Table 1 summarises climate change impacts per climate hazard (rows) and per dimension of the energy sector (columns). For example, high temperatures and heatwaves have substantial impacts on various dimensions of the energy sector, effects that are increasingly evident in recent events. For example, in June 2023, Texas experienced reduced wind power output during above normal temperatures for that period. Wind power generation can be affected by low wind speeds and decreased air density during high-temperature periods, leading to derating of wind turbines. This, combined with an increased demand for cooling and ventilation and the reduction of transmission capacity, as well as other factors, has strained the power grid, bringing it close to blackout⁽³⁾.

Moreover, thermal power plants encounter efficiency losses and derating during heatwaves, as higher intake water temperatures decrease their cooling efficiency and reach their operating limits. This was notably observed in Europe in 2018 when the continent faced a prolonged heatwave, leading to reduced thermal power generation capacity⁽⁴⁾. These impacts are not limited to electricity production; they extend to other energy sources, such as biofuel power plants, which suffer from crop yield losses due to heat stress and pests. These real-world examples highlight the detrimental effects of high temperatures on energy production and underline the need for adaptive measures to ensure a stable energy supply.

Irrespective of the climate hazards in Table 1, an increase in demand for securing critical infrastructure (e.g., during a prolonged blackout) is expected, as well as a rise in maintenance, repair and overhaul, with a possibly higher need for supplies, spare parts and staffing. Further, facilities and equipment will face delayed operations due to disturbances, malfunction or damage, absence or reduced performance of personnel, and higher operational costs and financial losses. Climate hazards can also cause oil and chemical spills, fires or explosions involving oil and gas infrastructure.

⁽³⁾ <https://www.reuters.com/world/us/texas-power-use-breaks-record-heat-wave-again-with-no-blackouts-2022-07-13/>

⁽⁴⁾ <https://www.powermag.com/intense-summer-heatwaves-rattle-worlds-power-plants/#:~:text=When%20the%20air%20temperature%20becomes,degree%5D%20C%20in%20the%20temperature>.

Table 1. Examples of possible direct and cascading effects induced by climate change on electricity, oil and gas production, storage, transmission, distribution and demand (based on Tavares da Costa et. al, 2023).

| | Energy production | Energy storage | Energy transport | Energy demand |
|---------------------------------|--|---|--|--|
| High temperatures and heatwaves | <p>Damage to structures ⁽¹⁾, equipment ⁽²⁾ or components ⁽³⁾ due to thermal stress, loss of load-bearing capacity and ground failure from permafrost thaw, (bio-)fouling, clogging and increased corrosion.</p> <p>Malfunctioning of equipment ⁽⁴⁾ (e.g., due to less oxygen, overheating), increase in false signals, derating and tripping of circuit breakers.</p> <p>Increase in evaporation losses, and losses due to leaks, and higher potential for technological accidents (e.g., chemical and oil spills, ignition of flammables by hot surfaces with potential for fires and explosions).</p> | | | <p>Increase in electricity demand due to an increase in ventilation, cooling, humidity control and refrigeration.</p> <p>Decrease of energy demand for heating and seasonal shift in peak demand for energy.</p> <p>Increase in fuel consumption for electricity generation, including backup power.</p> |
| | <p>Reduction of electricity generation:</p> <ul style="list-style-type: none"> — Solar power due to efficiency loss and haze. — Wind power due to low wind and decrease in air density, but also derating. — Hydropower due to seasonal flow change from rainfall, ice and snow melt and increase in water demand, and evaporation losses. — Thermal power plants due to generation efficiency loss, derating, higher intake temperature of water and decrease in cooling efficiency (including carbon capture), and restrictions in the discharge of warm water (heat sink). In coal-fired power plants due to coal self-combustion. In biofuel power plants due to crop yield loss due to heat stress and pests. <p>Refining process efficiency loss due to warmer air and water temperatures, restrictions in the discharge of warm water, and (bio-)fouling.</p> | <p>Lower fuel reserves.</p> <p>Efficiency reduction of batteries.</p> | <p>Efficiency reduction of transmission and distribution lines.</p> <p>Electricity transmission and distribution congestion.</p> <p>Decrease in pipeline transport capacity, increase in costs and aftercooling, pressure and flow rate fluctuations.</p> <p>Constraints in fuel supply and energy export restrictions ⁽⁵⁾.</p> | |
| Drought | Damage to structures ⁽¹⁾ , equipment ⁽²⁾ or components ⁽³⁾ due to ground failure from soil dry out. | | | Increase in electricity |

| | | | | |
|--------------|--|---|---|--|
| | <p>Reduction of electricity generation:</p> <ul style="list-style-type: none"> — Solar power due to water use restrictions for Concentrated Solar Power (CSP). — Hydropower due to low river flows, and restrictions associated with water use and environmental flows. — Thermal power plants due to water use restrictions for cooling and emissions control systems (including carbon capture), restrictions in the discharge of warm water, and due to limited inland water transport of fuels. In biofuel power plants due to crop yield loss. | <p>Reduction/restriction in the use of pumped-storage hydroelectricity.</p> | <p>Reduction of transmission and distribution efficiency of subsurface electric power lines and effectiveness of earth wires.</p> <p>Energy export restrictions (⁵).</p> | <p>demand due to an increase in water use for pumping, irrigation and desalination.</p> |
| Extreme cold | <p>Damage to structures (¹), equipment (²) or components (³) due to ice, snow and rain-on-snow loads (e.g., roof collapse), freeze-thaw, frost heave, thermal stress (e.g., cracked solar cells), glazing and wind-on-ice loads (e.g., downed power lines, toppled transmission towers), impact loads from drifting ice and falling debris (e.g., trees and branches), clogging (e.g., water intake, hydrate formation) and corrosion (e.g., condensation, internal flooding).</p> | | | <p>Increase in electricity demand due to an increase in heating demand.</p> |
| | <p>Malfunctioning of equipment (⁴) (e.g., stoppage and slow start of backup power), particularly process equipment not prepared to handle multiphase fluids, ice accumulation on insulators and flashover, increase in false signals, derating and tripping of circuit breakers.</p> | | | <p>Increase in fuel consumption for electricity generation, including for backup power generators, constraints in fuel supply.</p> |
| | <p>Increase in losses due to leaks and higher potential for technological accidents (e.g., chemical and oil spills).</p> | | | |
| | <p>Reduction of electricity generation:</p> <ul style="list-style-type: none"> — All power plants due to sustained damage. — Solar power due to cloudiness, fog and snow or ice deposition. — Wind power due to wind turbine blade icing and excessive vibration. — Hydropower due to frozen water bodies. — Thermal power plants due to fuel shortage and due to frozen water bodies. In coal-fired power plants due to frozen coal. In biofuel power plants due to | <p>Lower fuel reserves.</p> | <p>Electricity transmission and distribution congestion due to increased demand, failure of components of the power grid, possible fuel shortages and malfunctioning of equipment. It should be noted, however, that transmission efficiency increases with decreasing air temperatures.</p> <p>Possible restriction on</p> | |

| | | | | |
|---------------------------|---|---|--|------------------------------------|
| | <p>crop yield loss from frost.</p> | | <p>energy exports ⁽⁵⁾. Pressure and flow rate fluctuations in pipelines.</p> | |
| Heavy rainfall and floods | <p>Damage to structures ⁽¹⁾, equipment ⁽²⁾ or components ⁽³⁾ sitting in flood-prone areas at ground-level due to water action, impact loads from drifting debris, ground failure, including swamping and rainfall-triggered landslides, erosion (including exposure and damage of subsurface pipelines), abrasion (e.g., gates, hydroelectric turbines), sediment accumulation and clogging (e.g., water intake, drainage) and corrosion (e.g., condensation, internal flooding, seawater and salt deposits in the case of coastal floods). Flooding of open mines.</p> <p>Malfunctioning of equipment ⁽⁴⁾ and tripping of circuit breakers.</p> <p>Increase in losses due to leaks and higher potential for technological accidents due to the releases of dangerous substances from spent fuel dry casks, coal stockpiles, open cast mines, pipelines, fuel storage tanks (e.g., chemical and oil spills, wastewater, toxic or radioactive contamination, ignition of flammables by sparks or electric arcs with potential for fires and explosions). Malfunction of sump pumps and overflow of sump tanks.</p> | <p>Reduction of electricity generation:</p> <ul style="list-style-type: none"> — All power plants due to sustained damage. — Solar power due to cloudiness increase or fog. — Hydropower due to the forced use of floodways with loss of output, and increased silting of reservoirs and water intakes. — Thermal power plants due to fuel shortage. In coal-fired power plants due to coal drenching and coal transport disruption. In biofuel power plants due to crop yield loss due to water damage and salinisation (coastal). | <p>Displacement, deformation and fracture of storage tanks (e.g., flotation, roof collapse) due to water action. Lower fuel reserves.</p> | <p>Constraints in fuel supply.</p> |
| Windstorms and lightning | <p>Damage to structures ⁽¹⁾, equipment ⁽²⁾ or components ⁽³⁾ due to wind action, impact loads from airborne debris and hail (e.g., pipeline suspension bridges), lightning (e.g., wind turbine blades, inverters, fuel storage tanks), erosion (including exposure and damage of subsurface pipelines), abrasion (e.g., wind turbines, solar cells), sediment accumulation and clogging with debris and dirt. Combined strong wind and wave action damage, underwater landslides and corrosion from moisture and salt sprays (exacerbated by lightning damage), to structures, equipment or components located offshore or</p> | | | |

| | | |
|-----------|---|---|
| | <p>in low-lying coastal areas (e.g., tanker loading/unloading, submarine pipeline damage due to anchor dragging).</p> <p>Malfunctioning of equipment (⁴), increase in false signals due to lightning, debris and salt deposits, and tripping of circuit breakers.</p> <p>Increase in losses due to leaks and higher potential for technological accidents due to the releases of dangerous substances from spent fuel dry casks, pipelines, fuel storage tanks (e.g., chemical and oil spills, wastewater, toxic or radioactive contamination, ignition of flammables by sparks or electric arcs with potential for fires and explosions).</p> | |
| | <p>Change in electricity generation:</p> <ul style="list-style-type: none"> — All power plants may experience a reduction due to sustained damage. — Solar power may experience a reduction due to cloudiness increase or fog, dust and dirt deposition. On the other hand, may also experience an increase due to increasing efficiency with decreasing air temperature due to wind. — Wind power may experience a reduction due to increase in turbulence and excessive vibration. — Wave power may experience a reduction due to excessive wave heights. — Thermal power plants may experience a reduction due to fuel shortage because of sustained damage to oil and gas infrastructure. In biofuel power plants due to crop yield loss from wind damage. | <p>Uplift and displacement, deformation and fracture of aboveground storage tanks (including their roofs) due to wind action.</p> <p>Lower fuel reserves due to increase in losses from the failure of fuel storage tanks and sustained damage in oil and gas tank farms and terminals, pipelines and offshore oil and gas platforms.</p> |
| Wildfires | <p>Damage to structures (¹), equipment (²) or components (³) due to thermal stress, impact loads from airborne debris, ash and sediment accumulation, clogging and corrosion.</p> <p>Malfunctioning of equipment (⁴), increase in false signals due to fire, smoke, and airborne debris, and tripping of circuit breakers.</p> <p>Higher potential for technological accidents (e.g., ignition of flammables by hot surfaces with potential for explosions).</p> | |

| | | | | |
|--|---|--|---|--|
| | <p>Reduction of electricity generation:</p> <ul style="list-style-type: none"> — All power plants due to sustained damage. — Solar power due to smoke and airborne ash, and its deposition. — Wind power due to increase in turbulence and excessive vibration. — Thermal power plants due to fuel shortage. In biofuel power plants due to crop yield loss from fire damage. | <p>Efficiency reduction of transmission and distribution lines (e.g., power line sag, derating).</p> | <p>Pipeline depressurisation and purge.</p> | |
|--|---|--|---|--|

(¹) For example, power plants, substations, oil and gas tank farms and terminals, bridges and access roads, levees.

(²) For example, electricity poles, transmission towers, pipelines, oil and gas wells, pump/meter stations, storage tanks.

(³) For example, small-bore connections, welds, flanged joints, concrete anchor blocks, foundations.

(⁴) For example, transformers, inverters, electronics, meter, sensors, control systems, life-safety and security systems, such as pressure relief valves, water systems.

(⁵) For example, reduction of electricity interconnector capacity or curtailment of oil and gas exports.

4 The dunkelflaute

As renewable energy takes an ever increasing share of electricity generation, these weather-dependent energy sources pose new challenges to the smooth and reliable operation of the power grid. Often the focus is on the intermittency aspects of renewable energy, but the implications of prolonged periods of low generation due to certain weather conditions pose a very serious risk if countermeasures (e.g., energy storage) are not considered. In contrast, periods of extremely high generation can be avoided with the curtailment of wind and solar power, a measure typically used by operators to avoid power grid congestions, or alternatively, energy storage to use during periods of low renewable electricity generation.

A dunkelflaute event, in other words an extended period with high number of clouds (overcast conditions), and thus low insolation, compounded with low wind speeds, can cause significant electricity shortfall with serious consequences for operators (Li et al., 2021). These events, as other compound events, are often overlooked, particularly in the scientific community, nevertheless they occur relatively frequently (2 to 10 times per year, Li et al., 2021) and in different seasons. For example, the Netherlands experienced a dunkelflaute in April 2018, leading to a significant shortfall in renewable electricity generation and an emergency response by the operator (Li et al., 2020). More recently in the summer-autumn of 2021, Europe experienced a long period of low wind, although bright sky, which alone affected significantly wind power generation (ca. 32% less wind power than expected in the UK)⁵.

A dunkelflaute event can occur over large geographical areas and it is critical to improve our understanding and develop new forecasting capabilities for this “new” type of climate extreme. This is needed to dimension storage, demand response, sector coupling strategies and the demand flexibility contracted in the market accordingly, to overcome periods of low renewable electricity generation.

Europe has a single electricity market, which enables the efficient transport of electricity from where it is produced to consumers. This substantially helps operators to more easily tackle dunkelflaute events. Their strongest effect will be perhaps on the electricity market, as renewables reduce the price of electricity with their zero marginal cost for generation. This means that less renewable electricity in the market translate in an increase in electricity prices.

5 Conclusions

This study underscores the profound implications that climate change has for CEI, revealing a complex web of interconnected impacts. We argued that it is imperative for climate risk management to go beyond looking exclusively into direct impacts from isolated events, as this disregards the potential for compound events, the triggering of technological accidents and cascading effects. The departure from stable climate averages and more frequent and intense extreme weather events will challenge energy production and transmission/distribution, posing a substantial threat to the reliability and resilience of these vital systems. This may increase the risk of energy crises if risk reduction and resilience measures prove to be inadequate or insufficient. As the backbone of economic and societal functions, energy systems underpin essential services such as healthcare, transportation and communications, making their safeguarding imperative also for national security. Recalling that the energy sector itself also depends upon some of those essential services for continuity. On one hand, the urgency of reducing the emission of GHGs must be accompanied by a significant transformation of how the energy system is planned, operated and assessed, while on the other a more complete view of climate risk is needed to ensure a reliable and resilient energy system and the continued provision of energy in an era of escalating climate uncertainty.

References

- 1 Henry, C. L. and Pratson, L. F. Differentiating the Effects of Climate Change-Induced Temperature and Streamflow Changes on the Vulnerability of Once-Through Thermoelectric Power Plants. *Environmental Science & Technology* 53, 7, 3969–3976, 2019. <https://doi.org/10.1021/acs.est.8b05718>
- 2 Li, B., Basu, S., Watson, S. J. and Russchenberg, H. W. J. Mesoscale modelling of a “Dunkelflaute” event. *Wind Energy* 24, 5–23, 2021. <https://doi.org/10.1002/we.2554>

⁽⁵⁾ <https://www.cnbc.com/2021/09/29/sse-says-low-wind-dry-conditions-hit-renewable-energy-generation.html>

3 Li, B., Basu, S., Watson, S. J. and Russchenberg, H. W. J. Quantifying the Predictability of a 'Dunkelflaute' Event by Utilizing a Mesoscale Model, Journal of Physics: Conference Series 1618, 062042. <https://doi.org/10.1088/1742-6596/1618/6/062042>

4 Tavares da Costa, R., Krausmann, E. and Hadjisavvas, C. Impacts of climate change on defence-related critical energy infrastructure, Publications Office of the European Union, Luxembourg, 2023, JRC130884. <https://doi.org/10.2760/03454>

5 van der Vleuten, E. and Lagendijk, V. Transnational infrastructure vulnerability: The historical shaping of the 2006 European "Blackout". Energy Policy 38, 4, 2010. <https://doi.org/10.1016/j.enpol.2009.11.047>

2.14 Fragility assessment of power grid infrastructure towards climate resilience and adaptation

George Karagiannakis, Department of Architecture, Built Environment and Construction Engineering, Politecnico di Milano, Italy georgios.karagiannakis@polimi.it

Mathaios Panteli, Department of Electrical and Computer Engineering, University of Cyprus, Cyprus, panteli.mathaios@ucy.ac.cy

Sotirios Argyroudis, Department of Civil and Environmental Engineering, Brunel University London, UK, sotirios.argyroudis@brunel.ac.uk

Abstract

Natural hazards pose a significant risk to the robustness of the power grid. Climate-related hazards, in particular, are growing in both frequency and severity as a result of climate change. Statistical analyses demonstrate a noticeable increase in both the frequency of accidents owed to climate related stressors and their ensuing consequences in recent years. Consequently, it becomes crucial to understand and measure the resilience of infrastructure when confronted with external challenges, which is a pivotal stage in crafting successful strategies for adapting to climate change. To accomplish this objective, the creation of sturdy fragility models is absolutely necessary. These models function as instruments for assessing the extent of damage to assets and for quantifying losses using metrics related to hazard intensity.

Within this framework, we conduct a review of the existing fragility models tailored to transmission networks, distribution networks, and substations. Our review is structured into three primary sections: damage assessment, fragility curves, and recommendations for climate adaptation. The initial section offers a brief examination of damaging hazards, modes of failure and impacts. The subsequent section provides an overview of both analytical and empirical fragility models, underscoring the need for further investigations into compound and non-compound hazards, particularly windstorms, floods, lightning, and wildfires. Finally, the third section delves into climate adaptation investments within the context of climate change. This review can contribute to the enhancement of power grid asset resilience in the face of climate change. Its findings are pertinent to various stakeholders, including risk analysts and policymakers involved in risk modelling and the formulation of adaptation investments.

Keywords: power grid; fragility curves; climate resilience; adaptation investments

1 Introduction

The European power grid is vital for modern societies, supporting critical services like water, transportation, and communication, as well as facilities like healthcare. Yet, the resilience of roughly 509,000 km transmission network and 25,400 substations are continuously threatened by natural hazards e.g. windstorms and flooding. Ensuring uninterrupted electricity supply is crucial for community safety and prosperity. Natural hazards, including climate-related ones, threaten grid functionality annually. According to the European Network of Transmission System Operators for Electricity [1], 18–22% of disruptions in Europe during 2018–2021 resulted from climate hazards, potentially higher due to under-reporting [2]. Climate hazards were the leading cause of transmission network disruptions in this period, with no outages linked to power generation plants. A World Bank study [3] estimated 37% of power outages attributed to natural hazards from 2010–2016, lasting four times longer than non-natural outages. Global trends support these findings [4], with higher percentages in some regions [5]. Notable examples of grid vulnerability include the 2021 European floods and the 2019 California heatwave, causing extensive damage and prolonged power outages [6,7].

Evidence indicates a rising trend in accidents and their consequences, driven by climate change and grid complexity. In 27 EU+UK countries, the average interruption frequency due to extreme weather events more than doubled from 2004 to 2016 [8]. The North American Electric Reliability Corporation (NERC) reported that 69 out of 70 large power transmission events in the U.S. from 2016–2021 resulted from extreme weather, challenging the electricity system [9]. The Intergovernmental Panel on Climate Change (IPCC) 2023 report [10] confirmed increasing weather extremes due to global warming, expected to persist [11]. Expanding power grids, especially in coastal Mediterranean regions [12], heightens infrastructure exposure.

To understand power grid vulnerabilities, we need robust fragility models. Fragility Curves (FCs) facilitate risk analysis and loss assessment as well as quantification of resilience [13]. However, literature on power grid

fragility models against natural hazards, accounting for climate projections and multiple hazards, is limited. A review by [14] highlighted empirical, single-hazard models as predominant. Existing models focus largely on wind hazards, neglecting others like snow, lightning, floods, and wildfires [9,15]. European models remain mostly empirical, even for wind hazards [16,17]. Analytical FCs primarily target different infrastructure types [18,19].

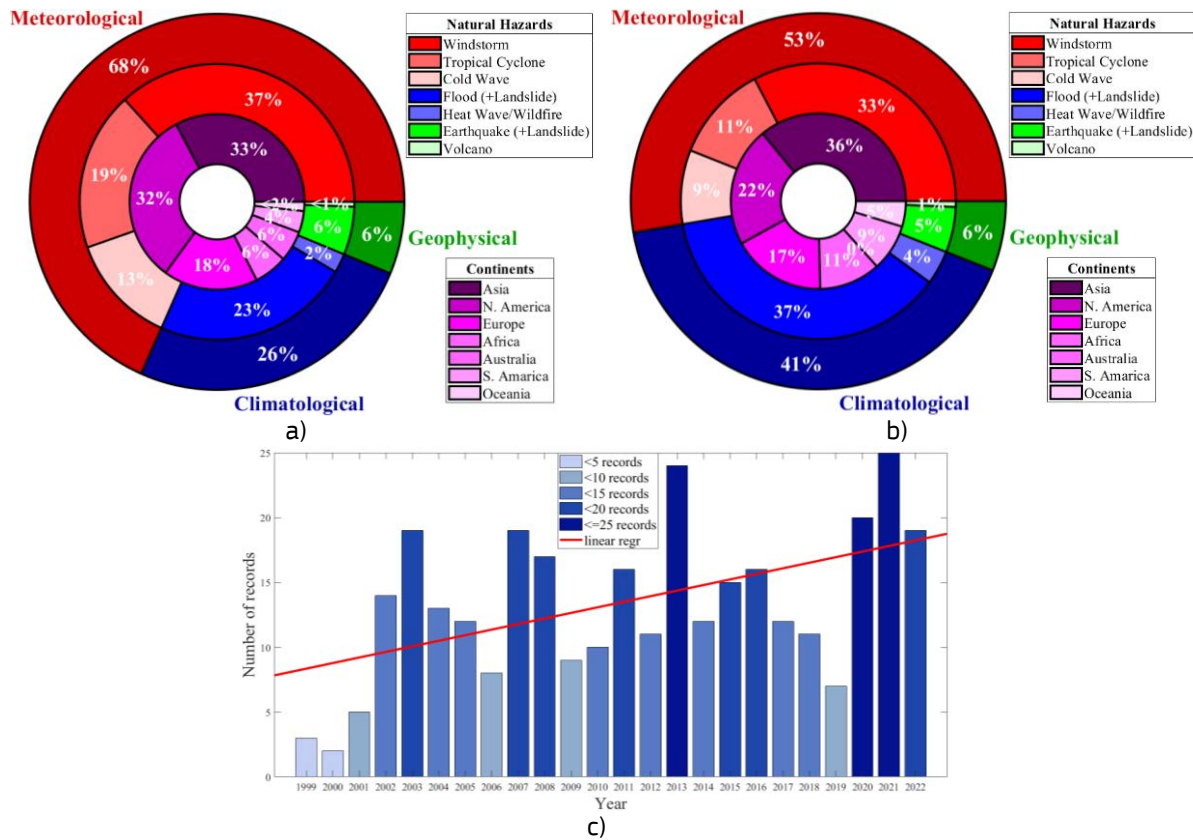
In view of the new EU Directive [20] that intends to enhance the resilience of critical entities, accounting for all-hazards, climate change and adaptation, this study aims to conduct a review of fragility assessment models and adaptation investments for power grid assets against critical natural hazards. Before doing so, a database analysis and damage assessment to identify the most damaging hazards, failure modes and impact is carried out.

2 Previous accidents on power grid due to natural hazards

2.1 Database analyses

The purpose of this section is to identify the most significant natural hazards that pose threat to the power grid network as well as the potential research gaps in available damage reporting and in the consideration of natural hazards for fragility assessment. The main challenge when carrying out a statistical analysis is that databases present different level of accuracy and detail. Numerous accidents are under-reported, and there is also inconsistency with respect to the information that is reported for each accident, which introduces bias into the statistical analysis. To reduce the bias, multiple databases and cross-checking with reports and media can be employed. In this study, data is extracted from two available accident databases: the International Disaster Database (EM-DAT) and the database of the Asian Disaster Reduction Center (ADRC). These choices were made, because the data are publicly available, while the level of detail allows the categorization of accidents. The accidents included in the analysis meet one or more of the following criteria in both databases: 5-10 or more fatalities, a minimum of 100 people affected and/or an international appeal for emergency assistance. The extracted records refer to accidents that occurred between 1999 and 2022.

Figure 36: Database analyses: percentage of natural hazards that have triggered a power outage and the allocation of accidents to each continent from a) EM-DAT and b) ADRC databases, and c) linear regression of the number of accidents per year based on EM-DAT and ADRC



Out of a total of 703 accidents, 177 and 151 accidents were selected from EM-DAT and ADRC, respectively. Using keywords, the accidents were categorized per each family of hazards (meteorological, climatological and geophysical), individual natural hazards and continent where the accident occurred. In Figure 36a&b, the outer circle of the pie charts represents the family of hazards, and it can be seen that the majority of accidents were triggered by meteorological hazards, followed by climatological and geophysical, for both databases. The databases agreed regarding the most damaging hazard, which was windstorms, accounting for approximately 33% to 37% of the accidents, followed by floods and cold waves. It is important to note that windstorms are compound hazards involving both wind and lightning, which have been found to cause significant damage to the power grid. A notable discrepancy between the databases was observed on the percentage of accidents caused by floods and tropical cyclones, which can be attributed to differences in the allocation of accidents. Although one-third of accidents occurred in Asia in both databases, the number of accidents that occurred in N. America was 10% less in EM-DAT, which may introduce some bias. Nearly one-fifth of accidents occurred in Europe in both databases, which could increase to 25% if hazards affected multiple countries were considered (omitted from this analysis due to lack of data). Among the least damaging hazards were heat waves and wildfires accounting for only 2% of the accidents. This percentage may be relatively biased due to under-reporting, considering the numerous and prolonged outages in wildfire-prone areas like California [23]. Wildfires are often localized events, and this might be a reason of the under-reporting; however, the risk of power grid damage due to wildfires is expected to increase considerably in areas with Mediterranean-line climate due to climate change [8,24].

Furthermore, a linear regression model was employed to estimate the number of accidents per year, taking into account data from both databases. This approach ensured that accidents reported in both databases were considered only once. As shown in Figure 36c, an increasing trend in the annual number of accidents is observed from 1999 to 2022. This outcome further highlights the importance of conducting risk assessment of power grid assets against natural hazards. Regarding the causes of failure, it can be confirmed that the most frequent cause was fallen trees on transmission towers or utility pylons due to excessive wind or snowfall, accounting for at least 15% of failures. It is noteworthy that approximately 25% of accidents were triggered by compound events such as combination of wind with rainfall, snow or lightning. These results provide valuable insights for the current review and future studies on risk and resilience assessment. Finally, regarding the failure modes, it is important to mention that, apart from conductor failures and the collapse of towers, pylons, or substations due to flooding, limited information was available for other failure modes. Therefore, the subsequent section will delve into reviewing damage assessment studies to gain a better understanding of these failure modes as well as other resilience aspects e.g. preparedness, restoration and recovery that contributed to increased losses.

2.2 Analysing failure modes and impact in major accidents

Table 4 presents information on significant power grid accidents linked to various destructive hazards, including snowstorms, heatwaves, windstorms, floods, and earthquakes. The objective is to emphasize the most common causes of failures and the consequences of these hazards on power grid assets and the economy. The first incident documented in the table concerns the 2005 Münsterland power blackout, which was triggered by a combination of factors, including ice and wind, as well as the aging infrastructure [25]. The event unfolded as a result of strong winds and heavy snowfall, leading to the accumulation of wet snow on overhead electrical lines in the form of snow rolls. This accumulation caused the failure of 82 high-voltage transmission towers. The power company responsible for the transmission system in the region initially labeled the failure as an unforeseeable "black swan" event. However, subsequent investigations by news media [26] and a forensic analysis conducted by [25] revealed that the tower collapse resulted from a combination of excessive ice and wind loading, coupled with the reduced capacity of the towers. The consequences of this blackout were substantial, affecting more than 250,000 individuals for a duration of 4 to 6 days, with estimated repair costs surpassing €130 million. This incident underscored the necessity of upgrading or replacing aging infrastructure and establishing effective communication channels between power operators and meteorological agencies to identify hazards and implement preventive measures to avert future accidents. Indeed, a power utility company proactively shut off electricity to approximately 3 million people in response to an impending threat of deadly wildfires and potential damage to the power grid due to a forecast of extreme weather conditions, which combined heat and wind hazards [6]. High temperatures can lead to short circuits because of line sagging, and wildfires front can damage directly power grid assets. While a post-event case study demonstrated that the prior shutdown by the company prevented a catastrophic outcome, it also revealed inadequacies in the preparedness of authorities and the resilience of the power grid. This was evident in the fact that it took over one month to fully restore power in all affected regions, primarily due to extensive inspections [27].

Table 4. A summary of failure modes and impact in major power grid accidents

| Natural Hazard | Event | Failure mode and contributing factors | Impact |
|--------------------------------------|---|--|--|
| Snowstorm (compound hazard) | <ul style="list-style-type: none"> • 2005 Münsterland power blackout • Affected country: Germany | <ul style="list-style-type: none"> • Transmission tower collapse due to excessive wind and ice load on the conductors | <ul style="list-style-type: none"> • Blackout experienced by 250,000 people for 4-6 days • Rupture of 82 transmission |
| Heat wave and wind (compound hazard) | <ul style="list-style-type: none"> • 2019 California shutoffs • Affected country: USA | <ul style="list-style-type: none"> • Pre-emptive shutdown as a response to the elevated wildfire risk • Substantial rise in California's population in wildfire-prone regions • Potential failure modes: short circuits due to line sagging and direct damage to assets from wildfire front | <ul style="list-style-type: none"> • Around 3 million people without power for up to a month • Disruption of rail transport services for two days |
| Windstorm (tropical cyclone) | <ul style="list-style-type: none"> • 2017 Hurricane Maria • Affected country: Puerto Rico | <ul style="list-style-type: none"> • Damaged power lines and inaccessibility to the sites due to fallen trees • Under-investment by the government: lack of vegetation management, redundancy and design of power lines for Hurricane Category 4 | <ul style="list-style-type: none"> • 70% of electricity customers without power • 18 billion of dollars for power grid restoration (direct damage) |
| Fluvial flood | <ul style="list-style-type: none"> • 2021 European floods • Affected countries: Germany, Netherlands | <ul style="list-style-type: none"> • Failure of equipment inside substations because of flood water • Very high quantity of water (the highest in 1000 years) | <ul style="list-style-type: none"> • Around 800,000 people without power for up to 8 weeks |
| Earthquake and tsunami | <ul style="list-style-type: none"> • 2011 Great East Japan earthquake and tsunami • Affected countries: Japan | <ul style="list-style-type: none"> • Collapse of steel-lattice transmission towers by tsunami-borne debris and landslides • Design level exceedance of generation plants, substations and equipment e.g. insulators, even for the most recently constructed power grid assets | <ul style="list-style-type: none"> • 10 million people without power, but reinstatement of 90% of the power grid within 6 days • Collapse 42 steel-lattice transmission towers (40 by tsunami-borne debris and 2 by landslide) • Half a billion \$ for restoration and demand curtailment during summer due to damage to power plants |

Furthermore, tropical cyclones, with hurricanes being a notable example, rank among the most destructive threats to the power grid. An illustrative case is the impact of Hurricane Maria in 2017, which inflicted severe damage on Puerto Rico's electrical infrastructure. Power lines and towers were collapsed because of severe wind and fallen trees, as a result of under-investment. Poor maintenance, vegetation management and inadequate design for Category 4 hurricanes were the primary causes of failure. Also, lack of redundancy was the main cause of prolonged outages. The endeavor to restore the power grid alone incurred costs as substantial as €18 billion, marking the highest expense among all the incidents delineated in Table 4. Owing to the grid's pronounced vulnerability, merely 20% of the transmission lines were back in operation after the initial month, and the restoration process extended over a year [28,29].

The 2021 European floods, which had a significant impact on Germany's power grid, underscored the high impact of flood hazards on numerous equipment inside substations for High Impact Low Probability (HILP) events. The power outage lasted for up to 8 weeks due to site inaccessibility and repair work [29,30]. Also, the 2011 Great East Japan earthquake inflicted extensive harm on transmission towers and substations, resulting in substantial financial losses. The earthquake and tsunami exceeded design levels even for the most recently constructed power grid assets. Transmission towers failed mostly due to tsunami-borne debris, but landslides caused damage as well. This catastrophe also had a profound impact on approximately 10 million individuals. It's worth noting that the power supply was swiftly reinstated in 90% of the affected area within a mere 6 days, underscoring the nation's commendable level of preparedness. Nevertheless, the remaining 10% of the region, where damage resulted from the tsunami and landslides, necessitated a month-long effort to fully restore the power supply [31,32]. TEPCO energy provider spent half a billion for restoration and issued summer power curtailments due to the loss of power plants.

3 Fragility models for European power grid assets

One of the requirements for assessing the resilience of power grid assets is the derivation of FCs, which are practical tools that describe the probability of exceedance of a certain level of damage given the intensity measure (IM) of a natural hazard [33,34]. As shown in the following sections, even though FCs have been derived for other critical infrastructures e.g. bridges and power plants [18,19], the literature is still scarce for power infrastructure. Dumas et al. [14] carried out a review of power grid vulnerability, which is one out of very few in the literature, and corroborated that the majority of the available models are empirical and single-hazard. Furthermore, by virtue of limitations of the lognormal distribution to capture efficiently the data that pertain to multiple-parameter or multiple-hazard events, the logit function is adopted instead [35,36]. There are four main methods for deriving FCs, namely empirical, analytical, judgmental and hybrid. Analytical methods are based on physical models or explicit demand-capacity relationships, while empirical and judgmental methods rely on observations, experiments, and expert judgments. Hybrid methods combine these approaches. The key advantage of analytical forecasting over empirical/judgmental methods is the auditability and verifiability of physical models, whereas empirical data are easier to handle. Table 2 summarizes all the available fragility models for transmission and distribution network as well as substations in the EU per natural hazard, fragility method and IM. This summary is part of a comprehensive review by [37] and relies only on peer-reviewed journal publications in the last two decades. Also, only publications that derive FCs are considered. Hence, resilience assessment studies that use FCs are not taken into account.

Table 5. Fragility models for power grid assets in the EU against different natural hazards

| Power grid asset | Hazard | Fragility model | IM |
|-------------------------|---------------|----------------------------------|---------------------|
| Transmission network | Wind | Analytical: [17] | 3-s gust wind speed |
| Distribution network | Wind | Empirical: [16] | Maximum wind speed |
| | Earthquake | Empirical: [38] | PGA |
| Substations | Earthquake | Analytical: [39] Hybrid: [40] | PGA: [39], [40] |

It can clearly be seen in Table 2 that the available models are limited per asset and hazard. This conclusion is especially true in Europe for all power grid assets and natural hazards, which renders the evaluation of impacts at an individual asset level inconsequential for planning recovery measures in a broader, EU-level policy framework. Prior FP7 projects e.g. RAIN, AFTER, ongoing HE e.g. ReCharged, R²D², HVDC-WISE, RISKADAPT and studies [41] have advanced the resilience assessment of power assets, but do not study new fragility models in a systematic way, disregarding structural- and hazard-induced uncertainties. Additionally, empirical models e.g. [16] and [38] are bound to specific regions, in contrast with numerical models, and cannot easily apply to other regions due to different typologies of assets and weather conditions e.g. multi-hazard or climate change effects. Numerical fragility functions are very limited, e.g. for the Nordic transmission power network against wind hazard [17] or for substations against earthquake hazard [39] and

[40], and case-specific with regard to asset typologies, ageing and design conditions. Therefore, it is evident that additional fragility studies are needed to evaluate the resilience of the EU power grid assets against all damaging natural hazards, including wind, flood, earthquakes, wildfires, lightning as well as compound events such as windstorms and snowstorms. The new fragility models can be used to reflect the impact of different adaptation investments e.g. structural upgrade, as discussed in the following section.

4 Adaptation investments for managing risks

Current EU regulations [42]<https://eur-lex.europa.eu/legal-content/EN/TXT/PDF/?uri=CELEX:32019R0941> focus mainly on the generation-demand balance, without providing well-informed methods on how energy infrastructure can be incorporated into national disaster risk assessments. The new EU Directive [20] and Adaptation strategy [43] stipulate that National Authorities shall identify critical entities, receive EU support and embrace grey, green and soft investments, especially because of climate change. Table 6 quotes different adaptation investments of power grid assets against natural hazards, which may exacerbate in frequency and/or intensity due to climate change depending on the region [11]. First, grey investments refer to engineering interventions that have low environmental footprint. These investments can be reflected on fragility and risk assessment models for evaluating whether the updated risk after the upgrade is acceptable or not. However, the literature lacks of such models, as demonstrated in the Section 3. Grey investments measures include structural upgrade, underground cabling, use of high-quality insulators, “low-sag” conductors, levee protection or relocation of assets, among others [44]. Green options are based on nature-based approaches and make use of the multiple services provided by natural ecosystems e.g. land-use planning for identifying alternative network paths, nature-based wind protection barriers, configuration of smart grids based on renewables to improve resilience and adaptation capacity.

Finally, soft options include policy, legal, societal, managerial and financial measures, capable of influencing human conduct and governance practices. For example, the improvement of legal status of EU member states regarding the development of smart grids, interconnection of transmission networks among member states for building redundancy and the consideration of power operators in the decision making of power infrastructure protection are soft measures. Additionally, cost-benefit analyses can be used to examine resilience trade-offs among different adaptation investments. For instance, a cost-benefit analysis can evaluate whether underground cabling is more cost-efficient than retrofitting or replacement options e.g. with pylons of different material in the long term in regions with extreme weather conditions [45]. This will result in money saving and higher safety of citizens. Also, vegetation management, maintenance and inspection of power grid assets should be part of a long-term financial planning of power operators in EU member states to prolong the lifetime of power grid assets and increase the resilience. Vegetation management, which includes trimming, removing hazard trees and other air-borne objects near overhead power lines to minimise interference risks, was identified as the most effective option for climate resilience enhancement by [46]. Finally, soft investments can play a key role in enhancing adaptive capabilities and raising awareness of local communities about climate change matters.

Table 6. Fragility models for power grid assets in the EU against different natural hazards

| Natural Hazard | Exacerbated by climate change | Adaptation measures |
|-----------------------|--|--|
| • Windstorm | • Yes (increase in intensity and/or frequency in some regions) | <ul style="list-style-type: none"> • Structural upgrade of towers/pylons, use of mechanical fuses to reduce conductor breakages and underground cabling • Exploration of alternative routes of overhead lines or ecosystem-based wind protection barriers • Establishing an efficient communication channel between power operators and meteorological agencies • Frequent inspection and maintenance, vegetation management • Effective decision-making based on cost-benefit analyses |
| • Lightning strikes | • Yes (increase is some regions) | <ul style="list-style-type: none"> • Surge arresters, high-quality insulators, shield wires and lightning masts • Vector shift protection • Load shedding with real time load assessment of feeders |

| | | |
|---|---|---|
| | | <p>using telecommunications</p> <ul style="list-style-type: none"> ● Grid reconfiguration |
| ● Heat waves and wildfires | ● Yes (Increase in intensity and/frequency) | <ul style="list-style-type: none"> ● Hardening, maintenance planning and vegetation management ● Installation of solar panels and mobile energy storage systems to increase redundancy, accounting for weather uncertainties ● Proactive generation redispatch and outage prediction modelling and shutoff due to wildfire progression ● System operators in the decision-making |
| ● Flood | ● Yes (Increase/decrease in intensity and/or frequency in some regions) | <ul style="list-style-type: none"> ● Substation relocation, equipment elevation or water-proofing ● Levee protection ● Shutdowns based on early warnings, surge mechanisms activation and positioning repair resources at the edge of flood zones |
| ● Earthquakes (inc. landslides, liquefaction and rockfalls) and tsunami | ● No | <ul style="list-style-type: none"> ● Seismic retrofitting of towers and equipment e.g. anchoring or flexible coupling among equipment items, use of bushings, surge arrestors and base isolation e.g. for transformers ● Installation of protection barriers all around transmission towers in tsunami run-up zones for debris protection ● Implementation of scour protection measures of equipment foundations |

5 Conclusions

Extended periods of power shortages and significant financial losses are evident in major accidents due to the absence of robust risk assessment models and preparedness. For transmission and distribution networks, the primary causes and contributing factors include falling trees and debris on overhead lines, wind loads surpassing design specifications and the effects of aging. Substations face challenges such as exceeding inundation levels, inadequate equipment maintenance, and the absence of protective barriers, which can lead to equipment damage and short circuits.

Hence, there is a need for new fragility models to enhance the assessment of power grid asset resilience against wind, flood, and wildfire hazards. For instance, there is a lack of analytical wind and multi-hazard models that can encompass the various types of transmission towers in different ecosystems. A similar deficiency is observed in the case of substations and flood hazards. While wildfire has been recognized as a significant threat, there is still limited research in this area. Given the aging infrastructure and the anticipated impact of climate change, particularly the intensification of wind, coastal and inland flooding, and heat waves, addressing these gaps becomes even more crucial.

Grey, green and soft adaptation investments should be considered to bolster asset resilience. The impact of climate-aware structural strengthening, wind or flood barriers, and mechanical fuses on conductors can be quantified through fragility models. Additionally, land-use planning for network relocation or expansion, emergency response planning, proactive line outages, and underground cables can significantly enhance asset resilience, all of which can be evaluated through cost-benefit analyses. However, it's important to note that the cost-benefit of these investments has not yet been quantified through resilience metrics specifically tailored to power grid assets, particularly in the case of transmission networks.

Acknowledgments

The second author received funding by the European Union HORIZON-MSCA-2021-SE-01 [grant agreement No: 101086413] ReCharged - Climate-aware Resilience for Sustainable Critical and interdependent Infrastructure Systems enhanced by emerging Digital Technologies. The third author received funding by the UK Research and Innovation (UKRI) under the UK government's Horizon Europe funding guarantee [Ref:

EP/X037665/1]. This is the funding guarantee for the European Union HORIZON-MSCA-2021-SE-01 [grant agreement No: 101086413] ReCharged project.

References

1. ENTSO-E. Incident Classification Scale Annual Report. European Network of Transmission System Operators for Electricity, Brussels. https://www.entsoe.eu/network_codes/sys-ops/annual-reports/. 2022;(September).
2. EC. Study on the quality of electricity market data of transmission system operators, electricity supply disruptions, and their impact on the European electricity markets, European Commission, Brussels. <https://energy.ec.europa.eu/study-quality-electricitymar>. 2018.
3. Hallegatte S, Rentschler J, Rozenberg J. Lifelines: The resilient infrastructure opportunity. Sustainable Infrastructure Series. World Bank, Washington, DC. <https://openknowledge.worldbank.org/handle/10986/31805>. 2019.
4. Zhaohong B, Yanl ng L, Gengfeng L, Furong L. Battling the Extreme: A Study on the Power System Resilience. Proc IEEE. 2017;
5. ENTSO-E. European Network of Transmission System Operators for Electricity, "Nordic Grid Disturbance Statistics 2012." 2013;1–92.
6. City-Journal. California Goes Dark, <https://www.city-journal.org/article/california-goes-dark>. 2019; Available from: <https://www.city-journal.org/article/california-goes-dark>
7. Koks EE, Van Ginkel KCH, Van Marle MJE, Lemnitzer A. Brief communication: Critical infrastructure impacts of the 2021 mid-July western European flood event. Nat Hazards Earth Syst Sci. 2022;22(12):3831–8.
8. Tavares da Costa R, Krausmann E, Hadjisavvas C. Impacts of climate change on defence-related critical energy infrastructure. Publications Office of the European Union, Luxembourg,; 2023.
9. NERC NARC. 2022 State of Reliability - An Assessment of 2021 Bulk Power System Performance, https://www.nerc.com/pa/RAPA/PA/Performance%20Analysis%20DL/NERC_SOR_2022.pdf. 2022;
10. IPCC. Intergovernmental Panel on Climate ChangeClimate Change 2023 - Summary for policy makers of the synthesis report, https://www.ipcc.ch/report/ar6/syr/downloads/report/IPCC_AR6_SYR_SPM.pdf. 2023;(2):2–5.
11. Stocker TF, Qin D, Plattner GK, Tignor M, Allen SK, Boschung J, et al. Climate Change 2013: The Physical Science Basis. Contribution of Working Group I to the Fifth Assessment Report of the Intergovernmental Panel on Climate Change. 2013;AR5(September 2014):1535.
12. Forzieri G, Bianchi A, Silva FB e, Marin Herrera MA, Leblois A, Lavalle C, et al. Escalating impacts of climate extremes on critical infrastructures in Europe. Glob Environ Chang. 2018;48(November 2017):97–107.
13. Mitoulis SA, Bompa D V, Argyroudis S. Sustainability and climate resilience metrics and trade-offs in transport infrastructure asset recovery. Transp Res Part D Transp Environ. 2023;
14. Dumas M, Kc B, Cunliff CI. Extreme Weather and Climate Vulnerabilities of the Electric Grid: A Summary of Environmental Sensitivity Quantification Methods. OAK Ridge National Laboratory. 2019.
15. Serrano R, Panteli M, Parisio A. Risk Assessment of Power Systems Against Wildfires. In: 2023 IEEE Belgrade PowerTech [Internet]. IEEE; 2023. p. 01–6. Available from: https://scholar.google.co.uk/citations?view_op=view_citation&hl=en&user=Ajm_SQAAAAAJ&sortby=pubdate&citation_for_view=Ajm_SQAAAAAJ:Tiz5es2fbqcC
16. Dunn S, Wilkinson S, Alderson D, Fowler H, Galasso C. Fragility Curves for Assessing the Resilience of Electricity Networks Constructed from an Extensive Fault Database. Nat Hazards Rev. 2018;
17. Scherb A, Garré L, Straub D. Evaluating component importance and reliability of power transmission networks subject to windstorms: methodology and application to the nordic grid. Reliab Eng Syst Saf. 2019;
18. Argyroudis SA, Mitoulis S, Winter MG, Kaynia AM. Fragility of transport assets exposed to multiple hazards: State-of-the-art review toward infrastructural resilience. Reliab Eng Syst Saf. 2019;
19. Karagiannakis G, Di Sarno L, Necci A, Krausmann E. Seismic risk assessment of supporting structures and process piping for accident prevention in chemical facilities. Int J Disaster Risk Reduct. 2022 Feb;69:102748.
20. CER Directive. Directive of the European Parliament and of the Council of 14 December 2022 on the resilience of critical entities and repealing Council Directive 2008/114/EC. 2022;
21. EM-DAT. The International Disaster Database - Centre for research on the Epidemiology of Disasters, Université catholique de Louvain, <https://public.emdat.be/> (Accessed in 25/05/2023).
22. ADRC. Asian Disaster Reduction Center, GLIDEnumber.net (Accessed in 25/05/2023).

23. Mitchell JW. Power lines and catastrophic wildland fire in Southern California. In: Conference Proceedings - Fire and Materials 2009, 11th International Conference and Exhibition. 2009.
24. Tavares da Costa R, Krausmann E. Impacts of Natural Hazards and Climate Change on Eu Security and Defence [Internet]. 2021. Available from: <https://www.preventionweb.net/publication/impacts-natural-hazards-and-climate-change-eu-security-and-defence>
25. Klinger C, Mehdianpour M, Klingbeil D, Bettge D, Häcker R, Baer W. Failure analysis on collapsed towers of overhead electrical lines in the region Münsterland (Germany) 2005. Eng Fail Anal. 2011;
26. Spiegel. The German power outage - Brittle giants [Internet]. 2005. Available from: <https://www.spiegel.de/international/spiegel/the-german-power-outage-brittle-giants-a-388759.html>
27. PG&E. Technosylva 2019 PSPS Event Wildfire Risk Analysis Reports, <https://www.cpuc.ca.gov/-/media/cpuc-website/divisions/safety-and-enforcement-division/documents/technosylva-report-on-pge-psps-eventoct-912-2019.pdf> [Internet]. 2021. Available from: <https://www.cpuc.ca.gov/-/media/cpuc-website/divisions/safety-and-enforcement-division/documents/technosylva-report-on-pge-psps-eventoct-912-2019.pdf>
28. Schweikert A, Nield L, Otto E, Deinert M. Resilience and Critical Power System Infrastructure; Lessons Learned from Natural Disasters and Future Research Needs. Policy Research Working Paper;No. 8900. © World Bank, Washington, DC. 2019; Available from: <https://openknowledge.worldbank.org/entities/publication/47095572-0e4e-5c0b-a591-69c91e1e4812>
29. NYT. European Floods are Latest Sign of a Global Warming Crisis [Internet]. 2021. Available from: <https://www.nytimes.com/2021/07/16/world/europe/germany-floods-climate-change.html>
30. News S. Germany and Belgium floods: More than 50 dead and over 70 missing after heavy rain [Internet]. 2021. Available from: <https://web.archive.org/web/20210715200906/https://news.sky.com/story/germany-and-belgium-floods-at-least-44-dead-and-more-than-70-missing-after-heavy-rain-12356134>
31. Cunha A, Caetano E, Ribeiro P, Müller G. Seismic Vulnerability of Power Supply: Lessons Learned from Recent Earthquakes and Future Horizons of Research. In: Proceedings of the 9th International Conference on Structural Dynamics, EURODYN 2014 Porto, Portugal, 30 June - 2 July 2014. 2014.
32. Eidinger J, Davis C, Tang A, Kempner L. M 9.0 Tohoku Earthquake March 11 2011 Performance of Water and Power Systems [Internet]. 6315 Swainland Rd Oakland, CA 94611; 2012. Available from: http://learningfromearthquakes.org/2011-03-11-tohoku-japan/images/2011_03_11_tohoku_japan/pdfs/Water-and-Power-Report-6.25.2012.pdf
33. Panteli M, Pickering C, Wilkinson S, Dawson R, Mancarella P. Power System Resilience to Extreme Weather: Fragility Modeling, Probabilistic Impact Assessment, and Adaptation Measures. IEEE Trans Power Syst. 2017;32(5):3747–57.
34. Panteli M, Mancarella P. The Grid: Stronger, Bigger, Smarter? Presenting a Conceptual Framework of Power System Resilience. IEEE Power Energy Mag. 2015;
35. Koutsourelakis PS. Assessing structural vulnerability against earthquakes using multi-dimensional fragility surfaces: A Bayesian framework. Probabilistic Eng Mech. 2010;
36. Reed DA, Friedland CJ, Wang S, Massarra CC. Multi-hazard system-level logit fragility functions. Eng Struct. 2016;
37. Karagiannakis G, Argyroudis S, Panteli M. Fragility modelling of power grid infrastructure for addressing climate change risks and adaptation, WIRES Clim. Change (preprint). 2023;
38. Yeşilyurt A, Okuyan Akcan S, Zülfikar AC. Rapid power outage estimation for typical electric power systems in Turkey. Chall J Struct Mech. 2021;
39. Pitilakis K, Crowley H, Kaynia AM. SYNER-G: Typology Definition and Fragility Functions for Physical Elements at Seismic Risk: Buildings, Lifelines, Transportation Networks and Critical Facilities. Geotech Geol Earthq Eng. 2014;157–85.
40. Cavalieri F, Donelli G, Pinho R, Dacarro F, Bernardo N, de Nigris M. Shake Table Testing of Voltage and Current Transformers and Numerical Derivation of Corresponding Fragility Curves. Infrastructures. 2022;
41. Panteli M, Mancarella P. Modeling and evaluating the resilience of critical electrical power infrastructure to extreme weather events. IEEE Syst J. 2017;11(3):1733–42.
42. EU. Regulation of the European parliament and of the Council of 5 June 2019 on risk-preparedness in the electricity sector and repealing Directive 2005/89/EC. 2019.
43. EC. COMMUNICATION FROM THE COMMISSION TO THE EUROPEAN PARLIAMENT, THE COUNCIL, THE EUROPEAN ECONOMIC AND SOCIAL COMMITTEE AND THE COMMITTEE OF THE REGIONS Forging a climate-resilient Europe - the new EU Strategy on Adaptation to Climate Change. 2021;
44. Najafi Tari A, Sepasian MS, Tourandaz Kenari M. Resilience assessment and improvement of

- distribution networks against extreme weather events. *Int J Electr Power Energy Syst.* 2021;
45. Salman AM, Li Y. Age-dependent fragility and life-cycle cost analysis of wood and steel power distribution poles subjected to hurricanes. *Struct Infrastruct Eng.* 2016;
46. Hou G, Muraleetharan KK, Panchalogarajan V, Moses P, Javid A, Al-Dakheeli H, et al. Resilience assessment and enhancement evaluation of power distribution systems subjected to ice storms. *Reliab Eng Syst Saf.* 2023;

2.15 Feasibility Study: Improving Low-Inertia Power System Resilience By Novel Load Shedding Method Including Control of Synchronous Condensers' Power Injections

Antans Sauhats, Andrejs Utans, Diana Zalostiba and Anna Mutule, Riga Technical University, Latvia,
antans.sauhats@rtu.lv, andrejs.utans@rtu.lv, diana.zalostiba@rtu.lv, anna.mutule@rtu.lv

Oskars Grigals, Augstsrieguma tikls AS, Latvia, oskars.grigals@ast.lv.

Dmitrijs Guzs, Vindr Latvia SIA, Latvia, dgpostbox@gmail.com

Abstract

The penetration of non-synchronous renewables and the abandonment of conventional power plants are bringing a number of power-system-related challenges such as: reduction of total system inertia; increasing rates of change of frequency (RoCoF); reduced frequency and angular stability and a decreasing number of generation units providing frequency regulation. The drop of the system inertia level has become a widely acknowledged issue, which can lead to a faster fall in frequency for the same power imbalance and may result in suboptimal operation of the traditional under-frequency load shedding (UFLS), causing an additional negative effect on system resilience. A novel, synchronous-condensers'-power-injection-based UFLS method is proposed by the authors. The preliminary test case and estimation has shown that the proposed rapid load shedding (RLS) approach significantly improves the post-contingency frequency response when compared with the traditional UFLS scheme. At present, a hardware platform, the operation algorithm and innovative scheme of the RLS system terminals are being tested in laboratory. The preliminary results have shown the advantages of the proposed innovative scheme of PS emergency control. Its implementation provides the opportunity to soften the restrictions regarding the selection of the maximum allowable capacity of synchronous generators and transmission network interconnections in the pre-emergency mode. Based on the usage of PS dynamic models and the NORDPOOL electricity market model, a methodology for assessing the economic benefit of applying the proposed solution has been developed. The case study of the Baltic power system (incl. analysis of power system operation modes) demonstrates the possibility of obtaining a positive economic effect due to optimal use of the capacities of the transmission network interconnections and economically efficient generation.

Keywords: power system inertia; resilience assessment; load shedding; frequency stability; synchronous condensers; feasibility study.

1 Introduction

To mitigate climate change and reduce greenhouse gas emissions, the European Union has introduced and started implementing the 2030 Climate & Energy Framework⁶. The proposed pathways consider transformation of energy infrastructures to meet 100% of the demand by means of renewable energy sources (RES). The transformation of the power system (PS) affects both the structure of the generation mix and its ability to withstand, and recover from, disturbances and contingencies. Substituting the traditional (fossil) power plants with renewable-energy power plants brings new challenges to PS operation, therefore strengthening the energy security and improving the resilience against new threats will only rise in importance on the way towards climate neutrality [1], [2]. The studies on the impact of non-synchronous RES generation on grid stability have brought forward the following challenges: reduction of total system inertia; increasing rates of change of frequency (RoCoF); inability to meet the requirements regarding peak demand and ancillary services with current system regulations; reduced frequency and angular stability and a decreasing number of generation units (rotational inertia) providing frequency regulation [3], [4], [2]. In the worst cases, frequency instability can trigger cascaded tripping of PS elements and even blackout of a power system or its part [5], [6]. The drop of the system inertia level has become a widely acknowledged issue concerning even power systems with historically sufficient inertia levels and stability reserves, such as ENTSO-E, the Nordic synchronous PS and the PS of the Baltic States [7]. The reduction of system inertia will

⁶) <https://www.consilium.europa.eu/en/policies/climate-change/2030-climate-and-energy-framework/>

lead to a faster frequency drop for the same power imbalance and may cause suboptimal operation of the traditional under-frequency load shedding (UFLS), resulting in an additional negative effect on system resilience [2], [7].

Equation (1), which is a form of swing equation [8], clearly shows that in order to improve the change in system frequency $d\omega/dt$, one can either increase the available system inertia H_{tot} by adding more synchronous machines (e.g., synchronous generators or/and synchronous condensers), by introducing synthetic inertia, or by providing a strong synchronous interconnection with a neighbouring PS — or else, one can decrease active power imbalance ΔP (e.g., by improving the efficacy of the existing UFLS):

$$\frac{d\omega}{dt} = \Delta P \frac{\omega_{syn}}{2H_{tot}} \quad (1)$$

As pointed out in [9], synchronous condenser technology (SC) can be used to increase system inertia and simplify the frequency control during loss-of-generation incidents. Besides, introduction of faster UFLS triggering would therefore be beneficial especially for PSs of medium and small size with low rotational inertia since the UFLS frequency thresholds are reached faster in such cases.

Different improvements of UFLS schemes are proposed in literature, making it possible to boost the efficacy of UFLS:

- semi-adaptive UFLS schemes — a triggering method utilising static frequency measurement and RoCoF thresholds instead of a frequency-only approach [9], [10], [11];
- adaptive UFLS schemes — triggering methods employing a dynamic combination of frequency and RoCoF; operating on the basis of a single estimation of the situation or constantly updating the estimation [10], [11], [12], [13]. Another type of method calculates the system inertia values or the total power imbalance and uses these for load shedding (LS) triggering together with frequency and RoCoF threshold values [11], [14] or even bus voltage threshold values [15], [16].

The above approaches use frequency measurements in one or another manner. Regardless of the merits of the adaptive UFLS in comparison with the traditional one, its use as system-wide protection is limited due to the complexity of a real PS and the difficulties in ensuring fast and accurate measurements of frequency and/or RoCoF, including the availability of data of the frequencies and inertia of various generators [13]. Therefore, a predictive approach to UFLS, as anticipated in [13], could be the next step in the development of UFLS. A novel synchronous-condensers'-power-injection-based UFLS method has been introduced by the authors [9] and motivates continuation of the work on the improvement of the resilience of a low-inertia power system (with high penetration of non-synchronous RES generation). The test case set provided in [16] has shown that the proposed rapid load shedding (RLS) method significantly improves the post-contingency frequency response and positively impacts the value of the quantitative resilience index [17] when compared with the traditional UFLS scheme.

This article is a continuation of the authors' work that was presented in [9], [16], [18]. The goal of this paper is to examine the feasibility of the proposed RLS from both technical and economic points of view. The remaining part of the paper is organised as follows: the novel RLS method and its principles are described in the next chapter, then automation concepts (including hardware structure and control terminal connection) and a case study are presented; finally, the conclusions are made.

2 The power system under consideration. Control principle and methodology

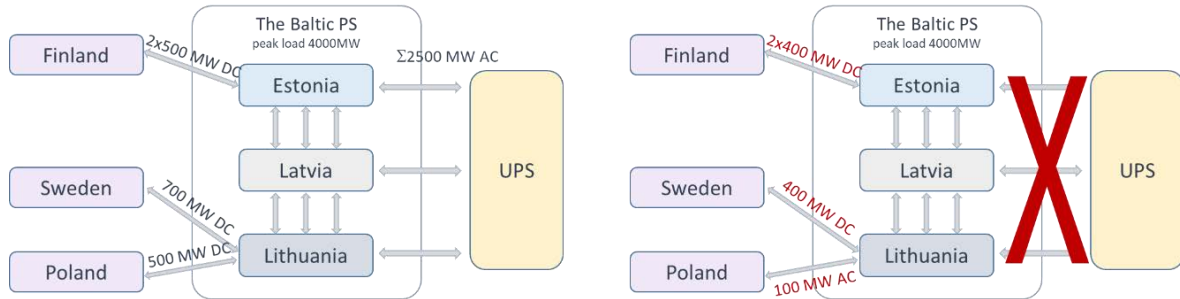
2.1 The Baltic power system

To test and demonstrate the feasibility of the proposed rapid load shedding, the Baltic power system has been chosen. It is well suited to illustrating the behaviour of a low-inertia PS; a simplified representation of the Baltic power system is shown in **Figure 37**. The Baltic power system is a relatively small PS with a peak load of ca. 4000 MW, historically synchronously operated with the Unified Power System of Russia (UPS), which provides vast frequency and inertia reserves (**Figure 37**, left part). To improve energy independence and security, it was decided⁷ to disconnect the Baltic PS from the UPS and to establish a new synchronous

(7) https://ec.europa.eu/commission/presscorner/detail/en/IP_19_3337

interconnection with the continental Europe network via Poland in early 2025 (through one double-circuit 400 kV AC line) [9]. The integration process has been started by introducing new HVDC connections with Finland, Sweden and Poland.

Figure 37. The Baltic PS (left part – present situation; right part - after disconnection from the UPS).



Source: RTU, 2023.

As has been pointed out in [9], after desynchronisation, the available transmission capacity on the AC link between Poland and Lithuania is planned to be only 100 MW (a thermal limit capacity of ca. 2000 MW). Any planned or unplanned outages of this AC interconnection will result in the operation of the Baltic PS in an island mode, only relying on its own inertia reserves, which are radically lower than today's available inertia of the UPS. The operation in the island mode is to introduce major challenges to the frequency stability of the Baltics. Moreover, power transfer over DC links needs to be reduced to approx. 400 MW, to ensure secure operation in the case of a loss-of-generation or DC link disconnection event (**Figure 37**, right part). Furthermore, a rapid shift towards renewable generation is expected, which additionally worsens the situation in case of frequency instability due to low inertia. To strengthen the Baltic PS, three synchronous condensers rated ca. 305 MVA each per each Baltic country will be installed by 2025⁸.

2.2 Determination of the imbalance of active power

An unexpected loss of active power results in deceleration of synchronously rotating machines. As stated in [9], the volume of the imbalance of active power ΔP at the very beginning of the process (prior to primary frequency control) is compensated by the injection of active power by each element of the PS possessing inertia:

$$\Delta P = \sum_{a=1}^{SC} \Delta P_{SC_a} + \sum_{b=1}^G \Delta P_{G_b} + \sum_{c=1}^L \Delta P_{L_c} \quad (2)$$

where ΔP_{SC_a} , ΔP_{G_b} and ΔP_{L_c} are the active power injections of every synchronous condenser, synchronous generator and frequency-dependent load (for example, electric motors) present in the PS; SC , G , L are the total numbers of these condensers, generators and frequency-dependent loads. To stop the frequency decline, it is necessary to restore the balance of generation and consumption, e.g. by disconnecting a load equal to ΔP . Nevertheless, due to the large number of elements in real power systems, it is a complex task to estimate the volume of this load by measuring all the ΔP s included in Equation (2). The problem can be simplified by assuming that Equation (2) can be represented as follows:

$$\Delta P = \left(1 + \frac{\sum_{b=1}^G \Delta P_{G_b} + \sum_{c=1}^L \Delta P_{L_c}}{\sum_{a=1}^{SC} \Delta P_{SC_a}} \right) \sum_{a=1}^{SC} \Delta P_{SC_a} = K_r \cdot \sum_{a=1}^{SC} \Delta P_{SC_a} \quad (3)$$

If the coefficient K_r is known, then, to estimate ΔP , it is sufficient to measure the power injections of all synchronous condensers $\sum \Delta P_{SC}$. In a real PS, the coefficient K_r is not a constant value and depends on the operating mode of the PS, its topology and also on the total system inertia level. However, as is mentioned in

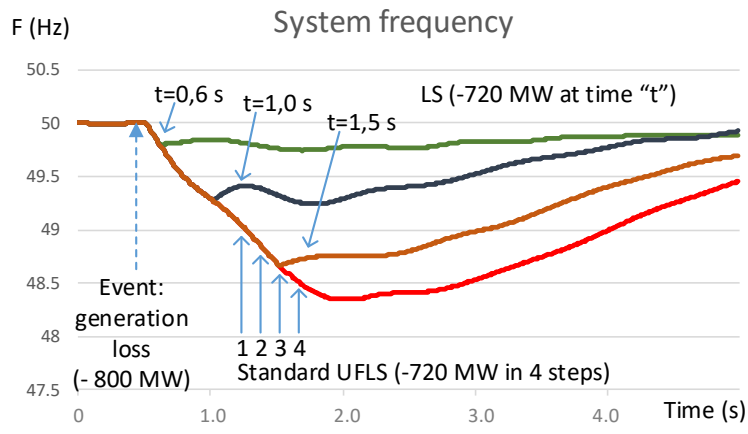
⁽⁸⁾ <https://www.ast.lv/en/projects/synchronisation-europe>

[9], in any case, we can assert that the measured $\sum \Delta P_{SC}$ can be taken as the basis for disconnecting the load for frequency stabilisation. This load shedding must be in a volume of not less than $\sum \Delta P_{SC}$. Such disconnection can significantly improve the efficiency of systems where the main source of inertia consists in synchronous condensers. Equation (3) will provide an opportunity to predict the frequency decline and therefore form the basis of the decision to initiate a fast triggering of the proposed LS scheme [9]. Monitoring of exclusively the SCs is achievable in practice and can be used as a basis for power imbalance and system frequency prediction. The implementation of such a concept would require using a Wide Area Measurement System and/or dedicated measurement units/terminals (see Chapter 0).

2.3 Rapid Load Shedding Method

Usually, standard multi-step UFLS is activated only after the frequency value reaches the set threshold/-s, gradually disconnecting load. As shown in **Figure 38** [16], for the same amount of disconnected load, the frequency nadir can be greatly improved if the load shedding is activated earlier. As to Equation (2), when any of the active power injections is measured, the same amount of load could be shed before the frequency reaches the first threshold.

Figure 38. System frequency profile depending on load shedding triggering time.



Source: RTU [16], 2023.

As mentioned above, we propose a novel synchronous-condensers'-power-injection-based UFLS method, which is based on a predictive approach, allowing much faster triggering of LS (up to 100-200 ms from the moment of the contingency) without using either frequency or RoCoF measurements [9]. The principle is based on the monitoring of the active power injections of the SCs. Our hypothesis is as follows: the active power injection of a SC in an AC power system contains information on the instantaneous shortfall of a major generation unit and the expected fall in frequency. SC active power injections can therefore be used as a set-off for rapid LS activation. Execution of such a rapid scheme of LS substantially reduces the frequency fall and the value of the frequency nadir, thus greatly reducing the risk of frequency limit violation in the given PS. The concept and the hypothesis were proved by performing PS dynamic simulation case studies; the results were demonstrated in [9], [18].

2.4 Resilience index

According to [19], power grid resilience characterises the system's ability to resist, prepare for, and adapt to changing conditions, withstand disruptions and rapidly recover from them. A quantitative resilience index, describing the resilience when system is transiting from an undisturbed state to a degraded state, was presented in [17]. The system frequency has been chosen as the first parameter to evaluate the transition phase (from the initial, steady-state condition towards a degraded one). The second parameter is the amount of load which has been shed during the transition state in an attempt to prevent instability and stop the decline of the system frequency. By combining both parameters, a part of the grid resilience concept, related to system transition from the initial, undisturbed state to the degraded yet stable state, could be assessed as [17]:

$$R_{trans} = \frac{f_{min}}{f_{rated}} \frac{L_{total} - L_{shed}}{L_{total}} \quad (4)$$

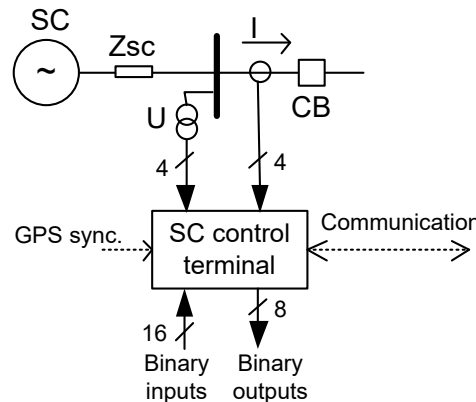
where f_{min} is the system frequency nadir, Hz; f_{rated} is the rated system frequency, Hz; L_{total} is the total load before the disruption, MW; L_{shed} is the amount of load that was shed during the transition stage. The index may vary between 0 and 1.0 with a higher value representing better performance.

To evaluate the impact that the reduced inertia has on the system's frequency stability two models of the Latvian 330 kV network have been used (see [17] for more detail). The frequency response described in the case study showed that decreased inertia in the Baltic PS after disconnection from the UPS produces a negative effect on frequency stability, thus decreasing the total resilience of the system. The authors conclude that an addition of the inertial reserves in the form of synchronous condensers improves the situation, yet nonetheless, these measures are insufficient and could not fully compensate for the absence of inertial response from the UPS power grid. Since the novel synchronous-condensers'-power-injection-based UFLS noticeably reduces the frequency fall and the value of the frequency nadir, its implementation can improve the resilience of the PS.

3 The structure of the control terminal's hardware and software. Technical feasibility

To control the SCs' power injection, the authors propose using a dedicated SC control terminal (SCCT), which measures SC currents and voltages and estimates the real power of the SCs (**Figure 39**).

Figure 39. SC control terminal connection.



Source: RTU, 2023.

Two options of SCCT operation are possible:

1. The SCCT continuously transmits estimated real power to the control and monitoring centre where all the SC's data are processed and the decision about the amount of load to be shed is taken in real time and commands are sent from the control centre;
2. If the active power value, exceeding which load shedding action must be taken, is known (as a result of simulating power system contingencies), then the SCCT can send a binary command to a predefined frequency relay, which disconnects a fixed amount of load.

3.1 Signal sampling. Fourier Transform and Phasor Computation

The operating principle of the proposed RLS is based on real power measurements, which are given by:

$$P = U \cdot I \cdot \cos(\theta) \quad (5)$$

where $\theta = \theta_U - \theta_I$ is the phase angle between voltage U and current I .

Equation (5) is ill-suited for direct measurements of power P . However, the phasor measurement technique allows overcoming this difficulty. To do that, another form of real power definition will be used:

$$P = \operatorname{Re}(\dot{S}) = \operatorname{Re}(\dot{U} \cdot \dot{I}) = \operatorname{Re}((U_r + jU_i)(I_r - jI_i)) = U_r \cdot I_i + U_r \cdot I_i \quad (6)$$

where \dot{S} is the complex power; \hat{I} is the complex conjugate of current I ; voltage and current are represented in complex form by real U_r, I_r and imaginary U_i, I_i components, respectively.

Sampled waveforms of SC's current and voltage will be processed by the full-cycle Discrete Fourier Transform (DFT) to derive the real and imaginary components of the voltage and current phasors (Equation (7); the formula is only given for the voltage phasor) [20], [21].

$$U_r = \sum_{k=1}^N u_k \cdot \cos(k \cdot 2\pi \cdot f_0 \cdot \tau) \\ U_i = \sum_{k=1}^N u_k \cdot \sin(k \cdot 2\pi \cdot f_0 \cdot \tau) \quad (7)$$

where f_0 is the rated frequency and N is the number of samples (results of ADC) in one period of the rated power system frequency. The sampling interval τ is selected by the terminal designer in the range of milliseconds.

It's worth noting that (7) can be implemented by only using the basic arithmetic operations, since sines and cosines can be calculated in advance and entered in the form of coefficients.

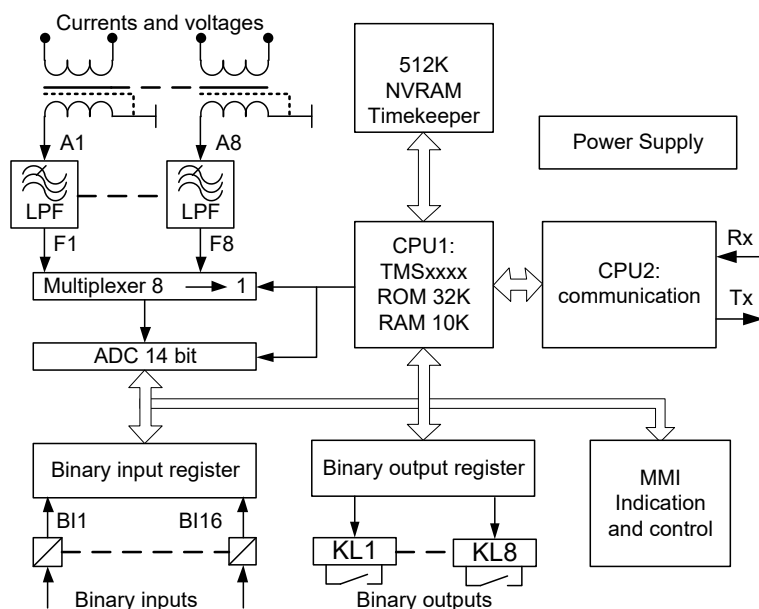
The implementation of the considered method of emergency automation is possible based on the use of the Phasor Measurement Unit (PMU) available on the electrical equipment market. However, to reduce the requirements for communication channels and block terminals in non-symmetric modes and/or in case of network failure, the decision to develop a dedicated terminal has been taken. The complexity and costs of the dedicated terminal are expected to be similar to those of widely used protection terminals.

3.2 Hardware SCCT

The proposed hardware structure of the SC control terminal (SCCT) is a typical power system IED (intelligent electronic device) structure with an analogue-to-digital conversion module, a binary input and output module, integrated MMI (man-machine interface), a dedicated digital signal processor and a communication processor (see **Figure 40**).

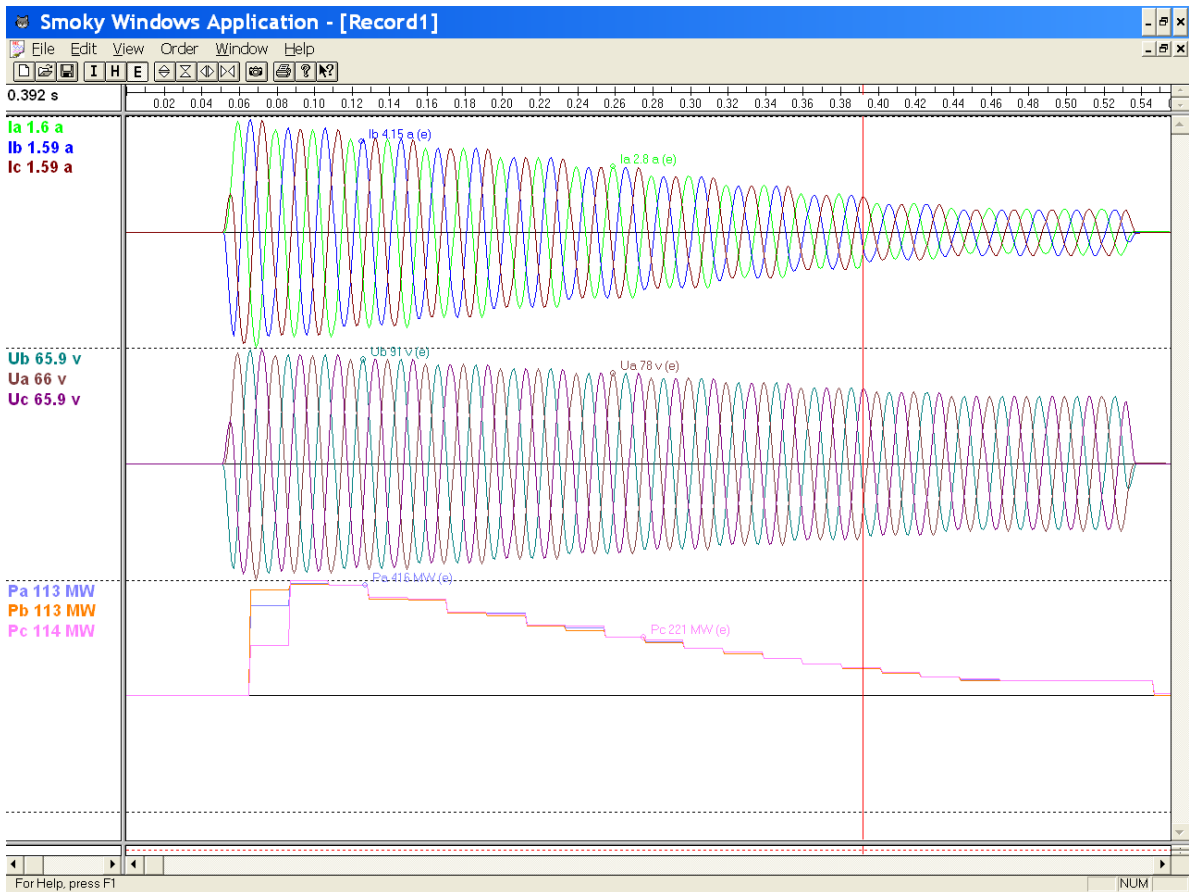
The SCCT is equipped with non-volatile memory (NVRAM) with a real-time clock intended for device settings and logging information storage. The SCCT is equipped with a high-speed disturbance recording function, which provides records of the instantaneous waveform of the controlled signals and the value of estimated active power.

Figure 40. SCCT hardware structure (CPU – Core Processing Unit, LPF – low-pass filter, RAM – data memory, NVRAM – non-volatile RAM, ROM – program memory, MMI - man-machine interface).



Source: RTU, 2023.

Figure 41. Voltages and currents step-up with consequent signal ramp.



Source: RTU, 2023.

The controlled signals (currents and voltages of the SC) are low-pass filtered to avoid the aliasing effect, multiplexed and sampled by an A/D converter. The signal sampling rate can be chosen between 4 and 64 samples per power system cycle. The signals' samples are processed by a Digital Signal Processor (DSP CPU1) implementing the DFT algorithm. More advanced algorithms could be used in determining the signals' phase angles, real and reactive power, waveform distortions and other complex quantities.

A prototype of the RLS automation terminal has been developed and is being tested in the laboratory. **Figure 41** illustrates an example of SCCT record, which was made and stored in digital form after applying currents and voltages to emulate the SC active power injection event. The three-phase currents and voltages are in secondary amperes and volts while the calculated and recorded active power is in primary units (MW).

4 Feasibility study: economic benefit

Based on the usage of PS dynamic models and the NORDPOOL electricity market model, a rough preliminary assessment of the economic benefit from applying the proposed solution can be carried out. The assessment has been done by using the Baltic PS case and model (see § 0). The following sub-tasks have been solved:

1. To evaluate the increase in the transfer capacity of the transmission network interconnections;
2. To calculate the economic benefit in monetary terms.

In general, cross-border transfer capacity is calculated by considering the peculiarities and technical limitations of the network, such as thermal limitations and stability issues. Implementation of advanced automation makes it possible to increase the stability limits and diminish the negative consequences of the emergency process. The proposed principle of RLS allows triggering load shedding much faster (without measurement of frequency or/and RoCoF), based on the active power injection of a synchronous condenser. As to **Figure 38**, the frequency responses clearly show that the same amount of disconnected load radically impacts the frequency nadir in case of faster triggering. In the case of the Baltic power system, the performed simulations and calculations have shown [9], [18] that the cross-border transfer capacity after

disconnection from the UPS can be maintained at the present level if RLS triggering occurs within 0.1–0.5 s from the moment of the contingency.

To evaluate the economic benefit in monetary terms, we predict electricity prices in the energy systems of the Baltic region (Latvia, Lithuania, Estonia, Sweden, Finland, Poland), set the structure of generators and consumers and, taking into account the rules of the NORDPOOL electricity market, perform a simulation of the operation of connected energy systems (more details on the methodology and electricity market model are presented in [22], [23]). The Baltic PS is modelled as a low-inertia system after disconnection from the UPS (with a high penetration of RES). The scenario considers PS operation with different transfer capacities of the high-voltage DC interconnection between Sweden and Lithuania (the NordBalt line).

Table 1 presents estimates of the impact of reducing the capacity of the NordBalt line on the average annual electricity prices in the Baltic price zone and also focuses on the operation costs of a reserve power plant. The presented results are preliminary and indicative in nature; however, the possibility of obtaining a significant economic effect (and thus increasing total welfare) is demonstrated. In comparison, the difference between the cases with and without availability of full transfer capacity of the NordBalt line leads to additional annual costs of 484,642,686 EUR or approx. 1,328,000 EUR per day.

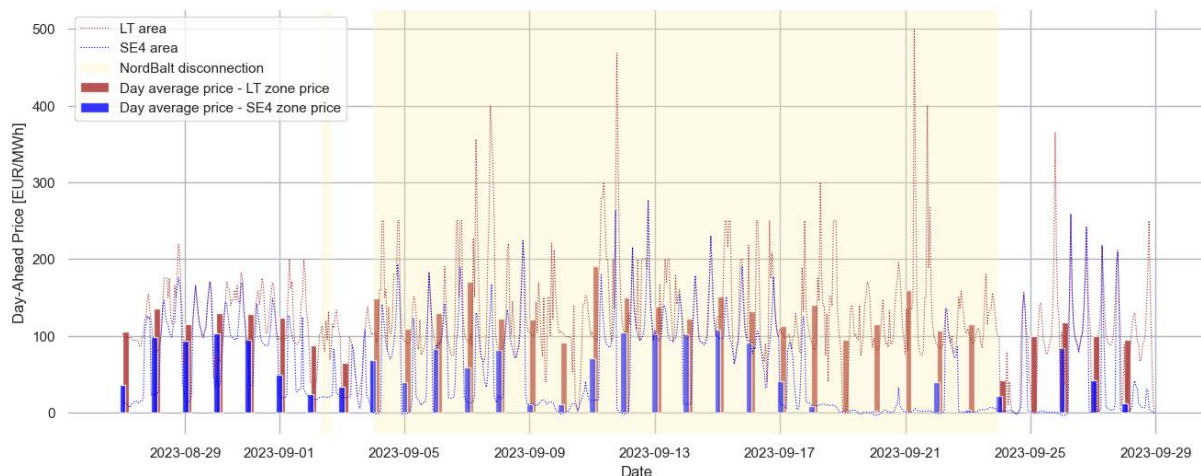
Table 1. The impact of reducing the capacity of the NordBalt line on the average annual electricity prices in the Baltic price zone and the operation costs of a reserve power plant.

| Scenario | Average price, EUR/MWh | Operation costs of reserve PP, EUR | Electricity produced by reserve PP, GWh |
|---------------------------------|------------------------|------------------------------------|---|
| Capacity of SE4-LT line: 0 MW | 139.75 | 1 055 770 167 | 3 199 |
| Capacity of SE4-LT line: 300 MW | 129.81 | 824 820 924 | 2 499 |
| Capacity of SE4-LT line: 500 MW | 122.59 | 690 438 594 | 2 092 |
| Capacity of SE4-LT line: 700 MW | 116.22 | 571 127 481 | 1 731 |

Source: RTU, 2023.

This conclusion is confirmed by (experimental) data obtained as a result of the forced disconnection of the NordBalt line (from 2023-09-04 till 2023-09-23). Prior to and after the disconnection, the power exchange over the NordBalt line (to Lithuania) was in full capacity. The NORDPOOL day-ahead prices and the day average prices in the Lithuania and Sweden price zones are shown in **Figure 42**. Thus, for example, on 9/23/2023 the average price was 2.91 EUR per MW·h in Sweden and 114.79 EUR per MW·h in the Baltic States; the energy demand in the Baltics was 29096 MW·h. If the NordBalt line had been in operation, an energy amount of 16800 (MW·h) could be (daily) transferred to Lithuania. Considering the difference between the zones' average prices ($114.79 - 2.91 = 111.88$ (EUR/MW·h)), the economic effect could be approx. 1,880,000 EUR. For the whole period (from 2023-09-04 till 2023-09-23), the economic effect would be EUR 26,794,439, or EUR 1,339,700 per day.

Figure 42. Day-Ahead Price.



Source: RTU, 2023.

Both examples demonstrate the possibility of improving the resilience of the Baltic PS and obtaining a positive economic effect due to optimal use of the interconnection capacity and economically efficient generation, thus increasing the total welfare.

5 Conclusions

Monitoring the active power of synchronous capacitors can be used to create high-speed emergency automation for power systems. Such automation will increase the allowed capacity of the power lines and will provide the opportunity to prioritise the use of the most efficient generators. The economic benefit can reach the order of hundreds of millions of euros per year. To implement automation, it is necessary to create a specialised terminal, the microprocessor implementation of which is close in complexity and cost to commonly used relay protection devices of high-voltage power lines.

Acknowledgements

This research is supported by the Latvian Council of Science, project SignAture (project No. Izp-2021/1-0227).

References

- [1] S. C. Johnson, J. D. Rhodes, and M. E. Webber, "Understanding the impact of non-synchronous wind and solar generation on grid stability and identifying mitigation pathways," *Appl. Energy*, vol. 262, no. December 2019, p. 114492, 2020.
- [2] K. Prabhakar, S. K. Jain, and P. K. Padhy, "Inertia estimation in modern power system: A comprehensive review," *Electr. Power Syst. Res.*, vol. 211, no. May, pp. 108–222, 2022.
- [3] E. Ørum *et al.*, "ENTSO Report - Future System Inertia," 2015.
- [4] ERCOT, "Inertia: Basic Concepts and Impacts on the ERCOT Grid," 2018.
- [5] D. Zalostiba, "Power system blackout prevention by dangerous overload elimination and fast self-restoration," in *4th IEEE/PES Innovative Smart Grid Technologies Europe, ISGT Europe*, 2013.
- [6] A. Sauhats, V. Chuvychin, G. Bockarjova, D. Zalostiba, D. Antonovs, and R. Petrichenko, *Detection and management of large scale disturbances in power system*, vol. 8985. 2016.
- [7] D. Guzs, A. Utans, A. Sauhats, G. Junghans, and J. Silinevics, "Resilience of the Baltic power system when operating in island mode," in *2020 IEEE 61st Annual International Scientific Conference on Power and Electrical Engineering of Riga Technical University, RTUCON 2020 - Proceedings*, 2020.
- [8] J. Machowski, J. W. Bialek, and J. R. Bumby, *Power system dynamics. Stability and Control*, 3rd ed. John Wiley & Sons, Ltd, 2012.
- [9] A. Sauhats, A. Utans, J. Silinevics, G. Junghans, and D. Guzs, "Enhancing power system frequency with a novel load shedding method including monitoring of synchronous condensers' power injections," *Energies*, vol. 14, no. 5, Mar. 2021.
- [10] B. Delfino, S. Massucco, A. Morini, and S. F. Silvestro, "Implementation and Comparison of Different

under Frequency Load-Shedding Schemes,” in *2001 Power Engineering Society Summer Meeting. Conference Proceedings (Cat. No.01CH37262)*, 2001, pp. 307–312.

- [11] K. Ben Kilani, M. Elleuch, and A. Haj Hamida, “Dynamic under Frequency Load Shedding in Power Systems,” in *14th International Multi-Conference on Systems, Signals & Devices (SSD)*, 2017, pp. 377–382.
- [12] U. Rudež and R. Mihalič, “Comparison of Adaptive UFLS Schemes in Modern Power Systems,” in *2011 IEEE Electrical Power and Energy Conference : IEEE EPEC 2011.*, 2011, pp. 233–238.
- [13] U. Rudež and R. Mihalič, “Trends in WAMS-based Under-Frequency Load Shedding Protection,” in *IEEE EUROCON 2017: 17th International Conference on Smart Technologies : conference proceedings : 6-8 July 2017, Ohrid, Macedonia*, 2017, pp. 782–787.
- [14] F. Zare, A. Ranjbar, and F. Faghihi, “Intelligent topology-oriented load shedding scheme in power systems,” in *ICEE 2019 : 27th Iranian Conference on Electrical Engineering*, 2019, pp. 652–656.
- [15] Z. Jianjun, Z. Dong, G. Yang, and Y. Zhihong, “Load shedding control strategy for power system based on the system frequency and voltage stability(Apr 2018),” in *China International Conference on Electricity Distribution, CICED*, 2018, no. 201804230000057, pp. 1352–1356.
- [16] A. Sauhats, A. Utans, D. Guzs, and L. Zemite, “Improving power system frequency response with a novel load shedding method,” in *60th ESReDA Seminar: Advances in Modelling to Improve Network Resilience*, 2022, pp. 1–6.
- [17] D. Guzs, A. Utans, and A. Sauhats, “Evaluation of the resilience of the Baltic power system when operating in island mode,” in *Proceedings of the 31st European Safety and Reliability Conference, ESREL 2021*, 2021, pp. 1876–1883.
- [18] D. Guzs, “COST EFFECTIVE INNOVATIVE SOLUTION FOR TRANSMISSION CAPACITY MANAGEMENT IN LOW-INERTIA WEAKLY INTERCONNECTED Doctoral Thesis Cost effective , innovative solution for transmission capacity management in low-inertia weakly interconnected power systems,” 2023.
- [19] Z. Bie, Y. Lin, G. Li, and F. Li, “Battling the Extreme: A Study on the Power System Resilience,” *Proc. IEEE*, vol. 105, no. 7, pp. 1253–1266, 2017.
- [20] A. G. Phadke *et al.*, “Synchronized sampling and phasor measurements for relaying and control,” *IEEE Trans. Power Deliv.*, vol. 9, no. 1, pp. 442–452, 1994.
- [21] M. Noroozian and G. Andersson, “Power flow control by use of controllable series components,” *IEEE Trans. Power Deliv.*, vol. 8, no. 3, pp. 1420–1429, 1993.
- [22] K. Baltputnis and Z. Broka, “Future scenarios of the Baltic power system with large penetration of renewables,” *Int. Conf. Eur. Energy Mark. EEM*, vol. 2023-June, pp. 1–7, 2023.
- [23] Z. Broka and K. Baltputnis, “Open-source electricity market modelling for the Baltic states: Review and requirements,” *Int. Conf. Eur. Energy Mark. EEM*, vol. 2023-June, pp. 1–6, 2023.

2.16 An innovative methodology for risk-based resilience assessment to prioritize grid interventions against natural threats in the Italian power system

Emanuele Ciapessoni, Diego Cirio and Andrea Pitto, Ricerca sul sistema Energetico – RSE S.p.A., Italy, {emanuele.ciapessoni; diego.cirio; andrea.pitto}@rse-web.it

Enrico Maria Carlini, Francesco Marzullo, Silverio Casulli, Federico Falorni, Francesca Scavo, Giuseppe Berrettoni, Greta Magnolia, Terna, Italy {enricomaria.carlini; francesco.marzullo; silverio.casulli; federico.falorni; francesca.scavo, giuseppe.berrettoni; greta.magnolia}@terna.it

Abstract

In recent years, the rise in both the frequency and intensity of extreme natural events demands heightened attention from grid operators. Accordingly, these events are increasingly becoming a key consideration in transmission network planning and management. In this context a risk-based methodology for power system resilience assessment in the grid planning context has been elaborated in a joint effort between the Italian TSO, Terna, and Ricerca sul Sistema Energetico RSE S.p.A.

The methodology is aimed to capture the benefit of grid hardening interventions in terms of increase in the resilience of the system exposed to natural threats, with the final objective to support Cost-Benefit Analyses (CBA) in resilience-enhancement plans, as required by the Italian regulatory authority to all electric utilities.

An innovative aspect of the methodology is to include climate change modelling in grid planning, together with the typical planning driver, i.e. security of supply, market efficiency and renewable integration. The probability of natural threats (e.g. wet snow, wind) of increasing intensity is evaluated taking into account climatological models. The methodology is wide ranging and it can be applied to any natural threat; up to now, it has been applied to wet snow and strong wind, which represent the two major causes of load disruptions in the Italian system, but the modelling framework is being expanded to include also hydrogeological threats.

The methodology adopts analytical physics-inspired models, based on international standards for component design, and on the National Normative Addendum, to simulate the vulnerability of components to the threats. This is another innovative aspect: unlike statistical models, analytical models can quantify the benefits brought by deploying countermeasures to the asset (e.g., antitorsional devices on overhead lines against wet snow). Specifically, the paper proposes an advanced model for the vulnerability of overhead lines to indirect effects of wet snow and strong wind, i.e. the potential actions these threats have on the vegetation which can interfere with the lines. The model integrates the information coming from Lidar systems of the operator, concerning the potential interferences of the vegetation with the right of way of the lines.

Combining the probabilistic models of extreme events with the vulnerability models of the components leads to the failure return periods (RP) of components exposed to the hazards, also accounting for the real extension of the threats via meteorological reanalysis. Starting from the failure RPs of grid assets and from the information about threat extension based on past natural events, the methodology selects a representative set of multiple contingencies.

The new resilience indicator is introduced in compliance with the guidelines of national standardisation and regulation bodies. It is used to define criteria and priorities for the selection of interventions on the national transmission system, quantifying the risk of power disruption for HV/MV substations. The risk metric requires the computation of the RP of substation outage, in turn depending on the failure RPs of the lines connected to the substation and on the meshing level of grid. Potential cascading trippings triggered by contingencies can contribute to the lack of supply to HV/MV substations: thus, they are properly simulated using a cascading outage simulator. The two main outputs of the methodology are the outage RP for each substation connected to the transmission grid and the Expected Energy Not Served (EENS) due to contingencies. The resilience benefit is given by the difference of EENS indicators before and after the deployment of grid interventions.

The application to a case study on one side demonstrates the effectiveness of the methodology in prioritizing the grid interventions for resilience enhancement plans based on a CBA informed by the proposed risk indicator; on the other side it shows the good alignment of the failure RPs of the overhead lines, computed

with the advanced vulnerability model, with actual faults recorded in the area of the Italian system under study.

1 Introduction

The climate change underway means that extreme atmospheric phenomena and the consequent risk of damage to the infrastructure dedicated to the transport of electricity are increasingly frequent. For this reason, the challenges facing TSOs (Transmission System Operators) related to climate change are increasingly urgent and entail two objectives: 1) to assess the risk of multiple employee disruptions and 2) to develop preventive or corrective countermeasures aimed at absorbing the effects of destructive events and rapid recovery, i.e. an increase in the resilience of the system [1]. The adaptation of the decision-making process at every level will be fundamental, in terms of resilience both in the operational and planning phases, reviewing analyses, methodologies, thus assessing the risk and comparing it with an acceptable threshold [2].

In the planning process, the transition from an "N-1" security criterion towards an "N-k" criterion, thus including the analysis of multiple contingencies and the evaluation of potential cascading effects, represents an innovative approach to adequately evaluate the level of resilience of the electricity system in the event of extreme weather events. In order to plan future interventions to increase grid resilience, a risk-based methodology was developed through the collaboration between Terna and RSE. The methodology is aimed at using prospective climate scenarios, to be scalable and replicable and to be used to analyse multiple weather threats. At present the methodology has been applied for the phenomena of strong wind and ice-snow threats which represent the two major causes of load disruptions in the Italian system.

Moreover, the methodology also makes it possible to assess, on a quantitative and objective basis, the investments that can lead to an increase in the resilience of the electricity grid, quantifying the technical benefits such as the reduction of: 1) probability of power asset outage and 2) risk indicators such as Expected Energy Not Supplied (EENS) [3].

This document presents the methodology mentioned above and its application to identify critical areas and the benefits of possible interventions. The paper is organized as follows: Section 2 recalls the methodology; Section 3 describes the prospective climate scenarios; Sections 4 and 5 respectively describe the vulnerability assessment and the efficient technique for the selection of N-k contingencies. Section 6 discusses a case study, and Section 7 presents the conclusions and future developments to include also hydrogeological threats.

2 The proposed methodology

The methodology for resilience assessment of the electrical transmission grid in Italy is developed by TERNA and RSE [3] and it can be applied to both wind and ice/snow threats, on the entire Italian electricity transmission grid. It is composed by 8 main steps:

1. Calculate the probability of occurrence of meteorological phenomena in the future, as a function of predefined intensity thresholds, using a climatological model.
2. Quantify the vulnerability of the grid components as a function of the intensity of the meteorological event considered, through the development of vulnerability curves applied to a georeferenced grid model.
3. Combine the probabilistic model of the weather event (derived in step 1) with the vulnerability curve (from step 2) of the grid components, specifically lines, which leads to the Return Period (RP) of the outages of the components in "pre-intervention phase" (RP_{PRE}) i.e. in the initial grid conditions.
4. Determine the Return Period ($RP_{PS,PRE}$) of the outages of the Primary Substations (PS) and the corresponding value of expected energy not served ($EENS_{PS,PRE}$) by applying a cascading outage simulator.
5. Identify possible interventions aimed at increasing resilience, based on the meteorological phenomena under analysis, the characteristics of the reference area, and the relevant lines, with reference to the critical primary substations in terms of outage RP and of load disruptions.
6. Evaluate the impact of the interventions identified in the previous step, measured in terms of increase in the RP of the lines (RP_{POST}) with respect to the previous value (RP_{PRE}).

7. Determine the Return Period ($RP_{PS,POST}$) of the Primary Substations (PS) and the corresponding value of expected energy not served ($EENS_{PS,POST}$) assuming that the interventions have been implemented, by applying a cascading outage simulator.
8. Calculate the resilience benefit associated with each identified intervention and perform the relevant economic evaluation. Currently the Cost-Benefit Analysis of the TSO is based on the economic valorisation of EENS reduction, which is used to quantify the benefit of a specific intervention on the grid.

Figure 43 shows a flow chart that summarizes the main phases of the methodology.

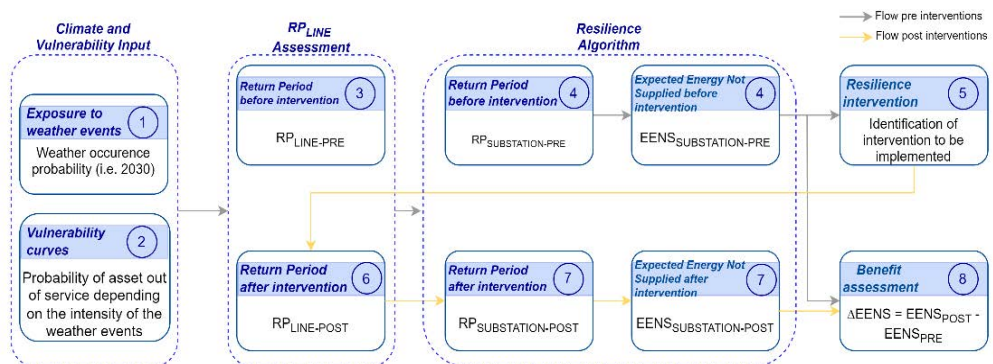


Figure 43– Architecture of the resilience assessment methodology

The presented methodology has been approved [4] by ARERA, the Italian Regulatory Authority for Energy, Networks and Environment, and is now part of Terna Grid code [5].

3 Climate maps

In the first stage of the methodology, climate models [6]-[8] are used to identify the exposure of the National Transmission Grid (NTG) to severe weather events expected in the coming decades.

Climate scenarios allow estimating future climate hazard at different levels of detail, calculating the probability that a phenomenon of a given intensity will occur in each area, over a certain period of time.

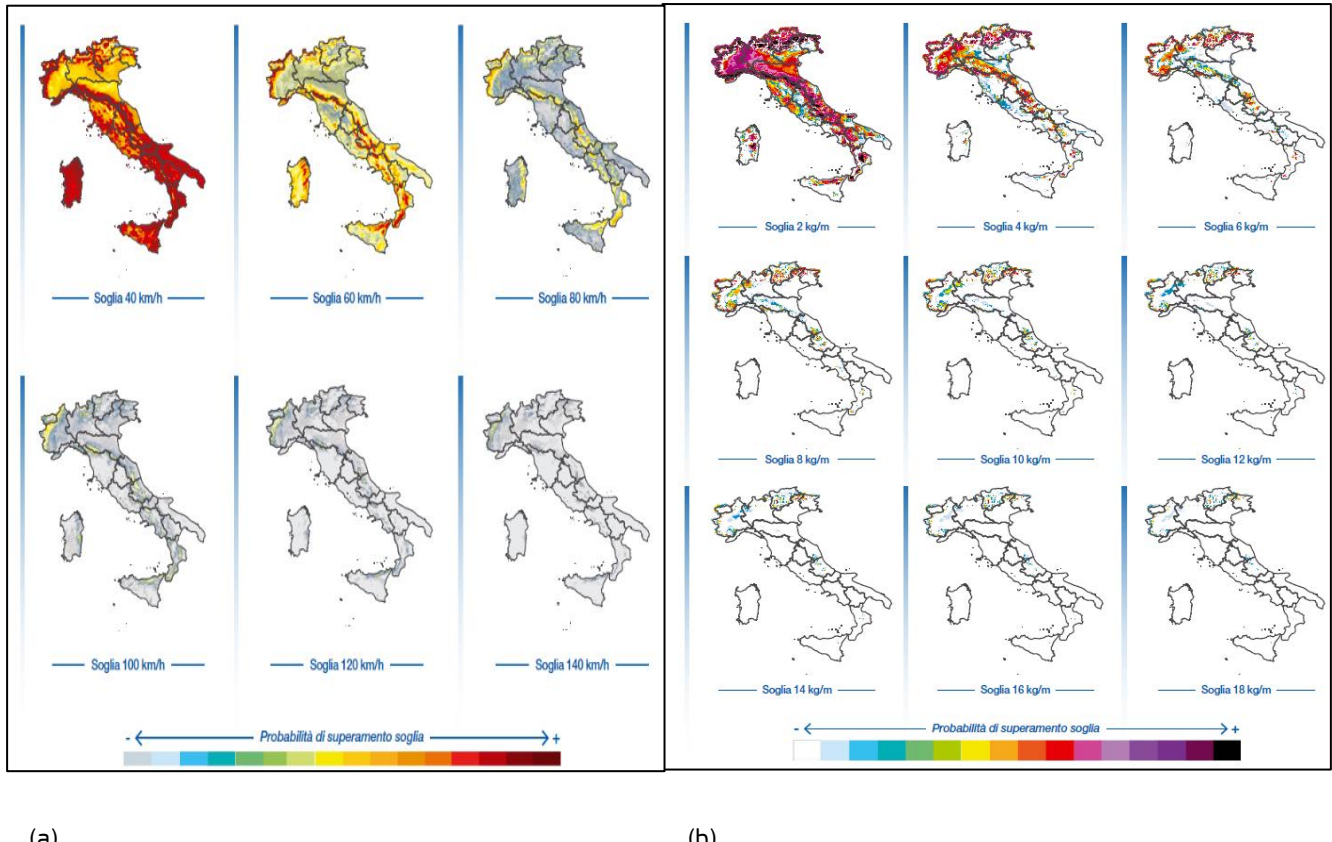
The climate projections are reproduced over the entire national territory with $4\text{km} \times 4\text{km}$ resolution which not only provide an overview of the expected evolution of the weather hazards, but also allow quantifying the risk to the NTG. This risk is evaluated by identifying its infrastructures with the highest probability of exposure to future severe weather events. Climate projections are determined for different time horizons, up to 2050 at 5-year intervals for wind and 10-year intervals for snow, as the annual probability of exceeding specific intensity thresholds of the considered weather threat.

The development of climate models involves four main steps:

1. Declining global historical climate data on a local scale: starting from model reconstructions of past climate, it is possible to “downscale” to the national level, obtaining local climate features with higher resolution. In the case of wind, 40 realizations of the CESM-LENS climate model [7] were used; in the case of the ice-snow phenomenon, Euro-CORDEX climate models [8] were used with the subsequent application of the Makkonen model for the estimation of the wet-snow sleeve phenomenon.
2. Bias correction: downscaled historical data require “bias-correction” where necessary to avoid systematic errors of underestimation or systematic overestimation of exposure thresholds. This correction is performed through data recorded at local weather stations or using meteorological reanalysis datasets. The correction of systematic model errors (e.g., over/underestimation with respect to observed local conditions) was made based on the provider's data availability: as far as

wind is concerned, the correction was made through the ERA-5 database [6], while in case of the ice-snow threat the MERIDA Optimal Interpolation [9] reanalysis dataset was used.

3. Processing of high-resolution climate projections: the results of climate models thus corrected are used to process future projections, rescaled to $4\text{km} \times 4\text{km}$ resolution for each region of interest and for selected future periods.
4. Calculation of the characteristic parameters of the expected weather event analysed: from the results of the downscaled and bias-corrected climate models, the probabilities of exceeding the threshold values of the stress variable at given future horizons are obtained (Figure 44).



(a)

(b)

Figure 44- a) Forecast maps to 2030, with $4\text{x}4\text{km}$ resolution, for wind, considering different thresholds of probability of exceeding the expected wind speed from 40 km/h to 140 km/h ; b) Forecast maps to 2030, with $4\text{x}4\text{km}$ resolution, for snow, considering different thresholds of probability of exceeding the expected sleeve load from 1kg/m to 18 kg/m .

The verification of such climatological models poses significant challenges to the researchers in the field: the verification has consisted in comparing the values of some quantities recorded in recent events (e.g. sleeve thickness) with the values of the same quantities evaluated in the scenarios developed by climatological models.

To estimate the exposure of the NTG with respect to the considered event, the results of climate projections are associated with the NTG, using the geo-referenced National Transmission Grid asset map, so as to deduce, for each line and each span under analysis, the probability values of exceeding the intensity thresholds for the analysed threat in the identified horizon year.

The adoption of climatological models allows to assess the effect of global warming on the trend of the main characteristics (severity and probability of occurrence) of weather events over the decades, also accounting for different emission scenario hypotheses.

Starting from multiple thresholds of weather threat (snow or wind) intensity, the CCDF (Complementary Cumulative Distribution Function) and CDF (Cumulative Distribution Function) are calculated: these

distributions combined with asset vulnerability models allow to calculate the failure return periods for Over Head Lines (OHL), as described in the sequel.

4 Vulnerability assessment

This section discusses the model proposed to quantify the vulnerability of OHLs to wet snow and wind threats. These models are characterised using real orographic and technical parameters of the NTG assets provided by the Italian TSO.

4.1 Vulnerability models of OHL spans against direct effects of wind and snow

The proposed approach, starting from CEI EN 50341-1 standard [10], expresses the vulnerability models as probabilities of component damage, in turn depending on two weather variables namely:

- wind speed w (in km/h), evaluated as the average value over 10 minutes at 10 m height from the ground;
- wet snow linear mass q (in kg/m) on reference conductors (22.8 mm and 31.5 mm diameters cover the large majority of existing conductors in the Italian transmission grid).

In particular, the model expresses the vulnerability of each span subcomponent as a function of the actions due to strong wind and snow loads. In fact, each weather variable (w and q) is converted into specific actions that the wind and snow apply to the different subcomponents of the OHL.

Specific mechanical actions are associated with the abovementioned subcomponents:

- Tension T_{pc} (in kN) on individual phase conductor
- Tension T_{sw} (in kN) on individual shield wire
- Resulting forces R_t (in kN) acting on the tower, derived by combining the vertical loads (due to the weight of the conductors and of potential wet snow/ice sleeves on contiguous spans, as well as to the altimetric coefficient K for the specific tower) and the horizontal ones (due to wind pressure on conductors, tower structure, shield wires, insulators/support, and to line deviation angle d)
- Stress variable for the tower foundations, consisting either in the overturning moment of the tower M_t (in $\text{kN} \times \text{m}$) in case of unique block foundations, or in the compression action on the ground (in N/m^2) for foundations with separate footings.

Vulnerability PV_i of i -th subcomponent to direct action is given in (1).

$$PV_i(w, q) = PV_i(A_i, Q_i) \quad (1)$$

where

- $A_i = G_i(\mathbf{r})$ is the action of wind and snow on subcomponent i , expressed in terms of the two weather variables in vector $\mathbf{r} = (w, q)$
- Q_i is (are) the parameter(s) which characterize(s) the vulnerability of subcomponent i to combined wind and snow actions.

Parameters Q_i are given by the expected values of:

- Rated Tensile Strength (RTS) in kN for phase conductors
- Rated Tensile Strength (RTS) in kN for shield wires.
- Breaking strength of supports in kN.
- Maximum overturning moment (in $\text{kN} \times \text{m}$) or maximum compression of the ground (in daN/cm^2), according to the type of foundations and to the typical design criteria.

Functions PV_i of the subcomponents of each individual line span represent the fragility curves of the subcomponents to the abovementioned actions. These functions are given by lognormal distributions of the action variables. To identify the parameters (mainly the maximum breaking strength) characterizing the vulnerability curves of the support, the following sources are exploited:

- the design criteria reported in CEI (Italian Electrotechnical Committee) 11.4 standard [11], and
- the mechanical utilization curves of the towers: these are piecewise linear curves in (C_m, d) and (C_m, K) planes, where: C_m is the average value of the lengths of the two adjacent spans, K is the altimetric

coefficient, and d is the deviation angle of the line in correspondence of the specific mean span length Cm.

Once the vulnerability model of each subcomponent i is available, then the vulnerability of each line span can be expressed as in (2) because the failure of any subcomponent of the span is assumed to cause the outage of the entire span.

$$PV_{span}(w,q) = 1 - \prod_i [1 - PV_i(w,q)] \quad (2)$$

The detailed equations of the forces acting on each sub-components (conductors, supports, shield wires, foundations, etc.) are reported in [12].

4.2 Vulnerability models of OHL spans against indirect effects of wind and snow

This subsection describes the model developed to quantify the vulnerability of OHL spans against indirect effects of wind and snow (i.e. the potential interference due to vegetation along the OHL route).

4.2.1 Base vulnerability modelling

The contact with trees is a frequent cause of failures in MV and HV grids, due to strong wind or snow. An analytical probabilistic model of the interactions between the line and the interfering vegetation in presence of wind and snow has been proposed by the authors in [13] and it accounts for:

- vertical contact due to trees in the Right-Of-Way (ROW) (an unlikely event because the Italian TSO fulfils the prescriptions of CEI 11-4 Std.),
- lateral contact due to fall of trees from outside the ROW,
- lateral contact between the line catenary (inclined with respect to the vertical axis) and the trees at the ROW boundaries (unlikely event, due to the strict prescriptions of the Italian standard CEI 11-4).

The main factors considered are: tree linear coverage density (no. of trees per km), clearance distance (horizontal distance between tree line and the closest phase conductor), tree species (trunk height, coniferous or broad leaf, maximum breaking strength, root-soil system features), orography (terrain slope), weather conditions (wind, snow, ice etc.).

The tree characteristics (mechanical properties e.g. the Young's modulus, the modulus of rupture, etc.) and the weather conditions affecting line sag (solar irradiation, wind speed) are treated as stochastic variables.

Figure 45 indicates the scheme of wind and snow induced forces in the interaction tree-OHL. The main cause of tree fall is the strong wind, which applies a lateral force that can cause tree stem bending and rotation of the root system: this can increase the component of the overturning moment due to the vertical forces to which the snow load contributes. In the following, the analytical model described in [13] is extended to consider the effects of wet snow on the interaction between vegetation and lines.

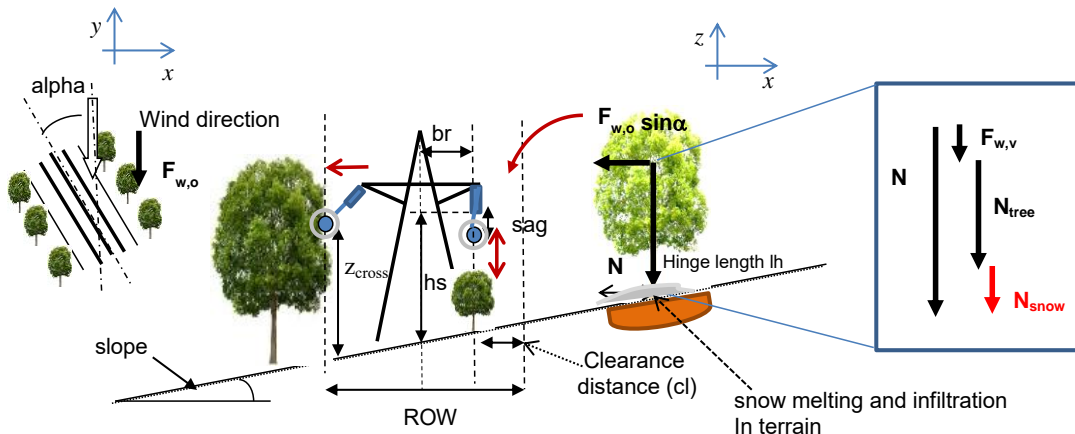


Figure 45. Scheme of wind and snow induced forces on OHL and interfering vegetation

The proposed vulnerability model is physics inspired and all the forces represented in Figure 2 (weights, wind and snow induced forces) are computed taking into account the abovementioned factors. More details on the model are reported in [12].

4.2.2 Advanced modelling integrating vegetation mapping from Lidar surveys

The base vulnerability model illustrated in the previous subsection employs the CORINE Land Cover database [14] to map the vegetation across Italy. Nonetheless, this database only provides average values for tree characteristics and does not offer precise insights into specific tree interference conditions along the OHL right-of-way.

To address this limitation, an advanced vulnerability model has been defined to integrate the vegetation mapping based on LiDAR systems [15] which are more accurate and updated compared to the CORINE approach. Terna employs its fleet of helicopters to conduct terrain mapping around the lines using LiDAR, a remote sensing system that allows to measure the distance of an object or surface from power lines using a laser pulse.

The primary goal of inspections is to accurately measure the actual distance between power lines and surrounding vegetation. This allows mapping potential tree interferences and planning preventive cutting actions. The LiDAR mapping covers a 50-meter width on each side of the line, with spatial resolution up to 1 m × 1 m. This mapping provides an accurate reconstruction of orography, of the presence and height of vegetation along the lines (see Figure 46). This information is updated annually through new surveys.

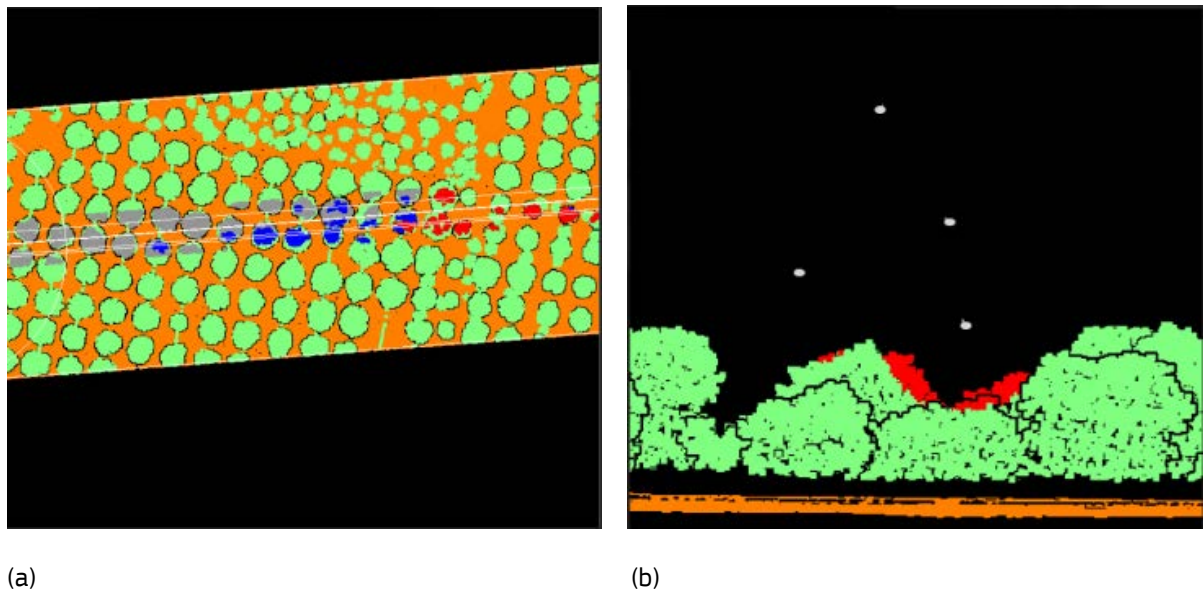


Figure 46 - a) Top view of the LiDAR survey reconstruction. In red the parts that are critical. b) View of the conductor section. In red the vegetation to be cut.

Within the data provided by LiDAR systems, the advanced model for OHL vulnerability to tree interference requires information about potential interactions between a cylindroid centred on the catenary of the wires (including conductors and shield wires) and potentially interference vegetation. These interactions are assessed both within and beyond the right-of-way, within each 1 m × 1 m cell along the path of each line span. Additional details are outlined in [16].

4.3 Evaluating the RP of the overall OHL

The evaluation of the return periods of substation outages starts from the assessment of the failure return periods of the lines which directly or indirectly connect the substation to the rest of the HV grid. The proposed resilience assessment methodology evaluates the return periods of the overhead line outages starting from the map of extreme values of the stress variables (snow loads and wind speeds) over different time horizons provided by climatological models [6], [17] as well as from the vulnerability models of the individual OHL spans.

More specifically, the combination of the vulnerability curves of each OHL span against both direct and indirect effects of wind and snow with the known return periods for specific values of the threat actions (e.g. wind and snow loads) allows to compute the return period of the outage of each OHL span due to direct and indirect effects of snow and wind. The flexibility of the modelling approach allows to separately consider the effects of wind and wet snow, thus computing two separate RPs for each OHL span.

After that, given the indications of Std. IEC 60826 [18] about the extension of the weather events, the line is divided into groups of N spans which are assumed to be simultaneously struck by the threat. The RP of each group is the minimum RP of the spans composing the group, while the RP of the line is obtained by computing the probability of the logical "OR" of the failure probabilities of each group.

4.4 Validating the Models

The validation process aims to verify whether the outputs of the entire methodology align with statistics related to OHL outages caused by extreme weather events, as derived from the actual operation of the power grid. Specifically, the areas subject to validation are the OHL vulnerability models and the climatological models, especially concerning one of the major threats affecting the Italian Extra High Voltage (EHV) grid, which is wet snow.

The validation process involves a comprehensive analysis of historical failure events that have occurred over the most recent 16-year observation period. From the complete failure database, the validation process selects only failures linked to direct or indirect impacts of a threat (such as wet snow) on the OHL components. Apart from ensuring the accuracy, completeness, and comprehensiveness of the available historical failure information related to OHLs, it is crucial to consider the history of "infrastructure upgrades" performed on these lines in recent years. Such upgrades lead to changes in vulnerability model parameters. Therefore, older failures might be due to higher vulnerability compared to what the methodology framework reconstructs based on the most current OHL parameters available in Terna databases. Hence, in the validation process, it is vital to filter out the lines whose behaviour with respect to the studied meteorological threat, evaluated using the methodology vs. reconstructed through historical failure records presents a discrepancy resulting from infrastructure changes implemented during the observation period.

For validation purposes, the "benchmark" comprises OHL failures caused by wet snow and documented during the observation period. The second comparison term consists of calculated outage return periods, which result from combining the OHL vulnerability model with a source of climatological or meteorological data, depending on the context of application. As the benchmark pertains to past failure events, the mentioned data source is based on the best available meteorological data, specifically the outcomes of the RSE meteorological reanalysis MERIDA-OI [9] with optimal interpolation of observed values.

Consequently, the validation process of the vulnerability model is divided into two steps:

1. Validation of the meteorological dataset against real wet snow events.
2. Validation of the calculated OHL outage return periods against empirical failure data.

The initial step is applied to recent and significant snowfall events that caused notable electrical disruptions. It involves comparing the wet snow loads recorded during these events with those reconstructed using the MERIDA OI dataset applied to the Makkonen accretion model.

The subsequent validation step involves comparing the statistics related to outage return periods calculated by the methodology with the corresponding statistics related to actual outages recorded in the grid.

Given the limited number of recorded OHL failure events within the available observation interval (approximately 16 years), the high number and the significant differences characterising the lines under analysis (the whole National Transmission Grid), the comparison between calculated and empirical outage return periods is conducted on clusters of lines grouped based on specific physical quantities. Creating line clusters allows identifying a sufficient number of failure events in each cluster, ensuring that the uncertainty regarding the empirical mean number of failures for the lines within each cluster remains adequately constrained.

The selection of physical dimensions is based on engineering judgment, involving the identification of physical parameters believed to significantly affect the outage return periods of OHLs for each specific threat. Particularly, concerning the wet snow threat, the physical quantities used for clustering are:

- Length of the line, to point out that longer lines have higher exposure to wet snow;
- Maximum altitude of OHL spans, to take into account that higher altitude leads to greater exposure to wet snow events;
- Voltage level, to consider that design characteristics affected by voltage levels strongly impact OHL response to wet snow loads.

The results obtained show that the clustering carried out allowed the lines to be grouped according to significant dimensions for which a very good matching is achieved with respect to the historical failure history: this permitted to successfully pass the validation. More detailed are reported in [3].

5 Efficient enumeration of multiple contingencies and power system response simulation

This section presents the modules for the efficient enumeration of multiple contingencies and for the assessment of their impact by simulating the power system response to the contingencies themselves.

5.1 Efficient enumeration of multiple contingencies

The methodology adopts an analytical probabilistic approach to enumerate the multiple contingencies which most contribute to the Expected Energy Not Served (EENS) risk indicator.

The enumerative process consists of the following steps:

- calculation of a correlation matrix, to account for the fact that a severe weather event can affect more than one line during the event duration (step 1),
- identification of clusters of lines with high correlation, based on the correlation matrix (step 2),
- identification of relevant contingencies, i.e. combinations of tripping and not tripping of lines with non-negligible probability within each cluster (step 3),
- calculation of the probability of multiple contingencies (step 4).

The steps are described in more detail in the sequel.

5.1.1 Calculation of correlation matrix

The method starts from an $[N_{events} \times N_{lines}]$ event matrix M evaluated as in (3), where N_{events} is the number of weather events when a specific intensity threshold has been overcome at least on one line of the set, N_{lines} is the total number of lines considered in the analysis.

$$M(i, j) = \begin{cases} 0 & \text{if } i\text{-th event does not strike } j\text{-th line} \\ 1 & \text{if } i\text{-th event strikes } j\text{-th line} \end{cases} \quad (3)$$

Matrix M allows to compute the event tables which report the number of weather events when the intensity threshold has been overcome on the lines, see example referring to lines L1 and L2 in TABLE VII.

Table VII. Event table for lines L1 and L2

| | L2 | not L2 | Totals |
|---------------|-----------|---------------|---------------|
| L1 | n_{11} | n_{10} | n_{1*} |
| not L1 | n_{01} | n_{00} | n_{0*} |
| Totals | n_{*1} | n_{*0} | |

where:

- n_{11} is the number of severe events for which both lines L1 and L2 are affected by a weather variable exceeding a threshold Th (in m/s for wind and kg/m for wet snow),
- n_{10} is the number of severe events for which line L1 is affected while line L2 is not affected by a weather variable exceeding a threshold Th ,
- n_{00} is the number of severe events for which neither line is affected by a weather variable exceeding a threshold Th ,
- n_{01} is the number of severe events for which line L2 is affected while line L1 is not affected by a weather variable exceeding a threshold Th .

The linear correlation coefficient between line L1 and L2 is computed as in (4).

$$\varphi_{12} = \frac{n_{11} \cdot n_{00} - n_{10} \cdot n_{01}}{\sqrt{n_{*1} \cdot n_{*0} \cdot n_{1*} \cdot n_{0*}}} \quad (4)$$

Repeating the computation in (4) for any pair of lines, the algorithm builds the line correlation matrix R for the whole set of lines.

5.1.2 Line clustering

The clustering algorithm represents a fundamental pillar for the efficient calculation of long-term resilience indicators. In fact, these indicators will be computed considering only a subset of N-k contingencies, which affect some representative “clusters” of lines. A sound dimensionality reduction starts from the selection of suitable line clusters, which represent a good trade-off between computational time and accuracy, taking into account the extension of past weather events over grid lines through matrix R.

To meet such requirements, this algorithm allows to create clusters with a user-defined threshold of minimum internal correlation between the lines in each cluster. Specifically, a hierarchical agglomerative algorithm is applied to cluster the lines based on correlation matrix R: in case the agglomerative algorithm provides very large clusters, these clusters are split into smaller ones considering topological information (e.g. the connection of the lines to the same substation).

5.1.3 Screening of contingencies

The previous clustering steps allow for a reduction in the number of possible N-k contingencies; however, the methodology applies an effective approach based on total probability theorem and copulas of binary variables to efficiently filter out multiple contingencies, also suitable for large power system applications.

In particular, the probability of the logical “AND” event related to the failures of n lines can be expressed in terms of a copula CDF of binary Bernoulli variables, each of which represents the probability of a specific status of each line (in service / out of service).

The above calculation of CDF values via copulas allows to filter out contingencies with negligible probability by exploiting the total probability theorem. In fact, given that a contingency consists in a combination of ns tripping and nns not tripping of lines, its probability is always lower than the probability of the logical AND of the ns trippings thanks to the total probability theorem. Thus, first, the algorithm computes the probability of an exhaustive set of combinations (logic AND) of trippings and discards all the ones for which the probability is lower than a given probability threshold. After that, all the contingencies which include any of the discarded AND combinations are also discarded by the algorithm.

5.1.4 Copula based calculation of contingency probabilities

Once identified the set of contingencies, their probabilities are computed by applying the theory of copulas for binary variables in each cluster. By Sklar's theorem [19] applied to discrete (particularly binary) variables which represent the statuses of the OHLs, the probability $prob_{ctg,h}$ of the occurrence of a generic h -th contingency meant as a combination of a set S of trippings and a set NS of not trippings, i.e. $P(S \& NS)$, can be written as an algebraic sum of the cumulative distribution of probability of the copula C evaluated at suitable points $\bar{s}^{(i)}$ in subset W_h of the binary variable space, according to the general formula indicated in (5) and related to a cluster of cardinality n and with a linear correlation matrix equal to R .

$$prob_{ctg,h} = P(\bar{X}^{(h)}) = \sum_{\bar{s}^{(i)} \in \Omega_h} sign(\bar{s}^{(i)}) \cdot C[F_1(s_1^{(i)}) \dots F_n(s_n^{(i)}), R] \quad (5)$$

where $\bar{X}^{(h)} = (X_1 = x_1^{(h)}, \dots, X_n = x_n^{(h)})$ is the vector of statuses of the OHLs in the h -th contingency $\bar{X} = (X_1 = x_1, \dots, X_n = x_n)$ and $\bar{s}^{(i)}$ is the i -th point with n components $s_1^{(i)} \dots s_n^{(i)}$ where generic term $s_m^{(i)}$ can be set to $x_m^{(h)}$ or $x_m^{(h)} - 1$. Function $sign(\bar{s}^{(i)})$ is evaluated as in (6).

$$sign(\bar{s}^{(i)}) = \begin{cases} 1 & \text{if } s_m^{(i)} = x_m^{(h)} - 1 \text{ for an even number of positions } m \\ -1 & \text{if } s_m^{(i)} = x_m^{(h)} - 1 \text{ for an odd number of positions } m \end{cases} \quad (6)$$

5.2 Power system response simulation

The power system response to contingencies selected in the previous step is evaluated using a cascading outage simulator which performs the following analyses:

- A post-contingency load flow analysis, with the identification of possible overloads caused on the surviving grid components,
- the identification of any additional line trippings due to previous overloads (cascading outage analysis),
- application of the re-dispatching of generation units aimed at relieving overloads and at bringing the lines back into a secure operational condition, quantifying any load shedding actions needed after the generation redispatch,
- registration of load disconnections at substations in case of each identified contingency and calculation of the related risk indicator Expected Energy Not Supplied on an annual basis (EENS – MWh/year), which is defined by ENTSO-E [20] as the expectation value of the amount of energy not being served to consumers on yearly basis, due to system capacity shortages or unexpected outages of assets.

The $EENS_{PSj}$ indicator at the j -th substation is computed as in (7):

$$EENS_{PSj} = \sum_{h=1}^{N_{ctg,j}} t_{recovery} \times Load_{j,h} \times prob_{ctg,h} \quad (7)$$

where $N_{ctg,j}$ is the number of contingencies causing a partial or total loss of supply at the j -th substation, $Load_{j,h}$ is the unserved load at the j -th substation for the h -th contingency, $prob_{ctg,h}$ computed in (5) is the annual probability of occurrence of the h -th contingency which determines the loss of load at the j -th substation, while $t_{recovery}$ is a conventional recovery time set to 16 hours.

6 Case study

This section presents a case study to demonstrate the effectiveness of the Terna-RSE methodology in identifying the critical and priority areas and in quantifying the benefits of the hardening interventions on the grid.

The analyses are based on the calculation of the Expected Energy Not Served (EENS) index, which represents the performance level of the grid. The EENS can measure the risk level associated with the outage of a substation connected to the HV grid, because it combines:

- the probability of occurrence of substation outage,
- the potential impact of the outage in terms of energy [MWh] not served to the affected customers.

Therefore, via the EENS index the TSO can identify and assess the high-risk area, i.e., the ones characterized by higher values of EENS, in order to define the priority interventions necessary to enhance the resilience and security of the grid and mitigate the loss of load risk. Moreover, the benefits achievable through the implementation of the interventions can be calculated in terms of reduction of EENS for the substations of the area under study.

6.1 Test system

The case study refers to a real portion of the transmission system which is critical for weather induced failures. In particular, Figure 47(a) and Figure 47(b), respectively, report a diagram of the grid portion under study and the linear correlation coefficients among the lines, which are derived from historical severe weather occurrences recorded close to the lines. The loads at the four primary substations (PSs) are evaluated based on the available historical series of power consumptions. In an “average loading grid condition” the loads at the PSs are reported in Figure 47(c).

The RPs of L1, L2 and L3 are 3, 13 and 13 years respectively, while L4 is found to be resilient for the threat analysed ($RP = \text{Inf}$)⁹. The analysis considers both direct and indirect effects of the weather threat considered on the OHLs.

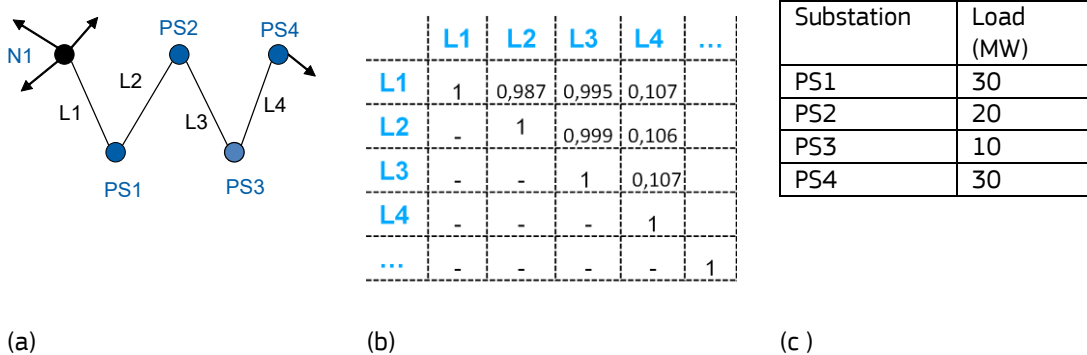


Figure 47. The data for the application example: (a) one line diagram of the portion of the grid vulnerable to weather events, (b) the correlation submatrix corresponding to the set of lines {L1, L2, L3, L4}, (c) loads at primary substations in an «average loading» condition of the grid. The black arrows represent the connections to the rest of the HV grid.

6.2 Evaluation of the EENS in the pre-intervention phase

In the pre-intervention phase, aimed at identifying the high-risk areas of the grid, the methodology enables to identify and assess all the possible and meaningful contingencies reported in TABLE VIII for increasing values of RP (column RP* in the table), quantifying their probability of occurrence Prob(ctg_n). This probability term depends both on the probability of occurrence of the impacting weather event and on the probability that, upon the occurrence of the weather event, those lines and no others are affected and experience an outage. Therefore, this probability of occurrence is a function of both the RP of the lines and of the level of meteorological correlation between them, which is evaluated considering the weather events that occurred on the lines over a multi-year historical horizon.

Table VIII. List of analysed contingencies for increasing RP values

| RP* | Ctg ID | Outaged lines | | | Prob(ctg _n) [p.u./year] |
|-----|--------|---------------|----|----|-------------------------------------|
| | | L1 | L2 | L3 | |
| 3 | A | 1 | 0 | 0 | 0.209877 |
| 13 | B | 0 | 1 | 0 | 0.000465 |
| | C | 1 | 1 | 0 | 0.018467 |
| | D | 0 | 0 | 1 | 0.000463 |
| | E | 1 | 0 | 1 | 0.018469 |
| | F | 0 | 1 | 1 | 0.000057 |
| | G | 1 | 1 | 1 | 0.055354 |

Afterwards, the response of the system to the abovementioned contingencies is analysed, assuming a conventional restoration time of the outages of 16 hours. Table IX reports the amount of unserved load, the yearly contingency probability of the failure occurrence and the EENS indicator for the three contingencies that cause the disconnection of PS1 substation. Of course, contingency G also causes the disconnection of PS2 substation, but Table III only lists the impact, probability and risk indicators (EENS) associated with PS1 substation. The methodology evaluates the EENS indicators for each substation of the grid portion under test. The total EENS associated with PS1 substation is equal to 44.3 MWh/year and the RP of PS1 substation

⁹ The correlation coefficients and the RPs mentioned above do not represent the real level of weather correlation or vulnerability of the lines which are part of the existing portion of the grid under examination. Hence the values exposed above have been defined for illustrative purposes.

outage is 11 years. It is worth noticing that the response of the system to multiple contingencies is simulated considering the model of the whole transmission system in the cascading outage simulator.

Table IX. Contributions of contingencies affecting PS1 substation to annual EENS.

| RP* | Ctg ID | Unserved load at “average loading” grid condition [MW] | Prob(ctg _n) [p.u./year] | EENS _n [MWh/year] |
|-----|--------|--|-------------------------------------|------------------------------|
| 13 | C | 30 | 0.018467 | 8.9 |
| | E | 30 | 0.018469 | 8.9 |
| | G | 30 | 0.055354 | 26.6 |

6.3 Evaluation of the EENS in the post-intervention phase and quantification of the benefit for CBA

After the identification of the critical and priority portions of the grid, the relevant areas are analysed to define the interventions necessary to increase the level of resilience of the transmission infrastructure and, consequently, of the substations.

Lines L2 and L3 present few spans with relatively low RP for the weather threat under study. In this specific case the most cost-effective solution identified via the CBA consists in the partial undergrounding of the lines, thus avoiding the exposition of critical line spans to the threat. This intervention makes lines L2 and L3 resilient to the threat under study. Alternative solutions involving the partial undergrounding of line L1 (with more spans exposed to the threat and a lower RP with respect to lines L2 and L3) are deemed less convenient by the CBA.

The capability provided by the methodology to punctually evaluate how the intervention on each line span can affect the overall resilience level of the system enables the TSO to identify the minimum hardening actions required, thus guaranteeing the cost-effectiveness of the grid planning process. Finally, applying again the methodology in the post-intervention scenario leads to a null value of the EENS for substation PS1 with reference to the specific threat, which means that the substation is completely resilient to the threat. In the end, the benefit of the intervention, in terms of EENS variation, is given by $\Delta\text{EENS} = \text{EENS}_{\text{POST}} - \text{EENS}_{\text{PRE}} = -44.3 \text{ MWh/year}$.

7 Conclusions

This paper introduced an innovative methodology, collaboratively developed by RSE and Terna, designed to assess long-term resilience indicators as a mean to prioritize grid hardening actions. This ground-breaking approach, forged through a close collaboration among experts in power systems, network planning, component design, and meteorology, is currently focused on addressing the primary causes of failures in the Italian EHV and HV grid, viz. wet snow and strong wind events. It accomplishes this by evaluating the outage return periods of HV/MV substations feeding distribution grids, starting from the return periods of outages in the lines connected to the substation and considering the grid meshing level. After a successful validation phase, the methodology has been approved by the Italian Regulatory Authority and it has been issued as an addendum of the grid code of the Italian TSO.

The methodology itself relies on a probabilistic framework. It combines probabilistic climatological models predicting extreme values of stress variables (such as snow loads and wind speeds) over various time horizons (up to the year 2050) with probabilistic analytical models assessing overhead line (OHL) vulnerability to both direct and indirect effects of wet snow and wind.

This collaborative effort, informed by a deep understanding of power grid resilience, by inputs from system operators and regulatory authorities, as well as by more challenging climate change scenarios, has spurred significant advancements in planning. Anticipating climate scenarios during the planning phase and considering all potential weather-related events and their combinations are deemed essential to effectively address climate change impacts on grid planning strategies.

The application of this methodology demonstrates its efficacy in assessing the return periods of line outages in alignment with operational experiences. It also effectively quantifies the benefits of grid interventions, expressed in terms of variations in Energy Not Supplied (EENS) and in the return periods of substation outages.

Moreover, the methodology is evolving to encompass additional threats, such as hydrogeological risks, thus further extending its applicability in ensuring the resilience of power grids.

Acknowledgements

For the part developed by RSE, this work has been financed by the Research Fund for the Italian Electrical System under the Three-Year Research Plan 2022-2024 (DM MITE n. 337, 15.09.2022), in compliance with the Decree of April 16th, 2018".

References

- [1] M. Panteli, P. Mancarella, "Influence of extreme weather and climate change on the resilience of power systems: Impacts and possible mitigation strategies", *El. Power Systems Research*, Elsevier, 2015.
- [2] E. Ciapessoni, D. Cirio, A. Pitto, M. Lacavalla, P. Marcacci, G. Pirovano, F. Marzullo, F. Falorni, F. Scavo, A. Lazzarini, C. Vergine, "A methodology to compute resilience indicators for the Italian Transmission System", Proc. of CIGRE 2021 Centennial Session, Paris, August 2021, pp.1-11.
- [3] E. Ciapessoni, D. Cirio, E. Ferrario, M. Lacavalla, G. Pirovano, A. Pitto, F. Marzullo, F. Falorni, A. Lazzarini, F. Scavo, S. Costa, S. Pierazzo, C. Vergine, "Validation and application of the methodology to compute resilience indicators in the Italian EHV Transmission System", Proc. of 2022 CIGRE Session, Paris, Aug 2022, p.1-14.
- [4] ARERA (Italian Regulatory Authority) Deliberation 9/2022/R/EEL of January 18, 2022, "Verifica di conformità del codice di trasmissione, dispacciamento, sviluppo e sicurezza della rete, in materia di valutazione dell'incremento di resilienza di progetti di sviluppo della rete" (in Italian).
- [5] Terna, "Metodologia per il calcolo del beneficio per l'incremento della resilienza della rete di trasmissione nazionale", Addendum A 76 of Terna Grid Code, 2022.
- [6] P. Faggian and G. Decimi, "An updated investigation about climate-change hazards that might impact electric infrastructures," Proc. of 2019 AEIT International Annual Conference (AEIT), Florence, Italy, 2019, pp. 1-5.
- [7] J. E. Kay, C. Deser, A. Phillips, A. Mai, C. Hannay, G. Strand, J. M. Arblaster, S. C. Bates, G. Danabasoglu, J. Edwards, M. Holland, P. Kushner, J.-F. Lamarque, D. Lawrence, K. Lindsay, A. Middleton, E. Munoz, R. Neale, K. Oleson, L. Polvani and M. Vertenstein, "The Community Earth System Model (CESM) Large Ensemble Project: A Community Resource for Studying Climate Change in the Presence of Internal Climate Variability", *Bulletin of the American Meteorological Society*, No. 96, pp 1333-1349, 2015.
- [8] D. Jacob, J. Petersen, B. Eggert, et al. "EURO-CORDEX: new high-resolution climate change projections for European impact research", *Reg Environ Change*, no. 14, pp. 563–578, 2014.
- [9] M. Lacavalla, R. Bonanno, S. Sperati. «A new high-resolution Meteorological Reanalysis Italian DAset: MERIDA», RMETS - Royal Meteorological Society, March 2019.
- [10] CEI EN 50341-1:2013-10, "Overhead electrical lines exceeding AC 1 kV - Part 1: General requirements - Common specifications", 2013.
- [11] CEI (Italian Electrotechnical Committee) Std 11-4, "Norme tecniche per la costruzione di linee elettriche aeree esterne", (in Italian), 1998-9.
- [12] E. Ciapessoni *et al.*, "Modeling the overhead line vulnerability to combined wind and snow loads for resilience assessment studies," *2021 IEEE Madrid PowerTech*, Madrid, Spain, 2021, pp. 1-6.
- [13] E. Ciapessoni, D. Cirio, A. Pitto, G. Pirovano and M. Sforza, "Modelling the vulnerability of overhead lines against tree contacts for resilience assessment," Proc of 2020 International Conference on Probabilistic Methods Applied to Power Systems (PMAPS), Liege, Belgium, 2020, pp. 1-6.
- [14] CORINE database (latest version: 2018). Available at: <https://land.copernicus.eu/pan-european/CORINE-land-cover/>
- [15] D.W. Wanik, J.R. Parent, E.N. Anagnostou, B.M. Hartman, "Using vegetation management and LiDAR-derived tree height data to improve outage predictions for electric utilities", *Electric Power Systems Research*, Vol. 146, pp. 236-245, 2017.
- [16] E. Ciapessoni, D. Cirio, A. Pitto, G. Pirovano – RSE SpA e e E. M. Carlini, F. Marzullo, S. Casulli, F. Falorni, F. Scavo, G. Magnolia – Terna SpA e G. Berrettoni – University of Cassino – "An innovative tree

- interference mapping with LiDar for overhead lines vulnerability assessment in the Italian power system”, Proc. of AEIT 2023 International conference, Roma, Italy, Oct 5-7, 2023, p. 1-6.
- [17] Jupiter Intelligence website available at: <https://jupiterintel.com>
 - [18] Std. IEC 60826, “Overhead transmission lines – Design criteria”, Edition no. 4, Feb 2017.
 - [19] R. B. Nelsen, An introduction to copulas, New York, Springer, 2006.
 - [20] ENTSO-E, “Winter Outlook 2022-2023”, technical report, 2022.

2.17 The Resilience Assessment in Electricity sector: How to get started, holistic or segmented view?

Maria Luisa Alberto and Manuela Gaivéo, EDP – Energias de Portugal, S.A., Portugal,
marialuisa.alberto@edp.com, manuela.gaiveo@edp.com

Abstract

Resilience is a multifaceted concept, used in many different domains and whose interpretation and definition vary in different organizations around the world, based on the type of discipline, implemented practices, and lived experiences.

In the complex context of the electricity sector which directly includes key critical sub-sectors such as Generation, Transmission, Distribution, and Trading, in addition to all the IT/OT support systems, human resources and supply chain, it is essential to assess where these complex systems stand in terms of resilience, considering that they evolve internally and interact with other equally complex systems.

This paper will address these issues, focusing on reflection on the best approach to follow – the holistic or segmented view – to define, establish and implement a methodology for assessing resilience in the electricity sector.

1 Introduction

Resilience has been gaining increasing prominence in the last decade [1], largely as a result of its identification as one of the principles assumed by the EU. We see it reflected in the preparation of the public and private sectors to face extreme weather events, in the capacity of critical infrastructures and entities to respond, in a sustainable manner, to disruptions and threats of different types, or how cities are capacitating themselves to react and recover from the impacts from natural disasters, to name a few examples.

The COVID-19 pandemic has brought it even further forward by highlighting the challenges that the management of critical infrastructures and services have faced, and the impact that the lack of resilience in different sectors may have on society and the economy, demonstrating the need to address resilience in a more holistic and articulated way [2].

The emergence of the geopolitical conflict in Eastern Europe in 2022, led by Russia and Ukraine, has increased the sense of urgency and the relevance of achieving an adequate level of resilience, but also of the need to develop the appropriate means for assessing and monitoring resilience in different contexts.

The dependency society and critical sectors, both public and private (e.g. security, health, water, communications), have on energy, leads to the acknowledgement of the electricity sector as highly critical. It is only natural that nations should recognize electricity-related infrastructures (generation, transmission, distribution) as national critical infrastructures (CI) and invest in ensuring that an appropriate level of resilience is met, as well as that of the services they're dependent on, often needing to articulate such efforts with private sector companies that are responsible for CI management and operation.

The first part of this article will be devoted to clarifying definitions and concepts, exploring of the methodologies that have been used to enhance and assess resilience, while the second part will be dedicated to analyzing electricity sector-related case studies of the application of methodologies that support the achievement of resilience and its assessment, to set the basis for a framework to address this issue.

2 Resilience theoretical foundations

While it's not this article's main objective to deep dive into the different definitions of resilience, or to provide yet another one, it is important to address resilience's characteristics and contexts, to develop a clearer understanding of the issues that arise when trying to establish a resilience development and assessment methodology.

2.1 Definitions

The definition of resilience is itself a challenge. A comprehensive concept, which, depending on the context, acquires its own particularities [3], has found application in mechanics, social sciences, engineering, national security, response to extreme events, or critical infrastructures, among other domains [1].

The UN Office for Disaster Risk Reduction (UNISDR), defines resilience as the “The ability of a system, community or society exposed to hazards to resist, absorb, accommodate, adapt to, transform and recover from the effects of a hazard in a timely and efficient manner, including through the preservation and restoration of its essential basic structures and functions through risk management.” [4], focusing on the capacity to timely identify and manage risks that might result in significant impacts (even though their probability may be low), increasing the robustness of the system, community or society while ensuring its flexibility in responding to events characterized by uncertainty to a larger or smaller extent.

EU's 2020 Strategic Foresight Report [5] is dedicated to resilience, assuming it as “a new compass for EU policies with the COVID-19 crisis” and discussing the need to ensure appropriate resilience monitoring. Within this context, resilience is defined as the “ability not only to withstand and cope with challenges but also to undergo transitions in a sustainable, fair, and democratic manner”, setting the tone for a broader approach to resilience, intimately related to Europe’s capability to respond to and recover from “current and future crises”, ensuring alignment with the UN’ Sustainable Development Goals.

In its *Hybrid Threats – A comprehensive resilience ecosystem* publication, the European Commission’s JRC and Hybrid CoE [1] refer to a generic definition of resilience such as “the ability of an entity to overcome adversity, with two main perspectives underpinning understanding of resilience: reactive and proactive”, highlighting the evolution of the concept over time from an approach of “controlling shocks by resisting and returning to equilibrium” to an approach of “overcoming shocks by adapting and moving towards a new stable equilibrium close to the original one”, which in turn points to the need to ensure the critical and systematized review of the ecosystem of measures adopted, and to promote the evolution and creation of new paradigms of resilience building, based on the learning carried out in the face of the different challenges and events experienced.

The concept of organizational resilience is addressed in detail in ISO 22316 [6], which establishes the principles and guidance that enable the development of a framework and strategy with an aim to develop, implement and evaluate organizational resilience. Defining organizational resilience as “the ability of an organization to absorb and adapt to a changing environment to enable the delivery of its objectives and to survive and prosper”, ISO 22316 [6] recognizes the importance of being able to identify and respond to threats and opportunities, as well as the role risk management plays in achieving resilience. It further highlights the necessity for a greater coordination between management disciplines (e.g. risk management, business continuity, supply chain management) to optimize efforts in achieving resilience, as well as a deeper understanding of stakeholders and interested parties, and existing dependencies, and how these impact organizational objectives.

Resilience definitions also abound in relation to critical infrastructures (CI) and entities, with emphasis on EU's Directive (EU) 2022/2557 on the resilience of critical entities [7], establishing resilience requirements the member states must enforce in managing their national critical infrastructures. In this regard, resilience translates into “a critical entity's ability to prevent, protect against, respond to, resist, mitigate, absorb, accommodate and recover from an incident”.

In 2019, OECD [8] thoroughly addressed the resilience of critical infrastructures, with special attention being given to its governance. Defining resilience as the “capacity of critical infrastructure to absorb a disturbance, recover from disruptions and adapt to changing conditions, while still retaining essentially the same function as prior to the disruptive shock”, this report argues that when facing a shock event, resilience can translate into the ability to limit the extent of the damages and of associated service downtime/interruption. Additionally, it recalls the key qualities that critical infrastructures must combine to achieve resilience, including robustness, redundancy, resourcefulness, and adaptability. In its Annex 3.B. Definition of Critical Infrastructure in OECD countries, this report demonstrates the multiplicity of definitions that might be adopted for the concept of critical infrastructure, which poses a supplementary challenge for an unified definition of what resilience can mean in this context.

The RESILIENS – Realising European ReSilienCE for Critlcal INFraStructure Project [9] – responsible for the development of the *European Resilience Management Guidelines* focusing on critical infrastructures-, defines resilience as “... the ability of a system or systems to survive and thrive in the face of a complex, uncertain and ever-changing future.”, underlining its usefulness in (i) minimizing disruption, (ii) ensuring timely recover, and (iii) adapting to an everchanging context, thriving under new and uncertain circumstances. It further states that “within the context of CI, the resilience process offers a cyclical, proactive and holistic extension to risk management practices”.

2.2 Related methodologies

It has been established that resilience – a multi-layered and wide-spanning concept-, can have various definitions, depending on the context and scope in perspective. Furthermore, it can describe a goal – achieving resilience- or a property – to be resilient.

The achievement of resilience can be accomplished through different approaches, often combined, to strengthen the overall ability to “resist, absorb, accommodate, adapt to, transform and recover” [4] to and from impactful events. These approaches typically offer the means to identify (i) critical assets, services and processes, and their exposure to (ii) threats and risks, that can be managed through (iii) directed strategies and measures, that once implemented, should result in an adequate level of resilience to relevant scenarios (e.g. business continuity plans).

Once resilience has been achieved, it's crucial to be able to evaluate its prevalence and extent. Being able to measure or assess resilience is key in ensuring adequate levels are maintained over time [6], identifying the need for adjustment or revision of resilience measures in order to react, respond and recover from threats and events of different natures, emerging in complex and uncertain contexts.

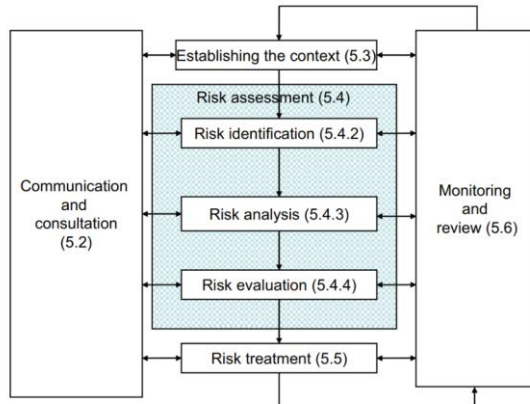
This chapter offers a brief overview of some methodologies that are commonly used to assist in attaining resilience, while simultaneously providing tools to ensure its structured assessment and improvement, focusing on risk management and business continuity as broad application methodologies that are prevalent in the electricity sector.

2.2.1 Risk Management

Risk management has long been considered a key practice in supporting the achievement and improvement of resilience, as clearly stated in UNISDR's definition of resilience [4], for instance.

By being able to timely detect threats and vulnerabilities, and offering a structured approach to evaluate exposure degree, likelihood, and potential consequences [10], the risk management process, Figure 48, allows for the anticipation of risk scenarios and mitigation of their impacts (including operational and financial impacts), in accordance with the organization's risk appetite profile.

Figure 48 - Risk management process



Source: ISO 31000

Risk treatment plans emerge as result of risk evaluation and often include measures and controls to limit negative consequences and decrease likelihood of such scenarios, by increasing robustness and resistance to external threats, and acting on internal vulnerabilities and flaws. The overall process will necessarily result in heightened resilience to the scenarios that were identified.

Additionally, since risk management assumes recurrence, for instance on an yearly basis, new and emerging risk scenarios can be promptly signalled and monitored, and the need to revise treatment strategies, identified.

Allowing for both top-down and bottom-up approaches, when aiming for the strengthening of resilience, risk management would benefit from a hybrid approach, in order to capture the specifics of each critical asset, infrastructure or process, at an operational level, while providing an outlook on wider risk scenarios.

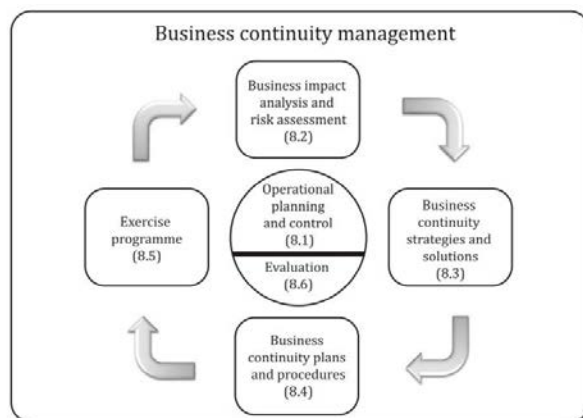
2.2.2 Business Continuity Management

Business Continuity is defined in ISO 22301 [11] as the “capability of an organization to continue the delivery of products and services within acceptable time frames at predefined capacity during a disruption”, concentrating on limiting the impact on critical services and processes and recovering these services, partially or completely, within an appropriate period.

In turn, business continuity management (BCM), provides an approach that enables the identification of disruption scenarios that may challenge organizational and infrastructure resilience, characterizing its impacts, enabling the development and adoption of strategies and measures to increase its resilience.

A critical part of the BCM process, Figure 49 [19], business impact analyses (BIA) aid organizations in identifying high-impact disruptive scenarios with a potential to significantly affect critical processes, services, and assets, with direct repercussions on the pursuit of business objectives.

Figure 49 - Elements of business continuity management



Source: ISO 22313

BIA therefore allows organizations to signal potential situations in which the reinforcement of their response and recovery ability with regard to severe incidents that might condition their activity, resulting in an increment in organizational resilience. The definition of RTO¹⁰, RPO¹¹, MBCO¹² and MTPD¹³ as outputs of the BIA process, provides objective goals against which recovery capacity and resilience can be measured [12].

In the same way as previously discussed regarding risk management, a BC risk assessment will complement and provide additional insight into threats and vulnerabilities which are being addressed in a sub-optimal way, and can be mitigated at an operational level to increase resilience when facing disruptions, by both decreasing exposure and improving response and recovery abilities (e.g. business continuity plans, contingency and disaster recovery plans).

Following the risk assessment (and treatment plan definition), the selection and design of adequate response and recovery strategies is crucial to develop business continuity, contingency and disaster recovery plans which will enable the organization to manage the impacts of a disruption, ensuring that the necessary resources to respond and recover are previously identified, prepared and tested before-hand.

⁽¹⁰⁾ RTO - recovery time objective

⁽¹¹⁾ RPO - recovery point objective

⁽¹²⁾ MBCO - minimum business continuity objective

⁽¹³⁾ MTPD - maximum tolerable period of disruption

Since returning to the same 'normal' situation that existed before the disruption is not always possible, or even appropriate, it's desirable that organizations develop the ability to rebuild their infrastructure, processes and services in a more robust and fail-safe way, guaranteeing that the adequate redundancies are put in place, thus learning from the disruptive situation and improving to better respond in the future.

In addition to the BIA, risk assessment and response/recovery planning, regular exercises that cover part or the whole of response and recovery strategies and resources, assist in evaluating operational and organizational resilience, enabling the identification of flaws and the need for improvement. Exercises in which other stakeholders – key suppliers, authorities, etc., are involved should be promoted, since they offer an integrated perspective on resilience associated with dependencies (e.g. intra and inter sectorial exercises), contributing to its increase.

3 Resilience assessment approach

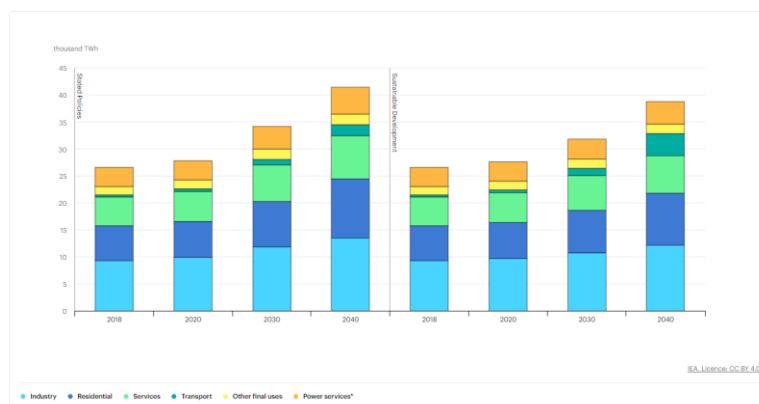
"The increasing complexity and interdependence between critical infrastructures and the increasing dependence on the electric energy infrastructure makes the resilience of the energy network a fundamental priority in safeguarding the economic and social growth of modern societies" [13].

Considering the complexity and diversity of the different methodologies described previously, it's this article's aim to present the basis for a framework that can be adapted and applied to the electricity sector, keeping in mind that "resilience is a proactive and comprehensive approach that involves developing organizational capabilities, fostering a culture of adaptability and innovation, and possessing the agility to respond to both expected and unexpected events [14]."

3.1 Electricity sector

It is an irrefutable truth that "Electricity is at the heart of modern economies, and it is providing a rising share of energy services. Demand for electricity is set to increase further because of rising household incomes, with the electrification of transport and heat, and growing demand for digital connected devices and air conditioning." as shown in Figure 50 [15].

Figure 50 - Electricity demand by sector and scenario, 2018-2040

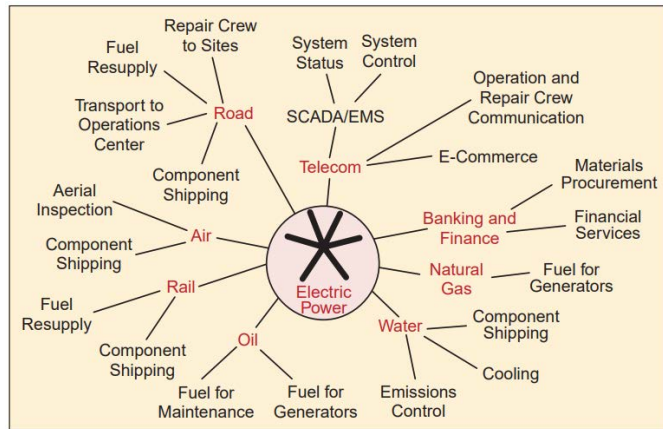


Source: International Energy Agency (IEA), 2019

The prospect of a substantial increase in electricity demand is gradually putting additional pressure on the electricity sector and inherently, in electricity companies, to invest and adapt their business, opting for a set of strategies, policies, methodologies, and organizational and operational measures that will allow them to continue to respond to the rapid-evolving demands of consumers (individuals and businesses), and society in general.

On the other hand, most sectors (e.g. water, transport, communications, etc...) depend on the electricity sector. Figure 51 [16] illustrates the concept of dependence between the various sectors of essential services of society, when operating in normal "business as usual" circumstances.

Figure 51 - Examples of electric power infrastructure dependencies



Source: IEEE Control Systems Magazine, 2001

However, in situations of constraint to, or disruption of essential services, it's crucial to strengthen the relations between infrastructures and their interdependencies, the monitoring of these facilities through risk management, and the identification of alternatives or contingency plans to be developed, in order to reduce and mitigate possible disasters.

Because of these interdependencies, any disruption to essential services, even if initially confined to one entity or sector, can have wider repercussions and result in widespread and long-term negative impacts on the delivery of services throughout the internal market. Serious crises have revealed the vulnerability and exposure of increasingly interdependent societies and sectors to risks with low probability of occurrence but with high impact [17].

Pursuing the path of organizational resilience is a strategy that many organizations are adopting since more resilient organizations can better anticipate and respond to threats and opportunities, arising from sudden or gradual changes in their internal and external contexts [18].

3.2 Implementation perspectives

Bearing in mind what was previously mentioned about the electricity sector, the dependencies and interdependencies between the various sectors, the fact it is delivering an essential service for society, and in addition, the particularity of the classification as critical entities [7], result in an even more complex decision regarding which path to follow in implementing resilience.

In the next chapters, possible approaches to this subject and different cases studies will be presented; these were selected regardless of the size and location of the organization, and consider mostly, but not only, the electricity sector, offering different resilience assessment perspectives (e.g. business continuity and recovery, critical infrastructure, crisis management, organizational resilience, supply chain, IT/OT¹⁴).

The case studies presented below are examples of the implementation of processes, methodologies, good practices, and legal obligations that can be used as steps/phases for a way to achieve resilience. It's not the intention of this article to present a single solution that will serve all contexts, but to indicate possible paths, or sections of thereof, alternatives and approaches that can help achieve the desired level of resilience.

Each case presents a different scope and point of view, highlighting some characteristics of resilience assessment tools (although in some cases, theoretical), to help understand the benefits of the selected approach.

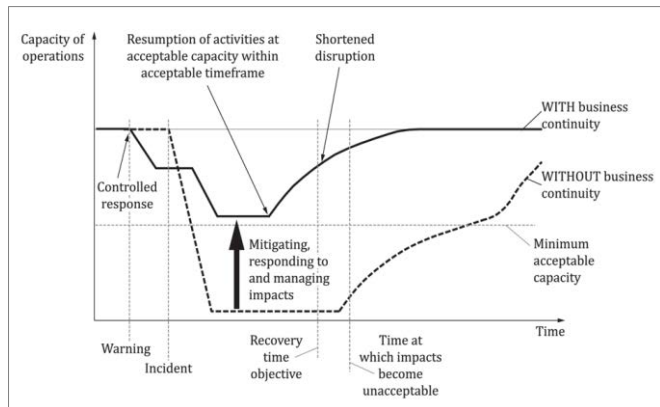
3.2.1 Business Continuity and Recovery

As defined in ISO22313 [19] "business continuity is the capability of the organization to continue delivery of products or services at acceptable predefined capacities following a disruption". Implementing a business continuity management process "increases the organization's level of preparedness to continue to operate

⁽¹⁴⁾ IT/OT – Information Technology / Operational Technology

during disruptions", as shown in Figure 52. "It also results in improved understanding of the organization's internal and external relationships, better communication with interested parties and the creation of a continual improvement environment."

Figure 52 - Illustration of business continuity being effective for gradual disruption



Source: ISO 22313

To strengthen its resilience, the EDP Group¹⁵ established, in an internal document, its framework for Business Continuity Management (BCM), Figure 53, also specifying the methodological approach to be observed, in alignment with the ISO 22301 [11], strengthening its ability to detect and appropriately respond to risks with potential impact on its activity.

The EDP Group defined a BCM network that promotes and facilitates cooperation between its Business Units, ensuring the existence of a common and combined effort to achieve the overall resilience necessary to face any disruptive incident.

Figure 53 - EDP Group BCMS framework



Source: EDP Group's Crisis Management and Business Continuity Model

Another example of this approach is the effective activation of the Business Continuity Plan of the Electricity Distribution System Operator in Portugal, (part of the EDP Group, E-REDES, formerly EDP Distribuição). When facing an extreme event, business continuity management was referred to as a key contribution to a

⁽¹⁵⁾ EDP Group, is a Portuguese a multinational, vertically integrated utility company, present in 29 markets around the world, and over 13.000 employees. With more than 40 years of history, provide electricity and gas to more than 9 million customers. Its activities cover the electricity value chain and the gas supply activity. EDP is one of the largest wind energy generation companies in the world and 87% of the energy produced was from renewable resources. Source: edp group | edp.com

successful performance [3]. As mentioned in [20] the company's level of preparation will determine how well it will perform under extreme conditions.

Key takeaway: In summary the implementation of a BCM, as part of a continuous improvement cycle allows organizational readiness when dealing with disruptive events, through the development of an evolutionary exercise program [21] combined with awareness and training sessions. However, only through cooperation with relevant internal and external stakeholders will it be possible to adequately increase resilience.

3.2.2 Critical Infrastructures in the energy sector

According to the definition of the European Union, Council Directive 2008/114/EC [17], Critical Infrastructure (CI) is "an asset, system or part thereof located in Member States which is essential for the maintenance of vital societal functions, health, safety, security, economic or social wellbeing of people, and the disruption or destruction of which would have a significant impact in a Member State as a result of the failure to maintain those functions".

This Directive focuses exclusively on the protection of such infrastructures and provides a procedure for the identification of European critical infrastructures in the energy and transport sectors, taking into account that possible disruptions or the destruction of associated assets would most translate into a significant cross-border impact in at least two Member States.

However, an assessment carried out in 2019 concluded that protective measures relating to individual assets alone are insufficient to prevent disruptions from taking place and, that would be necessary to shift the approach towards ensuring and strengthening the resilience of critical entities.

Thus, a new European directive was recently approved, Directive (EU) 2022/2557 of the European Parliament and Council of December 14, 2022, on the resilience of critical entities (repealing Directive 2008/114/EC with effect from October 18, 2024).

This normative document aims to address, in an in-depth and comprehensive manner, the resilience of those which are critical entities in respect to all hazards, whether they are natural or man-made, accidental, or intentional. [7]. Thus, resilience thinking acknowledges that there are events that cannot be planned for and encourages adaptability and flexibility when faced with unexpected events [3].

Therefore, it's necessary to (i) identify harmonized minimum rules to ensure the provision of essential services in the internal market, (ii) enhance the resilience of critical entities, and (iii) improve cross-border cooperation between competent authorities [7].

However, since 2008, much progress has been made when it comes to strategy implementation and institutional programs to address resilience, as offered in the Annex 3.A. *Critical infrastructure strategy or programme and lead institution in charge* [8].

Several examples of critical infrastructure disruptions (not exclusively from the electricity sector), contributed to the analysis and discussion about the shift in mentality about resilience in Annex 1.A. *Lessons learned from past critical infrastructure failures* [8]:

- The 2011 Great East Japan Earthquake and the subsequent tsunami significantly affected the energy sector in Japan. The nuclear meltdown of the Fukushima Daiichi Nuclear Power Plant and the following shutdown of the nuclear power plants throughout the country, led to a 50 % reduction in electricity production, causing substantial energy supply disruptions across the country
- The closure of European air spaces following the Eyjafjallajökull volcanic eruption in Iceland in 2010 led to more than 100 000 flight cancellations and rerouting around the world. As a result, many companies that depend on air cargo to deliver products and key components were unable to supply markets and production systems throughout Europe and beyond
- The Northeast United States and Canadian Power Outage in 2003 was caused by trees falling on a high-voltage power line in northern Ohio triggering cascading failures in south-eastern Canada and eight states in the Northeast United States impacting 50 million people in both the United States and in Canada at an estimated cost of USD 6 billion.

Furthermore, it is important to mention the role assumed by EDP Group in promoting the adoption of good practices in the management of critical infrastructures in the sector, through the dissemination of such practices, but also through collaboration with external entities (with special focus in the interaction with the Portuguese TSO), participating in exercises and workshops relevant to the topic [20]. In addition to the

examples given above, in the report [23] can be found 15 good practices examples that promote the work that different companies and countries are carrying out and have already implemented.

Key takeaway: In summary, we have evolved, at European level, from infrastructure protective measures relating to individual assets alone, to a deeper understanding and global resilience of critical entities. It's expected that this article might act as a catalyst for critical entities, and in particular the electricity sector, to continue to strengthen their capacity to provide services in challenging scenarios, further developing their resilience.

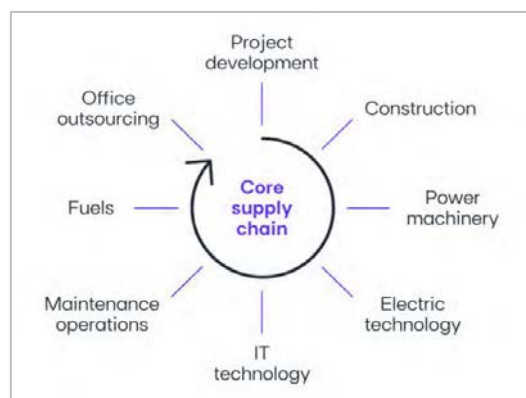
3.2.3 Supply chain

"In today's dynamic and interconnected operating environment, organizations face challenges that can disrupt their operations and threaten their survival. Whether it is a natural disaster, a cyberattack, supply chain disruptions, or another unforeseen event, the ability to navigate through such disruptions and maintain essential functions is crucial" [13].

Supply chain is defined by ISO22318 [24] as a "network of organizations that are involved, through upstream and downstream linkages, in the processes and activities that produce value in the form of products and services in the hands of the ultimate consumer." In this sense, the concept of resilience, particularly in supply chains, acquires relevance, as it is seen as the ability of organizations to cope with adversity, adapt and continuously accelerate as disruptions and crises arise over time.

"For an organisation like EDP Group, present in multiple markets and business areas, supply chains hide interdependencies, potentially leading to crises, where hidden interruptions may arise, unexpectedly impacting the company's business plan" [22]. There are four ESG risk segments (Electrical/Industrial technology, Technical Services and Construction, Corporate Services and IT, Fuels) in the supply chain that correspond to the purchasing categories of the value chain, as show in Figure 54.

Figure 54 - EDP's core supply chain



Source: EDP Annual Integrated Report, 2022

EDP Group has defined several Management tools to follow this subject (e.g Sustainable Purchasing Policy, Supplier's Code of Conduct, Sustainability in Purchasing Protocol (i. Due Diligence, ii. Risk analysis, iii. Assessments, audits, and annual appraisal, iv. Contractual clauses), Human and Employment Rights Policy, Climate and Environment Policy, Prevention and Safety Policy, Code of Ethics for contractors, Integrity Policy, Ethics and Speak Up Channels, Sustainable Purchasing Committee, Objectives and KPI policy).

As mentioned in the BCI report [25] "COVID-19 did indeed provide a shock lesson in supply chain resilience good practice. Management commitment to supply chain management is at an all-time high, while centralised reporting of supply chain disruptions and investment into specialist technology tools have also soared. However, work still needs to be done. Many organizations are still failing to make basic checks on the business continuity and resilience plans of their most critical suppliers, and reporting data on disruptions is frequently held in Excel spreadsheets and not shared throughout the organization."

Key takeaway: In summary, the dependency on suppliers to deliver critical products or services, is a known and assumed risk, shared by all organizations. Nevertheless, there is room for improvement in the

identification, assessment, follow-up and monitoring of critical suppliers, recognizing that the potential impact of the disruption of their activities will significantly impact the activities of the organization.

3.2.4 Organizational resilience

As mentioned in 2.2 *Resilience theoretical foundations*, organizational resilience is the ability of an organization to absorb and adapt in a changing environment, but also the result of the interaction of attributes and activities, and contributions made from other technical and scientific areas of expertise [18].

As argued throughout this article, there isn't a single approach to achieving resilience, and ISO 22316 [18] reflects this perspective by stating that existing established management disciplines contribute towards resilience but are, on their own, insufficient to safeguard an organization's resilience. It's then suggested that, the design, development and coordination of management disciplines, and their alignment with the organization's strategic objectives are fundamental to enhancing organizational resilience.

Table 1 summarizes some examples of relevant management disciplines referred in this standard, whose coordination would support and facilitate the achievement of resilience. However, in addition to these examples, disciplines such as sustainability and compliance management, can also be considered, given their relevance.

Table 1- Relevant management disciplines

| | | | |
|--------------------------------|--------------------------|---|-----------------------------------|
| asset management | emergency management | health and safety management | quality management |
| business continuity management | environmental management | human resources management | risk management |
| crisis management | facilities management | information security management | supply chain management |
| cyber security management | financial control | information, communications, and technology | strategic planning |
| communications management | governance | physical security management | sustainability (¹) compliance (¹) |

(¹) Disciplines not included in ISO22316

Source: ISO 22316

As an example of articulation between different disciplines (e.g health and safety, crisis management, communications management, human resources, business continuity, etc), was the EDP Group [26] concerted response to pandemic crisis. Since January 2020, an effective monitoring of the evolution of the pandemic situation began, with several dedicated monitoring groups being created, ensuring the participation of representatives from relevant areas to the topic.

"The management of the COVID-19 pandemic in the EDP Group is a paradigmatic case of the relevance of good communication in crisis, guiding the EDP Group by the best communication practices, which enabled the increase of proximity to its Customers, Employees and Service Providers in this very challenging period. The commitment to clear, targeted, internal and external communication, through the right channels and at the right times, has been decisive for the success of the management of the pandemic crisis and the implementation of responses to it. [26]"

Key takeaway: In summary, organizational resilience is a strategic goal that can be established as part of a set of good practices. Although the framework presents the subject as a more global approach, there should be an effective gradual alignment between the multiple management disciplines so that it results in strengthened resilience.

4 Discussion and Main Challenges

The broad applicability of the concept of resilience, proven by the case studies presented, represents in itself a challenge in establishing a transversal and aggregating approach to its achievement. Different contexts and perspectives will necessarily condition the selection of methodologies to better support the development of resilience and its maintenance over time, as well as to ensure its assessment.

When designing an assessment approach, it's important to note the nature and scope of the assessment. An initial assessment should concentrate on identifying existing measures, vulnerabilities and threats which are not yet being addressed, as well as pinpointing relevant risks. Subsequent assessments should provide

gradually deeper analyses, evolving in its scope, to encompass firstly physical infrastructures, then services, and finally the entity as whole, also considering its relations with relevant stakeholders.

Approaches to develop, enhance, and assess resilience will also vary according to the entity's maturity in operating and managing its critical infrastructures.

Entities with lower maturity will most likely find it more manageable to start by establishing practices to evaluate risks and impacts at an operational level, which would enable them to build resilience at a facility level, to begin with. Emergency and contingency management would be prevalent when facing disruptive events, in an effort to ensure minimal services.

As maturity increases, and operational risks are managed at facility level – since they've been subjected to risk treatment and are being consistently monitored-, a service perspective becomes more easily achievable, allowing for the analysis and addressing of risks associated with integration between facilities, other assets and organizational functions, as well as with dependencies, both internal and external. At this point, the conditions are met to promote intra-sector collaboration as a standard in managing critical infrastructures, and some inter-sector alignment should be accomplished. Business continuity should now be fully developed, in accordance with best practices, and the ability to respond to and recover from disruptions, containing impacts and resuming service to an acceptable degree in a pre-established time frame, is ensured.

A strategic management of critical infrastructures and services would then surface, with a somewhat developed ability to coordinate management disciplines in order to better take advantage of their integration in guaranteeing not only infrastructure and service resilience, but also resilience at an organizational level, tackling strategic and business risks. This will enable better inter-sector cooperation and integration, as well as an improved management of external dependencies, strengthening an entity's overall resilience. Business continuity is now ensured in all relevant aspects of the entity (critical and priority activities, as well as relevant support functions), including stress tests, as part of an broader exercise program, to evaluate and improve dependency management; crisis management is established, flexible and adaptative to respond to a wide range of scenarios, with appropriate escalation procedures.

Optimization would be the next step, with greater advantages from synergies being accomplished, and resilience considered in every part of critical infrastructure and services' lifecycle.

Other relevant challenges may include the development of a resilience culture to support the dissemination of resilience-relevant practices and policies, management commitment to resilience, adequate funding to ensure effective resilience methodology adoption and implementation, the emergence of new and more sophisticated threats, particularly when it comes to IT/OT, as well as geopolitical and economic instability.

5 Conclusions

Resilience has recently claimed a place in the limelight. Not that it hadn't already been one of the main concerns and objectives of both nations and organizations, for decades, but the challenges the world has been facing in recent years - with a special mention to climate-related events and natural disasters, the COVID-19 pandemic or the Russia-Ukraine conflict-, motivated by growingly powerful and far-reaching threat agents, resulted in an increased interest in the subject.

While there is not an unique definition of resilience, there is consensus in considering it key when it comes to critical infrastructures and entities, and associated essential services. The methods and approaches to achieve and enhance resilience are also varied, even though some organizational disciplines, such as risk management and business continuity are more times than not, referenced as essential.

There are different approaches that organizations can adopt to building and maintain resilience of critical infrastructures. It's often a combination of methodologies that can provide a robust framework that will cover the most significant aspects related to resilience.

Factors such as sector, context and maturity need to be taken into account when selecting methodologies to support resilience, as well as assess it. A purely segmented approach is often characteristic of entities still taking the first steps towards resilience, while progressively integrated and all-inclusive approaches typically translate a higher maturity. A gradual but steady evolution from a siloed perspective towards a holistic view of critical infrastructure and entities resilience, should be incentivized as the organization improves its resilience governance and articulation with its stakeholders.

Further research on this area should consider the definition of mechanisms to measure resilience, enabling the monitoring of metrics and indicators, and explore the definition of a maturity evaluation approach, as

outlined in this article, as complementary to the risk management - business continuity management framework, and provide a strategic roadmap to resilience enhancement.

References

- [1] Jungwirth R., Smith H., Willkomm E., Savolainen J., Alonso Villota M., Lebrun M., Aho A., Giannopoulos G., Hybrid threats: a comprehensive resilience ecosystem, Publications Office of the European Union, Luxembourg, 2023, doi:10.2760/37899, JRC129019.
- [2] OECD (2021) Building resilience: New strategies for strengthening infrastructure resilience and maintenance, <https://doi.org/10.1787/354aa2aa-en>
- [3] Dechy, N., Merad, M., Petersen, L., Pestana, M., Linkov, I., Dien, Y., Foresight for Risk Prevention and Resilience: to what Extent do they Overlap? Proceedings of the 53rd ESReDA Seminar, 14 – 15 November 2017, European Commission Joint Research Centre, Ispra, Italy
- [4] United Nations Office for Disaster Risk Reduction (www.unisdr.org/terminology/resilience)
- [5] 2020 Strategic Foresight Reports (https://commission.europa.eu/system/files/2021-04/strategic_foresight_report_2020_1_0.pdf)
- [6] International standard, ISO 22316:2017 Organizational resilience – Principles and attributes
- [7] Directive (EU) 2022/2557 of the European parliament and of the council of 14 December 2022 on the resilience of critical entities and repealing Council Directive 2008/114/EC, Official Journal of the European Union, 27 December 2022, L333/164
- [8] OECD (2019), Good Governance for Critical Infrastructure Resilience, OECD Reviews of Risk Management Policies, OECD Publishing, Paris. <https://doi.org/10.1787/02f0e5a0-en>
- [9] RESILENS: Realising European ReSILienCE for Critical INFraStructure (H2020 2014). <http://resilens.eu/resilens-outputs/> - D1.1 Resilience Evaluation and SOTA Summary Report
- [10] International standard, ISO 31000:2009 Risk Management – Principles and attributes
- [11] International standard, “Security and resilience — Business continuity management systems — Requirements”, ISO 22301:2019
- [12] International standard, “Security and resilience — Business continuity management systems — Guidelines for business impact analysis”, ISO 22317:2021
- [13] International Conference on Electricity Distribution, CIRED (<http://www.cired.net/cired-working-groups/resilience-of-distribution-grids>)
- [14] BCI Continuity and Resilience Report 2023 (<https://www.thebci.org/news/bci-launches-supply-chain-resilience-report-2023.html>)
- [15] International Energy Agency (<https://www.iea.org/reports/world-energy-outlook-2019/electricity>)
- [16] Steven M. Rinaldi, James P. Peerenboom, Terrence K. Kelly, (2001) Identifying, Understanding and Analyzing Critical Infrastructure Interdependencies, IEEE Control Systems Magazine, December 2001
- [17] Council directive 2008/114/EC of 8 December 2008 on the identification and designation of European critical infrastructures and the assessment of the need to improve their protection, Official Journal of the European Union, L345/75.
- [18] International standard, “Security and resilience — Organizational resilience — Principles and attributes, ISO 22316:2017
- [19] International standard, “Security and resilience — Business continuity management systems — Guidance on the use of ISO22301, ISO22313:2019
- [20] Ferreira, N., Lopes, H., Martins, C., Utilities response to extreme condition events – Edp Distribuição case 21st International Conference on Electricity Distribution, Frankfurt, 6-9 June 2011, paper0561
- [21] Alberto, P., Silva, I., Duarte, N., Rojão, T., Pestana, M., Increasing DSO's resilience by exercising business continuity plan 25st International Conference on Electricity Distribution, Madrid, 3-6 June 2019, paper13481
- [22] EDP 2022 Annual Integrated Report (<https://www.edp.com/en/2022-annual-integrated-report>)
- [23] International Conference on Electricity Distribution, CIRED, Resilience of distribution grids working group, ISSN 2684-1088, (<http://www.cired.net/files/download/204>)
- [24] International standard, “Security and resilience — Organizational resilience — Guidelines for supply chain continuity, ISO 22318:2015
- [25] BCI Supply chain Resilience Report 2023 ([BCI Launches Supply Chain Resilience Report 2023 | BCI \(thebci.org\)](https://www.thebci.org/))
- [26] EDP 2022 Sustainability report (https://www.edp.com/sites/default/files/2021-04/Sustainability%20Report%20EDP%202020_1.pdf)

2.18 Modelling of power disruption scenarios by PyPSA in the Baltic region

Isabel Asensio, Hrvoje Foretić, Vytis Kopustinskas, European Commission Joint Research Centre (JRC), Ispra, Italy



Modelling of power disruption scenarios by PyPSA in the Baltic Region

Isabel Asensio, Hrvoje Foretić, Vytis Kopustinskas

European Commission, Joint Research Centre (JRC)

63rd ESReDA Seminar, 25-26 October 2023

Objective and background

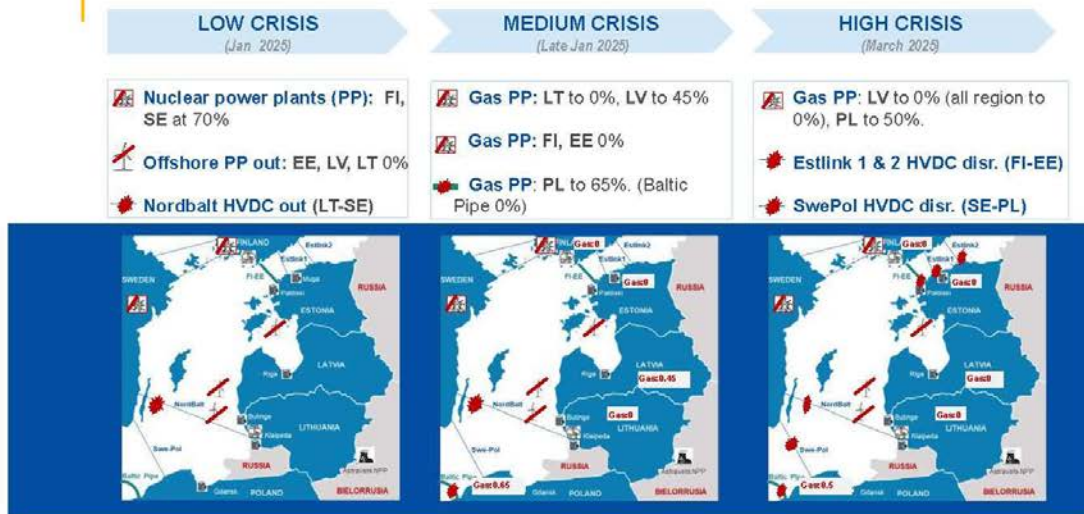
- This work was performed as a support activity for the tabletop exercise CORE23-B on **maritime critical energy infrastructure protection** that JRC co-organizes with NATO Energy Security Centre of Excellence
- The model simulates **electricity grid disruptions** stemming from incidents as defined in the exercise
- The **modeling results** indicate impact **to electricity supply in the Baltics**
 1. Which is the **critical energy maritime infrastructure** in the Baltics?
 2. Which are the **scenarios disruption** selected?
 3. How to assess the electricity grid disruptions? **Modelling by PyPSA**
 4. **Modelling results**

Critical Maritime Energy Infrastructure in Baltics 2025

| | Estonia | Latvia | Lithuania |
|----------------------|-------------------------|---------|----------------------|
| Offshore Wind | 500 MW | 1000 MW | 700 MW |
| Oil terminal | Paldiski, Muga | Riga | Butinge, Klaipeda |
| LNG terminal | | | Klaipeda FSRU |
| Power cable | Estlink1 / 2 (FI-EE) | | Nordbalt LT- SE |
| Gas pipeline | Baltic conn. FI-EE | | |
| Under Ground Storage | | | |



Three TTX Scenarios (consecutive from Jan to April 2025)



Modelling by PyPSA-Eur model

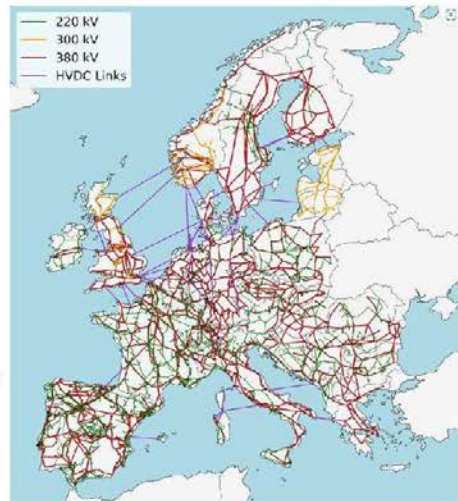
PyPSA-Eur is suitable for both **operational studies** and expansion planning studies

Modelling the European Network:

- 5000 buses
- 9600 (aggregated) generators
- 6000 AC lines & 60 HVDC links

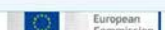
Main Features:

- Only freely available and **open data**
- Optimal power flow** w/ dispatch/unit commitment
- High temporal resolution** (hours-years)
- High spatial resolution** (from power plants to countries) & scope



Assumptions of input data: data source

| <u>Installed Capacity / demand applied</u> | <u>Other assumptions</u> | | | | | | | | |
|---|-------------------------------|-------------------------------|-------|------|-------|-----|-------|------|--|
| <ul style="list-style-type: none">• Installed capacity:<ul style="list-style-type: none">• Thermal: adapt to cap_entsoe2023.• RES: adjusted to 2025, based ERAA2022• Demand side response added (based on ERAA 2022)• Transmission lines capacities (TL)<table border="1"><thead><tr><th>Intercon countries</th><th>Interconnection capacity (MW)</th></tr></thead><tbody><tr><td>EE-LV</td><td>1100</td></tr><tr><td>LT-LV</td><td>950</td></tr><tr><td>EE-FI</td><td>1000</td></tr></tbody></table>• Demand: based on ERAA2022 (→ 2025) weather year 2016 | Intercon countries | Interconnection capacity (MW) | EE-LV | 1100 | LT-LV | 950 | EE-FI | 1000 | <ul style="list-style-type: none">• BRELL= 0.• Must-run for thermal PPs (OCGT/oil) in EE (FI/LT/LV) as per generation in ENTSO-E 2016.<ul style="list-style-type: none">• Relevant in EE (70% of inner generation based on oil shale units – must run units)• Hydro: initial level as of 2016• CCGT in LT: 1190 MW. Limited production as they are old (15% of max capacity) |
| Intercon countries | Interconnection capacity (MW) | | | | | | | | |
| EE-LV | 1100 | | | | | | | | |
| LT-LV | 950 | | | | | | | | |
| EE-FI | 1000 | | | | | | | | |



Model outcomes for the evaluation of grid disruptions

Energy flow



Electricity generation, cross border power exchange, interaction gas-oil

Lost load



Unserved energy
(generation adequacy)

Electricity Price



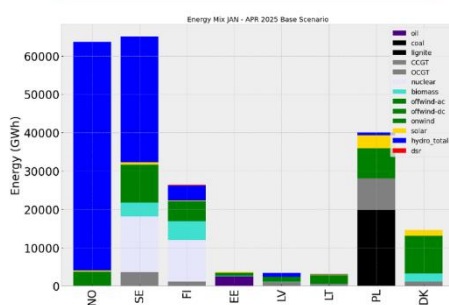
Wholesale market
price at perfect
competition (*)

(*) Sensitivity of CO₂ emissions (from 50 eur/ton to 0 eur/ton) has been also assessed



Base case (no disruption): generation & energy flow

Internal energy generation Jan-Apr (GWh)



Regional energy flow Jan-Apr 2025 (GWh)



INTERNAL GENERATION:

- Northern neighbours rely on hydro & nuclear (SE, FI)
- Baltics rely on off-shore wind, shale oil (EE) & gas (LV).
- PL relies on coal / lignite & gas

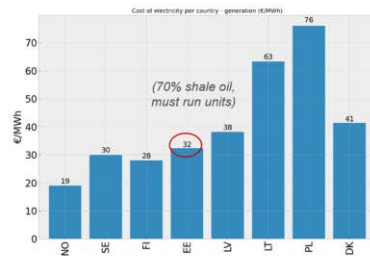
REGIONAL NET POSITION:

- Net exporters: NO, SE, EE, LV
- Net importers in the region: FI, LT, DK
- Load demand of EE, LV, LT is 5% of regional demand
- LT imports 30% of its demand from FI, EE, LV

Base case (no disruption): lost load & price

Average costs Jan-Apr 2025 (€/MWh)

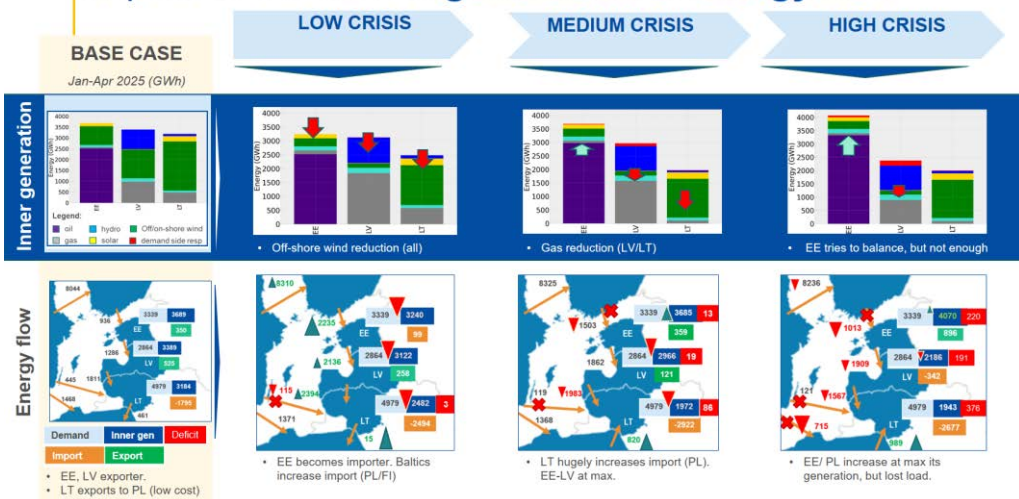
There is no lost load
in the base case

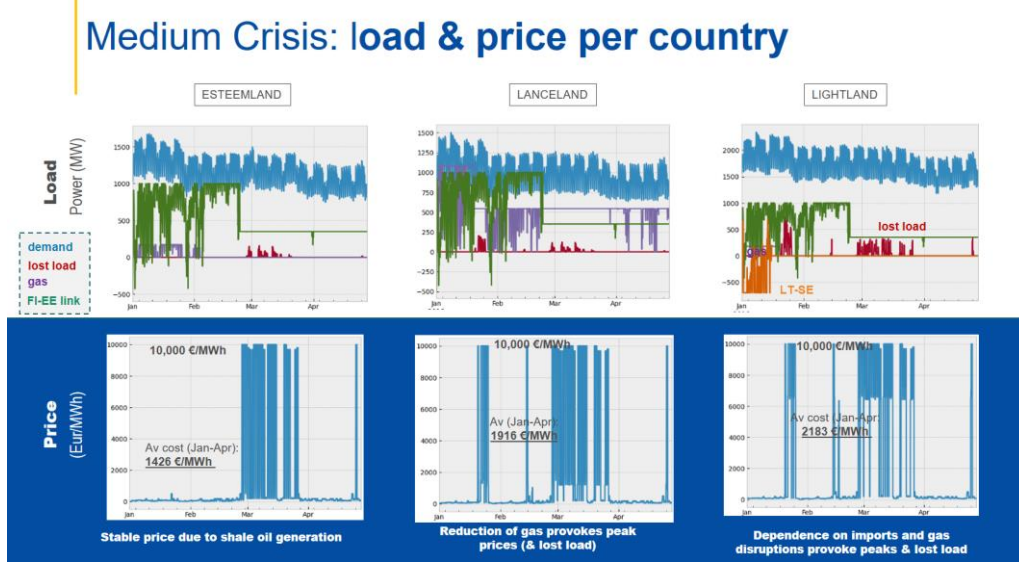
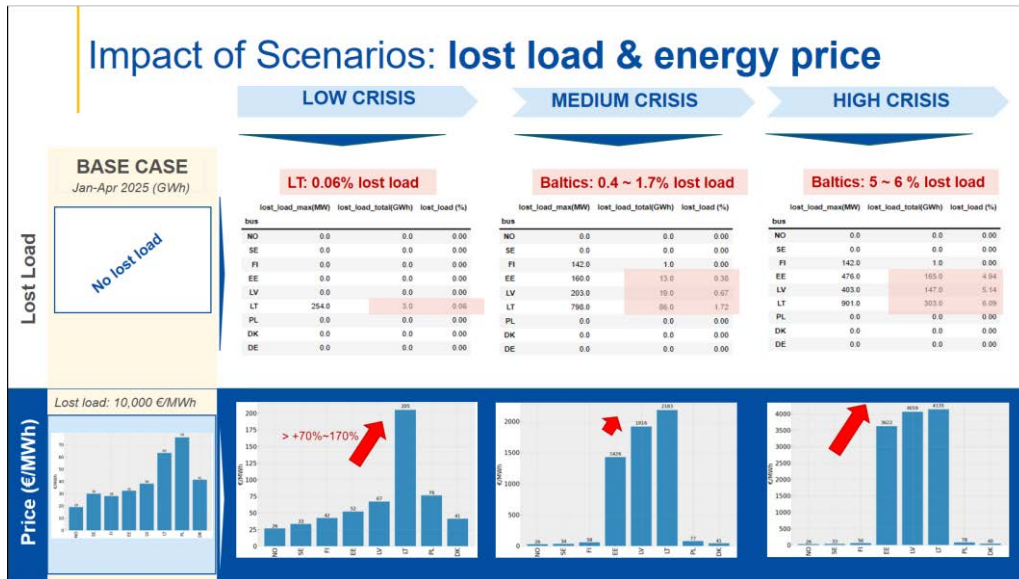


AVERAGE COSTS:

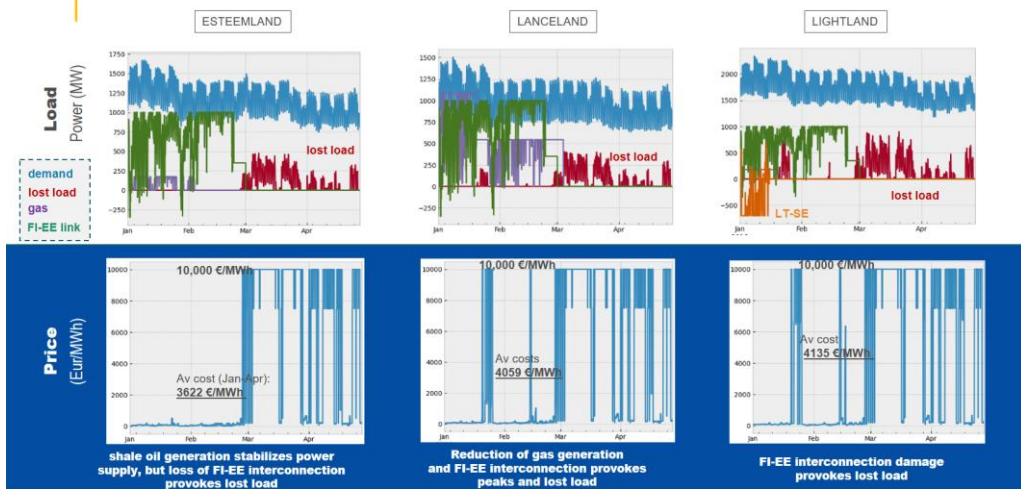
- There is no lost load
- The energy costs is lower in NO (mainly hydro) and higher in PL (relying on coal).
- Electricity generation in EE comes mainly from shale oil (70%), as these are must-run units. In EE, Unitary cost of electricity does not reflect the real cost (paid through heat / ancillary).

Impact of Scenarios: generation & energy flow

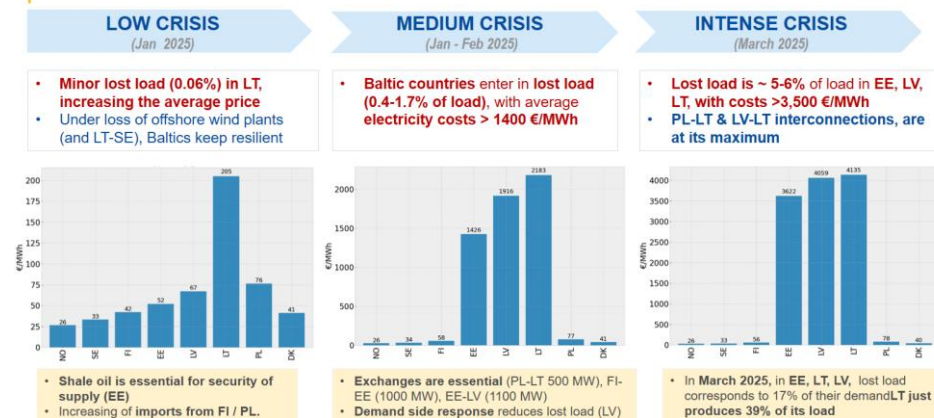




Intense crisis: load & price per country



Conclusions of electricity system disruptions impact (January – April 2025)



(*) Demand side response reaches 2% of LV load in Medium Crisis & 4% of load (8.3% of LV generation) in High Crisis Scenario

References

- 1 ENTSO-E Transparency Platform <https://transparency.entsoe.eu/>
- 2 European Resource Adequacy Assessment (ERA). 2022. <https://www.entsoe.eu/outlooks/eraa/>
- 3 Hoersch J., Hofmann F., Schlachtberger D., Brown T. 2018. PyPSA-Eur: An open optimisation model of the European transmission system. Energy Strategy Reviews, 22, 207-215.
- 4 Vasylius V., Jonaitis A., Gudžius S., Kopustinskas V. 2021. Multi-period optimal power flow for identification of critical elements in a country scale high voltage power grid, Reliability Engineering & System Safety, 216, 107959.

2.19 The Impact of Small Hydro Power Plants on the Adequacy of a Power System with High Penetration of Renewable Energy Sources

Jonas Vaičys, Saulius Gudžius, Audrius Jonaitis and Daivis Virbickas, Kaunas University of Technology, Lithuania, jonas.vaicys@ktu.lt, saulius.gudzius@ktu.lt, audrius.jonaitis@ktu.lt, daivis.virbickas@ktu.lt

Abstract

As the share of renewable energy sources in the power generation mix continues to rise, the necessity for dispatchable and sustainable renewable energy sources becomes crucial to maintain energy balance and ensure power system adequacy. With numerous countries, including Lithuania, aiming to achieve a 100% net share of renewable energy generation, an in-depth investigation is conducted to assess the adequacy of Lithuania's power system. This investigation emphasises small hydro power plants due to their dispatchable nature. The analysis is carried out at a national level, focusing on individual power systems without considering interconnections, and employs an open-source climate database provided by ENTSO-E. The adequacy model is formulated as a convex optimization problem, with the objective of minimizing energy not served. To enhance computational efficiency, clustering analysis is employed to identify the most representative climate years for the modelling process. In addition, separate day-ahead convex optimization models are integrated into the mathematical adequacy model to accurately simulate hourly generation for hydro pump storage and hydro run-of-river power plants. These separate models address the unique characteristics of these hydro power generation facilities. The findings of the analysis reveal that while the net generation of renewable energy sources may exceed 100%, the current storage capacities in island operation scenarios are inadequate in addressing power system adequacy concerns. Furthermore, the comparison between dispatchable and non-dispatchable hydro power plants generation strategies indicates that employing simple day-ahead optimization can lead to a reduction in energy not served by 0.001% per installed MW of small hydro power plant capacity. Lastly, the analysis demonstrates the point at which onshore wind and solar PV generation have a diminished impact on power system adequacy compared to small hydro power plants generation.

1 Introduction

Based on the findings from the IRENA World Energy Transitions Outlook 2023, it is evident that the global transition toward sustainable energy sources is currently falling short of expectations. To adhere to the critical 1.5-degree Celsius global temperature limit by the end of this century, a substantial and immediate reduction in global carbon emissions is imperative. This pressing need for change has accelerated the deployment of renewable energy sources (RES), which have significantly contributed to the composition of the final electricity supply mix over the past decade. Projections indicate that RES will continue to reshape the global energy supply landscape, reducing the reliance on fossil fuels, with a predicted increase from 28% to 91% of gross electricity production from renewables by 2050 (in the 1.5-degree scenario).[1].

While the electrification of the energy generation sector has yielded positive results in terms of emission reductions, the expansion of electrification into other industrial sectors has led to a substantial increase in energy demand. This surge in demand is expected to triple electricity generation between 2020 and 2050, necessitating a corresponding expansion in RES deployment. Accommodating these changes in generation dynamics, including decentralized generation, energy curtailment, and energy trading, becomes imperative.[2][3]

Energy production from wind and solar sources offers a sustainable alternative to fossil fuel-dominated generation, which has historically prevailed for centuries. However, the integration of these RES into the grid presents certain challenges. The primary challenge lies in the intermittent availability of energy production, often misaligned with energy demand. The high penetration of highly variable generation introduces grid vulnerabilities, elevating the risk of outages and grid instability. Ensuring grid stability requires both reliable energy production and energy sources capable of rapid adjustment in response to fluctuations in energy production. With the increasing production of RES, the demand for flexible generation has grown, with energy storage emerging as a widely adopted solution, encompassing batteries and hydro power plants.[4][5]

Following the closure of the Ignalina nuclear atomic power plant in 2007, which previously accounted for a significant portion of final energy consumption in the Baltic region (specific numbers pending verification), Lithuania became heavily reliant on Russian gas to maintain stable energy production. Over the past decade, Lithuania has embarked on a remarkable energy transition, transitioning from fossil fuel-powered power

plants to RES such as solar and wind.[6] As of 2023, Lithuania boasts close to 2 GW of installed RES capacity, with plans to more than triple this figure by 2030, reaching 7 GW of total installed capacity of RES. This transformative shift is epitomized by the ambitious 1400 MW Offshore Wind project, set to become the Baltic region's inaugural offshore wind farm.[7].

In 2012, aligned with the European Union and United Nations' commitment to the Paris Agreement and the evolving energy landscape, Lithuania set an ambitious target: achieving 100% of its electricity consumption and 80% of final energy consumption sourced from RES. This aligns with the EU Green Deal's overarching objectives of attaining climate neutrality by 2050.

The National Energy Independence Strategy [8] emphasizes the urgency of completing synchronization with the continental European electricity network by 2025. This strategic imperative is motivated by the goals of meeting electricity demand through sustainable energy sources and achieving energy independence, a particularly critical consideration given recent geopolitical developments. Energy self-sufficiency and grid stability have always been instrumental in upholding grid reliability. The synchronization with continental Europe, coupled with the expanding penetration of RES, has underscored the need for reliable must-run units [9] and enhanced flexibility.

As previously noted, the transition to RES highlights the pivotal role of fast-response power generation units in ensuring system reliability. Small hybrid power plants have long served as reliable distributed energy sources for many smaller towns and villages worldwide. Lithuania is no exception, with small hydroelectric power plants (HPPs) playing a significant role. In contrast to large-scale power plants, small HPPs do not require extensive dam infrastructure or large water reservoirs. Like their larger counterparts, small HPPs can be planned to be despatched and respond rapidly as needed, offering valuable grid support and flexibility.[10][11]

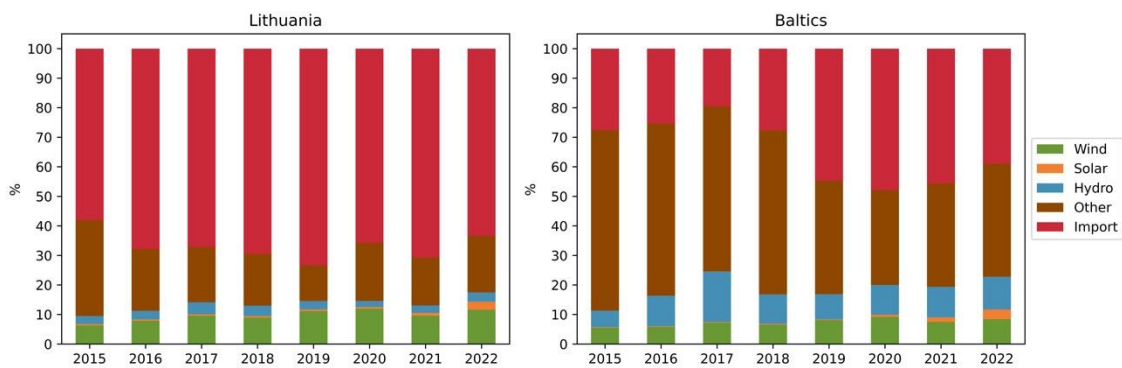
The aim of this paper is to illustrate the impact of small HPPs on the generation adequacy of Lithuania power system. This is particularly significant because the main traditional base generation units in Lithuania were decommissioned in 2007, leading to a heavy reliance on energy imports. The structure of the paper is divided in 4 main parts: problem statement, methodology, results, and conclusions. Case study and data used is described in problem statement part, whereas data analysis, adequacy model and sensitivity analysis flow chart are stated in the methodology part. Finally, results and conclusions are provided.

Comprehensive overview of the problem, methodology and outcomes of this research potentially can benefit future assessments of generation adequacy of any power system. The findings may play a crucial role in determining whether it is more advisable to decommission or reinvest in aging small HPPs.

2 Problem Statement

Since Ignalina Nuclear PP was shut down, the entire Baltic (Lithuania, Latvia, and Estonia) power system has increasingly relied on imports. Figure 1 demonstrates that during last 8 years there has been little substantial change in this trend and Lithuania is in local generation deficit by importing around 60 % of its energy needs from abroad. Additionally, the Lithuanian Hydro Association reports that nearly half of the currently installed small HPPs were constructed prior to the 2000s. As these aging small HPPs approach the need for refurbishments, including upgrades to their electrical and structural components, questions arise about whether to decommission them or invest in their renewal.

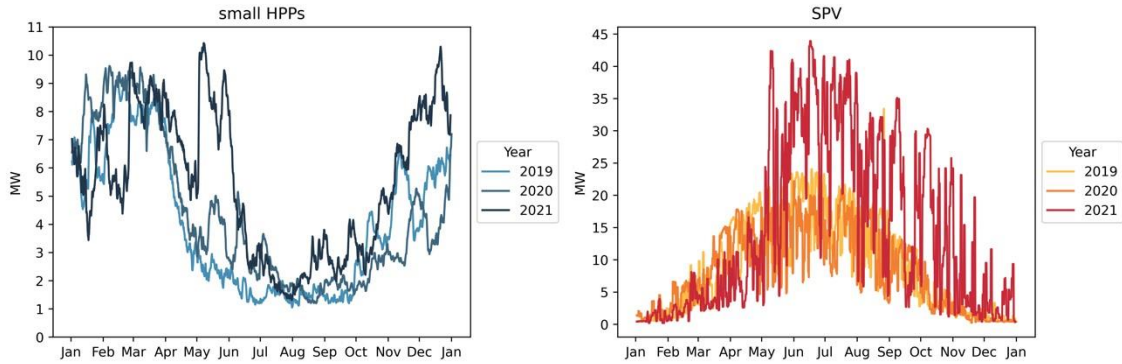
Figure 1. Total generation mix and imports in Lithuania (a) and Baltics (b) in 2015-2022.



Source: ENTSO-E, 2023.

HPPs contribute a relatively small share to the overall generation mix, however, they possess distinct characteristics compared to solar photovoltaics (SPV), onshore wind (OW), and offshore wind (OWO). Figure 2 illustrates the availability of primary energy sources for HPPs and SPV during different seasons from 2019 to 2022. During the summer season (Figure 1a), HPPs face challenges related to water inflow, while SPV generation predominates (Figure 1b), and vice versa. As a result, small HPPs have the potential to address the issue of low SPV generation during winter and transitional seasons.

Figure 2. 24-hour moving average of hourly generation of small HPPs (a) and SPV (b) in 2019-2022.



Source: Lithuanian Hydropower Association (a) and ENTSO-E (b), 2022.

According to the National Energy Independence Strategy [8], Lithuania plans to install a total capacity of 2 GW of solar PV, 3.6 GW of onshore wind, 1.4 GW of offshore wind, and 126 MW of hydro run-of-the-river (ROR) by 2030. As indicated in Table 1, when considering various RES capacity factors used for Lithuania by ENTSO-E in European Resource Adequacy Assessment (ERAA), this would potentially account for a 145.45% net share of Lithuania's end consumption, equivalent to 15 TWh. However, it is essential to highlight in this paper that achieving a renewable energy share of 100% or higher in the energy mix does not inherently guarantee power system adequacy. As previously discussed, different types of RES exhibit diverse seasonal patterns, and periods characterized by low wind and solar PV generation can occur. Addressing these challenges requires the integration of storage, base generation, or dispatchable generation sources.

The power system of Lithuania is quite unique due to its large energy storage setup, originally designed as a backup for Ignalina Nuclear PP. Kruonis Hydro Pump Storage (HPS) plant has a substantial capacity of 900 MW and can store 10.8 GWh of energy, equivalent to 12 hours of generator/pump mode at maximum capacity. While Kruonis HPS is vital for Lithuania's shift to green energy, we investigate whether it is sufficient to cover periods when wind and solar PV generation are low in 2030 by optimizing its charging/discharging patterns in power system adequacy model described in the methodology part.

Table 1. RES installed capacity and its net share in end consumption in Lithuania in 2030.

| Energy Source | Installed Capacity, MW | Capacity Factor | Net Share (%) |
|---------------|------------------------|-----------------|---------------|
| Solar PV | 2000 | 0.114 | 13.4 |
| Wind onshore | 3600 | 0.423 | 89.2 |
| Wind offshore | 1400 | 0.481 | 39.4 |
| Hydro (ROR) | 126 | 0.467 | 3.45 |

Source: National Energy Independence Strategy [8], 2018.

For a comprehensive modelling of various RES, this research leverages a large climate dataset made available through ENTSO-E ERAA 2022 [12]. This dataset covers a span of N=35 years, ranging from 1982 to 2016, and includes hourly data ($\Delta t=1$) for onshore wind, offshore wind, solar PV generation, and electricity

load. Additionally, it provides daily ($\Delta t=24$) records of water inflows in ROR HPPs. Importantly, this dataset takes into consideration the capacity factors (CF) of future technologies in Lithuania projected for the analysed year 2030.

Data analysis step is used as an initial and crucial step not only to understand the climatic patterns of Lithuania, but also to perform detailed research as efficiently as possible. Different clustering techniques, such as k-means, k-medoids and hierarchical (agglomerative and divisive) were employed prior to adequacy modelling. However, in the methodology, we focus on the selected clustering technique utilized for modelling purposes.

Two distinct adequacy models are developed to assess the significance of the small HPPs' dispatch capabilities. In one model, the generation from small HPPs is uniformly distributed across different hours of the day. In the second model, the total daily water energy inflow is optimized and dispatched on an hourly basis using convex optimization techniques. Subsequently, both adequacy models are used to calculate the energy not served (ENS) and a parameter denoted as γ . This parameter represents the reduction in ENS per installed RES megawatt (MW). The purpose of deriving parameter γ is to enable an objective comparison of the impact of various RES sources on power system adequacy. Emphasis is placed on identifying the threshold at which small dispatchable and nondispatchable HPPs have an equivalent impact on power system adequacy as solar PV and onshore wind. Further elaboration on the methodology is provided in subsequent sections, offering a more detailed explanation.

3 Methodology

The methodology consists of 3 main parts: different climate year analysis using hierarchical clustering technique, power system adequacy assessment as convex optimization problem statement, and the analysis of the impact of small HPPs on reducing ENS in comparison with other RES as the total installed capacity of each solar PV and onshore wind increases.

3.1 Clustering Analysis

Given that the climate years dataset spans across $N=35$ years, encompassing hourly data ($\Delta t=1$) for onshore wind, offshore wind, solar PV generation, and electricity load, along with daily data ($\Delta t=24$) for water inflows in ROR HPPs, the average climate year \mathbf{m} is computed as a vector comprising 5 average values, each representing one of the climatic variable:

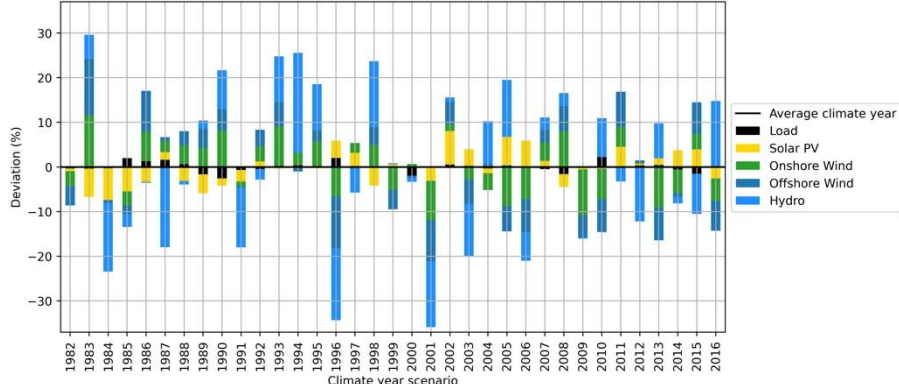
$$\mathbf{m} = \begin{bmatrix} m^{SPV} \\ m^{OW} \\ m^{OWO} \\ m^H \\ m^L \end{bmatrix} = \frac{1}{N} \begin{bmatrix} \sum_{n=1982}^{N=2016} \sum_{t=1}^{T=8760} SPV_{n,t} \\ \sum_{n=1982}^{N=2016} \sum_{t=1}^{T=8760} OW_{n,t} \\ \sum_{n=1982}^{N=2016} \sum_{t=1}^{T=8760} OWO_{n,t} \\ \sum_{n=1982}^{N=2016} \sum_{t=1}^{T=365} H_{n,t} \\ \sum_{n=1982}^{N=2016} \sum_{t=1}^{T=8760} L_{n,t} \end{bmatrix} \quad (1)$$

Then, the deviation matrix $\boldsymbol{\delta}$ of size equal to 35×5 is calculated and it consists of climate year deviations vectors $\boldsymbol{\delta}^*$, which represent to the difference between each climatic variable in climate year n and its corresponding value in the average climate year \mathbf{m} .

$$\boldsymbol{\delta}_n = \begin{bmatrix} \delta^{SPV} \\ \delta^{OW} \\ \delta^{OWO} \\ \delta^H \\ \delta^L \end{bmatrix} = \begin{bmatrix} \frac{\sum_{t=1}^{T=8760} SPV_{n,t} - m^{SPV}}{m^{SPV}} \\ \frac{\sum_{t=1}^{T=8760} OW_{n,t} - m^{OW}}{m^{OW}} \\ \frac{\sum_{t=1}^{T=8760} OWO_{n,t} - m^{OWO}}{m^{OWO}} \\ \frac{\sum_{t=1}^{T=365} H_{n,t} - m^H}{m^H} \\ \frac{\sum_{t=1}^{T=8760} L_{n,t} - m^L}{m^L} \end{bmatrix}, \forall n \in N \quad (2)$$

Deviation matrix $\boldsymbol{\delta}$ can be graphically represented as in Fig. 3, where each column represents climate year deviations vectors $\boldsymbol{\delta}^*$.

Figure 3. Deviations from average climate year of all climate years.



Source: ENTSO-E, 2022.

We start our cluster analysis by constructing an initial distance matrix that captures the dissimilarity between different climate years. This matrix is based on the Euclidean distance between climate year pairs, calculated using the following formula (Eq. 3):

$$d_{ij} = \sqrt{(\partial_i^{SPV} - \partial_j^{SPV})^2 + (\partial_i^{OW} - \partial_j^{OW})^2 + (\partial_i^{OWO} - \partial_j^{OWO})^2 + (\partial_i^H - \partial_j^H)^2 + (\partial_i^L - \partial_j^L)^2}, \forall i, j \in N \quad (3)$$

Then we continue clustering analysis by adopting Ward's Method as the linkage function to determine which climate years or their clusters to merge into a single cluster. This method operates by minimizing the Error Sum of Squares, denoted as $ESS(X)$ in Eq. 4. $ESS(X)$ represents the cumulative squared differences within the clusters and is designed to ensure that the growth in $ESS(X)$ is minimized at each merging stage in the agglomerative clustering. The distances between clusters are then computed according to Eq. 5

$$ESS(X) = \sum_{i=1}^{N_X} \left| x_i - \frac{1}{N_X} \sum_{j=1}^{N_X} x_j \right|^2 \quad (4)$$

$$d(X, Y) = ESS(X, Y) - ESS(X) - ESS(Y) \quad (5)$$

This cluster merging process is repeated until the hierarchical tree-like structure, known as a dendrogram, is formed. Fig. 3 represents the climate years clustering analysis results. The tree is cut at distance equal to 20 so that climate years are grouped into 8 clusters (typical years).

Figure 4. Climate year clustering dendrogram.

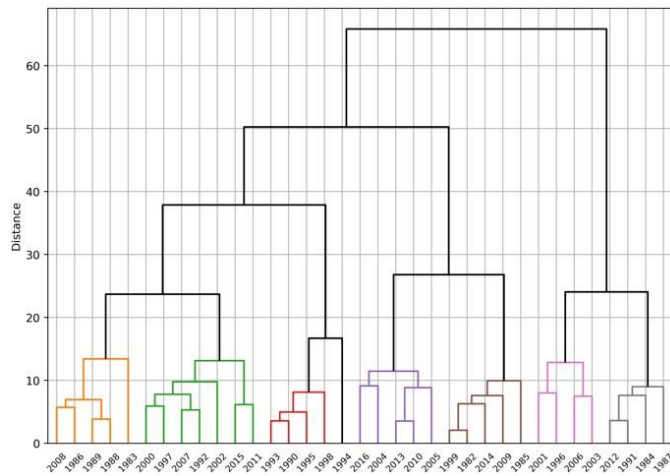


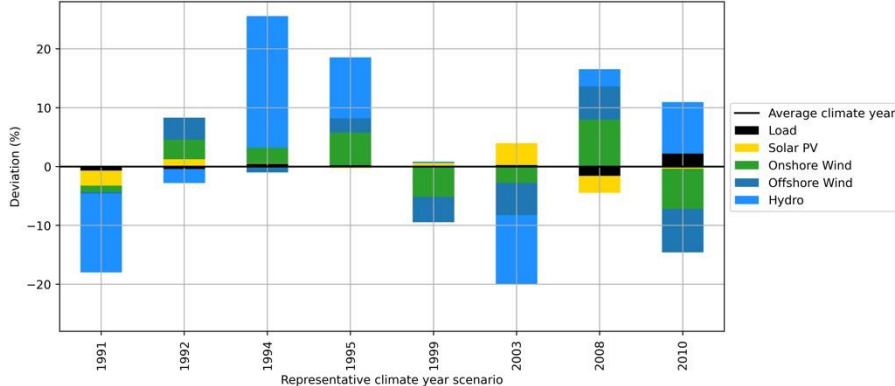
Table 1 shows which climate year is selected to represent each cluster and it also indicates that each cluster has different number of climate years. The number of climate years in cluster determines its weight. The weights are further used in power adequacy model when calculating weighted average of energy not served (ENS) of 8 representative climate years instead of calculating the average of all N=35 climate years.

Table 1. Clustering results and weights of each representative climate year.

| Cluster No. | Representative climate year | Number of climate years (Weight) |
|-------------|-----------------------------|----------------------------------|
| 1 | 1991 | 4 |
| 2 | 1992 | 7 |
| 3 | 1994 | 1 |
| 4 | 1995 | 4 |
| 5 | 1999 | 5 |
| 6 | 2003 | 4 |
| 7 | 2008 | 5 |
| 8 | 2010 | 5 |

Based on the outcomes of the clustering analysis, an improved version of Figure 3 (depicted as Figure 5) is generated. This updated figure showcases eight climate years that serve as representatives. Among these climate years, 2010 (weighted at 5) is characterized by higher load and reduced wind onshore and wind offshore generation. In contrast, 2008 (also weighted at 5) is associated with lower load and higher generation onshore wind, offshore wind, and hydro. The remaining climate years fall into transitional categories, exhibiting intermediate characteristics.

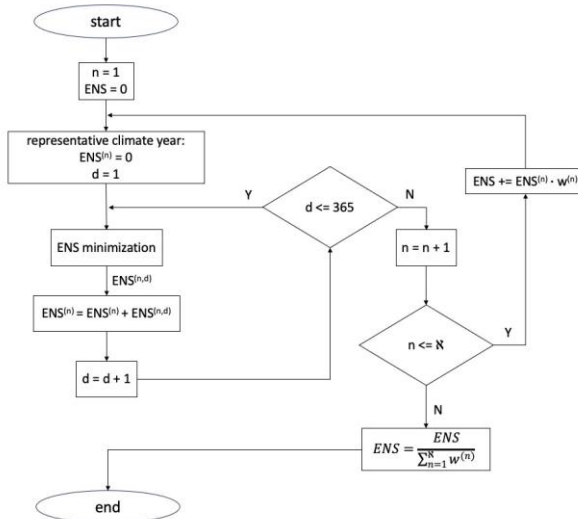
Figure 5. Deviations from average climate year of representative climate years.



3.2 Power System Adequacy Model

The power system adequacy analysis is performed following the process depicted in the flowchart presented in Figure 6. This flowchart illustrates the utilization of representative climate years and their corresponding weights in the final ENS calculation. Each climate year is subdivided into 365 days, thereby each day consists of 24 hourly data points for onshore wind, offshore wind, solar PV generation, and electricity load, as well as a single value for total daily water inflows in ROR HPPs. Central to this analysis is the power system adequacy model, which seeks to minimize ENS. Notably, the problem includes hourly energy storage optimization, which is expressed as a convex problem following the approach outlined by [13]. Furthermore, it is essential to underscore that the proposed power system adequacy model remains versatile and can be applied under various assumptions that align with, but are not limited to, the conditions delineated in Equations 6-7.

Figure 6. Power system adequacy analysis flow chart.



Although charging and discharging efficiencies and prices conditions can be relaxed, it is practical to express it as in Equations 6-7, where ϕ – curtailment penalization constant:

$$0 < \eta_{ch} < 1 < \eta_{dch} \quad (6)$$

$$c_{ch} < 0 < \phi < c_{dch} < VoLL \quad (7)$$

The power system adequacy model can be mathematically expressed as a linear (convex) problem, focusing on the minimization of ENS and operation costs over a 24-hour horizon (Equation 8). Given that the Lithuanian power system under examination comprises solely RES and energy storage, the objective function

can be simplified to minimize the costs associated with energy storage charging, discharging, generation curtailment, and ENS without individual pricing considerations for each RES component, as shown in Equation 8a. The prioritization of RES generation over energy storage and ENS is achieved through the power balance equation (Equation 8b). Further constraints are established to govern the minimum and maximum state of charge (SOC) of energy storage (Equations 8c-8d), as well as the minimum and maximum power limits of hydro power plants, energy storage charging and discharging, ENS, and curtailment (Equations 8e-8n).

Lastly, Equations 8o and 8p are used interchangeably when analysing the impact of small dispatchable and nondispatchable HPPs on Lithuanian power system adequacy. Equation 8o is used in case of small dispatchable HPPs as it introduces a constraint concerning a total daily water energy inflow in hydro power plants while Equation 8p. distributes total daily water energy inflows among all hours in a day equally.

o. f.:

$$\min_{p_H, p_{ch}, p_{dch}, ENS, p_{cu}} \sum_{t=1}^{T=24} p_{ch}^{(t)} c_{ch} - p_{dch}^{(t)} c_{dch} + p_{cu}^{(t)} \phi + ENS^{(t)} \cdot VoLL \quad (8a)$$

s. t.:

$$p_{OW}^{(t)} + p_{OWO}^{(t)} + p_{SPV}^{(t)} + p_H^{(t)} - p_{ch}^{(t)} + p_{dch}^{(t)} - p_{cu}^{(t)} + ENS^{(t)} = L^{(t)}, \forall t = 1, \dots, 24 \quad (8b)$$

$$E - E_0 + \sum_{n=1}^t (\eta_{dch} p_{dch}^{(n)} - \eta_{ch} p_{ch}^{(n)}) \leq 0, \forall t = 1, \dots, 24 \quad (8c)$$

$$E_0 + \sum_{n=1}^t (\eta_{ch} p_{ch}^{(n)} - \eta_{dch} p_{dch}^{(n)}) - \bar{E} \leq 0, \forall t = 1, \dots, 24 \quad (8d)$$

$$\underline{p}_H \leq p_H^{(t)} \leq \bar{p}_H, \forall t = 1, \dots, 24 \quad (8e-8f)$$

$$\underline{p}_{ch} \leq p_{ch}^{(t)} \leq \bar{p}_{ch}, \forall t = 1, \dots, 24 \quad (8g-8h)$$

$$\bar{p}_{dch} \leq p_{dch}^{(t)} \leq \bar{p}_{dch}, \forall t = 1, \dots, 24 \quad (8i-8j)$$

$$0 \leq ENS^{(t)} \leq L^{(t)}, \forall t = 1, \dots, 24 \quad (8k-8l)$$

$$0 \leq p_{cu}^{(t)} \leq p_{OW}^{(t)} + p_{OWO}^{(t)} + p_{SPV}^{(t)}, \forall t = 1, \dots, 24 \quad (8m-8n)$$

$$0 \leq \sum_{t=1}^{T=24} p_H^{(t)} \leq p_{H24} \quad (8o)$$

$$p_H^{(t)} = \frac{p_{H24}}{24} \quad (8p)$$

3.3 Analysis of Impact of Small HPPs on Power System Adequacy

As Lithuania strives to achieve its ambitious renewable energy goals by installing new solar PV, wind onshore and wind offshore capacities, the role of other RES with limited expansion potential, such as small HPPs, comes into question. The key point of this research is to determine the threshold at which small dispatchable and nondispatchable HPPs exert an equivalent influence on power system adequacy as solar PV and onshore wind. Despite the relatively low net share of small HPPs in the total generation mix, it is essential to assess their effectiveness in ensuring power system adequacy.

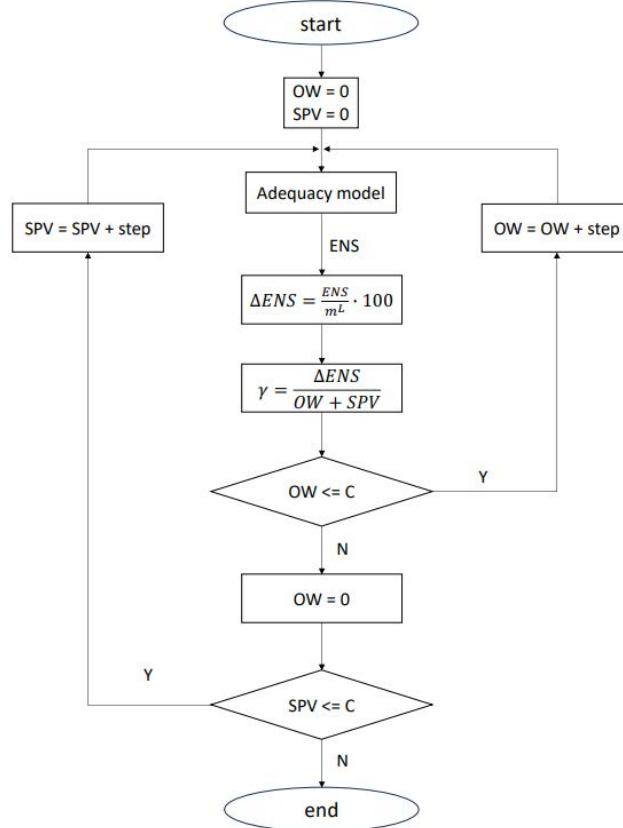
To perform such analysis, the adequacy models described in section 3.2 are used to calculate ENS and the γ parameter, as expressed in Equation 9. This parameter represents the reduction in ENS per installed solar PV and wind onshore megawatt (MW) and is expressed as a fraction in average climate year total load (15 TWh). As illustrated in the flow chart in figure 7, ΔENS and γ parameters are calculated across different levels of

solar PV and onshore wind penetration (up to installed capacity $C=4000$ MW), facilitating the creation of a heatmap depicting the γ parameter's behaviour under different scenarios.

$$\gamma = \frac{\Delta ENS}{SPV + OW}$$

9

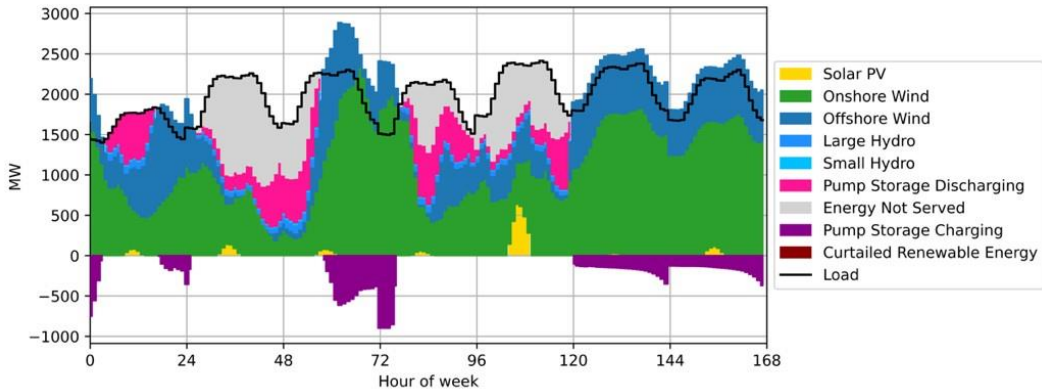
Figure 7. Analysis of impact of small HPPs on power system adequacy flow chart.



4 Results

As illustrated in Figure 8, it becomes evident that the power system adequacy model functions according to its design: it accurately represents the behaviour of solar PV, onshore wind, and offshore wind, allowing them to operate according to its weather conditions. It then activates HPPs and HPS only when necessary. Furthermore, in cases of surplus RES generation, the HPS is charged, aligning with expectations. The depicted sample week in Figure 8 serves as a potential realization of Lithuania's local generation mix in 2030, a year when the net share of RES in end consumption is projected to reach 145.45%. An analysis of the extended periods of ENS in grey reveals that even a 900 MW HPS operating for 12 hours cannot fully address the challenge of shifting variable RES generation to hours of low RES output.

Figure 8. Sample power adequacy modelling week in 2030

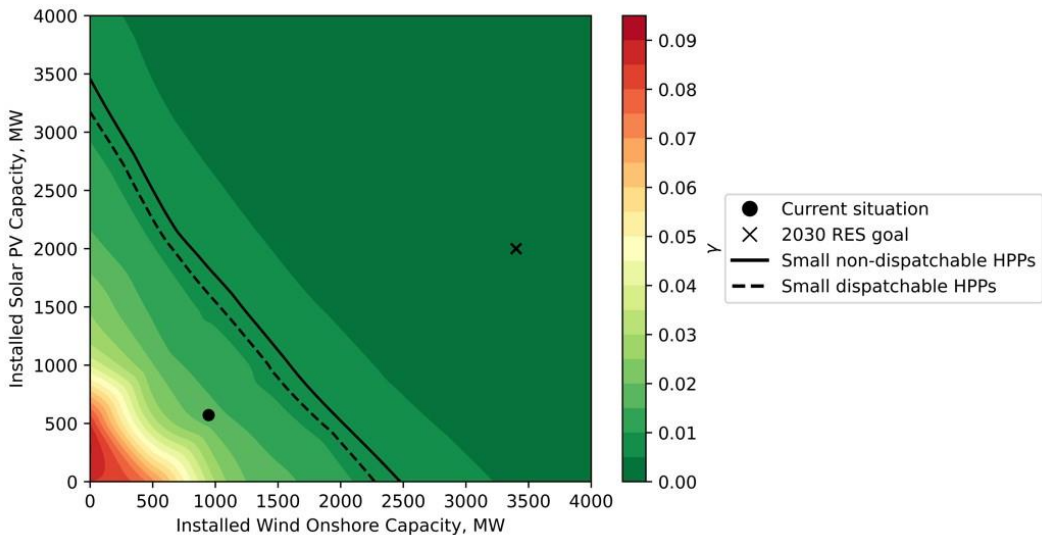


In Figure 9, we observe the γ parameter heatmap at varying levels of solar PV and onshore wind penetration. The pattern is clear: as the combined installed capacity of solar PV and onshore wind increases, the corresponding γ value decreases. It's worth noting that onshore wind tends to saturate slightly faster than solar PV. This is primarily since wind generation is more prominent during nighttime, coinciding with lower electricity demand, unlike solar PV generation.

However, the most critical takeaway from this illustration is that Lithuania's National RES goal for 2030 falls significantly short of achieving higher γ values. This suggests that even the addition of approximately 2 GW of either onshore wind or solar PV, or a combination of both, would have only a minimal impact on Lithuania's power system adequacy. Furthermore, it can be concluded that challenges with ENS, which we observed in Figure 8, can and should be solved effectively, i.e., by any other but not by weather based solar PV, onshore wind, or offshore wind generation.

Additionally, two threshold lines have been included to indicate the scenarios in which the installed capacities of onshore wind and solar PV would yield the same γ value as that of small non-dispatchable and small dispatchable HPPs. This analysis leads to the conclusion that investing in small HPP control systems, which utilize simple day-ahead optimization, could potentially reduce ENS by 0.001% for each installed MW of small HPP capacity. This reduction of ENS could result in significant socioeconomic benefit for Lithuania, considering the publicly available VoLL (4620 Eur/MWh). [14]

Figure 9. γ parameter heatmap at different penetration levels solar PV and onshore wind.



5 Conclusions

To model various RES generation in different climate conditions, large amount of data is necessary. In our analysis, clustering analysis is used to identify representative climate years to increase modelling efficiency. 8 typical climate years are selected to capture the variability in renewable generation patterns. Two threshold lines are drawn to indicate the scenarios in which onshore wind and solar PV generation have an equivalent impact on power system adequacy as small HPPs. This analysis underscores the potential effectiveness of small HPPs.

The study formulates a power system adequacy model as a convex optimization problem with the aim of minimizing energy not served (ENS), which is a key criterion in evaluating system adequacy and wise transition to RES. This model considers hourly generation, energy storage, and the unique characteristics of hydro power plants. The study highlights the challenges associated with integrating highly variable RES into the grid, including the need for flexible generation and energy storage solutions.

The study indicates that Lithuania's 2030 RES goals fall short of achieving higher levels of power system adequacy. Even the addition of 2 GW of onshore wind or solar PV, or a combination of both, would have a minimal impact on adequacy. On the other hand, if wind, solar PV, and flexible hydro generation would be considered as an integral whole, that could bring a significant positive impact on adequacy. Small HPPs emerge as valuable assets in addressing the intermittency of renewable generation, particularly during periods of low wind and solar output. The research demonstrates that employing simple day-ahead optimization can lead to a reduction in ENS by 0.001% per installed MW of small HPP capacity, potentially resulting in significant socioeconomic benefits.

The research focuses on the critical role of small HPPs in ensuring power system adequacy in the face of increasing RES integration. It emphasizes the need for a comprehensive approach that combines renewable generation, energy storage, and optimization strategies to meet the challenges of a transitioning energy landscape. Additionally, the study's findings provide valuable insights for future assessments of generation adequacy and investment decisions in the energy sector. Managerial implications of this study reveal that EU policy makers, when developing energy regulations and support schemes aimed at full transition to RES, should consider the wind, solar PV, and flexible generation (like hydro, which is already in place and does not require lengthy development) as an integral whole that could bring a significant positive impact on adequacy.

Acknowledgements

The authors would like to express their sincere gratitude to Dainius Markauskas for invaluable guidance and support throughout this research. The collaboration and insights from Lithuanian Hydro Association were instrumental in the success of this research.

References

1. IRENA, World Energy Transitions Outlook 2023: 1.5°C Pathway. International Renewable Energy Agency, Editions Eyrolles N° 1, Abu Dhabi, 2023.
2. Machado, R., et al. Estimating the Adequacy Revenue Considering Long-Term Reliability in a Renewable Power System. *Energy*, Vol. 243, 2022.
3. Ma, J., et al. Comprehensive Probabilistic Assessment on Capacity Adequacy and Flexibility of Generation Resources. *International Journal of Electrical Power & Energy Systems*, Vol. 145, 2023.
4. Xu,T., et al. The Implementation Limitation of Variable Renewable Energies and its Impacts on the Public Power Grid. *Energy*, Vol. 239, 2022.
5. Qays, M., et al. System Strength Shortfall Challenges for Renewable Energy-Based Power Systems: A Review. *Renewable and Sustainable Energy Reviews*, Vol. 183, 2023.
6. Sattich, T., et al. Searching for Energy Independence, Finding Renewables? Energy Security Perceptions and Renewable Energy Policy in Lithuania. *Political Geography*, Vol. 96, 2022.
7. Wind Europe, Lithuania Kicks off Offshore Wind with First 700 MW Auction. Brussels, 2023.
8. Ministry of Energy of the Republic of Lithuania, The National Energy Independence Strategy. Lithuania, 2018.
9. Didsayabutra, P., et al. Defining the Must-Run and Must-Take Units in a Deregulated Market. *IEEE Transactions on Industry Applications*, Vol. 38, 2002, pp. 596-601.
10. Doolla, S. and Bhatti, T. S. Automatic Generation Control of an Isolated Small-Hydro Power Plant. *Electric Power Systems Research*, Vol. 76, 2006, pp. 889-896.

11. Bulatov, Yu N., et al. Group Predictive Voltage and Frequency Regulators for Small Hydro Power Plant in the Context of Low Power Quality. *Renewable Energy*, Vol. 200, 2022, pp. 571-578.
12. ENTSO-E, European Resource Adequacy Assessment 2022 Edition. Brussels, 2022.
13. Garifi, K., et al. Non-Simultaneous Charging and Discharging Guarantees in Energy Storage System Models for Home Energy Management Systems. 2018.
14. ACER, Study on the estimation of the value of lost load of electricity supply in Europe. Brussels, 2018.

List of abbreviations and definitions

| | |
|-----|---------------------|
| CF | Capacity Factor |
| ENS | Energy Not Served |
| H | Hydro |
| HPS | Hydro Pump Storage |
| L | Load |
| OW | Wind onshore |
| OWO | Wind offshore |
| PP | Power Plant |
| ROR | Run-of-the-river |
| SPV | Solar photovoltaics |

2.20 Evaluation matrix to select appropriate countermeasures for Offshore Wind Farm protection

Babette Tecklenburg, Alexander Gabriel, Arto Niemi, Frank Sill Torres, The Institute for the Protection of Maritime Infrastructures, German Aerospace Center, Bremerhaven, Germany, Babette.tecklenburg@dlr.de

Abstract

The extension targets for the German offshore windfarms are quite ambitious. Until today around 8 GW of capacity is installed. The extension goal for 2030 is 30 GW in the North and Baltic sea. One option to increase the offshore capacity is to repower old Wind Turbines (WT). Even though that is a valid option also more areas need to be dedicated to the Offshore Wind Farms (OWFs). Because the offshore wind industry is not the only stakeholder within the German exclusive economic zone, it is possible that a co-use of the areas dedicated to the OWFs is introduced. In the end of April 2023, a collision between a WT and a vessel took place. It has to be noted that it seems like that the detection of the unauthorized vessel within the OWF has not been noticed. With this work it should be investigated how existing and future countermeasures can be evaluated. Therefore, this work presents an evaluation scheme to assess the suitability of a countermeasure. The focus thereby is to include multiple aspects for example the scope of the countermeasure, timely restrictions or mechanism of action considered. The developed framework has then been applied to exemplary countermeasures within OWFs and blind spots within the combination of multiple countermeasures have been determined.

1 Introduction

Offshore Wind Farms (OWFs) are characterized by their special location. Placing OWFs in the German North and Baltic seas enables a higher production rate in comparison to onshore wind farms. The average offshore Wind Turbine (WT) produces 5.9 MW. While the average onshore WT in the 40 largest windfarms in Germany only produces 2.25 MW. Due to the exposed location of OWFs other threats and risks are relevant than for an onshore wind farm. A previous work focused on the definition of threats for an OWF (see [1]). Among others the risk of a collision of a vessel into an offshore platform a WT have been stated by many interview participants [1].

That this is a realistic risk could be seen on April 24th 2023. The vessel "Peträ L" was on its way from Szczecin (Poland) to Antwerp (Netherlands) [2]. The Peträ L is a cargo vessel with a total length of 73,66 m and sails under the flag of Antigua Barbuda [3]. She was loaded with 1,500 tons of grain and was manned by 6 crew members (3 officers and 3 workers) [2, 4]. In that evening of the same day, she sailed using the autopilot in the German EEZ and entered the 500m safety zone of the wind farm "Gode Wind 1" (see Figure 55). It was neither noticed by the vessel crew nor by the control centre of the OWFs. The result was that the Peträ L rammed a wind turbine (WT) (see Figure 55) [2]. Damage occurred to the ship and wind turbine. A hole of about 5 by 3 meters was torn in the bow of the vessel but no one was injured [2, 5]. At the wind turbine, the boat landing was destroyed but only minor damages to the tower of the WT were caused [2]. The vessel interrupted the journey and headed towards the port of Emden [4] where it arrived in the morning of the 25th of April. What is interesting about this incident is that, according to media reports, the collision was not initially noticed in remote monitoring or on a distant working vessel [2].

This incident shows that the mechanism of action of a countermeasure does not always match the associated risk. Therefore, this paper focuses on the development of a multi-criteria evaluation approach for countermeasures in the offshore wind industry. The authors understand countermeasures in accordance to the resilience measures defined by the CER directive "resilience of critical entities" [21]. Following the directive resilience measures are for example the physical protection of infrastructures as well as the appropriate training for the employees. [c.f. 21] The evaluation approach should consider all infrastructure parts (WTs, Offshore substations, High voltage direct current converter station and entire OWF). In the second section the layout of OWFs is described. Furthermore, current approaches to assess the suitability of countermeasures are described. The third section describes the methods brainstorming and Key Performance Indicators (KPIs). In the following section the development process of the proposed framework is described. A case study is performed in the fifth section.

Figure 55: Schematic course of the Petra L



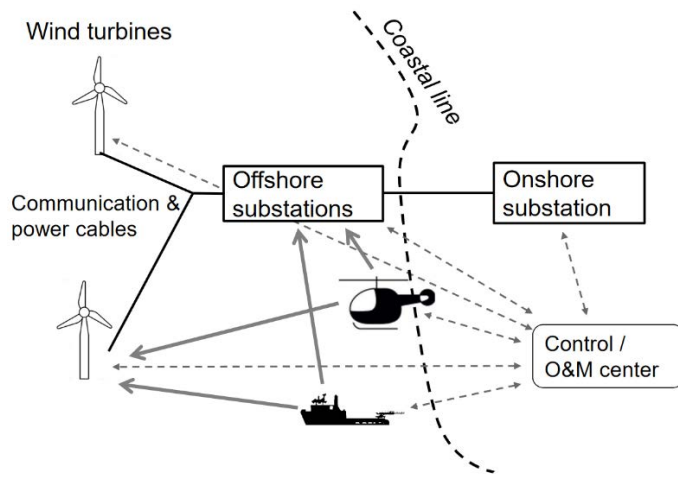
Source: by authors, following [6]

2 Background

2.1 Layout of an OWF

An OWF comprises of multiple WTs, an offshore substation and an underwater cable to connect the farm to shore (see Figure 56). The WTs produce the offshore electricity which is by the inner grid transported to the offshore substation. The Offshore Substation (OSS) transforms the energy. Then it is forwarded to the High Voltage Direct Current Converter station (HVDCC) which collects the energy of multiple OWFs and changes the type of current. In the last step, the energy is transported to the shore. An onshore substation feeds the electricity into the land based power grid. [7, 8] A loss of a HVDCC would have significant consequences, as the energy produced in multiple OWFs could not be fed into the grid. An HVDCC consists of a top structure which include workshops, operation rooms and accommodation facilities. The top structure is built onto a support structure. Staff and parts are transported to the HVDCC either by vessel or by helicopter. For these purposes the HVDCC has a pier and a helicopter landing deck. [8] The OWFs are monitored through an onshore control room. With a SCADA system the operators in the control room receive information about the current and past operating states of all infrastructure elements. Furthermore they also supervise the offshore crews and vessels in the windfarm. [9]

Figure 56: Schematic structure of an OWF



Source: [10]

2.2 Assessment of countermeasures

Different approaches exist to assess the suitability of a countermeasure. In this section the following should be presented: exercise/ experiment, simulation and theoretical approach. During the experimental approach the countermeasure of interest is studied in the real world. The countermeasure is installed in either the real application or in a laboratory environment. The experimenter then tests if the countermeasure detects attacks and how the countermeasure can be overcome. This approach is very common in IT security domain. Moro et al. for example studied the robustness of selected software schemes against fault injection on embedded programs. Thereby they focused on microcontroller. [11] The benefit of this experimental approach is that the countermeasure is tested in the real application conditions and that therefore cross sensitivities regarding for example lights or humidity can be excluded. Another approach would be to simulate the infrastructure and the planned countermeasures. A common approach is to study for example if the attacker is successful [12]. This approach is especially useful for large facilities where the installation on a trial basis is time consuming. The other advantage is that multiple configurations can be tested and the best suited one can later be installed. One example for this approach is Marroni et al. They determined fragility models for a chemical plant. The aim is to determine the likelihood that the Physical Protection Systems resist an explosive attack. Therefore they studied multiple scenarios. [13] The last approach is a theoretical approach. Thereby a set of criteria and categories are defined in advance. Then, each countermeasure is evaluated based on the criteria. After a comparison of the countermeasures the best suitable for the application is selected. The advantage of this approach is that it is a rather abstract approach. No detailed information about the infrastructure layout is necessary. One example is the work presented by Brauner et al. [12].

3 Method

The result of this work should be a visual evaluation scheme for the selection of countermeasures in OWFs. The evaluation scheme is based on KPIs to assess the characteristics of countermeasures. The KPIs have been developed based on a brainstorming.

3.1 Brainstorming

In 1953 brainstorming was introduced into the business world by the marketing expert Alex F. Osborn. Brainstorming is an intuitive-creative technique. [14] Thereby it is based on the principle of free association. It can either be performed individually or in a group. For a group brainstorming the ideal number of team members is between five and seven participants. [15] Antosch-Bardohn describes that instead of a group brainstorming, an individual brainstorming of the single team members with a following comparison of the results produces more ideas. One reason for this is, that the thought process of individual team members is interrupted or even disturbed by the expressed ideas by others. [14] Brainstorming is a fast technique. It should take between 20 and 40 minutes. [14, 15] The following four rules should be followed: let the thoughts run free (every idea is welcome, wrong or nonsense thoughts do not exist), switch off critic (evaluation of thoughts or ideas takes place later), quantity is more important than quality (not all ideas are useful, therefore the focus should be on many ideas) and take the ideas of the team members up (All ideas can be used by the other team members which leads to combination of ideas and improvement). [15]

3.2 Key Performance Indicators

KPIs were originally introduced by the business administration. Companies try to evaluate their performance with them. In the first approaches before 1992 only financial aspects were the focus. After 1992 three more aspects have been considered Customer, Internal Process as well as Learning and Growth. KPIs should support the management to determine whether or not the company is successful. Thereby the indicator can either be qualitative or quantitative. [16] Other authors as Peterson argue that KPIs should be a rate or a ratio or even a percentage but not a raw number. So that the statement of the number is more meaningful. [17] According to literature around 10 KPIs is a suitable number [16].

In recent years, the application of KPIs has not only been limited to the business administration discipline. It has been also introduced into other domains such as safety and security or maintenance. In the following, a few literature examples will be presented to show the variety of usage.

Gabriel and Sill Torres published a work which defines KPIs to determine the safety and security of an OWF. Thereby they focus on the following aspects: composition and layout, operation and maintenance, position and environment among others. An example one indicator evaluates the distance between the OWF and the coastline. Depending on the context of the indicator the rating schema has two or three options. [18]

Saihi et al. focused on the sustainability of maintenance. Their approach is thereby rather general and not limited to one infrastructure. First, they defined the KPIs and evaluated them with experts. They defined the three pillars “Environmental”, “Social” and “Economic”. Each pillar includes categories, sub-categories and indicators. In the pillar “environmental” for example the category “resource use” is included. One sub-category is “land use” with the indicators “Maintenance waste effect on land quality” and “Maintained systems waste effect on land quality”. Each indicator can be ranked on a scale from one to five. [19]

4 Development Framework

This section describes the development and the visualisation of the framework. In the beginning of the development process, the authors performed an individual brainstorming and later the researchers discussed the results of the brainstorming in the group. The topic thereby was the collection of possible criteria to assess the suitability of countermeasures. The research question for the brainstorming was: What are possible dimensions to determine the suitability of a countermeasure? The word cloud in Figure 57 shows the results of this comparison after the brainstorming.

Figure 57: word cloud with the results of the brainstorming



Source: Authors

Some of the ideas have a similar meaning but are used different words. One example is the involvement of a person and autonomous or not. Therefore, the possible indicators are organized into groups of the same main topic and some of them are renamed or even deleted (in case they were double). Also for each indicator the possible values are defined. Depending on the content of the indicator that can be either qualitative or quantitative. An overview of the categories and indicators including a description of the indicator and the scale can be seen in Table 10.

Table 10: Overview of the Categories and KPI's including a short description as well as a scale

| Category | Indicator | Description | Scale |
|----------------------|-------------------|---|-------------------|
| Financial | acquisition cost | Describes the cost to purchase the countermeasure including material and personal costs. | Low, medium, high |
| | maintenance costs | Describes the efforts to maintain the countermeasure material- and personal costs are included. | Low, medium, high |
| | Human yes/ no | Describes if staff members are necessary to conduct countermeasure. | Yes and no |
| Performance criteria | Selectivity | Describes how often false alarms take place. | Low, medium, high |

| | | | |
|-------------------|------------------------|--|--|
| | Effectivity | Describes the intended reaction of the countermeasure | No info, only info, loud alarm and countermeasure initiate |
| | Speciality | Describes against how many attack vectors the countermeasure is effective | Between 1 and 5 (below water, above water, air, land, internal) |
| Location | Infrastructure level | Describes in what infrastructure the countermeasure is implemented | HVDCC, OSS, WT and cable |
| | Effect level | Describes where the countermeasure is effective | HVDCC, OSS, WT and cable |
| Time | Preventive or reactive | Describes if the countermeasure can initiate a reaction or not | Preventive or reactive |
| | Downtimes | Describes the duration of downtime after a reaction of the countermeasure is triggered | Seconds, minutes, hours, days, weeks |
| Device properties | Stationary or portable | Describes if the countermeasure is moveable or not. | Stationary or portable |
| | Size of countermeasure | Describes the amount of room a countermeasure needs | No additional space, mm ³ , cm ³ , dm ³ , room filling or multiple rooms affected |

Furthermore, a documentation of the KPIs has been written. It describes the KPI in more detail than in Table 10. In addition, the evaluation categories are described in more detail. To illustrate them better, an exemplary classification is described. In the following an extract of the documentation regarding the "maintenance costs" is presented.

This category describes the maintenance costs (MC) for a countermeasure. This includes worn parts, such as filters, but also spare parts or, if necessary, personnel costs to carry out the countermeasure. Again, the values are divided into "Low", "Medium" and "High" (see Table 11). Low maintenance costs would be, for example, if it is only necessary to check once a year whether the functionality is still given. Medium maintenance costs are when worn parts have to be replaced to an appropriate extent. High maintenance costs exist if specialized personnel must be permanently employed or if high-quality spare parts and worn parts must be regularly replaced.

Example smoke detector without connection to the professional fire department: The maintenance costs are low, since the functionality only has to be tested every year or even less frequently.

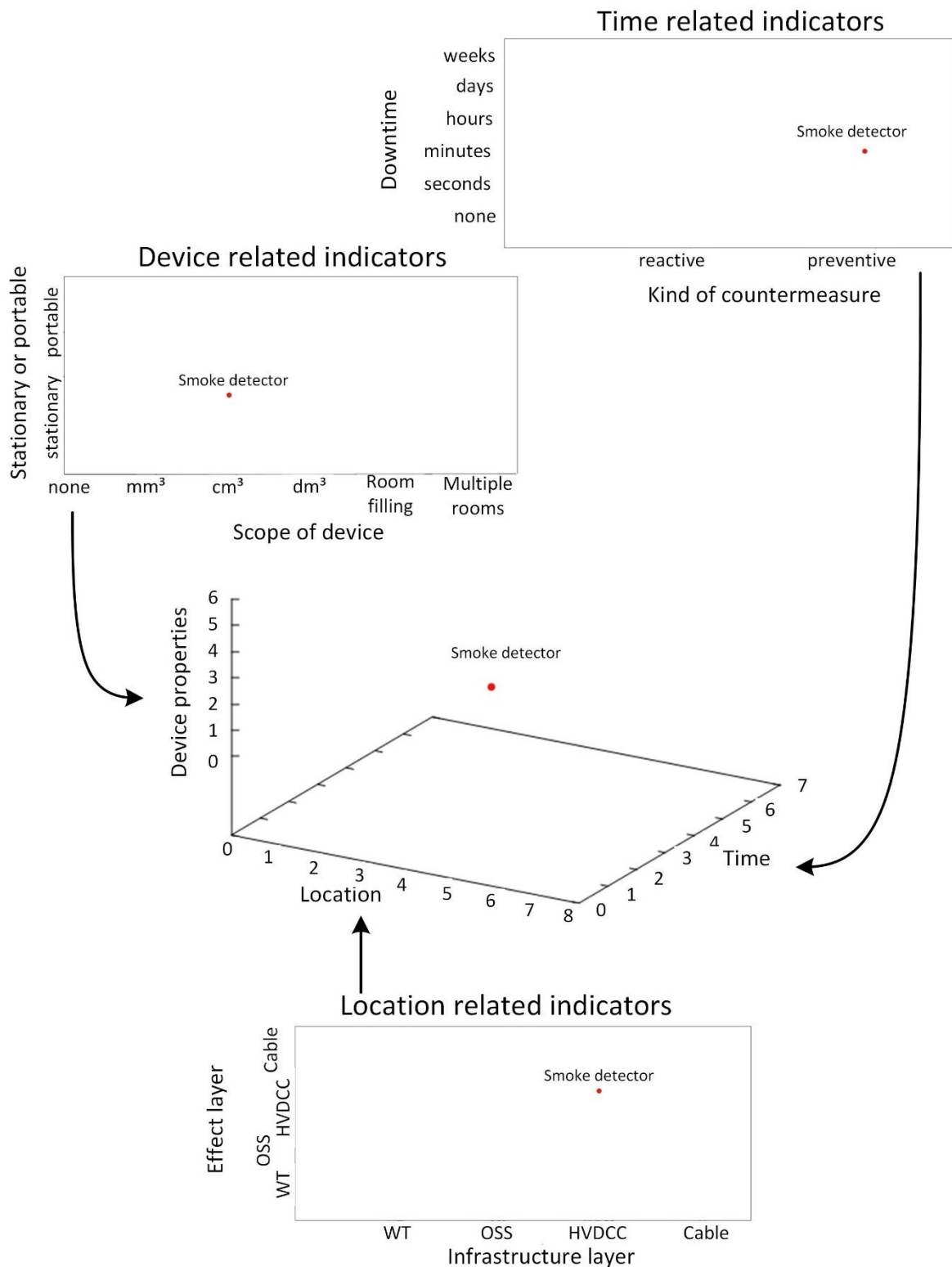
Table 11: Thresholds for the different values within the "maintenance costs" category

| Value | Threshold |
|---------------|--------------------------------------|
| Low | $\leq 100 \text{ €/ year}$ |
| Medium | $200 < MC/ year \leq 1000 \text{ €}$ |
| High | $> 1000 \text{ €/ year}$ |

In addition, a graphical representation of the KPIs has been developed. First for each category an overview of the related indicators has been designed. For selected combinations also two or three categories are compared. To summarize the indicators the length of the vector has been determined. Eq. (1) exemplarily shows the length for the category “time”. Depending on the content of the category depiction is either a two or three dimensional scatter diagram (see Figure 58).

$$Value_{Time} = \sqrt{Value_{downtime}^2 + Value_{preventiv or preactive}^2} \quad (1)$$

Figure 58: Different options to visualize the indicators



Source: Authors

5 Case study

For a case study the countermeasures in a generic OWF were studied. In 2021 the authors conducted interviews with stakeholders from the German offshore wind industry. In total 28 participants with different backgrounds like authorities, operators or maintenance companies were interviewed. For more information regarding the interviews see [20]. One part of the interview also focused on the countermeasures which the interview participants have installed. Figure 59 shows some of the mentioned countermeasures in the interviews.

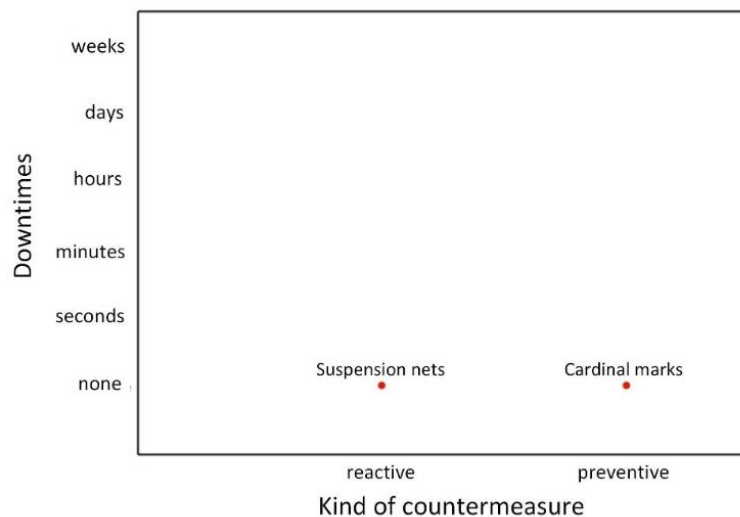
Figure 59: Mentioned countermeasures by the interview participants



Source: [20]

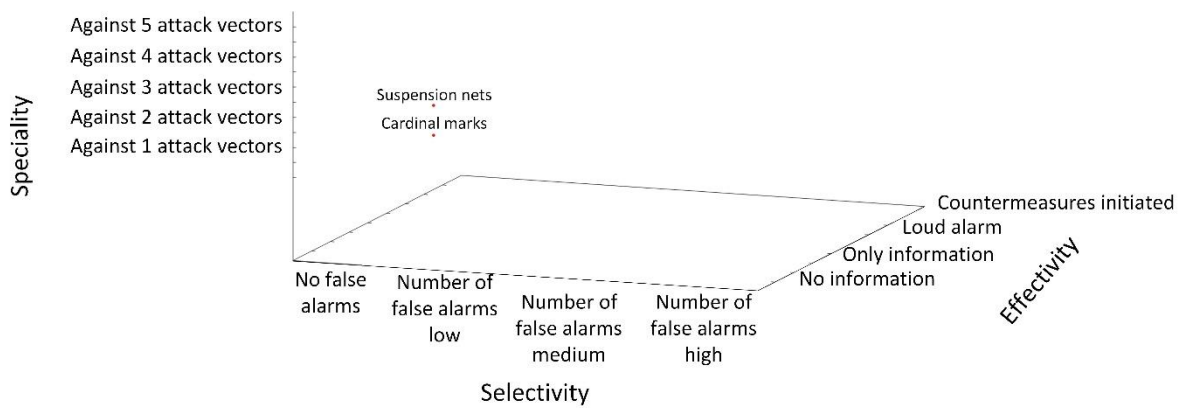
As a first comparison the authors picked cardinal marks. They are the green and red buoys to mark the waterway or point our hazardous areas. An interesting comparison partner would be suspension nets. As the name indicates they are metal nets which are stretched between infrastructures. The aim is to have a physical barrier that inhibits vessels or underwater vehicles to enter the protected area. Figure 60 shows the time related indicators for the countermeasure “suspension nets” and “cardinal marks”. It can be seen that both of the countermeasures cause no downtime. This can be explained by the fact that neither of them do not trigger any further actions. Assuming that they perform their intended use, the WTs can still produce energy. A difference between them is that cardinal marks belong to the preventive countermeasure. It informs the captains of the passing vessels about the presence of hazards. In case that the captain intentionally or unintentionally avoids this information, no further action originated from the buoys will take place. On the other hand, suspension nets belong to the reactive countermeasures. They do not only inform passing vessels and people that they cannot move on. They actively hinder vessels and people from entering to the protected area.

Figure 60: Comparison of cardinal marks and suspension nets in regard to time



Source: Authors

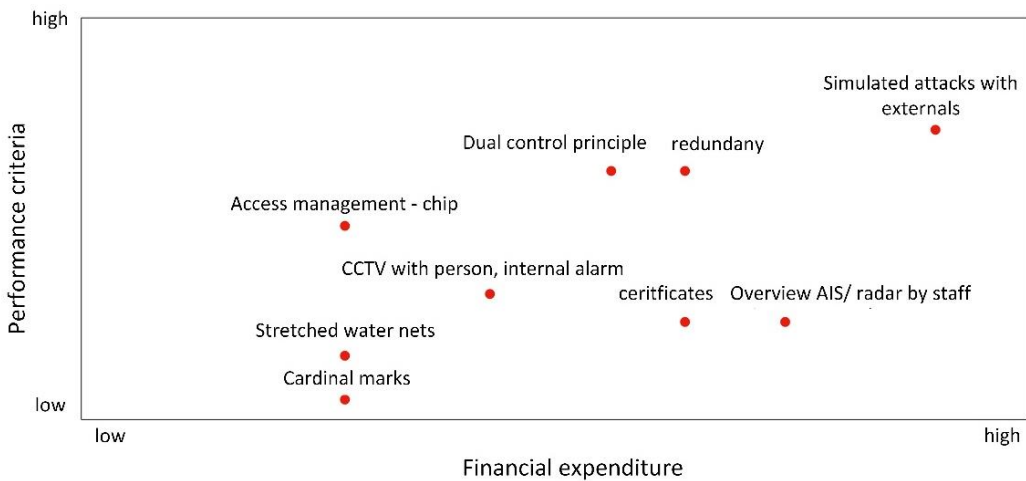
Figure 61: Comparison of cardinal marks and suspension nets in regard to the performance criteria



Source: Authors

Figure 61 illustrates the performance criteria of both countermeasures. It can be seen that both of them are quite similar in terms of selectivity and effectivity. But vary in terms of speciality. Cardinal marks only protect against one attack vector. While suspension nets prevent attacks against two attack vectors. For cardinal marks the attack vector is "above water". There the buoy's body can be seen. So, passing vessels receive the information where the hazard is located. Technically it can also be seen from the air. But the hazard it alerts to, is not relevant in the air vehicles. So "air" is not a relevant attack vector. Under water the chain is visible but the information where the hazard occurs is missing. Therefore "under water" cannot be accounted as a protected attack vector. In contrast, the suspension nets are stretched above the waterline but also a significant part is located below the waterline. Therefore, both attack vectors have been chosen. Against an internal attack this countermeasure is not effective because it is visible and therefore a possible attacker knows about it and will find other ways to reach the desired area.

Figure 62: Comparison of different countermeasures



Source: Authors

Figure 62 shows a comparison of different security-oriented countermeasures. For comparison the two main categories "performance criteria" and "financial expenditure" have been chosen. It can be seen that the countermeasures cover in terms of the financial expenditures mostly the middle part of the scale. With the outlier "simulated attacks" which are more at the end of the scale. In terms of the performance criteria the countermeasures cover almost everything from the bottom to the top of the scale. But with the majority of the countermeasures in the middle part of the scale. The left part and parts of the upper middle are empty. So, no countermeasures with the criteria are considered. In a real application that could mean no countermeasures with this portfolio have been installed. For the comparison of the "performance criteria" and "financial expenditure" it needs to be said that a high performance criteria with low financial expenditure is unlikely to be achieved.

6 Discussion and conclusions

With this work the authors propose a framework to determine the resilience capacity of possible countermeasures. This is highly relevant considering recent legislative developments in European Union. A directive on critical entities resilience was approved with following definition:

"Resilience' means a critical entity's ability to prevent, protect against, respond to, resist, mitigate, absorb, accommodate and recover from an incident" [21]

First, the definition names possible objects of application. An OWF consists of multiple infrastructures which are physically connected and share a common goal. Therefore, the authors would argue that an OWF is a system. Furthermore, the definition points multiple characteristics that a system should have, namely "resist, absorb, accommodate and recover".

Our proposed framework can help the operator to determine the resistance of the OWF. With for example the indicator "Speciality" provides information how many attack vectors are covered. The next characteristic in the definition is "to absorb". Here the author would like to point out the indicators "preventive/ reactive" and "effectivity". The relevant characteristic is "reactive" and "countermeasure initiated". These characteristics point out countermeasures which does not only identify a hazard but also interrupt the mechanism of attack or accident. So, the OWF "absorbs" the hazard. In this development stage the framework has no indicator that illustrates the characteristic "to accommodate". But through the depictions as examples are shown in Figure 62 "blind spots", which no countermeasure supports, can be determined and specifically searched for suitable countermeasures. The skill "recover" is presented through the indicator "downtime" which illustrates how quickly the countermeasure can operate again after triggering. With these criteria in mind the proposed framework can contribute to the resilience engineering of OWFs.

Moreover, based on multiple criteria such as costs or performance criteria the countermeasures can be evaluated. The framework has been applied to the offshore wind industry. Furthermore, uncovered spots in the protection landscape can be determined and suitable countermeasures can be searched purposefully. The framework has been tested in a first approach with countermeasures from the offshore wind industry. The

plan for future work is to validate the criteria and characteristic of the criteria with stakeholders in the offshore wind industry and test it in the real world example. Also interesting could be to test the framework with countermeasures from a different industry.

Acknowledgements

This conference contribution is part of the research project Applied Research on Resilience-driven Offshore Wind Farm Safety and Security (ARROWS) which is financed by the German Aerospace Centre.

References

1. Gabriel A, Tecklenburg B, Sill Torres F. Threat and Risk Scenarios for Offshore Wind Farms and an Approach to their Assessment. In: ISCRAM 2022 Conference Proceedings – 19th International Conference on Information Systems for Crisis Response and Management; 2022. p. 162–73 [last access: 2022 Nov 11]. Available from: URL: https://idl.iscram.org/files/alexandergabriel/2022/2407_AlexanderGabriel_eta2022.pdf.
2. Schiff fährt gegen Offshore-Windrad: Kollision offiziell bestätigt. NDR; 2023 [last access: 2023 Aug 8]. Available from: URL: https://www.ndr.de/nachrichten/niedersachsen/oldenburg_ostfriesland/Schiff-fahrt-gegen-Offshore-Windrad-Kollision-offiziell-bestaeigt,schiff1390.html.
3. marinetricc. Petra L; 2023 [last access: 2023 Aug 8]. Available from: URL: https://www.marinetraffic.com/en/ais/details/ships/shipid:361457/mmsi:304559000/imo:8205187/vessel:MARIA_G.
4. Täglicher Hafenbericht. Jetzt ermittelt die BSU zum Seeunfall „Petra L“; 2023 [last access: 2023 Aug 8]. Available from: URL: <https://www.thb.info/rubriken/maritime-sicherheit/detail/news/jetzt-ermittelt-die-bsu-zum-seeunfall-der-petra-l.html>.
5. Küstenmotorschiff läuft mit riesengroßem Loch in der Bordwand in Emdener Hafen ein: Offenbar Kollision mit Offshore-Windkraftanlage. NonstopNews; 2023 [last access: 2023 Aug 8]. Available from: URL: <https://www.nonstopnews.de/meldung/41767>.
6. Voytenko M. Stückgutfrachter kollidiert mit Windkraftanlage, beschädigt, Nordsee; 2023 [last access: 2023 Aug 8]. Available from: URL: <https://www.fleetmon.com/maritime-news/2023/41741/general-cargo-ship-collided-wind-turbine-damaged-n/>.
7. Hau E. Windkraftanlagen. Heidelberg: SpringerLink; 2014.
8. Robak S, Raczkowski RM. Substations for offshore wind farms: a review from the perspective of the needs of the Polish wind energy sector. Bulletin of The Polish Academy of Sciences: Technical Sciences 2018; 66(4).
9. MacAskill A, Mitchell P. Offshore wind-an overview. WENE 2013; 2(4):374–83.
10. Sill Torres F, Kulev N, Skobiej B, Meyer M, Eichhorn O, Schäfer-Frey J. Indicator-based Safety and Security Assessment of Offshore Wind Farms. In: 2020 Resilience Week (RWS); 2020. p. 26–33.
11. Moro N, Heydemann K, Dehibaoui A, Robisson B, Encrenaz E. Experimental evaluation of two software countermeasures against fault attacks; 2014 IEEE International Symposium on Hardware-Oriented Security and Trust (HOST) 2014.
12. Brauner F, Maertens J, Bracker H, Mudimu OA, Lechleuthner A. Determination of the effectiveness of security measures for low probability but high consequence events: A comparison of multi-agent-simulation & process modelling by experts. In: ISCRAM 2015: The 12th International Conference on Information Systems for Crisis Response and Management 24-27 May in Kristiansand, Norway; 2015 [cited 2023 Sep 11]. Available from: URL: https://idl.iscram.org/files/florianbrauner/2015/1322_FlorianBrauner_eta2015.pdf.
13. Marroni G, Landucci G, Tamburini F, Bartolucci A, Kuipers S, Broekema W et al. Development of equipment fragility models to support the security management of process installations. In: Proceedings of the 32nd European Safety and Reliability Conference. Singapore: Research Publishing; 2022.
14. Antosch-Bardohn J. Kreativität für die Wissenschaft: Wie Sie kreative Methoden in Forschung und Lehre einsetzen. Paderborn: Brill/Schöningh; 2021. (UTB; vol 5712). Available from: URL: <https://elibrary.utb.de/doi/book/10.36198/9783838557120>.
15. Hözl C. Mind Mapping: Vernetztes Denken als gehirngerechte Methode im Fremdsprachenunterricht [Diplomarbeit]. Graz: Karl-Franzens-Universität Graz; 2012.
16. Woolliscroft P, Jakábová M, Krajcovicová K, Púčiková L, Cagánová D, Čambál M. Global key Performance Best Practice. In: Proceedings For the 9th European Conference on Management Leadership and Governance; 2013. p. 346–56 [last access: 2023 Aug 14]. Available from: URL: <https://www.proquest.com/openview/e6070a317cfda0a3be628c48bd2202c4/1?cbl=1796418&pq-origsite=gscholar&parentSessionId=U71KAtBAWl2nGXcpsADuOFqSvlqy5QOTi7rEhyYViFA%3D>.
17. Peterson ET. The Big Book of Key Performance Indicators. 1st ed : Web Analytics Demystified Inc.; 2006.

18. Gabriel A, Sill Torres F. Navigating Towards Safe and Secure Offshore Wind Farms: An Indicator Based Approach in the German North and Baltic Sea. In: Proceedings of the 20th International ISCRAM Conference; 2023 [last access: 2023 Aug 14]. Available from: URL: https://idl.iscram.org/files/gabriel/2023/2551_Gabriel+Torres2023.pdf.
19. Saihi A, Ben-Daya M, As'ad R. An Investigation of Sustainable Maintenance Performance Indicators: Identification, Expert Validation and Portfolio of Future Research. IEEE Access 2022; 10:124259–76.
20. Tecklenburg B, Gabriel A, Sill Torres F. Perception of threats in Offshore Windfarms and possible countermeasures. In: Proceedings of the 33rd European Safety and Reliability Conference. Singapore: Research Publishing; 2023, pp. 565–571.
21. European Union. Directive (EU) 2022/2557 of the European Parliament and of the Council of 14 December 2022 on the resilience of critical entities and repealing Council Directive 2008/114/EC. URL: <http://data.europa.eu/eli/dir/2022/2557/oj>.

List of abbreviations and definitions

| | |
|-------|---|
| HVDCC | High Voltage Direct Current Converter station |
| KPI's | Key Performance Indicators |
| OSS | Offshore Substation |
| OWFs | Offshore Windfarms |
| WT | Wind turbine |

2.21 Addressing the Risk of Prolonged Periods of Low Renewable Generation in Power Systems Resilient Planning

Ektor-Ioannis Stasinios, National Technical University of Athens, Greece, stasinosektor@mail.ntua.gr

Mathaios Panteli, University of Cyprus, Cyprus, panteli.mathaios@ucy.ac.cy

Nikos Hatziargyriou, National Technical University of Athens, Greece, nh@power.ece.ntua.gr

Abstract

The growing concerns over mitigating climate change effects resulted in power system planning and generation expansion strategies that include increasing penetration of intermittent renewable energy sources (RES) to fulfil the national energy and climate plans (NECPs) of countries worldwide. These developments pose a "new" resilience threat to power systems, namely the existence of prolonged periods of low or zero RES output, and their impact on generation adequacy. Such phenomena are increasingly observed in Europe and worldwide. These events occur with low probability but they have high impact, especially on RES-dominated power systems. Thus, they belong to the High Impact Low Probability (HILP) events which are the focus of resilience studies, but they have not been extensively considered so far, as such. This paper revisits the classical generation capacity expansion method based on the Screening Curves Method (SCM), assuming spinning reserves, necessary to cope with prolonged periods of low RES generation, to guarantee power system resilience.

1 Introduction

Power system resilience is defined as the ability of a power system to anticipate, withstand, adapt and recover from high-impact low-probability (HILP) events [1], such as extreme weather events and natural disasters or man-made cyber or physical [2] malicious attacks. Climate change seems to increase the frequency and intensity of HILP events worldwide [3], thereby jeopardizing the reliable operation of power system and its infrastructure integrity. The very high penetration of Renewable Energy Sources (RES) in the generation mix however dictated by the power system transition towards a carbon free operation poses a new threat that needs to be considered in the resilient planning of modern power systems. This threat concerns the prolonged occurrence of very weak winds and dense cloud coverage for several days over large regions extending to large part of a power system and even affecting neighbouring power systems. It is clear that as the systems move to reach 100% RES operation by 2050 in several parts of the world [4], such events are detrimental to generation adequacy and system reliability, if the traditional planning philosophies are applied. It should be noted that such extreme weather events, usually occur in Europe 2 to 10 times per year, primarily between October and February, lasting an average of 50 to 150 hours per month, with their duration commonly exceeding 24 hours [5]. They have been noted in the last few years in Europe, namely in the Netherlands [6], [7], Belgium [8], [9], and Germany [10], which required major intervention from the system operators. Such extreme weather events fall in the category of HILP events, since they are relatively rare, with the main difference that they concern prolonged periods of very low RES output and therefore potential prolonged power supply deficits. This requires a fresh thinking in long term planning of the system, especially in scheduling the necessary spinning reserve or employing alternative methods to cover prolonged power deficits. This paper focuses on generation planning in order to withstand prolonged low RES output events.

Generation capacity expansion planning determines the necessary generation capacity considering future demand and supply scenarios, aiming to satisfy certain security standards, while minimizing the cost of investments and the system operational cost [11]. In that way, generation expansion strategies decide the kind of technology, capacity, size and location of power plants in order to ensure an equilibrium between future supply and demand, with environmental considerations. A simplified generation capacity expansion planning technique is the Screening Curve Method (SCM) used for the estimation of the least-cost generation mix [11-16]. References [13] and [14] expand the traditional SCM taking into account the thermal cycling and considering both existing and candidate power plants, respectively. [15] considers the resilience and flexibility of future demand and supply scenarios, while [16] additionally considers ancillary services.

This paper aims to examine the difference in generation expansion planning, if resilience against prolonged low RES output periods is ensured, using SCM. The difference in generation capacity is obtained by assuming a high spinning reserve margin able to supplement prolonged loss of RES generation (i.e., the resilient spinning reserve scenario) compared to the traditional spinning reserve policy. The results can be used for decision making on thermal generation decommissioning in RES-dominated power systems and for an estimation of the resilience cost for ensuring generation adequacy.

The paper is organized as follows: Section 2 introduces the SCM used to determine the optimal capacity of each thermal technology, while Section 3 introduces the results of the proposed methodology for the case study application. Finally, Section 4 concludes the paper.

2 The Screening Curve Method

Screening curves (SCs) have been used [17] to approximate the optimum mix of generating technologies for a given system's demand before engaging in more detailed production cost analyses [18].

More specifically, SCs are used to represent the total (i.e., both fixed and variable) annual costs of each generation technology as function of its annual capacity factor (*CF*). The *CF* is used as the scaling factor that represents the percentage of the yearly generator's utilization. The first step of the analysis is to construct the total annual cost (*TAC*) curves for each technology and then match it to a corresponding system load duration curve [19]. That is to determine the most cost-effective capacity portfolio.

Various cost parameters need to be incorporated to calculate the *TAC* of a generating technology. In this work, the power generation unit's *TAC* is defined as:

$$TAC = FixC + (VC + INFC + EC) \times CF \times 8760 \quad (1)$$

The fixed Cost (*FixC*) represents the investment recovery costs, plus a profit. It consists of the upfront capital cost (*CapC*), which is the annualized overnight capacity cost *OvC*, to construct the plant and the non-capital fixed cost (*NCFixC*), also known as fixed operation and maintenance (O&M) cost, which includes maintenance, property taxes, facility fees, insurance and overheads [12]. The *CapC* can be calculated according to (2).

$$FixC = CapC + \frac{OvC r}{1 - e^{-r Tl}} \quad (2)$$

In (2), *r* denotes the discount rate (in % per year) and *Tl* signifies the expected lifetime of the power plant (in years).

The variable Cost (*VC*) expresses the cost of energy production determined by the fuel price and the average heat rate [13]. The incremental non-fuel cost (*INFC*) is the annualized operating costs, such as labour [20]. *EC* indicate *CO₂* emissions cost. *VC*, *INFC* and *EC* compose the full variable cost of conventional units.

As observed in (1), the generators' *TAC* is a function of their annual utilization. This scaling factor is modelled via the generators' *CF* which reflects the percentage of the generators' annual utilization.

The first step of the SCM entails the creation of the *TAC* curves for each respective controllable power generation technology, as functions of their *CF* [21]. Thereafter, these curves must be matched to the system annual load duration curve to determine the most cost-effective energy capacity portfolio. In order to determine the enhanced load duration curve, we must also consider RES generation and spinning reserves. First, assuming that RES units are more cost-effective or are given priority dispatch, we deduct RES generation from the initial load duration curve. This creates the net load duration curve. Thereafter, spinning reserve requirements are added to the net load creating the augmented load duration curve. This is the load duration curve at which the *TAC* curves will be matched. Hence, thermal units are responsible for meeting the system's augmented load (i.e., net load plus the spinning reserve).

In order to take into account resilience considerations, two spinning reserve policies are considered: the classic spinning reserve practice ("classic reserves scenario"), which considers supply of additional 10% of the load and 20% of the forecasted aggregated RES generation to cover forecasting errors, and the resilient spinning reserves policy that considers again a 10% percentage of the load, but 80% of the forecasted RES generation to account for prolonged periods of low RES generation ("resilient reserves scenario").

3 Study Case

The IEEE 24-bus RTS System with a modified annual peak load is used to illustrate the presented framework. The power system model contains 3 thermal technologies, G1-Combined Cycle (CC), G2-Coal (C1) and G3-Steam Turbine (ST). The units' technical characteristics are presented in Table 1.

Table 12. Generation Units Parameters

| Unit | G1 (CC) | G2 (C1) | G3 (ST) |
|---------------|---------|---------|---------|
| Capacity (MW) | 750 | 800 | 493 |
| OvC (k\$) | 717 | 1511 | 860 |
| NCFixC (k\$) | 14 | 30 | 50 |
| VC (\$/MWh) | 40.80 | 20 | 26.50 |
| INFC (\$/MWh) | 4.45 | 5.31 | 5.17 |
| EC (\$/MWh) | 2.80 | 3.70 | 4.20 |
| r (%) | 10 | 10 | 10 |
| TL (y) | 30 | 30 | 35 |

In all scenarios the thermal generation remains fixed at 2043 MW. The Base Case scenario includes 40% of non-dispatchable RES in the generation mix, corresponding to a total maximum capacity of 1362 MW. Cases I, II, III and IV represent penetration levels of 50%, 60%, 70% and 80% RES, respectively, in relation to the total installed generation capacity of the system. It should be noted that such high-level penetration scenarios are aligned with declared EU policies of sustainable power systems for the years 2030 to 2050 [4]. The total power generation capacity for each of the five considered scenarios is as follows:

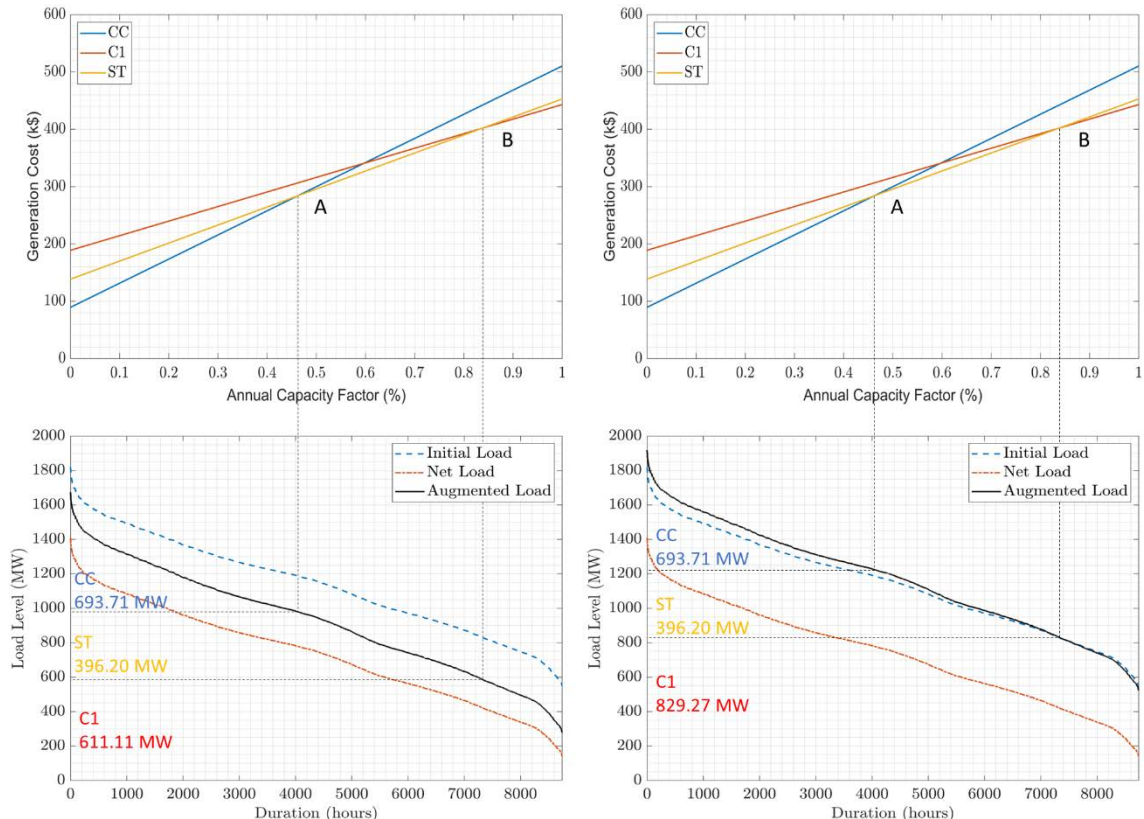
- Base Case 40% RES: 2043 MW Thermal / 1362 MW RES, 3405 MW in total
- Case I 50% RES: 2043 MW Thermal / 2043 MW RES, 4086 MW in total
- Case II 60% RES: 2043 MW Thermal / 3064.5 MW RES, 5107.5 MW in total
- Case III 70% RES: 2043 MW Thermal / 4767 MW RES, 6810 MW in total
- Case IV 80% RES: 2043 MW Thermal / 8172 MW RES, 10215 MW in total

For the Base Case of 40% RES integration, Figure 1 depicts the application of SCs for the thermal technologies assuming the classic and the resilient reserves policies. It should be noted that the spinning reserves must be supplied by thermal generators, as the RES units are non-dispatchable and thus, the capability of RES to provide reserves is not considered. The lower part of the figure displays the three load duration curves for the two reserve scenarios, namely the initial load curve, the net load curve (which is the initial load minus the actual renewable generation), and the augmented load duration curve (which is the net load plus the required spinning reserve). The thermal generation is called to satisfy the augmented load curve. The points of intersection (A and B) of the respective *TAC* curves of each technology signify the annual *CFs* beyond which each technology becomes less cost-effective than the other. In the case of the classic reserve scenario (left figures in Figure 1), for an annual *CF* less than or equal to point A, the CC technology is the most economical. Thus, this point can be subsequently benchmarked to the corresponding augmented load duration curve. The optimum CC installed capacity is determined as equal to 693.71 MW for the classic reserve scenario. The optimum C1 and ST installed capacities can be determined following a similar approach from the intersection of the two technologies' *TAC* curves at point B and its corresponding benchmarking to

the augmented load duration curve. Point B shows that the ST is the most economical at this point, and thus the optimum ST installed capacity is 396.20 MW, while the optimum C1 Capacity is 611.11 MW.

Following a similar logic in Fig 1b) the results with resilient reserves are determined as follows: CC and ST optimum capacities remain at 396.20 MW and 611.11 MW, respectively, while the C1 optimal capacity is 829.27, to cover the increased spinning reserve requirements.

Figure 63. SCM for the Base Case employing a) classic (left) and b) resilient (right) reserves policies.



Apparently, the resilient reserves form a higher augmented load duration curve, necessitating larger generation from the base units (Coal) to meet the augmented load requirements. Furthermore, in the resilient scenario, the least-cost generation mix requires capacity expansion for these units, as 829.27 MW are required, while their existing capacity is 800 MW. Elsewhere, the surplus 29.27 MW must be assigned to mid-merit units (ST), increasing the annual cost.

Based on the same principle, Figure 2 shows the formation of the augmented load duration curves for all considered scenarios, while Table 2 shows the corresponding optimum capacity of the thermal units.

Figure 64. Augmented load duration curves for all RES penetration cases.

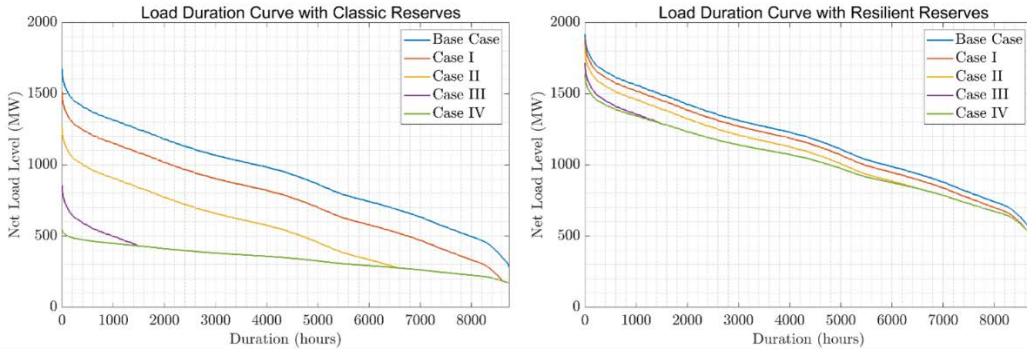


Table 13. Optimum capacities in MW for thermal technologies for all RES penetration cases.

| RES penetration cases | CC | ST | C1 |
|----------------------------|--------|--------|--------|
| Classic Reserve Scenario | | | |
| Base Case | 693.71 | 396.20 | 611.11 |
| Case I | 693.71 | 396.20 | 447.67 |
| Case II | 693.71 | 323.26 | 428.45 |
| Case III | 500.31 | 108.06 | 248.45 |
| Case IV | 189.91 | 108.06 | 247.73 |
| Resilient Reserve Scenario | | | |
| Base Case | 693.71 | 396.20 | 829.27 |
| Case I | 693.71 | 396.20 | 788.41 |
| Case II | 693.71 | 377.97 | 745.35 |
| Case III | 645.36 | 324.17 | 745.35 |
| Case IV | 567.58 | 324.17 | 745.35 |

It is obvious that the augmented load duration curves with resilient reserves require larger thermal generation, as shown in Table 2. Additionally, with the increase in RES integration, the augmented load duration curve declines, as a greater portion of the load demand is met by renewables. Figure 2 shows that, for both spinning reserves scenarios, the curves of Case I, II and III converge to the augmented load duration curve of Case IV at a specific point, which is different for each RES installation case. At these points, demand is entirely met by renewables, making the augmented load duration curve equal to the reserve requirements that thermal units must meet. This occurs for longer annual duration as RES integration increases. It should be noted that the proposed approach can be used to address the overall redundancy of the thermal generation. When a thermal technology reaches 100% redundancy, it can be decommissioned. This application will be further developed in a future paper.

4 Conclusions

This paper examines the impact of low probability, prolonged periods of low renewable generation in RES-dominated power systems, expanding the concept of resilience to such events. It utilizes the traditional SCM as a generation capacity expansion planning tool, using both a traditional and high spinning reserves able to supplement prolonged loss of RES generation. In this way, the most economical generation mix to face the increased requirements of resilient spinning reserves can be determined. This approach can be extended to provide recommendations for safe decommissioning of thermal units and as an indication of resilience cost, as will be shown in a future work.

References

- [1] M. Panteli and P. Mancarella, "The Grid: Stronger, Bigger, Smarter?: Presenting a Conceptual Framework of Power System Resilience," *Power Energy Mag.* IEEE, vol. 13, pp. 58–66, Jun. 2015, doi: 10.1109/MPE.2015.2397334.
- [2] T. V. Vu, B. L. H. Nguyen, Z. Cheng, M.-Y. Chow, and B. Zhang, "Cyber-Physical Microgrids: Toward Future Resilient Communities," *IEEE Ind. Electron. Mag.*, vol. 14, no. 3, pp. 4–17, Sep. 2020, doi: 10.1109/MIE.2019.2958039.
- [3] M. Panteli and P. Mancarella, "Influence of extreme weather and climate change on the resilience of power systems: Impacts and possible mitigation strategies," *Electr. Power Syst. Res.*, vol. 127, Oct. 2015, doi: 10.1016/j.epsr.2015.06.012.
- [4] G. Amanatidis, "European policies on climate and energy towards 2020, 2030 and 2050," 2020.
- [5] B. Li, S. Basu, S. J. Watson, and H. W. J. Russchenberg, "A Brief Climatology of Dunkelflaute Events over and Surrounding the North and Baltic Sea Areas," *Energies*, vol. 14, no. 20, Art. no. 20, Jan. 2021, doi: 10.3390/en14206508.
- [6] "Netbeheerder moet groot inkopen om stroomteekort op te vangen." Accessed: Aug. 20, 2023. [Online]. Available: <https://nos.nl/artikel/2229787-netbeheerder-moest-groot-inkopen-om-stroomteekort-op-te-vangen>
- [7] G. Ritzen, "Netbeheerder Tennet wendt landelijk stroomteekort af," NRC, Apr. 30, 2018. Accessed: Aug. 20, 2023. [Online]. Available: <https://www.nrc.nl/nieuws/2018/04/30/landelijk-stroomteekort-afgewend-door-netbeheerder-tennet-a1601355>
- [8] "Energy Transition in Belgium: Choices and Costs | EnergyVille." Accessed: Aug. 20, 2023. [Online]. Available: <https://www.energyville.be/energy-transition-belgium-choices-and-costs>
- [9] "Elia: Belgian's Electricity System Operator." Accessed: Aug. 20, 2023. [Online]. Available: <https://www.elia.be/en/>
- [10] S. Schultz, "Ökostrom knapp: Panikmache mit der Dunkelflaute," *Der Spiegel*, Feb. 07, 2017. Accessed: Aug. 20, 2023. [Online]. Available: <https://www.spiegel.de/wirtschaft/soziales/oekostrom-knapp-panikmache-mit-der-dunkelflaute-a-1133450.html>
- [11] W. Gandulfo, E. Gil, and I. Aravena, "Generation Capacity Expansion Planning under demand uncertainty using stochastic mixed-integer programming," in 2014 IEEE PES General Meeting | Conference & Exposition, Jul. 2014, pp. 1–5. doi: 10.1109/PESGM.2014.6939368.
- [12] N. Troy, E. Denny, and M. O'Malley, "Base-Load Cycling on a System With Significant Wind Penetration," *IEEE Trans. Power Syst.*, vol. 25, no. 2, pp. 1088–1097, May 2010, doi: 10.1109/TPWRS.2009.2037326.
- [13] T. Zhang, R. Baldick, and T. Deetjen, "Optimized generation capacity expansion using a further improved screening curve method," *Electr. Power Syst. Res.*, vol. 124, pp. 47–54, Jul. 2015, doi: 10.1016/j.epsr.2015.02.017.
- [14] Y. E. Güner, "The improved screening curve method regarding existing units," *Eur. J. Oper. Res.*, vol. 264, no. 1, pp. 310–326, Jan. 2018, doi: 10.1016/j.ejor.2017.06.007.
- [15] M. Panteli et al., "Analyzing the resilience and flexibility of power systems to future demand and supply scenarios," in 2016 18th Mediterranean Electrotechnical Conference (MELECON), Apr. 2016, pp. 1–6. doi: 10.1109/MELCON.2016.7495312.
- [16] T. Zhang and R. Baldick, "Consideration of ancillary services in Screening Curve Method," in 2015 IEEE Power & Energy Society General Meeting, Jul. 2015, pp. 1–5. doi: 10.1109/PESGM.2015.7286408.
- [17] M. Panteli et al., "Analyzing the resilience and flexibility of power systems to future demand and supply scenarios," in 2016 18th Mediterranean Electrotechnical Conference (MELECON), Apr. 2016, pp. 1–6. doi: 10.1109/MELCON.2016.7495312.

- [18] I. A. E. Agency, "Expansion Planning for Electrical Generating Systems," International Atomic Energy Agency, Text, 1984. Accessed: Oct. 16, 2023. [Online]. Available: <https://www.iaea.org/publications/1343/expansion-planning-for-electrical-generating-systems>
- [19] C. A. Charalambous, A. Milidonis, A. Lazari, and A. I. Nikolaidis, "Loss Evaluation and Total Ownership Cost of Power Transformers—Part I: A Comprehensive Method," IEEE Trans. Power Deliv., vol. 28, no. 3, pp. 1872–1880, Jul. 2013, doi: 10.1109/TPWRD.2013.2262506.
- [20] "PJM - Home." Accessed: Jul. 18, 2023. [Online]. Available: <https://www.pjm.com/>
- [21] "Power System Economics: Designing Markets for Electricity | IEEE eBooks | IEEE Xplore." Accessed: Jul. 20, 2023. [Online]. Available: <https://ieeexplore.ieee.org/book/5264048>

2.22 Assessing risk of water damage to buildings under current and future climates

Ola Haug, Claudio Heinrich-Mertsching, and Thordis Thorarinsdottir, Norwegian Computing Center, P.O. Box 114 Blindern, NO-0314 Oslo, Norway, ola@nr.no, claudio@nr.no, thordis@nr.no

1 Introduction

Climate and climate change is a major concern to the insurance industry through its weather-related risk exposure. For non-life insurance, the implications are immediate from physical damages to buildings and infrastructure as well as business interruptions.

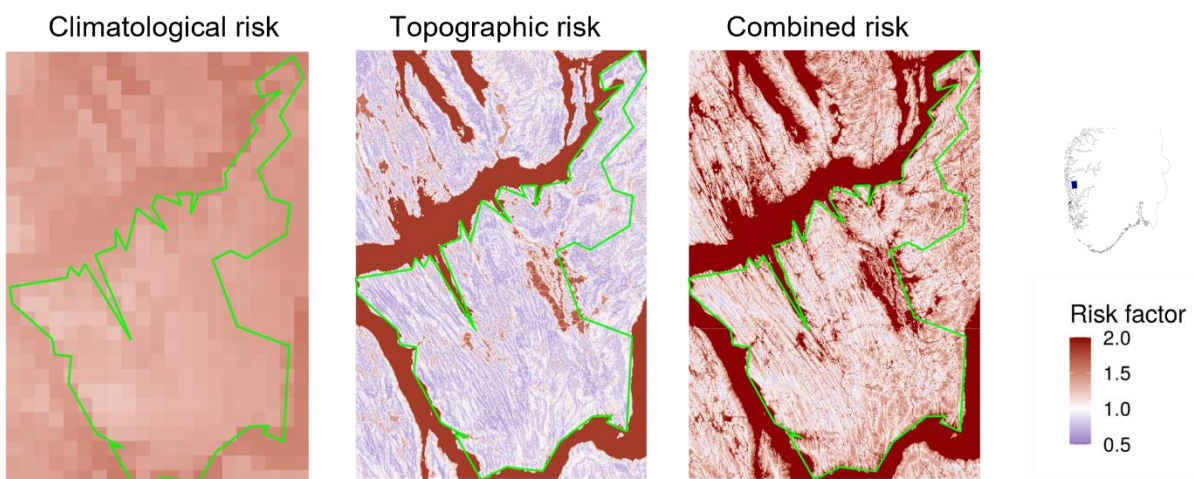
In Norway, claims related to surface water flooding, which is a sub-class of pluvial flooding, constitute roughly 50% of the weather-related damages to buildings over the past ten years [2]. Heavy rainfall, including cloudbursts, is the major driver for surface floods leading to water damage, but also long-lasting, not necessarily extremely intense, rainfall contributes to the damages considered in this study. The claim incidents are due to rainfall hitting directly or indirectly via surface water floods and manifest themselves via intrusion of water through the building shell above terrain, or via sewer-line backups.

Cloudburst events are anticipated to increase both in frequency and intensity in the decades to come [4]. Targeted efforts to prevent and mitigate the devastating effects of water intrusion are proven to save costs over subsequent restoration [6]. We address these endeavours by combining detailed knowledge of every single buildings' vulnerability with its external climatological exposure.

2 Background and novelty

In a recently published paper [5] and presentation [3], we develop a statistical model that quantifies building-specific risk of surface water flooding in Norway. A generalised additive model (GAM) [7] relates the number of water damages to a set of explanatory variables that can be categorised into building attributes, climatological index variables or granular topographic characteristics relevant to hydrological processes. This risk decomposition allows to highlight different sources of local risk, which is not only useful for insurance companies, but also for municipalities in their land-use planning. Figure 1 shows maps of the climatological and topographic partial risks for Osterøy municipality, as well as the product combining the two. Coupling the model with climate projections enables prediction of the locally varying impacts of climate change on the risk of surface water flooding, and in general, the GAM framework admits assessing sensitivity to specific perturbations in any of the partial risks from their training values.

Figure 65. Climatological, topographic and combined partial risks for Osterøy municipality on the western coast of Norway (see small map). The colorscale is centered at white, corresponding to the average risk, with below-average risk in blue and above-average risk in red.



The model in [5] expresses the long term, or pricing, risk of surface water flooding utilising climatological averages for precipitation and temperature on a quarterly time scale. This approach allows for robust assessment of present and future underlying water damage risk for any existing or planned building in Norway. Addressing instead the short-term risk aspect of surface water flooding to buildings, there is need for climatological information on a finer spatiotemporal resolution. This is for instance relevant in assessing risk and issuing alerts prior to upcoming extreme events, where apparently knowledge about seasonal average weather is of little use.

The potential of modelling weather-related water damage risk relies on availability of data with adequate quality and sufficient resolution in time and space. In the case study “Use of insurance loss data by local authorities in Norway” under the Climate Adapt project¹⁶, the need for accurate information on timing and location of insurance claims in adaptation planning is emphasised.

We devise an alternative idea that utilises climatological information on a scale in time and space that more precisely portrays damages caused by heavy rainfall incidents, directly or indirectly. Essentially, this approach abandons quarterly climatological indices in favour of appropriate indices down to sub-daily resolution generated from a high-resolution spatiotemporal precipitation data set obtained from assimilating radar data with in-situ measurements [1]. The risk model itself is restricted to daily resolution due to the registration practice adopted for the insurance claims, but we believe that incorporating sub-daily climatological indices better representing the intensity of short-term rainfall incidents will facilitate more precise modelling of the localised impacts of cloudburst events.

We envision producing risk forecasts up to 48 hours ahead, which is the time horizon of the detailed, hourly forecast provided by the national weather service in Norway. Taking into account the daily resolution of the risk model, separate risk forecasts will be generated for the first 24 hours and the period 25 – 48 hours ahead. The risk forecast can be updated each time a new weather forecast is issued, which for the Norwegian service is every six hours. This means that a first warning of a potentially high-risk water damage event reaches a homeowner 48 hours in advance (or 42 hours to be on the conservative side, considering that the event just escaped from the current weather forecast but shows up in the next forecast six hours later), leaving her two days to take precautionary measures like moving belongings away from exposed positions such as the basement. In an implementation of a warning system, risk forecasts evolve as new weather forecasts are produced, and supposedly the risk forecast 24 hours ahead is more reliable than the one 25 – 48 hours into the future, informing the homeowner how to adjust her efforts.

Combining the risk model with intensity, duration and frequency (IDF) curves for rainfall on a spatial grid, we envision producing risk maps expressing the spatially varying probability of having at least one rainfall-induced claim over a period of a certain duration, for instance 50 years. Such knowledge allows for targeted risk mitigation, again with application beyond the insurance sector.

3 Methodology

Utilising the high resolution of the new radar-based data set, we seek to develop a revised statistical model with suitable climatological covariates that better assesses, and even predicts from real-time weather forecasts, the localised water damage risk of cloudburst events.

The GAM from [5] produces a building-specific risk score representing the expected number of claims per day and insured value using a logarithmic link function. On original scale, the risk score r_i for building i can be written as the product of categorised partial risk scores,

$$r_i = r_0 \cdot r_i^{\text{clim}} \cdot r_i^{\text{topo}} \cdot r_i^{\text{b-s}} \cdot r_i^{\text{reg}} \quad (1)$$

where r_0 is a base risk that is common to all buildings, and the remaining four terms denote normalised representations of the climatological, topographic, building-specific and regional partial risks, respectively (cf [5] for details).

¹⁶ <https://climate-adapt.eea.europa.eu/en/metadata/case-studies/use-of-insurance-loss-data-by-local-authorities-in-norway>

For the new model, still on a daily temporal resolution, but now with sub-daily climatological indices, we formulate the risk as the probability p_i of building i having a claim on a certain day. In GAM, this is naturally modelled via a logistic regression with a logit link function, $\text{logit}(p_i) = \log\left(\frac{p_i}{1-p_i}\right)$, replacing the log-link of the original model in [5]. For small probabilities, like the ones that apply to our setting, the logit is well approximated with the log function. This implies that the suggested model retains the modular structure in (1), with the main difference being that interpretation turns from a formerly frequency- to a probability-based risk measure in the new model.

4 Summary

Cloudburst events are anticipated to increase both in frequency and intensity in the decades to come, and understanding and mitigating their impacts is imperative in developing resilient societies for the future. Based on a probabilistic water damage risk framework, we hope to contribute to this direction by developing a quantitative, asset-specific warning system that will help homeowners take precautionary measures based on short-term weather forecasts. Combining the risk model with gridded rainfall IDF curves, we will explore the idea of deriving probability risk maps for rainfall-induced damages corresponding to precipitation intensities reflecting specific return periods locally.

References

- [1] Dyrrdal, A. V., et al. Nedbør: SURF datasett og ekstremverdier, project presentation available from <https://www.nve.no/media/11210/dyrrdal-a.pdf>.
- [2] Finans Norge, Klimarapport Finans Norge 2023, <https://www.finansnorge.no/siteassets/statistikk-og-analyse/klimarapport/finans-norge---klimarapport-2023-enkeltsider.pdf>.
- [3] Haug, O., et al. Assessing probabilities and impacts of extreme events for the needs of insurance under climate change, CERIS - Disaster Resilient Societies Cluster Conference, Brussels 7 November 2022; https://home-affairs.ec.europa.eu/whats-new/events/ceris-disaster-resilient-societies-cluster-conference-2022-11-07_en.
- [4] Hanssen-Bauer, I., et al. Climate in Norway 2100 – a knowledge base for climate adaptation. NCCS report 1/2017, 2017, ISSN 2387-3027.
- [5] Heinrich-Mertsching, C., et al. Assessing present and future risk of water damage using building attributes, meteorology and topography, Journal of the Royal Statistical Society Series C: Applied Statistics, Vol. 72, Issue 4, 2023, pp. 809–828, <https://doi.org/10.1093/rssc/glad043>.
- [6] Pedersen, S., et al. Forprosjekt om den samfunnsøkonomiske verdien av å forebygge mot fysisk risiko som er utløst av klimaendringer, report 48/2022 Menon Economics, 2022, <https://www.menon.no/wp-content/uploads/2022-48-Forprosjekt-forebygging-fysisk-klimarisiko.pdf>.
- [7] Wood S. N. Generalized additive models: An introduction with R (2nd ed.), 2017, Chapman and Hall/CRC.

2.23 Flood resilience and sustainability in bridge climate adaptation

Stergios-Aristoteles Mitoulis, University of Birmingham, UK, S.A.Mitoulis@bham.ac.uk,
www.MetaInfrastructure.org

Sotirios Argyroudis, Brunel University London, UK, Sotirios.Argyroudis@brunel.ac.uk,
www.MetaInfrastructure.org

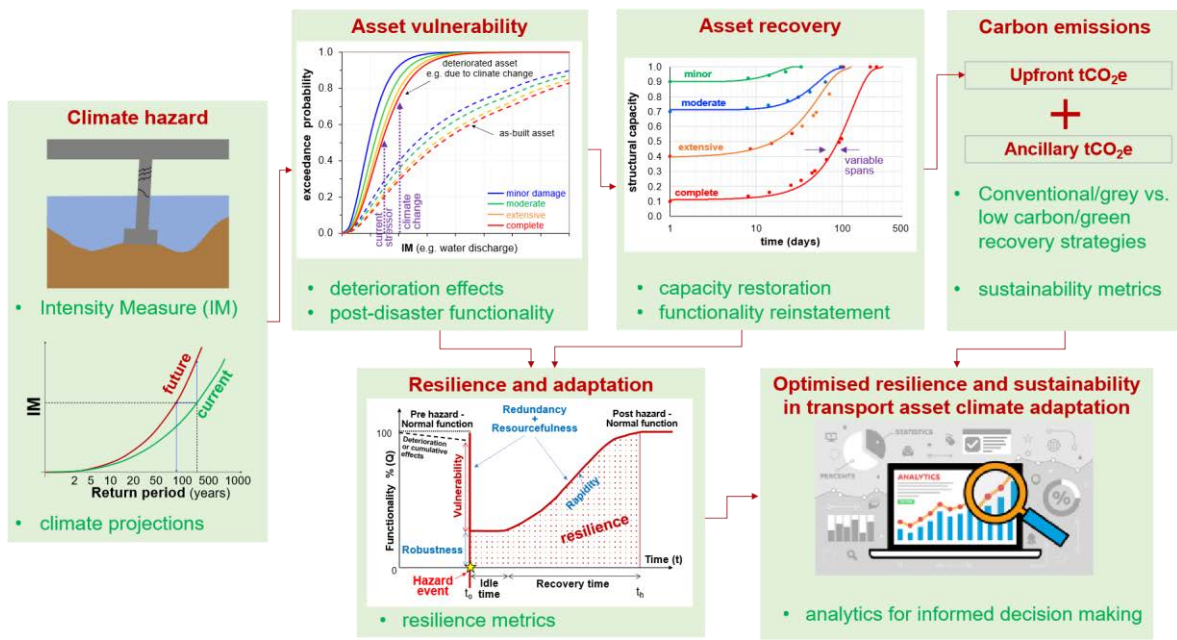
1 Introduction

Climate change exacerbates natural hazards and continuously challenges the performance of critical infrastructure (Pörtner et al. 2022). Thus, climate resilience of infrastructure is of paramount importance to maintain mobility and essential services that underpin the world economies. Though grey solutions have been streamlined since the concrete era, today we urgently need greener solutions that lead to less tCO₂e and more so in the structural sector to be on track with net-zero and sustainable requirements (Liu et al., 2022). Nevertheless, resilience and sustainability consolidation is neither adopted by current research and practice. The integration of these two principles has been introduced by previous frameworks (Penadés-Plà et al., 2016, Padgett and Tapia, 2023, Marchese et al., 2018). However, we still lack in practical metrics and representative case studies that facilitate both decision-making for efficient climate adaptation and lower tCO₂e in transport infrastructure sector, whilst accounting for limited finances and gradual deterioration of assets. To fill this gap, this paper applies a novel integrated framework for optimising resilience and sustainability metrics to minimise the cost using traditional and low-carbon grey restoration strategies in the event of floods affecting critical transport assets, with a focus on bridges (Mitoulis et al., 2023). This is the first output of the ongoing Horizon ReCharged (Ref: 101086413) and RISKADAPT (Ref: 101093939) research projects.

2 Methodology

The framework shown in Figure 1 describes the approach for quantifying ex-ante adaptation and post-ante recovery from the lenses of sustainability and resilience in a changing climate. The main steps of the framework are: **Step 1**. In this step, the hazard intensity measures (IM) are defined based on predicted, measured or estimated hazard data, using e.g., high-resolution flood maps to deduce probabilistic relationships of established IM, e.g. peak water depth, streamflow velocity, and discharge, for each one of the affected assets. The fluctuations in the IM, e.g., peak river flow, can be linked to the increased annual probability of exceedance, i.e., the frequency of the hazard, as a result of climate change projections. Based on these projections, information on the potential range of climate exacerbations of floods in the specific location, for different return periods, and emission scenarios can be defined. **Step 2**. The vulnerability for the as built and the deteriorated asset is estimated using fragility functions from the literature. The curves correlate the probability of exceeding given damage states (e.g. minor, moderate, extensive, complete) with the hazard IM. Regarding the generation of fragility curves for transport assets this can be found in e.g., Argyroudis et al. (2019), Argyroudis and Mitoulis (2021). **Step 3**. The asset recovery is evaluated based on restoration (structural capacity) and reinstatement (traffic capacity) models, which correlate the asset functionality to the recovery time after the event, considering its typology, damage state, available resources, and post-hazard idle times. In this paper, the modelling of the recovery strategies followed available models from the literature (Mitoulis et al., (2021)). **Step 4**. Carbon emissions are quantified considering grey and green restoration measures. Two main emission groups are considered: (i) the upfront emissions, correspond with the carbon associated with the construction works included in the restoration tasks; (ii) the ancillary emissions. refer to the environmental impacts related to traffic re-routing, pavement degradation, change in travel behaviours or recycling and reuse of materials from construction and demolition works within a restoration task. In **Step 5** the resilience to hazard occurrences is quantified with focus on the structural capability of the asset to withstand a hazard occurrence based on a probabilistic assessment, by calculating the weighted capacity using the occurrence probabilities of different damage states for a given IM (Argyroudis 2021). **Step 6** An integrated metric is proposed based on resilience, sustainability, and cost to create analytics for decision making.

Figure 1. Framework for resilience-based life-cycle management of transport assets.



3 Conclusions

The trade-offs between sustainability and resilience within design objectives reveals a spectrum of potential relationships. They can operate in synergy, stand independently, or even conflicting for priority with respect to the design targets. Notably, our study into post-flood restoration of bridges has brought forth a crucial finding: sustainability and resilience exhibit a lesser degree of interdependence, with the former often contending with cost constraints. Across all examined scenarios, the implementation of a low-carbon restoration strategy has proven itself beneficial. This strategy significantly reduces tCO₂e emissions by leveraging low-carbon materials, refining on-site practices, and optimising consumptions in transportation of materials, leading to an up to 50% increase in the infrastructure sustainability and resilience rating index. This can justify the additional investments for introducing greener adaptation strategies in transport infrastructure.

Acknowledgements

The authors received funding by the UK Research and Innovation (UKRI) under the UK government's Horizon Europe funding guarantee [Ref: EP/Y003586/1, EP/X037665/1]. This is the funding guarantee for the European

Union HORIZON-MSCA-2021-SE-01 [grant agreement No: 101086413] ReCharged - Climate-aware Resilience for Sustainable Critical and interdependent Infrastructure Systems enhanced by emerging Digital Technologies. The first author would also like to acknowledge funding by the UK Research and Innovation (UKRI) under the UK government's Horizon Europe funding guarantee [Ref: 10062091]. This is the funding guarantee for the European Union HORIZON-MISS-2021-CLIMA-02 [grant agreement No: 101093939] RISKADAPT - Asset-level modelling of risks in the face of climate-induced extreme events and adaptation.

References

- Argyroudis, S.A. (2022). Resilience metrics for transport networks: a review and practical examples for bridges. In Proceedings of the Institution of Civil Engineers-Bridge Engineering, 175(3).
- Argyroudis, S.A., Mitoulis, S.A. (2021). Vulnerability of bridges to individual and multiple hazards-floods and earthquakes. Reliability Engineering & System Safety, 210, 107564.
- Argyroudis, S.A., Mitoulis, S.A., Winter, M.G., & Kaynia, A.M. (2019). Fragility of transport assets exposed to multiple hazards: State-of-the-art review toward infrastructural resilience. Reliability Engineering & System Safety, 191, 106567.

4. Liu, Y., Wang, Y., Shi, C., Zhang, W., Luo, W., Wang, J., ... & Kite, S. (2022). Assessing the CO₂ reduction target gap and sustainability for bridges in China by 2040. *Renewable and Sustainable Energy Reviews*, 154, 111811.
5. Marchese, D., Reynolds, E., Bates, M. E., Morgan, H., Clark, S. S., & Linkov, I. (2018). Resilience and sustainability: Similarities and differences in environmental management applications. *Science of the total environment*, 613, 1275-1283.
6. Mitoulis, S.A., Argyroudis, S.A., Loli, M., Imam, B. (2021). Restoration models for quantifying flood resilience of bridges. *Engineering structures*, 238, 112180.
7. Mitoulis, S.A., Bompa, D.V., Argyroudis, S. (2023). Sustainability and climate resilience metrics and trade-offs in transport infrastructure asset recovery. *Transportation Research Part D: Transport and Environment*, 121, 103800.
8. Padgett, J.E., & Tapia, C. (2013). Sustainability of natural hazard risk mitigation: Life cycle analysis of environmental indicators for bridge infrastructure. *Journal of Infrastructure Systems*, 19(4), 395-408
9. Penadés-Plà, V., García-Segura, T., Martí, J. V., & Yepes, V. (2016). A review of multi-criteria decision-making methods applied to the sustainable bridge design. *Sustainability*, 8(12), 1295.
10. Pörtner, H.O., Roberts, D.C., Adams, H., Adler, C., Aldunce, P., Ali, E., Begum, R.A., Betts, R., Kerr, R.B., Biesbroek, R. and Birkmann, J. (2022). Climate change 2022: Impacts, adaptation and vulnerability. *IPCC Sixth Assessment Report*.

2.24 An Empirical Model for Predicting Landslide Runout Distance in Malaysia

Kwan Ben Sim, Faculty of Science & Engineering, University of Nottingham Malaysia, Jalan Broga 43500 Selangor, Malasya, evxks8@nottingham.edu.my

Min Lee Lee, Faculty of Science & Engineering, University of Nottingham Malaysia, Jalan Broga 43500 Selangor, Malasya, MinLee.Lee@nottingham.edu.my

Remenyte-Prescott Rasa, Faculty of Engineering, University of Nottingham, University Park, Nottingham NG7 2RD, United Kingdom, r.remenyte-prescott@nottingham.ac.uk

Soon Yee Wong, Faculty of Science & Engineering, University of Nottingham Malaysia, Jalan Broga 43500 Selangor, Malasya, SoonYee.Wong@nottingham.edu.my

Abstract

One of the critical components in landslide hazard and risk assessment is the reliable estimate of the runout distance of the sliding mass. The sliding mass and its propagation greatly impacts the region of impact, especially when landslides have a long travel distance. Due to climate change, this impact of landslides on structures and infrastructures is increasing. Hence, the development of a reliable model for the prediction of landslide travel distance for better landslide disaster risk assessment and management has become more critical than ever before. In Malaysia, the risk management of landslides is in its early stages. However, despite these endeavours the current efforts remain insufficient. A new empirical model for runout estimation in Malaysia is introduced in this paper. This novel model relies on empirical data and is recommended for adoption in Malaysia until analytical models are developed. Data on landslide events in Malaysia were collected, processed and analyzed in order to discuss the correlation and significance of various influential parameters on the travel distance and to establish its prediction model. The reliability of the proposed model was verified through a reasonable agreement between the actual runout and prediction values. Therefore, this new model is of potential practical use in Malaysia and other regions, with similar geomorphological and geological properties. In addition, this model also investigates the understudied yet influential parameter governing landslide travel distance i.e. retrogression distance, paving the way for a more accurate prediction model for Malaysia. This perspective not only advances the field of landslide prediction but also offers a different approach to enhancing safety and risk management for infrastructures in Malaysia. It is the authors' vision that the prediction model shall empower decision-makers and planners to implement proactive measures, ultimately safeguarding lives and critical infrastructure from the mounting challenges posed by climate change. Significantly, this study contributes to enhanced safety, risk assessment and disaster prevention by providing valuable prediction into the runout behavior of landslides.

1 Introduction

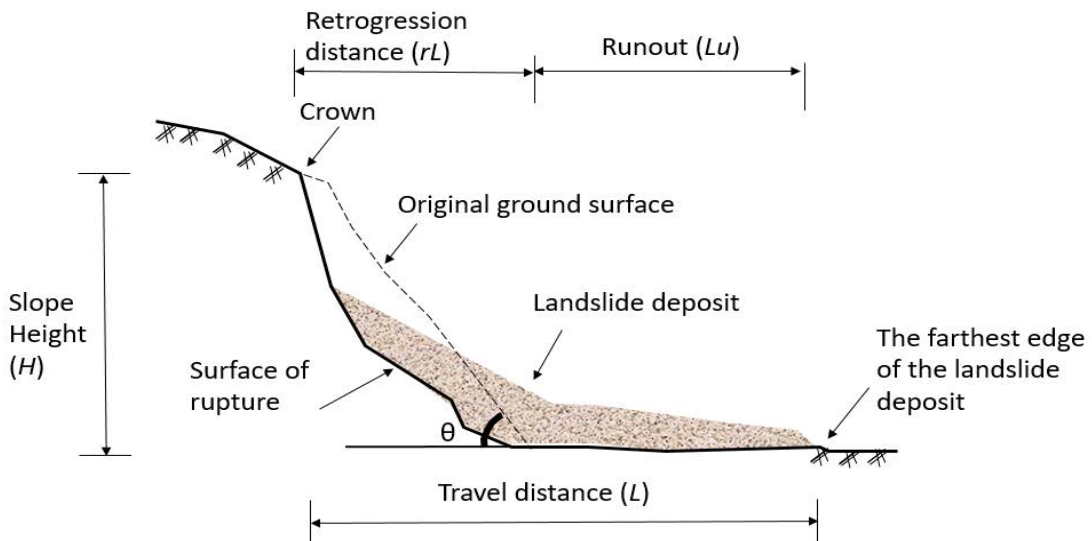
Landslides are significant geohazards that threaten human life and economy worldwide. They have caused tens of thousands of fatalities and an estimated annual economic loss of \$20 billion [1–3]. In tropical hilly regions like Malaysia, landslide hazard assessment research is crucial to reduce their impact on affected areas. Landslides have been a recurring and significant phenomena in Malaysia, resulting in property damage and threatening the lives of the population [4–6]. Malaysia is gradually implementing landslide risk management, but progress remains below-par [6]. Predictive methods, especially landslide runout analysis, play a vital role in risk assessment and mitigation as well as in pre-disaster preparedness and planning. [7].

Replicating and investigating landslide runout, which results from various causes and factors, is extremely challenging in laboratory models [8,9]. There are two common approaches for landslide runout prediction: empirical-statistical models, based on geometric parameter correlations, and numerical modeling, which simulates physical processes [7,10]. The distinction between the two methods is often insignificant due to the complexity of collecting universal guidelines for runout modeling [11,12]. Additionally, applying numerical models for landslide propagation is still too complex [8,13].

Empirical-statistical methods are useful for predicting landslide runout and the coverage impact area [14]. They rely on simple correlations between landslide parameters and runout [15] (Figure 66). Despite the simplified dynamics, these methods can provide reliable predictions of landslide propagation [8,16], aiding decision-making and complying with guidelines for landslide risk assessment [8,17]. In developing countries, with limited data, experts, and funding, these simple, low-cost procedures are imperative [8,18].

This paper focuses on the physical characteristics of landslides in Malaysia, establishing empirical correlations between travel distance, runout, retrogression distance, slope height, slope angle, and landslide volume. It presents an empirical procedure to determine runout distance, along with key findings and recommendations. Applying these empirical formulas will contribute to evaluating landslide hazard in Malaysia and supporting the national slope master plan for landslide disaster risk reduction.

Figure 66 Geometrical variables: height of slope (H), run out distance (L), slope angle (θ), retrogression distance (rL), runout (Lu)



Modified from: Hungr et al. 2005; Strand et al. 2017

2 Literature review

Analysing empirical relationships is the most regularly, yet efficiently, used method for estimating the runout distance of landslides. Numerous empirical correlations for predicting runout distance landslides have been described in literature. In order to study the most significant and easily available factors affecting runout distance, researchers usually conduct statistical analyses on the parameters that are to be utilized in their empirical models. A study by Legros [21] states that the best prediction model is when travel distance is directly proportional to the landslide volume (V). The limitation is that, the parameter (V) is normally not stated in existing landslide reports [22].

As stated by Qarinur [23], slope height exhibits linear correlation to the run out distance for Indonesia, i.e. run out distance will increase as the height of slope increases. However, the authors in [23] also suggested that a combination of slope angle with height will be more effective.

In a more recent study by Apriani et al. [22], it is stated that the parameter slope angle (θ) is not significant on the runout distance of Indonesian landslides. In addition, Apriani et al. [22] concludes their statistical study with the conclusion that the height of slope (H) has a stronger influence compared to the slope angle and volume of landslides towards runout distance.

In another study [24], it is recommended that the maximum runout distance for landslides in Canada to be in terms of Runout (Lu) and retrogression distance (rL).

Table 14 summarizes the empirical models for predicting the runout distance of landslides. There are more than 10 empirical equations proposed by 10 researchers. It can be seen that height of slope (H) is the most used parameter by researchers, as it is the most widely available worldwide, followed by landslide volume (V). Prediction models based on Runout (Lu) and retrogression distance (rL). are still relatively scarce and is one of the parameter that will be the focus of this study.

Table 14 Summary of empirical models for predicting landslide runout distance

| No. | Researcher(s) | Equations | | Parameters used |
|-----|---------------------|--|------|-----------------|
| 1 | Corominas [25] | $L = 1.03V^{0.105} H$ | (1) | V, H |
| 2 | Rickenmann [14] | $L=1.9V^{0.16} H^{0.8}$ | (2) | V, H |
| 3 | Legros [21] | $L=8V^{0.25}$ | (3) | V |
| | | $Lu = 8.8rl^{0.8}$ | (4) | rL |
| 4 | Locat [24] | $Lu= 4.4rl^{0.8}$ | (5) | rL |
| 5 | Guo et al. [26] | $L = 2.672 H - 208.31$ | (6) | H |
| 6 | Qarinur [23] | $L=1.267H^{1.027}$ | (7) | H |
| | | $L= 1.066H^{1.093}$ | (8) | H |
| | | $L = 1.448 H^{1.062} \tan \theta^{-0.482}$ | (9) | H, θ |
| 7 | Strand et al [20] | $Lu = 3.0 rL$ | (10) | rL |
| | | $Lu = 1.5rL$ | (11) | rL |
| | | $Lu = 0.5rL$ | (12) | rL |
| 8 | Samodra et al [27] | $L=1.65H+1.09$ | (13) | H |
| 9 | Zhou et al [28] | $L = 0.04 V^{1/3}$ | (14) | V |
| | | $L= 0.05 H^{0.43} V^{0.28}$ | (15) | $V H$ |
| 10 | Apriani et al. [22] | $L = 6.918 H^{0.84}$ | (16) | H |

Source: Corominas 1996; Rickenmann 1999; Legros 2002; Locat 2008; Guo et al. 2014; Qarinur 2015; Strand et al. 2017; Samodra et al. 2018; Zhou et al. 2019; Apriani, Credidi, and Khala 2022

3 Empirical Method for Runout Distance Prediction - Malaysia

The research location spans both East and West Malaysia, encompassing significant landslide events. The selection criteria for landslides in this study concern the ability to measure their extent and the availability of reliable geotechnical and geometric information. For this study, landslide data from 1993 to 2022 were collected based on satellite imagery interpretation, investigation reports, and descriptions from published papers and newspapers. Data collection encompassed mostly quantitative information of past landslide events in Malaysia (i.e. the runout distance, landslide volume etc.) allowing comprehensive analyses of the landslide parameters needed for developing the empirical models. The landslides in the dataset are those induced by rainfall.

Table 15 displays the distribution of landslides and their parameters, which were used to develop a statistical model for landslide runout distance. Among these parameters, data on slope height is the most widely available. However, obtaining data on other parameters, such as retrogression distance and landslide volume, proved to be challenging, as they are often absent from reports. Similar to Indonesia, where parameter landslide volume (V) is frequently neglected in reports [22], this scarcity of robust data exists. Despite this limitation, past studies have established empirical models using less than 20 cases [23,29–31]. Using IBM software SPSS, statistical analyses were employed to derive empirical equations for landslide runout distance, considering height of slope (H), travel distance (L), slope angle (θ), retrogression distance (rL), runout (Lu), and landslide volume (V).

4 Relationship between landslide runout distance and landslide parameters

Given the multitude of factors influencing landslide movement, it is imperative that the predictive model for landslide travel distance take into account the various influential parameters. To accomplish this, regression analyses were employed, supported by the application significance tests (i.e. F-tests and T-tests), to derive an optimized model for predicting landslide travel distance [22,26,31]. R-squared (R^2) values will be used to establish the correlation between the variables in the model. R^2 denotes the multiple correlation coefficient, indicating the degree of correlation between the dependent variable and its independent counterparts. The

computation of R^2 takes into account the variable count and serves as a means to assess the goodness of fit and accuracy across diverse regression models [26,31,32]. An R^2 value of 0.6 or higher signifies a strong correlation and suggests that the constructed regression models are reliable [22,28,33]. Moreover, the p-value served as a tool to examine statistical significance. Relationships with a p-value less than 0.05 will be deemed statistically significant [28,31].

4.1 Correlation between Slope height (H), volume (V) and total travel distance (L)

In Figure 67 and Figure 68, the relationship between landslide travel distance (L) and two variables, slope height (H) and landslide volume (V), respectively, is illustrated. Figure 67 shows a weak linear correlation ($R^2=0.271$) between slope height and landslide travel distance. Using the slope height alone to predict landslide travel distance is not sufficient due to the unknown positions of the toe of the failed mass and the crest of the sliding source before the landslide event [26]. Therefore, considering other influential factors simultaneously is recommended.

Figure 68 reveals a relatively strong linear correlation between landslide travel distance (L) and landslide volume (V) ($R^2=0.709$). The p -value = 0.035 < 0.05, indicating that landslide volume significantly affects travel distance. The results suggest an exponential correlation between travel distance and landslide volume, meaning that travel distance rapidly increases with landslide volume.

This observation supports the statement in [21] that "the travel distance depends primarily on the volume and not on the fall height, which just adds scatter to the correlation." The stronger correlation between volume (V) and travel distance (L) compared to slope height (H) and travel distance (L) suggests that landslide propagation is mainly influenced by their own volume rather than slope height.

The correlation's R^2 value is 0.879 (Figure 69), with the regression model being statistically significant (p -value < 0.05). Equation (20) can be further transformed into power law relationships.

$$L = 0.0078H^{1.46}V^{0.387} \quad (17)$$

Nonetheless, the coefficient of determination (R^2) of using a combination of H and V together is higher ($R^2=0.879$) than those using only the parameters of height of slope, H alone ($R^2=0.269$) or volume, V alone ($R^2=0.709$). This shows that multivariate runout relationship provides higher accuracy.

4.1.1 Correlation between Slope height (H) and Slope Angle (θ) and Runout Distance (Lu)

As there are two independent variables, slope height (H) and slope angle (θ), multiple linear regression is employed to analyse the data. The predictive equation of multiple linear regression analysis can be seen as follows:

$$L = 4.788 H^{0.898} \tan \theta^{0.048} \quad (18)$$

The coefficient of determination R^2 is 0.307 which is rather weak. In the study conducted by [23] it is stated that an equation form from a combination of slope height (H) and slope angle (θ) is a better landslide runout predictor compared to relying solely on slope height (H) due to the change of the value of R^2 . In this study, it should be noted that the rise of R^2 value obtained from using slope height (H) and slope angle (θ) ($R^2=0.307$), while the coefficient of determination R^2 of using only slope height (H) is only ($R^2=0.271$). This observation seems to concur with the results of [23].

In terms of significance, the model with a combination of slope height (H) and slope angle (θ) has an p -value value of $0.159 > 0.05$. The p -value of $0.159 > 0.05$ indicates that the model does not provide strong statistical evidence to reject the null hypothesis, implying that the relationship between variables is not be statistically significant. Furthermore, the p -value for slope angle parameter (θ) is found to be higher than 0.05 which further confirms that the slope angle parameter (θ) does not have a significant effect on the travel distance. Similar observations were seen in the recent empirical statistical study by [22].

Table 15 The parameters of rainfall triggered landslides in Malaysia

| No. | Name | slope angle,(θ), degrees | slope height (H), m | landslide volume (V), m ³ | Retrogression distance (rL), m | Runout, (Lu), m | Travel distance (L) , m | Source |
|-----|--|--------------------------|---------------------|---------------------------------------|--------------------------------|-----------------|-------------------------|---------|
| 1 | Highland tower 1993 | 20 °-30 ° | 48 | 40,000 | - | - | 120 | [3,34] |
| 2 | Bukit Antarabangsa 2008 | 45° - 50 ° | 65 | 101,500 | 120 | 210 | 330 | [34,35] |
| 3 | Batang kali 2022 | 45 ° | 70 | 450,000 | 330 | 270 | 600 | [36,37] |
| 4 | Taman Zooview, Ulu Kelang, 2006 | - | 60 | | - | - | 100 | [38] |
| 5 | Puncak Setiawangsa 2012 | 35°-66 ° | 42 | - | - | - | 71 | [39,40] |
| 6 | Failure investigation of a fill slope in Putrajaya, Malaysia, 6th of January 2001 | 22° to 25 ° | 25 | - | - | - | 50 | [41] |
| 7 | Cut slope in kedah | 45 ° | 27 | - | - | - | 250 | [42] |
| 8 | Filled Slope in Selangor | 22-45 ° | 21 | - | - | - | 120 | [42] |
| 9 | Kem Terendak, Melaka 2019 | 30 ° | 21 | - | - | - | 44 | [43] |
| 10 | Bukit Nanas 7th May 2013 | 30°-45 ° | 30 | - | 50 | 100 | 150 | [44] |
| 11 | Ialuan Seksyen 6, Jalan Sungai Ikan, Kampung Raja, Cameron Highland, Pahang , April 2019 | - | 38 | - | - | - | 108 | [45] |
| 12 | Ruan Changkul, Simunjan on the 28th January 2002. | 25°-40 ° | 76 | 20,000 to 22,000 | 130 | 92 | 222 | [46] |
| 13 | Slope Failure at Putrajaya 2007 | 45 ° | 50 | - | 23 | 25 | 58 | [47,48] |
| 14 | Bukit Lanjan 2003 | 70 ° | 70 | 35,000 | - | - | 160 | [49,50] |
| 15 | Taman Hillview 20 November 2002 | 20-30 ° | 60 | 25,000 | 110 | 90 | 200 | [51] |

Source: Shong et al. 1982; Hashim and Among 2003; Komoo and Lim 2003; Hussein and Mustapha 2004; Gue and Cheah 2008; Ooi 2009; Sapari, Nasiman and Tipol, Farah Hanan and Rahamat Noor, Nurul Farah and Mohamed Zaid 2011; Ahmed et al. 2012; Huat et al. 2012b; Qasim and Osman 2013; Osman et al. 2014; NAJIB 2016; Ismail and Yaacob 2018b; Alsubal et al. 2019; Khairul Anuar 2022; Lias et al. 2022; Sim et al. 2023; Halim et al. 2023

Figure 67 Landslide travel distance in relations with slope height

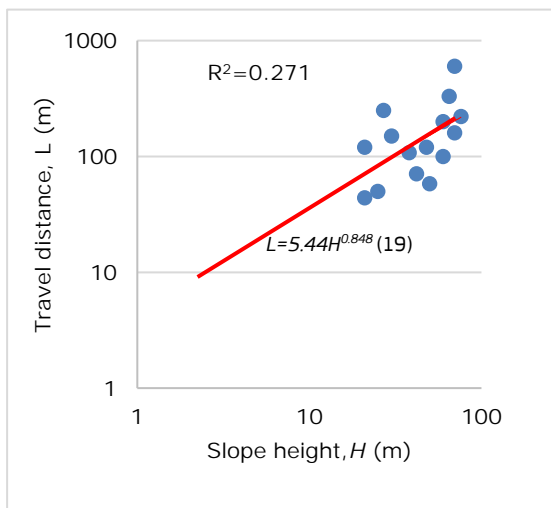


Figure 68 Landslide travel distance in relations with landslide volume

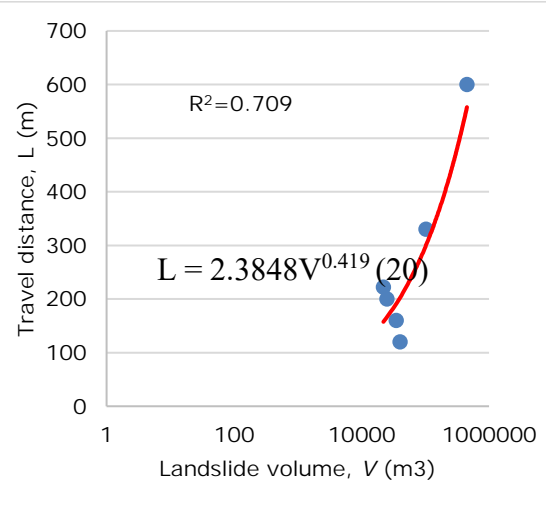
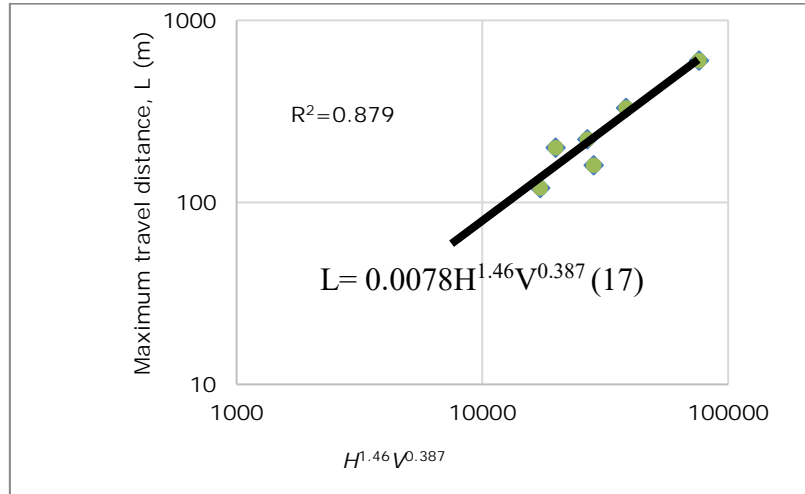


Figure 69 Relationship of maximum travel distance (L) versus slope height (H) and landslide volume (V)



4.2 Retrogression and Runout Distances, Lu and rL

There are currently no direct guidelines for determining rL in Malaysia. Therefore, slope stability analyses specific to Malaysia's conditions need to be conducted to investigate rL more thoroughly [20]. Figure 70 demonstrates a relatively strong relationship ($R^2=0.774$) between rL (retrogression distance) and Lu (runout), described by the power function: (dotted line in Figure 70):

$$Lu = 2.6697rL^{0.8051} \quad (21)$$

The upper limit for the studied cases is defined by the power function: (solid line in Figure 70):

$$Lu = 3.6322rL^{0.8475} \quad (22)$$

These equations align with those developed by [24]. The statistical analysis confirms the appropriateness of the model, p -value of $0.02 < 0.05$. Additionally, Lu can be estimated using the relationship from Figure 70 as follows:

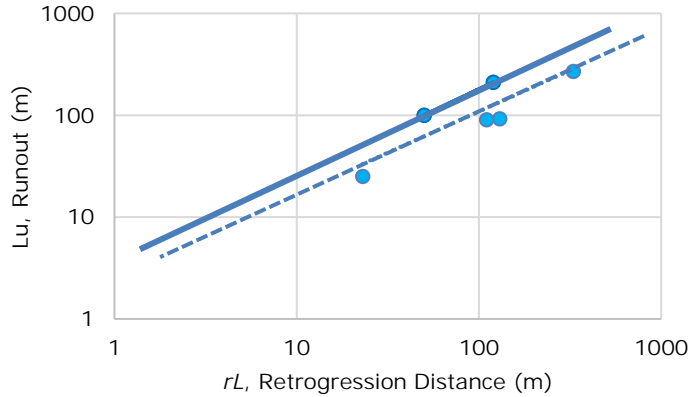
$$Lu = 0.9125rL \quad (23)$$

The upper limit/ maximum credible runout is defined by the following relationship (dash line in Figure 70) :

$$Lu = 1.787rL \quad (24)$$

Overall, one can conclude that the variable retrogression distance significantly affects the runout.

Figure 70 Relationship between runout, Lu , and retrogression distance, rL



4.3 Model validation

To further validate the proposed models, the runout/travel distance in each case study were back-calculated using the models developed by past researchers in

Table 14 as well as the newly developed ones. The estimation of errors of each landslide were obtained using the equation: $|L_{predicted} - L_{observed}| / L_{observed} \times 100\%$ (25). The average error for the models are shown in Table 16. The percentage shown in the table indicates the extent to which the predicted values differ from the actual values. For example, a 90% average error of means that, on average, the predicted value using model (1) differs by 90% from the actual value. This is not favorable, as a large average error suggests significant discrepancies.

Table 16 Landslide travel distance/runout prediction models and their comparisons

| Researcher(s) | Equations | Parameters used | Average error(%) |
|---------------------|--|-----------------|------------------|
| Corominas [25] | $L = 1.03V^{0.105} H$ (1) | $V H$ | 90% |
| Rickenmann [14] | $L = 1.9V^{0.16} H^{0.8}$ (2) | $V H$ | 45% |
| Legros [21] | $L = 8V^{0.25}$ (3) | V | 44% |
| Locat [24] | $Lu = 8.8rL^{0.8}$ (4) | rL | 242% |
| | $Lu = 4.4rL^{0.8}$ (5) | rL | 72% |
| Guo [26] | $L = 2.672 H - 208.31$ (6) | H | 195% |
| Qarinur [23] | $L = 1.267H^{1.027}$ (7) | H | 50% |
| | $L = 1.066H^{1.093}$ (8) | H | 47% |
| | $L = 1.448 H^{1.062} \tan \theta^{-0.482}$ (9) | H, θ | 44% |
| Strand et al [20] | $Lu = 3.0 rL$ (10) | rL | 192% |
| | $Lu = 1.5rL$ (11) | rL | 59% |
| | $Lu = 0.5rL$ (12) | rL | 51% |
| Samodra et al [27] | $L = 1.65H + 1.09$ (13) | H | 43% |
| Zhou et al [28] | $L = 0.04 V^{1/3}$ (14) | V | 308% |
| | $L = 0.05 H^{0.43} V^{0.28}$ (15) | $V H$ | 97% |
| Apriani et al. [22] | $L = 6.918 H^{0.84}$ (16) | H | 68% |

| | | | | |
|-------------------|---|------|-------------|--------|
| The present study | $L = 0.0078H^{1.46}V^{0.387}$ | (17) | H, V | 14.80% |
| | $L = 4.788 H^{0.898} \tan \theta^{0.048}$ | (18) | H, θ | 60% |
| | $L = 5.44H^{0.848}$ | (19) | H | 51% |
| | $L = 2.3848V^{0.419}$ | (20) | V | 25.17% |
| | $Lu = 2.6697rL^{0.8051}$ | (21) | rL | 32% |
| | $Lu = 3.6322rL^{0.8475}$ | (22) | rL | 75% |
| | $Lu = 0.9125rL$ | (23) | rL | 29% |
| | $Lu = 1.787rL$ | (24) | rL | 78% |

Source: Corominas 1996; Rickenmann 1999; Legros 2002; Locat 2008; Guo et al. 2014; Qarinur 2015; Strand et al. 2017; Samodra et al. 2018; Zhou et al. 2019; Apriani, Credidi, and Khala 2022

Based on the results in Table 16, it is not surprising that empirical expressions (19) and (18) show large errors, as they have low correlation coefficients of R^2 at 0.271 and 0.307, respectively. Notably, models (8) and (9) proposed by Qarinur [23], and empirical model (13) proposed by Samodra et al. [27], have similar accuracy with errors around $\pm 45\%$. This observation is understandable as both Indonesia and Malaysia are tropical countries with high rainfall throughout the year, and they share similar coastal plains, hills, and mountainous terrains. It should be noted that while geographical and climatic similarities might contribute to similar landslide behaviors, the accuracy of any model remains fundamentally rooted in the quality and relevance of the employed datasets.

Other models, such as those proposed by Zhou et al. [28] and Corominas [25], do not yield satisfactory results, with average errors of 97% and 308% respectively. The model by Zhou et al. [28] predicts longer travel distances than observed, but none smaller than the actual observations. This discrepancy might be because their dataset consists of debris flows in the earthquake-prone area of Wenchuan, China, whereas most landslides in Malaysia are rainfall-induced and involve different mechanisms. Similarly, the model by Corominas [25] may not be applicable to Malaysia due to differences in geological and hydrogeological conditions. More popular empirical models proposed by Rickenmann [14] and Legros [21] show relatively more reasonable average errors within $\pm 44\%$. The proposed models (17) and (20), using parameters H and V , exhibit good performance in predicting landslide travel distance, with relative errors within $\pm 15\%$ and $\pm 25\%$ respectively.

Comparative analyses reveal that models (21) and (23), which incorporate retrogression distance (rL), produce reasonably good performance in predicting landslide runout, with relative errors within $\pm 30\%$, consistent with studies in [22,26]. However, the upper limit empirical models (22) and (24) predict runout distances nearly 80% higher than actual values. These models are designed to be conservative and provide a safety margin for emergency situations, avoiding underestimation of risk and hazard. On the other hand, models proposed by Strand et al. [20] and Locat [24] do not yield satisfactory results, with average errors reaching overestimations as high as 242%. These models were tailored to flow slide of sensitive clays in Norway and Eastern Canada, which differ significantly from the landslides in Malaysia, possibly due to distinct geological and hydrogeological conditions.

Overall, the runout predictions in this study show the closest resemblance to observed values because they are based on local datasets, making them more applicable to specific ground conditions in Malaysia. They shall contribute to bolstering safety measures and enhancing decision-making support in landslide-prone regions. It is proposed that probabilistic slope stability analyses be conducted to determine the potential occurrence of landslides for any particular development in a specific region in the country. Following that, the retrogression distance (rL) will be used to determine the runout for the aforementioned landslide study, as (rL) can be determined through slope stability analyses. In addition, landslide volume would be a good parameter to use provided enough parameters i.e. landslide area is available for its derivation. Accurate runout predictions empower authorities and infrastructure planners to proactively implement tailored mitigation strategies. In addition, landslide runout predictions is crucial to establish safety measures when creating buffer zones, aiming to mitigate the effects of landslides [54,55].

5 Conclusions

Landslide runout distance is crucial for assessing landslide hazard and risk, particularly for identifying potentially affected elements. Predicting runout typically involves either empirical/statistical methods or analytical dynamic methods. However, obtaining reliable predictions requires sophisticated rheology models and material parameters, which are often unavailable, especially in developing nations such as Malaysia. In the absence of such data, it is highly recommended to estimate runout and landslide impacts using empirical methods [8,18,22,26,31,56].

In this study, we reviewed established and newly developed empirical models to estimate landslide runout in Malaysia. We based our recommendations on a comprehensive dataset of historical landslides in the country. We performed statistical analyses to assess the efficiency of various parameters, such as height of slope (H), travel distance (L), slope angle (θ), retrogression distance (rL), runout (Lu), and landslide volume (V). By comparing the constructed models with other established models using coefficients of determination (R^2) and other statistical parameters like p -values, we evaluated the accuracy of the newly developed models.

Our analyses revealed that multivariate equations, such as those combining V and H , yield better predictions than univariate models that only use parameter V . Univariate runout relationships are simpler but less accurate, while multivariate models offer improved accuracy. Notably, we found a strong relationship between retrogression distance (rL) and runout, as well as volume (V) and slope height (H) with runout. Determining landslide volume (V) can be challenging in practice. However, an equation ($V = 2.482 A^{1.024}$ (25)) with determination coefficient of 0.99 was proposed by Amirahmadi et al. [23] to estimate volume of landslides by analyzing the landslide area. This equation stated to be applicable globally as it utilizes data from diverse regions across different countries [22,23]. On the other hand, accurate rL values can be obtained through slope stability analyses.

Two new models were developed using retrogression distance, which provide reasonably good estimates of runout distance for Malaysia. However, it is essential to be cautious with an upper limit model, as it tends to overestimate runout distances.

The limitation of this study is that the more sophisticated parameters such as landslide types and soil parameters on travel distance were not studied. In addition, it would be interesting to be able to complete the missing geotechnical information for the dataset in Table 15 and to add more landslide cases. Data collection in Malaysia, as noted by Sim et al. [1] and Gue et al. [57], is a labor-intensive process involving mining information from various sources. Much information is scattered among different parties, and some of the documents are classified, either because they contain sensitive information or due to the trade secrets used by certain parties [57]. Despite all the challenges, the predicted results are in reasonable agreement with observations. Additional explorations are recommended to further refine the newly developed empirical models. It is encouraged for other researchers to utilize and add to this database continuously to enhance both the quantity and quality of the data, as statistical analyses rely on robust datasets. At present, the suggestions proposed in this paper can be utilized as an approximate estimation for landslide runout in Malaysia. The empirical model, although in preliminary stages, shows some promising results, holding the potential to significantly enhance safety measures. By providing reasonably accurate predictions, even in its early stages, this model equips decision-makers with a valuable idea for implementing proactive safety measures, thereby mitigating the risks associated with landslides.

References

1. Sim K Ben, Lee ML, Rasa RP, Wong SY. An Overview of Causes of Landslides and Their Impact on Transport Networks. In: Advances in Modelling to Improve Network Resilience [Internet]. 2022. p. 114–25. Available from: https://nottingham-repository.worktribe.com/index.php/preview/9903151/JRC130275_01.pdf#page=117
2. Froude MJ, Petley DN. Global fatal landslide occurrence from 2004 to 2016. Nat Hazards Earth Syst Sci. 2018;18(8):2161–81.
3. Sim K Ben, Lee ML, Wong SY. An Overview of Socioeconomic Impacts of Landslides. In: Proceedings of the IAIA 2023 conference. 2023.
4. Rahman HA, Mapjabil J. Landslides disaster in Malaysia: an overview. Health (Irvine Calif). 2017;8(1):58–71.
5. Lim CS, Jamaluddin TA, Komoo I. Human-induced landslides at bukit antarabangsa, hulu kelang, Selangor. Bull Geol Soc Malaysia. 2019;2019(67):9–20.
6. Sim K Ben, Lee ML, Rasa RP, Wong SY. Perception on landslide risk in Malaysia : A comparison between communities and experts â€™ surveys. Int J Disaster Risk Reduct [Internet]. 2023;95(July):103854. Available from: <https://doi.org/10.1016/j.ijdrr.2023.103854>

7. McDougall S. Landslide runout analysis — current practice and challenges. *Can Geotech J*. 2014;54(5):605–20.
8. Falconi LM, Moretti L, Puglisi C, Righini G. Debris and mud-ows runout assessment: a comparison among empirical geometric equations in the Giampilieri and Briga basins (east Sicily, Italy) affected by the event of 1st October 2009. *Reserach Sq* [Internet]. 2022;(October 2009):0–34. Available from: <https://doi.org/10.21203/rs.3.rs-2273092/v1>
9. Ward SN, Day S. Particulate kinematic simulations of debris avalanches: Interpretation of deposits and landslide seismic signals of Mount Saint Helens, 1980 May 18. *Geophys J Int*. 2006;167(2):991–1004.
10. Peruzzetto M, Mangeney A, Grandjean G, Levy C, Thiery Y, Rohmer J, et al. Operational estimation of landslide runout: Comparison of empirical and numerical methods. *Geosci*. 2020;10(11):1–35.
11. Scheidl C, Rickenmann D. Empirical prediction of debris-flow mobility and deposition on fans. *Earth Surf Process Landforms*. 2010;35(2):157–73.
12. Huang Y, Cheng H. A simplified analytical model for run-out prediction of flow slides in municipal solid waste landfills. *Landslides*. 2017;14(1):99–107.
13. Li WC, Deng G, Cao W, Xu C, Chen J, Lee ML. Discrete element modeling of the Hongshiyan landslide triggered by the 2014 Ms 6.5 Ludian earthquake in Yunnan, China. *Environ Earth Sci* [Internet]. 2019;78(16):1–18. Available from: <https://doi.org/10.1007/s12665-019-8438-2>
14. Rickenmann D. Empirical relationships for debris flows. *Nat Hazards*. 1999;19(1):47–77.
15. Jakob M, Hungr O, Jakob DM. Debris-flow hazards and related phenomena. Vol. 739. Springer; 2005.
16. Berti M, Simoni A. Prediction of debris flow inundation areas using empirical mobility relationships. *Geomorphology*. 2007;90(1–2):144–61.
17. Corominas J, van Westen C, Frattini P, Cascini L, Malet JP, Fotopoulou S, et al. Recommendations for the quantitative analysis of landslide risk. *Bull Eng Geol Environ*. 2014;73(2):209–63.
18. Guinau M, Vilajosana I, Vilaplana JM. GIS-based debris flow source and runout susceptibility assessment from DEM data - A case study in NW Nicaragua. *Nat Hazards Earth Syst Sci*. 2007;7(6):703–16.
19. Hungr O, Corominas J, Eberhardt E. State of the Art Paper #4, Estimating landslide motion mechanism, travel distance and velocity. *Landslide Risk Manag*. 2005;(February 2017):99–128.
20. Strand SA, Thakur V, L'Heureux JS, Lacasse S, Karlsrud K, Nyheim T, et al. Runout of landslides in sensitive clays. *Adv Nat Technol Hazards Res*. 2017;46(May):289–300.
21. Legros F. The mobility of long-runout landslides. *Eng Geol*. 2002;63(3–4):301–31.
22. Apriani DW, Credidi C, Khala S. An Empirical-Statistical Model for Landslide Runout Distance Prediction in Indonesia. *Pondasi*. 2022;27(1):15.
23. Qarinur M. Landslide Runout Distance Prediction Based on Mechanism and Cause of Soil or Rock Mass Movement. *J Civ Eng Forum*. 2015;1(1).
24. Locat P. Remaniement et mobilité des débris de glissements de terrain dans les argiles sensibles de l'est du Canada. 4th Can Conf Geohazards. 2008;1971:594.
25. Corominas J. The angle of reach as a mobility index for small and large landslides. *Can Geotech J*. 1996;33(2):260–71.
26. Guo D, Hamada M, He C, Wang Y, Zou Y. An empirical model for landslide travel distance prediction in Wenchuan earthquake area. *Landslides*. 2014;11(2):281–91.
27. Samodra G, Chen G, Sartohadi J, Kasama K. Generating landslide inventory by participatory mapping: an example in Purwosari Area, Yogyakarta, Java. *Geomorphology* [Internet]. 2018;306:306–13. Available from: <http://dx.doi.org/10.1016/j.geomorph.2015.07.035>
28. Zhou W, Fang J, Tang C, Yang G. Empirical relationships for the estimation of debris flow runout distances on depositional fans in the Wenchuan earthquake zone. *J Hydrol* [Internet]. 2019;577(July):123932. Available from: <https://doi.org/10.1016/j.jhydrol.2019.123932>
29. Costa JE. Floods from dam failures. *Flood Geomorphol*. 1988;439–63.
30. Edgers L, Karlsrud K. Soil Flows Generated By Submarine Slides - Case Studies and Consequences. *Behav Off-Shore Struct Proc Int Conf*. 1983;2(July):425–37.
31. Shan Y, Chen S, Zhong Q, Mei S, Yang M. Development of an empirical model for predicting peak breach flow of landslide dams considering material composition. *Landslides* [Internet]. 2022;19(6):1491–518. Available from: <https://doi.org/10.1007/s10346-022-01863-1>
32. Yang H, Pei Z, He Z, Lei J, Xia X. An empirical model for the travel distance prediction of deflection-type rock avalanches in the wenchuan earthquake area. *Front Earth Sci*. 2022;10(December).
33. Apriani DW, Salsabila AP, Khala CC, Silfiani M. Prediksi Jarak Luncur Longsoran Berdasarkan Parameter Geometri Lereng dan Tipe Batuan Landslide Distance Prediction Based on Slope Geometry and Rock Type Parameters. 2023;11(2):197–208.
34. Qasim S, Osman SBS. Causal factors of Malaysian landslides: A narrative study. *Res J Appl Sci Eng*

- Technol. 2013;5(7):2303–8.
35. Huat LT, Ali F, Ibrahim AS. An investigation on one of the rainfall-induced landslides in Malaysia. Electron J Geotech Eng. 2012;17 D(January 2012):435–49.
36. New Straits Times. Batang Kali landslide: How it happened? New Straits Times [Internet]. 2022 Dec 18; Available from: <https://www.nst.com.my/news/nation/2022/12/862066/batang-kali-landslide-how-it-happened>
37. Halim NZA, Abdullah N, Ghazali MD, Hassan H. The Possibility of Using Terrestrial-Based Ground Penetrating Radar (GPR) Technology for Supplying 3rd Dimension Information for A Search and Recovery Mission for Landslide Victims. Int J Geoinformatics. 2023;19(5).
38. Ooi TA. Some Cases of Fill Slope Failure and Rehabilitation in Malaysia. J Southeast Asian Geotech Soc [Internet]. 2009;1–10. Available from: http://seags.ait.asia/e-journal/1970-2012/GEJ_2009_v40n1-2-March_1-10.pdf
39. Ismail NI, Yaacob WZW. An investigation of landslides in Bukit Aman and Puncak Setiawangsa, Kuala Lumpur, Malaysia. AIP Conf Proc. 2018;1940(1):20031.
40. NAJIB FHB. SLOPE ANALYSIS AND REMEDIAL WORK ON LANDSLIDE AT TAMAN SETIAWANGSA KUALA LUMPUR [Internet]. Jurnal Algoritma. Universiti Teknologi Malaysia; 2016. Available from: <http://jurtek.akprind.ac.id/bib/rancang-bangun-website-penyedia-layanan-weblog>
41. Hussein AN, Mustapha AH. Failure Investigation of a Fill Slope in Putrajaya , Malaysia. Fifth Int Conf Case Hist Geotech. 2004;1–6.
42. Shong LS, & LCH, Leong LC. Four Landslide Investigations in Malaysia. 1982;1–6.
43. Lias R, Jais IBM, Lat DC. Climatic Influence on Slope Failure: A Case Study at Kem Terendak, Melaka. Int J Sustain Constr Eng Technol. 2022;13(1):39–49.
44. Osman K, Kasim N, Yusof MAM. Landslide Investigation : A Case Study of the Landslide in Bukit Nanas Lands slide Inv estigati on : A Case S Study o f the Lands slide in Bukit Nanas N F ore st Re eserve , Kuala Lump ur , Mala yasia. Proc World Landslide Forum 3. 2014;(2014):15–40.
45. Khairul Anuar MAF. Rainfall Impact on Slope Stability. Tech J Eng Appl Sci. 2022;1–14.
46. Hashim K, Among HL. Geological investigation on Ruan Changkul landslide. Bull Geol Soc Malaysia. 2003;46(May):125–32.
47. Alsubal S, Sapari N Bin, Harahap ISH, Ali Mohammed Al-Bared M. A review on mechanism of rainwater in triggering landslide. IOP Conf Ser Mater Sci Eng. 2019;513(1):0–12.
48. Ahmed J, Ghazali MA, Mukhlisin M, Alias MN, Taha MR. Effectiveness of horizontal drains in improving slope stability: A case study of landslide event in Putra Jaya Precinct 9, Malaysia. 5th Asia-Pacific Conf Unsaturated Soils 2012. 2012;2(July 2017):625–30.
49. Gue SS, Cheah SW. Geotechnical Challenges in Slope Engineering of Infrastructures. Int Conf Infrastruct Dev Putrajaya [Internet]. 2008;1–20. Available from: http://www.gnpgeo.com.my/download/publication/2008_04.pdf
50. Sapari, Nasiman and Tipol, Farah Hanan and Rahamat Noor, Nurul Farah and Mohamed Zaid SN. Joint Patterns in Granite And Its Relationship With Its Slope Failure : Bukit Lanjan Revisited. 2011;(October 1993):31–2.
51. Komoo I, Lim CS. Tragedi gelinciran tanah Taman Hillview. Bull Geol Soc Malaysia. 2003;46(October 2014):93–100.
52. Huat LT, Ali F, Ibrahim AS. An investigation on one of the rainfall-induced landslides in Malaysia. Electron J Geotech Eng. 2012;17 D(December 2008):435–49.
53. Ismail NI, Yaacob WZW. An investigation of landslides in Bukit Aman and Puncak Setiawangsa, Kuala Lumpur, Malaysia. In: AIP Conference Proceedings. AIP Publishing LLC; 2018. p. 20031.
54. Erfen HFWS, Musta B. Landslide Runout Distance Prediction of Pinousuk Gravel Slope in Mesilou Kundasang, Sabah Using Slope Characterization. IOP Conf Ser Mater Sci Eng. 2022;1229(1):12012.
55. Xu Z, Stark TD. Runout analyses using 2014 Oso landslide. Can Geotech J. 2022;59(1):55–73.
56. Guinau M, Pallàs R, Vilaplana JM. A feasible methodology for landslide susceptibility assessment in developing countries: A case-study of NW Nicaragua after Hurricane Mitch. Eng Geol. 2005;80(3–4):316–27.
57. Gue SS, Karnawati D, Wong SY. Policy and institutional framework for landslide mitigation and risk reduction. Landslides - Disaster Risk Reduct. 2009;531–54.

2.25 Complex Systems Resilience to Hybrid Threats

Frédéric Petit, European Commission, Joint Research Centre (JRC), Ispra, Italy
frederic.petit@ec.europa.eu

Stefano Ruberto, Commission, Joint Research Centre (JRC), Ispra, Italy
stefano.ruberto@ec.europa.eu

Monica Cardarilli, Commission, Joint Research Centre (JRC), Ispra, Italy
monica.cardarilli@ec.europa.eu

Georgios Valsamos, Commission, Joint Research Centre (JRC), Ispra, Italy
georgios.valsamos@ec.europa.eu

Extended abstract

The society constitutes a system-of-systems of physically and virtually linking components (e.g., social, economic, infrastructure, environmental, and governance) that influence and interact with each other. This complex system is in a fragile equilibrium where disruption of one component can result in cascading failures across all systems. The COVID-19 pandemic and extreme climatic events have emphasized the disparities in resilience and security capabilities and the need for more holistic strategies that address the interdependencies between infrastructures that make up these interconnected social, natural, and built environments across the European Union (EU). The society is contingent on its ability to manage complexities across critical entities and develop cohesive and concerted efforts to withstand and adapt to all hazards.

The consideration of hybrid threats adds another level of complexity especially through cascading effects. Resilience in the context of hybrid threats requires a perspective that goes beyond resilience in sectoral areas. Hence, the “whole-of-society” approach considering dependencies and interdependencies is needed. Developing the next generation of infrastructure interdependencies modelling requires multidisciplinary and collaborative approaches to enhance our understanding of operations of critical entities systems. Most research still focuses on assessing physical interdependencies to anticipate cascading failures for a limited number of infrastructure systems. Only a few works consider cyber, social, and governance aspects. Current assessments are limited by data availability, and they do not consider adaptation capabilities during a crisis. It is essential to lay the foundations to model the interactions among infrastructure systems in real-time to anticipate their impact on society’s mitigation and response capabilities to hybrid threats.

The JRC work on hybrid threats proposes an analytical framework to conceptualize the phenomenon and provide more comprehensive analytics to counter them. It proposes a broad suite of measures at the EU and national levels designed to assess and mitigate vulnerabilities, streamline policies and procedures, and harness advanced technologies and capabilities to counter hybrid threats effectively and holistically. Cognitive computing can also be used to enhance the understanding of interdependencies and how infrastructure systems adapt to various types of disruption. Artificial intelligence could improve our understanding of critical entities’ behaviour during a crisis, address current interdependencies modelling challenges, and assist human thinking and decision-making.

This presentation will discuss and illustrate existing techniques that can be used to enhance the resilience of critical entities by:

- Filling existing data gaps in identifying and understanding infrastructure interdependencies; and
- Analysing critical entities' resilience to hybrid threats.

3 Conclusions of the Seminar

We believe that the Seminar provided a glimpse of what the state of resilience is at the moment and likewise prospects in this field of research, which is tightly linked to reliability and risk analysis, assessment and management. The seminar highlighted the presence of multi-disciplinary group of scientists working on the subject that will be able to contribute to further works in the field, also within ESReDA activities.

The 63rd Seminar served also as an opening event for the new ESReDA project group, Resilience Assessment of Critical Infrastructure, which was approved by the General Assembly of ESReDA during the meeting in April 2023. This project group (PG) continues the work done in the previous ESReDA project group “Resilience Engineering and Modelling of Networked Infrastructure” during 2018-2021 period. This Seminar served as a forum to discuss the possible work directions of the project group, exchange ideas and set a work plan for the next years. A dedicated project group meeting was held on October 24, the day before the Seminar.

With that in mind, we envisage the need to continue this work on resilience within the new ESReDA project group. Therefore we invite all interested institutions to contact the organisers to develop a joint plan for future work in the field of resilience.

Annexes

Annex 1. Programme of the Seminar as presented.

Day 1. Wednesday 25 October

| Start | End | Agenda item |
|--------------|--------------|---|
| 08:00 | | Departure from the Hotel* to JRC (organised BUS) |
| 09:15 | 09:30 | Welcome to the participants (JRC, ESReDA) |
| 09:30 | 10:15 | PLENARY TALK I. Infrastructure Resilience: State of Science and Practice Igor Linkov |
| 10:15 | 12:00 | SESSION I. Resilience in the energy sector – part I Chair: Christophe Bérenguer |
| 10:15 | 10:30 | 1. The resilience of the Ukraine's critical energy infrastructure during the war with Russia Andrii Davydiuk |
| 10:30 | 10:45 | 2. On the resilience of the European Union natural gas system Rebecca Schill, Ricardo Fernández-Blanco, Nuria Rodríguez Gómez, Anca Costescu, Ricardo Bolado Lavín |
| 10:45 | 11:15 | Break |
| 11:15 | 11:30 | 3. Resilience enhancement of gas transmission system by remote control deployment of valves: methodology of indicator analysis and case study Bogdan Vamanu, Vytis Kopustinskas, Vladislavas Daškevičius and Andrius Dagys |
| 11:30 | 11:45 | 4. Application of metaheuristic algorithms for finding strategy of optimal response to natural gas supply disruptions Ivars Zalitis, Laila Zemite and Aleksandrs Dolgicers |
| 11:45 | 12:00 | 5. Hydrogen Electrolyzers as a flexible source for the optimal operation of the distribution grid Irina Oleinikova, Basanta Raj Pokhrel, Marius Rasmussen and Sofie Lorentzen |
| 12:00 | 13:15 | Lunch Break |
| 13:15 | 14:00 | PLENARY TALK II. Resilience analytical quantitative approaches to classify and rank first principle resilience and risk assessment and simulation options Ivo Häring |
| 14:00 | 15:00 | SESSION II. Indicators and metrics of resilience in critical infrastructures Chair: Myrto Konstantinidou |
| 14:00 | 14:15 | 6. Risk and resilience-informed decision-making for strategic territorial risk management : from methodologies to practical implementation for infrastructures exposed to mountain natural hazards Jean-Marc Tacnet, Simon Carladous, Nour Chahrour and Christophe Bérenguer |
| 14:15 | 14:30 | 7. Towards a modular co-simulation framework for the assessment of cascading effects among critical infrastructures and the impact on citizens Till Martini, Julia Rosin, Joanna Zarah Vetter, Stefan Neuhäuser, Eridy Lukau, Faruk Catal, Maurizio Boigk, Maik Simon, Michael Monteforte, Michael Gerold, Windy Phung, Steffen Dietze, Jörg Finger, Patrick Brausewetter and Steffen Nicolai |
| 14:30 | 14:45 | 8. Remaining Useful Life of hydraulic steel structures under high-cycle fatigue Presentation of the chair Medelia and preliminary study of a lock gate Julien Baroth, Vincent Michaud, Rafael Estevez and Arnaud Isaac |
| 14:45 | 15:00 | 9. Resilience Metrics for Interdependent Infrastructure Systems: Characterization in full-scale Application Paolo Trucco and Boris Petrenj |
| 15:00 | 15:30 | Break |

| | | |
|--------------|--------------|---|
| 15:30 | 16:30 | SESSION III. Resilience of critical assets and impact on urban infrastructures Chair: Jean-Marc Tacnet |
| 15:30 | 15:45 | 10. A territorial view to the resilience of infrastructures David Javier Castro Rodriguez, Micaela Demichela |
| 15:45 | 16:00 | 11. Use of Multi-Criteria Decision Analysis for assessing the resilience of Critical Entity systems Frédéric Petit |
| 16:00 | 16:15 | 12. The main topics of discussion and research on issues of modelling systemic changes in urban systems Katarzyna Goch, Przemysław Śleszyński and Andrzej Affek |
| 17:00 | | Departure from JRC to the Hotel* (organised BUS) |
| 19:00 | | Gala dinner at the Hotel* |
| | | End of Day 1 |

* Dolce Milano Malpensa Hotel

Day 2. Thursday 26 October

| Start | End | Agenda item |
|--------------|--------------|---|
| 08:00 | | Departure from the Hotel* to JRC (organised BUS) |
| 09:15 | 09:45 | PLENARY TALK III. Risk preparedness regulation in the electricity sector: aims and challenges Marta Poncela Blanco |
| 09:45 | 10:30 | SESSION IV. Resilience in the energy sector – part II Chair: Laila Zemīte |
| 09:45 | 10:00 | 13. Impacts of Climate Change on interdependent Critical Energy Infrastructure: Direct and Cascading Effects across Energy Production, Transport and Demand Ricardo Tavares da Costa, Elisabeth Krausmann and Marta Poncela |
| 10:00 | 10:15 | 14. Fragility assessment of power grid infrastructure towards climate resilience and adaptation Georgios Karagiannakis, Mathaios Panteli and Sotirios Argyroudis |
| 10:15 | 10:30 | 15. Feasibility Study: Improving Low-inertia Power System Resilience by Novel Load Shedding Method Including Control of Synchronous Condensers' Power Injections Antans Sauhats, Andrejs Utans, Dmitrijs Guzs, Diana Zalostiba, Anna Mutule and Oskars Grigals |
| 10:30 | 11:00 | Break |
| 11:00 | 12:00 | SESSION V. Resilience in the energy sector - part III Chair: Saulius Gudžius |
| 11:15 | 11:30 | 16. An innovative methodology for risk-based resilience assessment to prioritize grid interventions against natural threats in the Italian power system Emanuele Ciapessoni, Diego Cirio, Andrea Pitto, Silverio Casulli, Giuseppe Berrettoni, Federico Falorni, Francesca Scavo, Greta Magnolia, Francesco Marzullo and Enrico Maria Carlini |
| 11:30 | 11:45 | 17. The Resilience Assessment in Electricity sector: How to get started, holistic or segmented view? Maria Luisa Alberto and Manuela Gaivéo |
| 11:45 | 12:00 | 18. Modelling of power disruption scenarios by PyPSA in the Baltic region Isabel Asensio Bermejo, Hrvoje Foretić, Vytis Kopustinskas |

| <i>Start</i> | <i>End</i> | <i>Agenda item</i> |
|--------------|--------------|---|
| 12:00 | 13:15 | Lunch Break |
| 13:15 | 14:00 | SESSION VI. Resilience of the energy sector by renewable generation Chair: Hrvoje Foretić |
| 13:15 | 13:30 | 19. The Impact of Small Hydro Power Plants on the Adequacy of a Power System with High Penetration of Renewable Energy Sources Jonas Vaičys, Saulius Gudžius, Audrius Jonaitis and Daivis Virbickas |
| 13:30 | 13:45 | 20. Evaluation matrix to select appropriate countermeasures for Offshore Windfarm protection Babette Tecklenburg, Alexander Gabriel, Arto Niemi and Frank Sill Torres |
| 13:45 | 14:00 | 21. Addressing the Risk of Prolonged Periods of Low Renewable Generation in Power Systems Resilient Planning Ektor-Ioannis Stasinios, Mathaios Panteli and Nikos Hatziargyriou |
| 14:00 | 14:20 | Break |
| 14:20 | 15:20 | SESSION VII. Resilience of complex systems Chair: Micaela Demichela |
| 14:20 | 14:35 | 22. Assessing risk of water damage to buildings under current and future climates Ola Haug, Claudio Heinrich-Mertsching and Thordis Thorarinsdottir |
| 14:35 | 14:50 | 23. Flood resilience and sustainability in bridge climate adaptation Stergios Aristoteles Mitoulis and Sotirios Argyroudis |
| 14:50 | 15:05 | 24. An Empirical Model for Predicting Landslide Runout Distance in Malaysia Kwan Ben Sim, Min Lee Lee, Rasa Remenyte-Prescott and Soon Yee Wong |
| 15:05 | 15:20 | 25. Complex Systems Resilience to Hybrid Threats Frédéric Petit, Stefano Ruberto, Monica Cardarilli and Georgios Valsamos |
| 15:20 | 15:45 | Closing of the Seminar |
| 16:00 | | Departure from JRC to the Hotel* and Malpensa Airport (organised BUS) End of Day 2 and Seminar |

* Dolce Milano Malpensa Hotel

Annex 2. Plenary speakers

Speaker 1: Igor Linkov - Infrastructure Resilience: State of Science and Practice

Dr. Igor Linkov is Senior Science and Technology Manager with the US Army Engineer Research and Development Center (ERDC), and Adjunct Professor with Carnegie Mellon University. He is responsible for ERDC's project portfolio in the areas of crises mitigation and resilience. He develops methods and tools for measuring resilience in interconnected network and applies these tools to critical infrastructure, transportation, energy and cyber systems, supply chains as well as command and control systems. He is Army representative at the White House Networking and Information Technology Research and Development (NITRD) Program. He has published widely on environmental and technology policy, climate change, and risk and resilience analytics, including twenty five books and over 500 peer-reviewed papers and book chapters in top journals, like Nature, Nature Nanotechnology, Nature Climate Change, among others. Dr. Linkov is Elected Fellow with the American Association for the Advancement of Science (AAAS) and Society for Risk Analysis. Dr. Linkov has received multiple USACE, Army and DOD Awards and Civilian Service medals, including the highest Civilian Award in the US Army and 2023 Army's Humanitarian Assistance Medal, as well 2020 DOD Top Scientist Award. He received multiple awards from the Society for Risk Analysis (SRA), 2022 Edgeworth-Pareto Award from the International Society for Multi Criteria Decision Making (MCDM), 2022 IDRIM Distinguished Research Award, and 2021 Arthur Flemming Award for outstanding public service.



Speaker 2: Ivo Häring – Resilience Analytical Quantitative Approaches to Classify and Rank First Principle Resilience and Risk Assessment and Simulation Options

Dr. Ivo Häring gained his doctorate at Max-Planck-Institute for the Physics of Complex Systems (MPIPKS) and TU Dresden. Since 2004 he works at Fraunhofer Ernst-Mach-Institute (EMI), currently as Senior Scientist in the Department Safety and Resilience of Technical Systems. He lectures for the master courses Risk Engineering at Furtwangen University of Applied Science (HFU) and Sustainable Systems Engineering at the corresponding department INATECH of the Faculty of Engineering of the University of Freiburg. Research projects (set up) and corresponding publication record cover in 2023 25 million Euro research funding. Domains of interest include analysis of event probabilities and susceptibility, of hazards and damage, vulnerability, risks and resilience of socio-technical systems. Furthermore, concepts of technical risk and resilience analysis, engineering and management, functional safety analysis and related methods, in particular when applied to new domains, e.g. autonomous driving. Sample projects include EU projects in critical infrastructure resilience domain covering electricity (eFORT), gas networks and Storage (SecureGas, EDEN), telecommunication (RESISTO), transport (TRESPASS, XP-DITE), and urban infrastructure (EDEN, D-BOX, ENCOUNTER, VITRUV), countering of large-scale fires (AF3), as well as projects covering several CIs (RESILIENS, SnowBall). He (co-)authored 2 books, 24 articles, 68 conference papers and 7 book chapters.

**Speaker 3: Marta Poncela Blanco – Risk Preparedness Regulation in the Electricity Sector: Aims and Challenges**

Dr. Marta Poncela studied MSc electrical engineering at the University of Valladolid where she also obtained a PhD in information and telecommunication technologies. Currently she is Policy Officer at the European Commission, Directorate General for Energy, Energy Security and Safety unit. Previously she worked at the European Commission, DG Joint Research Centre for 9 years, in the Energy Security, Distribution and Markets Unit doing research for policy support on risk preparedness for the electricity sector, resource adequacy, smart grid laboratories and projects of common interest among other topics. Before joining the European Commission, she was for more than 10 years the responsible of the energy division at Cartif technology centre in Spain working on energy efficiency, renewable energy and hydrogen.



Her research areas include risk assessment for the electricity sector, resource adequacy and integration of renewable energies into the grid. She is an expert in modelling, forecasting techniques and statistical analysis applied to the energy system. She has worked in several R&D projects in the energy sector, and she is author of several reports, book chapters and scientific papers.

Annex 3: About the Seminar



European Safety, Reliability &
Data Association



63rd ESReDA Seminar
on
Resilience assessment: Methodological challenges
and applications to critical infrastructures

25-26 October 2023

JRC Conference Centre – bdg 36 – 1st floor, Module C
European Commission Joint Research Centre (JRC)
Via Enrico Fermi 2749, I-21027 Ispra (VA), Italy



A. Seminar organisation

The Seminar is jointly organised by ESReDA and JRC.

B. Location

European Commission Joint Research Centre (JRC)

Via Enrico Fermi 2749, I-21027 Ispra (VA), Italy

C. Chairperson of the Seminar

Kristine VLAGSMA (European Commission, Joint Research Centre)

D. Technical Programme Committee (TPC)

John ANDREWS, University of Nottingham, UK

Florent ARRIGNON, MAD-Environment, France

Anne BARROS, CentraleSupélec, France

Julien BAROTH, University of Grenoble, France

Christophe BÉRENGUER, University of Grenoble, France

Marko ČEPIN, University of Ljubljana, Slovenia

Nicolas DECHY, IRSN, France

Sebastien DELMOTTE, MAD-Environment, France

Mohamed EID, RiskLyse, France

Gianluca FULLI, JRC Directorate C – Energy, Mobility and Climate, Italy

Antonio J. GUILLÉN, Ingeman, Spain

Saulius GUDŽIUS, Kaunas University of Technology, Lithuania

Rainer JUNGWIRTH, JRC Directorate E – Space, Security and Migration, Italy

*Vytis KOPUSTINSKAS, JRC Directorate C – Energy, Mobility and Climate, Italy

Elisabeth KRAUSMANN, JRC Directorate E – Space, Security and Migration, Italy

Pierre-Etienne LABEAU, Université libre de Bruxelles, Belgium

Andre LANNOY, IMdR, France

Marcelo MASERA, Politecnico di Torino, Italy

Tomasz NOWAKOWSKI, Wroclaw University of Science and Technology, Poland

Rasa REMENYTÉ-PRESCOTT, University of Nottingham, United Kingdom

Sigitas RIMKEVIČIUS, Lithuanian Energy Institute, Lithuania

Antonio Jesus SANCHEZ HERGUEDAS, University of Seville, Spain

Giovanni SANSAVINI, ETH Zürich, Switzerland

John STOOP, Kindunos, Netherlands

Jean-Marc TACNET, University of Grenoble, France

Agnieszka TUBIS, Wrocław University of Science and Technology, Poland

Bogdan VAMANU, ‘Horia Hulubei’ National Institute of Physics and Nuclear Engineering, Romania

Laila ZEMITE, Riga Technical University, Latvia

**Technical Programme Committee chairperson*

E. Local Organisation Committee

Virginie PETITJEAN (JRC Directorate C – Energy, Mobility and Climate, Netherlands)

Isabel ASENSIO (JRC Directorate C – Energy, Mobility and Climate, Italy)

Hrvoje FORETIĆ (JRC Directorate C – Energy, Mobility and Climate, Netherlands)

Vytis KOPUSTINSKAS (JRC Directorate C – Energy, Mobility and Climate, Italy)

F. Scope of the seminar

Research in resilience of infrastructure systems has been constantly increasing during the last decade and is expected to grow further. Although the term resilience was used in material science already in 19th century, the current meaning of system resilience originates from research in ecology back in 70s. Self-repairable computer systems, being developed also in the same decade for space and defence applications, could be considered as examples of resilience applications in engineering. Resilience applications in technical systems domain have evolved most significantly during the last two decades and the term resilience has already been transferred to the policy domain, as the Directive on the Resilience of Critical Entities (CER Directive) went into force in January 2023 and replaced the Critical Infrastructure Directive, published in 2008.

Two fundamental points in resilience domain to be addressed by the Seminar are:

- The methodological development of resilience assessment from a conceptual framework to modelling approaches.
- The metrics for resilience assessment and development of quantitative tools for decision-making.

The 63rd ESReDA seminar will be a forum for exploring these points and other related questions. We aim to discuss theories, concepts, and experiences of resilience assessment methodologies and applications. Authors are invited to present their proposals and discuss successes and/or failures and to identify future needs in resilience research. We want to encourage new ideas, scientific papers, conceptual papers, case studies and cross-sectoral research on this topic with examples and applications of infrastructures exposed to both technological and natural threats, hazards. This seminar will bring together researchers, practitioners and decision-makers.

G. Target groups and domains of application (examples)

Papers for the seminar are welcome from various stakeholders (industry, academia, R&D consultancy organisations) and could address different infrastructure sectors:

- Energy sector (electricity, gas, hydrogen)

- Transport sector (rail, road, air and maritime)
- Other Critical infrastructures, networks and entities
- Urban development
- Public sector and government

This seminar is aimed at addressing resilience due to different hazards and threats, such as:

- Disruptions of infrastructures due to aging or random failures,
- Natural disasters,
- Intentional attacks or man-made hazards,
- Emerging threats (e.g. hybrid).

Interdependencies of infrastructures and cascading effects are also among the topics of the Seminar. It integrates as well technical, human, organizational, social, financial dimensions. Other topics may be included if they fit well within the topic on resilience assessment.

Annex 4: About ESReDA organisation and activities

European Safety, Reliability & Data Association (ESReDA)

European Safety, Reliability & Data Association (ESReDA) is a European Association established in 1992 to promote research, application and training in Reliability, Availability, Maintainability and Safety (RAMS). The Association provides a forum for the exchange of information, data and current research in Safety and Reliability. The contents of ESReDA seminar proceedings do not necessarily reflect the position of ESReDA. They are the sole responsibility of the authors concerned. ESReDA seminar's proceedings are designed for free public distribution. Reproduction is authorized provided the source is acknowledged.

ESReDA membership is open to organisations, private or governmental institutes, industry researchers and consultants, who are active in the field of Safety and Reliability. Membership fees are currently 1000 EURO for organisations and 500 EURO for universities and individual members. Special sponsoring or associate membership is also available.

For more information and available ESReDA proceedings please consult: <http://www.esreda.org/>.

ESReDA project group on Resilience Assessment of Critical Infrastructures

ESReDA is currently running a new project group (PG) on Resilience Assessment of Critical Infrastructure, approved by the General Assembly of ESReDA during the meeting in April 2023. This project group (PG) continues the work done in the previous ESReDA project group "Resilience Engineering and Modelling of Networked Infrastructure" during 2018-2021 years.

The aim of the PG is to develop and propose an integrated approach for quantitative resilience assessment including management decisions (comparison of solutions for investment, maintenance) in a context of uncertain scenarios (global change and emerging threats).

This Seminar served as a forum to discuss the work of the project group, exchange ideas and set a work plan for the next years. A dedicated project group meeting was held on October 24, the day before the Seminar. We invite all interested institutions to contact the organisers to develop a joint plan for future work in the field of resilience and contribute to the project group.

Getting in touch with the EU

In person

All over the European Union there are hundreds of Europe Direct centres. You can find the address of the centre nearest you online (european-union.europa.eu/contact-eu/meet-us_en).

On the phone or in writing

Europe Direct is a service that answers your questions about the European Union. You can contact this service:

- by freephone: 00 800 6 7 8 9 10 11 (certain operators may charge for these calls),
- at the following standard number: +32 22999696,
- via the following form: european-union.europa.eu/contact-eu/write-us_en.

Finding information about the EU

Online

Information about the European Union in all the official languages of the EU is available on the Europa website (european-union.europa.eu).

EU publications

You can view or order EU publications at op.europa.eu/en/publications. Multiple copies of free publications can be obtained by contacting Europe Direct or your local documentation centre (european-union.europa.eu/contact-eu/meet-us_en).

EU law and related documents

For access to legal information from the EU, including all EU law since 1951 in all the official language versions, go to EUR-Lex (eur-lex.europa.eu).

EU open data

The portal data.europa.eu provides access to open datasets from the EU institutions, bodies and agencies. These can be downloaded and reused for free, for both commercial and non-commercial purposes. The portal also provides access to a wealth of datasets from European countries.

Science for policy

The Joint Research Centre (JRC) provides independent, evidence-based knowledge and science, supporting EU policies to positively impact society



EU Science Hub

Joint-research-centre.ec.europa.eu



Publications Office
of the European Union